

Departement für Chemie  
Universität Freiburg (Schweiz)

**Controlling the supramolecular assembly of perfluorinated poly-  
condensed aromatic hydrocarbons by side chain engineering**

INAUGURAL-DISSERTATION

zur Erlangung der Würde eines *Doctor rerum naturalium* der Mathematisch-  
Naturwissenschaftlichen Fakultät der Universität Freiburg in der Schweiz

vorgelegt von

Olivier F. Aebischer

aus

Schmitten / FR

Dissertation Nr. 1575

Uniprint

2007

Von der Mathematisch-Naturwissenschaftlichen Fakultät der Universität Freiburg in der Schweiz angenommen, auf Antrag von Prof. Dr. Titus A. Jenny, Prof. Dr. Daniel Guillon (Université Louis-Pasteur, Frankreich), Prof. Dr. Hans Ulrich Güdel (Universität Bern, Schweiz) und Prof. Dr. Carl-Wilhelm Schlaepfer (Universität Freiburg, Schweiz), Präsident der Jury.

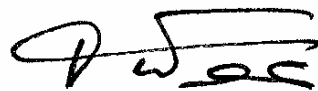
Freiburg, 26. Juli 2007

Dissertationsleiter und Dekan

A handwritten signature in black ink, appearing to read 'Titus Jenny'.

Prof. Dr. Titus A. Jenny

Vizedekan

A handwritten signature in black ink, appearing to read 'A. Weiss'.

Prof. Dr. Antoine Weiss

Für Myriam und meine Familie, Ruth und Charles





Aus Leidenschaft entsteht die Vision eines Zieles

Bruno Staffelbach



## Acknowledgement

This work has been realised under the guidance of Prof. Dr. Titus A. Jenny in the period of January 2004 until June 2007 at the Department of Chemistry, University of Fribourg (Switzerland)

I would like to express my deep gratitude to Prof. Dr. Titus A. Jenny for the kind acceptance in his research group and for the possibility to realise this work. The numerous and motivating discussions as well as the insightful guidance helped very much to realise this thesis.

I would also like to express my gratefulness to Prof. Dr. Daniel Guillon and Prof. Dr. Hans Ulrich Güdel for their kind acceptance as experts and for their valuable feedback.

The present and the previous heads of the department; Prof. Dr. Thomas Bally, Prof. Dr. Titus A. Jenny and Prof. Dr. Peter Belser are thanked for the availability of an assistantship position. Priv. Doc. Dr. Norbert Engel is appreciated for organizing the students' practical course. Prof. Dr. Titus A. Jenny is very deeply appreciated for the possibility to join the analytical service in the frame of the assistantship position as this experience proved to be extremely valuable.

I wish to express my sincere appreciation to all persons external to the University of Fribourg for their kind and valuable support, namely:

Prof. Dr. Hans Ulrich Güdel, Dr. Annina Aebischer and Dr. Karl Krämer (University of Bern) for the possibility to perform fluorescence experiments in their department and for all fruitful discussions and overall the competent technical support.

Prof. Dr. Daniel Guillon and Dr. Bertrand Donnio (University Louis Pasteur) for the TGA, DSC and XRD measurements as well as for the valuable discussions of the obtained data.

Dr. Massoud Dadras and Mireille LeBoeuf (University of Neuchâtel) for the possibility to perform cryo-SEM, SEM, TEM and AFM measurements as well as for their valuable technical support.

Prof. Dr. Walter Amrein, Dr. Oliver Scheidegger and Louis Bertschi (ETHZ) are kindly acknowledged for carrying out the numerous MALDI-TOF characterizations as well as the helpful discussions.

Prof. Bodenhausen, Dr. Jens Dittmer, Dr. Sasha Antonjevic and Simone Cavadini (EPFL) are thanked for their technical support to build up the SS-NMR facility at the University of Fribourg.

Prof. Robert Deschenaux and Dr. David Scanu (University of Neuchâtel) for the performance of DSC and POM investigations.

Dr. Arno Schneider (ETHZ) for the THz measurements and the kind demonstration of his facilities.

Prof. Eric Vauthey and Jakob Grilj (University of Geneva) for the performance of time resolved fluorescence and their valuable support for the interpretation of the obtained data.

Dr. Pierangelo Gröning, Dr. Oliver Gröning and Dr. Pascal Ruffieux (EMPA Thun) for the STM investigations and for their kind support in the field of electron emission.

Prof. Dr. Thomas Bally (University of Fribourg) for the performed calculation and the helpful discussions.

My special thanks goes to the analytical service of the University of Fribourg, namely to Freddy Nydegger (mass analysis), Felix Fehr (NMR analysis) and Inge Müller (general support) for the analytical support and their kind acceptance in their group.

Daniela Bossi, Martine Poffet, Mauro Schindler, Patrick Tondo are thanked for their patience to review the manuscript and for their support during this thesis.

Dr. Bassam Alameddine, Dr. Christophe Eggertswyler, Dr. Roger Mafua and Dr. Ludwig Muster are thanked for their support during this thesis and for their kind acceptance in the research group.

A special thank to those who participated to his project: Jean-Luc Débieux and Patrick Tondo (diploma thesis), and particularly to Mauro Schindler and David Muñoz (Master thesis) as well as Corinne Savary (central laboratory) and Benoît Dubray (advanced practical work)

An appreciation to all the Chemistry department and a special thank for all those whose kind support greatly facilitated this work: Jaques Hässler, Nils Zimmermann, Rafael Nussbaum, Jaime Lage Robles, Claire-Lise Ciana, Aurelien Crochet, Priscilla Brunetto, Laurent Mirolo, Fabienne Gschwind, Anne Schuwey and Verena Schwalm.

A special than also to Xavier Hanselmann, Lucienne Rouillet, Bernadette Khun-Piccand, Noelle Chassot, Philippe Rime and Hubert Favre of the central service. Many thanks to Verena Schwalm and Emerith Brügger (secretaries). Further Alphonse Crottet and Olivier Graber are thanked for the technical, electrical and mechanical support they offered. Michel Piccand is acknowledged for the poster impressions.

A special thank goes to my family, Ruth and Charles Aebischer, Myriam, Hildi and Peter Zbinden, Romy and Sepp Stadler, Christine and Sacha Volery and David Raemy for their support outside the University.

This project was supported by the Swiss National Science Foundation

## Table of contents

<b>Acknowledgement</b>	i
<b>List of abbreviations</b>	ix
<b>Summary</b>	1
<b>Zusammenfassung</b>	3
<b>I Theoretical Part</b>	5
<b>1 Introduction</b>	7
<b>2 Molecular interactions – self-assembly</b>	9
2.1 Introduction	9
2.2 $\pi$ - $\pi$ stacking	9
2.2.1 <i>General considerations</i>	9
2.2.2 <i>Discotic derivatives in solution</i>	11
<b>3 Charge carrier mobility</b>	13
3.1 Introduction	13
3.2 Molecular wires	13
3.2.1 <i>Formation of excitons</i>	14
3.2.2 <i>Charge injection</i>	14
<b>4 Applications in nanotechnology</b>	17
4.1 Introduction	17
4.2 Organic field effect transistors (OFET)	18
4.2.1 <i>Research development</i>	18
4.2.2 <i>Basic principle of OFET devices</i>	18
4.3 Organic light emitting diode (OLED)	20
4.3.1 <i>Research development</i>	20
4.3.2 <i>Basic principle of OLED devices</i>	20
4.4 Field emission display (FED)	22
4.4.1 <i>Basic principle of field emission displays</i>	22
4.4.2 <i>Field emission – the Fowler-Nordheim law</i>	23
4.4.3 <i>Metallic emission tips</i>	27

---

4.4.4	<i>CNT emission tips</i>	29
<b>5</b>	<b>Toward a new self-assembled molecular wire</b>	33
5.1	Possible application – OFET (organic field effect transistor)	34
5.2	Possible application – OLED (organic light emitting diode)	34
5.3	Possible application – FED (field emission display)	35
<b>6</b>	<b>Supramolecular wires</b>	39
6.1	Choice of the appropriate aromatic core	39
6.2	Crystallization of HBC bearing no lateral chains	40
6.3	Six-fold alkylated HBC derivatives	40
6.4	Variation of the number and the nature of the lateral chains	45
6.5	Functional sided chains allowing cross-linking or “double cable” formation	47
<b>7</b>	<b>Suppressing lateral aggregation by “fluorine coating”</b>	49
<b>8</b>	<b>Vision of the Thesis</b>	51
<b>II</b>	<b>Results and Discussion – Part 1: Synthetic Investigations</b>	53
<b>9</b>	<b>General aspects</b>	55
9.1	Retro synthesis of HBC derivatives	55
9.1.1	<i>Cyclodehydrogenation of HPB derivatives</i>	55
9.1.2	<i>Formation of HPB derivatives with <math>D_{6h}</math> symmetry</i>	60
9.1.3	<i>Formation of substituted tolane derivatives</i>	62
9.1.4	<i>Formation of perfluoroalkylated halogenaryl derivatives</i>	63
9.1.5	<i>Formation of HPB derivatives with <math>D_{3h}</math> symmetry</i>	64
9.1.6	<i>Formation of completely desymmetrized HPB derivatives</i>	66
9.2	Introduction to applied C-C cross coupling reactions	67
9.2.1	<i>Kumada, Suzuki cross-couplings</i>	67
9.2.2	<i>Heck cross-couplings</i>	69
9.2.3	<i>Sonogashira cross-couplings</i>	70
<b>10</b>	<b>HBC carrying linear alkyl / perfluoroalkyl side chains</b>	73
10.1	Introduction	73
10.2	HBC- $Rf_{2,6}$ and HBC- $Rf_{2,8}$	74
10.2.1	<i>Attempted direct synthesis of Tol-<math>Rf_{2,6}</math></i>	74
10.2.2	<i>X-Ph-<math>Rf_{2,6}</math></i>	74

10.2.3	<i>HPB-Rf<sub>2,6</sub></i>	75
10.2.4	<i>HBC-Rf<sub>2,6</sub></i>	78
10.3	<i>HBC-Rf<sub>3,6</sub> and HBC-Rf<sub>3,8</sub></i>	79
10.3.1	<i>Synthesis of X-Ph-Rf<sub>3,6</sub> and X-Ph-Rf<sub>3,8</sub></i>	79
10.3.2	<i>Synthesis of HPB-Rf<sub>3,6</sub> and HPB-Rf<sub>3,8</sub></i>	82
10.3.3	<i>Synthesis of HBC-Rf<sub>3,6</sub> and HBC-Rf<sub>3,8</sub></i>	85
10.4	<i>HBC-Rf<sub>4,4</sub>, HBC-Rf<sub>4,6</sub>, HBC-Rf<sub>4,8</sub> and HBC-Rf<sub>4,10</sub></i>	85
10.4.1	<i>Synthesis of X-Ph-Rf<sub>4,m</sub></i>	85
10.4.2	<i>Synthesis of HPB-Rf<sub>4,m</sub></i>	87
10.4.3	<i>Synthesis of Tol-Rf<sub>4,8</sub></i>	87
10.4.4	<i>Synthesis of HBC-Rf<sub>4,m</sub></i>	88
10.5	<i>HBC-Rf<sub>5,6</sub> and HBC-Rf<sub>6,8</sub></i>	89
10.5.1	<i>Synthesis of Ph-Rf<sub>5,6</sub> and Ph-Rf<sub>6,8</sub></i>	89
10.5.2	<i>Synthesis of HPB-Rf<sub>5,6</sub> and HPB-Rf<sub>6,8</sub></i>	91
10.5.3	<i>Synthesis of HBC-Rf<sub>5,6</sub> and HBC-Rf<sub>6,8</sub></i>	92
10.6	<i>HBC-Rf<sub>5,8</sub></i>	93
10.6.1	<i>Synthesis of X-Rf<sub>5,8</sub></i>	93
10.6.2	<i>Synthesis of HPB-Rf<sub>5,8</sub></i>	93
10.6.3	<i>Synthesis of HBC-Rf<sub>5,8</sub></i>	95
10.7	<i>HBC-Rf<sub>8,4</sub>, HBC-Rf<sub>8,6</sub> and HBC-Rf<sub>8,8</sub></i>	95
10.7.1	<i>Synthesis of X-Ph-Rf<sub>8,m</sub></i>	96
10.7.2	<i>Synthesis of HPB-Rf<sub>8,m</sub></i>	97
10.7.3	<i>Synthesis of HBC-Rf<sub>8,m</sub></i>	98
<b>11</b>	<b>HBC carrying branched perfluorinated side chains</b>	<b>99</b>
11.1	Introduction	99
11.2	<i>HBC-Rf<sub>3,3,6,6</sub> and HBC-Rf<sub>3,3,4,4</sub></i>	99
11.2.1	<i>Synthesis of Br-Ph-Rf<sub>3,3,6,6</sub> and Br-Ph-Rf<sub>3,3,4,4</sub></i>	99
11.2.2	<i>Synthesis of HPB-Rf<sub>3,3,6,6</sub> and HPB-Rf<sub>3,3,4,4</sub></i>	101
11.2.3	<i>Synthesis of HBC-Rf<sub>3,3,6,6</sub> and HBC-Rf<sub>3,3,4,4</sub></i>	101
11.3	<i>HBC-Rf<sub>(3,3,6,6)</sub>3 – a HBC derivative in D<sub>3h</sub> symmetry</i>	102
11.3.1	<i>Synthesis of m-substituted aryl derivatives</i>	103
11.3.2	<i>Threefold aryl-aryl Suzuki and Kumada cross-coupling reactions</i>	105
11.3.3	<i>Threefold aryl-alkyl Heck, Kumada or Sonogashira cross-coupling</i>	105

11.3.4	<i>Synthesis of an isomeric mixture of HBC-Rf<sub>(3,3,6,6)</sub><sub>3</sub></i>	107
<b>12</b>	<b>HBC primer</b>	109
12.1	Introduction	109
12.2	HBC-SCF <sub>3</sub>	109
12.2.1	<i>Synthesis of HPB-SCF<sub>3</sub></i>	110
12.2.2	<i>Synthesis of HBC-SCF<sub>3</sub></i>	111
12.3	HBC-CH <sub>2</sub> S- <i>t</i> -butyl and HBC-CH <sub>2</sub> S-C <sub>12</sub> H <sub>25</sub>	113
12.3.1	<i>Synthesis of HPB-CH<sub>2</sub>S-<i>t</i>-butyl and HPB-CH<sub>2</sub>S-C<sub>12</sub>H<sub>25</sub></i>	113
12.3.2	<i>Synthesis of HBC-CH<sub>2</sub>S-<i>t</i>-butyl and HBC-CH<sub>2</sub>S-C<sub>12</sub>H<sub>25</sub></i>	115
12.4	HBC-(CH <sub>2</sub> S- <i>t</i> -butyl) <sub>3</sub>	115
12.5	HBC-(CH <sub>2</sub> S- <i>t</i> -butyl) <sub>1</sub>	117
12.6	Concluding remarks on the synthetic part	118
<b>III</b>	<b>Results and Discussion – Part 2: Investigation of the Properties</b>	119
<b>13</b>	<b>Characterization of perfluoroalkylated HBC derivatives</b>	121
13.1	NMR spectroscopy in the liquid and solid state	121
13.2	MS spectroscopy	125
<b>14</b>	<b>Investigation techniques – cryo-SEM and fluorescence</b>	127
14.1	Cryo-SEM	127
14.1.1	<i>Scope and limitation</i>	127
14.1.2	<i>Sample preparation</i>	129
14.1.3	<i>Cryo-SEM versus SEM</i>	130
14.2	Fluorescence	131
14.2.1	<i>Introduction</i>	131
14.2.2	<i>Theoretical background</i>	132
14.2.3	<i>Excitation and luminescence spectrum of HBC derivatives</i>	133
14.2.4	<i>Luminescence spectrum of 1-D stacks and 2-D or 3-D lateral aggregated structures</i>	135
14.2.5	<i>Influence of oxygen</i>	137
14.2.6	<i>Ultrasonic treatment</i>	138
14.2.7	<i>Wavelength dependence of the excitation and luminescence</i>	139
14.2.8	<i>Fluorescence dynamics</i>	140
<b>15</b>	<b>Tuning the aggregation behaviour of HBC derivatives</b>	143
15.1	Engineering the medium	143



---

15.1.1 Solvent influence on the aggregation	143
15.1.2 Concentration influence on the aggregation	146
15.1.3 Effect of temperature and time on the aggregation	151
15.1.4 Complexation of the HBC core	152
15.2 Engineering the side chain	154
15.2.1 Variation of the alkyl spacer $n$ of linear chains in HBC-Rf <sub><math>n,m</math></sub>	154
15.2.2 Variation of the perfluoro spacer $m$ of linear chains in HBC-Rf <sub><math>n,m</math></sub>	164
15.2.3 Comparing the perfluoro / alkyl ratio	169
15.2.4 Branched perfluoroalkyl chains	170
<b>16 Morphology of HBC derivatives</b>	<b>175</b>
16.1 DSC and TGA investigations	175
16.2 X-ray investigations	177
16.2.1 Temperature dependence of X-ray	177
16.2.2 X-ray investigation at high temperatures	178
<b>17 Alternative techniques for the detection of self-aggregated stacks</b>	<b>187</b>
17.1 TEM investigations	187
17.2 THz investigations	189
17.2.1 General considerations	189
17.2.2 Generation of THz pulses and set up of the measurement	189
17.2.3 THz experiment on HBC derivatives	191
<b>18 Deposition attempts of primer HBCs</b>	<b>193</b>
18.1 Solution deposition on a gold-silicon wafer	193
18.2 Sublimation on a gold wafer	194
<b>IV Conclusion and outlook</b>	<b>197</b>
<b>19 Conclusion and outlook</b>	<b>199</b>
<b>V Experimental Part</b>	<b>203</b>
<b>20 General considerations</b>	<b>205</b>
<b>21 Synthesis of HBCs bearing linear alkyl / perfluoroalkyl side chains</b>	<b>209</b>
21.1 Synthesis of HBC-(Rf <sub>2,6</sub> ) <sub>6</sub>	209
21.2 Synthesis of HBC-(Rf <sub>3,6</sub> ) <sub>6</sub>	214

21.3	Synthesis of HBC-(Rf <sub>3,8</sub> ) <sub>6</sub>	218
21.4	Synthesis of HBC-(Rf <sub>4,4</sub> ) <sub>6</sub>	223
21.5	Synthesis of HBC-(Rf <sub>4,6</sub> ) <sub>6</sub>	228
21.6	Synthesis of HBC-(Rf <sub>4,8</sub> ) <sub>6</sub>	235
21.7	Synthesis of HBC-(Rf <sub>4,10</sub> ) <sub>6</sub>	239
21.8	Synthesis of HBC-(Rf <sub>5,6</sub> ) <sub>6</sub>	243
21.9	Synthesis of HBC-(Rf <sub>5,8</sub> ) <sub>6</sub>	250
21.10	Synthesis of HBC-(Rf <sub>6,8</sub> ) <sub>6</sub>	253
21.11	Synthesis of HBC-(Rf <sub>8,4</sub> ) <sub>6</sub>	260
21.12	Synthesis of HBC-(Rf <sub>8,6</sub> ) <sub>6</sub>	265
21.13	Synthesis of HBC-(Rf <sub>8,8</sub> ) <sub>6</sub>	271
<b>22</b>	<b>Synthesis of HBCs carrying branched perfluorinated side chains</b>	<b>277</b>
22.1	Synthesis of HBC-(Rf <sub>3,3,4,4</sub> ) <sub>6</sub>	277
22.2	Synthesis of HBC-(Rf <sub>3,3,6,6</sub> ) <sub>6</sub>	284
22.3	Synthesis HBC-(Rf <sub>3,3,6,6</sub> ) <sub>3</sub>	289
<b>23</b>	<b>Synthesis of HBC primers</b>	<b>301</b>
23.1	Synthesis of HBC-(SCF <sub>3</sub> ) <sub>6</sub>	301
23.2	Synthesis of HBC-(CH <sub>2</sub> S- <i>t</i> -butyl) <sub>6</sub>	304
23.3	Synthesis of HBC-(CH <sub>2</sub> S- <i>t</i> -butyl) <sub>3</sub>	307
23.4	Synthesis of HBC-(CH <sub>2</sub> S- <i>t</i> -butyl) <sub>1</sub>	310
23.5	Synthesis of HBC-(CH <sub>2</sub> S-dodecyl) <sub>6</sub>	314
<b>VI</b>	<b>Annexes</b>	<b>317</b>
<b>24</b>	<b>Index of main compounds</b>	<b>319</b>
<b>VII.</b>	<b>Curriculum Vitae</b>	<b>321</b>
<b>VIII.</b>	<b>References</b>	<b>325</b>

## List of abbreviations

6am4	bis(4-methyl phenyl)phenylamine
acac	Acetylacetonate
AIBN	2,2'-azobis(2-methylpropionitrile)
aliquat 336	tricaprylmethylammonium chloride
BATC	Benzyltriethylammoniumchloride
BTF	$\alpha,\alpha,\alpha$ -benzotrifluoride
CNT	carbon nanotube
cp	cross polarisation
Cp	cyclopentadiene
cpd	composite pulse decoupling
CRT	cathode ray tube
cryo-SEM	cryo-scanning electron microscope
CSA	chemical shift anisotropy
CVD	chemical vapour deposition
CW	continuous wave
DAST	4- <i>N,N</i> -dimethylamino-4'- <i>N'</i> -methyl stilbazolium tosylate
dba	dibenzylideneacetone
DBN	1,5-diazabicyclo[4.3.0]non-5-ene
DBPO	dibenzoylperoxide
DBU	1,8-diazabicyclo[5.4.0]undec-7-ene
DCTB	trans-2-[3-(4- <i>tert</i> -buthylphenyl)-2-methyl-2-propenylidene]malononitrile
DDQ	2,3-dichloro-5,6-dicyano-1,4-benzochinon
DMA	<i>N,N</i> -dimethylacetamide
DMF	<i>N,N</i> -dimethylformamide
DMSO	dimethylsulfoxide
dppf	1,1'-bis(diphenylphosphine)ferrocene
dppp	1,3-bis(diphenylphosphine)propane
EI	electron impact
ESI	electron spray ionisation
FAB	fast atomic bombardment
FED	field emission display
FEM	field emission microscope
FID	free induction decay
FWHM	full width at half maximum
GUAN	1,3,4,6,7,8-hexahydro-2 <i>H</i> -pyrimido(1,2- <i>a</i> )pyrimidine
HBC	hexa- <i>peri</i> -hexabenzocoronene

---

HBC-C <sub>x,y</sub>	HBC derivative carrying six identical branched alkyl chains, x indicating the number of carbon atoms of the longest chain whereas y is the sum of carbon atoms of the secondary chain.
HBC-Rf <sub>n,m</sub>	HBC-(Rf <sub>n,m</sub> ) <sub>6</sub> ; only other than six lateral chains are noted
HFB	hexafluorobenzene
HOMO	highest occupied molecular orbital
HOPG	highly oriented pyrolytic graphite
HPB	hexaphenylbenzene
IMes	<i>N,N'</i> -bis(2,4,6-trimethylphenyl)imidazol-2-ylidene
IPr	<i>N,N'</i> -bis(2,6-diisopropylphenyl)imidazol-2-ylidene
ITO	indium tin oxide
LCD	liquid crystal display
LUMO	lowest unoccupied molecular orbital
MA	magic angle
MALDI-ICR	matrix assisted laser desorption ionisation - ion cyclotron resonance
MALDI-TOF	matrix assisted laser desorption ionisation - time of flight
MAS	magic angle spinning
MWNT	multi-walled carbon nanotube
NBS	<i>N</i> -bromosuccinimide
NMR	nuclear magnetic resonance
OFET	organic field effect transistor
OFT	octafluorotoluene
OLED	organic light emitting diode
PAH	polyaromatic hydrocarbon
PEDOT	poly(3,4-ethylenedioxythiophene)
PF2	poly[9,9-bis(2-ethylhexyl)fluorene-2,7-diyl]
PIFA	bis(trifluoroacetoxy)iodobenzene
PR-TRMC	pulse-radiolysis time-resolved microwave conductivity
PSS	poly(styrene sulfonic acid)
Rf <sub>n,m</sub>	abbreviation for semi-perfluorinated chains: n indicating the number of alkyl carbons; m indicating the number of perfluorinated carbons
Rf <sub>n1,n2,m1,m2</sub>	abbreviation for branched semi-perfluorinated chains: n1 indicating the number of alkyl carbon before the branching point; n2 indicating the number of alkyl carbon after the branching point, including the later; m1 gives the number of perfluorinated carbons of one chain; m2 number of perfluorinated carbons of the second chain
SAFEM	scanning anode field emission microscope
SEM	scanning electron microscope
SPC	single photon counting
SWNT	single-walled carbon nanotube

---

<i>t</i> -Am	<i>tert</i> -amylate
TBB	3'',3'',3''-triiodo-1,3,5-tribiphenylbenzene
TCB	1,2,4-trichlorobenzene
TCNE	tetracyanoethylene
TCNQ	7,7,8,8-tetracyanoquinodimethane
TDDFT	time dependent density functional theory
TEA	triethylamine
TEG	triethylene glycol
TFA	trifluoroacetic acid
TMS	tetramethylsilane / trimethylsilane
TMSA	trimethylsilylacetylene
Tol	tolane
Tol-Rf <sub>n,m</sub>	Tol-(Rf <sub>n,m</sub> ) <sub>n</sub> ; only other than two lateral chains are noted
UV	ultraviolet
VIS	visible



---

## Summary

The possibilities of industry to process and to engineer materials at the nanometer level rapidly increase and products using materials engineered at the nanometer level emerge on the markets. In the long term, it is hardly possible to estimate, from the present point, where the ability to engineer materials on the nano-scale will lead human beings, whether the dream of a molecular nanotechnology with autonomous working machines, built with atomic precision, will ever become reality. Due to this promising development, nanotechnology is an ever increasing field of research.

This work focuses on the preparation and investigation of certain polycondensed aromatic hydrocarbons (PAH), showing a very high charge carrier mobility in the bulk. These PAH are known to form nano-scaled self-assembled columnar  $\pi$ - $\pi$ -aggregated structures offering thereby an access to nanometer sized electronic building blocks. Such self-assembled nanofilaments are promising candidates in the area of field emission displays or organic field effect transistors. They excel over other systems through their self-healing property, due to the  $\pi$ - $\pi$ -aggregation, and through the possibility of chemically synthesizing highly pure monomers able to form complex architectures.

Substituted disc-shaped perfluorinated hexa-*peri*-hexabenzocoronenes (HBC), known to self-assemble into conducting ordered architectures were synthesized and characterized. As highly fluorinated derivatives behave completely different than their purely alkylated counterparts, new synthetic strategies had to be developed to perform all syntheses. A systematic variation of the linear or branched perfluoroalkylated side chains was performed in order to improve their one dimensional self-aggregation. The fluorine mantle around the self-assembled stack, formed by the perfluoroalkylated tails of the side chains, endowed these HBC derivatives with a “Teflon-like” coating, preventing eventually the lateral aggregation of formed one dimensional architectures. Scanning probe microscope and optical investigations in solution (fluorescence and time resolved fluorescence) revealed the possibility of obtaining linear monostranded stacks. By systematic engineering of the side chains as well as the medium some control on the aggregation was gained. Powder X-ray as well as differential scanning calorimetry proved the liquid crystalline behaviour for most prepared HBC derivatives at elevated temperature.

In order to grow monostranded stacks of self-assembled HBC derivatives onto a metallic surface a primer HBC molecule was designed acting as a “docking station” for the perfluoroalkylated HBC derivatives. The primer derivatives were fitted with sulfur atoms in the lateral chain, known to have a good adhesion on gold surfaces. A variation of the number of the side chains as well as the nature of the protecting group was performed in order to find the ideal primer derivative. Vapour deposited monolayers on gold were prepared and investigated with a scanning tunnelling microscopy (still running).

Such self-assembled molecular wires are potential candidates for state of the art applications, such as field emission displays (FED), organic light emitting diodes (OLED) or field effect transistors (FET). Their most outstanding properties are the self healing effect as the individual constituents are not covalently linked and the possibility to obtain a defect free material is guaranteed by the chemical synthesis.



---

## Zusammenfassung

Nanotechnologie ist ein Begriff, dessen Bedeutung ständig wächst, da die Industrie täglich mehr Materialien auf den Markt bringt, welche im Prozess der Miniaturisierung bis in den Nanometerbereich entwickelt wurden. Vom heutigen Standpunkt aus ist es längst nicht mehr klar, wohin uns die Nanotechnologie noch führen wird. Kann der Traum von molekularen Maschinen, die mit „atomarer“ Präzision arbeiten, je einmal verwirklicht werden? Die Antwort kann momentan noch nicht gegeben werden, jedoch steht schon heute fest, dass solche „Nanotechnologie-Träume“ dieses interessante Forschungsgebiet rasch vorantreiben werden.

Diese Arbeit beschäftigt sich mit der Herstellung und den Eigenschaften von einigen auserwählten polykondensierten aromatischen Kohlenwasserstoffen. Diese Kohlenwasserstoffe besitzen die höchste Ladungsmobilität, welche bisher für organische Moleküle gemessen wurde. Des Weiteren sind diese Verbindungen durch  $\pi$ - $\pi$ -Wechselwirkungen in der Lage, selbst-aggregierende lineare Strukturen im Nanometerbereich zu bilden. Diese Nano-Strukturen sind sehr viel versprechende Kandidaten für die Konstruktion von Feldemissionsbildschirmen oder von organischen Feldeffekttransistoren. Der Vorteil dieser neuartigen Strukturen liegt in bisher unbekannten Eigenschaften, wie zum Beispiel deren Selbstheilung nach äußerer Störung. Weiter bestehen die selbst-aggregierenden Strukturen aus Monomeren, welche ihrerseits chemisch in sehr hoher Reinheit hergestellt werden können.

Hexa-*peri*-hexabenzocoronene Derivate (HBC), welche mit teilweise perfluorierten Seitenketten ausgestattet sind und mittels Selbstaggregation leitende Strukturen bilden, wurden in dieser Arbeit hergestellt und charakterisiert. Es ist bekannt, dass sich hochfluorierte Derivate im Vergleich zu alkylierten Verbindungen sehr unterschiedlich verhalten. Aus diesem Grund mussten die bestehenden und publizierten Synthesestrategien für alkylierte Derivate stark abgeändert werden. Um die Eigenschaft zur Bildung molekularer Fäden zu kontrollieren wurde die perfluorierte Seitenkette der HBC-Derivate systematisch verändert. Die perfluorinierten Endstücke der Seitenketten statten diese HBC-Verbindungen mit einer teflonartigen Hülle aus, welche das seitliche „Verkleben“ einzelner Fäden verhindern soll.

Die Eigenschaften der neu hergestellten Verbindungen wurden vor allem mikroskopisch (Rasterelektronenmikroskop) und mit optischen Messungen (Fluoreszenz und Zeit aufgelöste Fluoreszenz) ermittelt. Durch systematische Veränderung der Derivate sowie der Bedingungen (Lösungsmittel, Konzentration etc.) wurde eine Kontrolle über die Bildung molekularer Fäden sowie deren „Verkleben“ gewonnen. Des Weiteren haben dynamische Differenzkalorimetrie (DSC) und Pulver Röntgen Spektroskopie (XRD) nachgewiesen, dass die hergestellten Derivate bei erhöhter Temperatur flüssigkristalline Eigenschaften besitzen.

Um solche molekulare Fäden gezielt auf Oberflächen aufzubringen, benötigt man spezielle Verbindungen, welche „Andockstationen“ für die perfluorinierten HBC Derivate bilden können. Diese mit Schwefel ausgestatteten Verbindungen haben die Eigenschaft, mit Gold eine starke Wechselwirkung einzugehen und dadurch permanent auf der Goldoberfläche zu haften. Eine Variation der schwefelhaltigen Seitenketten wurde auch hier durchgeführt um das ideale „Andock-Molekül“ zu finden. Diese Eigenschaft wurde mit hochauflösenden Mikroskopen (Rastertunnelmikroskop (STM) und Rasterkraftmikroskop (AFM)) untersucht, wobei die hergestellten Derivate auf hochreine Goldoberflächen aufgedampft wurden. Diese Experimente jedoch sind noch nicht abgeschlossen.

Selbst-aggregierende molekulare eindimensionale Strukturen sind ideale Kandidaten für verschiedene Anwendungen, wie zum Beispiel Feldemissionsbildschirme, organische Lichtemissionsdioden oder organische Feldeffekttransistoren. Die aussergewöhnliche Eigenschaft dieser Verbindungen liegt darin, dass keine kovalenten Bindungen zwischen den einzelnen Monomeren vorhanden sind, unter anderem eine Voraussetzung für Selbstheilungseffekte.

## **I Theoretical Part**



## 1 Introduction

The conventional way of producing any sort of functional device was over centuries a manufacturing process respecting the physical laws of Newton. Up to now, human beings have formed and manufactured materials at their will, even though there is a steady ongoing miniaturization process. This may probably change in the near future, due to the engineering of “intelligent” self-organizing materials, endowed with properties such as self-healing or self-cleaning for example. Supramolecular self-assembly is the most promising bottom-up concept in nanotechnology. Precisely controlled molecular self-assembled architectures are potential candidates in fields like electronics, sensor techniques, material science and many others.

Moreover history teaches that normally the long term forecast of future revolutionary technologies was always underestimated. Thus, experts believed after the invention of the transistor that probably at one day the construction of a computer will be possible, made by semiconductors able to perform 5000 operations per second. Furthermore its weight was estimated around 1500 kg! Actual PC stations are nowadays in all respects much more powerful.

Future will show whether nanotechnology will be placed in this line of revolutionary techniques!



## 2 Molecular interactions – self-assembly

### 2.1 Introduction

The principle of self-organization is well known in biological systems and is the driving force in the formation of a wide variety of complex biological structures as for example the folding of proteins<sup>[1]</sup> but is a relatively new manufacturing concept for human beings to be precisely handled. Even though the number of publications concerning self-assembled materials increased enormously during the past years, applications of self-assembled functional derivatives are not yet numerous. Because of that, one of the great challenges in supramolecular chemistry is the development of individual molecular units that are capable of organizing into ordered geometries through weak intermolecular forces.<sup>[2]</sup> Self-assembly is emerging as a new strategy in chemical synthesis, with the potential of generating non-biological structures with dimensions up to several hundreds of nanometres.<sup>[3]</sup> As examples for intermolecular forces one could mention  $\pi$ - $\pi$  interactions,<sup>[4]</sup> hydrogen bonding,<sup>[5]</sup> donor-acceptor interactions<sup>[6]</sup> and reversible ligand-metal interactions.<sup>[7]</sup> Molecules which are promising self-assembling candidates with an application in advanced functional materials include liquid-crystals,<sup>[8]</sup> block copolymers,<sup>[9]</sup> hydrogen bonded complexes<sup>[10]</sup> and coordination polymers.<sup>[11]</sup>

Among supramolecular self-organizing systems, liquid crystals formed of disc shaped molecules, are of particular interest. They endow a great potential of incorporating different desirable chemical functionalities in their periphery and their physical properties may therefore be tuned at nanoscaled dimensions. Discotic derivatives containing large aromatic cores were of particular interest in this thesis. As a consequence of this, the most important non-covalent interaction of these large aromatic derivatives is  $\pi$ - $\pi$  stacking or the so called arene-arene interaction. A more detailed discussion in the following section concentrates on this weak interaction, whereas for the other interactions, the reader is referred to the existing literature cited previously.

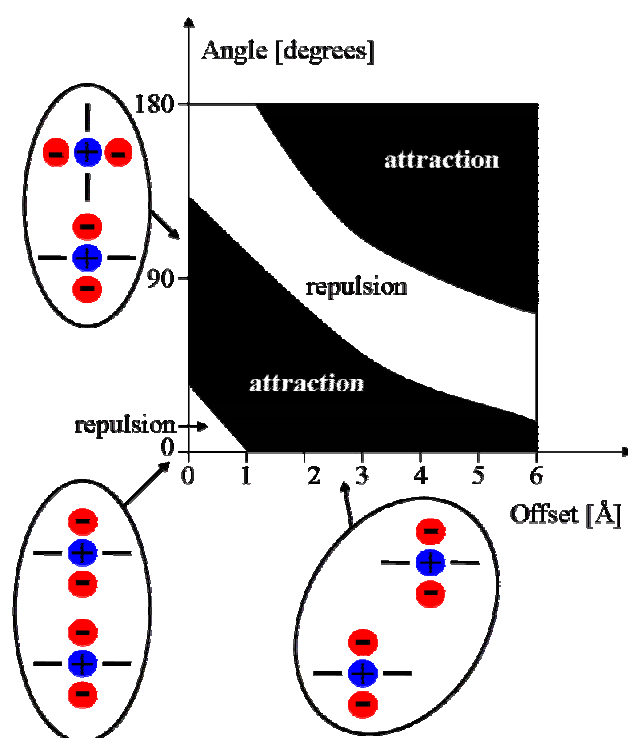
### 2.2 $\pi$ - $\pi$ stacking

#### 2.2.1 General considerations

Aromatic structures have generally one very important main feature being their stacking which has long been recognized as an important role in diverse areas. This is the reason why aromatic compounds were intensively studied by E. Clar,<sup>[12]</sup> J. Fetzer<sup>[13]</sup> and M. Zander.<sup>[14]</sup> Quantitative analysis of this interaction is complicated by the involvement of several factors including van der Waals,

solvophobic and electrostatic effects. Nevertheless some qualitative conclusions can be drawn due to the extensive research done in this field. First, the van der Waals and solvophobic interactions can greatly influence the aromatic stacking. Studies have shown that both the surface area<sup>[15]</sup> and the nature of the solvent strongly affect the strength of  $\pi$ - $\pi$  stacking.<sup>[4a, 16]</sup> Second, electrostatic interactions are also important, as it was shown that the aromatic association is influenced by the electronic characteristics of the substituents attached to the aromatic groups.<sup>[17]</sup>

The  $\pi$ - $\pi$  interaction may be explained by an electrostatic driving force which comes from the attraction between the positively charged  $\sigma$ -framework and the negatively charged electron clouds of the interacting units, which outweigh unfavourable contributions such as  $\pi$ -electron repulsion.<sup>[18]</sup> It has to be noted, that the  $\pi$ - $\pi$  interaction is strongly dependent of the geometry and may be concluded by the following statements: *i)*  $\pi$ -electron repulsion dominates in a face-to-face geometry; *ii)*  $\pi$ - $\sigma$  attraction dominates in an edge-on (T-shaped) geometry or in an offset  $\pi$ -stacked geometry; *iii)* the face-to-face stacked geometry is always favoured by van der Waals interaction and solvophobic effects. Figure 2.1 summarizes these statements which are based on experimental evidence from crystal structures of simple aromatic compounds, where normally two types of geometries are observed: edge-on geometries which give rise to the characteristic herring bone pattern and offset stacked structures.<sup>[19]</sup>



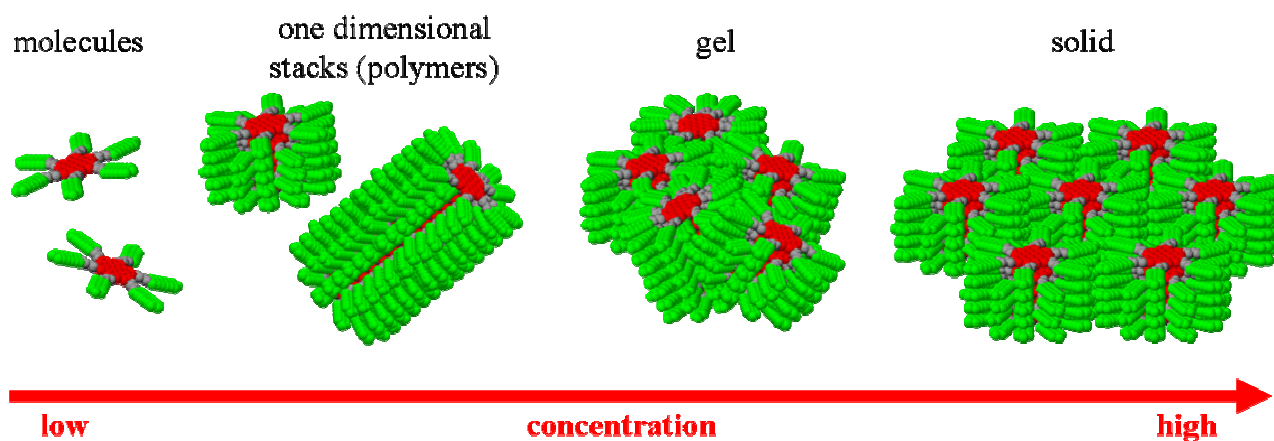
**Figure 2.1** – The interaction between two idealized  $\pi$ -atoms illustrated as a function of the orientation where two attractive geometries and the repulsive face-to-face geometry are shown<sup>[19]</sup>



### 2.2.2 Discotic derivatives in solution

The aromatic compounds considered until now carried no substituents in their periphery which could influence the adopted geometry. Aromatic discotic molecules in contrary often consist of a disc-shaped aromatic core surrounded in by a various number of flexible side chains. The anisotropy due to the flat aromatic core and the flexible side chains generates generally thermotropic liquid crystalline mesophases. The strong  $\pi$ - $\pi$  interaction between the aromatic cores controls the aggregation of the individual molecules. Due to the sterical hindrance exerted by the side chains of laterally substituted discotic derivatives, the only possible  $\pi$ - $\pi$  interaction is face-to-face stacking, sometimes to a certain extent offset or slightly of a herringbone type, depending of the side chains. Because of that, these discotic derivatives are the only type of liquid crystals able to form linear architectures. Other types of liquid crystals have normally ordering interactions of the same order of magnitude in two dimensions, which give rise to gels.

Discotic molecules in solution have normally an aromatic stacking interaction which is stronger than the inter-columnar side-on interaction due to the fact that the van der Waals interactions between the side chains are much weaker. Only at higher concentrations, the intercolumnar interactions become prominent and aggregation of the formed monocolumnar structures occur to form either gels or solids,<sup>[10]</sup> as shown in Figure 2.2.

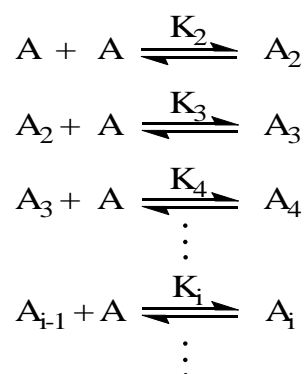


**Figure 2.2** – Self-assembly of disc shaped polycondensed aromatic molecules with the different aggregates given as a function of concentration

A powerful tool to investigate the stacking behaviour of aromatic compounds in solution is NMR spectroscopy because of the dependence of the chemical shift on the degree of aggregation. If aromatic compounds are close together due to  $\pi$ - $\pi$  stacking the nuclei's of each molecule are affected by the ring current magnetic anisotropy of the adjacent molecule, resulting in a shift of the resonance.<sup>[20]</sup> A typical feature of the  $^1\text{H}$ -NMR spectrum of discotic compounds is therefore the significant line broadening and shielding due to the aggregation, which provokes normally an up-field

shift of the aromatic resonances. Because of that  $^1\text{H}$ -NMR spectra are temperature and concentration dependent which allows for an interpretation of the underlining kinetics.

Further information on aggregation in solution is often drawn from fluorescence spectra, which are very sensitive to aggregation and give rise to red shifted bands on aggregation.<sup>[21]</sup> In order to obtain quantitative information about association strengths and association constants, experimental data from NMR or vapour pressure osmometry are usually applied to theoretical models.<sup>[22]</sup> A variety of different mathematical models have been reported so far to explain intermolecular associations.<sup>[23]</sup> In these models, the association process is normally described by a series of equilibrium equations. The most commonly used set of equations is shown in the following expressions (Equation 2.1), where the association is described as a successive addition of a monomer unit onto another monomer or an already existing aggregate (isodesmic growth).



**Equation 2.1** – Intermolecular association model describing the aggregation as a successive addition of monomers<sup>[23]</sup>

### 3 Charge carrier mobility

#### 3.1 Introduction

Charge transport and charge recombination processes are key features in a wide range of applications. The essential parameter in these systems is the charge carrier mobility  $\mu$ , which characterizes the transport of charge carriers. Its determination and interpretation has therefore occupied many authors during the past decades. Many different methods to measure the charge carrier mobility were developed and intensively discussed in the literature, out of which pulse-radiolysis time-resolved microwave conduction (PR-TRMC),<sup>[24]</sup> time-of-flight (TOF)<sup>[25]</sup> and time-resolved terahertz spectroscopy<sup>[26]</sup> are among the most dominant. The motion of charge carriers in terms of the mobility through an one dimensional molecular wire was described theoretically by different models<sup>[27]</sup> which differ by the shape for the one dimensional potential energy profile and in particular the mechanism. For detailed information about the different experimental techniques as well as mechanistic discussion the reader is referred to the specific literature available.<sup>[28]</sup>

#### 3.2 Molecular wires

It was shown in literature that the highest so far measured charge carrier mobility for organic systems was measured in organic single crystals, which are not suitable for large scale applications due to difficulties in their handling. With respect to the earlier discussed self-assembly potential of organic molecules, molecular wires are much more versatile for any kind of application. In terms of mobility, there is nevertheless a “mobility gap” between organic single crystals, which exhibit mobilities in the range of  $10^{-1}$  to  $1 \text{ cm}^2\text{V}^{-1}\text{s}^{-1}$ <sup>[29]</sup> as compared to the charge carrier mobility for monostranded molecular stacks, which were found to range between  $10^{-4}$  and  $1 \text{ cm}^2\text{V}^{-1}\text{s}^{-1}$ .<sup>[30]</sup>

The charge carrier mobility is influenced by several factors such as the chemical structure of the aromatic core (band gap)<sup>[31]</sup> nature of the side chain (liquid crystalline behaviour, supramolecular order),<sup>[32]</sup> the purity of the material as well as a defect-free long-range order (reduces possible trapping sites for charge carriers)<sup>[32a]</sup> and the  $\pi$ -overlap between the electronically active transport units,<sup>[33]</sup> which is probably the most important parameter for the charge-carrier transport process in organic systems. Because of this the most favourable approach towards high-mobility organic systems involves the use of columnar discotic liquid crystals. In these materials, the molecular units self-organize into columnar stacks providing a favourable face-to-face orientation of the aromatic cores, which leads to a larger  $\pi$ - $\pi$ -overlap between the adjacent molecular units and therefore a high charge carrier mobility.

### 3.2.1 Formation of excitons

The HOMO-LUMO band gap of aromatic derivatives suitable to form molecular wires ranges in between 2.0 and 4.0 eV.<sup>[31b]</sup> The magnitude of the band gap of benzenoid polyaromatic hydrocarbons (PAHs) is related to their aromaticity, i.e. to the number of aromatic resonant sextets present in the structure, which in turn is related to the spatial distribution of the hexagonal fused rings. The lower the band gap the easier an exciton formation occurs. On the other hand a low band gap signifies also a low stability of the compound due to a high tendency for degradation due to oxidation.

The intermolecular spacing of two adjacent discs in a self-assembled  $\pi$ - $\pi$  stack is around 3.5 Å. The binding between the molecules of such strands is therefore in most cases mainly due to van der Waals forces. As the orbitals extend only to roughly 1.5 Å out of the plane a direct electronic wave function overlap from one molecule into the positive core of a neighbouring molecule in the ground state is very weak. Nevertheless quantum fluctuation generating excitons may occur on short time scales ( $\sim 10^{-15}$  s). A neutral state undergoing a charge fluctuation, which originates on a single molecule, creates momentarily an exciton. This formed exciton has the possibility to split up, for example with the negative charge moving into a neighbouring molecule's LUMO leaving behind the positive partner charge. This formed excitonic pair moves preferably along the columns, but hops from column to column until recombination. By moving in the whole column the exciton is taking up more configuration space, which lowers its energy. In other words, the fact that the exciton has the possibility to move around the self-assembled strand lowers its kinetic energy i.e. lowers the cost in energy of creating the exciton. This finding is normally called electronic bonding.

Compared to a covalently bound semi-conductor, however, the gain in kinetic energy from such an exciton in a discotic liquid crystal is typically around 0.6 eV and therefore small in comparison to the energy needed to separate the initially strongly bound electron-hole pair (2.5-4 eV).<sup>[34]</sup> Once created, the exciton will normally recombine on a very fast time scale yielding a material where such short lived charge fluctuations give only small contributions to the binding energy with neighbours.

### 3.2.2 Charge injection

The situation is quite different when an electron is injected into the self-assembled stack. There are several techniques known in the literature to measure such a process, as mentioned previously (chapter 3.1).

By injecting an extra charge into a strand of self-organized molecules, the charge is localized first in the LUMO band which is much more weakly bound and the corresponding wave function is therefore extending further in space. This results in a better overlap with the potential of the neighbour-

ing molecule. Moreover, the overlap to the nearest neighbours is even enhanced due to the induction of a dipole in the two nearest neighbours, generating thereby an extra energy of about 1 eV.<sup>[34]</sup>

It has not yet been fully elucidated in literature, if a hole or an electron is migrating, and by which mechanism such a migration would occur. For the injected electron however, the induced charge-polarisation interaction is the same as for holes. Nevertheless some difference between hole and electron migration may be discussed: for electrons the negative charge still sees a highly screened neighbour. In the case of holes the situation is clearly different, as the hole may be described as a net positive charge. The hole attracts therefore the outer shell electrons of its neighbours which can jump into the hole.

To inject electrons into self-assembled stacks the lowest molecule of the strand has to be in close contact with a metal surface like gold or platinum. There can be a more or less strong electronic coupling between the  $\pi$ -electrons on the conjugated core and the s-electrons on the metal surface. Normally, this coupling is expected to be rather weak, as the Fermi level of a metal like gold will be roughly 1 eV above the valence band of the molecular columns, which depends strongly on the chemical structure of the organic molecules. The charge can therefore not easily flow in or out. At high voltages, however, it is possible to inject electrons from a metal electrode into the valence band of columns. Normally average fields in the order of  $10^5 \text{ V cm}^{-1}$  are required.



## 4 Applications in nanotechnology

### 4.1 Introduction

*“With the invention of the scanning tunnelling microscope (STM) in 1981 by G. Binnig and H. Rohrer,<sup>[35]</sup> the gate to the nanoworld was pushed open. The prospect to control matter and units on molecular and atomic level, inspired many scientists to think about new technological approaches – nanotechnology in the sense of Richard Phillips Feynman<sup>[36]</sup> became reality. Thus, nanotechnology is not only the next step of the miniaturisation following microtechnology – nanotechnology is an approach to investigate natural architectures and to mimic them for technological problems. Nanotechnology is an evolutionary process to our technological society with the potential to solve everyday problems with revolutionary concepts and devices”.<sup>[37]</sup>*

Many revolutions occurring during industrial evolution of the past two centuries were triggered by the ability to produce smaller and smaller devices with an increasing precision. In a retrospective, one observes an increasing rate of miniaturization during the past 40 years. Today, it is possible to fabricate micro-electromechanical systems of several hundred nanometres in size with few nanometer tolerances.

Chemistry in contrary has been working with sub-nano-objects already since its beginnings. Today, the “top down” approach of physics and the “bottom-up” approach of chemistry are meeting at the point where the macro-domain meets the nano-domain, as illustrated in Figure 4.1.

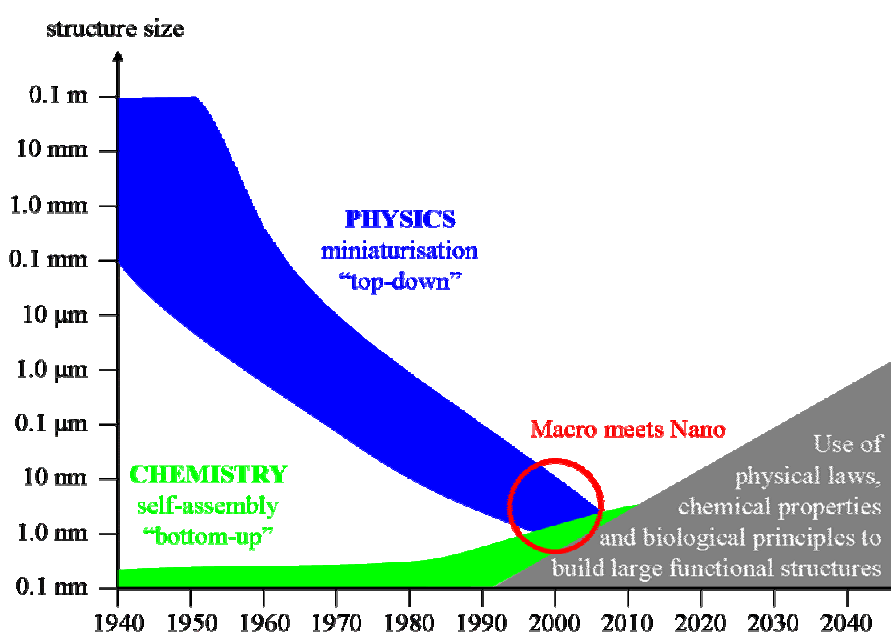


Figure 4.1 – “Top-down” approach of physics and “bottom-up” approach of chemistry<sup>[37]</sup>

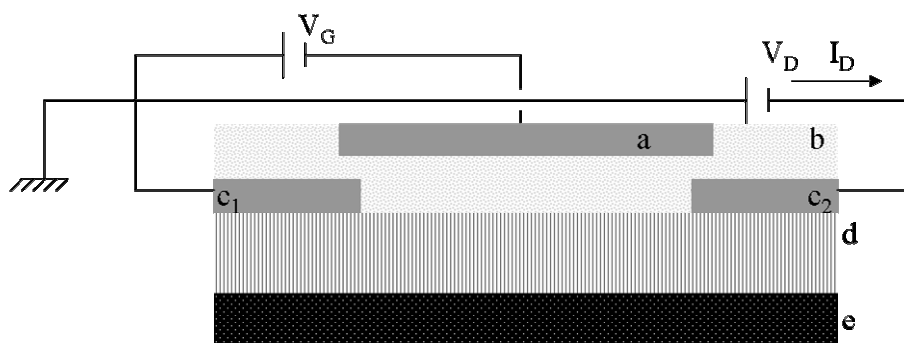
## 4.2 Organic field effect transistors (OFET)

### 4.2.1 Research development

The interest in organic semiconductors arose in the late 1940s, however only in the year 2000 the noble prize in Chemistry was awarded to Alan J. Heeger for his contribution to organic semiconducting materials. Most notably the high cost pressure in industry for electronic circuits supports the use of cheap organic semiconductors such as pentacene based devices for example. Moreover would the use of organic semiconductors as active layer enable the preparation of lightweight, large-area and flexible electronics products. Over the past ten years the most promising progress was done especially with pentacene,<sup>[38]</sup> which has a high charge carrier mobility<sup>[39]</sup> together with a high on-off rate of the source-drain current,<sup>[40]</sup> due to the extended  $\pi$  system which enhances the intermolecular overlap of the  $\pi$ - $\pi$  systems in the solid state. However, the common problematic with linear acenes is their chemical instability as they are influenced by ultraviolet light, temperature, water vapour and oxygen.<sup>[41]</sup> Another class of substrates well reported in literature are conducting polymers<sup>[42]</sup> or CNT.<sup>[43]</sup>

### 4.2.2 Basic principle of OFET devices

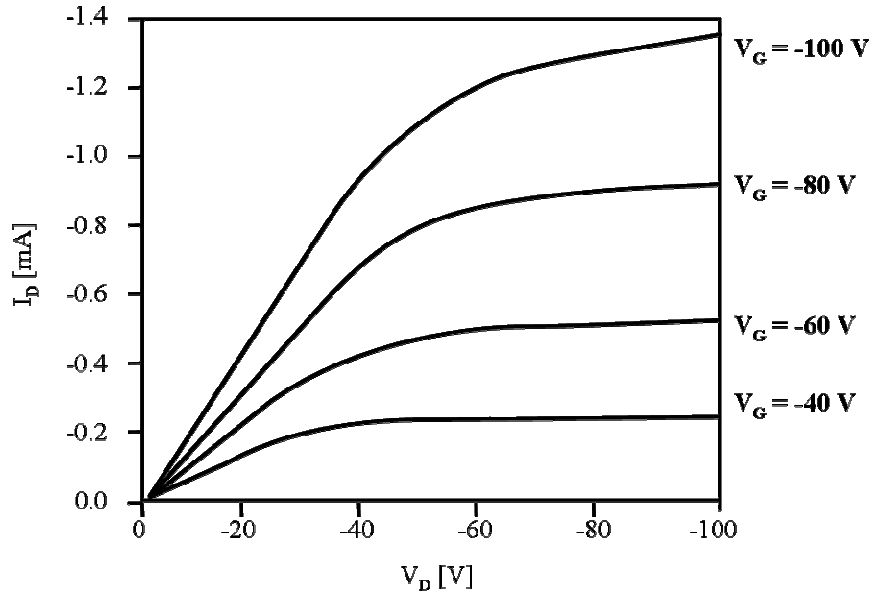
As in traditional inorganic semiconductors, organic materials can function either as p- or n-type semiconductors. The difference arises in the charge transport, as in p-type semiconductors the carriers are holes, whereas in n-type devices the carriers are electrons.<sup>[44]</sup> In an OFET device at least one active layer is composed of an organic semiconductor. In principle, the operation of an OFET needs as a usual transistor the connection of three different contacts. Two contacts (source and drain), over which the current will flow are connected to a necessary potential. A further potential is needed between the source contact and the third gate contact. This potential is responsible to open and to close the conductive path in the active layer which connects drain and source. For clarity an OFET is sketched schematically in Figure 4.2.



**Figure 4.2** – Schematic device structure of an OFET; a) gate electrode (Al); b) insulator ( $\text{SiO}_2$ ); c<sub>1</sub>) source electrode (Au); c<sub>2</sub>) drain electrode (Au); d) p-type organic semiconductor (pentacene); e) substrate (Si)



Pentacene OFETs, as shown in Figure 4.2, exhibit normally p-type behaviour, i.e. the majority of all charge carriers are holes. When the gate electrode is biased positively compared to the source electrode, the channel region is depleted of carriers resulting in high channel resistance and yields the off state as no charge flows due to the reduction of carriers in the transistor channel. In contrary by using a negatively biased gate electrode with respect to the source the device is operating in the accumulation mode. Because of that a large concentration of carriers is accumulated in the transistor channel, resulting in low channel resistance, the so called on state. In this state the charge flow is allowed.<sup>[45]</sup>



**Figure 4.3** – Output characteristics (plot of drain current  $I_D$  versus drain voltage  $V_D$  at various gate voltages  $V_G$ ) of a OFET bearing a pentacene active layer<sup>[44]</sup>

A typical plot of the output characteristics of an OFET composed of polycrystalline pentacene as active layer is shown in Figure 4.3. The graphic consist of the plot of the drain current  $I_D$  versus the drain voltage  $V_D$  at various gate voltages  $V_G$ . The application of a negative voltage to the gate increases the negative drain current. At low drain voltage, the drain current increases linearly with  $V_D$  (linear regime) and is approximately determined from Equation 4.1:<sup>[44]</sup>

$$I_D = \frac{WC_i\mu}{L} \left( V_G - V_T - \frac{V_D}{2} \right) V_D$$

**Equation 4.1** – Approximation of the drain current

$L$  is the channel length and  $W$  the channel width of the active layer,  $C_i$  is the capacitance per unit area of the insulating layer,  $V_T$  is the threshold voltage and  $\mu$  the charge carrier mobility. For high values of the drain voltage, the drain current tends to saturate (saturation regime).<sup>[44]</sup>

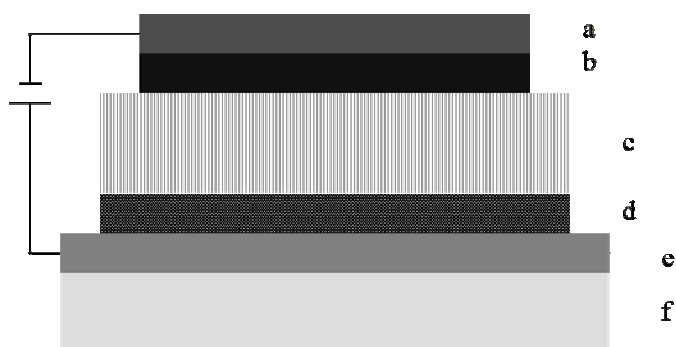
## 4.3 Organic light emitting diode (OLED)

### 4.3.1 Research development

Over the past years organic light emitting diodes have gained increased interest due to their potential application for the fabrication of flat panel devices, large-area light sources and particularly for small-scale applications such as cellular phones or digital cameras.<sup>[46]</sup> OLED devices offer many attractive features as compared to conventional devices such as LCDs, including a wider viewing angle, bright emission and low power consumption.<sup>[47]</sup> The realisation of red, green, and blue OLEDs is sophisticated; nevertheless red OLEDs are dependent upon improving the operational stability.<sup>[46a]</sup> At the same time, white OLEDs (WOLED)<sup>[48]</sup> have gained an increased interest in industry, which allows the preparation of devices with a broad white emission.<sup>[46b, 49]</sup>

### 4.3.2 Basic principle of OLED devices

Figure 4.4 shows a cross section of an OLED device consisting of a single emissive layer.



**Figure 4.4** – Cross section of an OLED; a) cathode (Al); b) electron transport layer (Ca), c) emissive layer consisting of a conductive polymer, for example (PF2/6am4); d) hole transport layer (PEDOT/PSS); e) ITO; f) glass substrate<sup>[50]</sup>

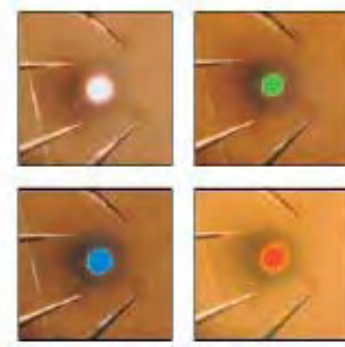
Onto a glass substrate (f) the transparent anode (ITO) (e) is deposited, onto which a hole transport layer is added (d). The hole transport layer may be composed for example of PEDOT/PSS (PEDOT: (Poly(3,4-ethylenedioxythiophene), PSS poly(styrene sulfonic acid)). The next coating is the emissive layer (c) which may be composed of a variety of organic materials. In this case a conducting polymer PF2/6am4 (PF2: poly[9,9-bis(2-ethylhexyl)fluorene-2,7-diyl], 6am4: bis(4-methylphenyl)phenylamine) was used. On top of the emissive layer the electron transport layer (b) is added, for instance Ca. The aluminium cathode (a) finishes the device<sup>50</sup>.

The luminescence of an OLED device is created in the following way. Electrons are injected in the LUMO from the cathode, whereas holes are produced simultaneously at the anode. Hole and electron drift through the organic film under the influence of the applied electrical field and recombine

optimally in the emissive layer to produce luminescence. In this case PEDOT acts as hole transport medium whereas PSS is responsible to lower the injection barrier for holes as it smoothes the surface and hinders the diffusion of indium.

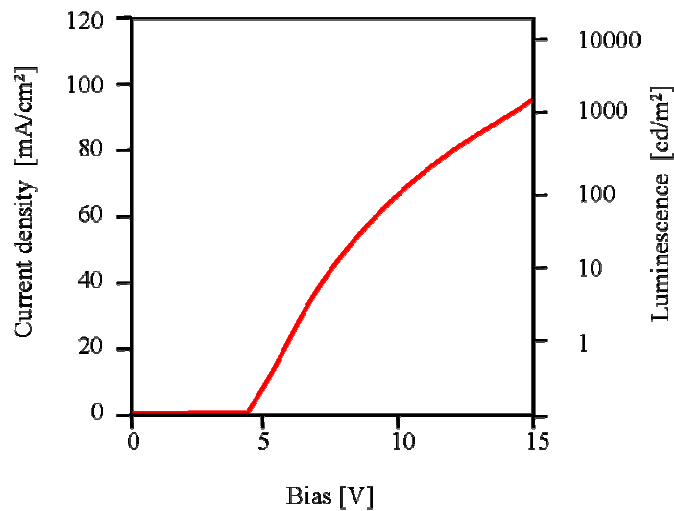
The research to increase the performance of OLEDs is still ongoing as the quality of an OLED is dependent of many different parameter such as for example HOMO and LUMO values for electron- and hole transport layer, high carrier mobility, high quantum efficiency, stability or turn-on voltage.

A WOLED may be constructed by separately energized red, green and blue regions. The device therefore consist of three separate OLEDs (red, green and blue) to control the emission of each colour independently which allows for an independent tuning of the colour mix as shown in Figure 4.5.



**Figure 4.5** – WOLED which produces red, green, blue or white light<sup>[46b]</sup>

Figure 4.6 shows the typical luminescence versus voltage characteristics of a modern OLED device out of which the typical features may be acquired: *i*) the turn-on voltage which is the lowest voltage required for the device to produce any emission; *ii*) reduction of the intensity by increased voltage due to the heating process; *iii*) the decrease of the intensity after some time (furnishes information on the life time). The rather short lifetime is the biggest disadvantage of OLED devices.



**Figure 4.6** – OLED display characteristics illustrated through current-voltage-luminescence measurements

#### 4.4 Field emission display (FED)

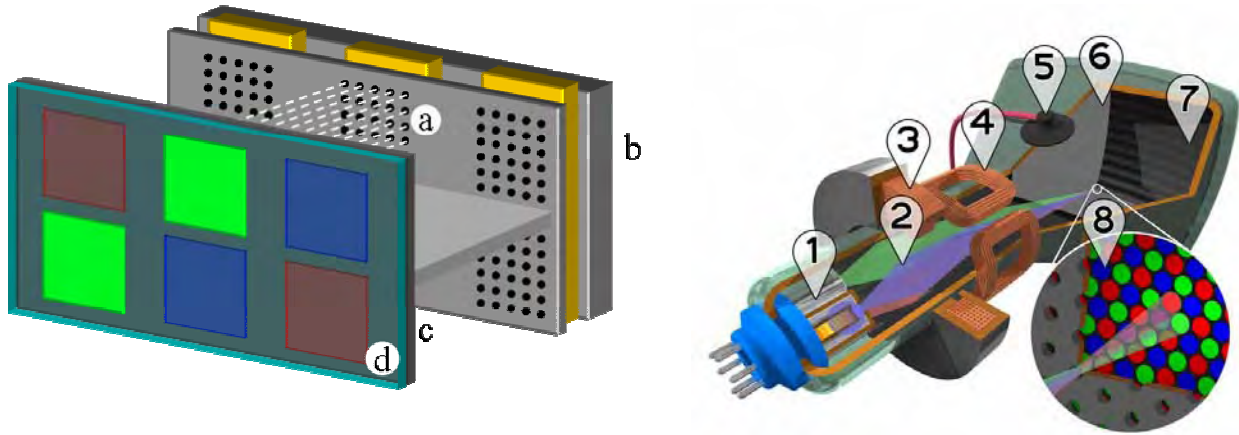
An enormous research effort was performed over the past years in order to develop new liquid-crystal displays (LCD). The investigated materials require to be transparent as well as easily and very quickly oriented in an electric field. In spite of the fact that over the past years many suitable materials were produced to fit these criteria the dominance of LCDs in the area of flat panel displays is now being challenged by rapid improvements in carbon nanotube (CNT) devices and other organic material based techniques. Motorola for example announced: “*Carbon nanotube displays that outperform today’s flat-panel televisions are ready to move out of the lab and into factories*”.<sup>[51]</sup>

The advantages over standard flat panel screens are the followings:

- Field emission displays uses the ballistic motion of electrons which is based on cold emission. Because of that, no heat is produced and as a consequence no heat has to be dissipated.
- Better viewing angle up to 160 °C
- Flatter screen
- Lower power consumption
- No background illumination needed

##### 4.4.1 Basic principle of field emission displays

FEDs work like conventional cathode ray tubes, except that each single pixel is illuminated by its own addressable, miniaturized electron source, which is directly located behind it. Each electron source is composed of several hundreds of electron emitters which illuminate one pixel. This arrangement allows the fabrication of displays of only a few millimetre thickness which still have the same outstanding image quality as cathode ray tubes. Classical CRT use thermionic electron sources operating at temperatures between 950 and 2000 °C, making miniaturization impossible due to the lack of dissipation of the created heat. In contrast to this, field electron emitters operate at room temperature and hold therefore a great potential for miniaturization.<sup>[37]</sup> Both FED and CRT are sketched schematically in Figure 4.7.



**Figure 4.7 – Left:** sketch of 6 pixels of a field emission display (FED) where two pixels (green) are illuminated; a) emitted electrons; b) cathode; c) phosphorescent coating; d) transparent anode (ITO);<sup>[37]</sup> **right:** cathode ray tube, 1) hot cathode; 2) electron beam; 3) focalizing coils; 4) deviation coils; 5) anode; 6) pinhole; 7) phosphorescent screen; 8) zoom of the phosphorescent screen<sup>[52]</sup>

#### 4.4.2 Field emission – the Fowler-Nordheim law

Already in 1928 R. H. Fowler and L. W. Nordheim<sup>[53]</sup> found the first generally accepted explanation for field emission in the newly developed theory of quantum mechanics. According to the Fowler-Nordheim theory, the local field emission current density  $j$  is a function of the electric field  $E$  and the emitter work function  $\Phi$  according to the following generalized equation:

$$j = \frac{e^3}{4(2\pi)^2 \hbar \phi} E^2 \exp\left(-\frac{4\sqrt{2m_e}}{3\hbar e E} \phi^{1.5}\right)$$

**Equation 4.2 – Fowler-Nordheim equation**

where  $E$  and  $\Phi$  are the local field and the work function, respectively, for the emitting surface,  $e$  is the elementary charge,  $\hbar$  the reduced Planck constant and  $m_e$  the electron mass. A simpler way of description is the following:

$$j = \frac{a}{\phi} E^2 \exp\left(-\frac{b}{E} \phi^{1.5}\right)$$

**Equation 4.3 – Simplified Fowler-Nordheim equation**

where  $a$  and  $b$  are given by the universal constants:

$$a = \frac{e^3}{4(2\pi)^2 \hbar} = 1.54 \cdot 10^{-6} \text{ AeV}^2$$

$$b = -\frac{4\sqrt{2m_e}}{3\hbar e} = 6.83 \cdot 10^9 \text{ eV}^{-1.5} \text{ Vm}^{-1}$$

**Equation 4.4 – Constants  $a$  and  $b$  used in the Fowler-Nordheim equation**

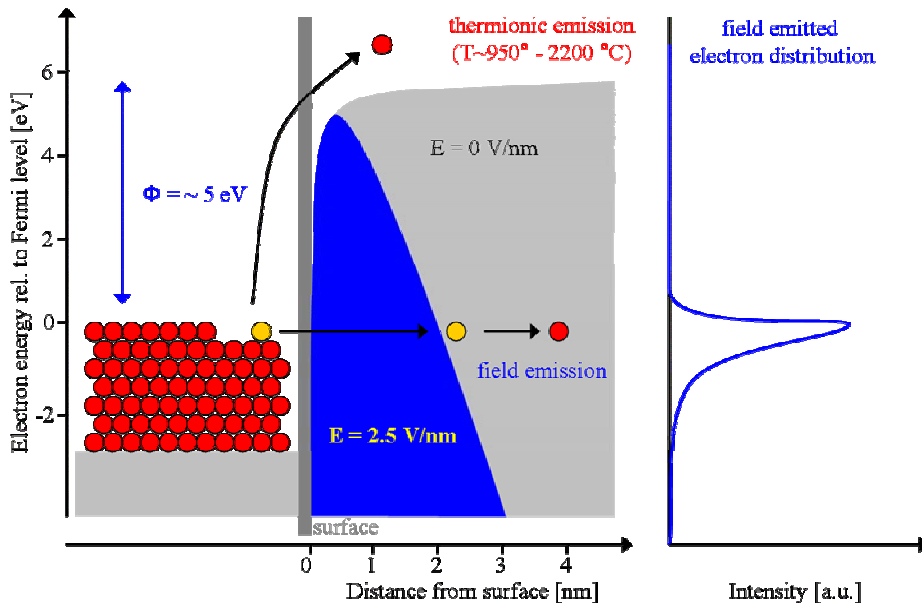
The current density can vary strongly with the position, especially by using small emitters. To get an expression for the current from a single emission site the emission area  $A$  has to be taken into account and Equation 4.3 can be written in the following way:

$$I(E) = \frac{A \cdot a}{\phi} E^2 \exp\left(-\frac{b}{E} \phi^{1.5}\right)$$

**Equation 4.5** – Expression for the current density

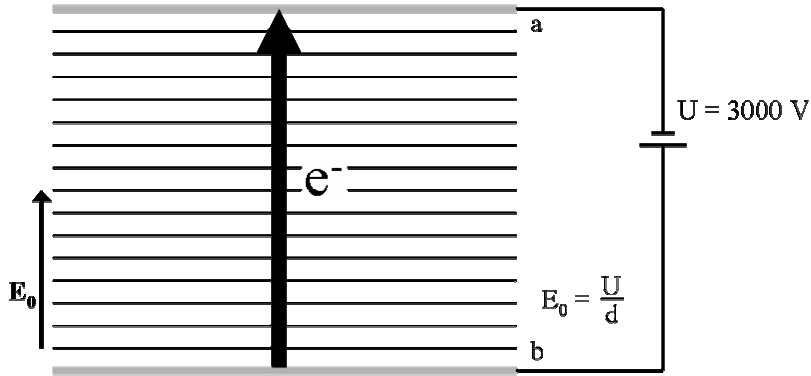
In summary, the emission current of a single emitter is characterized by the emitting surface  $A$ , the work function  $\Phi$  and the electric field  $E$ .<sup>[37]</sup>

Figure 4.8 shows schematically a metal under field emission condition: on the left, the electron distribution under Fermi-Dirac conditions at 300 °C is sketched. By applying a strong electric field, which in this case is around  $2700 \text{ V}\mu\text{m}^{-1}$ , the surface potential step retaining the electrons in the solid becomes a triangular shaped barrier, as shown in the middle section by the blue part. If the width of this surface potential barrier approaches the tunnelling distance of about 2.5 nm, the tunnelling probability of electrons near the Fermi energy is large enough to let them escape into vacuum. The resulting energy distribution of the emitted electrons is depicted on the right side of Figure 4.8. The high energy side of the peak shows thermal broadening of the electron distribution at the Fermi energy which at 0 K should result in a sharp cut-off.<sup>[54]</sup>



**Figure 4.8** – **Left:** electron emission from a metallic surface; **middle:** potential barrier under field emission conditions; **right:** energy distribution of the emitted electrons

For a perfectly flat metal surface with a typical work function  $\Phi$  of 5 eV the minimum field to get measurable emission currents is in the range of  $3000 \text{ V}\mu\text{m}^{-1}$ , which is the major drawback in the domain of electron field emission.<sup>[55]</sup> The situation for electron emission at a flat metallic surface is depicted in Figure 4.9.



**Figure 4.9** – Electron emission at a perfectly flat metallic surface; a) anode; b) cathode;  $E_0$  is the electrical field;  $U$  is the applied voltage;  $d$  is the distance in between anode and cathode

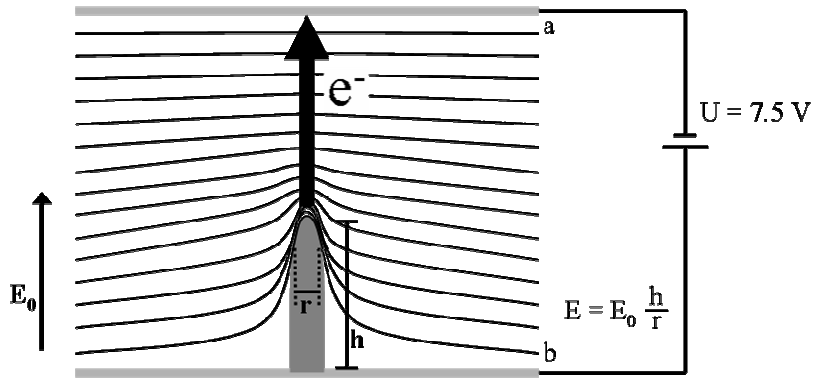
To solve the problem of the high voltages required to extract electrons out of a flat metallic surface, it was found that tip-like structures on the surface were able to produce the necessary field at the apex by applying a much smaller voltage. In a first approximation the field enhancement obtained at the apex of a needle-shaped object of the height  $h$  and the radius  $r$  can be expressed in the field enhancement factor  $\beta$ <sup>[56]</sup> which is equal to the aspect ratio as shown in Equation 4.6:

$$\beta = \frac{h}{r}$$

**Equation 4.6** – Field enhancement factor  $\beta$

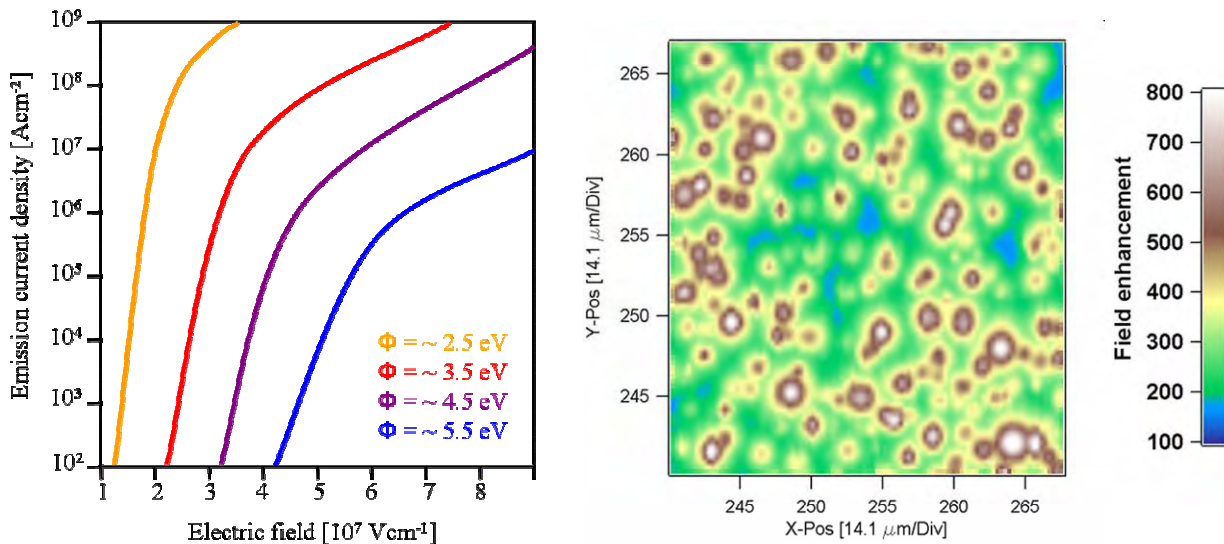
A needle like tip with a diameter of 3 nm and a length of  $1.2 \mu\text{m}$  for example exhibits a field enhancement factor  $\beta$  of 400. The required electrical field to generate the emission is lowered therefore from the beginning  $3000 \text{ V}\mu\text{m}^{-1}$  to only  $E_0 = \frac{E}{\beta} = 7.5 \text{ V}\mu\text{m}^{-1}$ , which is relatively low. There-

fore the higher the field enhancement factor  $\beta$  is, the smaller the effective emission area of the tips becomes, as the radius of curvature decreases. Although the field emission current density can easily exceed  $10^6 \text{ Acm}^{-2}$ , the total emission current per single tip remains small as the emitting area, being the apex of the enhancing tip, is small as illustrated in Figure 4.10.



**Figure 4.10** – Electron emission out of a metallic surface carrying needle-shaped tips; a) anode; b) cathode;  $E_0$  is the reduced electrical field;  $E$  is the resulting electrical field;  $U$  is the applied voltage;  $h$  is the height of the tip;  $r$  is the aspect ratio of the tip

By analyzing the Fowler-Nordheim equation Equation 4.2 it is obvious that only small variations of the work functions or the electric field, which may be provoked by unequal lengths of the emission tips, yield very strong variations in the emission current.<sup>[57]</sup> For an illustration the emission current is drawn for four different work functions in dependence of the electric field in Figure 4.11.<sup>[54a]</sup> Another way to demonstrate the tremendous sensibility of the emission current is a field enhancement map created by investigation of an array of field emitters by a SAFEM (scanning anode field emission microscope).<sup>[54a]</sup> A SAFEM is a scanning probe microscope working with a micrometer sized tip which is scanned at constant distance over the cathode surface together with an applied fields high enough for field electron emission.



**Figure 4.11** – **Left:** dependence of the emission current from the work function; **right:** field enhancement map measured by a SAFEM<sup>[54a]</sup>



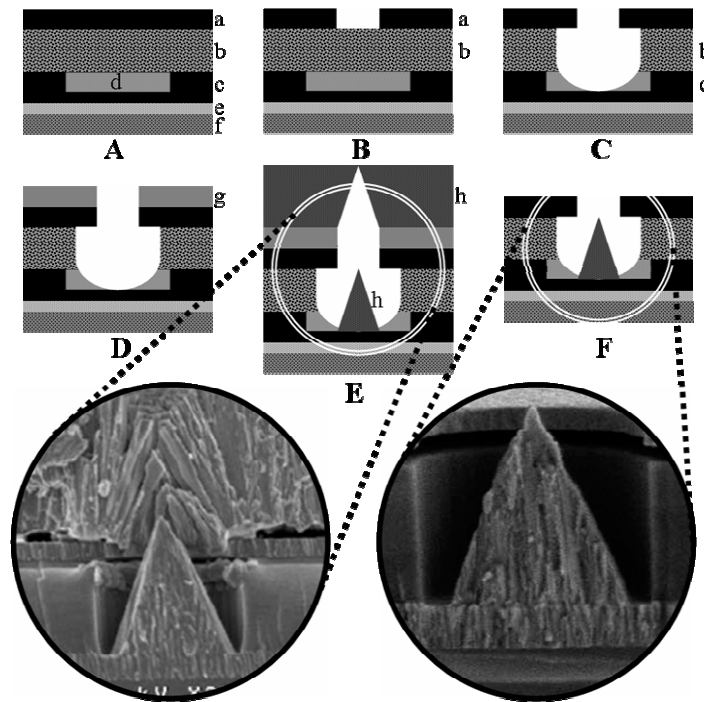
To produce field emission displays consisting of a uniform illumination it is crucial to have a very regular array of emission tips with respect to the height. Because of that the development of field emission was hampered for half a century. There are several techniques developed in the past to produce regular field emitting surfaces including the following ones:<sup>[58]</sup>

- Bulk diamond
- Pure bulk graphite
- Diamond crystallites embedded in amorphous carbon
- Metallic spint tips
- Carbon nanotubes

Different diamond-like carbon emitters were tested in the past and it was shown that they were characterized by the lowest turn-on voltages,<sup>[59]</sup> although at low current densities. These materials never reached the manufacturing stage mainly due to the fact that two new classes of tips, namely metallic emission tips and carbon nanotubes excelled with their properties over the others listed. The reason is the following: needed are field emitter sources of thigh current density approaching  $1 \text{ Acm}^{-2}$ , which is possible by integrating a large number of individual emitters. In order to achieve such high values, each tip has to exceed a current density of about  $10^{-8} \text{ Acm}^{-2}$  which limits the size of the emitters to even sub-micron dimensions. Today, they are only two mature techniques to produce such field emitter arrays: metallic spindt tips and CNT.<sup>[51, 60]</sup>

#### 4.4.3 Metallic emission tips

Many field emission structures prepared from different metals have been investigated in recent years using various micro-fabrication techniques.<sup>[58]</sup> The Spindt tip or so called “cone-in-a-well” emitter structures were the best choice for FED applications in the 1990s. Spindt tips consist of a metal cone with a tip radius less than  $300 \text{ \AA}$  which is deposited by electron beam evaporation into emitter wells. The process for the production necessities several steps and is schematically sketched in Figure 4.12.



**Figure 4.12** – Schematic sketch for the fabrication process of a spindt emission tip, produced at Motorola<sup>[61]</sup>

(A) The fabrication process starts with the deposition of a  $\text{SiO}_2$  /  $\text{SiN}$  layer (e) onto a glass substrate (f) which serves as a diffusion barrier to alkali metals stored in the glass substrate. Next the column metal (c) and the amorphous Si layer (d) are deposited by sputtering, followed by the deposition of the  $\text{SiO}_2$  dielectric gate (b) which is deposited by chemical vapour deposition (CVD). Finally, the first production step is terminated by the deposition of the Mo gate electrode (a), which is added by CVD too.

(B) The emitter wells are formed in the next sequence of steps, beginning with the removal of the gate metal (a) up to the oxide (b) by dry etch chemistry.

(C) The oxide (b) is then etched by applying a different type of dry etch chemistry. The oxide (b) is removed down to the amorphous Si layer (c).

(D) Finally the emitter cones are formed by first depositing an Al separation layer (g).

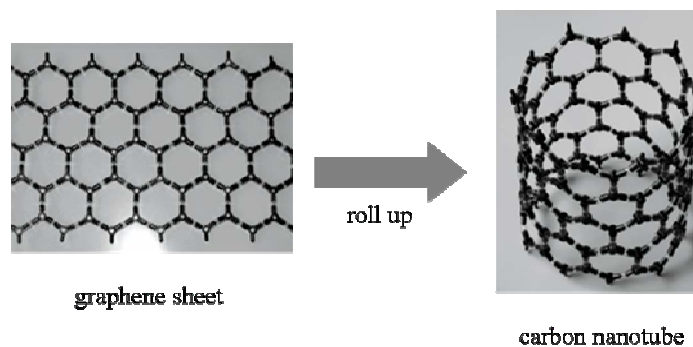
(E) Direct evaporation of Mo (h) creates the emission cone which is shown in the zoom in the form of a SEM picture.

(F) The last step consists of the removal of the Al separation layer (g) by an acid lift-off yielding the completed spindt emission tip, which is again shown as a SEM picture in the zoom.<sup>[61]</sup>

Despite the fact that spindt emitters comprise many advantage there are nevertheless several major unresolved challenges such as: *i*) scaling the production method to large area substrates, larger than 40 cm per side. Such scale up is necessary for economic reasons even if small area displays are produced; *ii*) producing spindt emitters that do not require fine photolithography or thin film technology; *iii*) increase the stability of spindt emitters which is considerably low due to chemical contamination (mostly oxidation) of the metallic tips, which provokes usually an increase of the work function.<sup>[62]</sup> The first generation of FED composed of metallic spindt emission tips is based on thin film technology as shown in this section. Despite the success in achieving FED based on metallic spindt emission, including adequate colour purity and brightness there are many opportunities to improve such FED. The most significant advances are being made by developing a second generation of FED, able to produce larger and moreover less costly devices.

#### 4.4.4 CNT emission tips

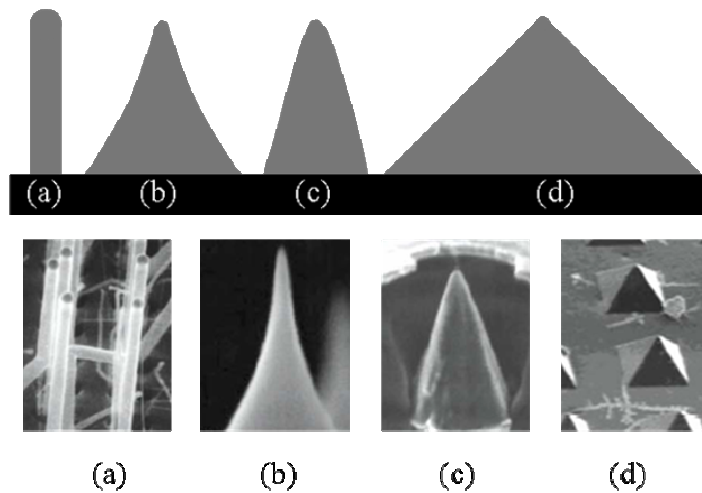
Carbon nanotubes are a unique form of carbon, in which the graphene walls roll up to form tubes<sup>[63]</sup> as shown in Figure 4.13.



**Figure 4.13** – Rolling up of a graphene sheet into a carbon nanotube<sup>[64]</sup>

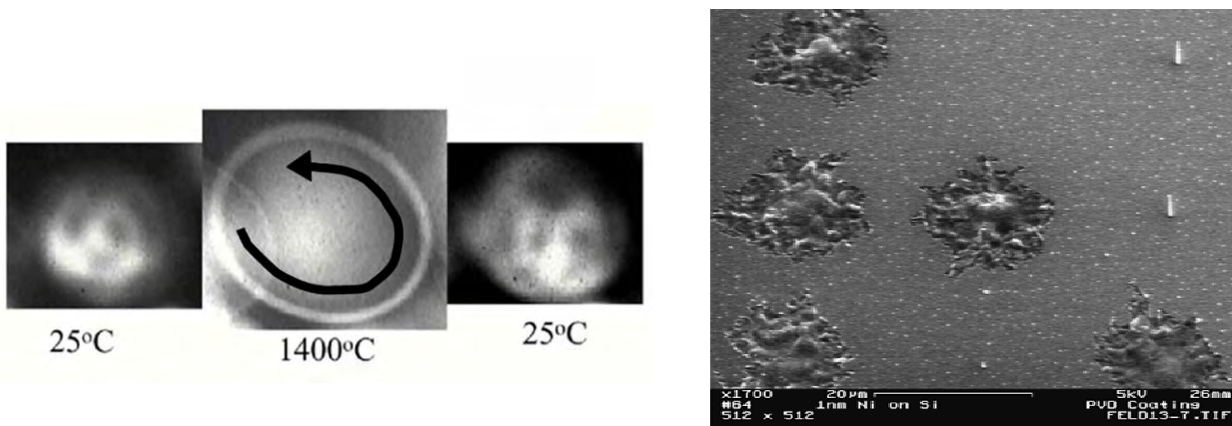
Single-walled CNTs (SWNT) can either be semiconducting or metallic-like depending upon the way in which they “roll-up”, where in contrast multi-walled CNTs (MWNT) are semi-metallic like graphite. The number of reports concerning preparation (arc discharge between two carbon electrodes,<sup>[63]</sup> laser ablation from a carbon target<sup>[65]</sup> and CVD techniques<sup>[66]</sup> for example) and purification<sup>[67]</sup> of CNTs was ever increasing in the past.

Carbon nanotubes endow many outstanding properties<sup>[68]</sup> out of which several allow CNT to be extraordinary materials for field emission:<sup>[69]</sup> *i*) SWNT or MWNT being semi-metallic exhibit high electrical conductivity at room temperature;<sup>[70]</sup> *ii*) CNT have a high aspect ratio and a very favourable whisker-like structure,<sup>[71]</sup> which proved to be the best tip shape for field emission.<sup>[71]</sup> Different possible tip shapes which were evaluated are shown in Figure 4.14.



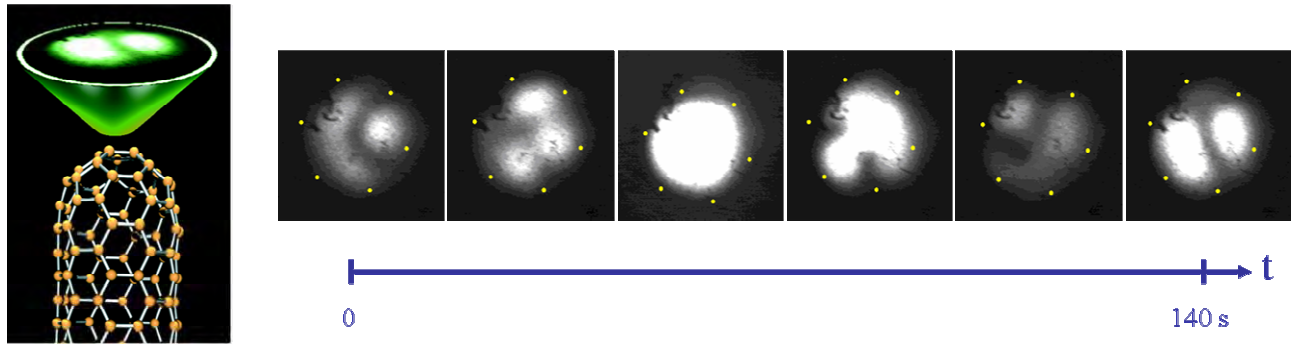
**Figure 4.14** – Various shapes of field emitters ordered from best (a) to worst (d); a) rounded whisker (silicon whiskers); b) sharpened pyramid (oxidation sharpened etched Si tips); c) hemi-spheroidal (spindt Mo tips); d) pyramidal (diamond)<sup>[71]</sup>

CNT are quite stable emitters even at high temperatures. It was demonstrated, that a MWNT could be heated up by its emitted current up to 2000 K without loss of stability.<sup>[72]</sup> One reason for the thermal stability of CNTs is most probably their ability to open and close reversibly their aspect as observed by FEM (field emission microscope). Figure 4.15 illustrates this observation using the FEM technique.<sup>[54a, 73]</sup> Nevertheless irreversible degradation was observed too which is mostly due to an overheating of the emission tip which provokes the melting of the cathode, as shown in Figure 4.15.



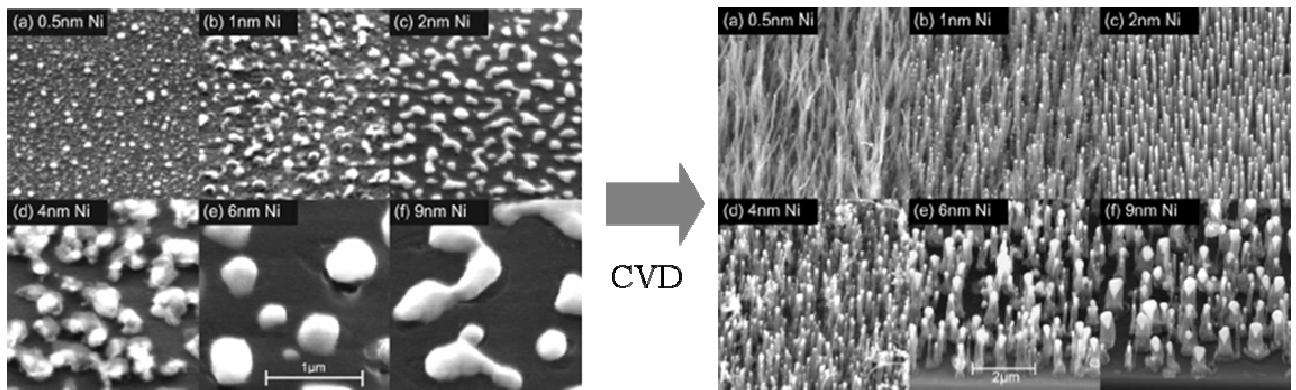
**Figure 4.15** –Left: morphology of CNT under heating;<sup>[54a]</sup> right: overheated CNTs<sup>[54a]</sup>

Nevertheless a fluctuation of the emission current up to a factor of 10 was observed, due to the low environmental stability of CNTs. Under environmental stability one understands the interaction of the electron emitter with the gaseous environment in which it is operating. Figure 4.16 shows FEM patterns commonly observed from SWNTs and MWNTs. These emission patterns are not stable in time but show fluctuation of the emission current intensity. The fluctuation frequency increases with higher currents and is in the order of 1 Hz.<sup>[74]</sup>



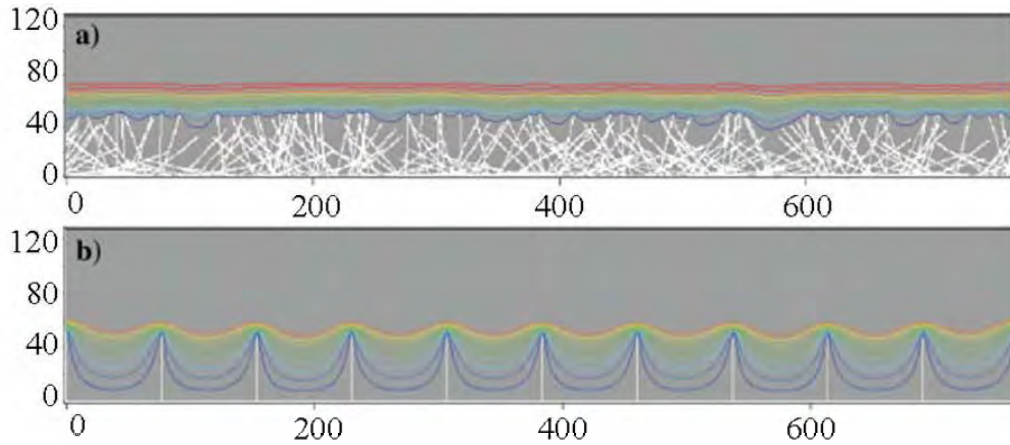
**Figure 4.16** – Left: Sketched emission of a SWNT at 300 K; right: some examples of a large variety of fluctuation during electron emission, where the intensity may vary by a factor of ten<sup>[74]</sup>

In order to be able to use CNT as field emitters or other applications their alignment on a substrate is of particular importance. The first report of well aligned CNTs on a glass substrate was in 1998, where the plasma-enhanced CVD technique was used.<sup>[75]</sup> The nanotubes are produced by depositing a thin nickel layer onto the substrate as catalyst, followed by the growth of the nanotubes. Figure 4.17 shows a SEM micrograph of such an array of CNTs at the beginning of the exploration of this technique.



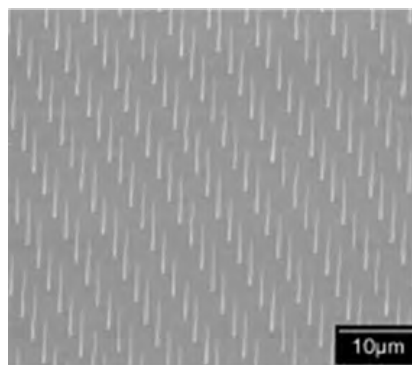
**Figure 4.17** – Left: Formation of Ni nanoclusters after heating thin films to 700 °C; right: CNT grown on the nanoclusters shown on the left<sup>[76]</sup>

As stated earlier such well aligned CNTs should make excellent field emitters. However, as shown by different authors<sup>[77]</sup> such close packed arrays of CNTs are not ideal at all for field emission applications as the close packing of the tubes screens the applied field effectively which reduces the field enhancement created by the high aspect ration of the tubes. It was found, that the geometrical arrangement of the CNTs has a detrimental influence on the field emission properties as a too high or too low density of CNTs decreases the emission property tremendously. These findings are illustrated in Figure 4.18.



**Figure 4.18** – Sketch showing the high electrical field screening of dense CNT (a) and a minimized field screening of spaced CNT (b)<sup>[64]</sup>

In order to avoid the undesired field screening and to achieve maximum field emission, it is highly desirable that the emitters are spaced by twice their height.<sup>[77b]</sup> Further the structural variation between emitters should be as small as possible in order to achieve a uniform emission. Plasma enhanced CVD offers nowadays a well-controlled technique for the production of such vertically aligned, well spaced CNTs. This technique allows further the control over height, and diameter of the nanotubes<sup>[78]</sup> and is well described in literature.<sup>[54b, 76]</sup> Briefly, the substrates are prepared by sputtering a thin film Ni catalyst onto a Si substrate. The substrate is then transferred to a plasma enhanced CVD chamber which is evacuated to  $10^{-2}$  mbar and heated to 700 °C. Under these conditions the Ni thin film forms nanoclusters due to the surface tension effects. The spacing and average size of the clusters increases with the original thin film thickness which is easily controlled.<sup>[64]</sup> The formed nanoclusters seeds then the growth of the CNTs which is performed by plasma enhanced CVD of acetylene and ammonia, which etches the amorphous carbon by-products.<sup>[79]</sup> An example of such a well ordered uniform array of CNTs produced by CVD is shown in Figure 4.19.



**Figure 4.19** – Array of CNT which may be used for FED<sup>[78b]</sup>

Over the past years many successful reports of carbon nanotube field emission displays have been published using the above mentioned methods or similar ones.<sup>[80]</sup>

## 5 Toward a new self-assembled molecular wire

Provided that supramolecular wires could be prepared at will, i.e. homogeneous strands of the same length, which could be attached to a metal cathode or anode, the applications described in this chapter are reasonable. As discussed in the previous chapter (chapter 4.4) CNT based FEDs are pretended to be ready to go for production as stated by Motorola.<sup>[51]</sup> Nevertheless CNT suffers of a main disadvantage: They are made by a physical process, which is meanwhile very well controlled to obtain clean homogeneous nanotubes. Nevertheless it is impossible to achieve a defect-free material in which all nanotubes have exactly the same diameter and length together with a high purity. Until now there exists no synthetic route which allows the control of the chirality of the tubes. As consequence, every batch of grown CNTs usually contains metallic and semi-conducting tubes. Processes for separation of metallic and semi-conducting tubes are recently being developed with modest success.<sup>[81]</sup>

A possible solution for this problem may be the use of organic molecules as electronic building blocks. Organic derivatives can relatively easily and reproducibly be synthesized with extremely high purity. In addition, they may be functionalized in a great variety. Molecular architectures formed by self-assembly of individual building blocks are very promising candidates for supramolecular structures with desired electronic or optical properties. Furthermore a self-assembled molecular structure does not contain any covalent bond in between the different disc-like monomeric units as compared to CNTs or polymers; their lifetime should be enhanced as an overheating of a formed strand would lead to a so-called “self-healing” effect. The overtop molecules are able to dissipate during the overheating process and to re-self-assemble onto a neighbouring stack. If nanostrands would be prepared from a chemically synthesized monomer, as for example a PAH a defect-free uniform self-organized molecular wire would be available, as shown in Figure 5.1. Unfortunately next to the large benefit from using pure molecules with tailored properties, adding electric contacts to these molecules remains the enormous challenge in integrating specific molecules for a functional architecture.

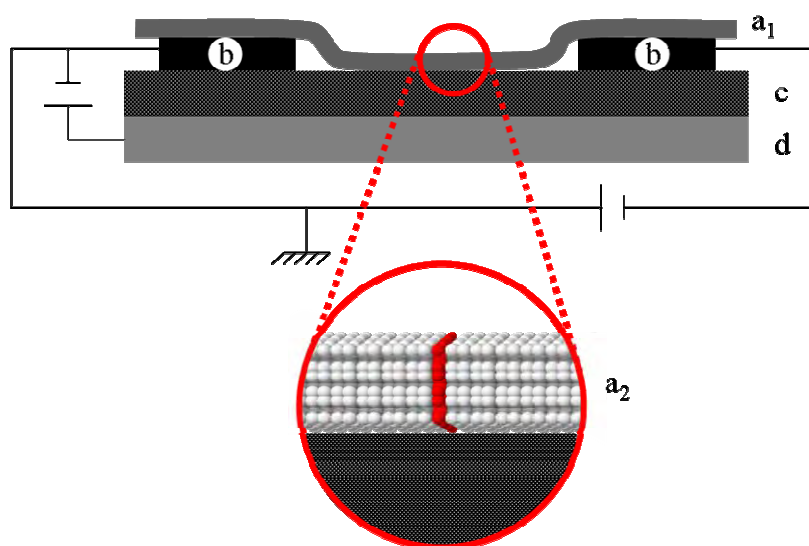


**Figure 5.1** – Sketch of a molecular wire formed by self-assembling of individual PAHs



## 5.1 Possible application – OFET (organic field effect transistor)

The realization of single-molecule devices has proved to be challenging, largely due to difficulties in achieving electrical contact to individual molecules as mentioned previously. The construction of an OFET, consisting of a self-assembled molecular wire could be done in two ways: *i*) either the conducting self-assembled material is grown onto a substrate as already done with different derivatives as shown previously in Figure 4.2; *ii*) deposition of growth of a single self-assembled molecular wire onto two metal electrodes as shown in Figure 5.2.<sup>[82]</sup> By applying a voltage to the gate electrode, the molecular wire could be switched from conducting to isolating.<sup>[83]</sup> This behaviour was already tested and reported for CNT<sup>[84]</sup> and HBC derivatives.<sup>[85]</sup> In order to construct an OFET device out of self-assembled derivatives they have to be assembled “edge-on” onto the substrate.



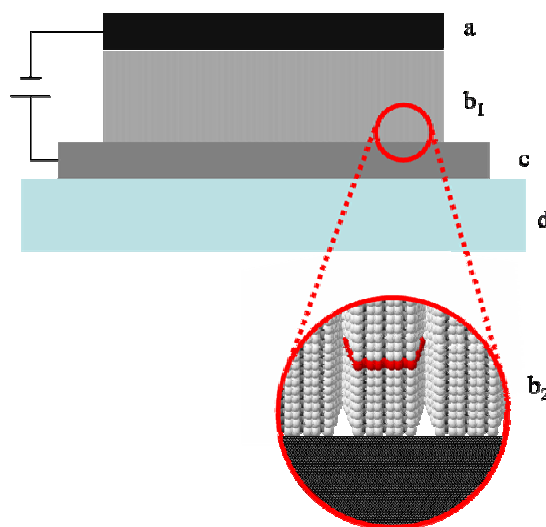
**Figure 5.2** – OFET device made of a single supramolecular wire: a<sub>1</sub>) self-assembled molecular wire; a<sub>2</sub>) zoom of the self-assembled molecular wire out of which one molecule is coloured in red for clarity; b) Pt electrodes (drain and source); c) insulator (SiO<sub>2</sub>); d) Si gate electrode

## 5.2 Possible application – OLED (organic light emitting diode)

The simplest possible OLED device would be made of a single emissive layer, as introduced earlier (see chapter 4.3). A device based on self-assembled discotic molecules could hence be fabricated in the following way: as anode, ITO on a glass substrate would most probably be suitable due to its high transparency for visible light and for the high working function to ensure efficient hole injection. The organic material which is able to form self-assembled supramolecular wires could be grown onto the ITO to form the active layer. The growth of the active layer has to be done “face-on”, i.e. the columnar structure has to be oriented perpendicular to the anode. It has to be noted, that lateral aggregation does most probably not hamper the proper functioning of the device. As cathode



of the device, gold could be evaporated onto the organic material. The cathode in contrary to the anode has a low working function to enhance electron injection.



**Figure 5.3** – OLED device constructed with a self-assembled organic material. a) Mg/Al alloy as cathode; b<sub>1</sub>) organic material as active layer; b<sub>2</sub>) zoom of the self-assembled active layer with one molecule marked in red for clarity; c) ITO anode; d) glass substrate;

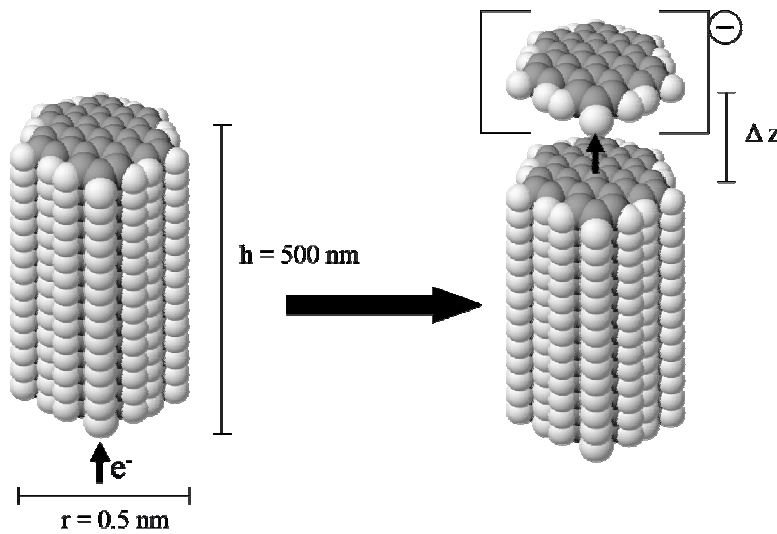
### 5.3 Possible application – FED (field emission display)

The use of self-assembled molecular wires for the construction of FEDs consists of several advantages but also some disadvantages as compared to the recently developed devices using CNTs. As already discussed, on one hand the advantages lie in the chemical synthesis of the constituents which afford pure compounds allowing a variety of substituents. Further a so called “self-healing” (see introduction of chapter 5) effect may increase the overall lifetime of the molecular wires. On top of that, the design of a primer PAH containing sulfur in its lateral chain allows the deposition of “docking stations” onto which other PAH may be deposited. This would ensure not only a good conductivity due to the developed contact but also induce the desired spacing in between the columns.

On the other hand a disadvantage could be the lengthy chemical synthesis of molecules as compared to the low cost physical preparation for CNTs. Furthermore the spacing or the lateral interactions are crucial parameters for the device to work properly and so far it is not clear, how difficult such a control would be.

An open question for the application of self-assembled strands in the domain of FEDs is the stability of such stacks during the electron emission. The following calculation may give an idea on the forces which are needed in order to remove the top molecule of a HBC stack under field emission

conditions. The only possibility for a molecule to be ripped off the stack would be by assuming a completely polarised supramolecular wire, i.e. injection of an electron from the cathode which moves along the strand. The strand is then totally polarised when the electron arrives at the last molecule, which is at this moment charged and therefore attracted by the anode. Unfortunately it has not yet been elucidated if this mechanism is correct. Another possibility would be that an electron is ripped off the top molecule leaving a net positive charge wandering to the cathode. Under these conditions no force at all is exerted on the top molecule. The situation is depicted in Figure 5.4.



**Figure 5.4** – Removal of a monomer from a self-assembled stack in an electrical field

The force, which is applied by elongation by  $\Delta z$  of a needle like tip in an electrical field  $E$ , with the distance between anode and cathode being  $d$ , is described by the following set of equations: Equation 5.1 expresses the change of the total energy  $\Delta U$ , which is given by the integral of the energy density of the electrical field, where  $\epsilon_0$  is the vacuum permeability and  $r$  the diameter of the stack.

$$\Delta U = \int_{\Delta V} d^3 \vec{r} \frac{\epsilon_0}{2} E^2(\vec{r})$$

**Equation 5.1**

Under the approximation that the electrical field is constant, Equation 5.1 may be rewritten resulting Equation 5.2, where  $A$  is the area of one molecule.

$$\Delta U \approx \Delta z A \frac{\epsilon_0}{2} E^2 = \Delta z \pi r^2 \frac{\epsilon_0}{2} E^2$$

**Equation 5.2**

The force is now nothing else than the energy change divided by the elongation, which furnishes Equation 5.3.

$$F = \frac{\Delta U}{\Delta z} = \pi \cdot^2 \frac{\varepsilon_0}{2} E^2$$

**Equation 5.3**

By taking into account the field enhancement ( $\beta$ ) the electrical field may be expressed in the following way (Equation 5.4):

$$E = \frac{V}{d} \beta = \frac{V}{d} \cdot \frac{h}{r}$$

**Equation 5.4**

By combining Equation 5.3 and Equation 5.4 the used force is obtained in a simple form, as shown in Equation 5.5 where the values for a column of HBC derivatives were used directly as shown in Figure 5.4, by assuming an applied voltage of 10 kV.

$$F = \frac{\pi \varepsilon_0 h^2}{2d^2} V^2 = 1.4 \cdot 10^{-9} N$$

**Equation 5.5**

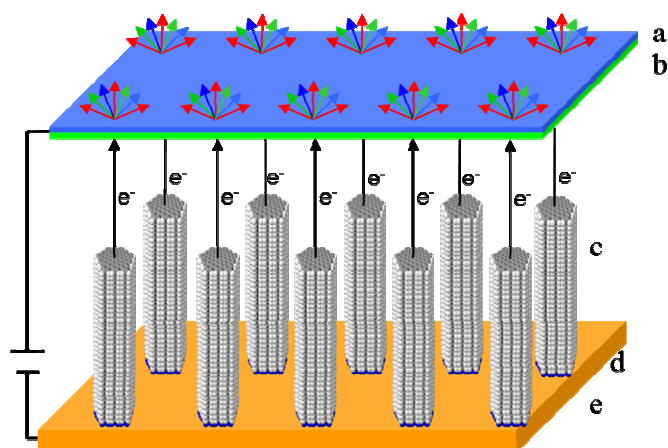
As the calculated force does not tell anything and is not comparable a transformation to the tensile strength is performed by applying Equation 5.6.

$$P = \frac{F}{A} = 1.4 \text{ GPa}$$

**Equation 5.6**

It has to be noted, that no experimental values for the dissociation under field-emission conditions of self-assembled systems is known. Nevertheless this value seems reasonable as for example Kevlar has a tensile strength of 3 GPa as example. Moreover the study of HBC stacks by means of theoretical calculations is not yet possible, as up to now mostly only dimers were treated in literature. Wesolowski *et al.* for example calculated the binding energy of several nitrogen containing PAHs and found a rather strong interaction of about 9 kcal/mol.<sup>[86]</sup>

If one assumes on the other hand, that the electron emission occurs from the top molecule, one would create a charge molecule whose adhesion to the next molecule in the pile would be greatly enhanced, an assumption which has not been taken into account in our calculation. Finally, there are so many hypothetical parameters, that only the experiment will shine light onto the stability of supramolecular wires under field emission conditions.



**Figure 5.5** – FED made of self-assembled molecular wires. a) transparent anode (ITO); b) phosphorescent layer; c) stacks of self-assembled molecules; d) primer molecule used as “docking station”; e) cathode

The exceptional large class of PAH has started to attract the interest of researchers long ago. A steady number of publications describing the synthesis and the properties of new PAH was reported since then, out of which the textbooks of E. Clar<sup>[12]</sup> and J. C. Fetzer<sup>[13]</sup> are noted as examples of accurate summaries of many different PAHs. The most intensively investigated and most promising PAHs are two discotic liquid crystals: triphenylene<sup>[92]</sup> and hexabenzocoronene.<sup>[90]</sup> For both compounds many different derivatives bearing various substituents have been prepared and investigated in the past.

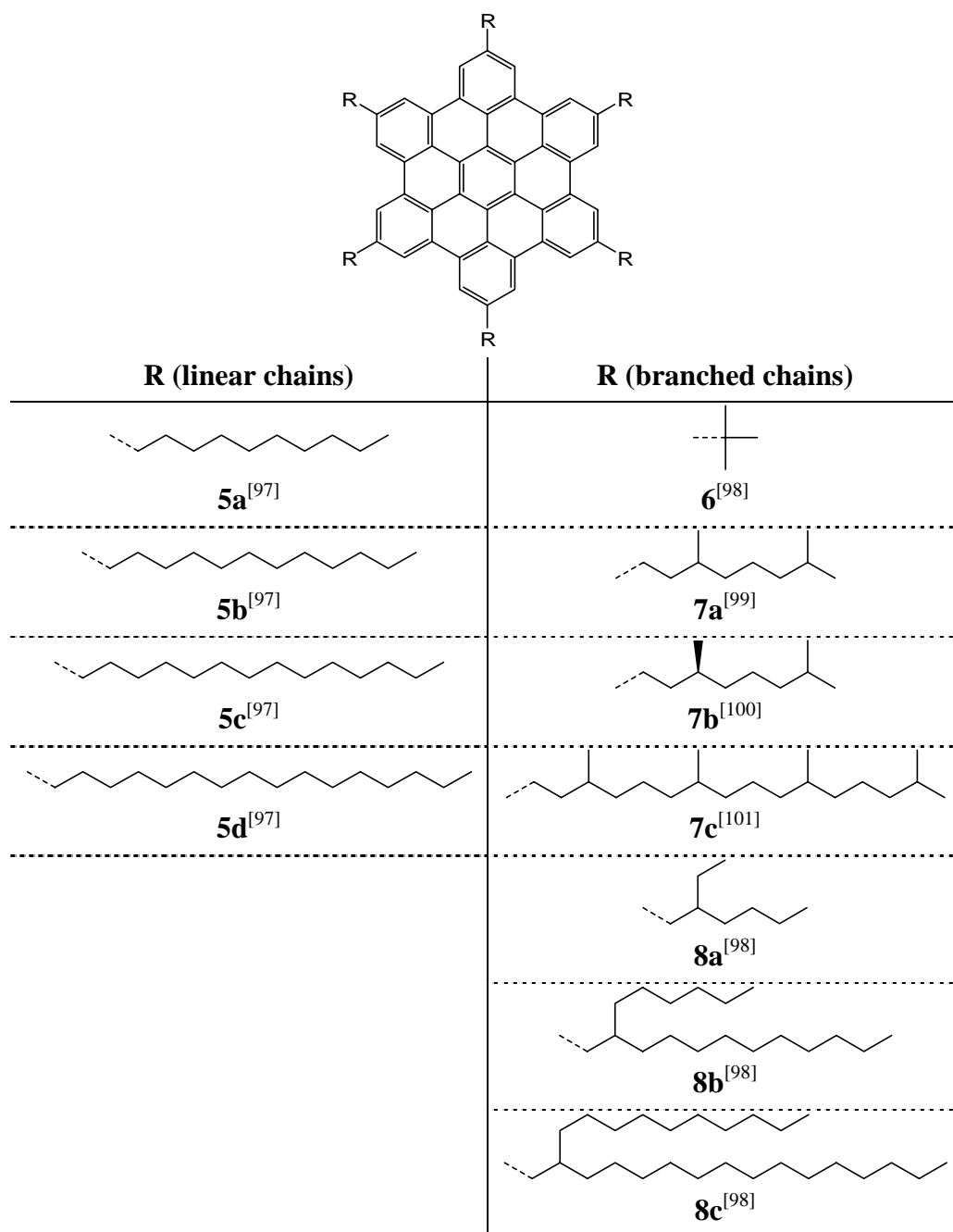
Finally hexabenzocoronene (HBC) was chosen for all investigations presented in this thesis. HBC is priming over triphenylene most notably due the larger aromatic core which results in a more favourable HOMO-LUMO gap and an increased stability for  $\pi$ - $\pi$  aggregation. Moreover HBC derivatives are the first discotic material with a charge carrier mobility over  $1 \text{ cm}^2 \text{V}^{-1} \text{s}^{-1}$ .<sup>[93]</sup> Most probably larger analogues of HBC would result in even higher charge carrier mobility in combination with a larger mesophase over an extended temperature range which would favour the practical application. Nevertheless the solubility of larger derivatives is expected to decrease to rapidly, which hampers their purification and hinders the formation of a liquid phase or formation of solutions in organic solvents which are needed for most deposition techniques.<sup>[94]</sup>

## 6.2 Crystallization of HBC bearing no lateral chains

The crystal structure of the unsubstituted HBC was first published in 1961<sup>[95]</sup> using diffraction data collected from HBC needle like crystals obtained by recrystallization of HBC from molten pyrene / mesitylene. As expected HBC crystallized in a herringbone or so called  $\gamma$ -motive.<sup>[96]</sup> This typical face / face and face / edge  $\pi$ - $\pi$ -aggregation of large unsubstituted PAH derivatives is, as mentioned previously (chapter 2.2), an unfavourable property for the preparation of molecular wires which should be oriented like coins in a stack. The only way to hinder the formation of a herringbone packing is to bestow HBCs with lateral chains, which increases at the same time the solubility of the derivative tremendously and offers therefore the possibility to process these derivatives in solution.

## 6.3 Six-fold alkylated HBC derivatives

Over the past twenty years a large variety of six fold alkylated HBC derivatives were reported in the literature. The alkyl chains vary from simple linear *n*-alkyl to highly branched and even chiral chains, as shown in Figure 6.2 by illustrating some typical examples.



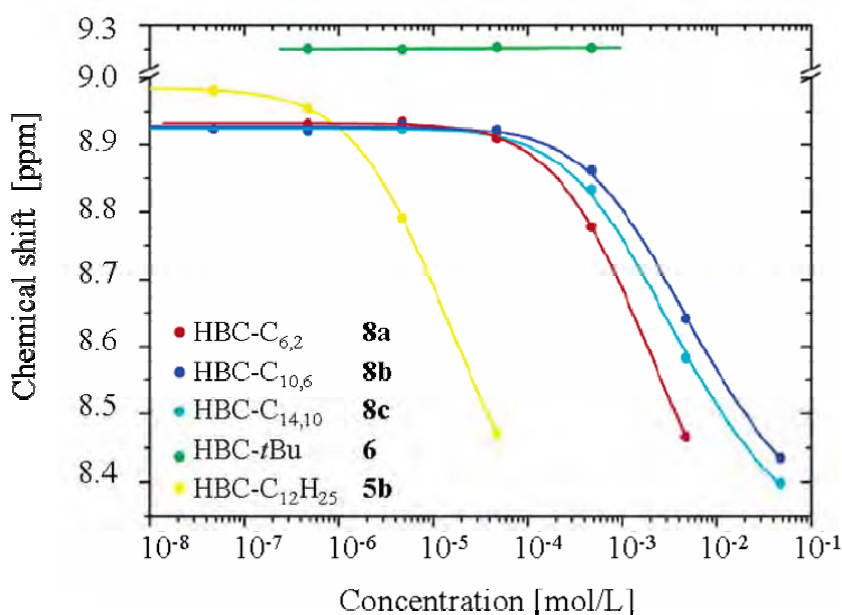
**Figure 6.2** – Overview of alkylated HBC derivatives known in literature

HBC derivatives carrying linear alkyl chains (**5a-d**) are soluble in common organic solvents and passes silica gel if eluted by hot toluene. In contrast, HBCs bearing branched alkyl chains (**7a-c** and **8a-c**) are even soluble in highly unpolar solvents, such as hexane, which allows column chromatography purification at room temperature yielding very pure samples.

The thermal behaviour of these compounds has well been investigated and *n*-alkylated HBCs have remarkable large liquid crystalline phases, in the range of 300°C. Compound **5a** for example has a melting point at 60°C and the resulting mesophase reaches the isotropic melt at 399°C.<sup>[97]</sup> Other *n*-alkylated HBC derivatives were shown to have the isotropization temperature well above 420°C, a

temperature around which decomposition starts.<sup>[100, 97]</sup> Prior to reach the liquid crystalline phase, *n*-alkylated HBCs show a minor transition which is due to alterations of the crystalline alkyl chain packing, which only slightly changes the electronic properties of the material.<sup>[102]</sup> The use of branched alkyl chains allowed the shift of the isotropization temperature to 231 °C for compound **7c** together with an onset of the mesophase at -36°C. Due to the high solubility of HBCs like **7** and **8**, they are obtained in high purity and may be processed easily from the isotropic state.<sup>[101, 103]</sup>

The self-aggregation of alkylated HBC derivatives was intensively studied by using the concentration dependence of <sup>1</sup>H-NMR chemical shifts and photo-physical measurements.<sup>[104]</sup> The chemical shift data provides an insight to the stacking in solution. Concentration dependent <sup>1</sup>H-NMR spectra of compound **5b** in 1,1,2,2-tetrachloroethane-*d*<sub>2</sub> for example showed a plateau at 10<sup>-6</sup> M for the aromatic resonances, which indicated monomeric species as shown in Figure 6.3.<sup>[98]</sup> The solution aggregation of HBC **5b** was found to be significantly more pronounced compared to derivatives bearing branched chains **8a-c**, while HBC-*t*Bu **6** failed to exhibit any association in solution.



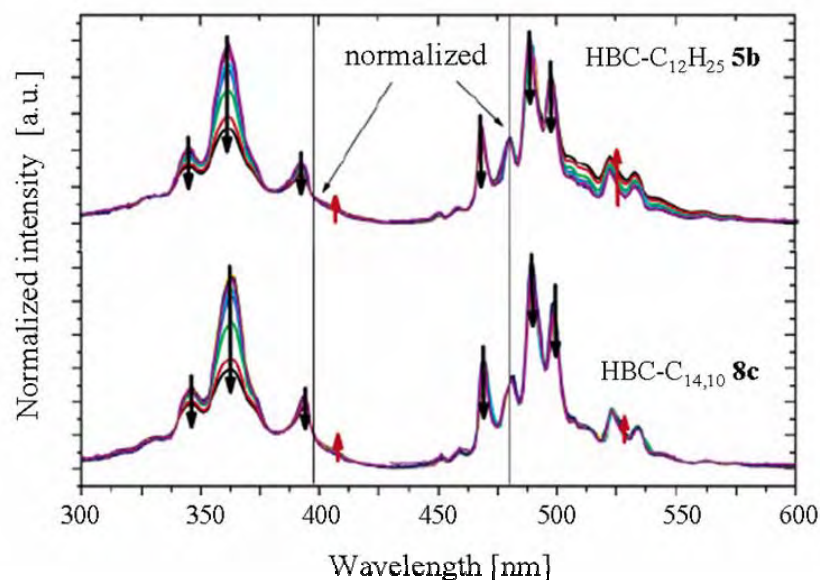
**Figure 6.3** – <sup>1</sup>H-NMR concentration dependent chemical shifts, recorded in 1,1,2,2-tetrachloroethane-*d*<sub>2</sub><sup>[98]</sup>

The influence of temperature was investigated too by using <sup>1</sup>H-NMR techniques and revealed a strong temperature dependence of the aggregation, which was higher for all tested derivatives at lower temperature.<sup>[98]</sup>

Alkyl HBC derivatives were also investigated using absorption spectroscopy, which showed only small differences upon concentration changes in between 10<sup>-7</sup> M and 10<sup>-4</sup> M. Excitation and luminescence spectra in contrast showed a more pronounced effect. By increasing the concentration the bands at 469, 489 and 497 nm decreased for all investigated HBCs in the luminescence spectrum. In contrast, the red-shifted broad band around 500 nm increased slightly, indicating the formation of

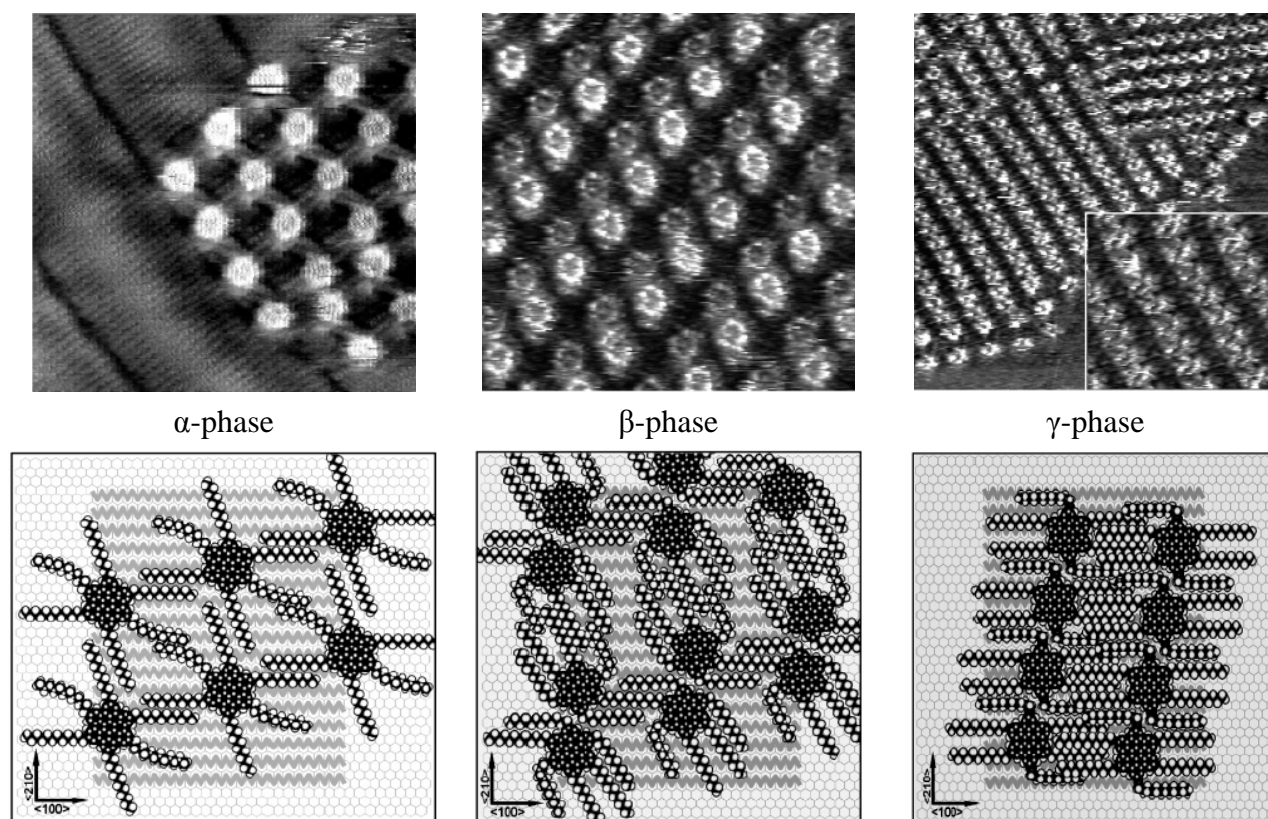


aggregates. The same behaviour was observed in the excitation spectrum as shown in Figure 6.4.<sup>[98]</sup> The concentration dependence was found to be much more pronounced in the excitation spectrum, which is to our own experience only partially true, as the decrease of the 360 nm band at high concentration in the excitation spectrum is most probably due to an artefact, provoked by the high concentration.



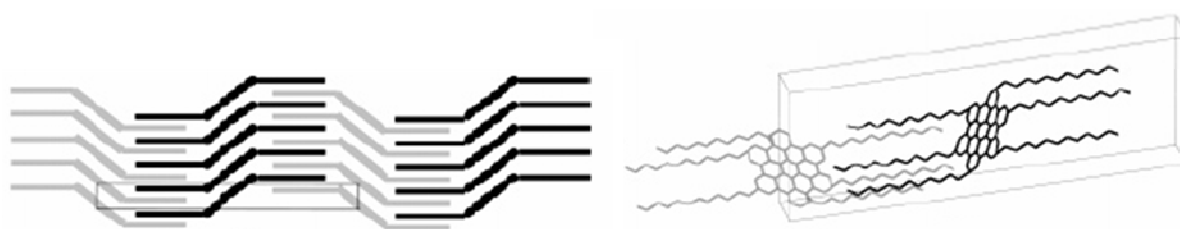
**Figure 6.4** – Excitation and emission spectra of HBC- $C_{12}H_{25}$  **5b** and HBC- $C_{14,10}$  **8c** in  $CHCl_3$  in a concentration range between  $10^{-4}$  M and  $10^{-7}$  M. Normalization was done at 480 and 398 nm, respectively. Arrows point in the direction of increasing concentration<sup>[98]</sup>

Nevertheless, alkylated HBCs have a main drawback, which is their lateral aggregation due to a crystallization of the side chains as shown by STM investigations. Deposition of *n*-alkylated HBC **5b** onto *n*- $C_{50}H_{102}$ -HOPG (highly oriented pyrolytic graphite onto which a  $C_{50}H_{102}$  monolayer was self-assembled) showed morphological, time depended phase transitions with formation of three different phases. In the first hour after the deposition the molecules arrange into the  $\alpha$ -phase which is depicted in Figure 6.5. During the second hour after the deposition the  $\alpha$ -phase transforms slowly into a dimer like aggregation, called  $\beta$ -phase. A further transition occurring after 6 hours leads to the final row structure ( $\gamma$ -phase).<sup>[105]</sup>



**Figure 6.5** – Upper images: STM images recorded after 1 h (left), 2 h (middle) and 6 h (right) showing the transitions between  $\alpha$ -,  $\beta$ - and  $\gamma$ - phase; lower images: Possible packing model of the  $\alpha$ -,  $\beta$ - and  $\gamma$ - phase<sup>[105]</sup>

Further it was shown by solid state MAS spectroscopy that the *n*-alkylated HBC **5b** crystallizes in a herringbone structure as shown in Figure 6.6, identical to the one of unsubstituted HBC, indicating that *n*-alkyl chains do not endow HBC derivatives with the most promising properties<sup>[106]</sup> needed for electronic applications.

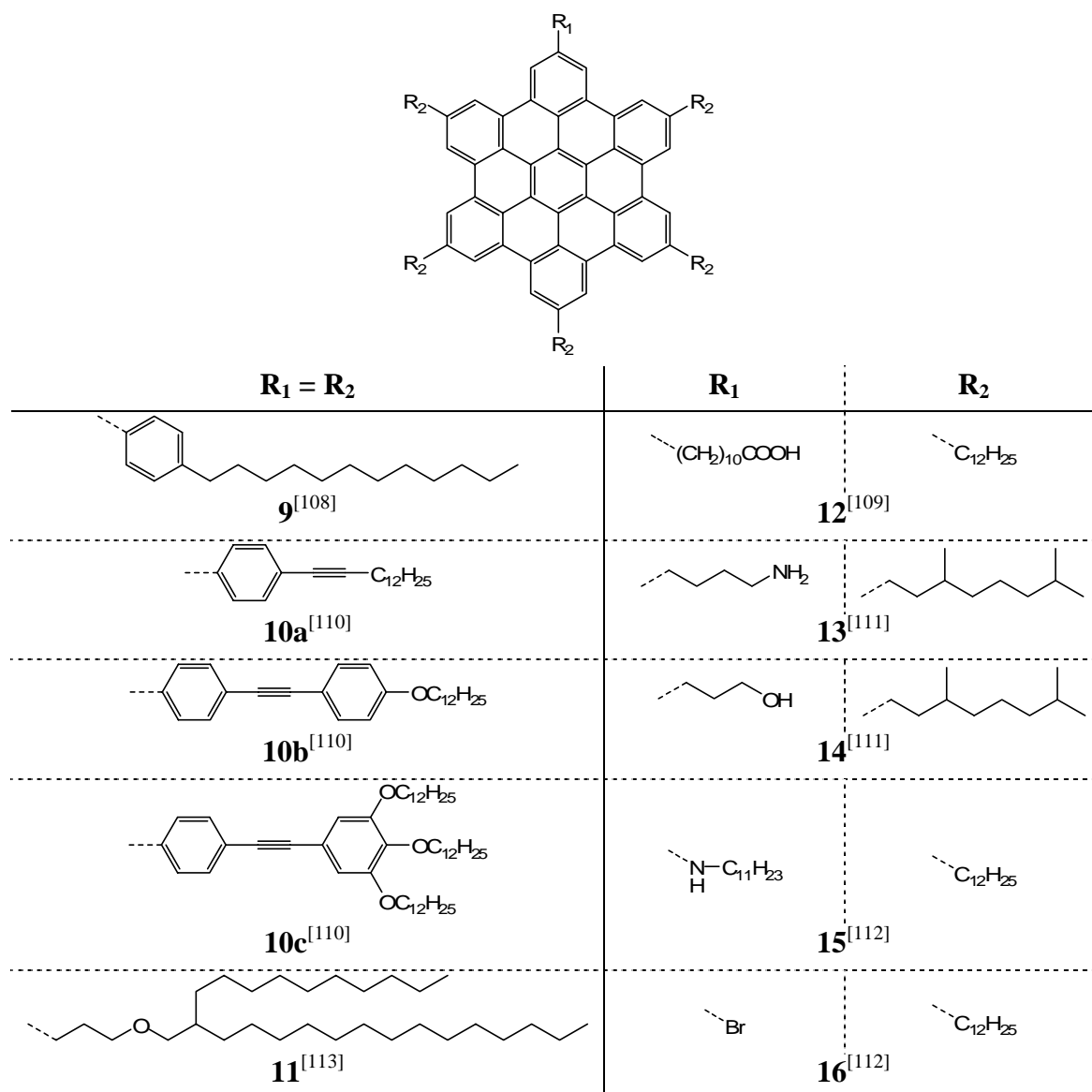


**Figure 6.6** – Illustration of the herringbone arrangement of HBC **5b**; left: the crystallized side chains are indicated with straight lines, whereas for readability, every other stack is grey and black; right: idealized unit cell

The prevention of the lateral aggregation of adjacent monocolumnar HBC stacks, i.e. the separation of the individual stacks is of tremendous importance for the charge carrier mobility. The charge recombination via intercolumnar electron tunnelling through the alkyl mantle was found to be highly influenced by the length of the alkyl chain as shown by PR-TRMC measurements. The life time of the charge carriers was found to increase from a few hundred nanoseconds to almost a milli-second, as the length of the alkyl chain was increased from 6 (**8b**) to 14 (**8c**) carbon atoms.<sup>[107]</sup>

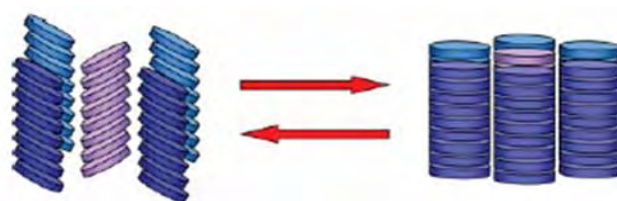
### 6.4 Variation of the number and the nature of the lateral chains

The realization of long range order is crucial for any application in organic electronics. A well pronounced linearity of self-assembled structures may be achieved by introduction of functionalities in the periphery which bring additional intracolumnar interactions, as for example dipole-dipole interactions or hydrogen bridges. With this prime concern in mind many publications were reported in the past. Figure 6.7 summarizes the most important derivatives out of many, which have been prepared in the past decade.



**Figure 6.7** – Overview of the most important HBC derivatives bearing other than pure alkyl chains

By comparing the charge carrier mobility of the *n*-alkylated HBC derivative **5b** and its analogue **9** and **10a**, carrying an additional aromatic ring in its periphery, an interesting observation was reported: HBC **9** had a constant charge carrier mobility of  $0.3 \text{ cm}^2\text{V}^{-1}\text{s}^{-1}$  over a large temperature domain whereas the charge carrier mobility of **5b** dropped from  $1.0 \text{ cm}^2\text{V}^{-1}\text{s}^{-1}$  to  $0.3 \text{ cm}^2\text{V}^{-1}\text{s}^{-1}$  by entering the mesophase. The reason of this behaviour was explained with the aid of solid state experiments. HBC **5b** forms in its crystalline phase a herringbone structure which is ideal for the charge carrier mobility due to an increased  $\pi$ - $\pi$  aggregation. By entering the liquid crystalline phase the HBC rings start to rotate around their axis<sup>[97, 108]</sup> and adopt therefore another geometry with a reduced  $\pi$ - $\pi$  aggregation which causes the charge carrier mobility to drop. The crystalline phase as well as the mesophase is sketched schematically in Figure 6.8.<sup>[82]</sup> In the case of HBC **9** the formation of a herringbone structure is hindered, which is the reason for the lower, but stable mobility.<sup>[114]</sup> Further, Müllen asserts that HBC derivatives bearing phenyl spacers form more stable columns due to the hindered gliding of adjacent HBC disks, shown by solid state NMR.<sup>[108]</sup> Nevertheless, it has not been proven up to now, that such structures were more stable. On the other hand an anisotropy with respect to the orientation of the deposited HBCs was found to be much higher for HBCs bearing a lateral phenyl spacer.<sup>[115]</sup>

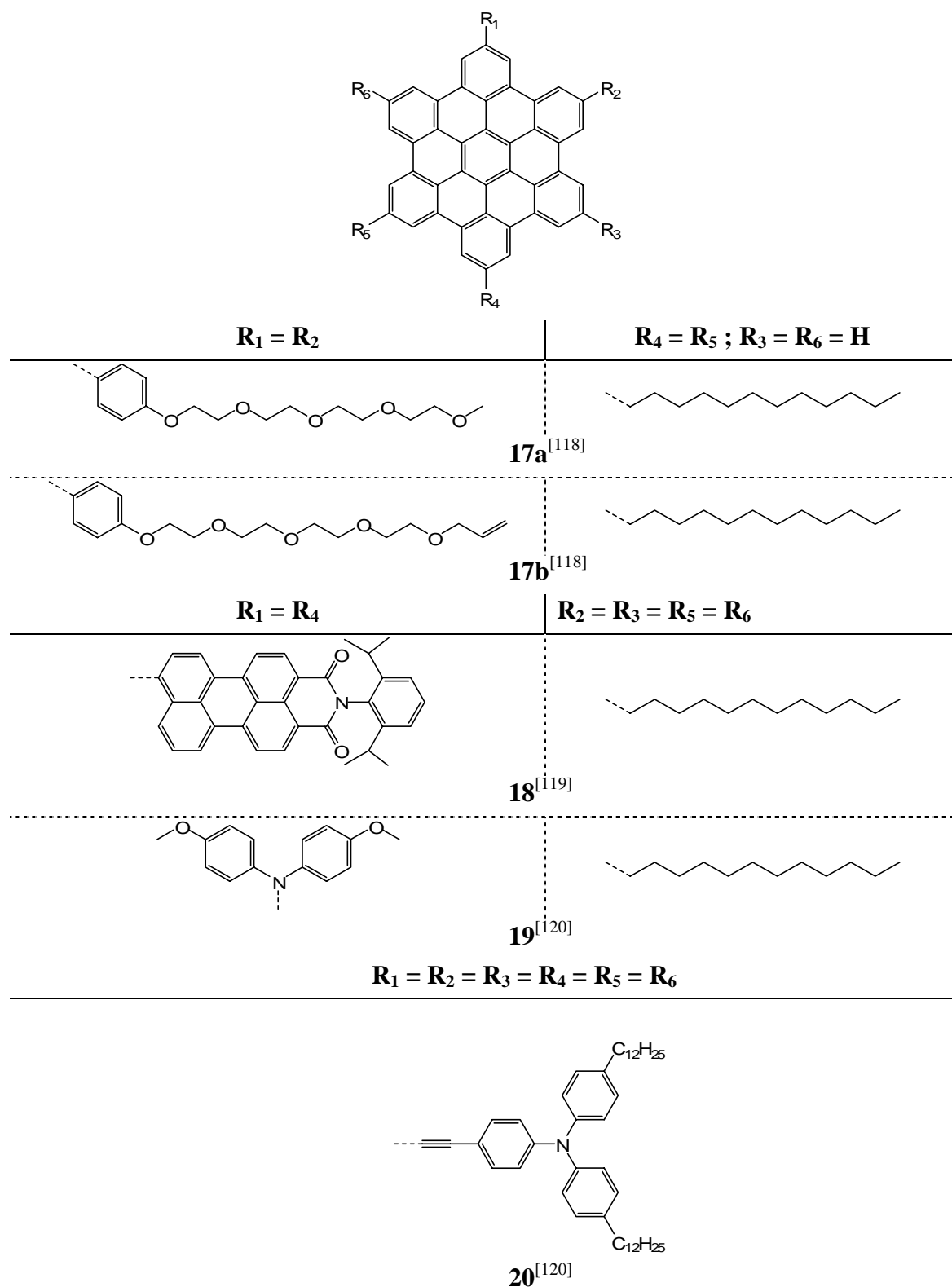


**Figure 6.8** – Schematic sketch of stacked HBC derivatives; **left**: “crystal phase” (tilted); **right**: mesophase (disks perpendicular to column axis) where HBC are oriented like coins in a stack<sup>[82]</sup>

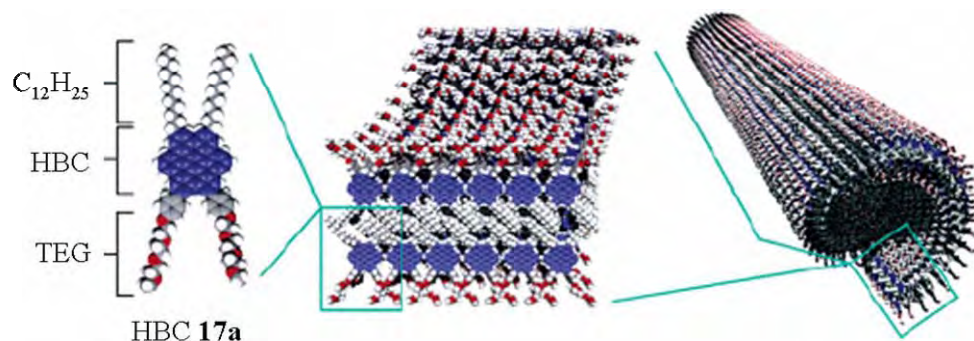
By substituting the HBC core with phenylalkoxy chains (**10b** and **c**) a crystallization in a herringbone pattern is also prevented<sup>[110, 116]</sup> because of the sterical hindrance as already shown for compound **9**. Due to the alkyne spacer of the lateral chain and the additional phenyl ring the charge carrier mobility is supposed to be slightly higher in derivatives **10b** and **c** compared to **9**. The incorporation of heteroatoms, as for example oxygen, in the side chain (**11**) increased the tendency of the corresponding HBC to grow in a pronounced linear alignment. This is most probably due to the interaction of the oxygen with the glass or aluminium substrate. The increased linearity of the obtained stacks was observed in both, “face-on” and “edge-on” deposition. Nevertheless this improvement does not prevent lateral aggregation of the formed stacks.<sup>[113]</sup>

A synergetic combination of  $\pi$ -stacking and hydrogen bonds was achieved by replacing one alkyl chain by a carboxylic acid. By the formation of hydrogen bonds, the degree of freedom of the movements of individual HBC molecules is reduced. This leads to stronger intermolecular or inter-columnar interactions and thus to an improved order in the bulk and a higher transition temperature to the mesophase.<sup>[109, 112, 117]</sup>

## 6.5 Functional sided chains allowing cross-linking or “double cable” formation

**Figure 6.9** – Small selection of HBC derivatives bearing functional side chains

Aida reported recently another approach to deal with the usually undesired lateral intercolumnar interaction by making use of it to build up another type of nanotube as shown in Figure 6.10.<sup>[121]</sup>



**Figure 6.10** – Schematic sketch of the formation of rolled HBC nanotubes; **left**: structure of HBC **17a**; **middle**: self-assembled bilayer; **right**: rolled-up nanotube<sup>[121]</sup>

HBC **17a** and **b** carry two long alkyl chains on one side and two triethylene glycol (TEG) chains on the other. The nanotubes are now formed by helical rolling-up of a HBC bilayer prepared by lateral interaction of the alkyl chains. The hydrophilic TEG chain cover therefore both, the inner and outer surface of the tube. In order to stabilize the formed tube it is possible to use alkene end groups (**17b**) which are cross-linked in a metathesis reaction<sup>[118, 121, 122]</sup> after the self-assembly has been completed. Charge carrier mobility measurements were not yet published. Nevertheless this new approach is an interesting way to stabilize the self-aggregated structures. But it has to be noted, that the self-healing property is inherently lost by covalently linking self-assembled structures.

A combination of HBC derivatives with their high charge carrier mobility and perylene diimide dyes which possess high electron mobilities,<sup>[123]</sup> would make such derivatives very interesting for the preparation of solar cells where donor (HBC) and acceptor (perylene diimide) are combined in the same molecule. Such “coaxial” derivatives **18** - **20**, able to form “double-cable” structures have been prepared in the past with several modifications, as shown in Figure 6.9.<sup>[119, 120]</sup>

## 7 Suppressing lateral aggregation by “fluorine coating”

Introduction of fluorine into a molecule tends to generate novel, sometimes hardly predictable behaviour but is nevertheless often used to influence the properties of a derivatives in a simple but highly effective way. The incorporation of large numbers of fluorine atoms, so-called perfluorination, has even more pronounced effects as shown during this thesis.

Fluorine combines the highest electronegativity and a low polarizability. Further fluorine and hydrogen differ quite strongly in the van der Waals radius which is 1.47 vs. 1.20 Å, respectively. Perfluorinated compounds are known to be sterically more demanding and much stiffer than their alkyl counterparts.<sup>[124]</sup> The cross-section of a perfluoroalkyl chain (30 Å) differs strongly from a normal alkyl chain (20 Å).<sup>[125]</sup> Moreover the typical planar “zigzag” structure of alkanes becomes rather helical and much more rigid in perfluorinated analogues.<sup>[126]</sup> Furthermore, perfluorinated chains have considerably more hydrophobic character than alkyl chains and have the unique attribute of being lipophobic as well.<sup>[127]</sup>

Due to all these very characteristic and unique properties, the incorporation of fluorine into a molecule is a common way to provoke phase segregation and hence the formation of liquid crystals, micelles or many other well defined structure formed due to the combination of completely different chemical groups in one molecule.

HBCs bestowed with partially perfluorinated end parts of the side chains should therefore have a reduced tendency for lateral interaction of formed one dimensional structures. The formed fluorine mantle around the HBC core, comparable to a Teflon-like coating, should isolate the formed stack from all interactions with neighbouring columns due to the following reasons: *i*) the much stiffer conformation of perfluorinated derivatives does not allow a crystallization as observed with purely alkylated chains; *ii*) reduction of the Van der Waals interaction in between the fluorines. Furthermore there should be no alteration of the desired  $\pi$ - $\pi$ -stacking, implying that the charge carrier mobility should neither be hindered.

The outstanding properties of fluorine may also be a possible reason why perfluoroalkylated HBCs have much higher transition temperatures to the mesophase as compared to their purely *n*-alkylated counterparts,<sup>[128]</sup> indicating the difficulties in melting the side chains due to their stiffness. As decomposition arises prior to the isotropization point of perfluoroalkylated HBC derivatives, no statement on the spread of the mesophase can be made. Nevertheless it is strongly probable that the stability and the mesophase range is increased comparing perfluorinated HBC derivatives to their alkylated counterparts, as these findings were observed for other derivatives.<sup>[129]</sup>

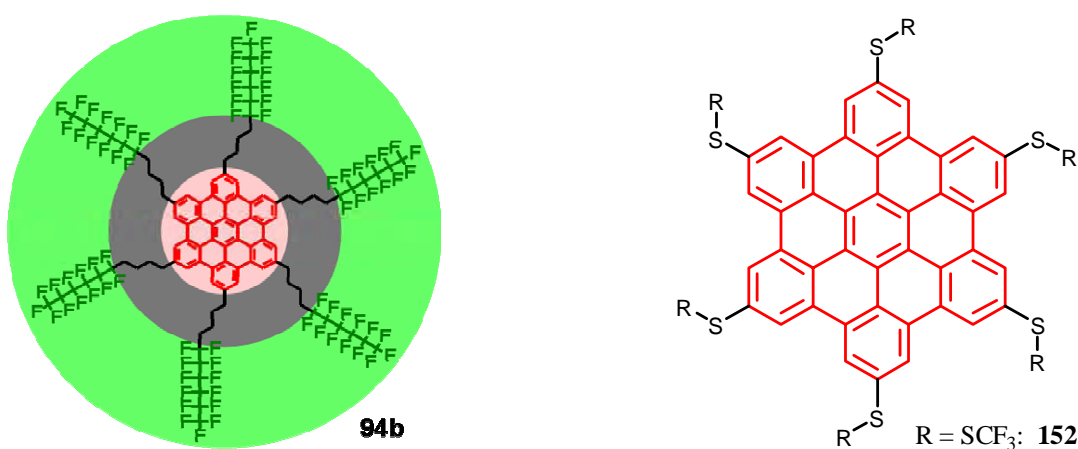
Aliphatic spacers, placed between the HBC core and the perfluoroalkylated side chain turned out to be crucial for synthetic reasons<sup>[130]</sup> as they shield the HBC core from the electron withdrawing effect of the perfluorinated substituents. A minimum spacer of two CH<sub>2</sub> groups is minimally needed in order to complete the synthesis. Preliminary investigations showed that the perfluoro / alkyl ratio turned out to be a crucial parameter for the lateral aggregation.<sup>[128, 131]</sup> Probable reasons may be the influenced solubility or the phase segregation in between the aromatic core, the paraffin-like alkyl part and the perfluorinated part. It has to be noted that the length and the ratio of perfluorinated parts has a much greater influence of the morphology of the derivative than the modification of a pure alkyl chain.<sup>[132]</sup>



## 8 Vision of the Thesis

The preparation of perfluoroalkylated and sulfurated HBC derivatives is envisioned. These compounds are composed of three main parts as shown in Figure 8.1.

- The HBC core, allowing for the  $\pi$ -aggregation and charge transport.
- The flexible paraffinic alkyl part, endowing the molecule with the needed flexibility to adopt the desired conformation for the  $\pi$ -aggregation. Further the alkyl part shields the core from the electron withdrawing effect of the fluorinated parts and enables the synthetic preparation.
- The perfluorinated tail of the side chain which endows the molecule with a fluorine coating reducing the lateral aggregation.
- The perfluorinated part may be replaced by a sulfur atom to create primer HBC derivatives used as docking stations.

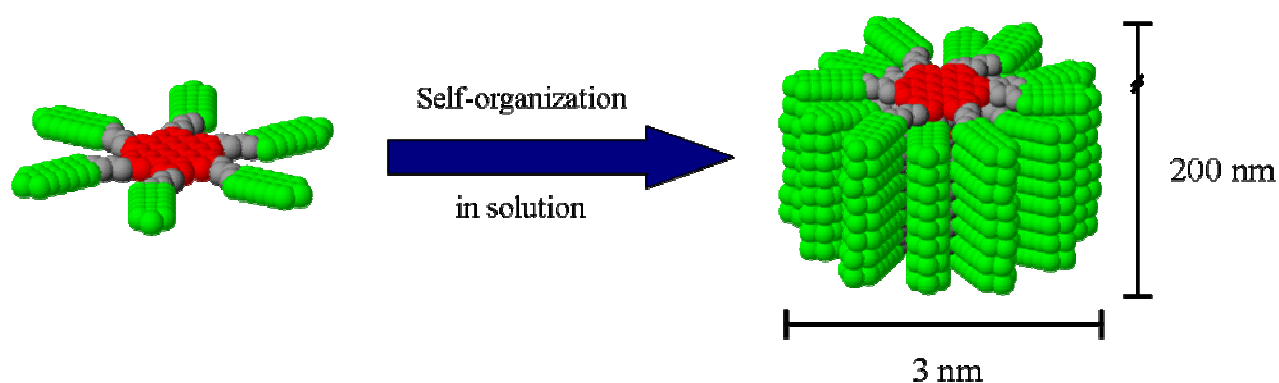


**Figure 8.1** – Left: HBC derivative carrying a semi-perfluorinated decoration (HBC-Rf<sub>4,6</sub>, **94b**) separating the derivative in three parts: red: polycondensed aromatic core; grey: flexible alkyl part; green: perfluoroalkylated isolating end part; right: HBC derivative carrying protected ( $R = SCF_3$ , **152**) sulfurated lateral chains

A systematic preparation of different derivatives carrying a variety of perfluoroalkylated and sulfurated side chains has to be done where the latter are intended for deposition attempts on gold surfaces. A further important point is the constitution of the side chain. Are linear perfluorinated chains ideal for self-assembled structures or would branched chains prime, as they increase the fluorine amount as well as the sterical hindrance tremendously? Up to now only D<sub>6h</sub> HBCs were prepared in our group. Perhaps a reduced number of side chains in combination with the use of branched chains endow HBCs with the desired property of forming well organized one dimensional stacks.

Further, analytical tools have to be found which allow the analysis of the morphology of these derivatives in solution and on surfaces. Interpretation of these results will allow eventually to find the ideal HBC moiety forming self-assembled structure with long range order in combination with a reduced tendency to aggregate laterally.

By engineering the side chain geometry, tuning the fluorination level and variation of the solvent, some control on the long range one-dimensional aggregation, as well as the lateral aggregation is intended to gain in order to produce self-assembled molecular wires in solution at will as shown in Figure 8.2.



**Figure 8.2** – One dimensional self-organization of HBC derivatives (**94b**) carrying semi-perfluoroalkylated lateral chains

## **II Results and Discussion – Part 1: Synthetic Investigations**



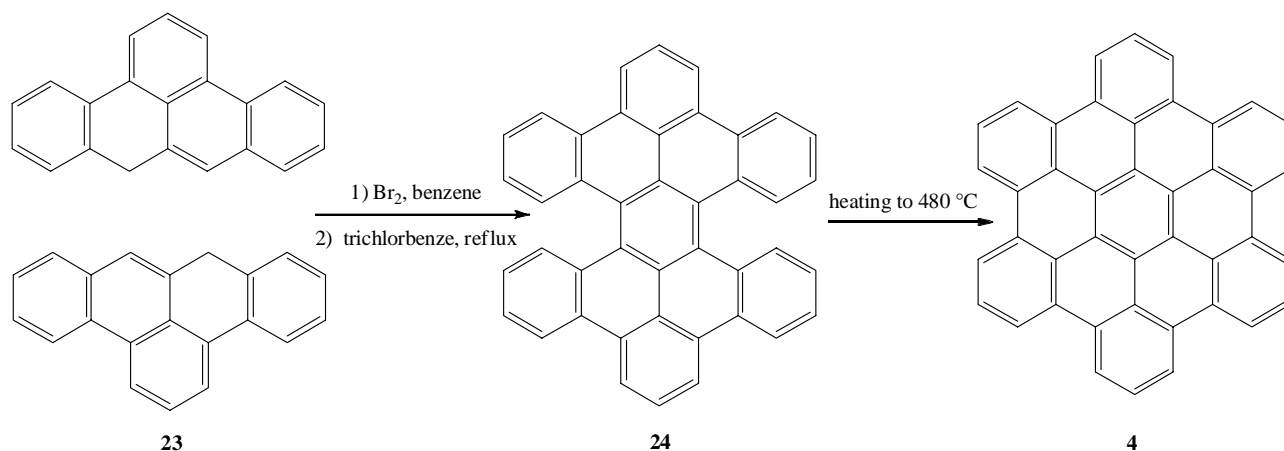
## 9 General aspects

### 9.1 Retro synthesis of HBC derivatives

Three main pathways for the preparation of HBC derivatives are used most commonly, depending on the symmetry of the target HBC which may be: *i*) completely symmetric derivatives, bearing six identical side chains ( $D_{6h}$ ); *ii*) derivatives bearing exactly three identical side chains ( $D_{3h}$ ); *iii*) desymmetrized derivatives bearing one to six different lateral chains ( $D_{2h}$ ,  $C_{2v}$ ). Nevertheless, the final step of all three strategies consists of a cyclodehydrogenation of the hexaphenylbenzene derivative under Kovacic conditions. The latter conditions, however, prevent the preparation of HBC derivatives in which perfluorinated side chains are directly attached to the aromatic core. An alkyl spacer of at least two carbons, or an ether or thioether linkage is required to reduce the electron-withdrawing effect of the perfluorinated side chain to an acceptable level for the mild iron(III)chloride reagent to be successful.<sup>[128]</sup> The preparation of a hexaiodo- or hexabromo HBC, to which the perfluoroalkylated chains are attached in a six-fold cross-coupling did not succeed as the decreasing solubility, induced by each additional highly fluorinated chain, hampered the completion of the reaction too severely.

#### 9.1.1 Cyclodehydrogenation of HPB derivatives

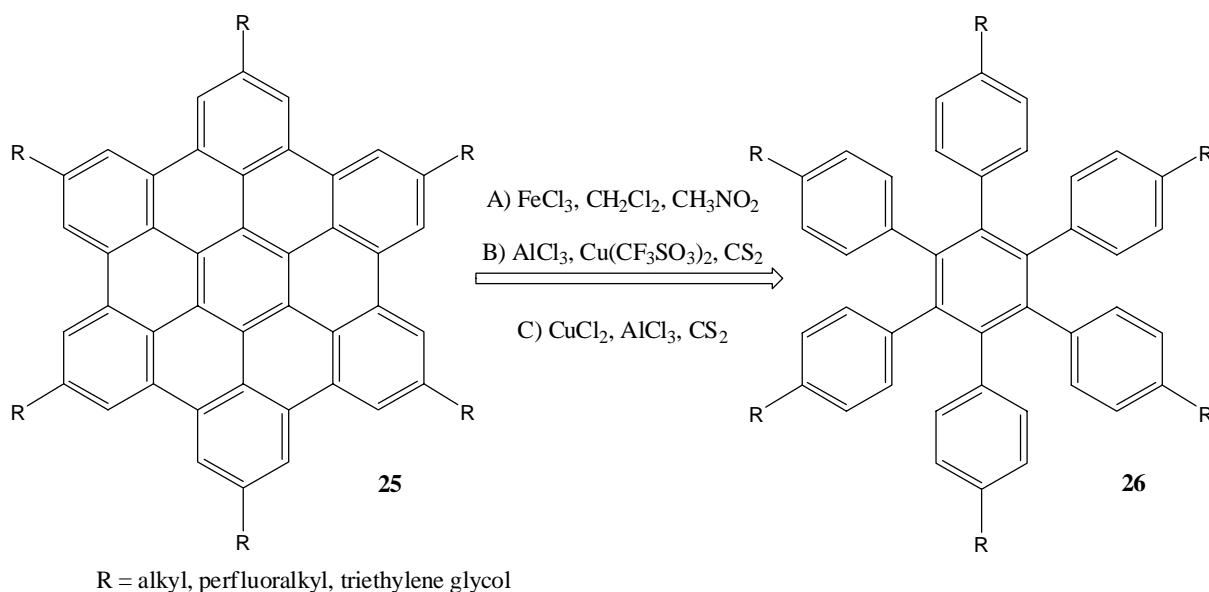
As introduced, the key step of the synthesis of HBC derivatives consists generally of the final oxidation of the HPB derivative yielding the planar HBC moiety. Nevertheless it is worth mentioning, that already in 1959 a different strategy for the synthesis of hexa-*peri*-hexabenzocoronene was reported by Clar.<sup>[12c]</sup>



**Scheme 9.1** – Formation of HBC performed by Clar in 1959.

Reacting 8H-benzo[*fg*]tetracene **23** in benzene with bromine yields a perbromide which eliminates HBr under heating in trichlorobenzene to form the hexabenzo[*a,cd,f,j,lm,o*]perylene **24** which under evolution of hydrogen yields the HBC derivative **4**. Halleux reported just a year before in 1958 the preparation of the parent HBC by cyclodehydrogenation of HPB in a  $\text{AlCl}_3\text{-NaCl}$  melt in very low yield (1-3%),<sup>[133]</sup> furnishing the basis of the current conditions.

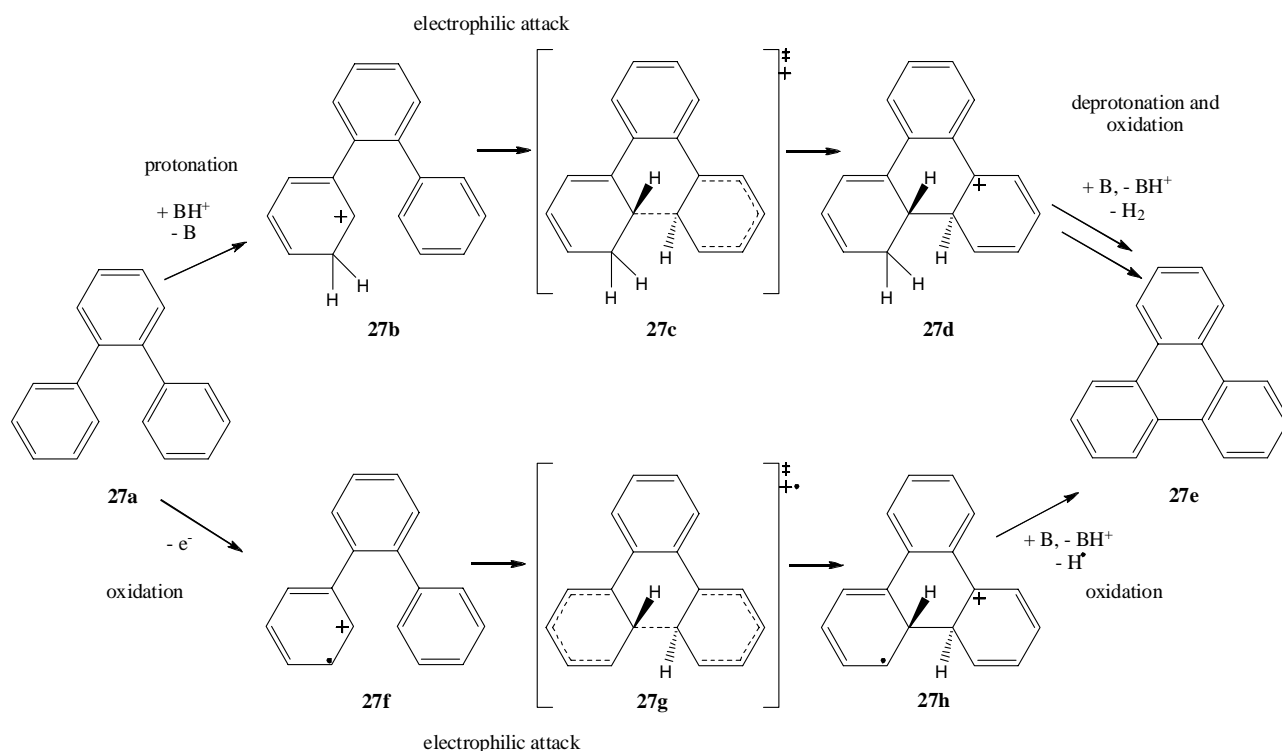
Nowadays different strategies exist for the preparation of HBC derivatives out of which the most popular is the acid-catalyzed oxidative condensation of HPB derivatives, known as the intramolecular Scholl reaction.<sup>[134]</sup> The Kovacic conditions<sup>[135]</sup> for this reaction, which use transition metal salts such as  $\text{MoCl}_5$ ,<sup>[136]</sup>  $\text{CuCl}_2$ <sup>[137]</sup> or  $\text{FeCl}_3$ ,<sup>[138]</sup> are most widely used. It is worth mentioning, that besides these conditions, other systems are used, involving for example vanadium salts<sup>[139]</sup> such as  $\text{VOCl}_3$  or  $\text{VOF}_3$ , thallium salts,<sup>[140]</sup> photocyclizations in the presence of iodine,<sup>[141]</sup> DDQ<sup>[142]</sup> or even palladium-charcoal catalyzed reactions.<sup>[143]</sup>



**Scheme 9.2** – Planarization of HPB derivatives

The most commonly used conditions reported for the formation of HBC derivatives (**25**) from HPB (**26**) moieties are: *i*)  $\text{FeCl}_3$ ,  $\text{CH}_3\text{NO}_2$ ,  $\text{CH}_2\text{Cl}_2$ ; *ii*)  $\text{AlCl}_3$ ,  $\text{Cu}(\text{CF}_3\text{SO}_3)_2$ ,  $\text{CS}_2$ ; *iii*)  $\text{CuCl}_2$ ,  $\text{AlCl}_3$ ,  $\text{CS}_2$ . Whereas the former are much milder than the later as the risk of chlorination is highest in the case of  $\text{AlCl}_3$ .<sup>[99, 103, 144]</sup>

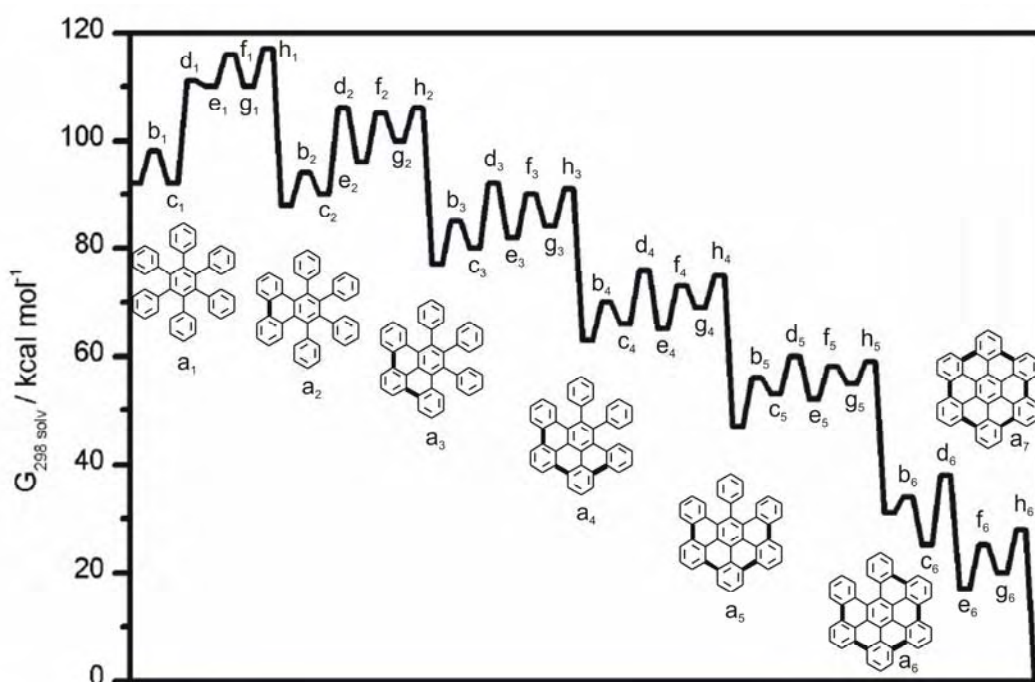
Recently Rempala<sup>[145]</sup> proposed a mechanism for the intramolecular Scholl condensation, which is based on computational and experimental data. Two main reaction pathways are possible for the oxidation of large aromatic compounds, using the Scholl reaction: the arenium or the radical cation based one,<sup>[146]</sup> illustrated in Figure 9.1 at the example of *o*-terphenyl for simplicity.



**Figure 9.1** – Arenium cation and radical cation *o*-terphenyl condensation pathways

The exact nature of the proton transfer and the oxidative dehydrogenation transition state [TSs] is not obvious. Because of this, these TSs were not calculated, but literature values were adopted instead.<sup>[147]</sup> The trans C-C bond-forming TSs **27c** and **27g** are significantly lower in energy than their cis counterparts. The calculated vacuum and solvated data suggest that the arenium cation pathway is preferred over the radical cation pathway. Protonated *o*-terphenyl ( $\text{BH}^+$ ) is the acid, which corresponds to a catalytic amount of a strong Brønsted acid in a weakly basic solvent.

On the basis of the *o*-terphenyl results, the arenium cation-based mechanism is more likely to occur during the oxidation of hexaphenylbenzene derivatives than a radical pathway, which has been calculated and is illustrated in Figure 9.2. In summary, the intramolecular Scholl reaction of hexaphenylbenzene may proceed by the following way: protonation (*ortho* and *para* protonation are nearly equivalent in energy), electrophilic attack, deprotonation, and subsequent oxidation. C-C-bonds are likely formed stepwise and contiguously, with the first being formed the slowest.



**Figure 9.2** – Reaction coordinate diagram for the oxidation of HPB (**28**) into HBC (**4**), considering ortho protonation. Labels: a<sub>j</sub> as shown; b<sub>j</sub> protonation TS; c<sub>j</sub> arenium cation; d<sub>j</sub> C-C bond formation TS; e<sub>j</sub> protonated dihydro intermediate; f<sub>j</sub> deprotonation TS; g<sub>j</sub> neutral dihydro intermediate; h<sub>j</sub> oxidation TS<sup>[145]</sup>

The above stated theoretical finding was corroborated by our experiences, as usually HBC derivatives were found with varying amounts of starting HPB, without any trace of partially oxidized derivatives, as shown by MALDI-ICR-MS experiments. The reaction is increasingly exergonic, possible due to increasing resonance energy per  $\pi$  electron,<sup>[148]</sup> and it is likely that therefore the utility of the Scholl reaction for the formation of large PAHs arises from the slippery slope phenomenon, as shown in Figure 9.2.

The proposed arenium cation pathway seems to be a plausible explanation of the mechanism, consisting nonetheless of two weaknesses: *i*) there is no strong acid in the reaction medium used ( $\text{FeCl}_3$ ,  $\text{CH}_2\text{Cl}_2$  and  $\text{CH}_3\text{NO}_2$ ), capable for protonating the first HPB derivative; *ii*) there is no HCl formed during the reaction, a proven reaction product by Kovacic<sup>[149]</sup> and Müllen.<sup>[150]</sup> A catalytically amount of acid may probably be formed by the reaction of iron(III)chloride with traces of moisture as shown in Scheme 9.3



**Scheme 9.3** – Formation of monohydrated iron(III)chloride acting as acid



Other authors who investigated the intramolecular Scholl reaction favoured a radical pathway with radical cation intermediates, according to Figure 9.3. It has to be noted that instead of  $\text{FeCl}_3$ , a mixture of  $\text{AlCl}_3$  and  $\text{CuCl}_2$  had been taken into account for their calculations, which should not alter the mechanism.

After the formation of the coupled radical intermediate **27h**, both remaining protons are ejected in a two-step process. Initially, the Lewis base  $\text{CuCl}_2^-$  abstracts one proton to give the neutral species **27i**. To release the second proton, a new cation must be formed in the presence of the second  $\text{CuCl}_2$  reagent. The final loss of the second proton from **27j** in the presence of  $\text{CuCl}_2^-$  gives the planarized derivative **27e** together with two molecules of  $\text{HCl}$ . The advantage of this mechanism is the explanation of the formed  $\text{HCl}$ . Which reaction mechanism takes place exactly may only hardly be predicted up to now.

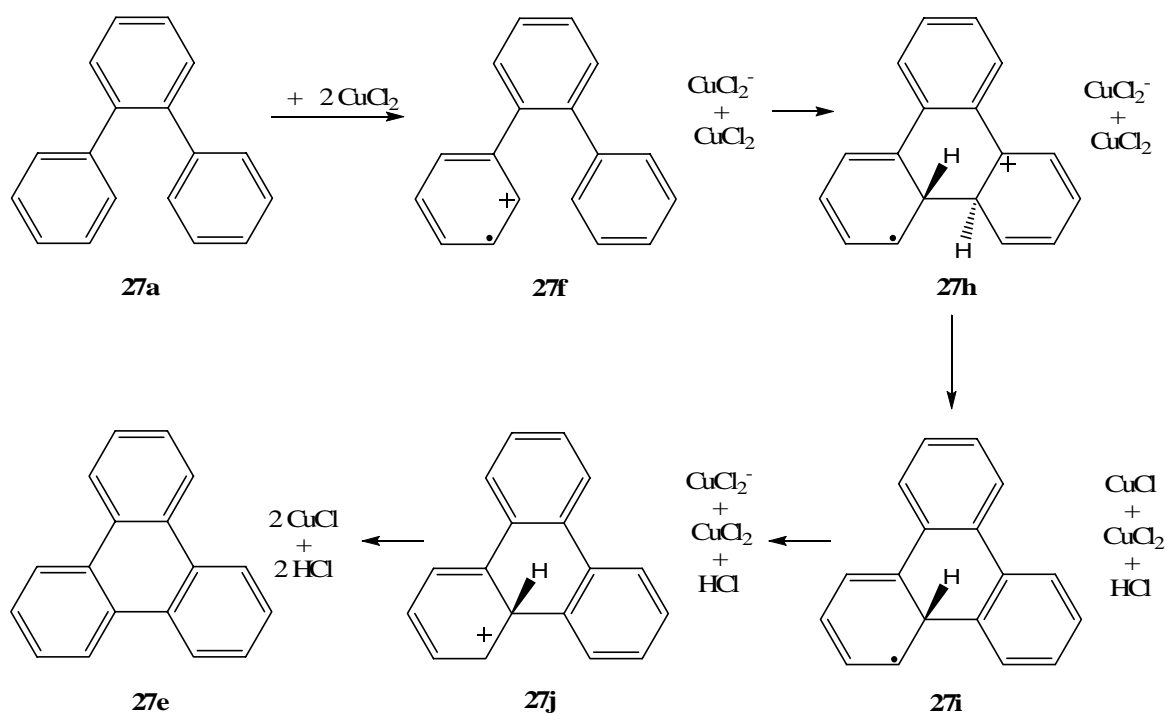
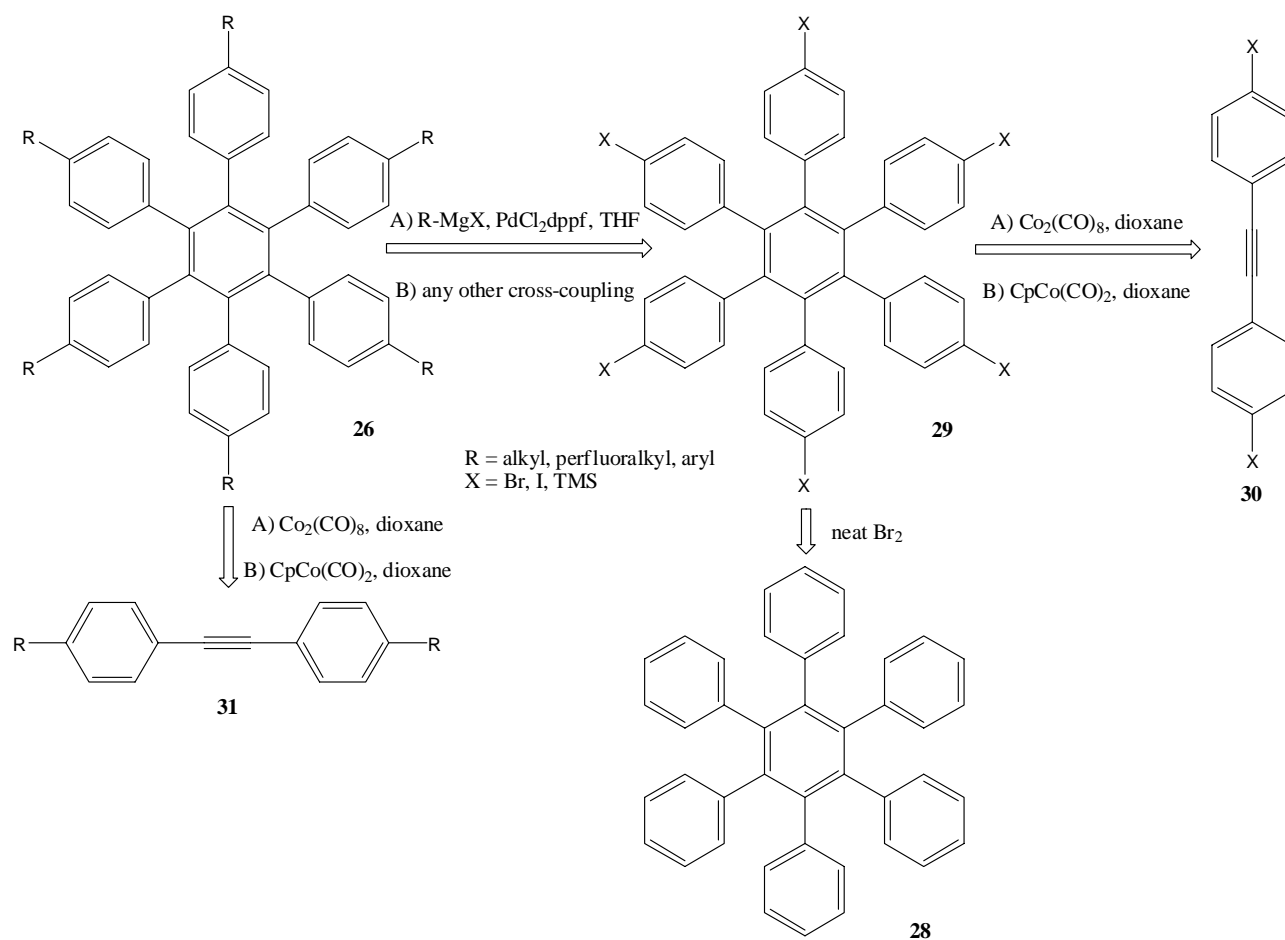


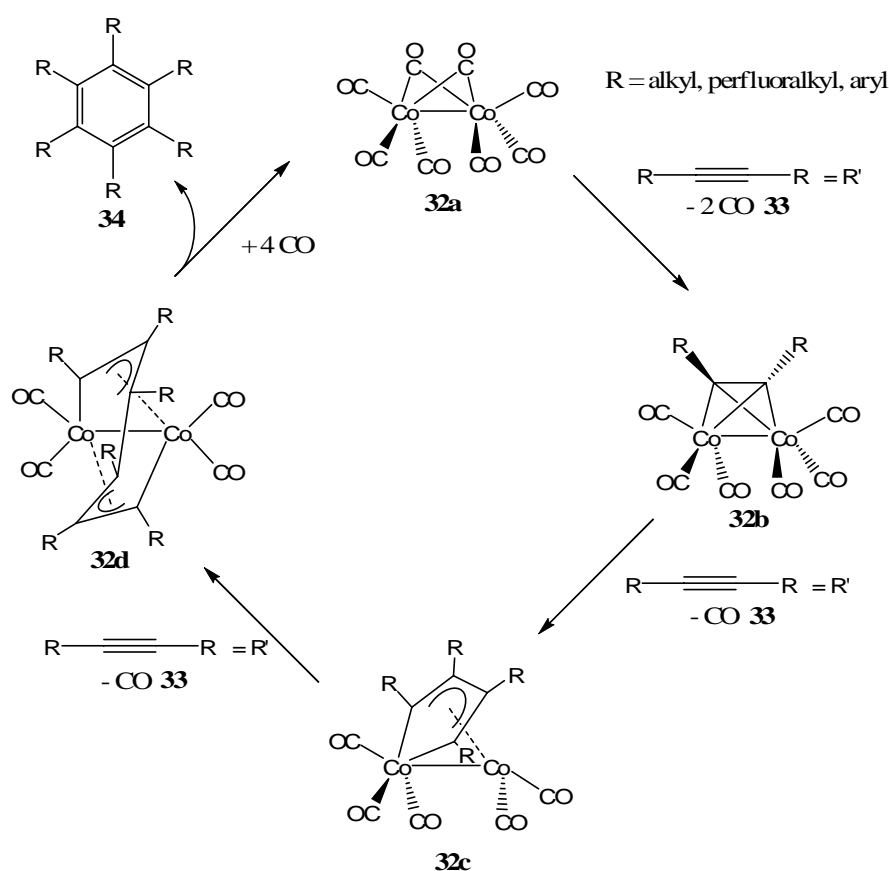
Figure 9.3 – Oxidation of terphenyl via a radicalic mechanism<sup>[150]</sup>

9.1.2 Formation of HPB derivatives with D<sub>6h</sub> symmetryScheme 9.4 – D<sub>6h</sub> HPB derivative formation

A very elegant way of synthesizing symmetrical hexaphenylbenzene consists of a cyclotrimerization of alkyne derivatives, such as **30** or **31**.<sup>[100, 103, 110, 151]</sup> Berthelot reported already in 1866 on the thermal cyclization of acetylene to benzene.<sup>[152]</sup> High temperatures (ca. 400°C) are required and a mixture of products is formed. In 1949, Reppe described the first transition metal catalyzed version of this transformation, where nickel was employed, and which under certain conditions leads to the predominant formation of cyclooctatetraene.<sup>[153]</sup> Although many transition metals, such as nickel<sup>[154]</sup> or even silicon<sup>[155]</sup> catalyze the cyclotrimerization of alkynes to arenes, Co<sub>2</sub>(CO)<sub>8</sub> and CpCo(CO)<sub>2</sub> are among the most efficient.<sup>[156]</sup> The mechanism of the Co<sub>2</sub>(CO)<sub>8</sub> mediated process has been studied extensively<sup>[157]</sup> and is shown in Figure 9.4. The first intermediate formed under mild conditions is the  $\mu$ -alkyne complex Co(CO)<sub>6</sub>(R') **32b**, containing a bridging acetylene ligand (**33** (R')). On further heating with excess acetylene, **32b** is converted to the complex Co<sub>2</sub>(CO)<sub>5</sub>(R'<sub>2</sub>) **32c**, which contains a cobalt-cyclopentadiene unit  $\pi$  bonded to the other cobalt atom. Subsequent reaction with the third acetylene gives the complex Co<sub>2</sub>(CO)<sub>4</sub>(R'<sub>3</sub>) **32d**, which has been identified by X-ray crystallography<sup>[158]</sup> and contains a bridging unit linking three alkyne units in a so-called

“fly-over” arrangement: such complexes thermally degrade to give the desired benzene derivative **34** and regenerate the active cobalt species.<sup>[159]</sup>

It is worth mentioning, that structures of the type **32c** form air-stable orange crystals, published in the case of  $\text{Co}_2(\text{CO})_5(\text{C}_8\text{H}_{12})_2$  bearing two cyclooctyne moieties<sup>[160]</sup> and may be formed at the end of the reaction, when not enough free acetylene derivative is present to accomplish the full catalytic cycle. Because of this, it is crucial to choose the amount of catalyst in the right range. We found, that by using loadings higher than 10%  $\text{Co}_2(\text{CO})_8$  the yield decreased, most probably due to the presence of large quantities of structures such as **32b** and **32c**. On the other hand using less than 6% usually led to an incomplete transformation.



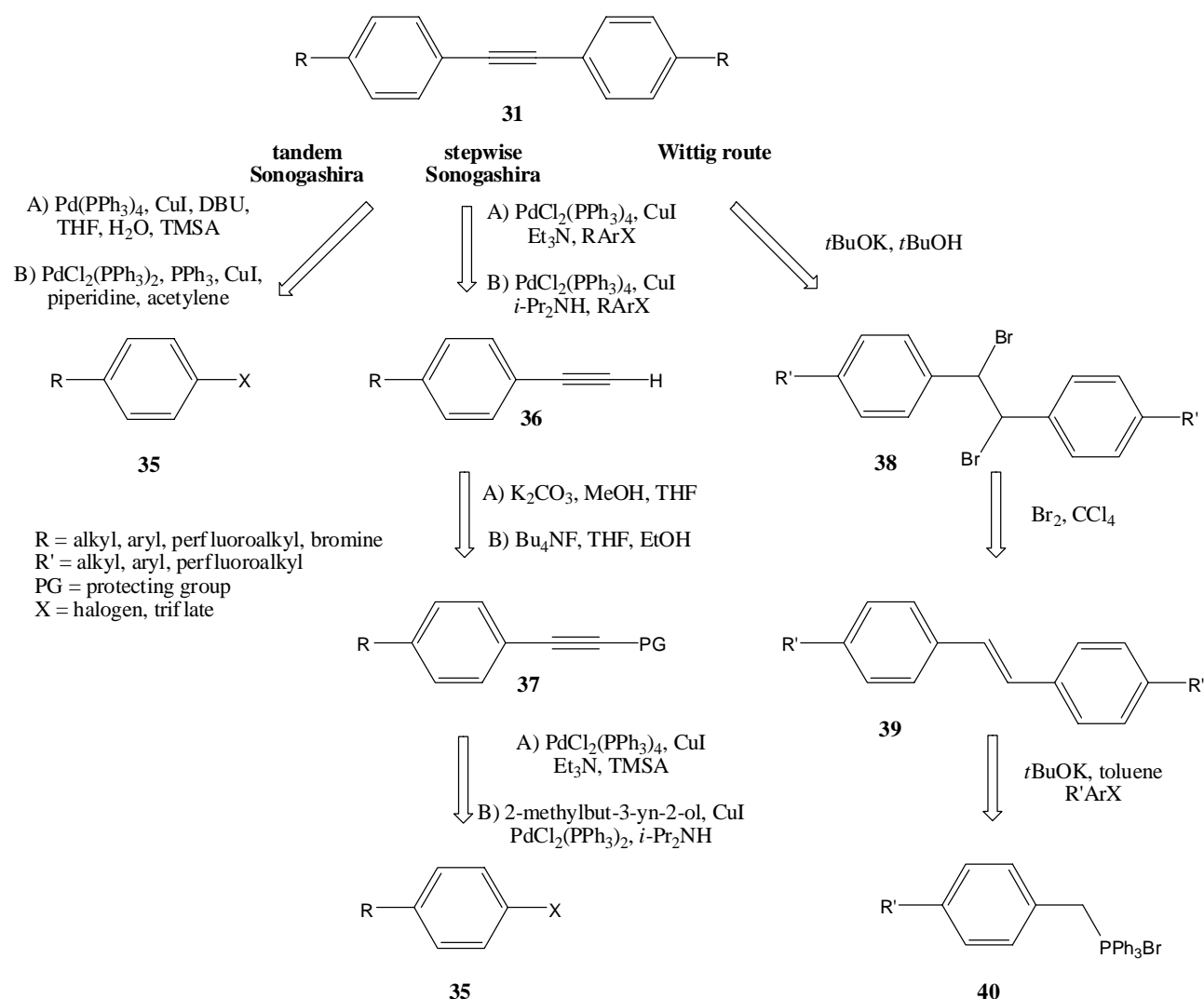
**Figure 9.4** – Mechanism of  $\text{Co}_2(\text{CO})_8$  mediated cyclotrimerization

Another, shorter possibility to produce symmetrical HBP derivatives, consist in the preparation of hexaiodo- or hexabromo HPB, which can subsequently be reacted in six fold cross-couplings to afford substituted HPB moieties. The preparation of hexahalogenated HPB **29** can either be achieved by the already investigated cyclotrimerization of halogenated tolane derivatives **30**<sup>[161]</sup> or by reacting commercially available hexaphenylbenzene with neat bromine.<sup>[110]</sup> Nevertheless, the problematic part remains by the six fold cross-coupling, working well by using aryl-aryl Suzuki couplings,<sup>[110]</sup> Grignard reactions with benzophenone<sup>[162]</sup> or by Sonogashira cross coupling reactions.<sup>[163]</sup> Unfortunately aryl-alkyl couplings are less favourable, but exclusively needed during this

work. Moreover they are reported only for Sonogashira reactions.<sup>[104]</sup> Furthermore these reactions turned out to be even more hindering for the preparation of HPB derivatives bearing perfluoroalkylated side chains, due to severe solubility problems.

As discussed in the previous section the most favourable way to prepare perfluoroalkylated HPB derivatives is by cyclotrimerization of the appropriate tolane derivatives. There are mainly three different strategies to prepare the desired bisarylethyne, or the so called tolane derivative bearing appropriate substituents: *i*) direct tandem or one-pot Sonogashira coupling of two halogenated aryl derivatives; *ii*) stepwise Sonogashira coupling of two halogenated aryl derivatives; *iii*) Wittig reaction of adequate phosphonium salts followed by bromination and dehydrobromination.

### 9.1.3 Formation of substituted tolane derivatives



**Scheme 9.5** – Different alternatives to form a substituted tolane derivative. A and B denotes different possible conditions

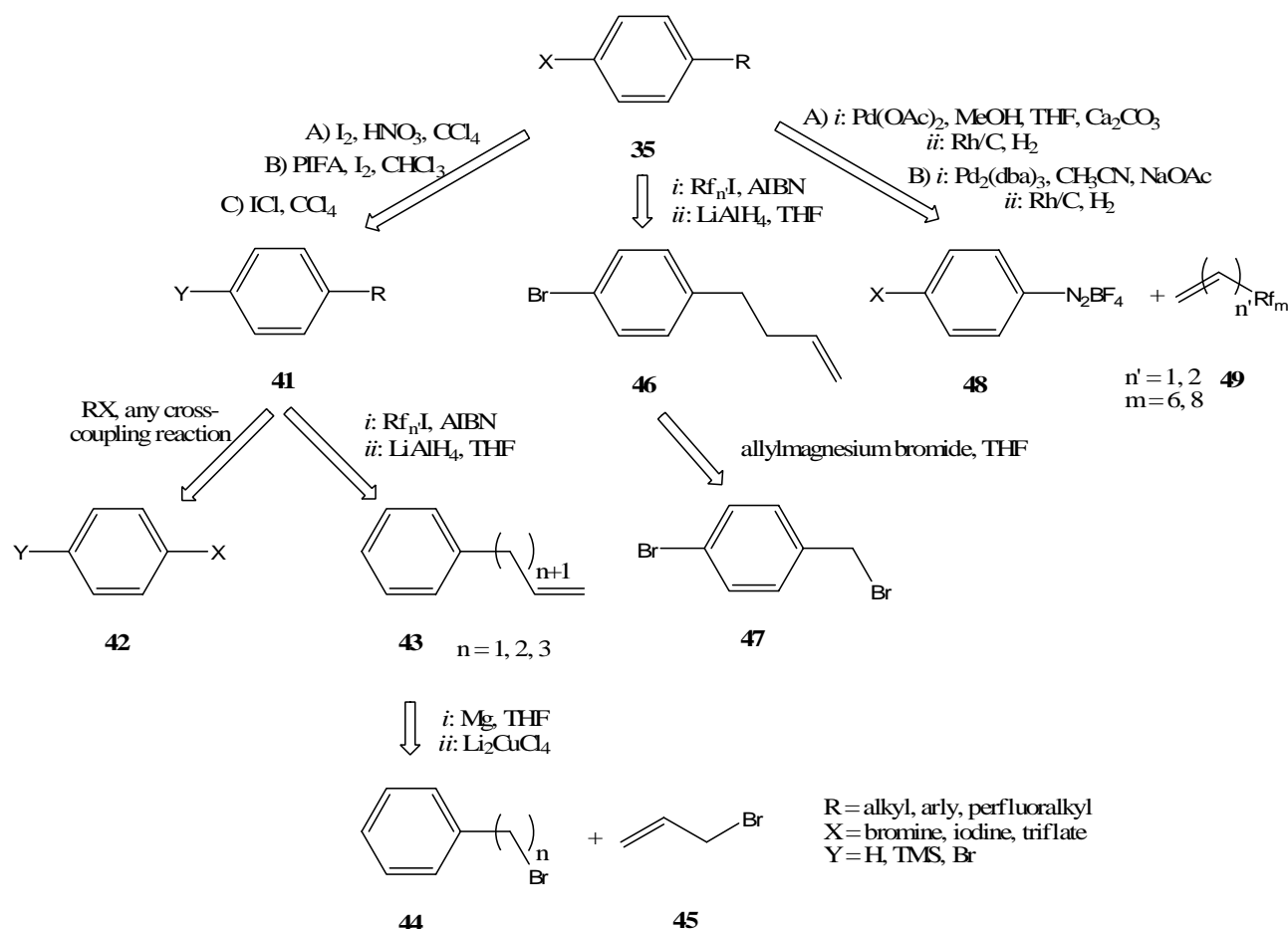
The shortest access is obviously by applying one-pot Sonogashira conditions, which involves either trimethylsilyl acetylene,<sup>[164]</sup> 2-methyl-3-butyne-2-ol<sup>[165]</sup> or acetylene<sup>[166]</sup> to install the triple bond. It has to be noted that by using one-pot conditions the risk of homocoupling of free arylacetylene derivatives rises, even though normally homocoupling occurs only in the presence of oxygen<sup>[167]</sup> or by applying adapted conditions incorporating chloroacetone as oxidant for example.<sup>[168]</sup> It is worth noting, that even unsymmetrical bisarylethynes may be produced in high purity and yield in one-pot reactions, by adding first the palladium catalyst, CuI, base, solvent, TMSA and the appropriate halogenaryl. After several hours of reaction the formed TMS protected arylacetylene is deprotected *in situ* by the addition of DBU and water. At the same time a second, different arylhalogenide is added which terminates the cross-coupling.<sup>[164]</sup> By applying these conditions a wide range of different bisarylethynes, bearing a variety of different functional groups, was reported.

A similar, but longer strategy consist of a stepwise Sonogashira reaction, where in principle the above mentioned reaction steps are performed identically, but with additional isolation of the intermediate products. The literature offers a large number of different approaches for the three step synthesis, allowing a variety of functionalities and protecting groups.<sup>[168, 169]</sup> The disadvantage of this route lies in the general lower yield compared to the tandem approach and the additional time needed for the purification.

A third, completely different approach is based on the halogenation and subsequent dehalogenation of appropriate stilbene derivatives **39**. Symmetrically or unsymmetrical substituted stilbene derivatives are easiest accessible by a Wittig or a Horner-Emmons reaction, respectively.<sup>[170]</sup> Generally the dibrominated derivative **38** is formed in nearly quantitative yield and can be dehydrobrominated by *t*-BuOK to establish the triple bond.<sup>[112, 171]</sup>

#### 9.1.4 Formation of perfluoroalkylated halogenaryl derivatives

The formation of substituted aryl derivatives may be performed by a large variety of different pathways, out of which the ones used during this thesis are presented as an overview in Scheme 9.6. A very effective way was found by using a Heck reaction of an appropriated alkene **49** with a halogenated aryldiazonium salt **48** which proved to be very reactive.<sup>[172]</sup> Nevertheless not every substrate was found to afford the desired product **35** in high yield as with an increased alkyl part (longer than butene) the reaction produced a considerable amount of an *exo*-isomer (compare to chapter 11.3.1).

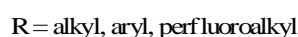


**Scheme 9.6** – Different possibilities to prepare perfluoroalkylated halogenaryl derivatives

Another elegant approach is the formation of halogenated derivatives such as **46** bearing the desired side chain with a terminal alkene onto which the desired perfluorinated part may be added.<sup>[173]</sup> The same is possible by inserting the *para*-halogen latter, as for the formation of **41**. Here, the disadvantage lies in the selective insertion of the halogen into the *para* position of the aromatic core. As last approach a Kumada cross-coupling of the desired brominated lateral chain on 4-bromo-1-iodobenzene for example may be cited which usually affords the desired product in good yield and selectivity.<sup>[174]</sup>

#### 9.1.5 Formation of HPB derivatives with $D_{3h}$ symmetry

Desymmetrisation is a very effective and important concept of organic chemistry which covers not only the loss of symmetry through the introduction of an asymmetric centre into a molecule, but also a reduction of symmetry due to constitutional modifications. This loss of symmetry affects the chemical and material properties of the resulting compound, as different parts of the molecule can interact differently with other molecules or with surfaces.

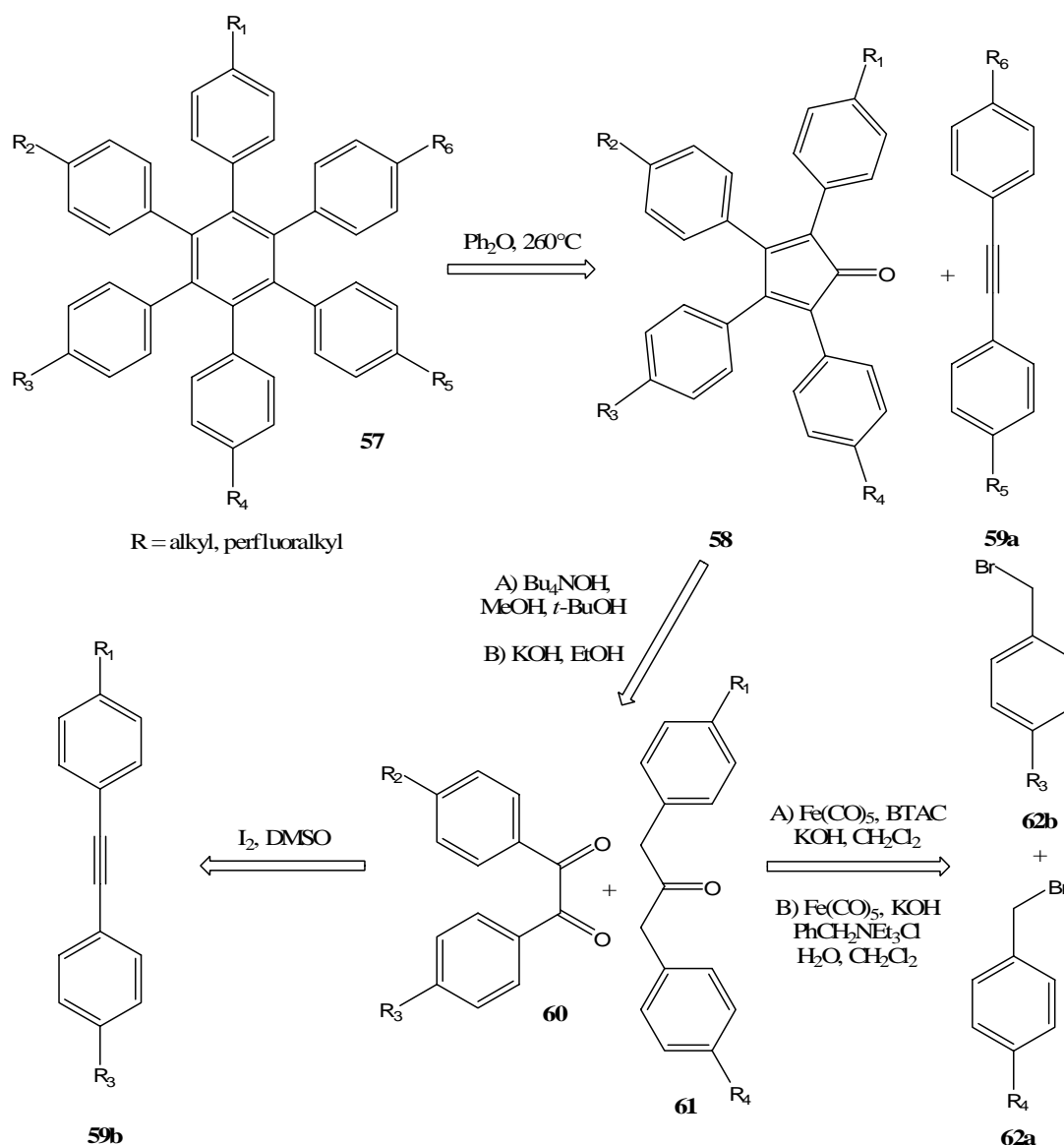


**Scheme 9.7** – Preparation of  $D_{3h}$ -HPB derivatives

The final step for the preparation of such derivatives consists in a three fold cross-coupling (Suzuki, Sonogashira or Kumada) on the triiodo derivative **51**.<sup>[138, 175]</sup> The triiodo derivative **51** is most favourably prepared by either a trifluoromethylsulfonic-acid mediated trimerization of 2-bromoacetophenone (**53**)<sup>[138]</sup> followed by a Suzuki reaction<sup>[175]</sup> or by two subsequent Suzuki cross-couplings starting from 1-bromo-2-iodobenzene and 3-(trimethylsilyl)phenylboronic acid (**56**).<sup>[120]</sup> Replacement of the three TMS groups is done very effectively using ICl.<sup>[175]</sup>

## 9.1.6 Formation of completely desymmetrized HPB derivatives

A slightly more elaborated strategy is needed for completely desymmetrized HPB derivatives, where all six substituents may be varied independently. The last step consists of a Diels-Alder addition<sup>[175, 176]</sup> between a suitable tolane **59a** or **b** derivative and a cyclopentadienone **58**, which itself is prepared by a two fold Knoevenagel condensation<sup>[112]</sup> of diarylacetone **61** with a substituted benzil **60** derivative. The disubstituted diarylacetone **61** is obtained by the coupling of appropriate substituted 4-bromobenzyl derivatives **62a** and **b** with iron pentacarbonyl,<sup>[177]</sup> affording evidently a mixture of three products ( $R_1/R_1$ , 25%;  $R_1/R_2$ , 50%;  $R_2/R_2$  25%) which have to be separated. Benzil derivatives are favourably prepared by oxidation of an appropriate tolane **59a** or **b** derivative with iodine and DMSO.<sup>[178]</sup> It has to be pointed out, that the overall yield varies from moderate to good, depending on the nature of the substituents.

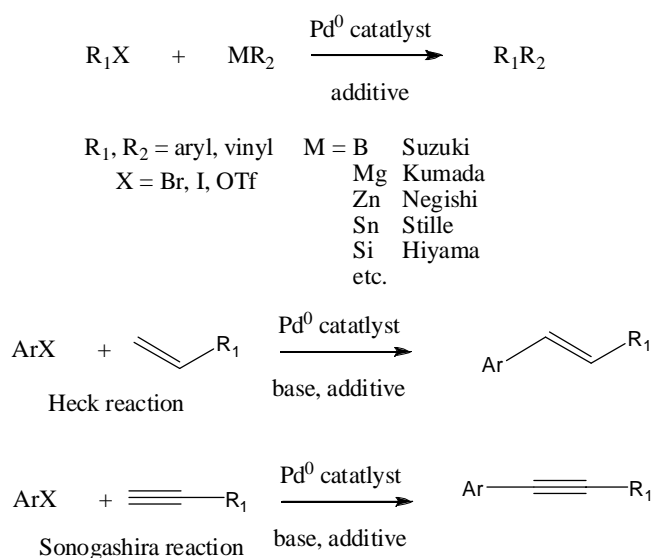


Scheme 9.8 – Preparation of desymmetrized HPB derivatives



## 9.2 Introduction to applied C-C cross coupling reactions

During the final quarter of the twentieth century, palladium catalysts emerged as extremely powerful tools for the construction of carbon-carbon, as well as carbon-heteroatom, bonds. An overview of the most used cross coupling reaction is given in Figure 9.5.<sup>[179]</sup> Until recently, nearly all reports of palladium-catalyzed couplings described the use of organic bromides, iodides, and triflates as substrates. Organic chlorides were noticeably uncommon partners, despite the fact that, among the halides, chlorides are the most useful class of substrates, because of their lower cost and the wider diversity of available compounds. During the past years the number of publications increased reporting on mild conditions which allow even the reaction with chlorides.<sup>[180]</sup> Usually such conditions need the previous preparation of elaborated non-commercial ligands.



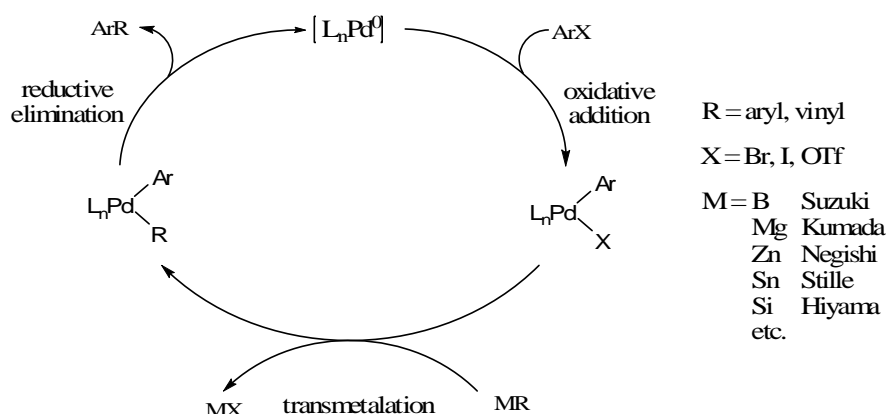
**Figure 9.5** – Overview of the most important cross-coupling reactions

### 9.2.1 Kumada, Suzuki cross-couplings

As the mechanism of the Suzuki, Kumada, Negishi, Stille and Hiyama cross coupling are very similar they are treated together. Furthermore only the Suzuki<sup>[181]</sup> and the Kumada<sup>[180, 182]</sup> coupling is discussed in this paragraph in more detail, as the other cross couplings were not used in this work and are mentioned only for completeness. The palladium-catalyzed cross-coupling of aryl and vinyl halides/triflates with organometallic reagents serve as a straightforward and powerful method for the formation of C-C bonds, as shown in Figure 9.6. The R<sub>2</sub> group of the organometallic reagent can be any out of a variety of saturated or unsaturated groups, for example, aryl or alkyl. Mostly magnesium, tin and zinc reagents are sufficiently reactive to undergo transmetalation with palladium without the need for an additive. Boron and silicon reagents, on the other hand, are usually reluctant to transmetalate in the absence of an activator. As a consequence, Suzuki and Hiyama

cross-couplings are typically carried out in the presence of an additive, the role of which is to form a higher valent, more reactive complex.

Among palladium-catalyzed cross-coupling processes, the Suzuki reaction of aryl and vinyl halides/triflates with boronic acids is emerging as a favourite. Nevertheless it has to be noted, that during this work, the Kumada cross-coupling reaction was used preferentially. One of the reasons is certainly the non existence of functional groups in the target molecules used herein, incompatible with a Grignard reagent, as this is often the limiting factor of a Kumada cross-coupling.

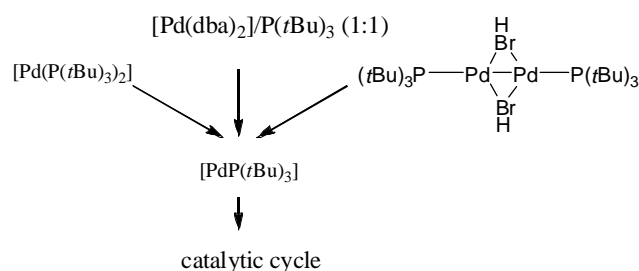


**Figure 9.6** – General accepted mechanism of the above mentioned cross-coupling reactions

The Suzuki and Kumada coupling reactions are generally thought to proceed through a mechanism that involves three distinctive steps:<sup>[183]</sup> *i*) first, an aryl halide reacts with the palladium(0) centre through an oxidative addition reaction. Sterically demanding ligands have the ability to stabilize low-coordination palladium complexes (in particular monoligated species) which are more reactive due to their low electron count. On the other hand, electron donating ligands generate an electron-rich metal complex which undergoes faster oxidative addition reactions; *ii*) this is followed by a transmetalation reaction to yield a palladium(II) complex which contains the two moieties to be coupled; *iii*) the final step is the reductive elimination of the product with the concomitant regeneration of the active palladium (0) catalyst. It is generally accepted that this step is faster when the palladium is coordinated to electron withdrawing and sterically demanding ligands. It is often found that in this mechanism, the oxidative addition is the rate-limiting step, above all if aryl chlorides and unactivated aryl bromides are used.

In the majority of all cases, the catalytically active palladium species has to be formed *in situ* during the reaction, as normally stable palladium(II) precursors of the catalytically active species are used. Several authors have shown that even when the same phosphine or carbene ligand is used in a particular reaction, the source of palladium employed has an important influence on the catalytic rates. Their investigations strongly suggest that the active species  $[\text{PdL}]$  is formed by any of their tested  $[\text{PdL}_2]$  precursors, as shown in Figure 9.7 for the example of  $[\text{PdP}(t\text{Bu})_3]$  as active species.<sup>[184]</sup> Fur-

the tetrakis(triphenylphosphine)palladium(0), which exists in an equilibrium with tris(triphenylphosphine)palladium(0) and free triphenylphosphine in solution, is frequently employed. The loss of a second phosphine ligand leads to the catalytically active bis(triphenylphosphine)palladium(0). However, palladium(II) complexes such as bis(triphenylphosphine)palladium dichloride or palladium acetate, which are easily reduced in the reaction medium, are more commonly employed for convenience, as they are inherently stable towards air.

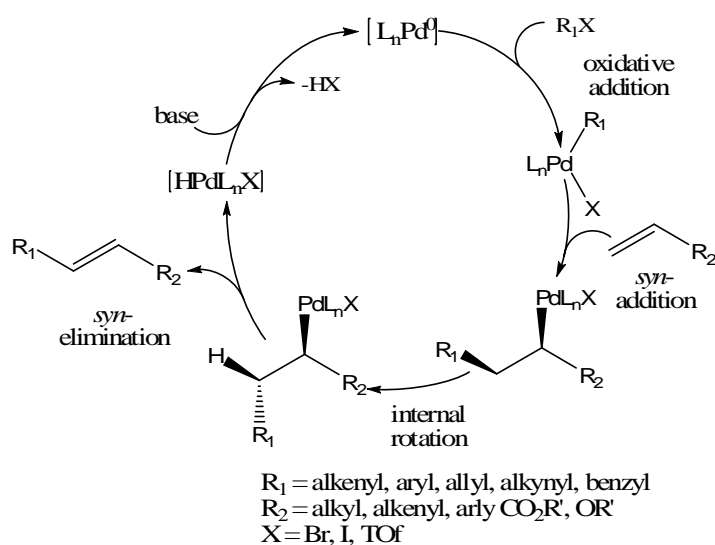


**Figure 9.7** – Formation of the catalytically active Pd<sup>0</sup> species

The possibility to choose the adequate catalyst and additive has increased over the past years, as several groups have proposed new palladium species that show high catalytic activity in cross-coupling reactions. Standard palladium or other transition metal catalysts for the Suzuki and Kumada reactions consist of: Pd<sub>2</sub>(dba)<sub>3</sub> / PPh<sub>3</sub>.<sup>[185]</sup> CpFe(PiPr<sub>2</sub>)<sub>2</sub>PdCl<sub>2</sub> / K<sub>2</sub>CO<sub>3</sub>,<sup>[186]</sup> Fe(acac)<sub>3</sub>,<sup>[187]</sup> Ni(dppp)Cl<sub>2</sub>,<sup>[188]</sup> [Pd(IPr)Cl<sub>2</sub>]<sub>2</sub> / KOtAm<sup>[189]</sup> mentioning only few examples out of many.

### 9.2.2 Heck cross-couplings

The mechanism of the Heck reaction is similar to the accepted mechanism for the Kumada and Suzuki reaction. Nevertheless is the mechanism shown in Figure 9.8 for clarity.



**Figure 9.8** – General accepted mechanism of the Heck cross-coupling

Analogous to the previously discussed mechanism, a coordinatively unsaturated 14-electron palladium(0) complex, usually coordinated with weak donor ligands, has meanwhile been proved to be the catalytically active species, which is mostly generated *in situ*.<sup>[190]</sup>

The general accepted mechanism of the Heck reaction consists of five steps:<sup>[191]</sup> *i*) in the first step of the sequence a haloalkane or haloarene is commonly assumed to add oxidative to the coordinatively unsaturated palladium(0) complex, generating an arylpalladium(II) complex;<sup>[192]</sup> *ii*) as the electrophilicity of this complex is enhanced, it more readily accepts an alkene molecule in its coordination sphere, probably by exchange for another ligand. Subsequent *syn*-insertion of the  $\sigma$ -aryl-palladium bond into the C-C double bond occurs to yield a  $\sigma$ -( $\beta$ -aryl)palladium complex *via* a four-centred transition state; *iii*) the  $\beta$ -hydride elimination of the next step can occur only after an internal rotation around the former double bond, as it requires at least one  $\beta$ -hydrogen to be oriented *synperiplanar* with respect to the halopalladium residue;<sup>[193]</sup> *iv*) the subsequent *syn*-elimination yielding an alkene and a hydridopalladium halide is reversible, however, and therefore the thermodynamically more stable (*E*)-alkene is generally obtained when the coupling reaction is performed with a terminal alkene; *v*) reductive elimination of HX from the hydridopalladium halide, assisted by the added base, regenerates the active catalyst and thereby completes the catalytic cycle; it has to be noted that this mechanism has not been proven in all details, and especially the rate-determining step has not been identified unequivocally. Frequently, the oxidative addition has been assumed to be rate-determining, however, some doubt has been cast on this hypothesis as well.

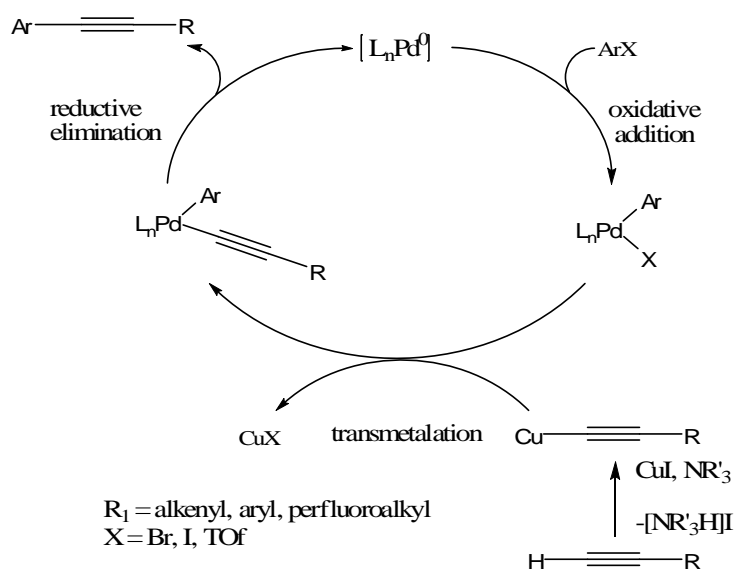
Commercially available palladium compounds in the presence of various ligands were frequently used as catalyst. The most commonly used are the following: Pd(OAc)<sub>2</sub>,<sup>[194]</sup> PdCl<sub>2</sub>,<sup>[195]</sup> Pd<sub>2</sub>(dba)<sub>3</sub>,<sup>[196]</sup> Pd(PPh<sub>3</sub>)<sub>4</sub>,<sup>[197]</sup> Pd(PPh<sub>3</sub>)<sub>2</sub>Cl<sub>2</sub>,<sup>[198]</sup> together with solvents such as DMF, DMA, CH<sub>3</sub>CN, DMSO and MeOH.

### 9.2.3 Sonogashira cross-couplings

Over the past few decades, the Pd-catalyzed alkynylation has emerged as one of the most general and reliable method for the synthesis of alkynes.<sup>[199]</sup> Currently, the most widely used is a hybrid of the Cu-promoted Castro-Stephens<sup>[200]</sup> reaction and the alkyne version of the Heck reaction, which is known as the Sonogashira reaction<sup>[201]</sup> originally reported in 1975.<sup>[202]</sup>

The standard three-step catalytic cycle has been proposed already in the 1970s for the Sonogashira reactions and is shown in Figure 9.9 consisting of the following steps: *i*) oxidative addition of a palladium(0) complex with an organic electrophile, identical to the oxidative addition discussed in the previous sections for the Kumada, Suzuki and Heck cross-couplings; *ii*) transmetalation to generate the diorganopalladium derivative. It has to be noted that the transmetalation step occurs from an alkenyl-copper species, formed upon treatment of the alkyne with an amine and copper(I)iodide.<sup>[156d]</sup>

As mentioned earlier, the stoichiometric amount of copper has been used in the Castro-Stephens reaction without the use of a palladium catalyst, while only a catalytic amount of copper is used in the Sonogashira reaction; *iii*) reductive elimination which expels the cross-coupled alkyne and regenerates simultaneously the catalytic active  $\text{Pd}^0$  species. Commonly used catalysts are for example  $\text{Pd}(\text{OAc})_2 / \text{CuI} / \text{IMes}$ ,<sup>[203]</sup>  $\text{Pd}(\text{PPh}_3)_2\text{Cl}_2 / \text{Net}_3 / \text{CuI}$ <sup>[204]</sup> or  $\text{Pd}(\text{PPh}_3)_4 / \text{CuI}$ .<sup>[199]</sup>



**Figure 9.9** – Generally accepted mechanism of the Sonogashira cross-coupling



## 10 HBC carrying linear alkyl / perfluoralkyl side chains

Despite that only few synthetic strategies are applicable for the preparation of perfluoroalkylated HBC derivatives any minor change of the perfluoro / alkyl ratio influenced the properties of the obtained derivative tremendously. Because of that the performed syntheses are presented in groups of similar products or reaction pathways.

### 10.1 Introduction

As no computational data is available concerning the influence arising from the nature of the side chain of substituted HBC derivatives a systematic HBC-Rf<sub>n,m</sub> series has been synthesized, carrying side chains with different perfluoro / alkyl ratios, in order to investigate their exerted influence in the  $\pi$ - $\pi$  stacking behaviour. It has to be noted that not only the perfluoro / alkyl ratio plays an important role for  $\pi$ -aggregation but also the tremendous sterical and solubility change exerted by varying the perfluoro / alkyl ratio. Table 10.1 summarizes the successfully prepared HBC derivatives bearing all linear perfluoroalkylated side chains.

As described earlier<sup>[130]</sup> the minimum spacer between the HBC core and the perfluorinated part of the side chain consists of two methylene groups in order to shield sufficiently the electron withdrawing effect of the fluorines.

**Table 10.1** – Synthesized HBC-Rf<sub>n,m</sub> derivatives with their respective perfluoro / alkyl ratio (perfluorinated carbons divided by purely alkyl carbons) of the side chains

<b>m \ n</b>	<b>2</b>	<b>3</b>	<b>4</b>	<b>5</b>	<b>6</b>	<b>8</b>
<b>4</b>			1			0.5
<b>6</b>	3	2	1.5	1.2	1 <sup>a</sup>	0.75
<b>8</b>	4 <sup>a</sup>	2.67	2	1.6	1.34	1
<b>10</b>			2.5			

<sup>a</sup> the synthesis of these two derivatives was carried out by B. Alameddine and is described elsewhere<sup>[130]</sup>

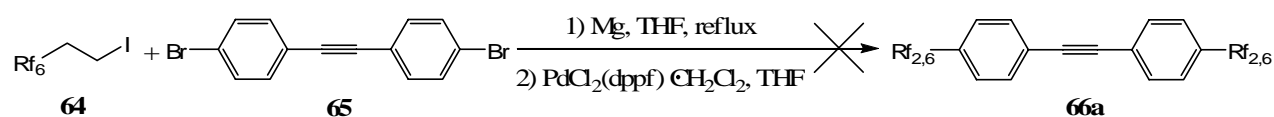
## 10.2 HBC-Rf<sub>2,6</sub> and HBC-Rf<sub>2,8</sub>

*Synthetic strategy:* The desired HBC derivative HBC-Rf<sub>2,6</sub><sup>[205]</sup> **63a** was prepared using as key step the Heck reaction of vinylperfluorohexane and 4-bromobenzendiazonium tetrafluoroborate with a subsequent tandem Sonogashira cross-coupling.

### 10.2.1 Attempted direct synthesis of Tol-Rf<sub>2,6</sub>

The first two HBC derivatives synthesized were HBC-Rf<sub>2,6</sub> **63a** and HBC-Rf<sub>2,8</sub> **63b**, bearing each two CH<sub>2</sub> spacers in combination with six and eight perfluorinated carbon atoms respectively, affording a side chain with a total length of eight or ten carbon atoms. The synthesis of HBC-Rf<sub>2,8</sub> **63b** has been performed by B. Alameddine and is described elsewhere.<sup>[128, 130]</sup>

The shortest way to synthesize the needed tolane derivative Tol-(Rf<sub>2,6</sub>)<sub>2</sub> requires a two fold Kumada cross coupling reaction as key step. The Grignard derivative of 1*H*,1*H*,2*H*,2*H*-perfluorooctyliodide **64** was prepared by heating freshly activated magnesium turnings together with **64** in dry THF for several hours. During this period the magnesium was clearly consumed, underlining the formation of the desired Grignard derivative<sup>[206]</sup> which was then added to the 4,4'-dibromotolane **65** and the palladium catalyst. Unfortunately the desired tolane derivative Tol-Rf<sub>2,6</sub> was not present at all after the work up. Probably the electron withdrawing effect of the perfluorinated Grignard reagent hindered the transmetalation step of the cross coupling reaction as the Kumada cross-coupling yielded the desired product only by using a minimum spacer of 4 aliphatic carbon atoms, as shown in section 10.4.3. Because of this, the Kumada cross coupling reaction sequence was not further investigated, as other, more promising alternatives exist.



**Scheme 10.1** – Attempted direct synthesis of tolane **66a**

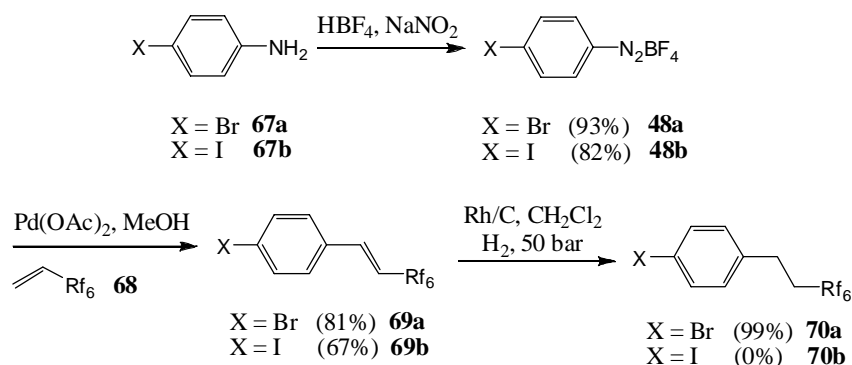
### 10.2.2 X-Ph-Rf<sub>2,6</sub>

Another way to form the strategic bond between an aryl and a semi-perfluorinated chain is the use of the Heck reaction, as shown in Scheme 10.2. Because the difficulties encountered by performing a two-fold Heck reaction onto a 4,4'-bromotolane **65** or 4,4'-diazotolane **81** (c.f. chapter 10.3.2), a one-fold Heck reaction was performed onto halogenated benzenediazonium salts.<sup>[172a]</sup> The preparation of halogenated diazonium salts from bromo- or iodoaniline **66a** and **b** worked<sup>[172b]</sup> for both derivatives well. The obtained salts were crystallized from methanol / ether to afford white crystals which can be stored under inert atmosphere and in a freezer for years without decomposition.



Subsequent Heck reaction of the diazonium salts with 1*H*,1*H*,2*H*-perfluorooctane **68**, in a mixture of methanol and THF, the later for solubility reasons, afforded the desired cross-coupled products **69a** and **69b** in fairly good yields. The iodinated derivative **69b** was provided in lower yield, as the bis-coupled product was formed too in about 15% yield and had to be removed by column chromatography. The mechanism of the Heck reaction was discussed earlier (c.f. chapter 9.2.2) together with the most widely used ligands, leaving groups and addends. For cross-couplings using perfluorinated derivatives it was found that the reaction proceeds only reliably by using a diazonium salt derivative as aryl halogenides are probably not reactive enough. Furthermore Pd(OAc)<sub>2</sub> proved to be useful by coupling the very reactive vinyl-perfluoroderivative **68**, but proved to be less performing by coupling allyl derivatives **75**, where Pd<sub>2</sub>(dba)<sub>3</sub><sup>[207]</sup> was used instead.

Hydrogenation of the double bond without dehalogenation of the aromatic core can not be achieved by using a palladium catalyst but was realised by using less reactive rhodium on carbon<sup>[172a]</sup> at room temperature under 50-60 bar of hydrogen. Brominated precursors yielded the saturated derivative in quantitative yield after one night of reaction, whereas iodinated precursors furnished a mixture of four compounds: starting material **69b**, hydrogenated derivative **70b**, dehalogenated saturated and unsaturated derivatives. It seemed that the iodine on the aromatic core is too reactive and was cleaved off during the reaction and on top poisoned the catalyst, which could explain the presence of starting material after the reaction.



**Scheme 10.2** – Formation of halogenaryl derivatives bearing the desired perfluoroalkylated side chain

### 10.2.3 HPB-Rf<sub>2,6</sub>

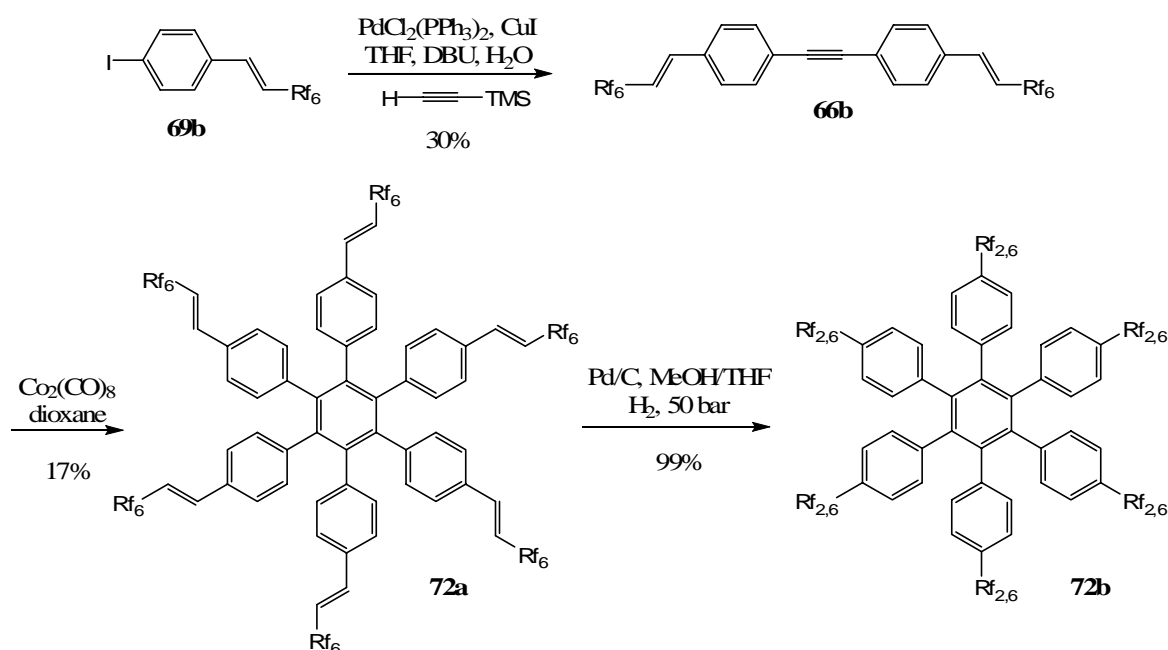
The formation of the desired HPB derivative **62b** was performed in two different ways using the two available precursors: the iodinated aryl derivative **69b** bearing a double bond in the side chain; the brominated saturated aryl derivative **70a**.

Starting with **69b**, a modified two-fold Sonogashira cross-coupling was applied. A wide range of catalysts, such as PdCl<sub>2</sub>(PPh<sub>3</sub>)<sub>2</sub> or PdCl<sub>2</sub>dppf as Pd<sup>2+</sup> examples or Pd<sub>2</sub>(dba)<sub>3</sub> (this catalyst needs 10 Mol% of PPh<sub>3</sub>) or Pd(PPh<sub>3</sub>)<sub>4</sub> as Pd<sup>0</sup> examples furnishes nearly the same result.<sup>[164]</sup> The same is true

for a variety of solvents, as for example benzene, toluene, dioxane, THF, DMF or acetonitrile, and bases, such as DBU, TEA, DABCO, DBN. Generally the formation of tolane (bisarylethynylenes) derivatives requires often systematic silane protection/deprotection of terminal ethynylenes<sup>[169b]</sup> as discussed earlier (c.f. chapter 9.1.3). Although a variety of strategies for *in situ* base-mediated deprotection and cross coupling have been reported, all these methods require prior installation of protecting groups or supplementary reagents.<sup>[165, 208]</sup> Only few exceptions of two-fold Sonogashira couplings were found which use continuous acetylene purging through the reaction mixture.<sup>[166d-e]</sup>

An elegant way was found in a newly reported protocol, where the utilization of an amidine base, such as DBU, and the presence of substoichiometric amounts of water were central. Most probably, after proceeding through the commonly accepted cross-coupling chemistry, the silane-protected arylethynylene converges with  $\text{Cu}^+$  and a water/DBU salt, resulting in protodesilylation to yield the terminal ethynylene derivative.<sup>[209]</sup>

Purification of the crude tolane **66b** was performed by filtration over a silica gel plug under reduced pressure followed by recrystallization from ether / ethanol. The solubility of tolane **66b** was found to be high enough for silica gel filtration, but it is worth mentioning that with tolanes bearing eight perfluorinated carbon atoms in their side chain, this purification procedure does not work at all.



Scheme 10.3 – Four step synthesis of HPB **72b**

Cyclotrimerization afforded the HPB derivative **72a** only in very moderate yield probably due to some interferences of the cobalt catalyst ( $\text{Co}_2(\text{CO})_8$ ) with the double bond which is known to participate in the Pauson-Khand reaction.<sup>[210]</sup> Hydrogenation of **72a** to **72b** was performed by using

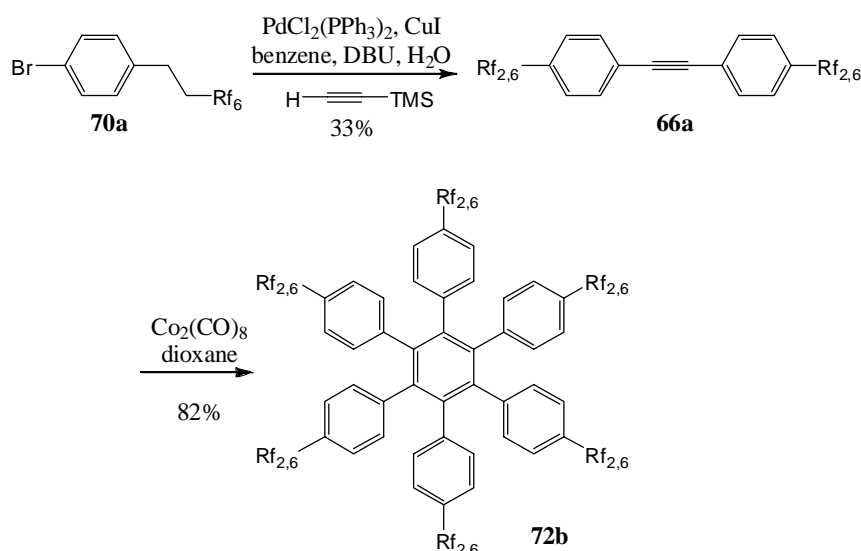
Pd/C as catalyst and a mixture of MeOH/THF as solvent. The choice of solvent was crucial for the success of the reaction, as shown in Table 10.2, where all attempts are summarized.

**Table 10.2** – Summary for the different conditions used for the hydrogenation of **72a**

Entry	Subst.	Catalyst [mol%]	Solvents [mL]	H <sub>2</sub> [bar]	Temp. [°C]	Time [h]	<b>72b</b> [%Yld]
1	<b>72a</b>	Pd/C (10)	EtOH (2) CH <sub>2</sub> Cl <sub>2</sub> (3)	2	r.t.	25	- <sup>a</sup>
2	<b>72a</b>	Pd/C (10)	EtOH (2) EtAc (1)	3	r.t.	3	- <sup>a</sup>
3	<b>72a</b>	Pd/C (10)	MeOH (1) THF (1)	3	r.t.	6	99

<sup>a</sup> quantitative recovery of **72a**

Another, shorter route to prepare HPB **72b** is by using the brominated saturated starting material **70a** instead of the iodinated unsaturated **69b**.



**Scheme 10.4** – Three step synthesis of HBP **72b**

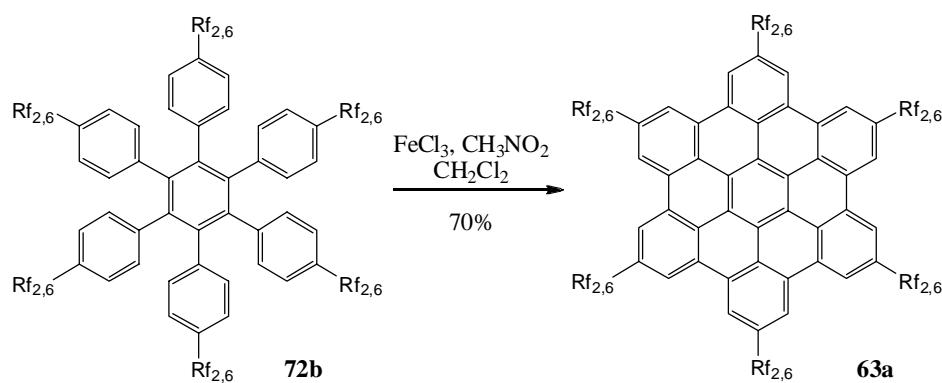
As listed in Table 10.3 several attempts of the one-pot Sonogashira cross-coupling were carried out in order to synthesize tolane **66a**. The yields of the reaction were generally around 30%. Furthermore, each time a considerable amount of starting material was found in combination with the desired tolane. It has not yet been clarified why the reaction did not run to completion, as even by doubling the reaction time (entry 3) the yield could not be improved. Moreover the literature offers by far higher yields for similar reactions, using alkyl instead of perfluoroalkyl substrates.<sup>[164]</sup> Cyclotrimerization in contrary yielded the desired HPB **72b** in good yield as white solid.

**Table 10.3** – Summary of all performed Sonogashira attempts to prepare tolane **66a**

Entry	Subst.	Reagent [eq]	Catalyst [mol%]	Additive [eq]	Solvent	Temp. [°C]	Time [d]	66a [%Yld]
1	<b>70a</b>	TMSA (0.5)	PdCl <sub>2</sub> (PPh <sub>3</sub> ) <sub>2</sub> (6) CuI (10)	DBU (6) H <sub>2</sub> O (0.4)	benzene <sup>a</sup>	80	3	33
2	<b>70a</b>	TMSA (0.5)	PdCl <sub>2</sub> (PPh <sub>3</sub> ) <sub>2</sub> (6) CuI (10)	DBU (6) H <sub>2</sub> O (0.4)	benzene	80	3	12
3	<b>70a</b>	TMSA (0.5)	PdCl <sub>2</sub> (PPh <sub>3</sub> ) <sub>2</sub> (6) CuI (10)	DBU (6) H <sub>2</sub> O (0.4)	benzene	80	7	25
4	<b>70a</b>	TMSA (0.5)	PdCl <sub>2</sub> (PPh <sub>3</sub> ) <sub>2</sub> (6) CuI (10)	DBU (6) H <sub>2</sub> O (0.4)	benzene	80	4	32

<sup>a</sup> 0.2 M solution of **70a**10.2.4 HBC-Rf<sub>2,6</sub>

For the cyclodehydrogenation of HPB derivatives bearing partially perfluoroalkylated side chains it proved to be sufficient to use the mild FeCl<sub>3</sub> conditions.<sup>[130]</sup> But it is worth mentioning that for all successful oxidations, a slightly modified protocol had to be adopted: normally, the HPB is dissolved in dichloromethane and a solution of FeCl<sub>3</sub> in nitromethane is added at room temperature followed by heating to 40 °C for 15 minutes to 1 hour. This procedure yielded mostly unreacted starting material together with traces of the desired HBC compound even when extending the reaction time to days. By injecting the FeCl<sub>3</sub>-nitromethane solution slowly (2-3 hours) into the warm (35°C - 45°C) dichloromethane-HBC solution, however, moderate to good HBC yields were obtained after several hours of reaction. Furthermore it proved to be crucial to bubble the reaction mixture with argon through a Teflon capillary during all the time in order to remove the formed HCl. Moreover the addition of HFB as co-solvent afforded higher yields when very insoluble derivatives (short alkyl spacers in combination with long perfluorinated tails) were used. Afterwards the reaction medium was quenched by the addition of methanol (typically half of the amount of dichloromethane) which completed the precipitation of the desired HBC derivative, which was collected by suction filtration over Millipore<sup>®</sup> under reduced pressure. The obtained black compound was then purified by sonication in different organic solvents (methanol, pentane, ether, THF, dichloromethane, nitromethane etc.) and by precipitation from BTF solutions by adding ether, and was finally obtained as yellow powder, soluble in highly fluorinated solvents, such as HFB, BTF, OFT. Characterization was severely hampered by the low solubility, even in HFB. Because of that only <sup>1</sup>H-NMR, UV, fluorescence and MALDI spectra could be collected.

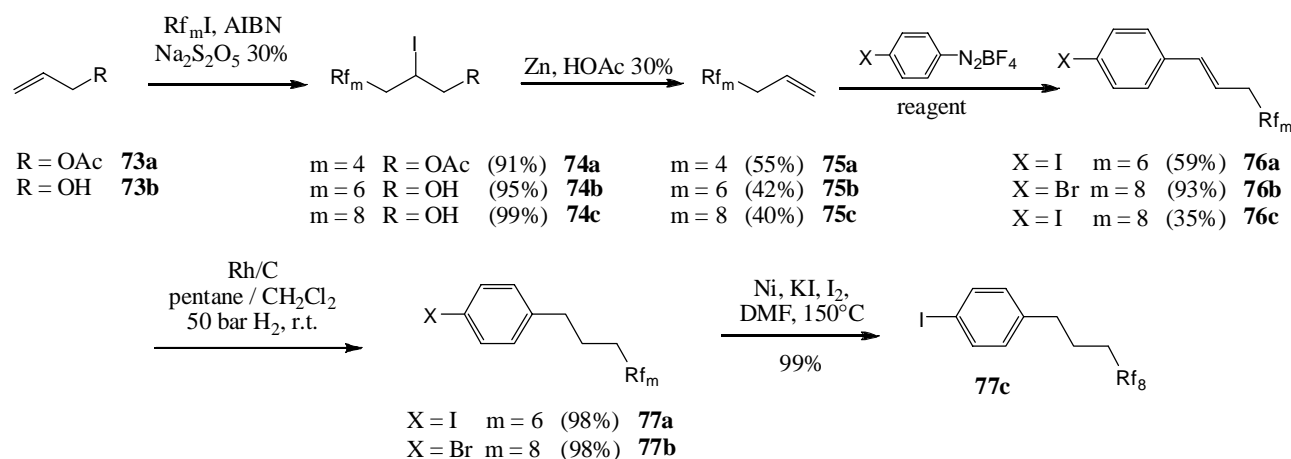
Scheme 10.5 – Formation of HBC **63a**

### 10.3 HBC-Rf<sub>3,6</sub> and HBC-Rf<sub>3,8</sub>

*Synthetic strategy:* In order to fix a perfluorinated three alkyl-carbon spacer to an aromatic halide either a Heck or Kumada cross-coupling may be applied. It turned out to be favourable to use the Heck coupling, similarly as in the formation of HBC-Rf<sub>2,6</sub> **63a**, because the yields largely exceeded those obtained by the Kumada cross-coupling.

#### 10.3.1 Synthesis of X-Ph-Rf<sub>3,6</sub> and X-Ph-Rf<sub>3,8</sub>

Three strategies for the preparation of iodinated aryl derivatives bearing perfluorinated chains together with a three carbon alkyl spacer could be applied: Kumada or Suzuki cross-coupling of an appropriate bromo- or iodo-perfluoroalkane, or a Heck reaction of an allyl-perfluoroalkane derivative. The Kumada cross-coupling reaction is severely hampered due to the electron withdrawing effect of the perfluorinated part, despite the three alkyl carbon spacer. The maximum yield of all attempted Kumada cross-couplings on either 1-bromo-(4-trimethylsilyl)benzene (one fold coupling) or 4,4'-dibromotoluene **65** (two fold coupling) never exceeded 19%.<sup>[211]</sup> Most probably a Suzuki cross-coupling would suffer from exactly the same problem. The Heck reaction is by far less sensitive to the fluorine effect and worked excellent for vinyl spacers, as shown in the previous section for the reaction of a diazonium salt **48a** and **48b** with a vinylperfluoroalkane derivative **68**. As the allyl perfluoroalkanes **75a**, **75b** and **75c** are not commercially available, contrarily to their vinyl analogues, several strategies were explored for their preparation, summarized in Table 10.4. Unfortunately, allyl perfluoroalkane **75b** was only accessible at best in moderate yield, which is also confirmed in the literature.<sup>[212]</sup>



**Scheme 10.6** – Reaction sequence using a Heck cross-coupling as key step to afford compounds **77a** and **c**

The most favourable way is a two step sequence, starting with the reaction of allylic alcohol<sup>[212a, 213]</sup> or allyl acetate<sup>[212b]</sup> with the appropriate perfluoroiodide in presence of a 30% aqueous solution of sodium metabisulfite and AIBN, followed by a reductive elimination / dehalogenation to install the allyl functionality. The radical addition reaction is induced by means of the radical initiator (AIBN), which abstract the iodine atom from  $\text{Rf}_m\text{I}$  forming an  $\text{Rf}$  radical that adds irreversibly to the alkene. This is an exothermic step, since the  $\pi$ -bond of the alkene is broken in favour of a stronger  $\sigma$ -bond. Finally, a transfer of the iodine atom from  $\text{Rf}_m\text{I}$  to the radical adducts gives the product and a secondary  $\text{Rf}$  radical that may continue the reaction chain.<sup>[214]</sup> A great increase in the reaction rate was achieved by the synergic action of sodium metabisulfite and AIBN. It has been proposed, that bisulfite suppresses side reactions that slow down the  $\text{Rf}_m\text{I}$  addition.<sup>[212a]</sup>

The second step consists of the reductive elimination / dehalogenation which can be accomplished by treatment with zinc powder in acetic acid, a method which is not very efficient. The reaction goes rapidly to completion, but there is significant formation of by-products, most probably and predominantly  $\text{Rf}_m\text{CH}_2\text{CH}_2\text{CH}_2\text{OH}$ .<sup>[212a]</sup> As shown in Table 10.4, the literature offers many different one step approaches for the formation of **75b**, without really improving the yield. Allylbromide may for example be reacted with  $\text{Rf}_6\text{I}$  in the presence of  $\text{KOH}$  and AIBN yielding **75b** only in low yield<sup>[215]</sup> (entry 1). As the active species is thought to be some peroxide traces in  $\text{KOH}$ , an addition of  $\text{KO}_2$  was attempted, which did not increase the yield (entries 2 and 3). Kumada cross coupling of  $\text{Rf}_6\text{I}$  and allylmagnesium bromide was also unsuccessful under various conditions (entries 4 and 5).

The only one step synthesis affording a competitive yield of **75b** was found by using  $\text{Rf}_m\text{I}$ , allyl acetate and DBPO as radical initiator.<sup>[212b]</sup> In contrast to the previously described procedure the intermediate product has not to be isolated and is directly injected onto a slurry of zinc powder in methanol affording the desired allyl derivative after distillation.

**Table 10.4** – Attempted conditions for the formation of **75b**

Entry	Subst.	Reagent [eq]	Additive [eq]	Temp. [°C]	Time [h]	75b [%Yld]
1	Rf <sub>6</sub> I	allyl- bromide (2)	KOH (3) AIBN (0.03)	80	5	15
2	Rf <sub>6</sub> I	allyl- bromide (2)	KO <sub>2</sub> (0.1)	80	0.5	-
3	Rf <sub>6</sub> I	allyl- bromide (2)	KOH (3) AIBN (0.05) KO <sub>2</sub> (0.05)	80	0.5	12
4	Rf <sub>6</sub> I	allyl-magnesium bromide (1.3)	PdCl <sub>2</sub> (dppf) (0.05) THF	r.t.	5	-
5	Rf <sub>6</sub> I	allyl-magnesium bromide (1.3)	PdCl <sub>2</sub> (dppf) (0.05) THF	75	4	-
6	Rf <sub>6</sub> I	allyl- acetate (1)	1) DBPO (0.02) 2) Zn (2), MeOH	65	1	45
7	Rf <sub>6</sub> I	allyl- alcohol (1.03)	1) AIBN (0.02), Na <sub>2</sub> S <sub>2</sub> O <sub>5</sub> 30% 2) Zn (1.5), CH <sub>3</sub> COOH	80	1	40
8	Rf <sub>6</sub> I	allyl- alcohol (1.03)	1) Pd(PPh <sub>3</sub> ) <sub>4</sub> (0.04), hexane 2) Zn (1.5), CH <sub>3</sub> COOH	r.t. 80	2	29

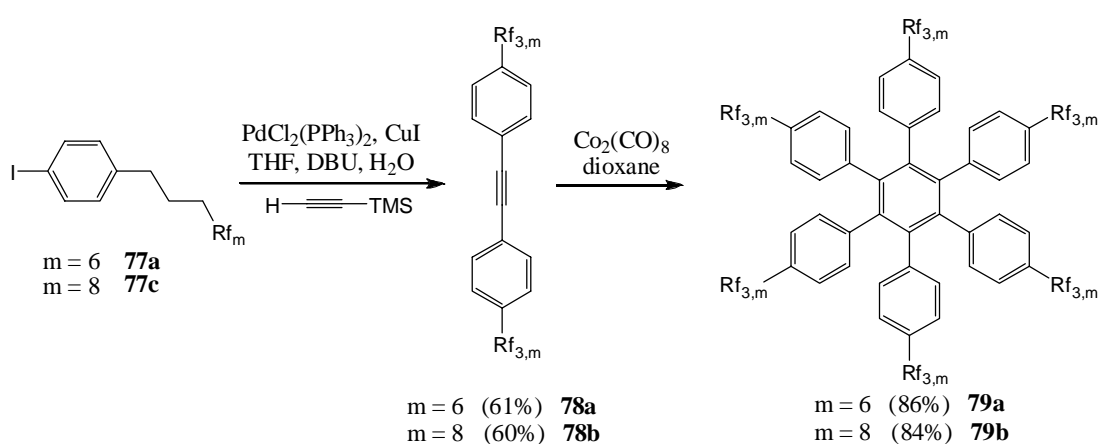
The corresponding perfluoroallyl derivatives **75b** and **75c** were reacted subsequently via a Heck coupling with bromo- or iodobenzene tetrafluoroborate, respectively. As shown in Scheme 10.6, the brominated derivative **76b** was afforded in very good yield (93%) whereas its iodinated analogues **76a** and **76c** were afforded in moderate yield only. The reason consisted in the fact that the more reactive iodine tends to react too, confirmed by the isolation of the bis-coupled product.

Subsequent hydrogenation of the double bond worked surprisingly with both precursors, in contrary to the difficulties encountered by hydrogenating an iodinated precursor, as discussed in the previous section for the preparation of I-Ph-Rf<sub>2,6</sub> **70b**.

Final exchange of the bromine in **77b** into an iodoaryl derivative **77c** was performed by reacting the former in presence of nickel, potassium iodide and iodine in DMF. Although a nickel to aryl bromide ratio of 5 to 1 was employed in the reaction, far less may be used as the nickel is acting as a catalyst in the exchange reactions. The purpose of using an excess of nickel powder is to raise the reaction rate by increasing the nickel surface. Furthermore, a small amount of I<sub>2</sub> was added to the reaction, with the aim of crating a fresh nickel surface from the reaction of I<sub>2</sub> with the nickel powder. Although the strength of the carbon-iodide bond in aromatic compounds is weaker than that of the carbon-bromide bond, the lack of solubility of KBr relative to KI in DMF drives the exchange

reaction in favour of the aryl iodide. The reaction mechanism involves  $\pi$ -adsorption of the aryl halide by the nickel surface in the first step, followed by the nucleophilic attack of an external halide ion at the aromatic halide carbon to give a negatively charged intermediate. Expulsion of one of the two halides and the subsequent desorption completes the exchange reaction.<sup>[216]</sup> The  $\pi$ -coordination of the aromatic ring to the metal surface greatly reduces the electron density on the ring and facilitates the nucleophilic displacement reaction.<sup>[217]</sup>

### 10.3.2 Synthesis of HPB-Rf<sub>3,6</sub> and HPB-Rf<sub>3,8</sub>



**Scheme 10.7** – Formation of HPB derivatives **79a** and **79b**

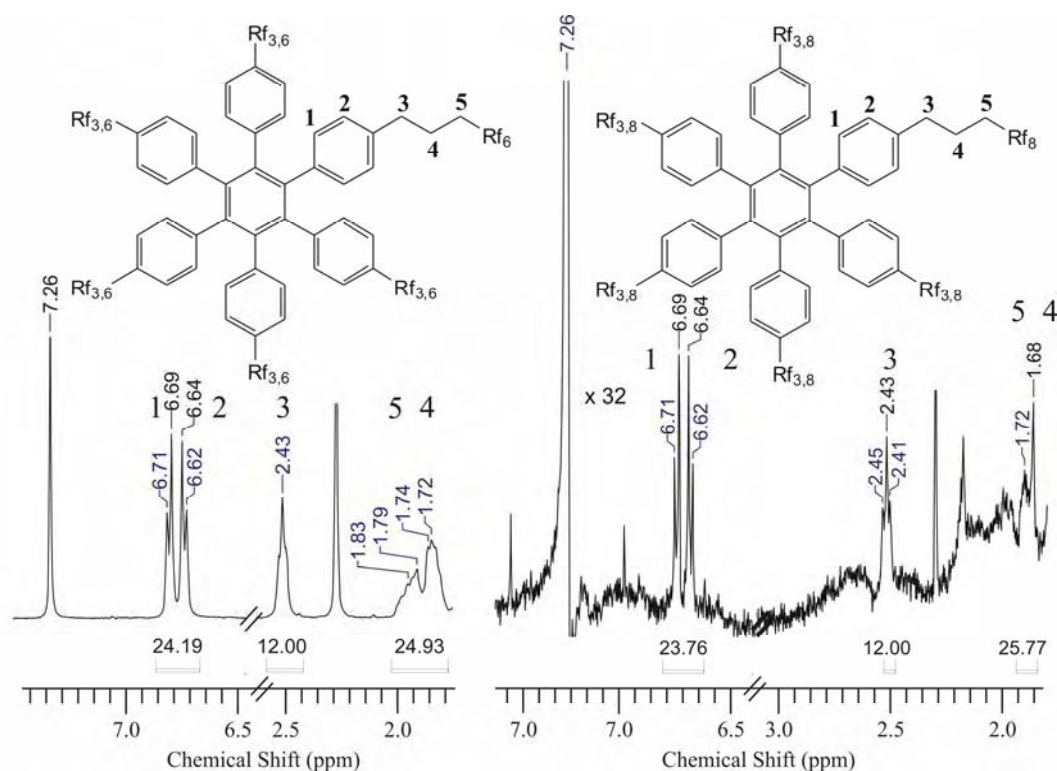
The tolane formation was performed for both derivatives, **78a** and **78b** by applying the one-pot Sonogashira conditions. The different conditions used are listed in Table 10.5.

**Table 10.5** – Reaction conditions for the Sonogashira cross-coupling

Entry	Subst.	Reagent [eq]	Catalyst [mol%]	Additive [eq]	Solvent	Temp. [°C]	Time [d]	Product [%Yld]
1	<b>77a</b>	TMSA (0.5)	Pd(PPh <sub>3</sub> ) <sub>4</sub> (6) CuI (10)	DBU (6.0) H <sub>2</sub> O (0.4)	THF	65	1	<b>78a</b> 61
2	<b>77c</b>	TMSA (0.5)	Pd(PPh <sub>3</sub> ) <sub>4</sub> (6) CuI (10)	DBU (6.0) H <sub>2</sub> O (0.4)	THF	70	2	<b>78b</b> 27
3	<b>77c</b>	TMSA (0.5)	Pd(PPh <sub>3</sub> ) <sub>4</sub> (6) CuI (10)	DBU (6.0) H <sub>2</sub> O (0.4)	THF	55	6	<b>78b</b> 31
4	<b>77c</b>	TMSA (0.5)	Pd(PPh <sub>3</sub> ) <sub>4</sub> (6) CuI (10)	DBU (6.0) H <sub>2</sub> O (0.4)	THF	50	1	<b>78b</b> 60



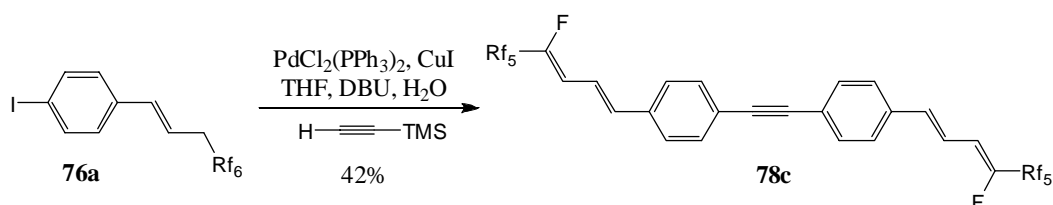
Subsequent cyclotrimerization under the usual conditions afforded the desired HPB derivatives for both target molecules **79a** and **79b** in moderate to fair yields. It has to be noted that the very low solubility of **78b** and **79b** hampered the completion of the reaction on the one hand, and the purification of the obtained product on the other hand. Because of this, the trimerization of the Tol-Rf<sub>3,8</sub> **78b** had to be repeated several times as the desired HPB **79b** was either lost during purification on silica gel, or was obtained as an inseparable mixture together with the starting material. In addition a decrease of solubility with increasing purity was observed. To overcome these difficulties two modifications had to be applied: first HFB was added as co-solvent to prevent an incomplete reaction due to incorporation of starting material in the precipitated product; second, the crude product had to be purified by silica gel filtration over an ultra short plug using hot BTF as solvent. The enormous difference in solubility between HPB **79a** and **79b** (about two orders of magnitude), induced by the elongation of the side chain by only two additional perfluorinated carbon atoms, is clearly demonstrated by the <sup>1</sup>H-NMR spectra of saturated solutions of these compounds in CDCl<sub>3</sub>, as shown in Figure 10.1.



**Figure 10.1** – Left: HPB-Rf<sub>3,6</sub> **79a** in a saturated CDCl<sub>3</sub> solution; right: HPB-Rf<sub>3,8</sub> **79b** in a saturated CDCl<sub>3</sub> solution, whereas the spectrum of **79b** was multiplied by a factor of 32 to compare the effect of the fluorine's on the solubility

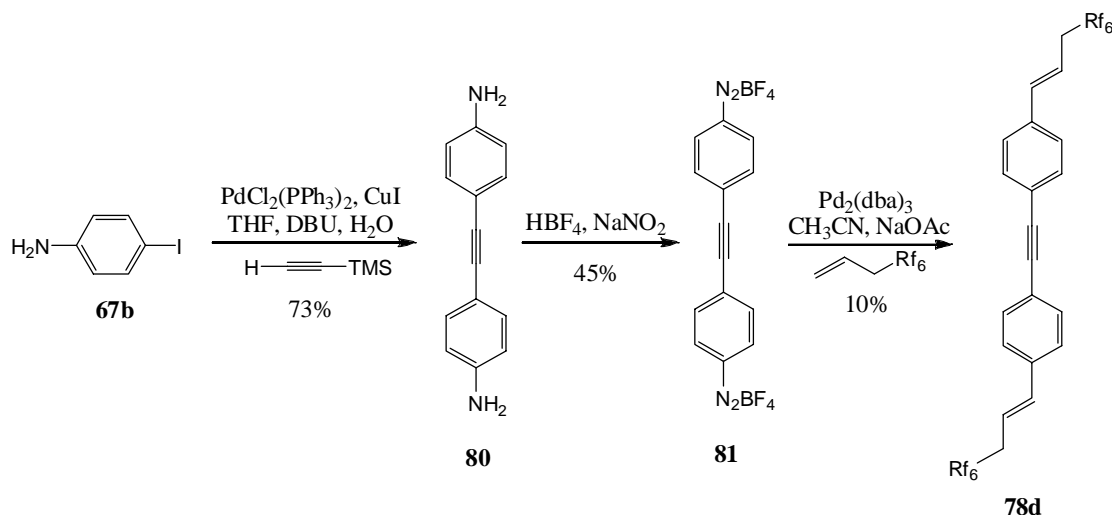
It is worth mentioning that the formation of a tolane derivative starting from **76a** bearing an allylic side chain did not yield the desired product at all, in contrary to the product containing a vinyl spacer between the aromatic core and the perfluorinated side chain (c.f. section 10.2.3). Analysis of the obtained reaction mixture of the one pot Sonogashira cross-coupling revealed that exclusively tolane **78c** was formed instead of **78a**. Most probably the catalyst performs first the reaction in the

usual way forming tolane **78d**. Then complexation of the allyl spacer by the palladium catalyst yields most probably an  $\eta^3$ -allyl complex, which by  $\beta$ -elimination expels a HF molecule. The cleavage of the very strong C-F bond is not a very usual reaction, but is in this case thermodynamically favoured by taking into account the formed hydrofluoric acid and the second conjugated double bond.



**Scheme 10.8** – Undesired main compound formed by one-pot Sonogashira cross-coupling of **76a**

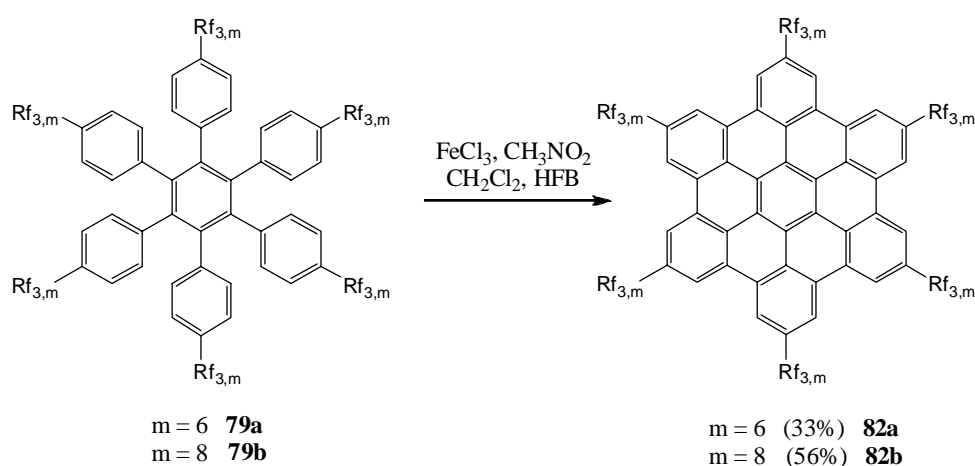
Because of these difficulties encountered in preparing tolane **78d** an alternative route was tested in order to compare the overall yield and to search for a more favourable general reaction pathway. As shown in Scheme 10.9 iodoaniline **67b** was reacted under standard tandem Sonogashira conditions to yield 4,4'-diaminotolane **80**. Surprisingly the amino group did not hinder this reaction at all. Tolane **80** was further transformed into its corresponding double diazonium salt **81**. It has to be noted that due to the low solubility of **80** the reaction had to be carried out in an ultrasonic bath. Heck coupling of tolane **81** and allyl **75b** afforded finally the desired tolane **78d** carrying the perfluorinated side chain with an allyl spacer. By comparing the overall yield of the original strategy (14%) and the one presented below (3%) it is evident that the shortened new pathway did not improve the procedure. Moreover it is known that diamino derivatives such as **80** suffer from an extremely high toxicity. Because of all this, no further attempts were performed along this strategy.



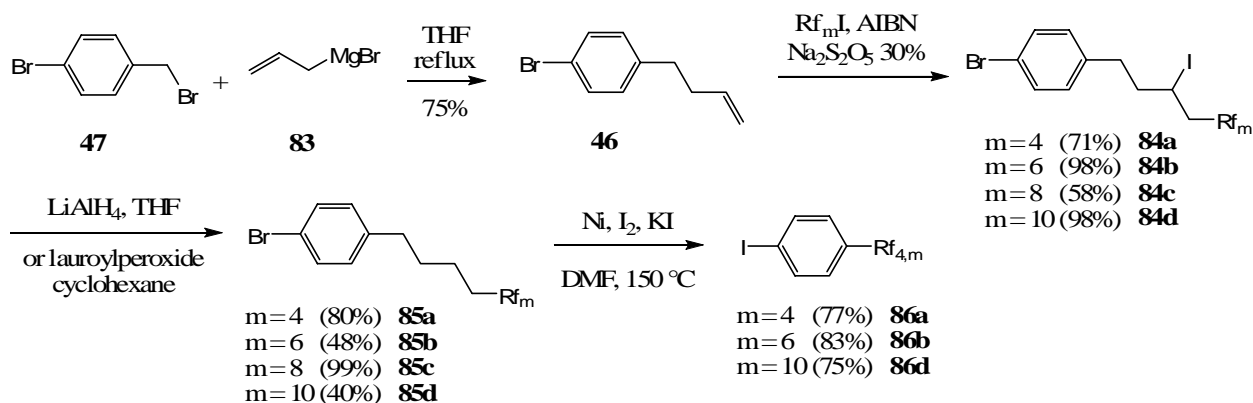
**Scheme 10.9** – Alternative pathway to form tolane **78d** carrying an unsaturated perfluoroalkylated chain

10.3.3 Synthesis of HBC-Rf<sub>3,6</sub> and HBC-Rf<sub>3,8</sub>

The planarization of HPB derivatives **79a** and **79b** afforded the desired HBC derivatives in moderate yield, as shown in Scheme 10.10. The oxidation of HPB **79b**, bearing eight perfluorinated carbons per side chain, afforded the desired HBC free of any starting material contamination, if HFB was added as co-solvent.

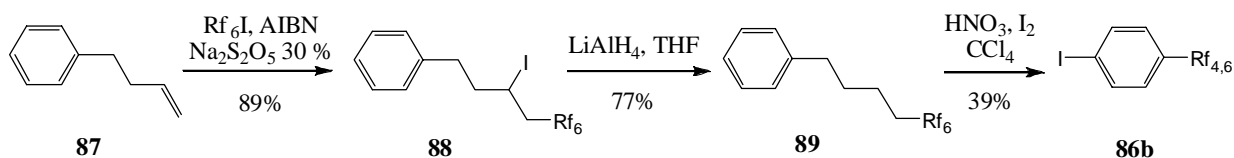
Scheme 10.10 – Oxidation to prepare HBCs **82a** and **82b**10.4 HBC-Rf<sub>4,4</sub>, HBC-Rf<sub>4,6</sub>, HBC-Rf<sub>4,8</sub> and HBC-Rf<sub>4,10</sub>10.4.1 Synthesis of X-Ph-Rf<sub>4,m</sub>

The preparation of halogenated aryl derivatives, carrying four hydrogenated alkyl spacers in the side chain in combination with a varying number (4, 6,<sup>[205]</sup> 8 and 10) of perfluorinated carbons is outlined in Scheme 10.11.

Scheme 10.11 – Short and high yielding approach to prepare derivatives **85c** and **86a**, **86b**, and **86d**

The different target compounds are obtained by this four step sequence in overall yields ranging between 22% and 43%. The first step consists of a Wurtz type coupling between allylmagnesium bromide **83** and 4-bromobenzyl bromide **47a**<sup>[173]</sup> affording compound **46**, which was reacted subsequently with the corresponding Rf<sub>m</sub>I. The removal of the iodo group of the side chain was carried out with LiAlH<sub>4</sub><sup>[213]</sup> or lauroylperoxide in cyclohexane yielding the desired aryl bromides (**85a-d**). This iodine reduction by lauroylperoxide is achieved by an unusual hydrogen atom transfer from cyclohexane. The key and rate determining step is the hydrogen abstraction from cyclohexane.<sup>[218]</sup> The cyclohexane radical removes the iodine of the starting product to form iodocyclohexane. The newly formed product radical lies in equilibrium with cyclohexane to afford the desired product and to reform a cyclohexane radical.<sup>[219]</sup> Unfortunately the yield of this elegant and mild strategy was lower than the one using LiAlH<sub>4</sub> and was therefore not further investigated. It has to be noted that by using the LiAlH<sub>4</sub> conditions only a small excess of hydrides is taken as otherwise the aromatic core would be dehalogenated. The radical mediated halogen exchange furnished finally the iodoaryl derivatives (**86a**, **86b** and **86d**).

An alternative approach was tested, consisting in a three step reaction sequence affording the desired iodoaryl **86b** in almost the same overall yield. The reaction started by addition of Rf<sub>6</sub>I **90b** to commercially available 4-phenyl-1-butene **87** which was dehalogenated with LiAlH<sub>4</sub>. The introduction of the aromatic iodo group in *para*-position proved to be tricky. Several conditions (shown in Table 10.6) were tested, out of which fuming HNO<sub>3</sub> together with I<sub>2</sub> in CCl<sub>4</sub> was chosen due to the highest obtained yield and the low cost of the reagents. Nevertheless a mixture of *para* and *ortho* substituted products was afforded which had to be separated by repetitive column chromatography on silica gel.



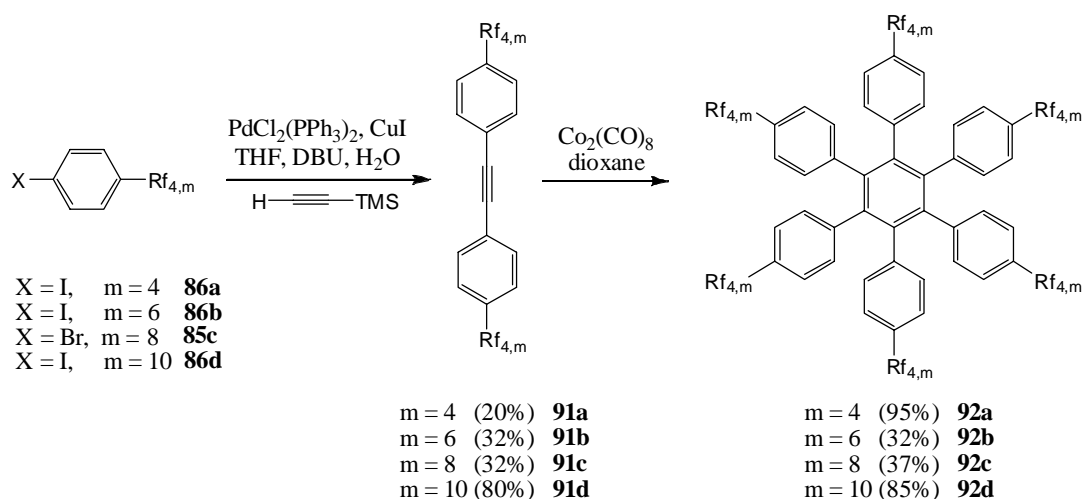
Scheme 10.12 – Formation of compound **86b**

Table 10.6 – Different attempts performed for the *para*-iodination of the aryl derivative **86b**

Entry	Subst.	Reagent	Additive [eq]	Solvent	Temp. [°C]	Time [d]	<b>86b</b> [%Yld]
1	<b>89</b>	I <sub>2</sub> (0.5)	PIFA (0.55)	CHCl <sub>3</sub>	60	3	36
2	<b>89</b>	I <sub>2</sub> (0.5)	PIFA (0.55)	CHCl <sub>3</sub>	60	1	25
3	<b>89</b>	I <sub>2</sub> (0.6)	HNO <sub>3</sub> (2.2)	CCl <sub>4</sub>	90	2	16
4	<b>89</b>	I <sub>2</sub> (0.6)	HNO <sub>3</sub> (2.2)	CCl <sub>4</sub>	90	2	39

10.4.2 Synthesis of HPB-Rf<sub>4,m</sub>

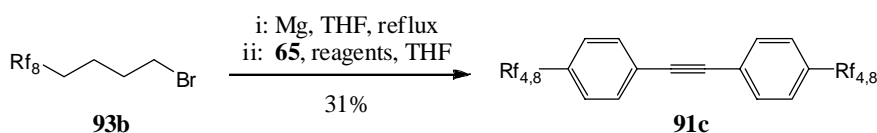
As shown in Scheme 10.13, the corresponding tolane derivatives were obtained from one-pot Sonogashira reactions in moderate yield except for Tol-Rf<sub>4,10</sub> **91d** which was obtained in high yield as a white solid. The surprising high yield of **91d** could not be explained, as the extremely low solubility of derivatives bearing ten perfluorinated carbons is expected to hamper the reaction and to drop the yield instead of increasing it. Furthermore it is worth mentioning that the mass balance is respected for all Sonogashira reactions as usually large quantities of unreacted starting material were recovered after the reaction. Hexaphenylbenzene formation was achieved by cobalt mediated cyclotrimerization of the corresponding tolane derivatives and yielded the desired HPB in moderate to excellent yield, depending mostly on the purity of the starting tolane and not on the nature of the side chain.



Scheme 10.13 – Tolane and HPB formation followed by cyclotrimerization

10.4.3 Synthesis of Tol-Rf<sub>4,8</sub>

In order to shorten the reaction sequence for 4,4'-disubstituted tolane derivatives the Kumada cross-coupling of perfluoroalkyl bromides with 4,4'-dibromotolane **65** was investigated. As shown in Table 10.7, the most efficient conditions were found to be PdCl<sub>2</sub>(dppf) as catalyst without any additive.<sup>[100]</sup> The yield could not be improved compared to the Sonogashira reaction discussed earlier. Moreover the very long reaction time and the unreliable yields together with the fact that side products such as the homocoupled Grignard derivative and monocoupled tolane were produced made this sequence less interesting than the previously discussed Sonogashira reaction.

Scheme 10.14 – Formation of tolane **91c** by two fold Kumada cross-coupling

The main difficulty of the Kumada cross-coupling is most probably the slow and incomplete Grignard formation, possibly due to micelle formation.<sup>[220]</sup> Different techniques, i.e. the addition of iodine as activator, the use of freshly activated (HCl) magnesium turnings and the formation of a magnesium mirror in the reaction vessel by stirring magnesium turnings in the empty reaction vessel, were tried in order to improve the yield of the reaction, but unfortunately no systematic improvement was obtained. Even the addition of fluorinated solvents, such as perfluorohexane or trifluorotoluene did not improve the obtained yields.<sup>[221]</sup>

**Table 10.7** – Formation of tolane **91c**

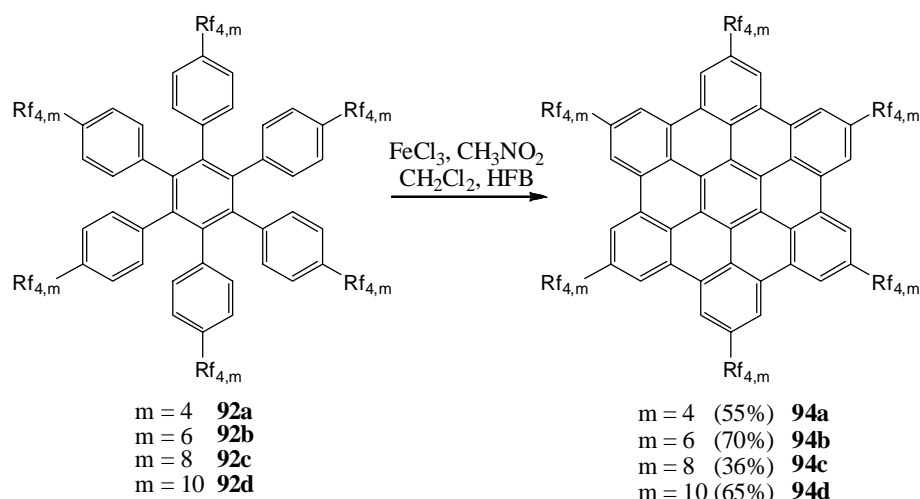
Grignard formation					C-C cross coupling					
Ent.	93b [mmol]	Mg [eq]	T. [d]	Solv.	65 [eq]	Catalyst [Mol%] <sup>a</sup>	Addend [Mol%] <sup>a</sup>	Temp. [°C]	T. [d]	91c [%Yld]
1	0.4	1.1	1	THF	0.25	PdCl <sub>2</sub> (dppf) (15)	-	75	7	-
2	0.9	1.2	1	THF	0.25	PdCl <sub>2</sub> (dppf) (15)	-	80	5	30
3	9.0	1.2	1	THF	0.25	PdCl <sub>2</sub> (dppf) (15)	-	80	6	41
4	3.6	1.2	1	THF	0.25	PdCl <sub>2</sub> (dppf) (15)	-	80	9	13
5	1.7	1.2	1	THF	0.25	Pd <sub>2</sub> (dba) <sub>3</sub> (2)	IPrHCl (4)	80	1	-
6	0.4	1.2	1	THF	0.33	Pd <sub>2</sub> (dba) <sub>3</sub> (2)	IPrHCl (8)	-78 to rt.	3	-
7	0.4	1.2	1	THF	0.4	Pd <sub>2</sub> (dba) <sub>3</sub> (2)	IPrHCl (8)	-78 to 40	2	-
8	3.0	1.0	1	THF	0.25	PdCl <sub>2</sub> (dppf) (10)	-	77	6	25
9	0.5	1.2	1	THF	0.25	NiCl <sub>2</sub> (dppp) (2.5)	-	75	7	-

<sup>a</sup> with respect to compound **65**

#### 10.4.4 Synthesis of HBC-Rf<sub>4,m</sub>

The final oxidation to the desired HBC derivatives was performed by applying the mild FeCl<sub>3</sub> condition. It has to be noted that for the well soluble HPB **92a** and **92b** only CH<sub>2</sub>Cl<sub>2</sub> was used as solvent, whereas for the HPB bearing longer side chains (**92c** and **92d**) HFB was added as inert co-solvent to prevent an incomplete reaction due to precipitation.

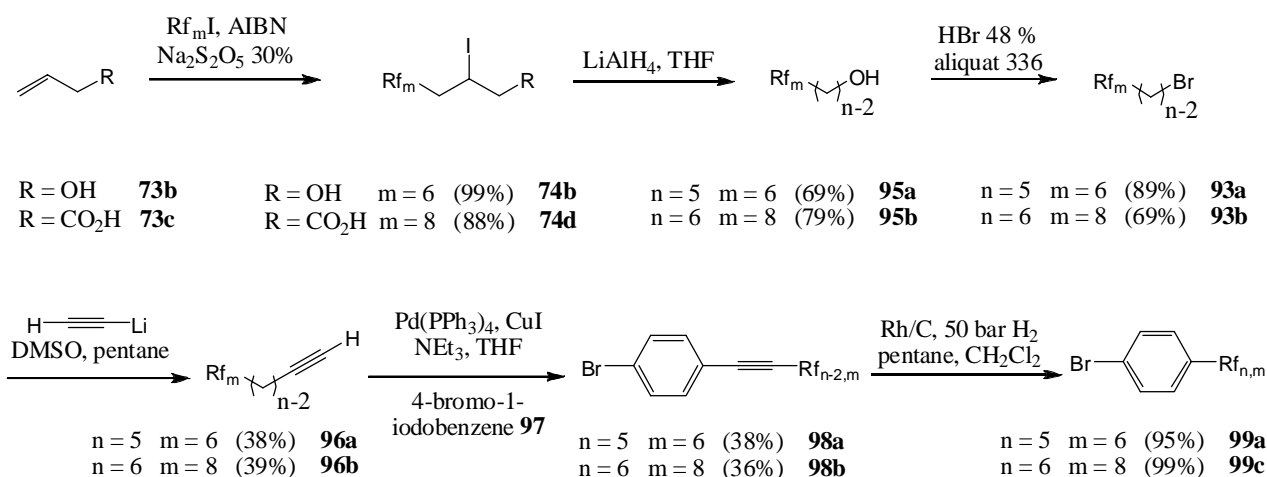
It has to be noted that the four carbon aliphatic spacer, independent on the perfluoro part, proved to be ideal for purification as precipitation from BTF and HFB afforded all derivatives as very bright yellow solids. No explanation could be found for this observation.

Scheme 10.15 – Scholl reaction affording the desired HBC derivatives **94a-d**

### 10.5 HBC-Rf<sub>5,6</sub> and HBC-Rf<sub>6,8</sub>

*Synthetic strategy:* The preparation of both derivatives was attempted with two different approaches: first formation of a perfluoroalkylated alkyne derivative, which was subsequently coupled under Sonogashira conditions to afford the key bromoaryl intermediate bearing the appropriate side chain; the second strategy envisaged to add any perfluorinated part prior to form the strategic alkyl-aryl bond. The above mentioned longer strategy, however, proved to be more adequate.

#### 10.5.1 Synthesis of Ph-Rf<sub>5,6</sub> and Ph-Rf<sub>6,8</sub>

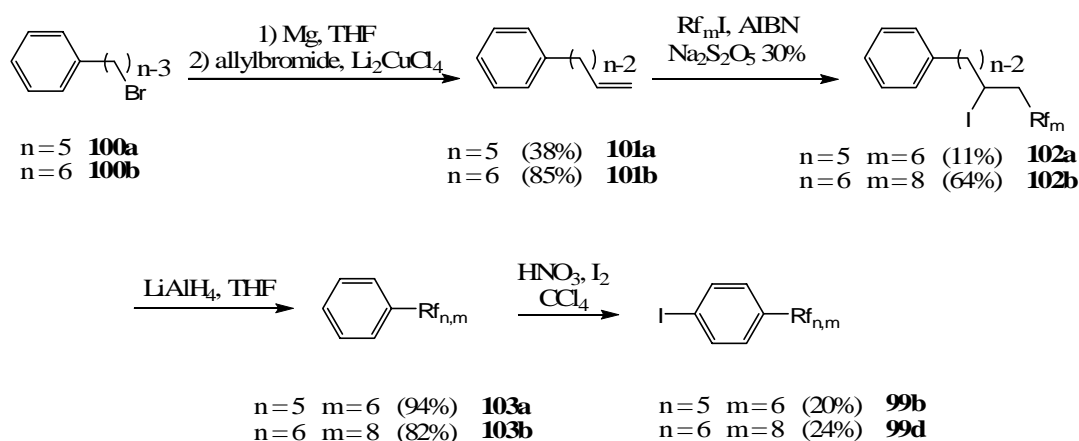
Scheme 10.16 – Formation of arylperfluoroalkanes **99a** and **c** via a Sonogashira cross-coupling

The preparation of the key compounds **99a** and **b** is shown in Scheme 10.16. Allylic alcohol **73b** or 4-pentenoic acid **73c** are reacted with the corresponding perfluoroiodide **90b** and **90c**, respectively, to afford the desired radical addition products **74b** and **74d**. These are reduced in the presence of

$\text{LiAlH}_4$  in THF yielding the alcohol derivatives **95a** and **95b**, which are subsequently refluxed in HBr 48% in the presence of aliquat 336 as phase transfer catalyst. Both perfluoroalkane bromides **93a** and **93b** are obtained as colourless oils in fair to good overall yield, 61% and 48%, respectively.<sup>[213]</sup> The elongation of the brominated alkanes by an acetylene group was achieved by treatment of the former with lithium acetylide ethylenediamine complex in DMSO.<sup>[222]</sup> In order to improve the homogeneity of the reaction mixture, the starting bromides were diluted with pentane prior to the addition yielding the perfluoroalkynes **96a** and **96b** as colourless, very volatile liquids. It has to be noted, that the pentane used for extracting the reaction mixture had to be removed by distillation through a vigreux column under normal pressure instead of usual rotary evaporation in order to prevent a major loss of product due to the high volatility. The high volatility is due to high partial pressures, which is a known property of perfluorinated compounds, despite their normally quite high boiling points.<sup>[223]</sup> In the case of **96a** and **b** or **98a** and **b** this property is even enhanced, as the acetylene endows the molecule with a high rigidity, reducing therefore the van der Waals interactions even more.

The subsequent unfavourable Sonogashira cross-coupling, unfavourable because the alkyne bears an alkyl and not an aryl substituent, was performed with  $\text{Pd}(\text{PPh}_3)_4$  as catalyst on 1-bromo-4-iodobenzene **97**. It is worth to mention that even at  $80^\circ\text{C}$  no trace of any biscoupled product, i.e. reacting at the bromide as well, was found. Even though the yields of this cross coupling are rather low, they were the result of a systematic investigation, summarized in Table 10.9, chapter 10.7.1. Subsequent hydrogenation of the alkynes **98a** and **98b**, under 50 bar of  $\text{H}_2$ , afforded the reduced perfluorinated bromoaryl key products **99a** and **99c** in quantitative yield as colourless oils.

As the overall yield for the lengthy preparation of perfluoroalkylated arylbromides **99a** and **b** was only 8% and 7%, respectively, another strategy was explored in parallel, shown in Scheme 10.17.



**Scheme 10.17** – Formation of arylperfluoroalkylated derivatives **99b** and **d** via iodination of the aromatic core

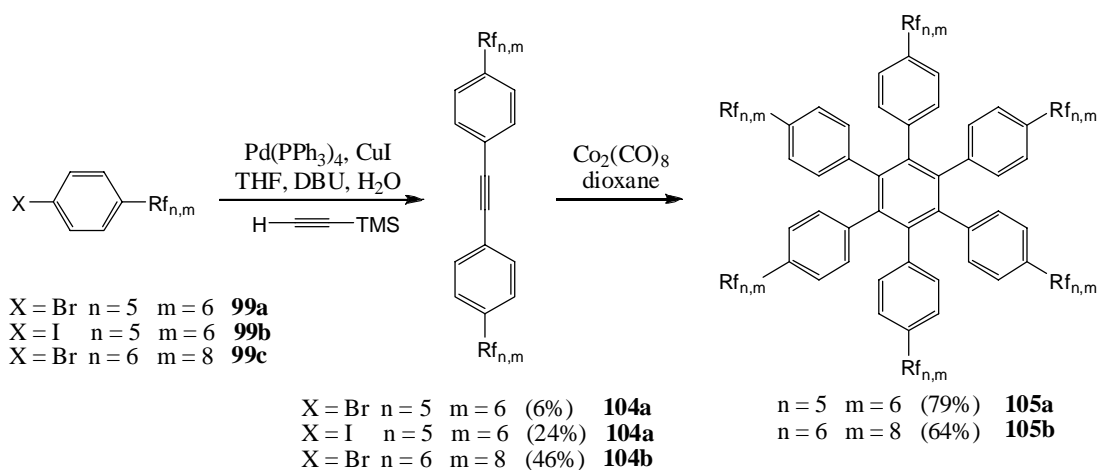


The main advantage of the second strategy is the presence of the strategic alkyl-aryl bond in the precursor, which eliminates in turn the difficult alkyne formation and its subsequent Sonogashira reaction.

Allylation of the precursors **100a** and **100b** was performed by a Grignard coupling using allyl bromide. In the case of 2-bromoethyl benzene **100a** no additional catalyst was needed, whereas for 3-bromopropyl benzene **100b**  $\text{Li}_2\text{CuCl}_4$  was added as catalyst.<sup>[173b, 224]</sup> The terminal alkene was then reacted with the corresponding perfluoroiodide using AIBN as radical initiator. It is worth mentioning that in the case of compound **101a**, bearing five carbons in the lateral chain, the yield was found to be very low. Increasing the reaction time and repetitive additions of AIBN and perfluoroiodide did not improve the result. The most plausible reason is the intramolecular complexation of the alkene by the aromatic core, as a five carbon chain was found to be ideal in arene-olefine cycloadditions.<sup>[225]</sup> This assumption is underlined by the fact, that already one additional  $\text{CH}_2$  in the alkyl chain (**101b**) allowed for a much better yield. Reduction of the iodo group was achieved by treatment with  $\text{LiAlH}_4$  followed by *para*-iodination of the aromatic core to yield the desired perfluoroalkyl aryl iodide **99b** and **99d**. The overall yield of this second approach is 1% for **99b** and 11% for **99d**. As conclusion the second strategy is two steps shorter but affords similar yields for **99d** and clearly lower for **99b**.

#### 10.5.2 Synthesis of HPB- $\text{Rf}_{5,6}$ and HPB- $\text{Rf}_{6,8}$

As shown in Scheme 10.18 both tolane derivatives **104a** and **b** were prepared by a one-pot Sonogashira cross-coupling. In the case of the brominated or iodinated precursor **99a** and **b**, the corresponding tolane **104a** was afforded in very low yield only, probably due to the quality of the catalyst, as large amounts of the starting material were recovered. In contrary **99c** afforded the corresponding tolane in good yield for a one-pot coupling. Subsequent trimerization furnished both HPB derivatives **105a** and **b** in high yield as white solids.

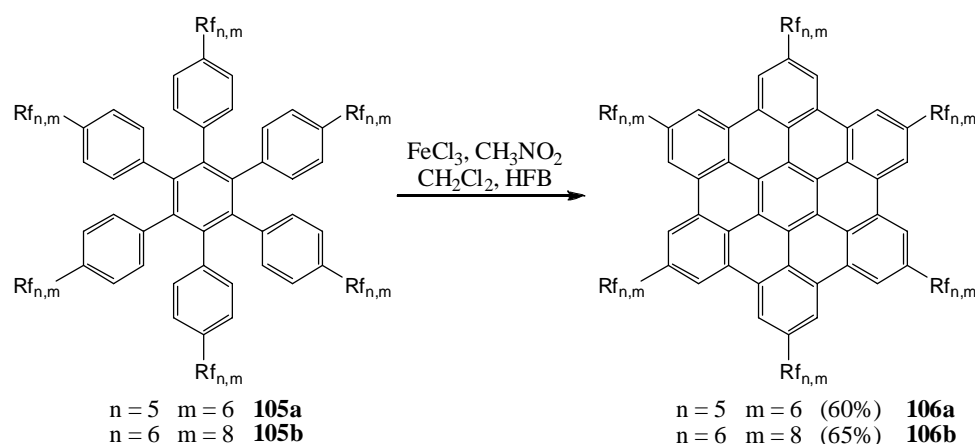


**Scheme 10.18** – One pot Sonogashira reaction followed by cyclotrimerization

10.5.3 Synthesis of HBC-Rf<sub>5,6</sub> and HBC-Rf<sub>6,8</sub>

The oxidation of HBC **106a** and **b** was performed using the standard mild conditions together with a 1:1 mixture of solvents (CH<sub>2</sub>Cl<sub>2</sub> / HFB). After the reaction the crude mixture was quenched by the addition of methanol which provoked the precipitation of the desired HBC as brown solids. Precipitation from common organic solvents (ether, dichloromethane, nitromethane and ethanol) and a fluorinated solvent (BTF) afforded after suction filtration over Millipore<sup>®</sup> the desired HBCs in high yield as yellow solids.

Nevertheless the following two observations are worth to mention: *i*) if one uses a mixture of HFB and nitromethane as solvents the formed HBC **106b** yielded a black, completely insoluble powder. Characterization of this powder was not possible, which proved the necessity of adding dichloromethane as co-solvent; *ii*) the use of FeCl<sub>3</sub> containing a very faint amount of water (shown by the presence of traces of yellow hydrated FeCl<sub>3</sub>) increased generally the yield. It is possible that hydrated FeCl<sub>3</sub> assists the beginning of the Scholl reaction by acting as acid.



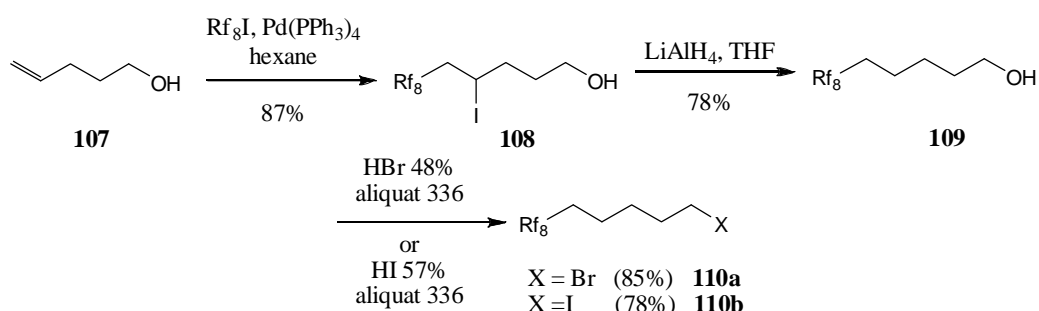
**Scheme 10.19** – Oxidation to obtain the desired HBC derivatives **106a** and **b**

10.6 HBC-Rf<sub>5,8</sub>

*Synthetic strategy:* This HBC derivative was prepared by using a Kumada cross-coupling of the perfluoroalkyl bromide **110** with 4,4'-dibromotolane **65**. Different catalytic systems were tested in order to improve the yield of this coupling, but the two fold Kumada coupling remains an unreliable reaction when used in combination with perfluoroalkylated substrates.

10.6.1 Synthesis of X-Rf<sub>5,8</sub>

A different preparation of the side chain was employed as compared to the previously presented ones. Pent-4-en-1-ol **107** was reacted with perfluorooctyliodide **90c** in a radical addition, initiated by Pd(PPh<sub>3</sub>)<sub>4</sub>. This reaction is known to be carried out under extremely mild conditions, giving high yields but requires long reaction times.<sup>[213]</sup> Subsequent reduction with LiAlH<sub>4</sub> afforded the corresponding alcohol **109** which was refluxed in either hydrobromic acid or hydroiodic acid yielding the according perfluoroalkyl halogenides **110a** and **b**, respectively, in high yields as colourless oils.



**Scheme 10.20** – Preparation of iodinated and brominated perfluoroalkanes

10.6.2 Synthesis of HPB-Rf<sub>5,8</sub>

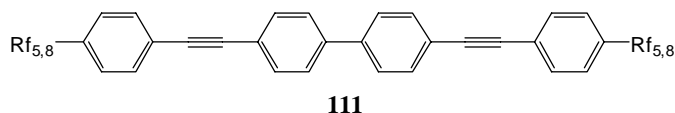
As mentioned earlier the Kumada cross coupling of a perfluoroalkyl bromide with 4,4'-dibromotolane **65** is a rather unreliable reaction yielding at best moderate yields. Because of that a systematic investigation was performed by testing different catalytic substrates, including brominated as well as iodinated precursors. Table 10.8 summarized the performed attempts.

**Table 10.8** – Conditions used in the two fold Kumada cross-coupling for preparing tolane **112**

Grignard formation					C-C cross coupling					
Ent.	<b>110a</b> [mmol]	Mg [eq]	T. [d]	Solv.	<b>65</b> [eq]	Catalyst [Mol%] <sup>a</sup>	Addend [Mol%] <sup>a</sup>	Temp. [°C]	T. [d]	<b>112</b> [%Yld]
1	0.9	1.2	1	THF	0.25	PdCl <sub>2</sub> (dppf) (15)	-	80	5	- <sup>b</sup>
2	0.2	1.2	1	THF	0.25	Pd <sub>2</sub> (dba) <sub>3</sub> (2)	IPrHCl (8)	-10	2	16 <sup>c</sup>
3	0.2	1.2	1	THF	0.25	Pd <sub>2</sub> (dba) <sub>3</sub> (2)	IPrHCl (8)	0	2	24 <sup>c</sup>
4	0.2	1.2	1	THF	0.25	Pd <sub>2</sub> (dba) <sub>3</sub> (2)	IPrHCl (8)	r.t.	2	22 <sup>d</sup>
5	0.2	1.2	1	THF	0.25	Pd(OAc) <sub>2</sub> (4)	IPrHCl (8)	80	3	15 <sup>e</sup>
6	0.2	1.2	1	THF	0.25	Pd(OAc) <sub>2</sub> (4)	IPrHCl (8)	-78 to rt.	3	18 <sup>e</sup>
7	0.2	1.2	1	THF	0.25	Pd(OAc) <sub>2</sub> (4)	IPrHCl (8)	-78 to 40	3	3 <sup>e</sup>
8	3.0	1.2	1	THF	0.25	PdCl <sub>2</sub> (dppf) (10)	-	76	6	83
9	1.2	1.2	1	THF	0.25	PdCl <sub>2</sub> (dppf) (10)	-	75	5	- <sup>b</sup>
10	10	1.2	1	THF	0.25	PdCl <sub>2</sub> (dppf) (10)	-	80	6	15 <sup>e</sup>

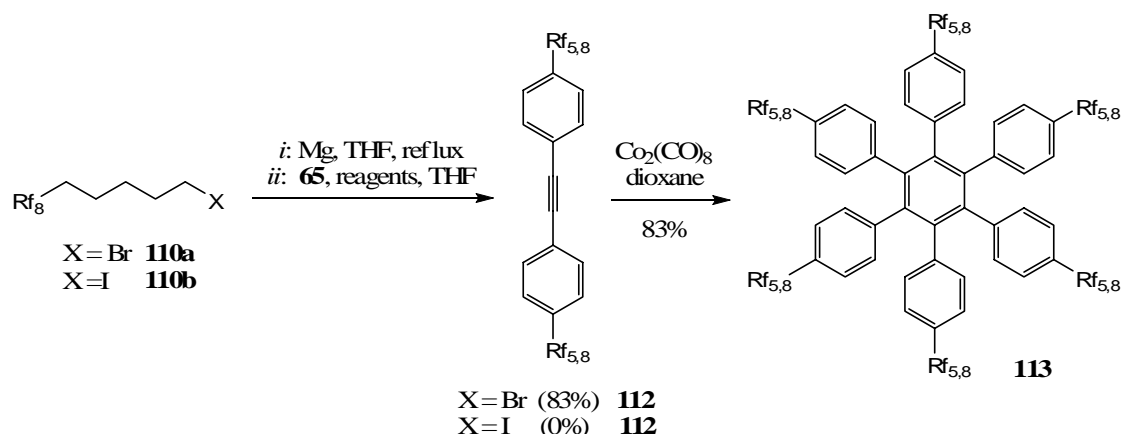
<sup>a</sup> with respect to **65**; <sup>b</sup> only **65** was recovered; <sup>c</sup> traces of homocoupled product **111** were found (the structure is shown in Scheme 10.21); <sup>d</sup> starting material **65** together with the alkene analogue of **110a** were found; <sup>e</sup> starting material **65** was found

PdCl<sub>2</sub>(dppf)·CH<sub>2</sub>Cl<sub>2</sub><sup>[226]</sup> proved to be the most promising catalyst, event though some runs were performed which yielded no desired product at all. Only in one entry (8) tolane **112** was obtained in high yield. The fluctuation of the yields points out that not all reaction parameters were under control. The use of recently developed catalytic systems was tried too, as already discussed in the previous section (c.f. chapter 10.4.3), without improving the yields.

**Scheme 10.21** – Homocoupled by-product formed during the Kumada cross-coupling

Due to the formation of many side products while using Pd<sub>2</sub>(dba)<sub>3</sub> or Pd(OAc)<sub>2</sub>,<sup>[189, 227]</sup> different temperatures (-10°C, 0°C and r.t.) were tested, revealing that at lower temperature a cleaner reaction is observed. Unfortunately nearly every run revealed the presence of some unreacted starting tolane **65** together with a homocoupled reaction product **111**, which would be very unfavourable for the subsequent trimerization.

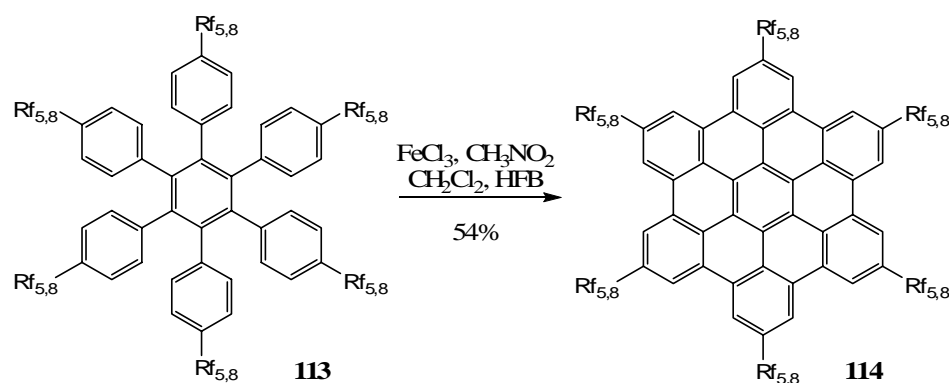
Only the use of highly pure tolane **112** allowed the preparation of the desired HPB derivative **113** in good yield as white powder.



**Scheme 10.22** – Tolane formation via Kumada cross-coupling followed by cyclotrimerization to obtain HPB **113**

### 10.6.3 Synthesis of HBC- $\text{Rf}_{5,8}$

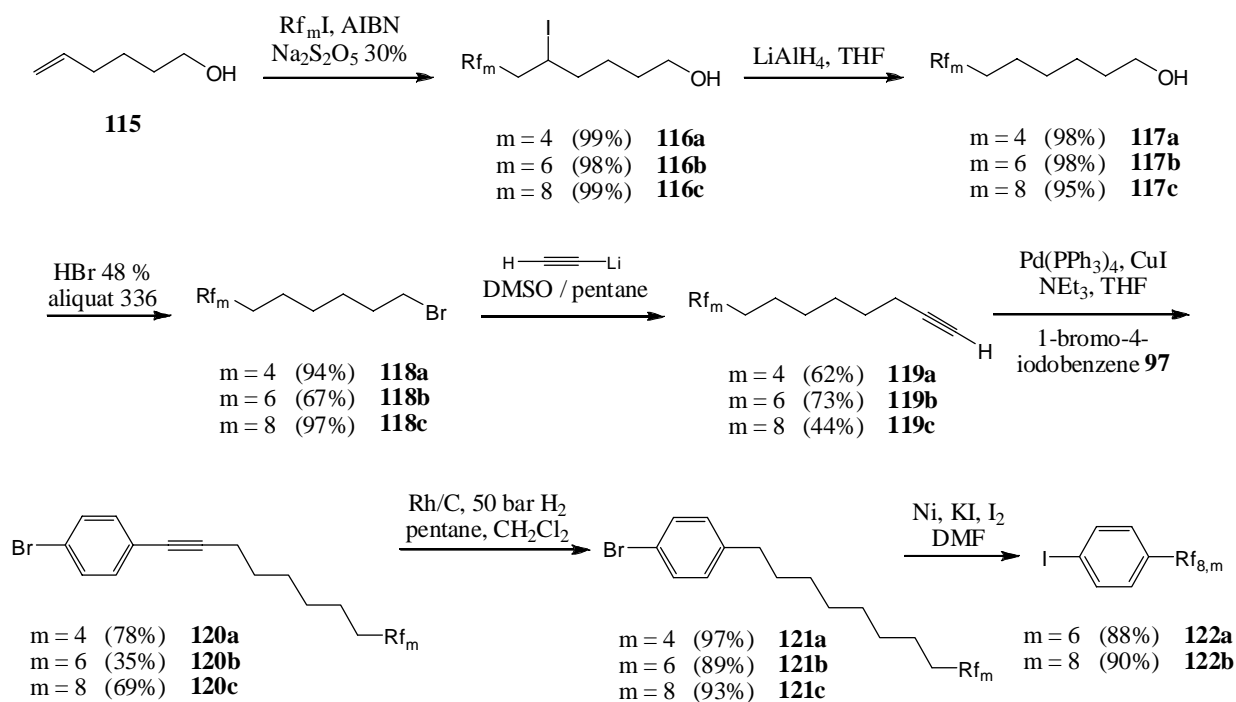
Planarization of HPB **113** was performed first by using iron(III)chloride in nitromethane and dichloromethane as solvent yielding only the starting compound, as the solubility was too low for a reaction to occur. Only by adding HFB as co-solvent the desired HBC **114** was obtained as slightly brown-yellow powder after several re-precipitations from BTF and HFB.



**Scheme 10.23** – Oxidation towards HBC **114**

## 10.7 HBC- $\text{Rf}_{8,4}$ , HBC- $\text{Rf}_{8,6}$ and HBC- $\text{Rf}_{8,8}$

*Synthetic strategy:* The synthesis of HBC derivatives bearing eight aliphatic carbon atoms as spacers in the lateral chains was realized *via* formation of perfluoroalkylated alkynes, which were coupled with a Sonogashira reaction to afford the substituted key bromoaryl derivatives. The Kumada cross coupling would have been an alternative, as using these long aliphatic spacers the electron withdrawing effect of the fluorines is completely eliminated and the solubility is increased at the same time. Unfortunately, the desired oct-7-en-1-ol is very expensive and its preparation proved to be laborious.<sup>[211b]</sup>

10.7.1 Synthesis of X-Ph-Rf<sub>8,m</sub>

**Scheme 10.24** – Reaction sequence to afford arylhalogenides carrying perfluorinated side chains in combination with eight hydrogenated carbons as spacer

Hex-5-en-1-ol **115** was reacted with the adequate perfluoroiodide **90a-c** using AIBN as radical initiator, which afforded after reduction with  $\text{LiAlH}_4$  the corresponding perfluoroalkyl alcohol **117a-c**. Bromination by hydrobromic acid with aliquat 336 as phase transfer catalyst furnished the halogenated derivatives **118a-c**, which were substituted with lithium acetylide to yield the desired eight aliphatic carbon spacer. Alkynes **119a-c** were subsequently coupled to 1-bromo-4-iodobenzene (**97**) in a Sonogashira reaction affording the brominated aryl analogues **120a-c**. It is worth mentioning that the yields of the alkyne formation as well as the consecutive Sonogashira reaction were well above the yields discussed in the earlier sections for similar products (c.f. chapter 10.5.1). One probable reason is the enlarged size of the aliphatic spacer, which certainly reduces the volatility due to increased Van der Waals forces. The Sonogashira cross-coupling was attempted several times under various conditions in order to improve the yield. As shown in Table 10.9, the simplest conditions (entry 3) primed over the more complicated ones (entry 2, 4 and 5), which involved *in situ* preformed zinc derivatives as active transmetalation species.

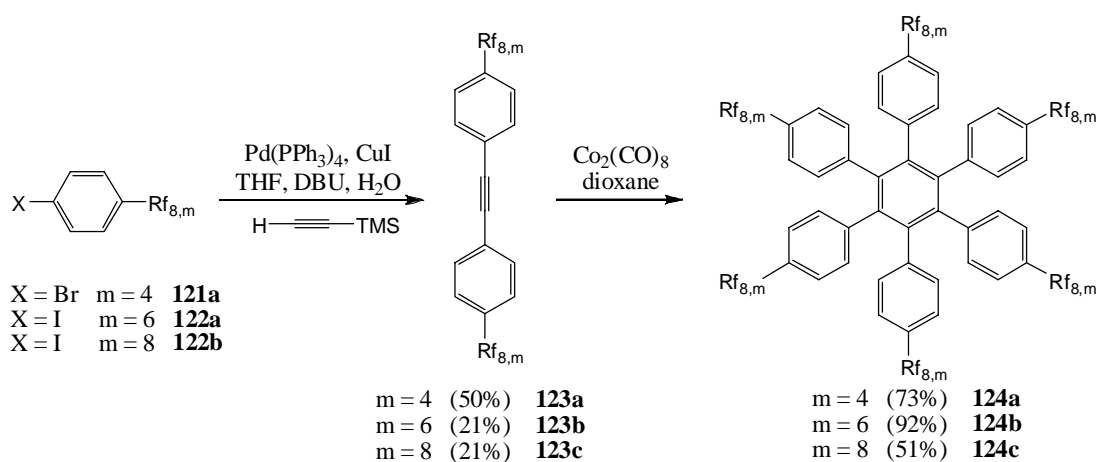
Final reduction of **120a-c** was achieved by treatment with rhodium on carbon under 60 bar of hydrogen. Halogen exchange was performed for two derivatives **121a** and **121b**.

**Table 10.9** – Optimisation for the Sonogashira cross-coupling between **97** and **119c**

Entry	Subst.	Addend [eq]	Catalyst [Mol%]	Solvent	Temp. [°C]	Time [d]	120c [%Yld]
1	<b>119c</b>	<b>97</b> (0.9) TEA (6)	Pd(PPh <sub>3</sub> ) <sub>4</sub> (6) CuI (10)	THF	r.t.	1	16
2	<b>119c</b>	<b>97</b> (0.8) TEA (4.8)	Pd(PPh <sub>3</sub> ) <sub>4</sub> (5) ZnBr <sub>2</sub> (1.2)	THF	r.t.	0.5	14
3	<b>119c</b>	<b>97</b> (1.0) TEA (6)	Pd(PPh <sub>3</sub> ) <sub>4</sub> (6) CuI (10)	THF	75	3	44 <sup>a</sup>
4	<b>119c</b>	<b>97</b> (0.8) TEA (4.8)	Pd(PPh <sub>3</sub> ) <sub>4</sub> (5) ZnBr <sub>2</sub> (1.2)	THF	75	3	28
5	<b>119c</b>	<b>97</b> (0.8) LDA (1.0)	Pd(PPh <sub>3</sub> ) <sub>4</sub> (5) ZnBr <sub>2</sub> (1.2)	THF	r.t.	3.5	10

<sup>a</sup> no starting material was found during the purification10.7.2 Synthesis of HPB-Rf<sub>8,m</sub>

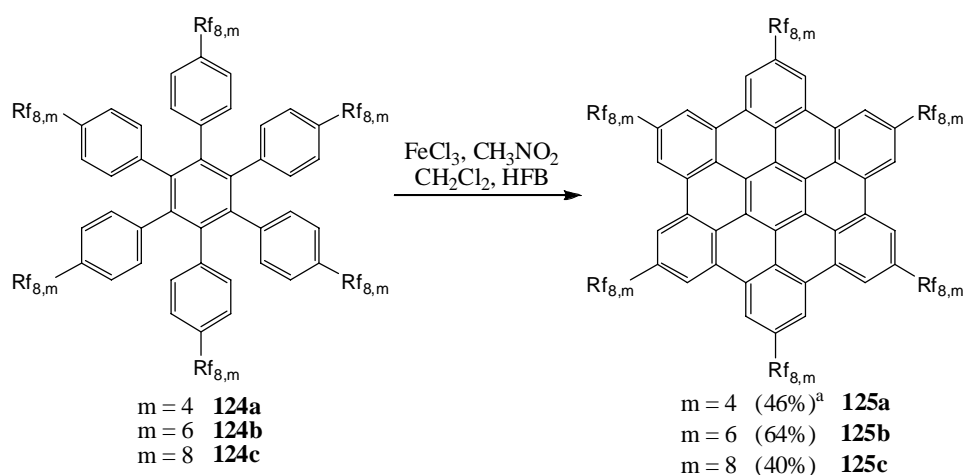
Tandem Sonogashira reaction using the brominated **121a** or the iodinated precursors **122a** and **122b** yielded the corresponding tolans **123a-c** in moderate to good yields. It seemed that the influence of the more reactive iodo group as compared to bromine is negligible in the presence of bulky perfluoroalkylated chains. Cobalt mediated cyclotrimerization afforded all three derivatives **124a-c** in moderate to good yields. It has to be noted that these HPB derivatives, bearing an eight carbon alkyl spacer terminated by a short perfluorinated part of four or six carbons (**124a** and **b**), are the first ones being oily instead of solid. This behaviour was up to now only reported for HBP derivatives bearing long and purely hydrogenated alkyl chains in their periphery.<sup>[103]</sup> HPB **124c**, carrying eight perfluorinated carbon atoms, was obtained again as powder.

**Scheme 10.25** – Tolane formation succeeded by cyclotrimerization yielding HPB derivatives

10.7.3 Synthesis of HBC-Rf<sub>8,m</sub>

The oxidation of the very soluble oily HPB derivatives **124a** and **124b** was carried out under standard conditions whereas for HPB **124c** a small amount of HFB had to be added in order to obtain a homogeneous solution. All three HBC derivatives were collected at the end of the reaction by suction filtration on Millipore® as very dark powders. Despite of the fact that the HBCs **125a** and **125b**, bearing short perfluorinated parts, were even moderately soluble in common organic solvents such as ether or dichloromethane, their purification proved to be even more time consuming. Due to the high solubility silica gel filtration using hot BTF, hot toluene, ether or dichloromethane was attempted with the result that the HBC stacked irreversibly to the silica gel. Separation over preparative TLC plates afforded an observable separation but it was found impossible to recover the compound from the solid support afterwards. Because of that, standard procedures were applied, consisting of the formation of suspensions and subsequent filtrations yielding HBC **125b** as dark yellow solid whereas HBC **125a** remained a dark powder. MALDI-TOF analysis of HBC **125a** revealed finally chlorination (up to five times) of the target HBC. Probably the chlorine insertion was provoked by the high solubility of the corresponding HPB derivative, as even at room temperature chlorination occurred.

HBC **125c** with its eight perfluorinated carbons showed a rather low solubility. Because of that purification was directly attempted by suspending HBC **125c** in common organic solvents followed by suction filtration over Millipore®. Unfortunately the black impurity could not be removed by this way. Only repeated precipitations out of refluxing 1,2,4-TCB afforded HBC **125c** as dark yellow solid.



**Scheme 10.26** – Planarization affording HBC derivatives **125**; <sup>a</sup> mixture with chlorinated derivatives



## 11 HBC carrying branched perfluorinated side chains

### 11.1 Introduction

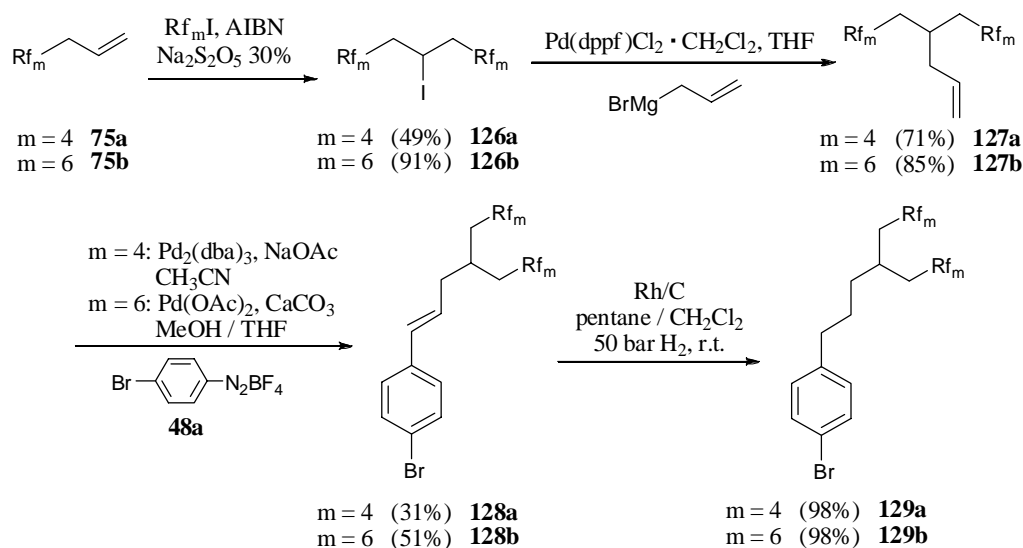
In order to further increase the fluorine coating of the HBC columnar stack, another class of HBC derivatives carrying branched perfluoroalkylated side chains was designed. The branched six carbon aliphatic spacer carries two perfluorobutyl or perfluorohexyl parts, which decrease the perfluoro / alkyl ratio, and therefore the density of the fluorine coating enormously. Moreover, a derivative carrying only three side chains instead of six was prepared.

### 11.2 HBC-Rf<sub>3,3,6,6</sub> and HBC-Rf<sub>3,3,4,4</sub>

*Synthetic strategy:* The lateral branched perfluoroalkylated side chain is most favourably made with a terminal double bond as only functional group. Because of that, the key step of this synthesis consists in the performance of a successful Heck cross-coupling between the unsaturated chain and a brominated aryl diazonium salt. It was nevertheless found, that the large and stiff perfluorinated parts hinder the reaction of the unsaturated chains.

#### 11.2.1 Synthesis of Br-Ph-Rf<sub>3,3,6,6</sub> and Br-Ph-Rf<sub>3,3,4,4</sub>

The addition of a second perfluorinated tail onto perfluoroalkylated allyl derivatives **75a** and **75b** proved to work smoothly but required in general longer reaction times and addition of several portions of the radical initiator.



**Scheme 11.1** – Preparation of branched perfluoroalkylated side chains and their subsequent Heck reaction

The subsequent Kumada reaction was found to be very tricky as the reaction was very sensitive to the applied condition. It is crucial, that the allylmagnesium bromide addition was carried out slowly over several hours at 0°C as otherwise many side products were formed.

Molecular modelling of compound **127b** showed a rather stiff T-shaped geometry of the perfluorinated part which renders the whole molecule sterically very demanding. This is certainly the reason for the difficult Heck reaction between **127a** and **127b** and a reactive aryl diazonium salt. Even the optimized and modified protocol afforded the desired compound in only moderate yield at best, as summarized in Table 11.1. Subsequent hydrogenation of the double bond afforded the desired aryl derivative carrying branched perfluoroalkylated side chains quantitatively.

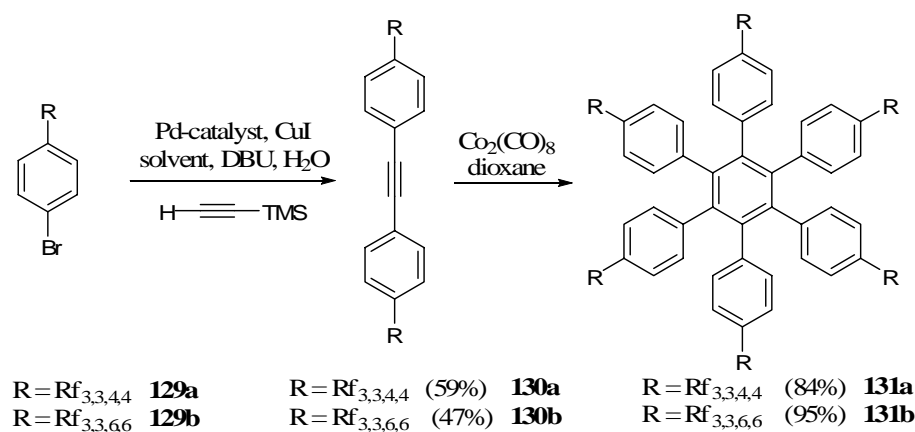
**Table 11.1** – Various conditions applied on the Heck coupling

Entry	Subst.	Reagent [eq]	Additive [eq]	Solvent	Temp. [°C]	Time [h]	Product [%Yld]
1	<b>127b</b>	<b>48a</b> (1)	Pd(OAc) <sub>2</sub> (0.01)	MeOH	40	2	- <sup>a</sup>
2	<b>127b</b>	<b>48a</b> (1)	Pd(OAc) <sub>2</sub> (0.02) CaCO <sub>3</sub> (1)	MeOH	40	4	<b>128b</b> 24
3	<b>127b</b>	<b>48b</b> (1)	Pd/CaCO <sub>3</sub> (0.02) CaCO <sub>3</sub> (1)	MeOH	40	2	- <sup>a</sup>
4	<b>127b</b>	<b>48b</b> (1)	Pd(OAc) (0.02) Cs <sub>2</sub> CO <sub>3</sub> (1) IPr HCl (0.04)	MeOH	40	1	- <sup>a</sup>
5	<b>127b</b>	<b>48a</b> (0.5)	Pd(OAc) (0.1) P( <i>o</i> -Tol) <sub>3</sub> (0.4) NEt <sub>3</sub> (1.5)	toluene	50	5	- <sup>a</sup>
6	<b>127b</b>	<b>48a</b> (1)	Pd(OAc) (0.02)	MeOH THF	50	1	- <sup>a</sup>
7	<b>127b</b>	<b>48a</b> (1)	Pd(OAc) (0.02) CaCO <sub>3</sub> (1)	MeOH THF	45	48	<b>128b</b> 51
8	<b>127a</b>	<b>48a</b> (1.1)	Pd <sub>2</sub> (dba) <sub>3</sub> (0.015) NaOAc (3.5)	CH <sub>3</sub> CN	r.t. to 60	16	<b>128a</b> 31

<sup>a</sup> compound **127b** was recovered quantitatively

11.2.2 Synthesis of HPB-Rf<sub>3,3,6,6</sub> and HPB-Rf<sub>3,3,4,4</sub>

Conversion of the brominated aryl derivatives **129a** and **129b** with their branched chains to the corresponding tolans was performed by tandem Sonogashira reactions. Purification was achieved for both derivatives by column chromatography over silica gel using pentane as eluent. It is worth mentioning that tolans **130a** and **130b** are the first tolans, which passed easily silica gel. Other derivatives i.e. Tol-Rf<sub>4,8</sub> (**91c**) have been lost on column as even with ether the product remained absorbed on the silica gel. Moreover, the branched T-shaped lateral chain seems to impede considerably the  $\pi$ - $\pi$ -aggregation of the central part as **130a** and **130b** are the first reported tolans, which are obtained as oils instead of solids. Due to the high solubility and purity of the corresponding tolans, Co<sub>2</sub>(CO)<sub>8</sub> mediated cyclotrimerization afforded the desired hexaphenylbenzene derivatives **131a** and **131b** in high yield, again as oily compounds, which had to be purified by column chromatography. The oily consistence of HPB derivatives was already mentioned in literature for compounds, which carry long linear (>C<sub>12</sub>) or branched alkyl chains in their periphery.

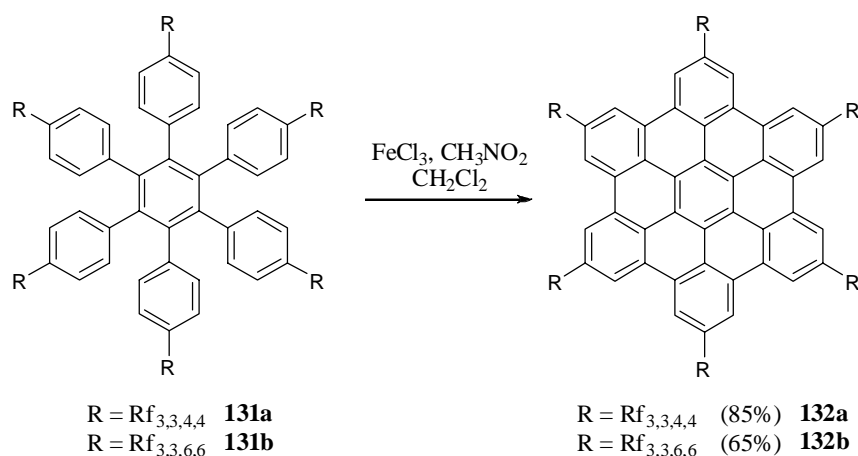


Scheme 11.2 – Sonogashira reaction and subsequent cyclotrimerization

11.2.3 Synthesis of HBC-Rf<sub>3,3,6,6</sub> and HBC-Rf<sub>3,3,4,4</sub>

The oxidation of HPB **131a** and **131b** was performed under mild FeCl<sub>3</sub> conditions. As solvent dichloromethane was largely sufficient as both starting materials were oils and therefore readily dissolved in dichloromethane. The purification of HBC **132a** was performed by the usual way of precipitating the HBC from BTF and HFB solution by the addition of ether, pentane and methanol, which yielded finally the desired HBC **132a** as yellow powder.

In the case of HBC **132b**<sup>[205]</sup> the obtained product behaved like a molten glass, which rendered Milipore<sup>®</sup> filtration impossible. Because of that different organic solvents such as ether, pentane or methanol were added. The suspensions were then treated in an ultrasonic bath and after sedimentation of the oily HBC the solvents were removed by canula decantation yielding finally HBC **132b** as a dark oily substance.

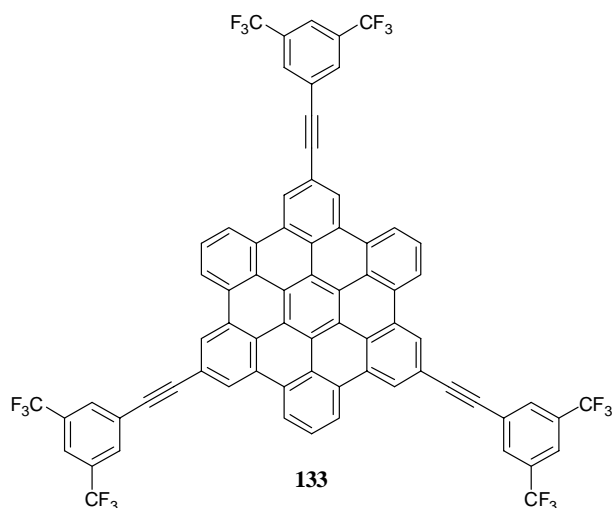


**Scheme 11.3** – Oxidation towards HBC derivatives carrying branched lateral chains

### 11.3 HBC-Rf<sub>(3,3,6,6)</sub><sub>3</sub> – a HBC derivative in D<sub>3h</sub> symmetry

HBC moieties carrying six identical lateral chains suffer from increased sterical hindrance of the  $\pi$ - $\pi$  stacking, especially in the case of branched chains (HBC **132a** and **132b**) due to the stiffness of the perfluoroalkylated end parts. By reducing the number of chains from six to three, one can imagine a reduction of the sterical hindrance occurring in the self-assembly process as from one disc to the other a 60° turn would place each lateral chain into the gap of the neighbouring molecule.

To investigate derivatives with D<sub>3h</sub> symmetry, a completely new compound was designed, where furthermore the perfluoroalkylated side chains were replaced by a completely stiff geometry consisting of an alkynearyl carrying two CF<sub>3</sub> groups. This HBC derivative is the first of a new class, bearing an alkyne in the lateral chain, a motive which is impossible to achieve in the traditional approach using cyclotrimerization. The synthesis and investigation of this HBC (**133**, shown in Scheme 11.4) was performed by Mauro Schindler during his Master Thesis.<sup>[228]</sup>



**Scheme 11.4** – HBC derivatives bearing rigid phenyl acetylene side chains

### 11.3.1 Synthesis of *m*-substituted aryl derivatives



Nevertheless new conditions were found in the literature and tested subsequently. The first method, known as the Jeffery conditions, uses common Pd(OAc)<sub>2</sub> as catalyst under solid-liquid phase transfer conditions (tetrabutylammoniumbisulfate as the phase transfer agent and sodium bicarbonate as base<sup>[229]</sup>). As shown in entry 1 of Table 11.2 these conditions failed again in our case. The only conditions which afforded the desired derivative **135a**, were the use of a very reactive catalyst known as Herrmann-Beller palladacycle,<sup>[230]</sup> which was employed at a level of only 0.1 Mol%. A binary DMF / BTF solvent system was used to ensure a homogenous mixture. The reaction was then heated to 125°C for 4 days. It has to be noted, that the reaction commonly furnished three isomers (**135a-c**), out of which **135a** and **b** yield an identical product after hydrogenation, whereas **135c** had to be eliminated by column chromatography. The formation of **135c** should theoretically

be prevented by the addition of an additional ligand which hinders the formation of palladium black, made responsible for the undesired product, or by variation of the base.<sup>[191a]</sup> The different conditions applied are summarized in Table 11.2.

Hydrogenation of **135a** and **b** was first attempted with Rh/C under 60 bar of hydrogen, which is known to be a very mild hydrogenation catalyst. As shown in Table 11.2 this was not at all the case by using TMS substituted aryl derivatives, as not only the TMS group was cleaved off, but the aromatic core was hydrogenated too. It could not be elucidated, why the mild rhodium hydrogenated even the aromatic core, yielding the cyclohexane derivative **136c** bearing the branched perfluorinated chain. By using Pd/C as catalyst under 3 bar of hydrogen in methanol / THF, a mixture of the desired compound **136a** was found in combination with the desililated derivative **136c**. By reducing both the hydrogen pressure to 1.5 bar and the time to 15 minutes the yield of compound **136a** could be increased to 99%.

The TMS group was then subsequently transformed either into an iodo group by treatment with ICl, or into the boronic acid analogue as illustrated in Scheme 11.5.

**Table 11.2** – Optimization of the Heck reaction and the subsequent hydrogenation of the double bond

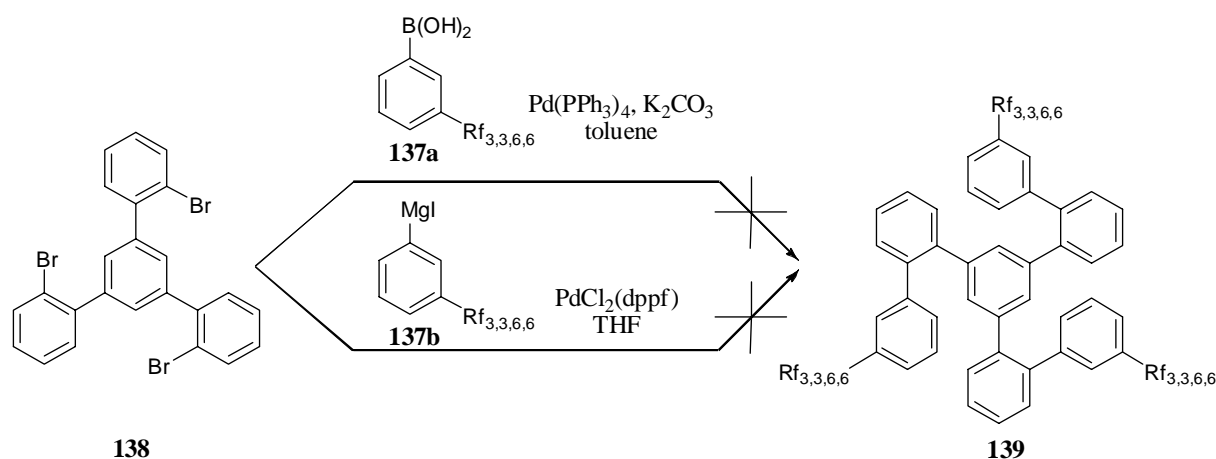
Ent.	Subst. [eq]	Catalyst [Mol%]	Additive [eq]	Solvent	Temp. [°C]	Time [h]	Product [%Yld]
1	<b>134</b> (1)	Pd(OAc) (4)	NaHCO <sub>3</sub> (2.5)	DMF	90	96	<b>135a</b> (-)
	<b>127b</b> (0.25)		<i>n</i> -Bu <sub>4</sub> NHSO <sub>4</sub> (1)	BTF			
2	<b>134</b> (1)	Palladacycle (0.1)	KOAc (1.3)	DMF	125	96	<b>135a</b> (22) <sup>a</sup>
	<b>127b</b> (0.25)			BTF			<b>135b</b> (16)
3	<b>134</b> (1)	Palladacycle (0.1)	KOAc (1.3)	DMF	125	24	<b>135c</b> (9)
	<b>127b</b> (0.8)			BTF			<b>135a</b> (35)
4	<b>135a</b> (1)	Rh/C (5)	H <sub>2</sub> 60 bar	pentane	r.t.	17	<b>136c</b> (95)
5	<b>135a</b> (1)	Pd/C (10)	H <sub>2</sub> 3 bar	CH <sub>2</sub> Cl <sub>2</sub>	r.t.	4	<b>136a</b> (74)
				MeOH			<b>136b</b> (21)
6	<b>135a</b> (1)	Pd/C (10)	H <sub>2</sub> 1.5 bar	THF	r.t.	15 min	<b>136a</b> (99)

<sup>a</sup> determined by GC-MS

## 11.3.2 Threefold aryl-aryl Suzuki and Kumada cross-coupling reactions

The Suzuki cross-coupling was attempted using standard conditions, i.e.  $\text{Pd}(\text{PPh}_3)_4$ , and an aqueous solution of  $\text{K}_2\text{CO}_3$  in toluene. After the reaction only the starting compound **138**<sup>[138]</sup> was found together with compound **136b**, which had lost the boronic acid. No trace of the coupled product was found by  $^1\text{H}$ -NMR analysis. The negative result may be explained by sterical hindrance and the deactivating *meta* substituents.

A Kumada cross-coupling was attempted as second strategy. First, the iodoaryl **137b** was transformed to its Grignard derivative. Addition of iodine and dibromoethane was needed in order to observe the consumption of the magnesium turnings. But at the end only the starting compounds **138** and **137b** were recovered, indicating that the Grignard derivative had not been formed at all. Moreover, the recovery of the unreacted starting materials underlines the low reactivity of the compounds as else at least the iodo group should have been cleaved off by the palladium catalyst. Due to the difficulties encountered another strategy was attempted, described in the next chapter.



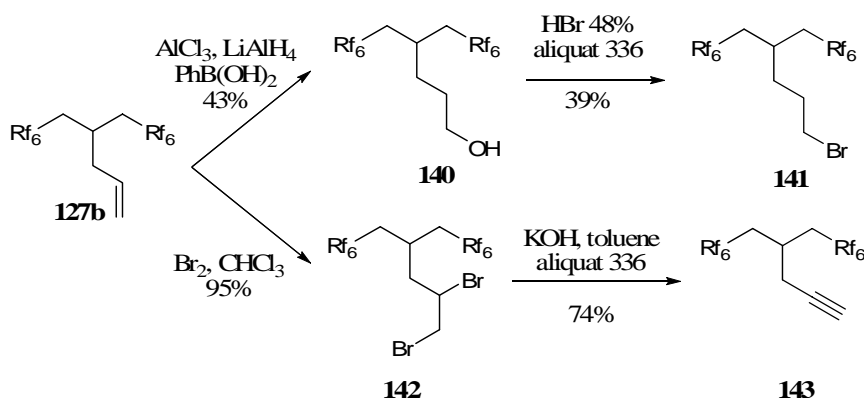
Scheme 11.6 – Suzuki and Kumada cross-coupling attempts for the preparation of **139**

## 11.3.3 Threefold aryl-alkyl Heck, Kumada or Sonogashira cross-coupling

As an alternative strategy for the preparation of HPB **139** remained several threefold cross-coupling reactions directly onto the previously prepared core structure **144**<sup>a</sup>. Heck, Kumada and Sonogashira coupling reactions were attempted, which needed the preparation of the appropriate perfluoroalkylated branched side chains, as described in Scheme 11.7. Anti-Markovnikov functionalization of an olefin was performed by a highly regio-selective organoborane-catalyzed hydroalumination yielding exclusively the desired isomer **140** in moderate yield,<sup>[231]</sup> which was subsequently transformed into **141** by exchange of the alcohol by bromide.

<sup>a</sup> the synthesis of **144** is described elsewhere<sup>[228]</sup>

The conversion of alkenes to alkynes is best performed by bromination (yielding the corresponding 1,2-dibromoalkene derivative **142** in excellent yield) and subsequent double elimination of hydrogen bromide (affording the terminal alkyne **143**). Many different protocols for the elimination had been reported, most of them using  $\text{KO}t\text{Bu}$  as base,<sup>[232]</sup> which proved ineffective for perfluorinated derivatives such as **142**. Another protocol, however, using  $\text{KOH}$  in toluene together with a phase transfer catalyst<sup>[233]</sup> finally afforded **143** as exclusive product in good yield.



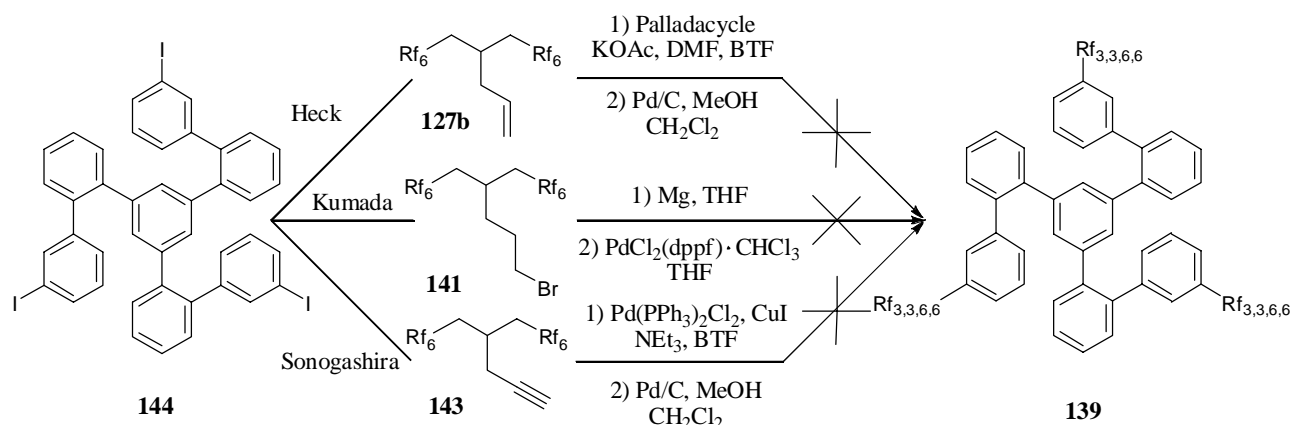
**Scheme 11.7** – Preparation of alkyne and bromide analogue of **127b** for Kumada and Sonogashira cross-coupling attempts

Heck reaction of **144** with **127b** was attempted by the optimized conditions, described previously (chapter 11.3.1). Unfortunately the reaction did not yield any trace of the desired product **139**; both starting materials were recovered. It seems that either compound **144** is still deactivated through the hindering *meta* effect, or that the sterical hindrance of **144** is too large for a successful transformation.

The Kumada cross-coupling reaction was attempted with the Grignard derivatives of **141**. For this reaction the optimized conditions obtained during the twofold Kumada cross-coupling of toluene derivatives (c.f. chapter 10.4.3) were used. Unfortunately only the starting material **144** together with the debrominated analogue of **141** were found in the crude reaction mixture, as shown by  $^1\text{H}$ -NMR spectroscopy.

Finally the Sonogashira reaction was tried, known to be a versatile and reliable cross-coupling method. The conditions had previously been optimized with the reaction of **143** and 1-bromo-4-iodobenzene. The optimal conditions noted in Scheme 11.8 afforded a nearly quantitative transformation for the test reactions but did not allow the preparation of **139**. It is hence probable that compound **144** is sterically too hindered.



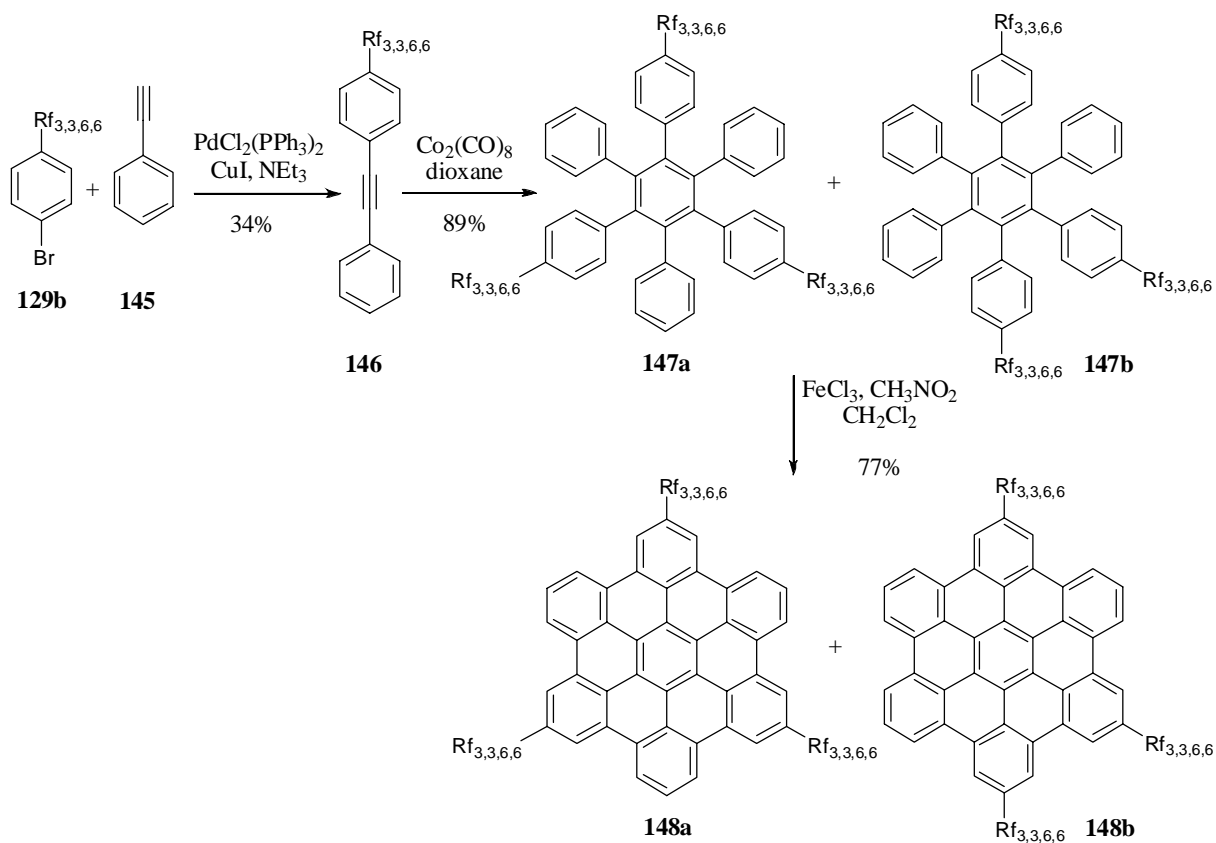


**Scheme 11.8** – Heck, Kumada and Sonogashira attempt for the preparation of **139**

#### 11.3.4 Synthesis of an isomeric mixture of HBC- $\text{Rf}_{(3,3,6,6)}_3$

The reason for the attempted preparation of HBC **148a** was the unknown influence of a reduced number of side chains in the periphery of the HBC core. As all attempts of the direct preparation of HPB **139** failed so far, a different strategy was attempted affording two isomers, HPB **147a** and **147b**. But even the mixture of these compounds will give an insight of the influence of the number of substituents.

A Sonogashira cross-coupling between the bromo aryl **120b** and phenylacetylene **145** afforded under standard conditions the unsymmetric tolane **146** which was cyclotrimerized using  $\text{Co}_2(\text{CO})_8$ . The two possible isomers **147a** and **147b** were obtained in a one to one ratio, which is quite surprising since isomer **147b** is sterically much more hindered than its counterpart **147a**. A separation of the two products was attempted by column chromatography but even with a pentane – ether mixture (49:1) both compounds eluted as inseparable mixture. Oxidation of the mixture was finally done using the mild  $\text{FeCl}_3$  conditions which furnished after standard work-up HBCs **148a** and **148b** as bright yellow powder.



**Scheme 11.9** – Preparation of the HBC derivatives **148a** and **b** bearing three branched perfluorinated chains

## 12 HBC primer

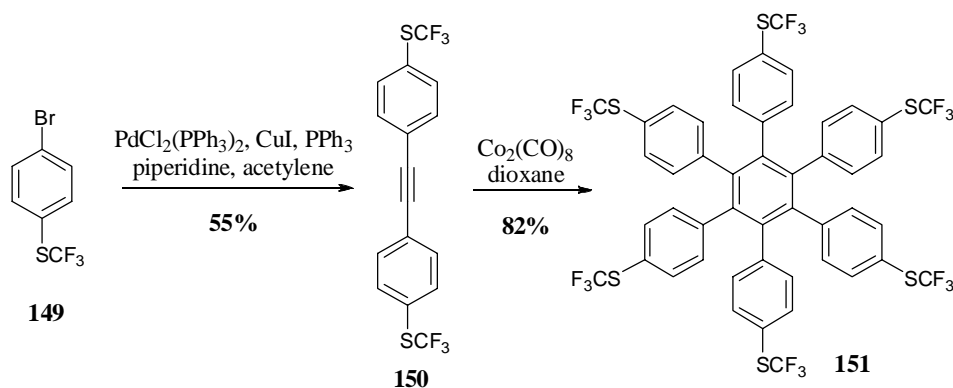
### 12.1 Introduction

The aim for the synthesis of HBC primer derivatives is to use them as template molecules, or so called “docking stations” on a specific substrate, onto which other HBC derivatives bearing long perfluoroalkylated side chains can be deposited in order to create a well ordered, regular array of monocolumnar architectures. A possible substrate for such deposition attempts would be a gold surface. Because of this we attempted to prepare HBC moieties bearing sulphur atoms in their periphery, as sulphur is known to have a good adhesion on gold.<sup>[234]</sup> Up to date no HBC derivative bearing sulphur in the periphery is known in the literature, whereas oxygenated HBCs have already been reported.<sup>[121, 235]</sup> HBCs bearing an alkoxy substituent directly attached to the aromatic core have the disadvantage that they cleave in many cases their alkyl substituents during the final oxidation to form quinonoid like structures.<sup>[236]</sup> Because of this it is very likely, that sulfurated analogues react in a similar way. Therefore our primer HBCs were designed with respect to the following concepts: *i*) attachment of a substituted sulphur, which can not loose its substituent easily as for example SCF<sub>3</sub>; *ii*) intercalation of a benzyl carbon between the heteroatom and the aromatic core in order to prevent the quinonoid formation. Further the benzyl offers yet another advantage as a further degree of freedom is offered to the anchoring sulphur atom, which can now much better bind to the gold surface.

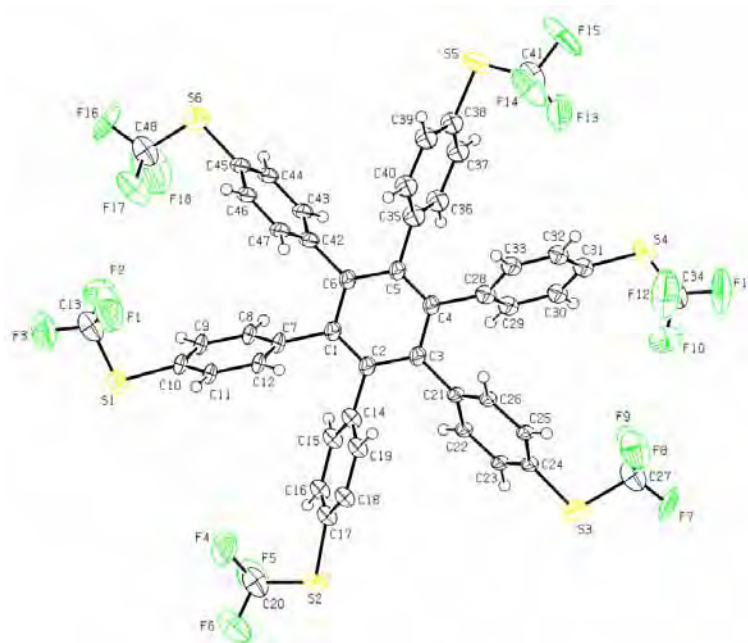
Another important point is the choice of an appropriate protecting group for the sulphur atom, which should respect the following three criteria: *i*) stable enough to resist the applied reaction conditions to stay intact until the desired HBC is formed; *ii*) reactive enough to cleave easily on the gold surface; *iii*) cleave at the right position, *i.e.* the sulphur has to stay on the HBC moiety. The synthesis of several derivatives was envisaged bearing all a benzyl spacer except for one derivative.

### 12.2 HBC-SCF<sub>3</sub>

*Synthetic strategy:* Due to the fact that the arylbromide bearing the desired SCF<sub>3</sub> group is commercially available, only the one-pot Sonogashira cross-coupling remains a competitive strategy and offers a direct access to the desired HBC in only three steps. HBC **152** has already been reported in the thesis of Bassam Alameddine<sup>[130]</sup> with a slightly different synthesis.

12.2.1 Synthesis of HPB-SCF<sub>3</sub>Scheme 12.1 – Preparation of SCF<sub>3</sub> substituted HPB **151**

The one-pot Sonogashira reaction producing tolane **150** was performed slightly different than previously discussed. The starting bromide **149** was reacted in the presence of  $\text{PdCl}_2(\text{PPh}_3)_2$ ,  $\text{CuI}$ ,  $\text{PPh}_3$  and piperidine with acetylene which was bubbled through the reaction mixture for several hours before stirring was continued without further bubbling. Standard work up afforded tolane **150** as slightly yellow needles after crystallisation in good yield. Subsequent trimerization under standard condition afforded HPB **151**. As HBP **151** was the only hexaphenylbenzene derivative which crystallized suitably, a single crystal X-ray crystallography structure determination was performed in order to compare the conformation of **151** with literature structures of other HPB derivatives.<sup>[161]</sup> The phenyl rings in the six arms of the star adopt a “paddle-wheel” configuration with twist angles out of the plane of the central benzene ring between 55 and 75°, identical to the values obtained by other groups<sup>[237]</sup> for other HPB derivatives. The molecular structure is shown in Figure 12.1.

Figure 12.1 – X-ray structure of HPB **151**

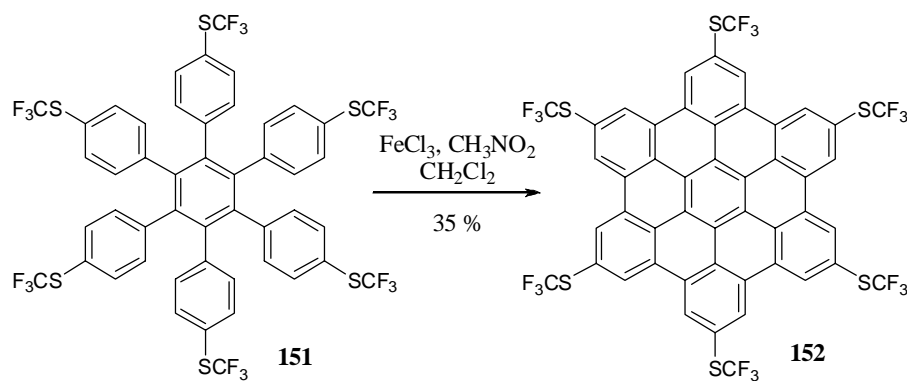
12.2.2 Synthesis of HBC-SCF<sub>3</sub>

Despite the fact that hexaphenylbenzene **151** is very soluble in dichloromethane and should therefore readily react in the oxidation reaction using FeCl<sub>3</sub> severe problems were encountered. Table 12.1 summarizes all attempts to prepare HBC **152**. As it can be noted, different variations including the amount of FeCl<sub>3</sub>, nitromethane / dichloromethane ratio, reaction time, iron(III)chloride addition speed, iron(III)chloride addition temperature and additive were attempted in order to optimize the reaction conditions. Unfortunately no systematic effect could be deduced. Even by applying “exotic” conditions as H<sub>2</sub>SO<sub>4</sub> without CH<sub>3</sub>NO<sub>2</sub><sup>[238]</sup> or AlCl<sub>3</sub> no systematical improvement was observed.

Table 12.1 – Attempts for the oxidation of HPB **151**

Entry	Subst.	Reagent [eq/ eq <sup>a</sup> ]	Additive [mL]	Solvent	Temp. [°C]	Time [h]	<b>152</b> [%Yld]
1	<b>151</b>	FeCl <sub>3</sub> (48/4)	CH <sub>3</sub> NO <sub>2</sub> (14)	CH <sub>2</sub> Cl <sub>2</sub> (50)	r.t. to 45 <sup>b</sup>	9	- <sup>c</sup>
2	<b>151</b>	FeCl <sub>3</sub> (90/7.5)	CH <sub>3</sub> NO <sub>2</sub> (14)	CH <sub>2</sub> Cl <sub>2</sub> (60)	r.t. to 45 <sup>b</sup>	8	- <sup>c</sup>
3	<b>151</b>	FeCl <sub>3</sub> (18/1.5)	H <sub>2</sub> SO <sub>4</sub> (0.01)	CH <sub>2</sub> Cl <sub>2</sub> (1)	r.t.	14	-
4	<b>151</b>	FeCl <sub>3</sub> (60/5)	CH <sub>3</sub> NO <sub>2</sub> (3)	CH <sub>2</sub> Cl <sub>2</sub> (35)	r.t. to 45 <sup>b</sup>	168	26 <sup>d</sup>
5	<b>151</b>	FeCl <sub>3</sub> (60/5)	CH <sub>3</sub> NO <sub>2</sub> (3) BTF (20 mL)	CH <sub>2</sub> Cl <sub>2</sub> (20)	r.t. to 45 <sup>b</sup>	12	- <sup>c</sup>
6	<b>151</b>	FeCl <sub>3</sub> (60/5)	CH <sub>3</sub> NO <sub>2</sub> (35)	CH <sub>2</sub> Cl <sub>2</sub> (200)	45 <sup>e</sup>	96	35 <sup>d,f</sup>
7	<b>151</b>	FeCl <sub>3</sub> (90/7.5) <sup>g</sup>	CH <sub>3</sub> NO <sub>2</sub> (12)	CH <sub>2</sub> Cl <sub>2</sub> (54)	r.t. to 45 <sup>b</sup>	16	-
8	<b>151</b>	AlCl <sub>3</sub> (36/3)	Cu(OTf) <sub>2</sub> (36 eq)	CS <sub>2</sub> (25)	r.t. to 35 <sup>b</sup>	15	-

<sup>a</sup> equivalents per hydrogen to be removed; <sup>b</sup> the FeCl<sub>3</sub> / CH<sub>3</sub>NO<sub>2</sub> solution was added at r.t.; <sup>c</sup> the starting HPB **151** was isolated quantitatively; <sup>d</sup> no confirmation by MALDI-ICR but absorption revealed typical HBC bands; <sup>e</sup> addition at 45°C; <sup>f</sup> impure material; <sup>g</sup> added with the syringe pump over 8 hours; entries 3, 7 and 8 were performed by Benoît Dubray during his practical work

Scheme 12.2 – Oxidation of HPB **151**

A further problematic point appearing after the oxidation was the difficulty in characterization of the obtained yellow product. Absorption spectroscopy indicated very nicely the characteristic bands of an HBC core. Nevertheless this is not sufficient to prove the presence of the desired HBC **152**. Unfortunately neither MALDI-ICR nor MALDI-TOF revealed the desired molecular peak. Either the substance is only hardly ionized or the presence of impurities hampers the ionization process. MALDI-ICR spectra were only available from a bright yellow powder, obtained from the pentane filtrate of a Millipore® filtration of the crude sample (Table 12.1, entry 6). This highly soluble substance contained effectively HBC cores, which had suffered chlorination that rendered them soluble due to a hindered  $\pi$ - $\pi$  stacking induced by the bulky chlorines in the periphery.

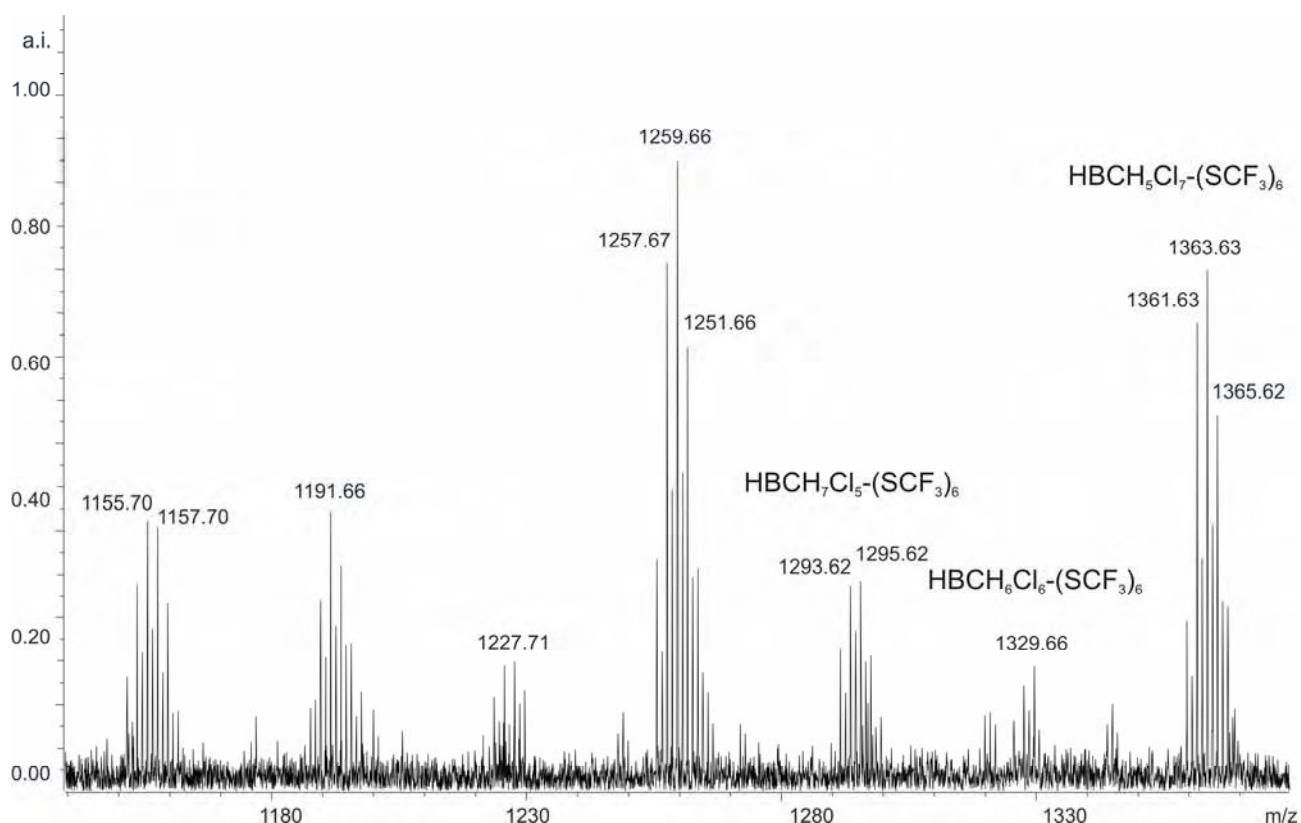
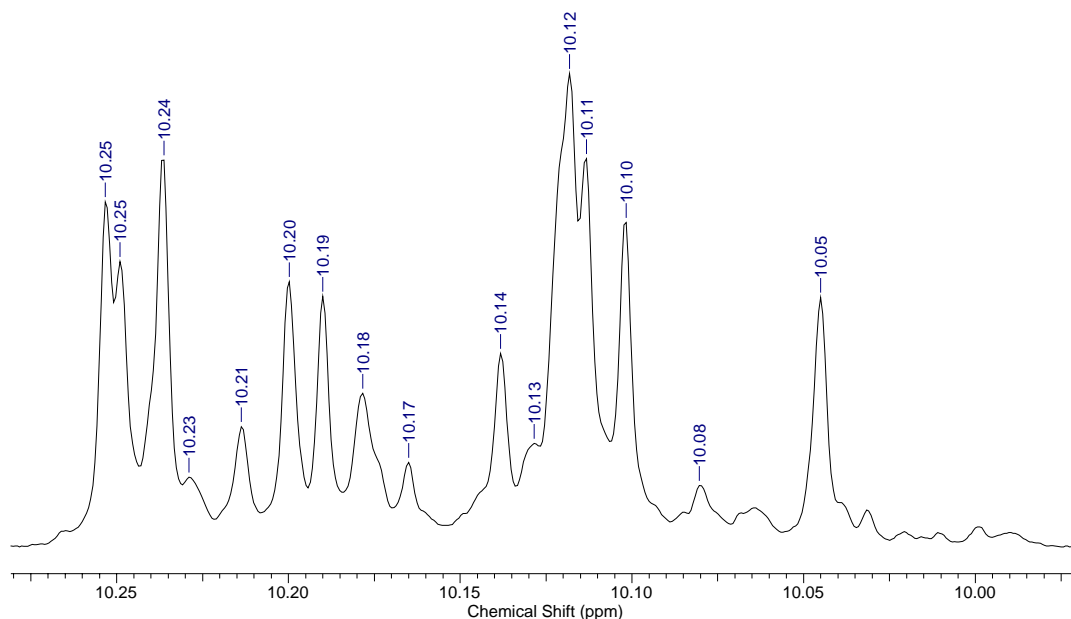


Figure 12.2 – MALDI-ICR spectrum of HBC **152**

Figure 12.2 shows a part of such a spectrum, revealing the presence of a series of HBC-(SCF<sub>3</sub>)<sub>6</sub> species bearing 5, 6 or even 7 chlorines in their periphery. The number of chlorines was deduced by comparing the isotopic pattern with simulated ones. The other signals shown in the spectrum could not definitely be attributed. It could not be elucidated if the signals are due to fragmentation during the MALDI-ICR measurement, or if they are produced during the oxidation.

Furthermore, the <sup>1</sup>H-NMR spectrum reveals only the presence of several HBC derivatives, as indicated by the large number of singlets in the aromatic region underlining the presence of several different HBC derivatives as shown in Figure 12.3. Unfortunately their chemical shift does not allow for attributing structures.



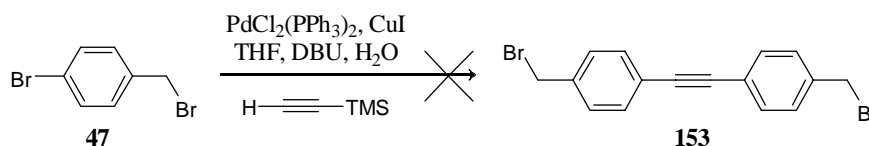
**Figure 12.3** –  $^1\text{H}$ -NMR spectrum of impure HBC **152**, measured in  $\text{CDCl}_3$

### 12.3 HBC- $\text{CH}_2\text{S}$ -*t*-butyl and HBC- $\text{CH}_2\text{S}$ - $\text{C}_{12}\text{H}_{25}$

*Synthetic strategy:* The preparation of benzylthio substituted HBC derivatives is very closely related to the strategy followed in the previous section for the preparation of HBC **152** with the only difference that the desired aryl derivative had first to be synthesized.

#### 12.3.1 Synthesis of HPB- $\text{CH}_2\text{S}$ -*t*-butyl and HPB- $\text{CH}_2\text{S}$ - $\text{C}_{12}\text{H}_{25}$

Because it was *a priori* not clear, if a thiobenzyl derivative, such as **155a** or **155b**, would resist the Sonogashira cross-coupling conditions, the preparation of a 4,4'-dibenzylbromide-tolane **153** was planned. Bromobenzyl bromide **47a** proved to be too reactive to resist the reaction conditions, since a polymer was formed at room temperature even prior to the TMSA addition.



**Scheme 12.3** – Attempted unsuccessful Sonogashira reaction of bromobenzyl bromide **47a**

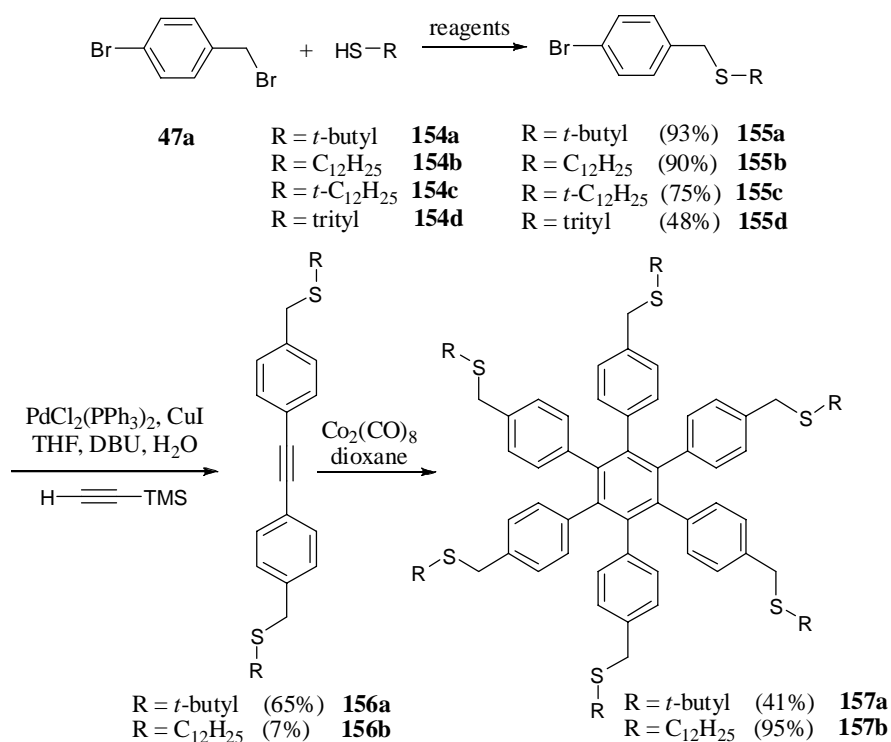
Different successful attempts were carried out to react a thiol with bromobenzylbromide **47a**. As summarized in Table 12.2 the cheapest access to derivatives of this type is the use of sodium carbonate in DMF together with bromobenzyl bromide **47a** and an appropriate thiol. These rather mild conditions allowed even the preparation of a trityl protected derivative.

**Table 12.2** – Conditions used for the preparation of substituted bromobenzyl thiol derivatives

Entry	Subst.	HS-R [eq]	Additive [eq]	Solvent	Temp. [°C]	Time [h]	155x [%Yld]
1	<b>47a</b>	<i>t</i> -butyl (1.1)	KH (1)	THF (100)	0 to r.t.	16	<b>a</b> (93)
2	<b>47a</b>	trityl (1)	KH (1)	THF (100)	0 to r.t.	17	<b>d</b> (45) <sup>a</sup>
3	<b>47a</b>	trityl (1)	Na (1.02)	EtOH (12)	80	16	<b>d</b> (65)
4	<b>47a</b>	trityl (1.2)	Cs <sub>2</sub> CO <sub>3</sub> (2)	DMF (8)	r.t.	16	<b>d</b> (-) <sup>a</sup>
5	<b>47a</b>	trityl (1.2)	Cs <sub>2</sub> CO <sub>3</sub> (2)	DMF (8)	r.t.	3	<b>d</b> (48)
6	<b>47a</b>	<i>t</i> -dodecyl (1.3)	Cs <sub>2</sub> CO <sub>3</sub> (2.6)	DMF (40)	r.t.	3	<b>d</b> (75) <sup>b</sup>
7	<b>47a</b>	dodecyl (1.3)	Cs <sub>2</sub> CO <sub>3</sub> (2.6)	DMF (20)	r.t.	3	<b>d</b> (90)
8	<b>47a</b>	dodecyl (1.3)	Na <sub>2</sub> CO <sub>3</sub> (2.6)	DMF (2)	r.t.	3	<b>d</b> (86)

<sup>a</sup> many side product were detected; <sup>b</sup> mixture of isomers

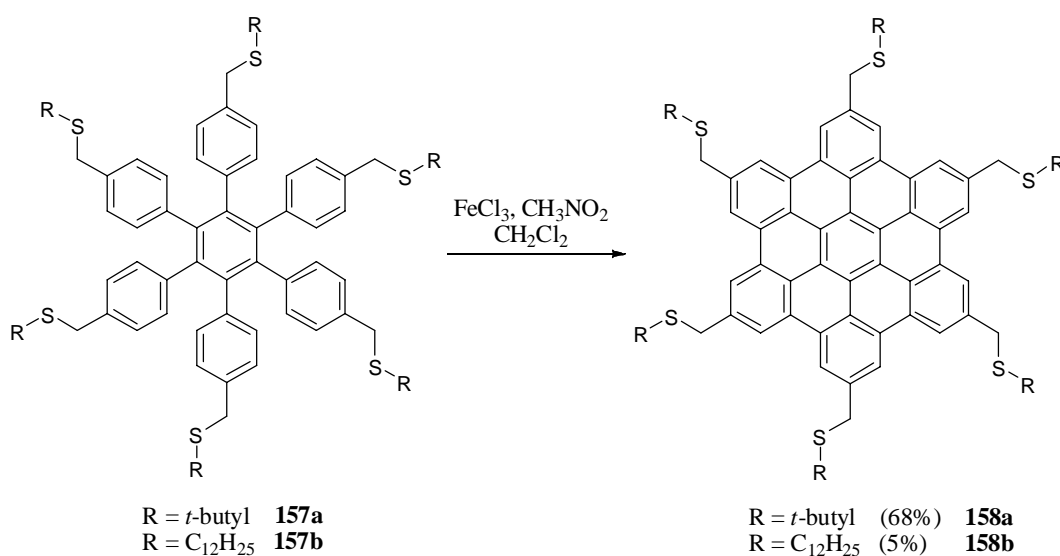
One-pot Sonogashira conditions afforded the desired tolans in high yield only for the *t*-butyl derivative **156a**. In the case of the dodecylthiol only 7% of the desired tolane **156b** was obtained. Either the sulfurated lateral chain hampered the reaction or was cleaved during the reaction. For both other derivatives **155c** and **155d** the desired tolans could not be synthesized. Compound **155c** consisted of so many isomers, due to the impossibility of buying pure *tert*-dodecylthiol (**154c**), that identification of any tolane was impossible and the trityl group did not resist the Sonogashira cross coupling conditions. Subsequent cyclotrimerization of tolans **156a** and **156b** yielded the desired HPB derivatives in moderate to good yields.

**Scheme 12.4** – Formation of sulfurated benzyl derivatives and subsequent reaction to HPB **157a** and **157b**



12.3.2 Synthesis of HBC-CH<sub>2</sub>S-*t*-butyl and HBC-CH<sub>2</sub>S-C<sub>12</sub>H<sub>25</sub>

The oxidation to the sulfurated HBC derivatives was performed under the mild FeCl<sub>3</sub> condition as it was *a priori* not clear if the benzylsulfide would resist the cyclodehydrogenation. As both HPB derivatives **157a** and **157b** were well soluble in dichloromethane, no co-solvent was needed. The reactions were quenched as usual with methanol, which completed the precipitation of the desired HBC derivatives **158a** and **158b**. Purification was attempted for both derivatives by refluxing them in different solvents followed by suction filtration over Millipore®. In the case of HBC **158a**, which was obtained as a bright yellow and nearly insoluble solid, this purification method worked rather well. For HBC **158b**, despite of the several repetitions it was not possible to remove the dark brown colour. Unfortunately the sulfur prevented the collection of MS data even by use of various additives such as silver salts. Because of that, the UV/Vis spectra remained the only way of characterization for both HBC derivatives.



Scheme 12.5 – Oxidation towards sulfurated HBC derivatives

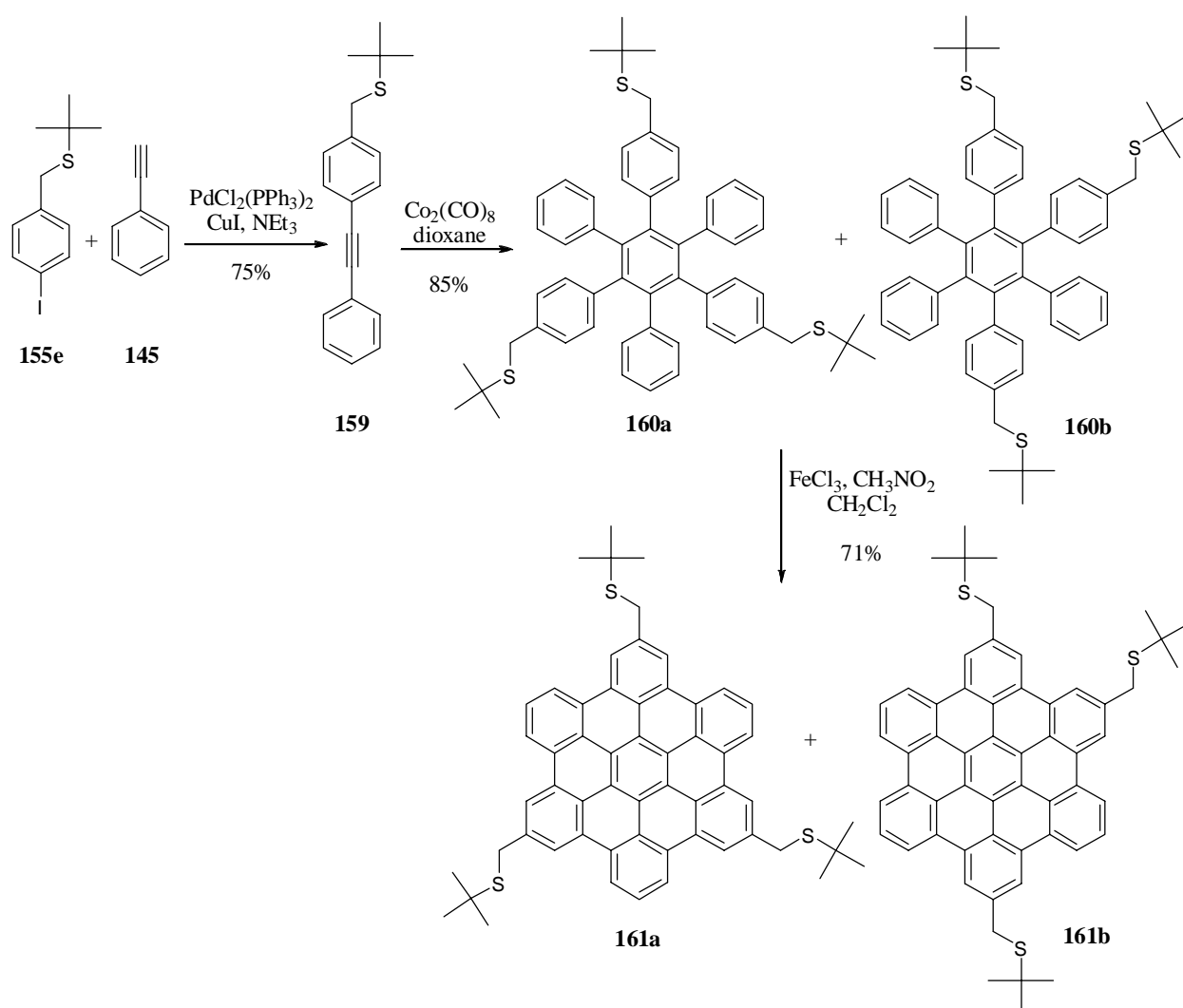
12.4 HBC-(CH<sub>2</sub>S-*t*-butyl)<sub>3</sub>

As the deposition onto Au(111) gave no result by using HBC **158a**, carrying six lateral chains, new derivatives bearing three or one chain were prepared, as the number of side chains may influence the sublimation onto the surface tremendously.

As shown in Scheme 12.6 the synthesis started by a Sonogashira reaction between the iodinated aryl **155e** and phenylacetylene **145** under “solvent free” conditions by using NEt<sub>3</sub> as base and solvent affording tolane **159** in high yield as soluble white powder. Subsequent cyclotrimerization furnished the two HPB isomers **160a** and **160b** as inseparable one to one mixture as shown by quanti-

tative  $^{13}\text{C}$  NMR. Column chromatography using even pure pentane was not able to separate the derivatives. Despite of the isomeric mixture the derivatives **160a** and **160b** are still very useful as the question to be answered is whether the deposition works better by taking a threefold substituted derivative or not.

Final oxidation of HPB **160a** and **160b** afforded the desired HBC derivatives **161a** and **161b** again as inseparable and very insoluble mixture. Even after many purification attempts in different organic solvents such as toluene and 1,2,4-trichlorobenzene for example, HBCs **161a** and **161b** were afforded as brownish solid. Again, the characterization afforded no clear results from MS measurements, where most of the different matrices were tried.

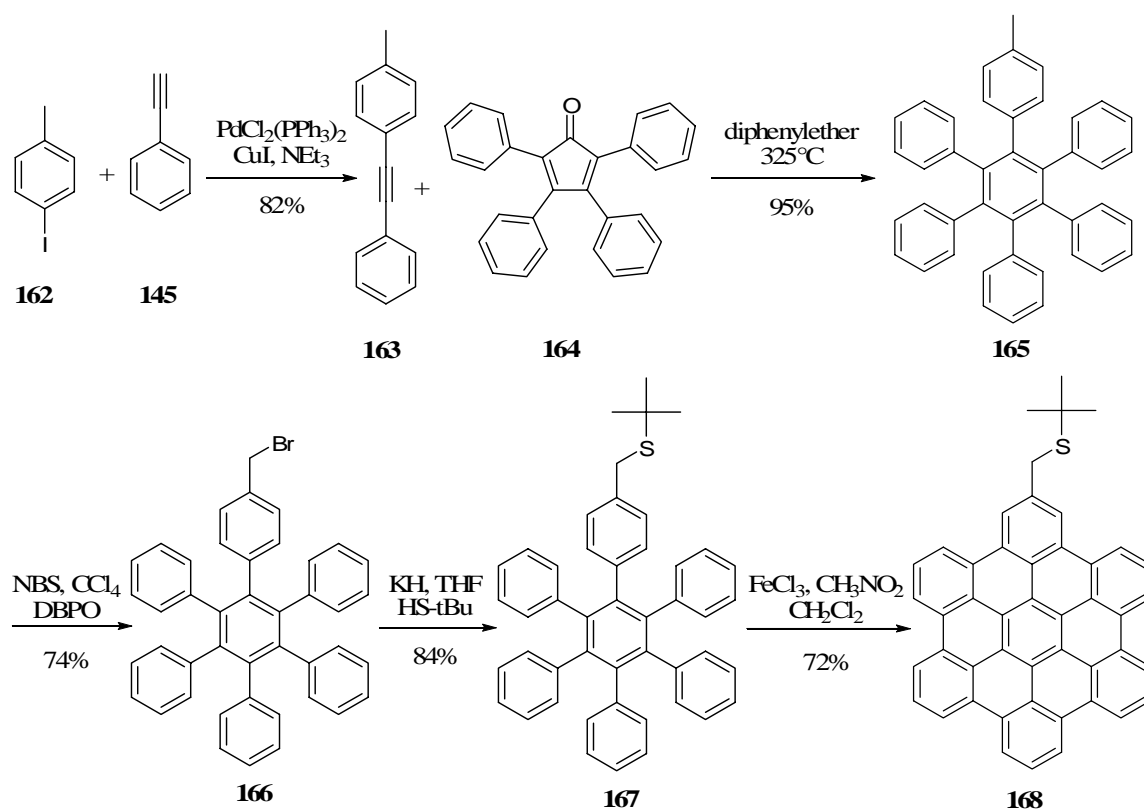


**Scheme 12.6** – Reaction pathway for the preparation of HBC **161a** and **b**

12.5 HBC-(CH<sub>2</sub>S-*t*-butyl)<sub>1</sub>

The preparation of a HBC carrying only one side chain is best prepared by a Diels-Alder reaction. The shortest procedure would involve the reaction of tolane **159**, bearing the desired side chain, with tetraphenylcyclopentadienone **164**. Unfortunately the *t*-butyl protecting group did not resist the high temperatures and was cleaved off during the reaction. Even the use of a microwave oven to reduce the temperature was not efficient. Due to this, the synthesis had to be changed as shown in Scheme 12.7, where the key point is to introduce the sulfur after the Diels-Alder reaction.

Tolane **163** was prepared by a Sonogashira reaction of 4-iodotoluene **162** and phenylacetylene **145** at room temperature using NEt<sub>3</sub> as base and solvent. The highly crystalline tolane was subsequently reacted with the tetraphenylcyclopentadienone **164** by refluxing in diphenylether which yielded the methylated HPB derivative **165** in nearly quantitative yield as white crystals. Selective bromination of the methyl group was performed with NBS and DBPO yielding HPB **166** as crystalline solid. The newly formed reactive benzyl group was thereafter transformed into the desired *t*-Bu-sulfur by reaction of **166** with KH and HS-*t*Bu. Again the purification was performed simply by crystallization which allowed the preparation of HPB **167** in high purity. Final cyclodehydrogenation afforded the desired HBC **168** as very insoluble brownish compound even after exhaustive purification attempts. MALDI analysis was again hampered most probably due to the incorporation of the benzyl sulfur group or due to the remaining impurities.



Scheme 12.7 – Preparation of HBC **168** bearing one lateral side chain

## 12.6 Concluding remarks on the synthetic part

The preparation of perfluoroalkylated HBC derivatives carrying six identical linear or branched side chains was found to work best by previous preparation of the adequate halogenated phenyl derivatives. Subsequent tolane formation *via* a twofold Sonogashira cross-coupling showed to be a reliable strategy. Cyclotrimerization followed by mild ( $\text{FeCl}_3$ ) oxidation furnished finally the desired HBC derivatives. Derivatives of  $D_{3h}$  symmetry are easiest prepared by cyclotrimerization of desymmetrized tolane derivatives. Unfortunately this strategy furnished an inseparable mixture of two regio-isomers. Other reaction pathways able to produce isomerically pure derivatives failed completely.

HBC primer derivatives bearing six identical side chains are synthesized in exactly the same way, namely by preparation of the desired phenyl derivative first, which is subsequently transformed into the desired HBC derivative. HBC primer derivatives of  $D_{3h}$  symmetry are either prepared by cyclotrimerization of desymmetrized tolane derivatives or by Diels-Alder reaction of the corresponding tolane with tetraphenylcyclopentadienone. For the later reaction pathway the desired sulfur group has to be inserted after the Diels-Alder reaction as the sulfur does not resist the required high temperatures.

### **III Results and Discussion – Part 2: Investigation of the Properties**



## 13 Characterization of perfluoroalkylated HBC derivatives

The investigation of the properties of the newly prepared HBC derivatives is described in this chapter with main focus on their ability to form one, two and three dimensional aggregated structures. Moreover new techniques, such as THz spectroscopy or Cryo-SEM, not very often discussed in literature, are introduced shortly. Although well known, fluorescence spectroscopy is discussed in more details, as many contradictory articles were published during the past few years on the excitation and luminescence spectra of HBC. Because of this, our point of view is discussed to clarify the subsequent discussion of such spectra.

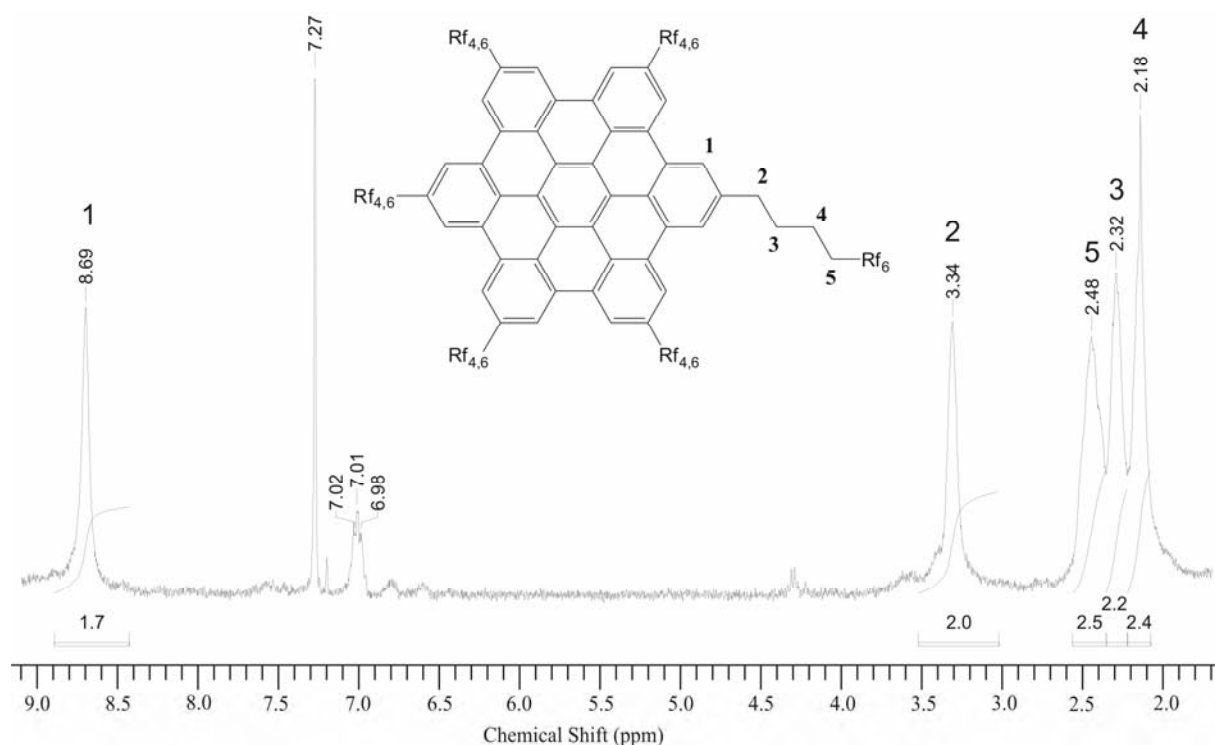
Further a discussion on the characterization of the commonly very sparingly soluble perfluorinated HBC derivatives is done by treating different techniques, their scope, limitation and adaptations performed in the frame of this thesis.

Most semi-perfluorinated HBC derivatives are only sparingly soluble in common organic solvents, such as acetone, ether, tetrahydrofuran, carbon disulfide, toluene, dichloromethane or pentane, hampering therefore seriously their characterization. Only highly halogenated aromatic solvents like 1,2,4-trichlorobenzene (TCB), benzotrifluoride (BTF) and hexafluorobenzene (HFB), showed an increased capacity in solubilizing fluorinated HBC derivatives. In the following section the scope and limitation of the applicable three techniques (NMR, MS and optical spectroscopy (see chapter 14.2 for the optical spectroscopy)) for the characterization of HBC derivatives is discussed.

### 13.1 NMR spectroscopy in the liquid and solid state

Not very well-resolved  $^1\text{H}$ -NMR spectra could be collected in hexafluorobenzene together with a minor amount of  $\text{CDCl}_3$ , the later being used for the lock signal. As an example the  $^1\text{H}$ -NMR spectrum of HBC-Rf<sub>4,6</sub> (**94b**) is shown in Figure 13.1. The low field resonance of the aromatic HBC protons is at 8.69 ppm, indicating already aggregation of the individual HBC disks, as the typical resonance of HBC monomers is around 9.0 ppm ( $10^{-7}$  M solution of HBC-C<sub>12</sub>H<sub>25</sub> **5b** in 1,1,2,2-tetrachloroethan-*d*<sub>2</sub>).<sup>[98]</sup> A typical feature of the  $^1\text{H}$ -MNR spectra of HBC derivatives is hence the significant line broadening and shielding due to the aggregation, which is sensitive to concentration and temperature.<sup>[104]</sup> A decrease in the concentration from  $51.16 \cdot 10^{-3}$  to  $1.35 \cdot 10^{-3}$  at constant temperature results in a downfield shift by almost 0.5 ppm, as shown for HBC-C<sub>12</sub>H<sub>25</sub>.<sup>[104]</sup> A less pronounced downfield shift can be observed for the  $\alpha$ -CH<sub>2</sub> protons of the lateral chain. The additional signals in the aromatic domain around 7 ppm are due to impurities in hexafluorobenzene, consisting most probably of benzene and pentafluorobenzene.

The low solubility of perfluorinated HBC derivatives in deuterated solvents, adequate for  $^{13}\text{C}$  NMR, prevented the collection of  $^{13}\text{C}$ -NMR data completely, as HFB proved to be an inadequate solvent due to the very intensive multiplets in the aromatic region.



**Figure 13.1** –  $^1\text{H}$ -NMR spectrum of HBC **94b** in a mixture of HFB and  $\text{CDCl}_3$

The only way to collect information on the carbon skeleton of perfluorinated HBCs is to perform solid state NMR. In the liquid state, the rapid and random rotation of molecules tend to average out the line broadening due to the dipole-dipole interactions between nuclear spins, making possible the observation of high resolution features in the NMR spectrum. There is an experimental technique which, under many circumstances, has a similar effect for solid samples: magic-angle spinning (MAS). Not only the dipole-dipole interaction, but also other sources of line broadening, such as chemical shift anisotropy (CSA), have an interaction containing a factor  $(3\cos^2\theta-1)$ , where  $\theta$  is the angle between the external magnetic field and the spin. If the sample spins along an angle

$\theta = \arccos\left(\sqrt{\frac{1}{3}}\right) = 54.73^\circ$ , it is obvious, that under these spinning conditions, at this particular angle

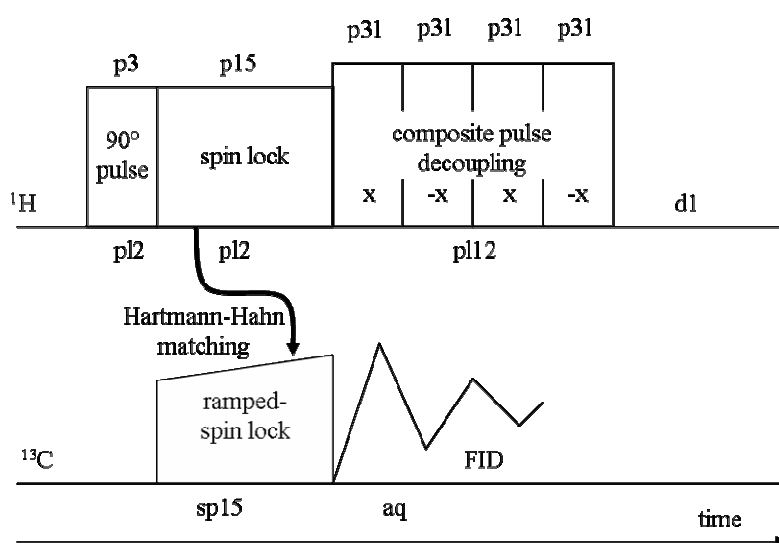
the interactions average to zero. For more information, the textbooks of Stejskal<sup>[239]</sup> and Duer<sup>[240]</sup> give very detailed explanations.

As the collection of solid state  $^{13}\text{C}$ -MAS spectra is not very effective (low  $\gamma$ ), it is important to use a supplementary technique in combination, called cross polarisation (*cp*), which uses the fact that the gyromagnetic ratio  $\gamma$  H is approximately 4 times larger than  $\gamma$  C. Therefore, the basis feature of the



measurement consisted of a cross-polarisation, the transfer of magnetization from an abundant spin ( $^1\text{H}$ ) to a rare spin ( $^{13}\text{C}$ ). Cross-polarisation is achieved by spin-locking in the rotating frame and transferring the magnetization by applying a matched radio frequency field to both spin systems, meeting the so-called Hartmann-Hahn conditions. It has to be noted that one of the two spin-lock pulses should favourably be ramped in order to reduce mismatching. After the spin lock pulses, of a typical length of 1 ms, the FID can be collected as soon as the decoupling started. Earlier, standard high power decoupling, so called continuous wave (CW) decoupling, was used. But composite pulse decoupling (*cpd*) proved to be much more efficient and uses far less power. It is worth mentioning that all the above mentioned parameters summarized in Figure 13.2 have to be adjusted previous to the measurement in order to achieve an acceptable spectrum. The combination of the magic-angle spinning with cross-polarisation leads to an enormous improvement of both resolution and sensitivity.

Due to the non-availability of a pulse sequence in the Bruker spectrometer used, containing at the same time a ramped *cp* and the *cpd* decoupling, such a sequence was created by ourselves, called *cprampcpd*<sup>[241]</sup> and is shown schematically in Figure 13.2.<sup>b</sup>

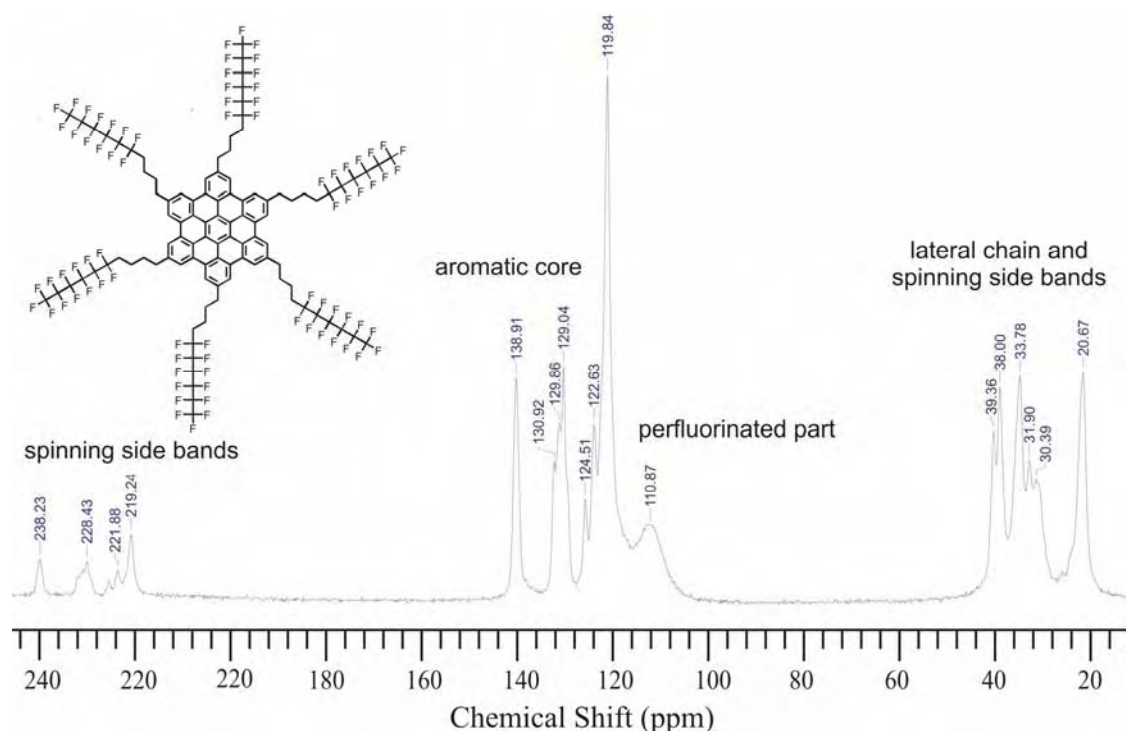


**Figure 13.2** – Used *cprampcpd* pulse sequence for solid state MAS NMR. p3 = 90° pulse (4  $\mu\text{s}$ ); p15 = contact pulse (600  $\mu\text{s}$ ); p31 = length of cpd pulse (7.4  $\mu\text{s}$ ); x = phase shift of cpd pulse (15°); pl2 = power level for 90° pulse and  $^1\text{H}$  spin lock pulse (6.7 dB); pl12 = power level for cpd decoupling (0 dB); sp15 = power level for  $^{13}\text{C}$  ramped spin lock pulse (7.0 dB); aq = acquisition time (35 ms); d1 = delay between two pulse sequences (5 s). The values in parentheses represent typical values.

<sup>b</sup> Technical support for the programation was given by S. Antonijevic, group of Prof. Bodenhausen, EPFL Lausanne.

However, the most crucial parameter to set is the exact value of the magic angle. A common way to adjust it is to optimize the envelope of the  $^{79}\text{Br}$  rotational echoes in KBr. Recently a new method was published by Bodenhausen,<sup>[242]</sup> which is by far more sensitive. The angle can be adjusted to an accuracy of  $|\Delta\theta| < 0.01^\circ$  ( $\Delta\theta$  = derivation of the magic angle) by minimizing the residual  $^2\text{H}$  quadrupolar splitting in a MAS spectrum of a deuterated sample, such as  $[\text{D}_6]\alpha$ -oxalic acid dihydrate. The residual splitting (quartet) allows the angle to be tuned to a miss-set of less than  $|\Delta\theta| = 0.01^\circ$  where a singlet is obtained.

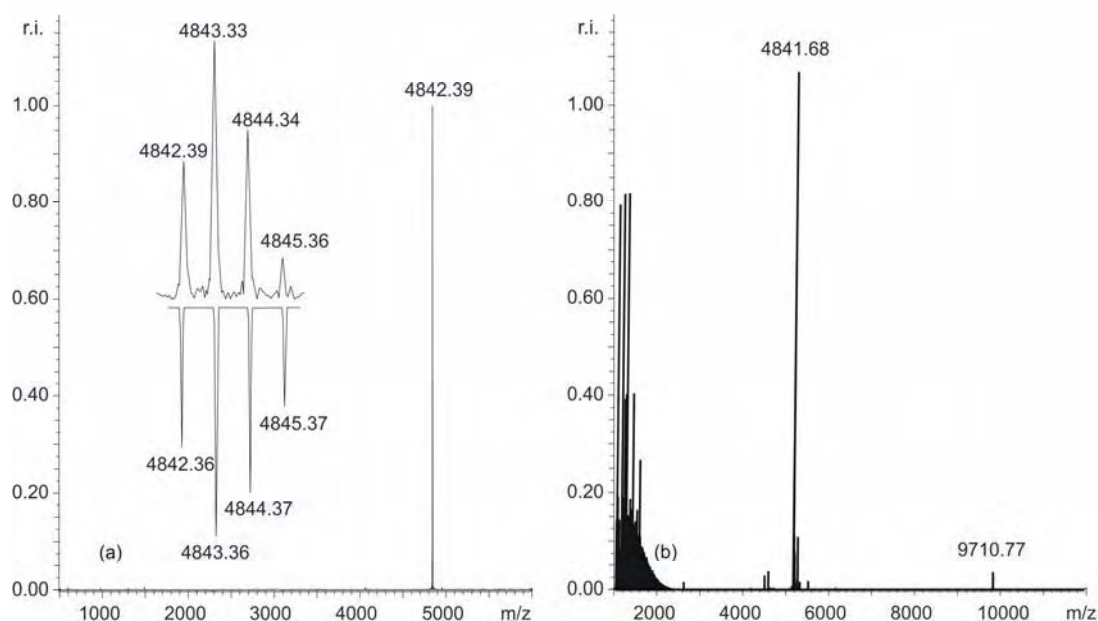
Figure 13.3 shows the solid state MAS spectrum collected by 12000 successive scans with a rotation of 10 KHz around the MA using the *cprampcpd* pulse sequence. It has to be noted, that even by using highly optimized parameters, the obtained resonances are much broader as compared to liquid NMR. Nevertheless, the aromatic carbons (119.84 – 138.91 ppm), the perfluorinated ones (110.87 ppm) and the lateral chain carbons (20.67 – 39.36 ppm) are clearly visible. The low field signals around 220 ppm together with the additional signals in the aliphatic region (30.39 and 31.90 ppm) are rotational side bands of the aromatic carbons exactly at a distance of 10 kHz from the central peaks. As limitation of solid state NMR remains the large amount of sample needed, typically 50 mg and the low resolution of the resonances.



**Figure 13.3** – SS MAS spectrum of HBC **94b**, collected with the *cprampcpd* pulse sequence on a Bruker DPX 400 at 100.62 MHz.

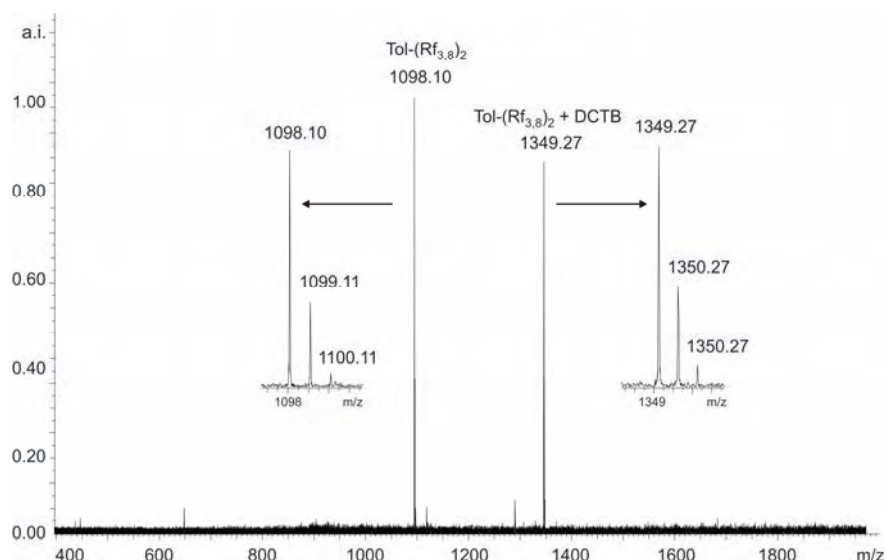
## 13.2 MS spectroscopy

The very low solubility of perfluorinated HBC derivatives prevents their characterization by conventional MS techniques, such as ESI-MS (solubility problems, difficult protonation or complex formation with metals, such as Ag, Hg to form charged particles), EI-MS (too low volatility) or FAB (no suitable matrix). Only the MALDI technique could be applied. Since MALDI sample preparation also requires some solubility of the analyte and matrix molecules, it had to be modified. Instead of solubilizing analyte and sample, a new sample preparation<sup>[243]</sup> was used consisting in mechanically mixing analyte and matrix by grinding, in a ratio of approximately 1:500 without any solubilization procedures. It was found, that especially this solvent-free MALDI sample preparation of perfluorinated HBC derivatives were highly sensitive to the purity of the sample, as the ion intensity on the ICR spectrometer rapidly decreased in the presence of even trace amounts of impurities. Furthermore even the morphology of the analyst solids *i.e.* the way of precipitation of the HBCs may influence the ion yield, as shown recently for other substances.<sup>[244]</sup> Nevertheless most HBC derivatives yielded intensive mass peaks when applying solvent free conditions while no signal at all was obtained if only a minor trace of solvent was added. As matrices mainly DCTB and TCNQ were found to give best results.



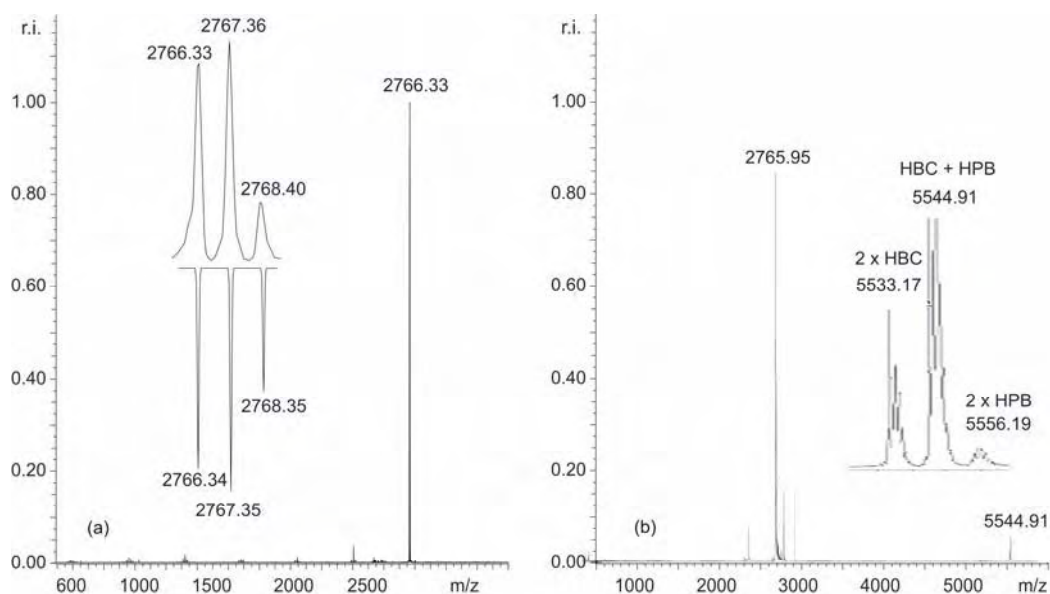
**Figure 13.4** – MALDI-MS analysis of HBC-Rf<sub>3,3,6,6</sub> **132b**. (a) ICR spectrum; inset: measured (top) and calculated isotopic pattern (upside down); (b) TOF spectrum.

MALDI-ICR gave as expected highly resolved peaks ( $\pm 10$  ppm), and excellent mass accuracy and typically no fragments, while MALDI-TOF spectra generally showed small fragment peaks and in most case higher aggregates (c.f. Figure 13.4), not seen in the ICR spectra due to the limited mass range ( $\leq 5000$  for 4.7 Tesla). As illustrated in Figure 13.5 ICR measurements show only, if at all, analyte – matrix aggregates.



**Figure 13.5** – MALDI-ICR of Tol-(Rf<sub>3,8</sub>)<sub>2</sub> **78b**, calculated for C<sub>36</sub>H<sub>20</sub>F<sub>34</sub> (**78b**) = 1098.10, and C<sub>53</sub>H<sub>39</sub>F<sub>34</sub> N<sub>2</sub> (Tol(Rf<sub>3,8</sub>)<sub>2</sub> + DCTB + H) = 1349.26

The MALDI-TOF measurements revealed often aggregated species as shown in Figure 13.6. The aggregation surprisingly occurred preferentially between a HBC derivative and its HPB precursor, present in minor quantities (below 5%). This observation suggests that HBC and HPB derivatives self-assemble in the gas phase after desorption. The presence of HPB aggregates underlines very clearly that MALDI measurements may prove the presence of the desired derivative, but do not account for its purity as the intensities are not reliable. This is especially due to the fact that each derivative has its characteristic ionization properties. Furthermore, by varying the lengths of the alkyl spacer and of the perfluorinated part, the intensity of the mass peaks changed tremendously.



**Figure 13.6** – MALDI-MS analysis of HBC-Rf<sub>4,6</sub> **94b**. (a) ICR spectrum; inset: measured (top) and calculated isotopic pattern (upside down). (b) TOF spectrum; inset: different dimers formed from HBC **94b** and HPB **92b**.

## 14 Investigation techniques – cryo-SEM and fluorescence

In this section cryo-SEM, fluorescence and THz spectroscopy (see chapter 17.2 for THz spectroscopy) are introduced in more details as these methods are either not yet common techniques in organic chemistry (cryo-SEM and THz) or contradictory descriptions are found in the literature (fluorescence). Moreover cryo-SEM and fluorescence are used during the whole discussion afterwards which is the reason for a larger introduction with the incorporation of some own results.

### 14.1 Cryo-SEM

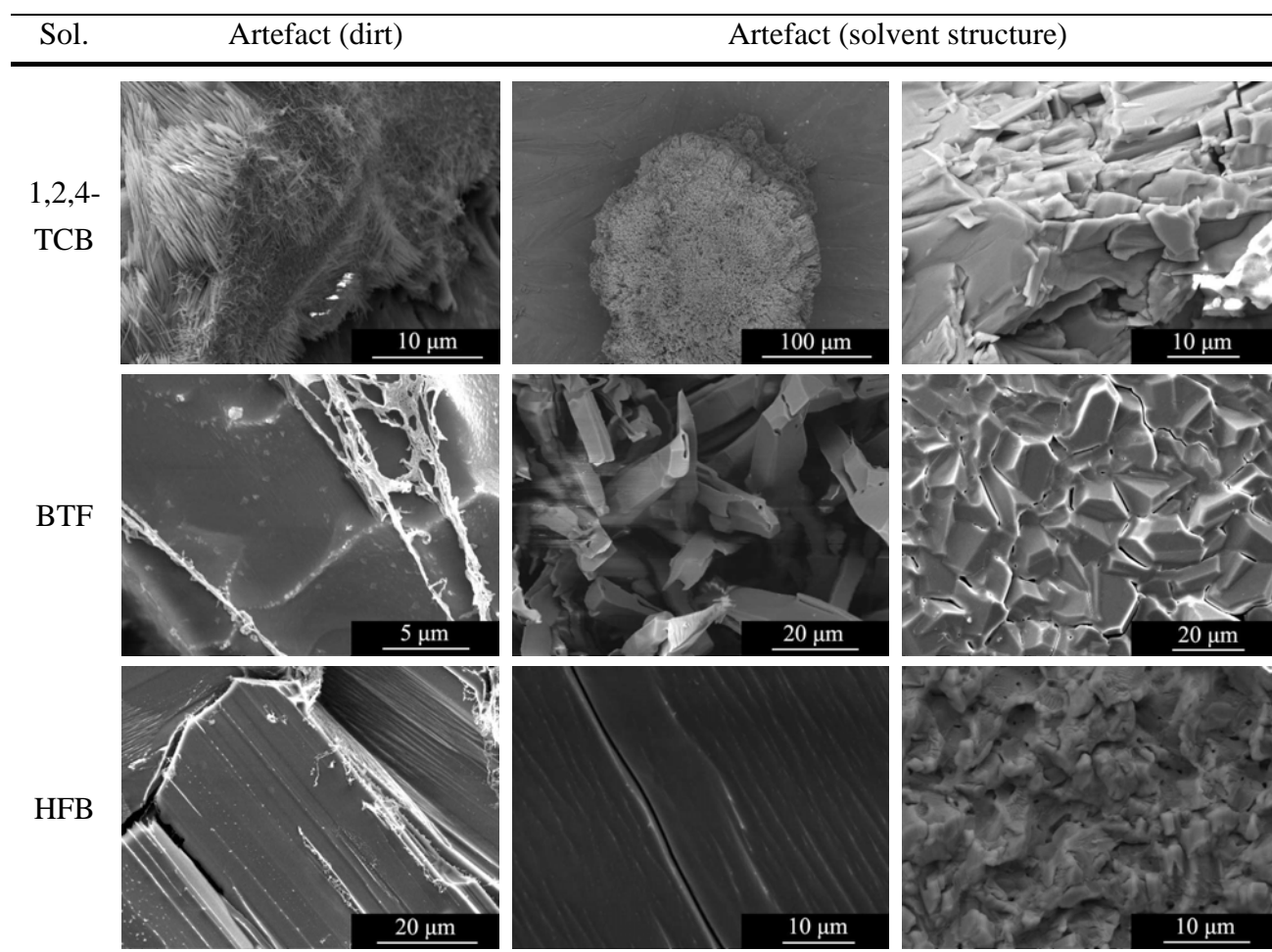
Micro- and nanoscopy, such as SEM, cryo-SEM, TEM, STM and AFM for examples, are the only experimental methods to visualize the aggregation behaviour of aggregated molecules in a direct way. Cryo-SEM measurements proved to be one of the most important techniques used in the investigation of the properties of HBC derivatives and is therefore treated in more detail. Other techniques, such as fluorescence for example, monitor the aggregation behaviour in an indirect way, as no direct image of the adopted structure is shown.

#### 14.1.1 Scope and limitation

Cryo-SEM, very closely related to normal SEM, is the technique favoured by biologists to investigate cryogenated biological cell samples.<sup>[245]</sup> Self-assembled HBC structures show a dynamic equilibrium of various aggregated HBC architectures, which are very sensitive to concentration variations occurring during deposition techniques used in SEM, such as spin coating for example. In contrast, by shock freezing solutions containing the desired self-assembled structures in liquid nitrogen, the formed aggregates are preserved and may be observed under the microscope after a part of the solvent has been sublimed off.

SEM as well as cryo-SEM require a conducting sample. Because of that the whole sample is sputtered with a layer of about 20 nm of platinum in order to render the sample conducting. The amount of sputtered metal is only approximately determined, which renders the thickness measurements of very small structures delicate. The thickness of the observed features is crucial for the distinction between laterally aggregated structures and monostranded stacks. A further limitation is the resolution of the cryo-SEM used for our investigations, which has to be situated around 10 nm. It is obvious, that the interpretation of the collected data depends very delicately on the distinction between artefacts or solvent structure and real data. Several artefacts and solvent structures collected from pure solvent are shown in Figure 14.1 as examples. It is worth to note that even by identical cryo-

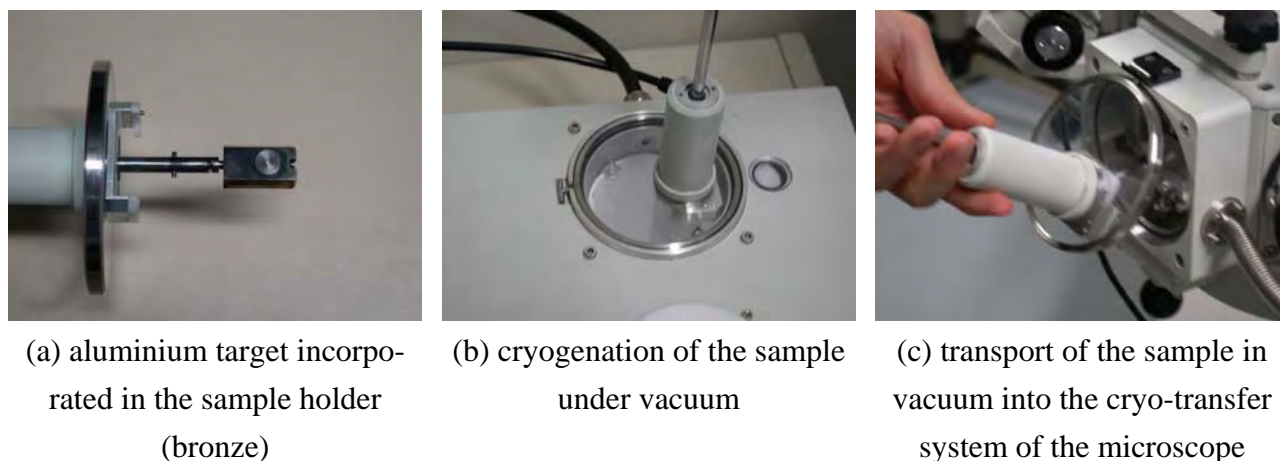
generation conditions the solvent structure after the sublimation process may change. 1,2,4-TCB was found to exist either in flat plate like structures or to form flower like architectures which are most probably due to the sublimation. In contrast to this, BTF showed either a smooth surface or highly fragmented structures, containing individual structures of various size and shape. In contrast to this HFB revealed either an amorphous surface or flat domains with a pronounced orientation. Artefacts on the other hand consisted mostly of spider web networks of filamentous structures. As they were observed randomly in several measurements they stem most probably of some tiny amounts of dirt incorporated in the solvent already.



**Figure 14.1** – Cryo-SEM micrographs showing artefacts observed in pure solvent

## 14.1.2 Sample preparation

The solutions in 1,2,4-TCB, BTF and HFB were prepared in such a way that the concentrations range from  $10^{-2}$  M to  $10^{-8}$  M depending on the solubility of the corresponding HBC. The dilutions were performed starting from the most concentrated solution by diluting it repetitively by a factor of 10. For observation one drop of the solution was applied with a Pasteur pipette on the aluminium target (a, d, e)<sup>c</sup> and was immediately shock frozen in liquid nitrogen at  $-195^{\circ}\text{C}$  and further cooled below  $-210^{\circ}\text{C}$  by pumping ( $10^{-2}$  mbar) (b, f). The sample holder and the cryogenation process are shown in Figure 14.2 and Figure 14.3.

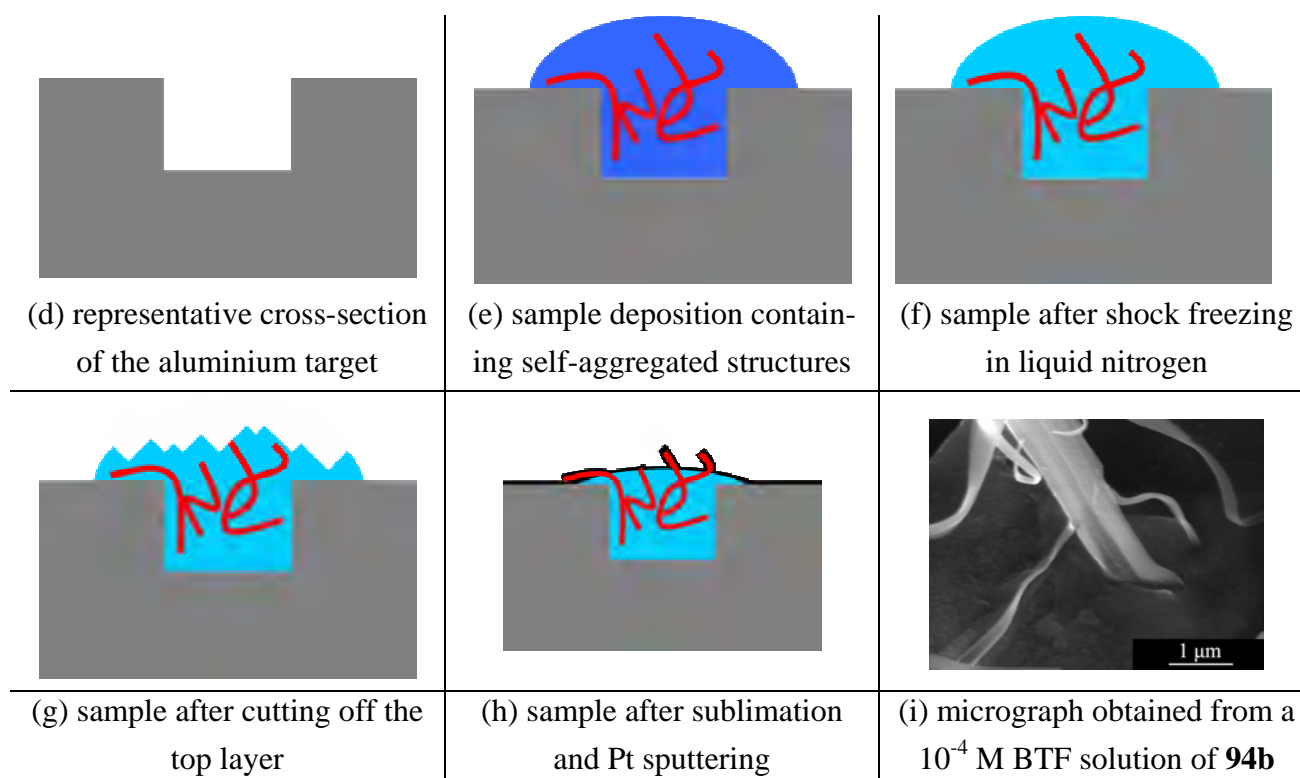


**Figure 14.2** – Images of the cryo-SEM microscope

The frozen sample is then transferred under vacuum to the cryo-transfer system (c). In order to remove the ice, which could have been formed during the shock freezing on the surface, the top layer of the frozen sample was removed with a knife installed in the microscope pre-chamber (g). Afterwards, the temperature was raised from  $-150^{\circ}\text{C}$  to  $-95^{\circ}\text{C}$ . By partially subliming the solvent at  $10^{-4}$  –  $10^{-5}$  mbar directly in the cryo pre-chamber, the pre-existing architectures are exposed on the recoiling frozen solvent surface (h, i). The sublimation process was carried out for 20 minutes, before the temperature was lowered again to  $-150^{\circ}\text{C}$ . In order to render the target conducting, a platinum coating of about 20 nm had to be applied (h). The finished sample was thereafter transferred under vacuum into the microscope chamber and observed. Figure 14.3 (g) illustrates the result of the cryo-SEM technique at the example of a micrograph of HBC-Rf<sub>4,6</sub> (**94b**) obtained from a  $10^{-4}$  M BTF solution. The recoiling frozen BTF surface is very clearly shown in dark grey whereas pre-existing laterally aggregated HBC structures, shown in light grey, are “protruding” out of the solvent.

<sup>c</sup> the lettering refers to Figure 14.2 and Figure 14.3





**Figure 14.3** – Schematic sketch of the cryo-procedure

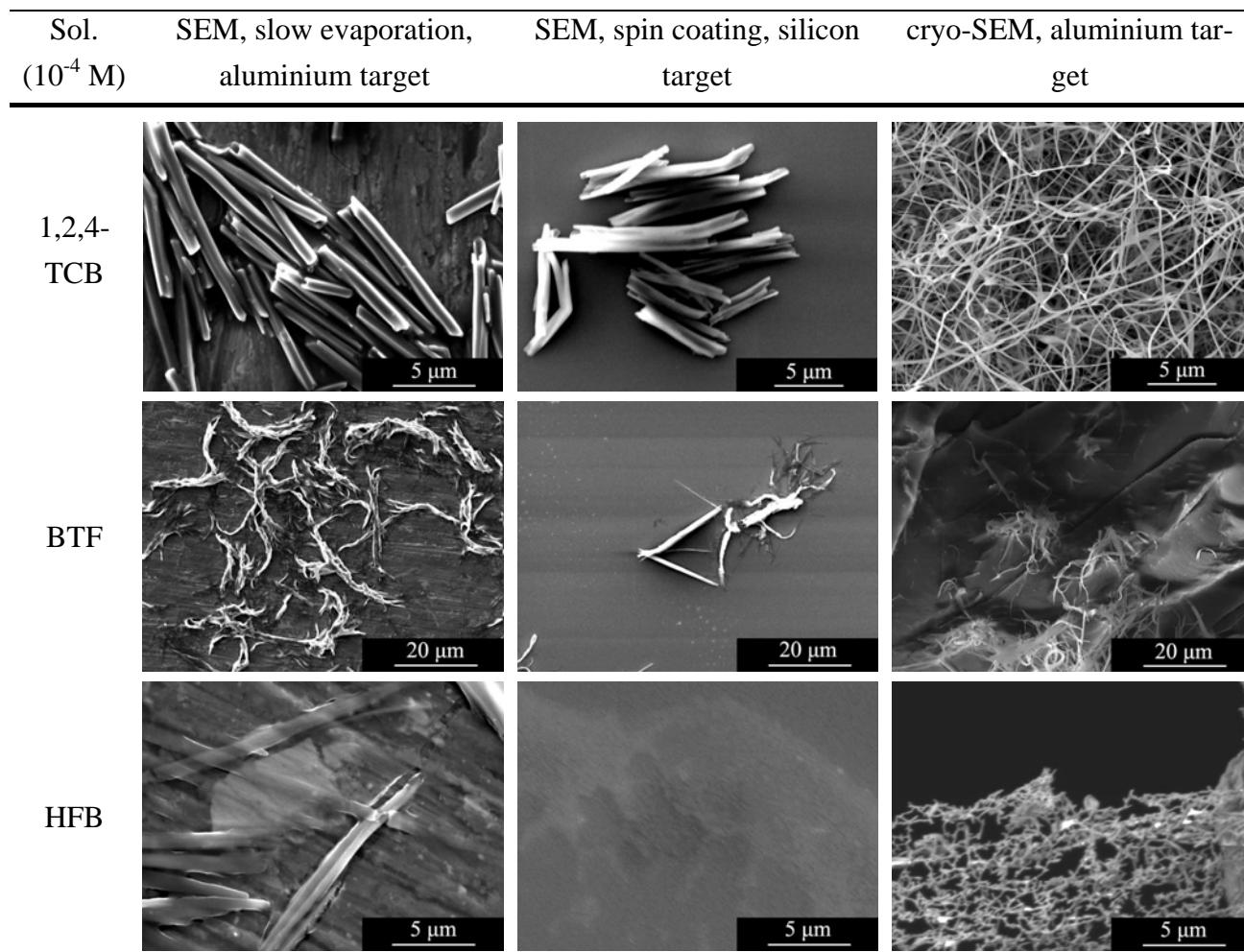
After the measurement, the aluminium target was cleaned by high-speed grinding on a Struers LaboPol 21, followed by polishing on a Planapol-V using a leather slap together with aqueous  $\text{Al}_2\text{O}_3$  grinding powder (first 3000 Å, followed by 200 Å). Afterwards the aluminium target was washed with distilled water, isopropanol and acetone, sonicated for 10 minutes in a 1:1:1 mixture of the previously mentioned solvents and dried with compressed air.

#### 14.1.3 Cryo-SEM versus SEM

In order to compare the performance of SEM and cryo-SEM and to prove the advantages of the cryogenated sample preparation for the observation of HBC solutions in 1,2,4-TCB, BTF or HFB, HBC **94b** samples were prepared with both techniques. For the collection of SEM micrographs two deposition techniques were used: *i*) a freshly cleaned aluminium target was loaded with a droplet of HBC solution followed by slow evaporation under normal pressure of the solvent. The residue was coated in the microscope pre-chamber with platinum and observed thereafter; *ii*) a droplet of solution was added on a fresh silicon wafer and spin coated on a Delta 6 RC BM, for 1 minute at 4000 rpm. The results of the different approaches are summarized in Figure 14.4. It is clearly visible, that in all three tested solvents the observed structures are much larger in diameter when the solvent evaporated completely, either slowly or by spin coating. One has the impression, that during the evaporation process, dissolved monomeric HBC or short structures aggregated to form tubular (1,2,4-TCB), distorted and twisted (BTF) or rectangular (HFB) architectures. In contrast to this, the shock frozen samples showed in all three solvents well defined and much narrower structures, un-



derlining that in cryo observation the pre-existing architectures are preserved. Because of that, all samples are examined with the cryo-SEM technique rather than with the standard SEM technique.



**Figure 14.4** – Cryo-SEM micrographs obtained by three different methods: slow evaporation SEM (left column); spin coating SEM (middle column); cryo-SEM (right column)

## 14.2 Fluorescence

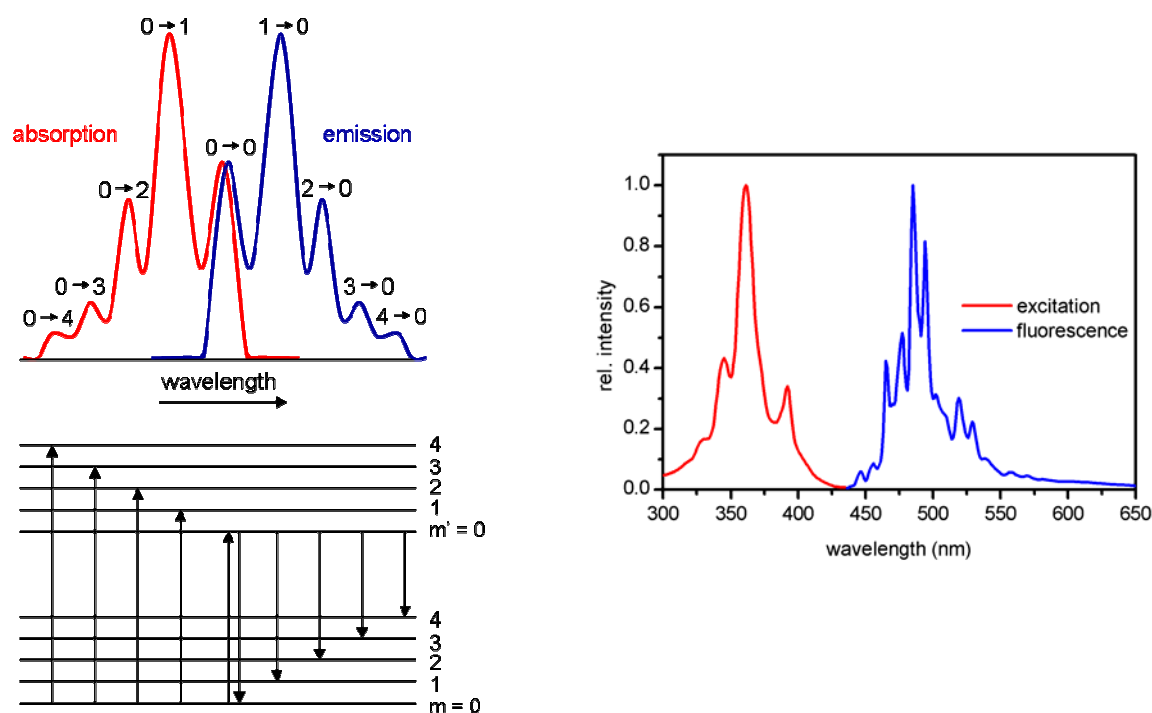
### 14.2.1 Introduction

Fluorescence spectroscopy is a very sensitive tool to differentiate monomers from aggregated structures, since the influence of neighbouring chromophores provokes red or blue shifted bands. A short theoretical introduction is given below, as several terms will be used to discuss the collected spectra. Moreover there are many controversial articles concerning the fluorescence of HBC derivatives which have been published in the past.<sup>[246]</sup> Further and more detailed general information on the background of fluorescence may be found in the specialized literature.<sup>[247]</sup>

## 14.2.2 Theoretical background

In Figure 14.5 the sequence of steps involved in absorption and fluorescence is illustrated (the left hand side illustrates the theoretical model, whereas on the right hand side the emission and fluorescence spectrum of HBC-Rf<sub>4,6</sub> (**94b**) is shown). The absorption of a photon takes the molecule to an excited electronic state and populates there the different vibronic levels. Through collisions of the excited molecule with the surrounding solvent, the former releases energy nonradiatively and steps down the ladder of vibrational levels to the lowest level of the electronically excited molecular state. If the neighbouring molecules are not able to accept the large energy difference to lower the excited molecule to its ground electronic state it may survive long enough to undergo spontaneous emission, and emit the remaining excess energy as radiation.

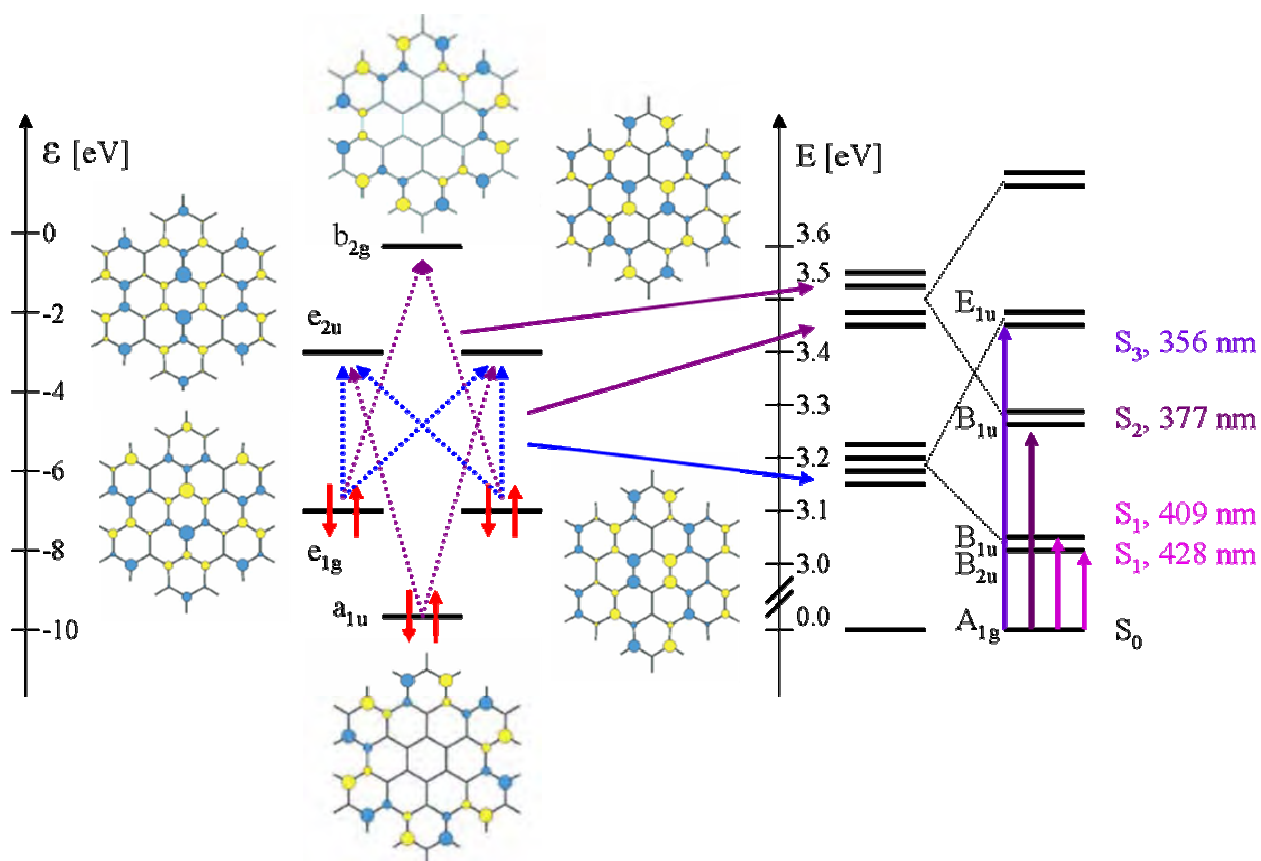
Provided they can be observed, the 0-0 absorption and fluorescence transitions can be expected to be coincident as often emission and absorptions behave like image and mirror image. The absorption spectrum arises from 0→0, 0→1, 0→2 etc. transitions and the peaks occur at progressively lower wavelength, *i.e.* higher energy. The intensities are governed by the Franck-Condon principle because the transition intensity is proportional to the square of the magnitude of the transition dipole moment, which is known as the Frank-Condon factor for the transition. It follows that the greater the overlap of the vibrational state wavefunctions, the greater the absorption intensity of that particular transition. The fluorescence spectrum arises then inversely from 0→0, 1→0, 2→0 etc downward transitions, and hence the peaks occur with increasing wavelengths.



**Figure 14.5** – Left:  $S_0$ - $S_1$  (red) and  $S_1$ - $S_0$  (blue) transitions with their corresponding vibronic structure; **right**: excitation spectrum ( $\lambda_{\text{det}} = 485$  nm) and fluorescence spectrum ( $\lambda_{\text{ex}} = 360$  nm) of a  $10^{-6}$  M solution of HBC-Rf<sub>4,6</sub> **94b** in BTF. Both spectra are arbitrarily scaled, excitation at 360 nm and fluorescence at 485 nm.

## 14.2.3 Excitation and luminescence spectrum of HBC derivatives

The situation in the highly symmetric HBC derivative is not as simple as depicted in Figure 14.5, and was because of this reported in different ways in the literature. As consequence, the corresponding orbital energies and transitions have been calculated using the TDDFT B3LYP/6-31G\*<sup>d</sup> technique in order to confirm our point of view, which is shown in Figure 14.6. TDDFT was used instead of other algorithms due to the incorporation of the dynamic electron correlation in this technique.



**Figure 14.6** – **Left:** Energy diagram of the frontier orbitals of HBC; **right:** corresponding configuration interaction diagram

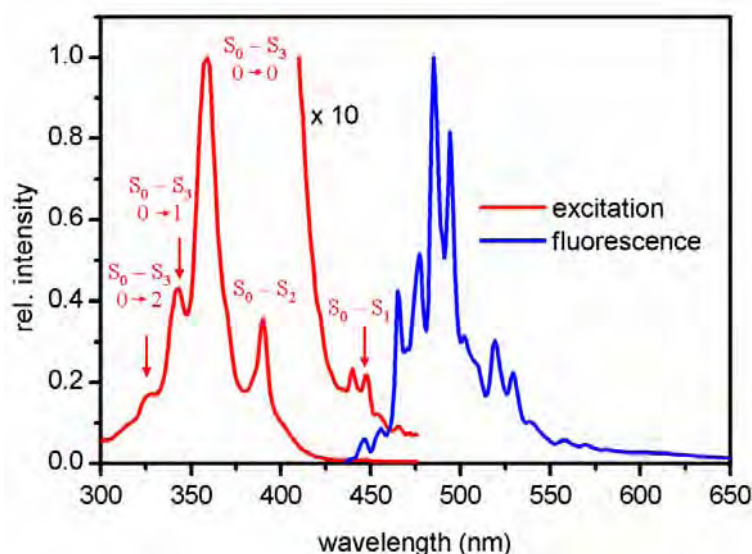
The energy situation of the HOMO-1, HOMO, LUMO and LUMO+1 orbitals in HBC is quite similar to the situation in benzene with the only difference that the six orbitals are closer together on the energy scale due to a larger number of carbons present in HBC. As consequence, in benzene only HOMO/LUMO interactions have to be considered<sup>[21]</sup> contrary to HBC where HOMO-1 and LUMO+1 interact too.

<sup>d</sup> The TDDFT calculation was performed by Prof. Thomas Bally, University of Fribourg

The HOMO-1 orbital with an  $a_{1u}$  symmetry has a relative energy of -9.42 eV. It has to be noted that orbital energies calculated with TDDFT are normally slightly too high. Further there are two degenerated HOMO orbitals ( $e_{1g}$  symmetry) with an energy of -7.96 eV. For the virtual orbitals, first two degenerated LUMOs ( $e_{2g}$  symmetry) at -1.3 eV followed by the LUMO+1 ( $b_{2g}$  symmetry) at nearly 0.0 eV were found. The calculation revealed further that there exist four  $e_{1g}$  to  $e_{2u}$  transitions (dashed blue lines) yielding a degenerated state indicated by the blue arrow towards the configuration interaction. The transitions  $a_{1u}$  to  $e_{2u}$  and  $e_{1g}$  to  $b_{2g}$  (dashed violet lines) furnish another set of nearly degenerate states (violet arrows). The splitting of these new states gives rise to several configuration interactions out of which four transitions were elucidated:  $S_0$ - $S_1$  (2x),  $S_0$ - $S_2$  and  $S_0$ - $S_3$ .

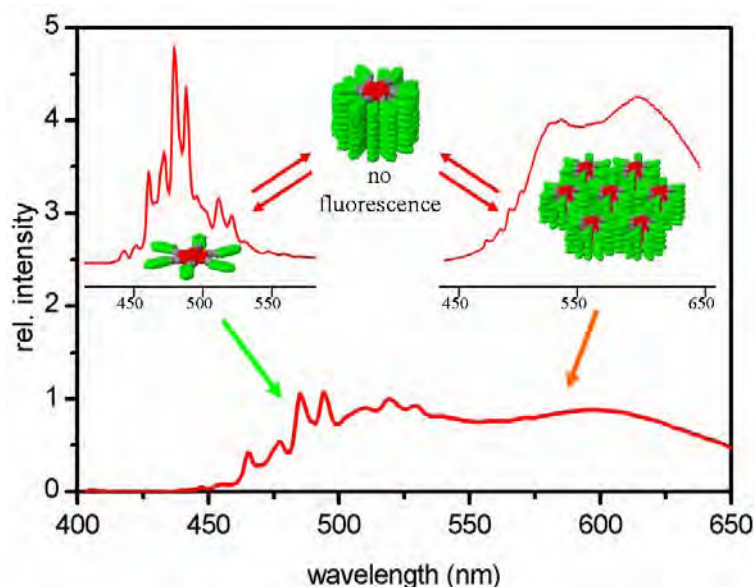
The dipole forbidden  $S_0$ - $S_1$  band at 448 and 439 nm (theoretical 428 and 409 nm) appear at the highest wavelength. The  $S_0$ - $S_2$  band at 392 nm (theoretical 377 nm) is of intermediate wavelength and intensity while still dipole forbidden, whereas the very intense allowed  $S_0$ - $S_3$  band at 361 nm (theoretical 359 nm) possesses the lowest wavelength. The two additional peaks at 343 and 325 nm are due to the vibronic fine structure of the intense  $S_0$ - $S_3$  transition. As illustration the excitation as well as the luminescence spectra of HBC is depicted in Figure 14.7. The luminescence spectrum looks normally like a mirror image of the  $S_0$ - $S_1$  transition. As the  $S_0$ - $S_1$  transition is dipole forbidden and moreover eventual vibronic structures are covered by the  $S_0$ - $S_2$  and  $S_0$ - $S_3$  transitions, the mirror like behaviour was not observed. Further, no explanation of the apparent splitting of the luminescence spectrum can be given at this moment.

Clar<sup>[12a, 247b]</sup> introduced in 1964 the empirical nomenclature  $\alpha$ -,  $p$ -, and  $\beta$ -band for aromatic compounds which were correlated to the “ortho” and “para” reactivity. Several authors used this nomenclature to describe the HBC spectrum, which is in our opinion not allowed, as nobody approved this assignment so far. Due to this, the Clar nomenclature will not be used in this description.



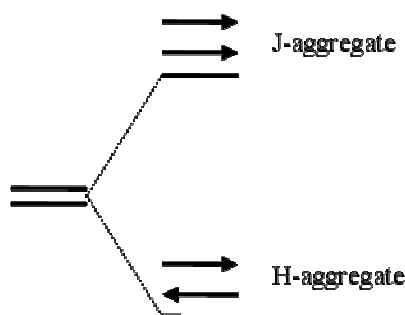
**Figure 14.7** – Excitation ( $\lambda_{\text{det}} = 485$  nm) and emission ( $\lambda_{\text{ex}} = 360$  nm) spectrum of a  $10^{-6}$  M BTF solution of HBC **94b**

## 14.2.4 Luminescence spectrum of 1-D stacks and 2-D or 3-D lateral aggregated structures



**Figure 14.8** – **Lower part:** luminescence spectrum ( $\lambda_{\text{ex}} = 360$  nm) of a  $10^{-4}$  M BTF solution of HBC-Rf<sub>4,6</sub> (**94b**); **upper left part:** luminescence spectrum of a  $10^{-6}$  M BTF solution of HBC-Rf<sub>4,6</sub> **94b**; **upper middle part:** “dark” HBC column; **upper right part:** luminescence spectrum of a  $10^{-3}$  M HBC-Rf<sub>4,6</sub> (**94b**) suspension in BFF

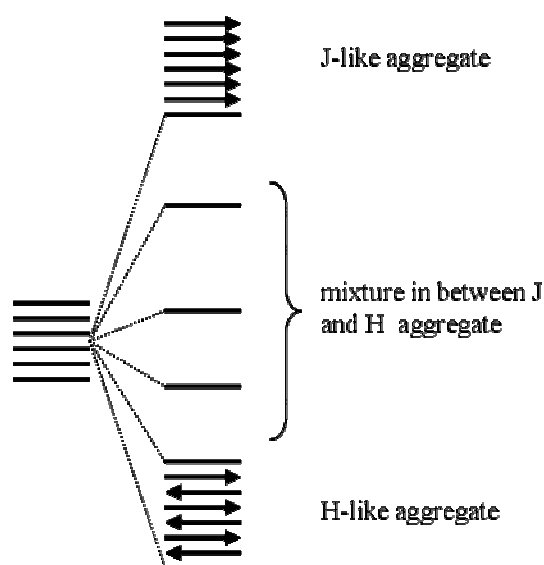
At the bottom of Figure 14.8 the luminescence spectrum of HBC-Rf<sub>4,6</sub> (**94b**) in BTF at  $10^{-4}$  M is shown. The spectrum is composed of the part containing well resolved bands between 400 and 550 nm, belonging to the green emission of the monomeric HBC. Further large broad bands in the region of 500 to 650 nm were revealed, which could be attributed to aggregated HBC columns yielding two- or three- dimensional architectures. These findings were underlined by a fluorescence spectrum of a  $10^{-3}$  M BTF suspension, shown on the upper right part of Figure 14.8. As shown later (section 15.1.2) a BTF solution of HBC-Rf<sub>4,6</sub> (**94b**) at  $10^{-4}$  M consist of three main “forms” of HBC which are in equilibrium: monomers, 1D-stacks and laterally aggregated 1D-stacks forming two-dimensional or three-dimensional structures. This implies that the fluorescence of one-dimensional stacks is missing (not emissive) as all observed bands are explained. HBC columns can therefore not be revealed by the fluorescence technique. Further experimental data underlining this theory will be given later (chapter 15.1.2). The strongly different fluorescence behaviour of one-dimensional stacks as compared to their laterally aggregated counterparts and monomers, respectively, may be explained in the following way:



**Figure 14.9** – J- and H-aggregates formed by parallel and anti-parallel alignment of the transition dipole moments

The energy level diagram of a stable HBC dimer, which has not to be confused with an excimer existing only in the excited state, formed by  $\pi$ - $\pi$  interaction of the aromatic cores is depicted in Figure 14.9. The transition dipole moments of the two molecules have to be considered at the same time, which yields two different states, parallel or anti-parallel, produced by linear combinations. If the dipole moments point in the opposite direction, a so-called H-aggregate is formed. Due to the favourable electrostatic interaction H-aggregates are lower in energy than the initial state and would give rise to a red shifted fluorescence band. Unfortunately the two dipole moments cancel each other and prevent therefore any fluorescence (symmetry forbidden transition). The energy dissipation has hence to occur radiationless.

The other arrangement of the dipole moments arises when the two transition dipole moments points in the same direction, creating a so called J-aggregate. Due to the unfavourable electrostatic interaction, the energy of J-aggregates is always higher than the initial state. The J-aggregate would give rise to a very intense blue shifted luminescence but is energetically unfavoured and therefore often not observed.

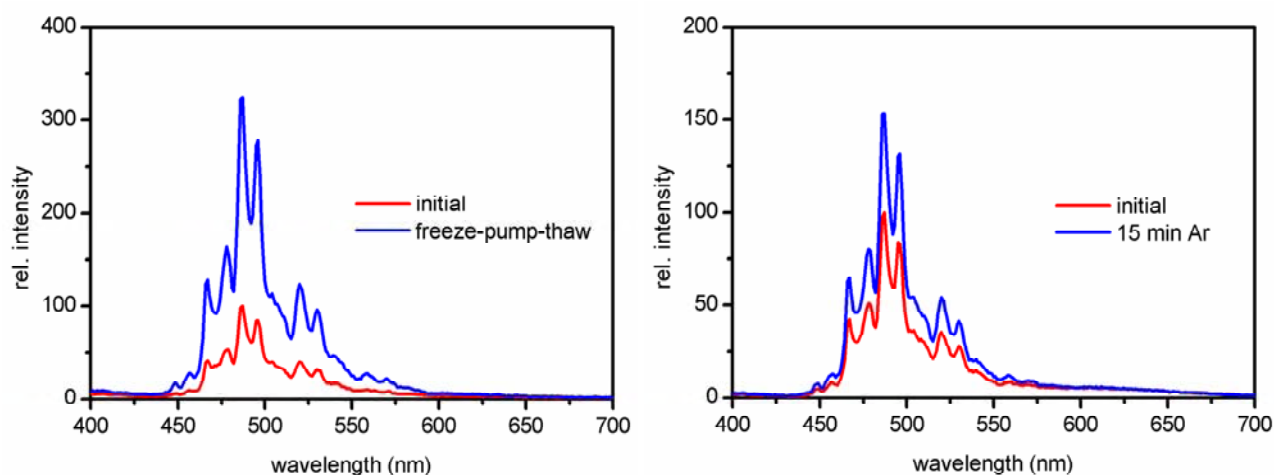


**Figure 14.10** – J- and H-like aggregates formed in a HBC hexamer by linear combinations of the transition dipole moments

By extrapolating the dimer situation to a stack consisting of six HBC units as shown in Figure 14.10, the same reasoning may be applied. The energy of the HBC hexamer splits up in six distinguished states, where the lowest state may be called H-like aggregate. In this state, the sum of the six transition dipole moments will be as small as possible, whereas in the energetically highest state a J-like aggregation is formed. Here the sum of the six transition dipole moments will be as big as possible. Due to energetic reasons only the lower states are populated in one-dimensional HBC stacks, explaining the very low fluorescence quantum yield. HBC columns were therefore not observed in fluorescence and behave like a “dark material”. Laterally aggregated architectures in contrary regain their fluorescence due to defects present in the structures, hindering the formation of net H-aggregates.

#### 14.2.5 Influence of oxygen

The fluorescence of the well structured monomer band (450 – 550 nm) is efficiently quenched by oxygen as depicted in Figure 14.11. On the left of Figure 14.11, the red curve was taken from a  $10^{-6}$  M aerated BTF solution containing HBC-Rf<sub>4,6</sub> (**94b**), whereas the blue curve shows the luminescence of the same solution after three freeze-pump-thaw cycles. An increase of the intensity of nearly 350 % could be observed proving that it is favourable to degas the solutions prior to the measurements but that it is not absolutely necessary as all bands are affected in the same way. A similar but less pronounced effect was found by bubbling argon through a BTF solution prior to the measurement. As expected the effect is exactly the same only less pronounced due to a lower efficiency to exchange oxygen. Nevertheless an increase of nearly 50 % could be achieved. It has further to be noted that the effect on the broad band around 600 nm was found to be completely negligible. The reason may be that these large aggregates are already quite big, and hinder therefore the access for oxygen to quench the fluorescence.



**Figure 14.11** – Luminescence spectra ( $\lambda_{\text{ex}} = 360$  nm) of HBC-Rf<sub>4,6</sub> (**94b**)  $10^{-6}$  M BTF solutions; **left**: aerated sample (red) and sample after freeze-pump-thaw deoxygenation (blue); **right**: aerated sample (red) and sample after 15 min. of argon sparking (blue); both graphs were normalized at 488 nm to 100% (red curves)

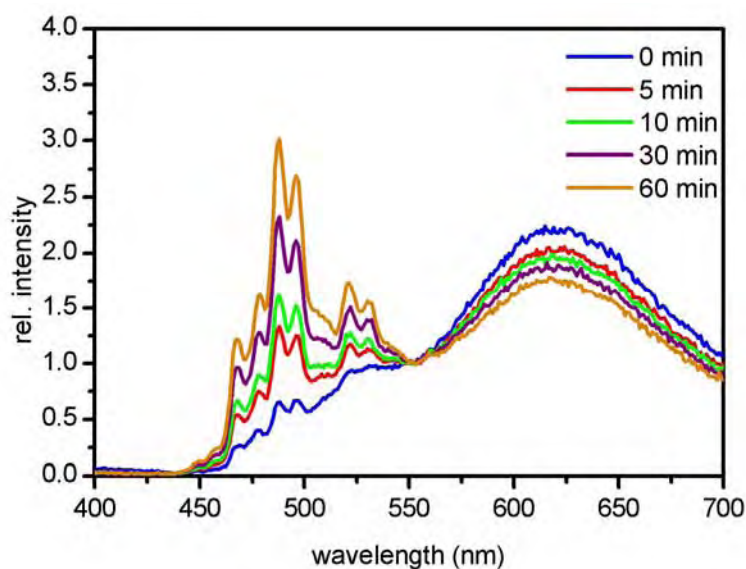


#### 14.2.6 Ultrasonic treatment

The fluorescence of a  $10^{-4}$  M BTF solution of HBC-Rf<sub>4,6</sub> (**94b**) was measured after different intervals of ultrasonic bath treatment. As depicted in Figure 14.12, the initial solution (blue curve) shows a pronounced large band around 600 nm, attributed to laterally aggregated HBC stacks together with less intense bands around 500 nm, due to HBC monomers.

By applying an ultrasonic treatment the broad red shifted band disappears very slowly, signifying that some HBC monomers are released from the aggregates. At the same time the liberated HBC monomers provokes a pronounced increasing of the corresponding band around 500 nm. By comparing the decrease of the 600 nm band with the increase of the 500 nm band it is obvious that their relation is not equal. It is known that ultrasonic waves interact much better with 1-D stacks than with large aggregated architectures. Because of that we suggest that to some extend aggregated structures are dissolved but at the same time 1D-stacks are broken, which liberate HBC monomers from a “dark material”. This could explain why the increase in monomer emission intensity exceeds the decrease in emission from aggregated structures.

In conclusion ultrasonic treatment readily dissolves 1D-stacks whereas aggregates are dissolved much less rapidly.



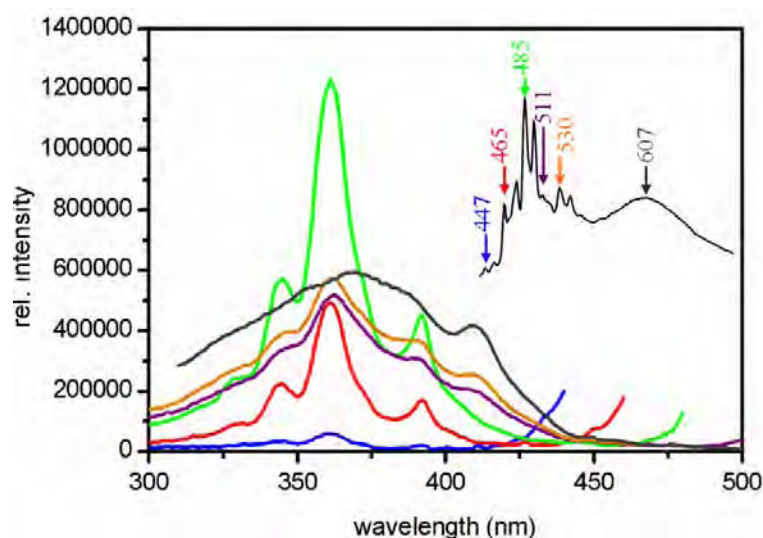
**Figure 14.12** – Fluorescence ( $\lambda_{\text{ex}} = 360$  nm) of  $10^{-4}$  M BTF solutions of HBC-Rf<sub>4,6</sub> (**94b**) after treatment in an ultrasonic bath for different periods; all spectra were normalized at 551 nm



### 14.2.7 Wavelength dependence of the excitation and luminescence

The excitation spectrum taken by detection at the high energy end of the luminescence at 447 nm (blue) reveals only the feature of monomeric HBC, which is not astonishing at all because the observation wavelength is well in the domain of the luminescence of the monomers (see chapter 14.2.4). The same is true by observing at 465 nm (red curve) and 485 nm (green curve), with the only difference of the later excitation spectra being much more intense.

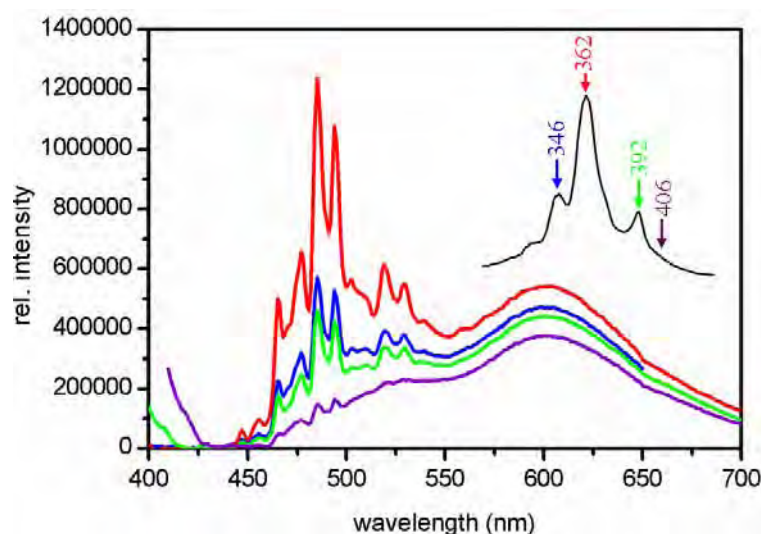
By detecting in between the region of monomer and aggregate at 511 nm (violet curve) and 530 nm (orange curve), the excitation spectrum reveals features of the monomeric HBC together with red shifted signals around 410 nm, attributed to aggregates. The pure aggregate excitation spectrum is then recorded by shifting the detection to 607 nm (grey curve). This spectrum shows a well resolved band at 406 nm together with a broad band around 370 nm. These observations are shown in Figure 14.13, which underlines in a complementary way the distinction between monomers and aggregates. Moreover if the excitation spectrum of the monomer is collected, the ideal wavelength is 485 nm, whereas for aggregate detection a wavelength around 600 nm has to be taken.



**Figure 14.13** – Excitation spectra of a  $10^{-5}$  M BTF solution of HBC-Rf<sub>4,6</sub> (**94b**) taken by varying the detection wavelength. The inset shows in the corresponding colour the detection on the luminescence spectrum of the same solution. No normalization was done.

The first three spectra in Figure 14.14, recorded by excitation at 346 nm (blue), 362 nm (red) and 392 nm (green), respectively, reveal intense part of the monomeric HBC together with a considerable superposition of the aggregated structures. This is not astonishing as the various excitation spectra shown in Figure 14.13 revealed that the aggregate is present in the whole range between 300 and 450 nm. Only by shifting the excitation wavelength to 406 nm (violet) the characteristic monomer structure is decreasing in favour of the large red shifted band around 600 nm as shown in Figure 14.14. The wavelength dependency of the fluorescence underlines that the attributions of

monomer as well as aggregate bands were done judiciously. Furthermore the optimal excitation wavelength to observe intense bands, enriched in monomer fluorescence, is 362 nm, whereas for aggregate detection at 406 nm or higher wavelengths is appropriate.



**Figure 14.14** – Luminescence spectra of a  $10^{-5}$  M BTF solution of HBC-Rf<sub>4,6</sub> (**94b**) recorded by variation of the excitation wavelength. The inset shows in the corresponding colour the used excitation wavelengths. The spectra were not normalized.

#### 14.2.8 Fluorescence dynamics

Time-dependent fluorescence was performed in order to get a deeper insight into the dynamics of the fluorescence<sup>e</sup>. The fluorescence lifetime  $\tau_r$  (radiative life time) is typically a few nanoseconds for allowed transitions and up to several hundred nanoseconds for forbidden transitions. This lifetime  $\tau_{nr}$  is related to the radiative rate constant  $k_r$  and the nonradiative rate constant  $k_{nr}$  by the following equation:<sup>[248]</sup>

$$k_{\text{exp}} = k_r + k_{nr} = \frac{1}{\tau_r} + \frac{1}{\tau_{nr}} = \frac{1}{\tau_{\text{exp}}}$$

**Equation 14.1** – Relation of lifetime and rate constant

The relation between the radiative lifetime  $\tau_r$  and the absorption and emission spectra of a chromophore is known as the Strickler-Berq equation,<sup>[249]</sup> which depends further on the refractive index due to the polarizability of the medium surrounding the chromophore.

<sup>e</sup> All shown time-dependent fluorescence experiments were performed by Jakob Grilj, group of Prof. Vauthey, University of Geneva

$$\frac{1}{\tau_r} = k_r = 2.88 \cdot 10^{-9} n^2 \frac{\int I(\tilde{\nu}) d\tilde{\nu}}{\int I(\tilde{\nu}) \tilde{\nu}^{-3} d\tilde{\nu}} \int \frac{\varepsilon(\tilde{\nu})}{\tilde{\nu}} d\tilde{\nu}$$

**Equation 14.2** – Strickler-Berg equation

In Equation 14.2  $n$  is the refractive index,  $I$  the fluorescence emission,  $\varepsilon$  the extinction coefficient and  $\tilde{\nu}$  the wave number. The fluorescence lifetime  $\tau_{nr}$  and the radiative lifetime  $\tau_r$  are related through the quantum yield  $\Phi$  in the following equation:

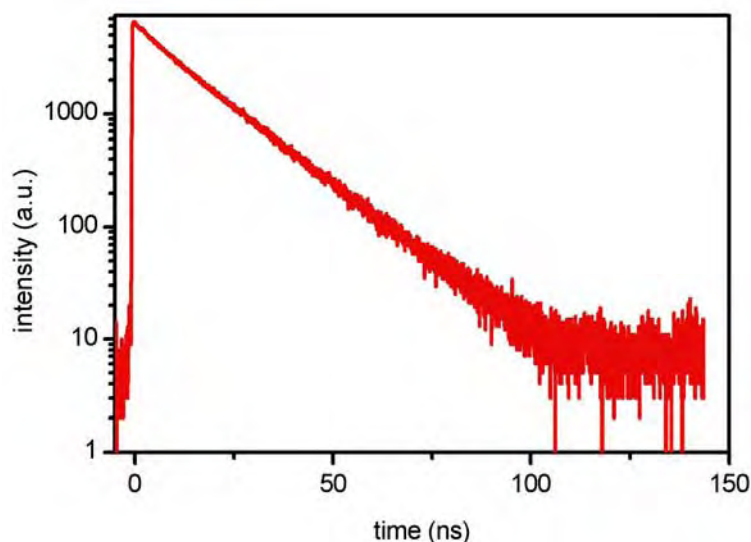
$$\Phi = \frac{\tau_{nr}}{\tau_r} = \frac{k_r}{k_r + k_{nr}}$$

**Equation 14.3** – Fluorescence quantum yield

Using the Strickler-Berg equation (Equation 14.1) with an estimated oscillator strength of  $f = 0.01$  and an experimentally determined fluorescence quantum yield  $\Phi = 0.05$  (using anthracene in cyclohexane  $\Phi = 0.3$  as standard) the following values for  $k_r$ ,  $k_{nr}$ ,  $\tau_r$  and  $\tau_{nr}$  were obtained:

$$\begin{aligned} k_r &= 1.0 \cdot 10^6 \text{ s}^{-1} & k_{nr} &= 2.0 \cdot 10^7 \text{ s}^{-1} \\ \tau_r &= 960 \text{ ns} & \tau_{nr} &= 50 \text{ ns} \end{aligned}$$

The kinetics of HBC-Rf<sub>4,6</sub> (**94b**) have been measured<sup>f</sup> in HFB and BTF at various concentrations for HFB and at one concentration for BTF as for this solvent the obtained precipitate hampered the experiment at high concentrations ( $10^{-5}$  M and higher). A single photon counting spectrum is shown in Figure 14.15 as example for a  $10^{-5}$  M HFB solution of HBC **94b**.

**Figure 14.15** – Fluorescence decay of HBC-Rf<sub>4,6</sub> (**94b**) in HFB ( $10^{-5}$  M) at 500 nm

<sup>f</sup> The kinetics were determined by Jakob Grilj, group of Prof. Vauthey, University of Geneva

The experimental SPC data was fitted to a bi-exponential decay equation (Equation 14.4) of the form:

$$I = I_0 + A_1 \cdot e^{(-t/\tau_1)} + A_2 \cdot e^{(-t/\tau_2)}$$

**Equation 14.4** – Fitting of the experimental data

The obtained values for the resulting amplitudes  $A_n$  and the corresponding lifetimes  $\tau_n$  are given in Table 14.1 for experiments using different band pass filters in order to choose a particular part of the fluorescence spectrum.

**Table 14.1** – Radiative lifetimes of HBC-Rf<sub>4,6</sub> (**94b**) at various concentration in BTF and HFB

Solvent	Conc. [mol/l]	filter	$\tau_1$ [ns]	$A_1$	$\tau_2$ [ns]	$A_2$
BTF	$10^{-5}$	500	<b>39</b>	0.7	<b>3</b>	0.3
		540	<b>14</b>	0.35	<b>5</b>	0.65
		610	<b>13</b>	0.32	<b>5</b>	0.68
HFB	$5 \cdot 10^{-5}$	500	<b>17</b>	0.77	<b>7</b>	0.23
		650	<b>20</b>	0.53	<b>5</b>	0.47
		700	<b>21</b>	0.48	<b>6</b>	0.52
HFB	$10^{-4}$	500	<b>16</b>	0.79	<b>7</b>	0.21
		700	<b>20</b>	0.50	<b>6</b>	0.50
HFB	$10^{-3}$	500	<b>15</b>	0.78	<b>4</b>	0.22
		700	<b>17</b>	0.51	<b>5</b>	0.49

The obtained radiative lifetimes, shown in Table 14.1 underline the findings discussed earlier. In BTF, the region of 500 nm is mostly due to the fluorescence of monomers (7 : 3) whereas at longer wavelengths (540 nm and 610 nm) the fluorescence is more and more due the aggregated architectures (3 : 7). The numbers in brackets refer to the calculated amplitudes of Equation 14.4. Moreover, the fluorescence of the monomers was found to be long-lived (between 20 and 40 ns), which is in agreement with the low oscillator strength. In contrast to this, the lifetime of the aggregates is rather small, most probably due to the fact, that there are much more pathways for an aggregate to dissipate its energy.

In HFB exactly the same behaviour was observed. Furthermore it was found that the kinetics are identical over a concentration range between  $10^{-5}$  and  $10^{-3}$  M. Higher concentration could not be measured as the solutions started to be turbid. As shown from concentration dependent fluorescence, the formation of aggregates starts to be important around  $10^{-3}$  M in HFB.

## 15 Tuning the aggregation behaviour of HBC derivatives

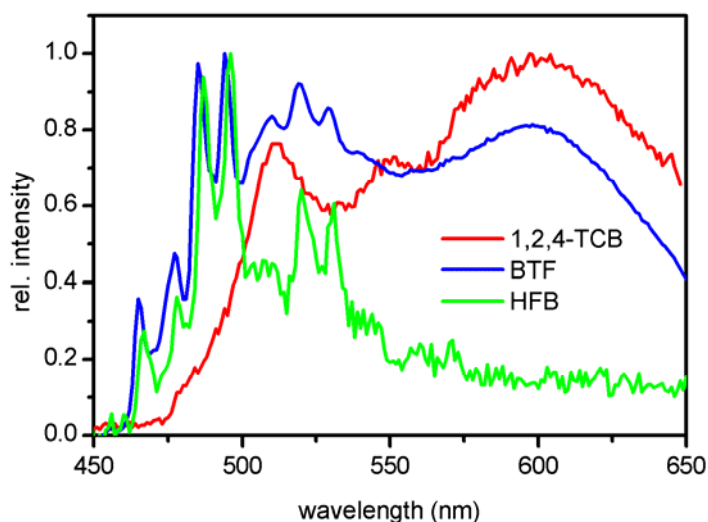
### 15.1 Engineering the medium

#### 15.1.1 Solvent influence on the aggregation

In this section, the effect of different solvents on the molecular aggregation of perfluorinated HBC derivatives is examined. The aggregation is a result of more favourable HBC-HBC interactions over HBC-solvent interactions.<sup>[250]</sup> If the interaction between solutes and solvent molecules is stronger than HBC-HBC and solvent-solvent interactions, there would be very few aggregates in solution and hence mostly monomers. On the contrary, if the molecule-solvent interaction is weak, there would be very few monomers present in solution, as HBC would tend to assemble.

Figure 15.1 shows the fluorescence spectra of HBC-Rf<sub>4,6</sub> (**94b**) at 10<sup>-4</sup> M in the three main solvents used for this investigation: 1,2,4-TCB, BTF and HFB, noted in the order of increasing capacity to dissolve HBC derivatives carrying perfluoroalkylated side chains. HBC-Rf<sub>4,6</sub> (**94b**) shows no traces of monomeric HBC in TCB, *i.e.* at this concentration only aggregated HBC structures are present, illustrated by the three bands (500; 540; 600 nm). Two factors are responsible for this behaviour: *i*) the low solubility of HBC-Rf<sub>4,6</sub> **94b** in TCB which favours aggregation; *ii*) the low tendency for  $\pi$ - $\pi$  complexation of TCB to the HBC derivatives which allows the formation of very extended structures. It is worth mentioning that the three bands observed suggest the presence of different kinds of aggregates coexisting at the same time. It could not be elucidated in what the aggregates differ.

Accordingly, in BTF solutions a dynamic equilibrium between aggregated and monomeric HBC-Rf<sub>4,6</sub> (**94b**) is observed as features of both species are revealed. On the other hand, the fluorescence spectrum of **94b** in HFB shows almost exclusively HBC monomer emission. Again two reasons might be responsible for this observation: *i*) the high solubility of the monomer, and *ii*) the high end-capping tendency of HFB, which favours short aggregated structures and hinders the formation of very long columns, which reduces inherently the formation of lateral aggregates. In addition it is worth to note that the luminescence intensity is reduced by two orders of magnitude in this solvent, as compared to BTF, which is most probably due to the presence of short “dark” supramolecular fibres as discussed earlier (chapter 14.2.4).



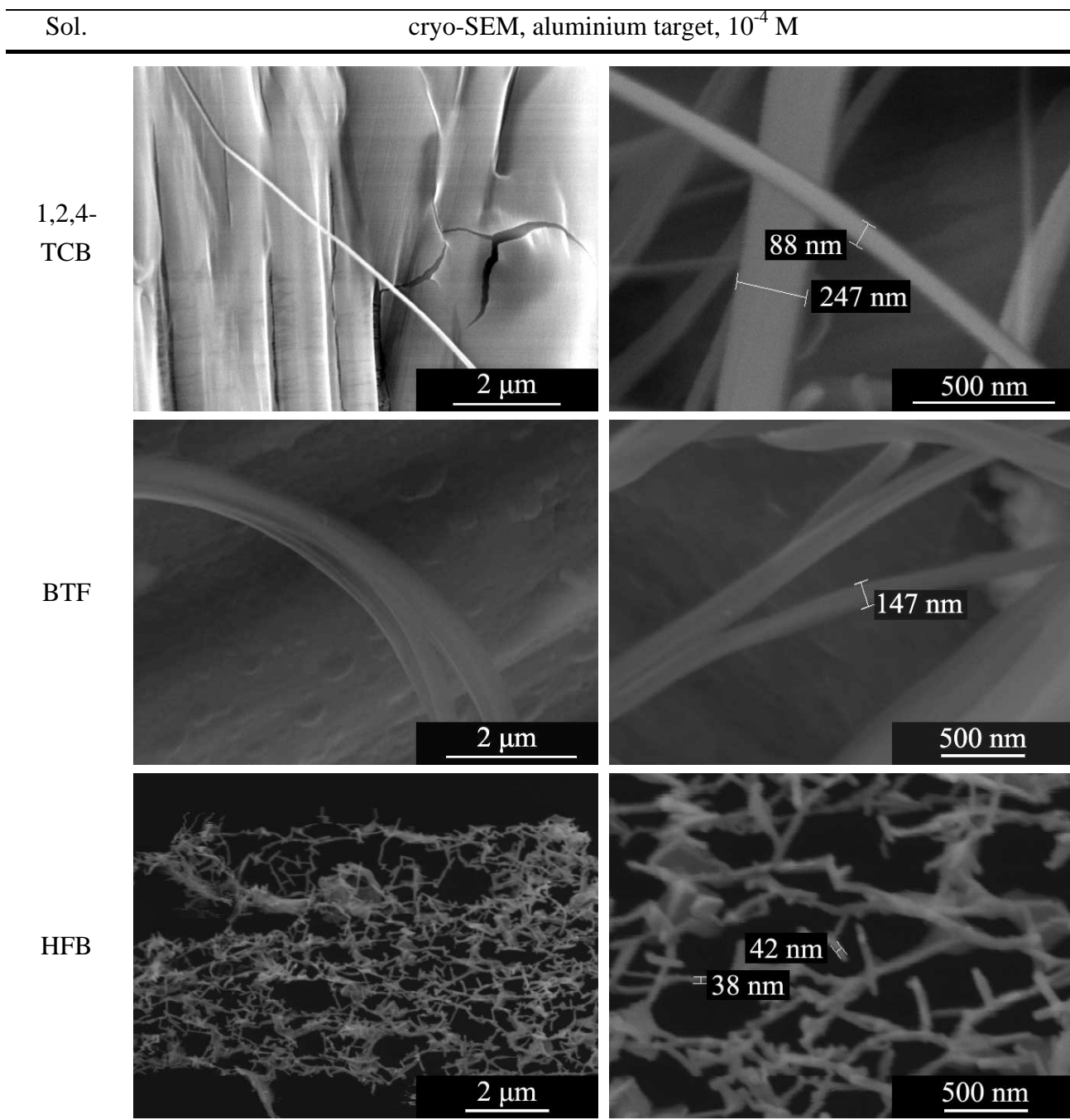
**Figure 15.1** – Luminescence spectra ( $\lambda_{\text{ex}} = 360$  nm) of  $10^{-4}$  M HBC-Rf<sub>4,6</sub> (**94b**) solutions in various solvents. The spectra are arbitrarily normalized

Cryo-SEM micrographs of the same samples ( $10^{-4}$  M in TCB, BTF and HFB) are depicted in Figure 15.2. HBC-Rf<sub>4,6</sub> (**94b**) in TCB reveals the presence of very long structures of rectangular cross section, presumably formed by lateral aggregation of HBC fibres into sheets, which stack to form piles. The remarkable length (average 20  $\mu\text{m}$ ) of these structures corroborates with the assumption of a low  $\pi$ - $\pi$  complexing tendency of TCB, leading to no end-capping. The typical cross section of these flat rectangular structures is about 100 nm  $\times$  250 nm, which corresponds to approximately 2000 laterally aggregated HBC filaments.

However, the samples obtained from BTF solutions result in structures showing a much wider range of different forms as compared to those obtained from TCB solutions. Large bundles of laterally aggregated HBC columns with an average length of about 20  $\mu\text{m}$  and a cross section of up to 500  $\times$  200 nm, were observed. In addition, the previously observed completely regular fibres in TCB show now several splittings into smaller strands that rapidly taper off in samples obtained from BTF solutions.

In contrast, from solutions of the same concentration in HFB, the compound only shows thin regular strands with a diameter of 40 nm (mostly Pt shading) and a typical length of 200 nm, 100 times shorter than in the other solvents. The observed uniform diameter of about 40 nm indicates the presence of monostranded HBC stacks, as for the observation in cryo-SEM a platinum coating of approximately 20 nm was applied. The observed short columns corroborate with our assumption of a pronounced  $\pi$ - $\pi$  complexation by this solvent, resulting in an efficient end-capping of the columns by HFB.<sup>[251]</sup>

In conclusion, the one-dimensional aggregation as well as the lateral aggregation is strongly influenced by the solvent as shown by fluorescence and cryo-SEM of HBC-Rf<sub>4,6</sub> (**94b**) in 10<sup>-4</sup> M TCB, BTF or HFB solutions. The solvent influences the aggregation by its capacity of solubilizing monomers as well as columns and its  $\pi$ - $\pi$ -complexation tendency towards HBC, which favours end capping.



**Figure 15.2** – Cryo-SEM micrographs of 10<sup>-4</sup> M HBC-Rf<sub>4,6</sub> (**94b**) solutions in three different solvents

### 15.1.2 Concentration influence on the aggregation

The effect on the aggregation as a function of concentration was investigated by fluorescence spectroscopy in solutions of HBC-Rf<sub>4,6</sub> (**94b**) at concentrations ranging from  $10^{-3}$  to  $10^{-10}$  M in TCB, BTF and HFB, shown in Figure 15.3. In TCB at  $10^{-4}$  M three large red shifted bands (510 nm, 550 nm and 600 nm) are observed which can be attributed to laterally aggregated HBC structures by comparison with cryo-SEM micrographs of the same concentration (as shown in Figure 15.4). On lowering the concentration the intensity of the three aggregate bands decreases as expected. It is worth mentioning that the monomer emission never appears, even by lowering the concentration to  $10^{-7}$  M. This is underlining the discussion from the previous chapter (chapter 15.1.1) concerning the low solubility and low end-capping tendency of TCB favouring the presence of long strands at the expense of monomer.

In BTF, below  $10^{-6}$  M only the resolved fluorescence features of monomeric HBC could be observed. As the concentration increases two new bands (510 and 600 nm) appeared at the red side of the fluorescence spectrum. These peaks are related to the fibrous structures observed in cryo-SEM. In addition the number and size of aggregates increases with concentration, as seen in the enhancement of the red-shifted emission and by comparing to the cryo-SEM micrographs of identical solutions.

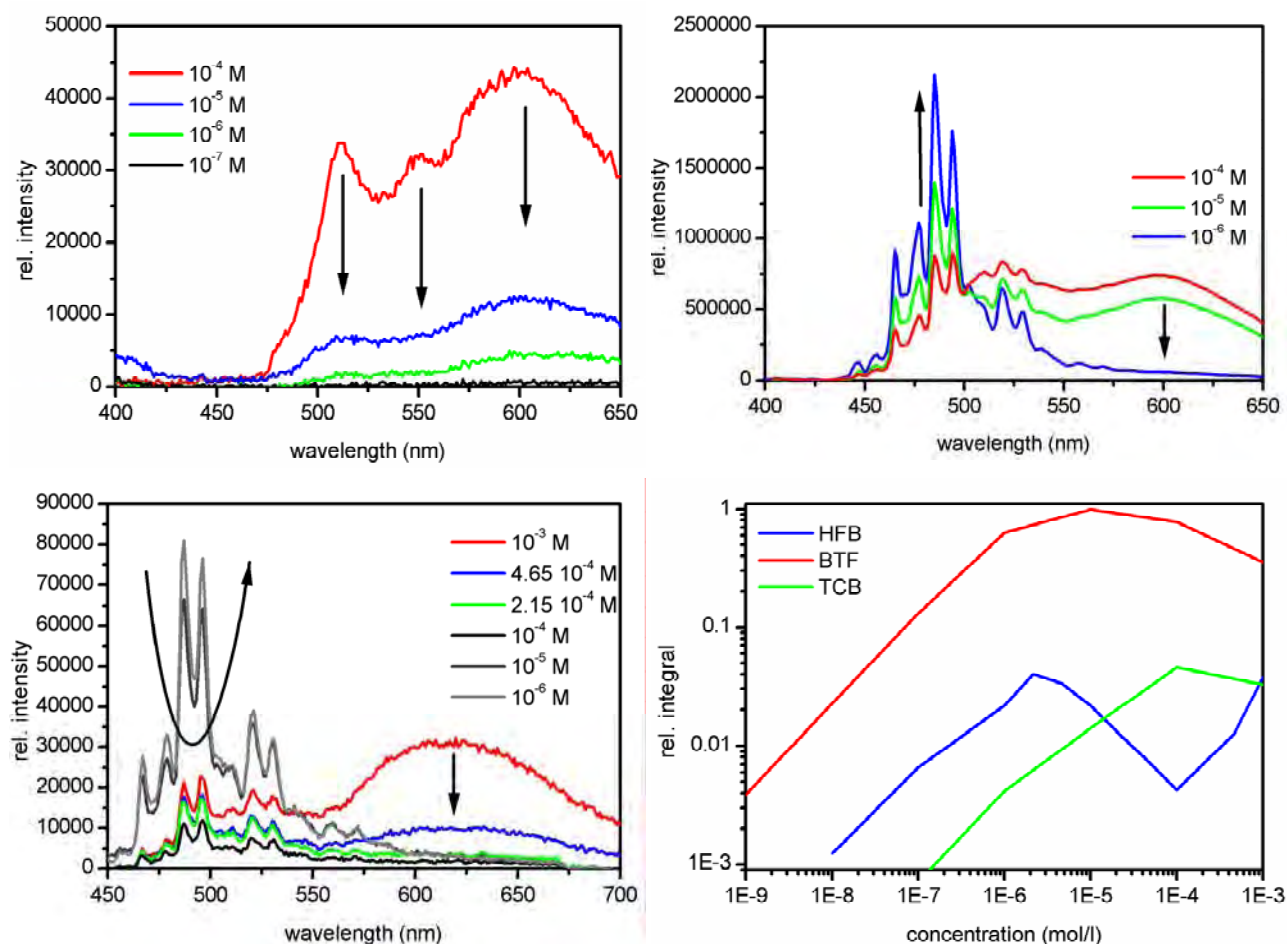
In HFB the behaviour is slightly different. At very high concentration, as expected from the cryo-SEM data depicted in Figure 15.4 mostly laterally aggregated architectures are present. This corroborates nicely with the red bands (510 nm, 615 nm) observed in fluorescence. By lowering the concentration by a factor of two, the red shifted bands loose nearly 75% of their intensity and reach nearly zero by reducing the concentration by a factor of 2 again. Surprisingly the monomer emission does not rise as observed in the case of BTF solutions but decreases slightly. At  $10^{-4}$  M the intensity of the 485 nm band reaches a minimum, whereas in cryo-SEM monostranded HBC columns were observed. By lowering the concentration by a factor of 10 further to  $10^{-5}$  M the 485 nm band shows a huge increase in intensity by a factor of 6. By lowering even further the concentration ( $10^{-6}$  M) the intensity of 485 nm reaches a maximum and decreases thereafter by further lowering the concentration. It seems that in this particular solvent the three distinctive HBC structures are present: *i*) at very high concentrations ( $10^{-3}$  M) the predominant species are large laterally aggregated structures, revealed by the red-shifted band in the emission spectrum; *ii*) at high concentrations ( $10^{-4}$  M) the predominant structures are monostranded stacks which do not fluoresce as discussed earlier (chapter 14.2.4); *iii*) on further lowering the concentration the monostranded stacks disassemble to monomers which are revealed by the very strong 485 nm band which may even be increased by lowering the concentration to  $10^{-6}$  M.



In order to visualize the “missing” fluorescence due to the formation of HBC stacks (predominantly in HFB) the luminescence spectra were integrated from 400 to 660 nm for all concentrations. The obtained curves are shown in Figure 15.3. As expected, in TCB the intensity increases linearly with the concentration up to  $10^{-4}$  M where the intensity decreases due to the inner filter effect provoked by the turbid solution containing too many aggregated particles, which diffract the light.

In BTF the changing point from increasing to decreasing is much less pronounced and starts already at  $10^{-6}$  M. This decrease is not explicable by the presence of aggregated structure with diffract the incident light as the solution at  $10^{-6}$  M is completely transparent. This underlines the idea of one-dimensional stacks, formed at lower concentrations than aggregates, which behave like “dark matter”. In BTF solutions the formation of monostranded stacks starts around  $10^{-6}$  M and is accompanied at  $10^{-5}$  M by the formation of aggregates.

By using HFB as solvent the domain of monostranded stacks and aggregates is well separated, as illustrated by the integration. The linear increase of intensity is suddenly interrupted and the intensity is even decreasing an order of magnitude by concentrating a hundred times. At  $10^{-4}$  M the intensity is again increasing and would probably start to decrease at higher concentrations due to the inner filter effect. The HFB experiment underlines very clearly the formation of non-emissive one-dimensional stacks at low concentration which aggregate laterally at much higher concentration. Interestingly, the highest overall intensity is observed in BTF indicating with this probably the least pronounced interaction between HBC molecules and the solvent reducing therefore any quenching of the fluorescence.



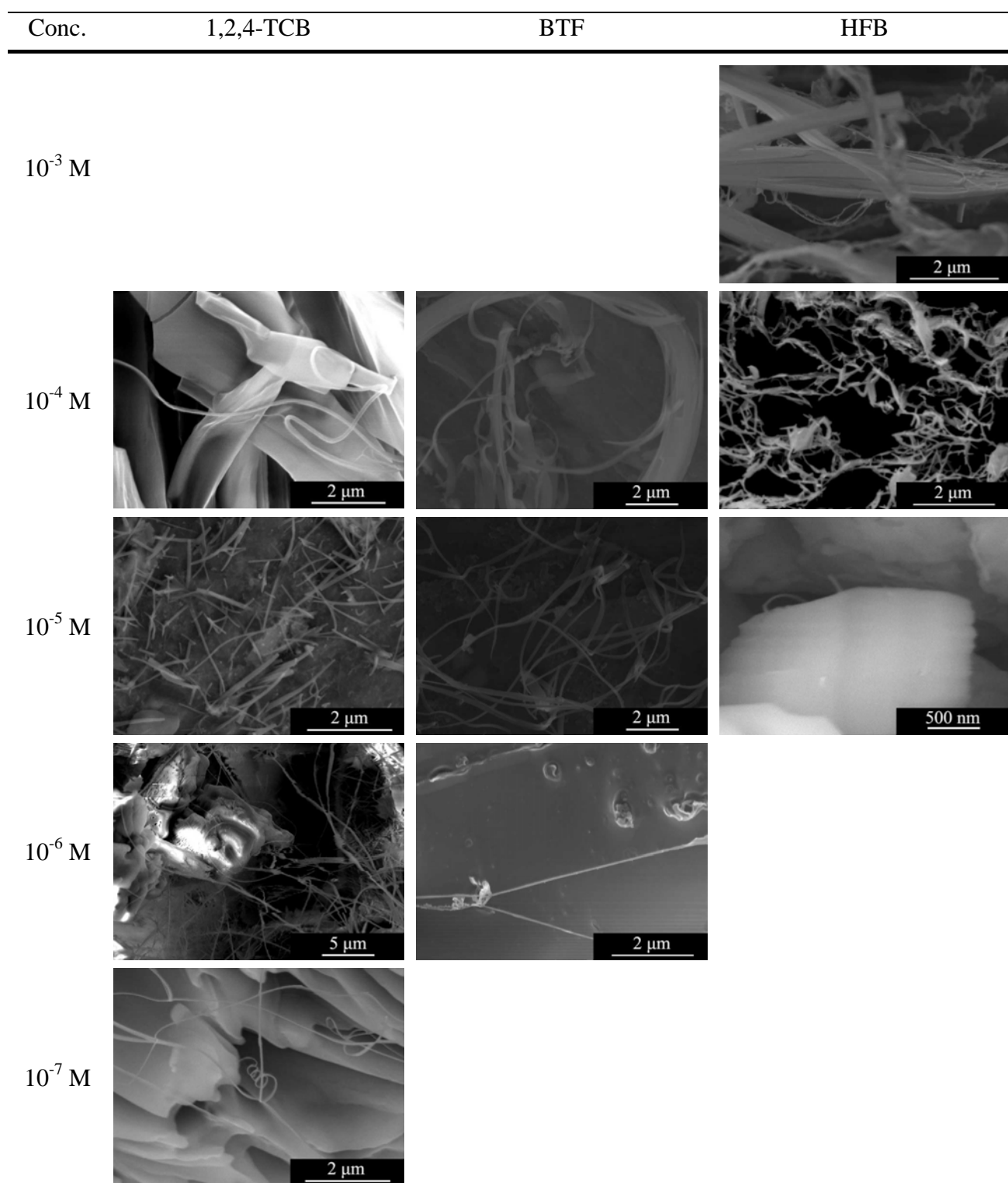
**Figure 15.3** — Fluorescence spectra ( $\lambda_{\text{ex}} = 360$  nm) of HBC-Rf<sub>4,6</sub> (94b) in various solvents and concentrations: **upper left:** TCB; **upper right:** BTF; **lower left:** HFB; **lower right:** integration of the emission between 400 and 700 nm. The fluorescence spectra are not scaled, contrarily to the integrated curves (without variation of the relative intensities).

The cryo-SEM observations corroborate very well with the fluorescence data. In TCB at 10<sup>-4</sup> M long, barely ramified but largely aggregated structures are expelled on top of the solvent. By lowering the concentration these structures slowly decrease in thickness whereas the length is more or less conserved to obtain at 10<sup>-7</sup> M thin long structures of various thicknesses. This indicates the presence of aggregated fibres even at this fairly low concentration. Moreover the observed monostranded stacks observed at 10<sup>-7</sup> M start to curl under the electron beam if they have a loose end which is not frozen in the solvent.

The 10<sup>-4</sup> M BTF solution reveals in contrary much thicker and less uniform structures. An enormous variety of linear and branched architectures is present. On lowering the concentration the uniformity of the structures rises as they keep approximately their length but reduce their cross-section. Only at 10<sup>-6</sup> M monostranded HBC stacks are observed.

In HFB solutions the situation is slightly different. The high solubility of HBC-Rf<sub>4,6</sub> (**94b**) in HFB allowed the preparation of a  $10^{-3}$  M solution which consists of large laterally aggregated structures which taper off rapidly in combination with monostranded long stacks. Already at  $10^{-4}$  M lateral aggregated structures are no longer visible. Only monostranded short columns are found all over the frozen solvent surface entangled in spider network like architectures. It has to be noted that this is the first observation of such a high amount of monostranded stacks without any presence of lateral aggregation. Finally by lowering the concentration to  $10^{-5}$  M nearly all structures are disassembled into small units, not visible in cryo-SEM. Only rarely some monostranded columns stacks stand out of the frozen solvent.

One concludes that the variation of the concentration has the expected effect: at high concentrations ( $\geq 10^{-5}$  M for BTF and  $\geq 10^{-3}$  M for HFB), large structures are dominant whereas on lowering the concentration (around  $10^{-5}$  M for BTF and  $10^{-4}$  M for HFB) lateral aggregation first decreases to yield mostly monostranded HBC stacks, which disassemble into their molecular components on further lowering the concentration. It is worth mentioning that in HFB the three domains monomer / column / aggregate are well separated whereas in TCB and BTF this is not the case. Moreover the micrographs depicted in Figure 15.4 are in agreement with the solvent effect discussed in the previous section (chapter 15.1.1).

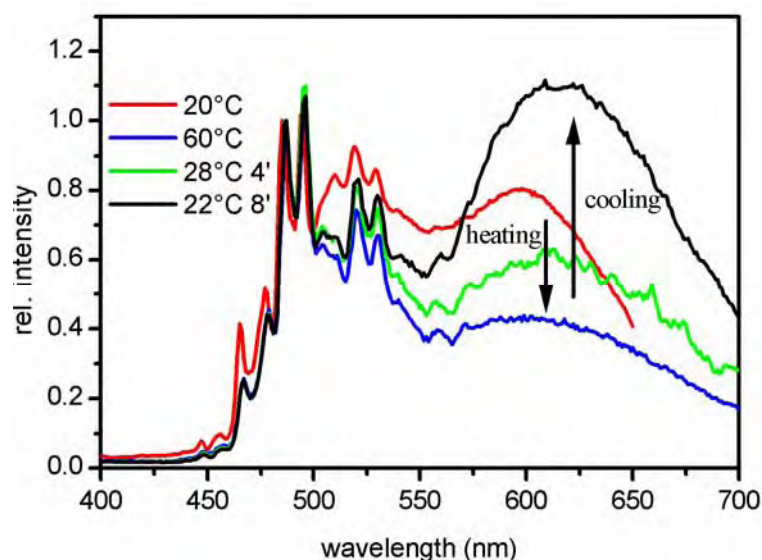


**Figure 15.4** – Cryo-SEM micrographs illustrating the morphology of HBC-Rf<sub>4,6</sub> (**94b**) at various concentrations in three different solvents

## 15.1.3 Effect of temperature and time on the aggregation

An increase of temperature induces most usually a higher solubility of the compound in question. In our case this signifies that the increased solubility reduces the lateral aggregation and moreover disassembles also the monostranded HBC structures. Upon heating a  $10^{-4}$  M BTF solution of HBC-Rf<sub>4,6</sub> (**94b**), the red aggregate bands are clearly reduced which signifies the dissolution of aggregated structures into monostranded stacks, which dissolves further into monomers. On regaining room temperature the red-shifted band re-evolves quickly and its maximum rises even slightly higher than the starting point. It has to be noted that the whole process is fully reversible, even though the red-shifted band do not match a hundred percent before and after the heating. This mismatch is most probably due to the fact that the exact nature of the aggregated substance may vary and has not yet been fully elucidated. It is therefore possible that different geometries of aggregates coexist in solution and more time is needed to regain the initial equilibrium. Moreover the initial solutions were prepared by heating each sample individually which proved to yield on repetitive samples identical spectra.

Furthermore it was observed that at higher temperatures, the fluorescence intensity decreases slightly, most probably due to the fact that the monomer emission quantum yield is lower at this temperature. This may be explained by the solvent influence, which changes upon heating its properties, such as the viscosity, and improves therefore the possibility for the excited molecule to loose its energy radiationless.<sup>[252]</sup>



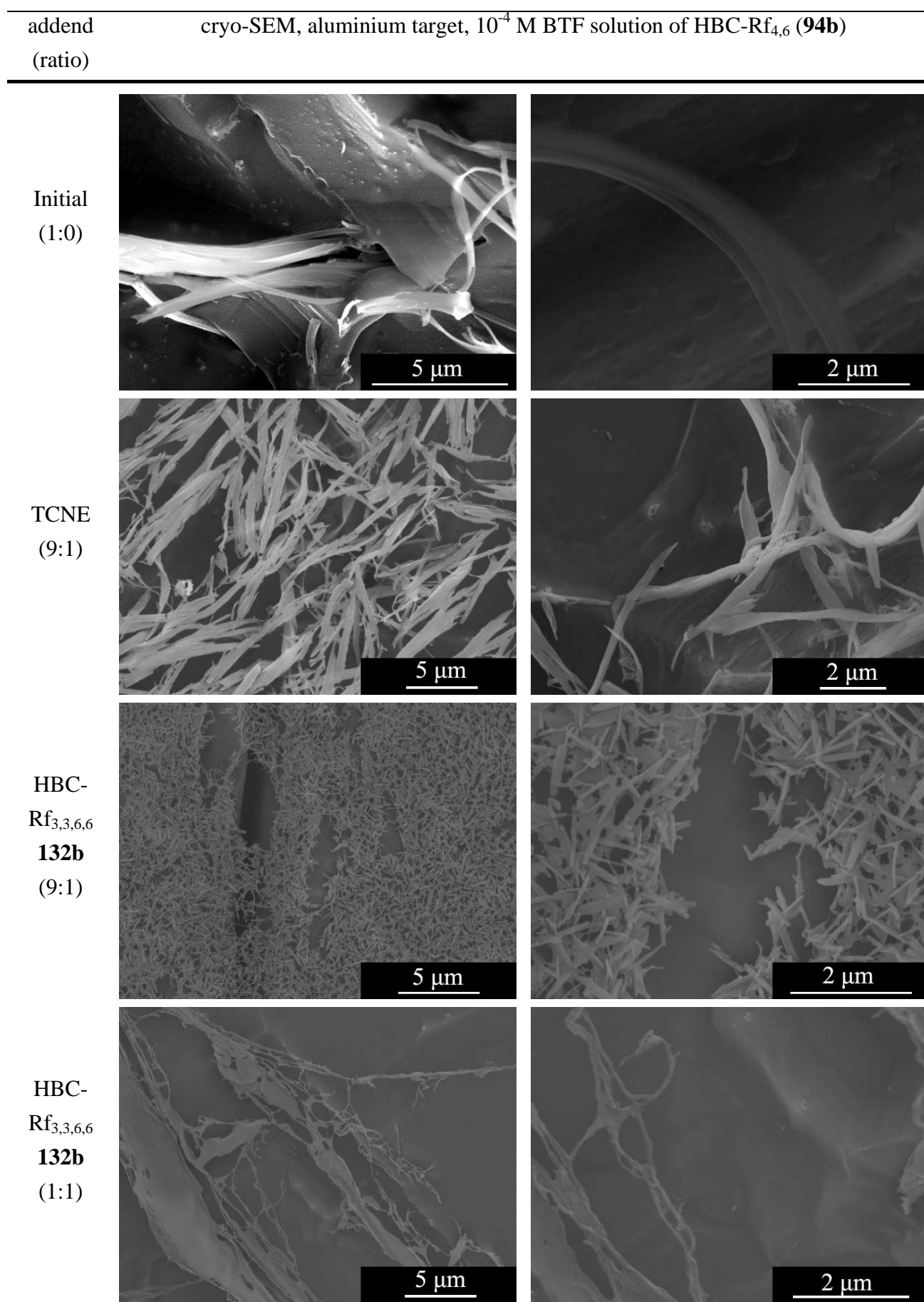
**Figure 15.5** – BTF solution ( $10^{-4}$  M) of HBC-Rf<sub>4,6</sub> (**94b**) at different temperatures with the corresponding cooling time for the last two measurements, ( $\lambda_{\text{ex}} = 360$  nm)

#### 15.1.4 Complexation of the HBC core

By the addition of “stopper molecules”, capable of complexing HBC derivatives, the geometry of the obtained aggregates was influenced and monitored by cryo-SEM. The added complexing agent should increase the end-capping probability and reduce therefore the length of the formed structures. As a consequence the obtained shorter architectures should exhibit a much lower lateral aggregation.

The first addend was TCNE, known to form stable charge-transfer complexes with aromatic systems.<sup>[253]</sup> TCB, BTF and HFB containing each 10% TCNE showed no coloration in the case of BTF and HFB and a deep yellow-orange colour for TCB. This indicated a strong interaction of TCNE with TCB and renders this solvent inappropriate for this sort of investigation. Out of the remaining solvents BTF was chosen as solvent as this was the standard solvent for many other performed measurements. The  $10^{-4}$  M solution was prepared in the usual way by heating HBC-Rf<sub>4,6</sub> (**94b**) in BTF followed by sonication with the only difference of the added 10% of TCNE. The amount of TCNE was chosen purposely so high, in order to provoke a clear effect as shown in Figure 15.6. Compared to the micrographs obtained from a pure BTF solution, the formed structures are shorter and thinner by a factor of almost ten. Nevertheless the geometry of the aggregates seems to stay the same as they contain branching points and taper off in almost the same way. In consequence the addition of TCNE has the same effect as a reduction of the concentration.

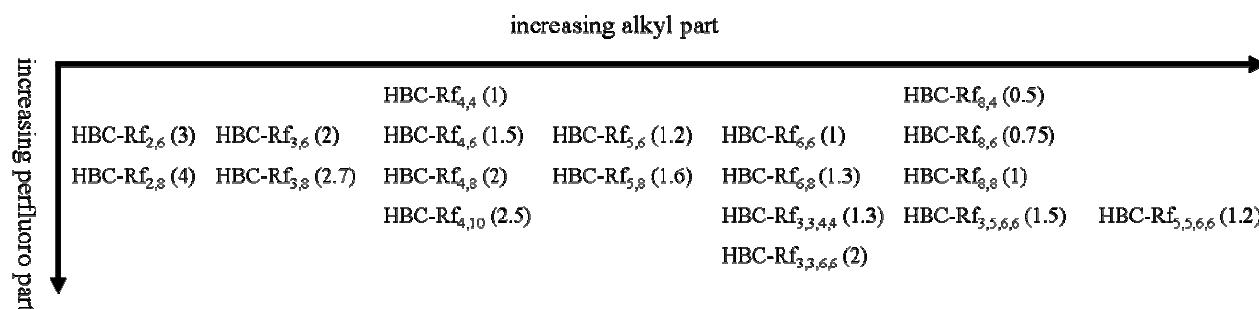
An even stronger effect was achieved by adding 10% of a second HBC derivative (HBC-Rf<sub>3,3,6,6</sub> **132b**), carrying perfluoroalkylated pony tails in the periphery. It seems that the incorporation into the monostranded stacks of only a small amount of HBC **132b** reduces tremendously the lateral aggregation. This is not surprising as TCNE acted only on the end-capping capacity to reduce lateral aggregation by formation of shorter structures, whereas HBC **132b** prevents lateral coagulation with its sterically demanding chains. As consequence much uniform structures were generated with tremendously reduced lateral aggregation as compared to the initial solutions. The original structures (500 nm x 200 nm) consisted approximately of about 10'000 laterally aggregated monostranded stacks whereas the “mixed” structures (100 nm x 100 nm) are only made of approximately 500 laterally aggregated columns, which means a reduction by a factor of 20. By increasing the amount of added HBC **132b** the lateral aggregation may even totally be prevented as depicted in Figure 15.6.



**Figure 15.6** – Cryo-SEM micrographs of  $10^{-4}$  M BTF solutions of HBC-Rf<sub>4,6</sub> (**94b**) with different complexing agents

## 15.2 Engineering the side chain

Figure 15.7 gives an overview of the synthesized HBC derivatives carrying linear and branched perfluorinated chains. The variation of the alkyl and the perfluoroalkyl part is investigated using fluorescence spectroscopy and the cryo-SEM technique. HBC-(Rf<sub>3,3,6,6</sub>)<sub>3</sub> (absent in Figure 15.7) carrying only three side chains will be used to investigate the influence of the number of lateral chains.



**Figure 15.7** – Overview of all HBC derivatives carrying perfluoroalkylated side chains (numbers in parentheses refer to the perfluoro / alkyl ratio (number of perfluorinated carbons divided by the number of alkylated ones))

### 15.2.1 Variation of the alkyl spacer n of linear chains in HBC-Rf<sub>n,m</sub>

The influence of the length of the alkyl spacer is discussed in this section. As shown in Figure 15.7 the shortest alkyl spacer used contains two CH<sub>2</sub> (**63a** and **b**) whereas the longest one is made of eight CH<sub>2</sub> (**125a-c**). The lower end of this range is given by the synthesis, as shorter alkyl spacer hinder the formation of the desired HBC, whereas the upper end is principally open.

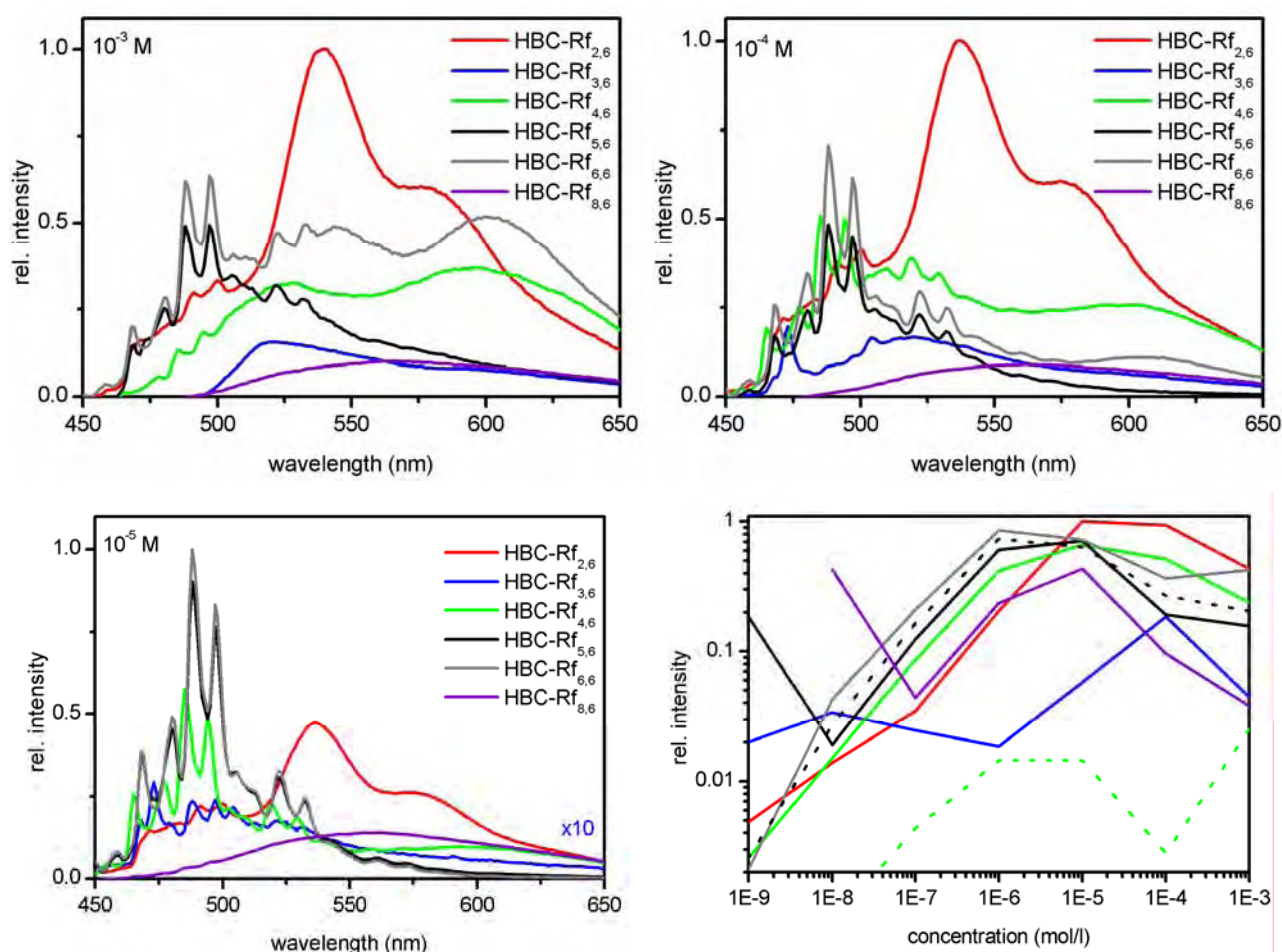
Figure 15.8 summarized the luminescence data collected of every synthesized HBC derivative carrying a linear perfluoroalkylated side chain in combination with a six carbon perfluorinated end part. 10<sup>-3</sup> M BTF solutions are found to be generally too concentrated as in all cases only lateral aggregated species are present, as shown by the large bands in between 500 and 650 nm. Nevertheless a general trend concerning the lateral aggregation may be drawn. Starting with HBC-Rf<sub>2,6</sub> (**63a**), very large broad bands are observed indicating a strong lateral aggregation which decreases slowly by increasing the alkyl spacer. The red bands are strongly blue shifted for HBC-Rf<sub>3,6</sub> (**82a**) without any large increase of the monomeric part of the spectrum. For HBC-Rf<sub>4,6</sub> (**94b**) the aggregate band has decreased already considerably as indicated by the equal intensities of the bands around 525 nm and 600 nm. The addition of one supplementary CH<sub>2</sub> (HBC-Rf<sub>5,6</sub> **106a**) reduces the lateral aggregation once more as shown by the large increase of the monomer luminescence. The fluorescence of HBC **106a** shows a minimal lateral aggregation as compared to the other discussed HBC's. By further increasing the alkyl spacer (HBC-Rf<sub>6,6</sub> **169**, and HBC-Rf<sub>8,6</sub> **125b**) the lateral aggregation starts to increase smoothly, nicely indicated by comparing HBC-Rf<sub>4,6</sub> (**94b**) and HBC-Rf<sub>6,6</sub> (**169**) which have nearly the same luminescence spectrum.



At  $10^{-4}$  M in BTF the situation is almost identical, only slightly shifted towards the emission of monomeric HBC. Nevertheless the luminescence spectrum of HBC-Rf<sub>2,6</sub> (**63a**) consists still mostly of aggregated species. But a clear reduction of side-on aggregation is already observed in HBC-Rf<sub>3,6</sub> (**82a**), which is even more dominantly reduced for HBC-Rf<sub>4,6</sub> (**94b**). Again HBC-Rf<sub>5,6</sub> (**106a**) consists of the least amount of luminescence due to aggregates. For HBC-Rf<sub>6,6</sub> (**169**) and HBC-Rf<sub>8,8</sub> (**125c**) the red bands are increasing again, whereas HBC-Rf<sub>6,6</sub> (**169**) is comparable with HBC-Rf<sub>4,6</sub> (**94b**).

At  $10^{-5}$  M a similar situation is encountered. The fluorescence spectrum of HBC-Rf<sub>2,6</sub> (**63a**) still reveals most predominantly the features of aggregated structures, whereas for HBC-Rf<sub>3,6</sub> (**82a**) the red bands are clearly reduced in favour of the monomer emission. Even HBC-Rf<sub>4,6</sub> (**94b**) still contains small parts of the aggregate fluorescence. HBC-Rf<sub>5,6</sub> (**106a**) and HBC-Rf<sub>6,6</sub> (**169**) are nearly identical and do not show any traces of aggregates any more, whereas HBC-Rf<sub>8,8</sub> (**125c**) has only slightly changed with respect to the more concentrated samples as the red band is still predominant.

In order to reveal any difference in the aggregation behaviour, each luminescence spectrum was integrated between 400 and 700 nm. All substances discussed above are illustrated in Figure 15.8 in a doubly logarithmic graph. The luminescence increases for most derivatives continuously until  $10^{-6}$  M. Exceptions are HBC-Rf<sub>3,6</sub> (**18a**), which has a more or less steady fluorescence over the whole concentration range, a behaviour which could not be explained. Furthermore HBC-Rf<sub>5,6</sub> (**106a**) and HBC-Rf<sub>8,8</sub> (**125c**) show a decrease of the fluorescence at very low concentrations which is most probably an artefact due to the presence of impurities in these dilutions. After reaching a maximum of the emission in between  $10^{-5}$  and  $10^{-6}$  M the luminescence intensity decreases for all derivatives (exception HBC **82a**) indicating the formation of HBC columns as already discussed in chapter 14.2.4 and chapter 15.1.2. Only two substances (HBC-Rf<sub>5,6</sub> **106a** and HBC-Rf<sub>6,6</sub> **169**) showed a stabilization of the fluorescence or even an increase of the fluorescence (**169**) on further increasing the concentration indicating the beginning of the lateral aggregation of HBC strands. Two substances (HBC-Rf<sub>4,6</sub> **94b** and HBC-Rf<sub>5,6</sub> **106a**) were measured also in HFB yielding an identical behaviour for HBC **106a** whereas HBC **94b** showed some differences. As already discussed the stability domain of monostranded HBC stacks is largely enhanced by the use of HFB as solvent in the case of HBC **94b** (see chapter 15.1.2). Furthermore the lower general intensity of the integration curve indicates too the presence of non-emissive matter in this sample.



**Figure 15.8** – Emission spectra ( $\lambda_{\text{ex}} = 360$  nm) of BTF solutions of HBCs differing by the number of  $\text{CH}_2$ 's of the lateral chain having all six perfluorinated carbon atoms; **upper left**:  $10^{-3}$  M; **upper right**:  $10^{-4}$  M; **lower left**:  $10^{-5}$  M; **lower right**: integration of the emission between 400 and 700 nm, dashed lines are the respective HBCs in HFB, the colours match with the other legends; all spectra are arbitrarily scaled without varying the relative intensities

An overview of cryo-SEM micrographs of  $10^{-4}$  M solutions of the above discussed HBC derivatives is given in Figure 15.9. The micrographs obtained from HBC-Rf<sub>2,6</sub> (**63a**) corroborates well with the previously discussed fluorescence data. The material is not organised in long uniform filaments but forms clumpy aggregates. No uniform direction of growth may be seen. Most probably this HBC never forms monostranded stacks and the material exists in equilibrium of aggregates and monomers. Moreover the equilibrium lies on the side of the aggregates due to the low solubility.

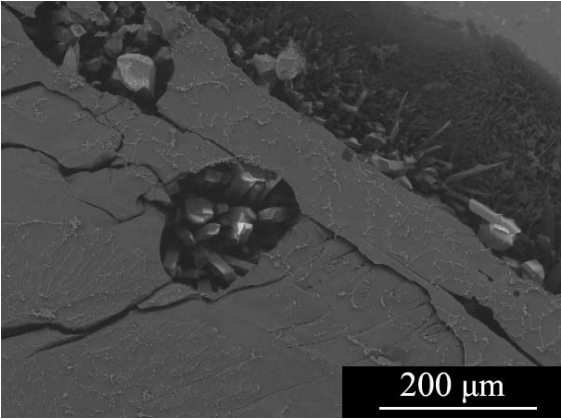
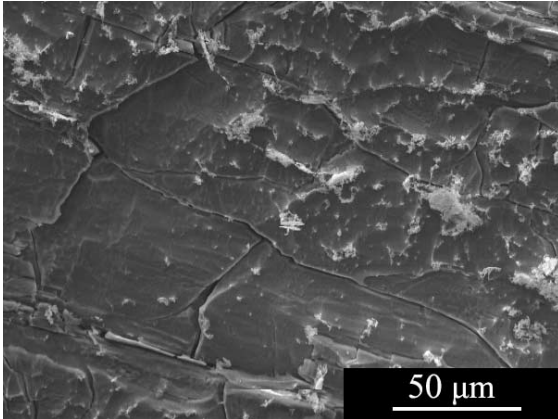
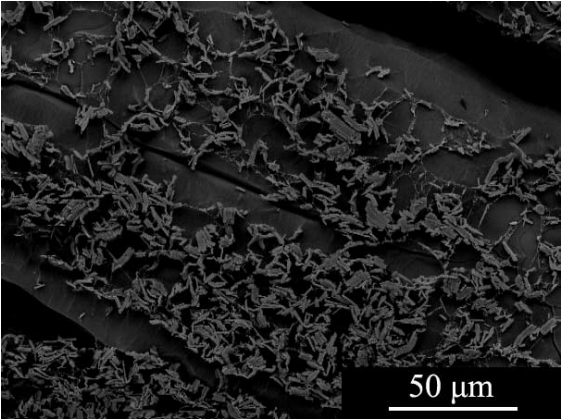
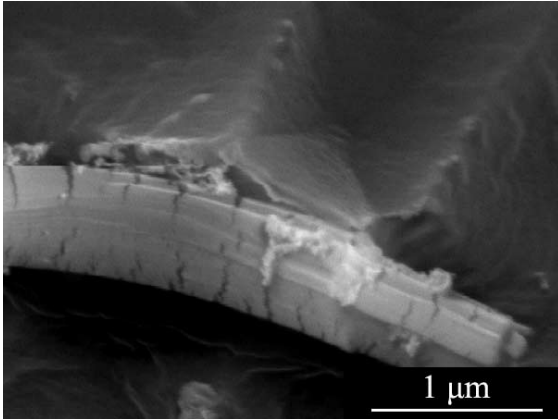
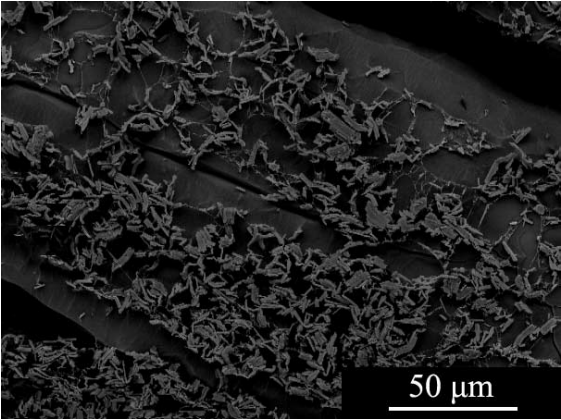
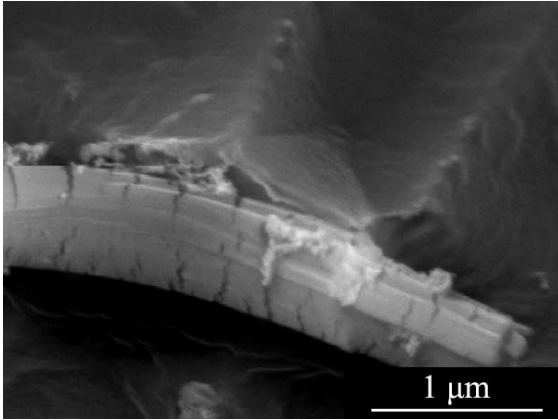
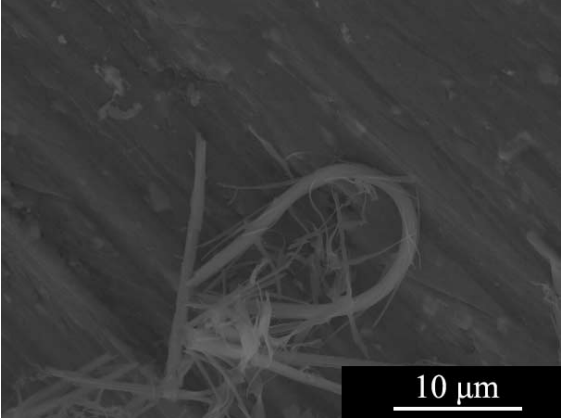
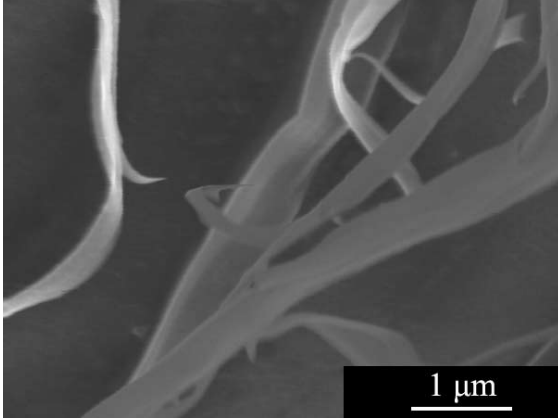
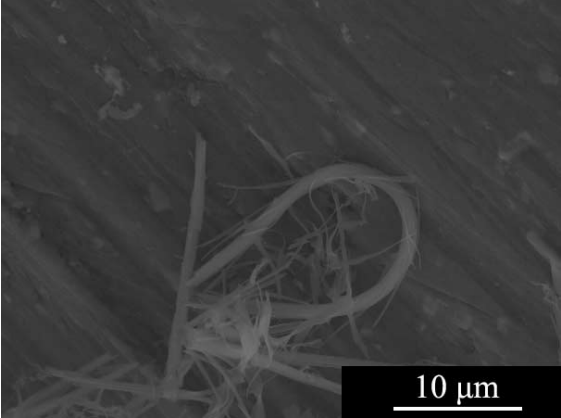
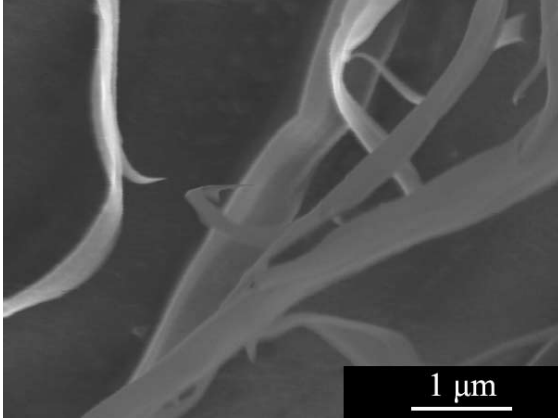
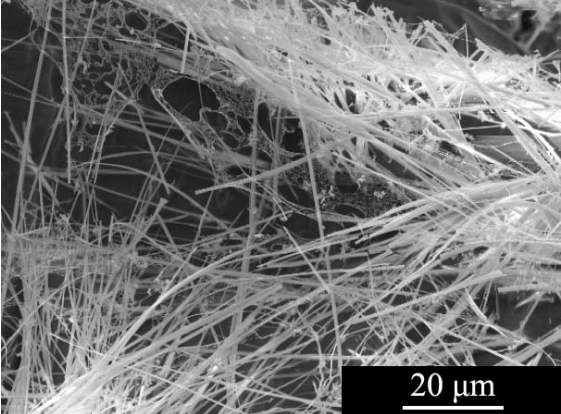
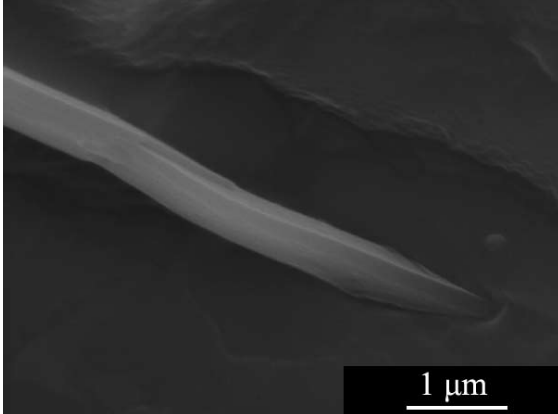
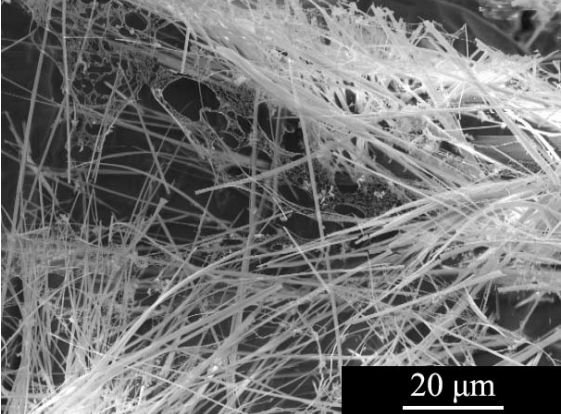
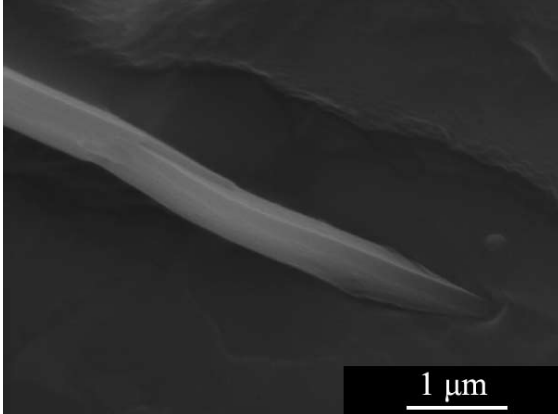


HBC-Rf<sub>3,6</sub> (**82a**) was found to exist in uniform, not branched but thick structures of a typical length of 10  $\mu\text{m}$  and a diameter of approx. 1  $\mu\text{m}$ . Several structures consist of sudden and sharp bends where the growing direction abruptly changes by almost  $90^\circ$ . Probably this behaviour is provoked when two pre-existing structures are combined together. The diameter of the observed structures is more or less uniform as no thin monostranded structures were observed. Interestingly these HBC aggregates start immediately to break when being focused with the electron beam indicating an instability in the direction of the linear growing.

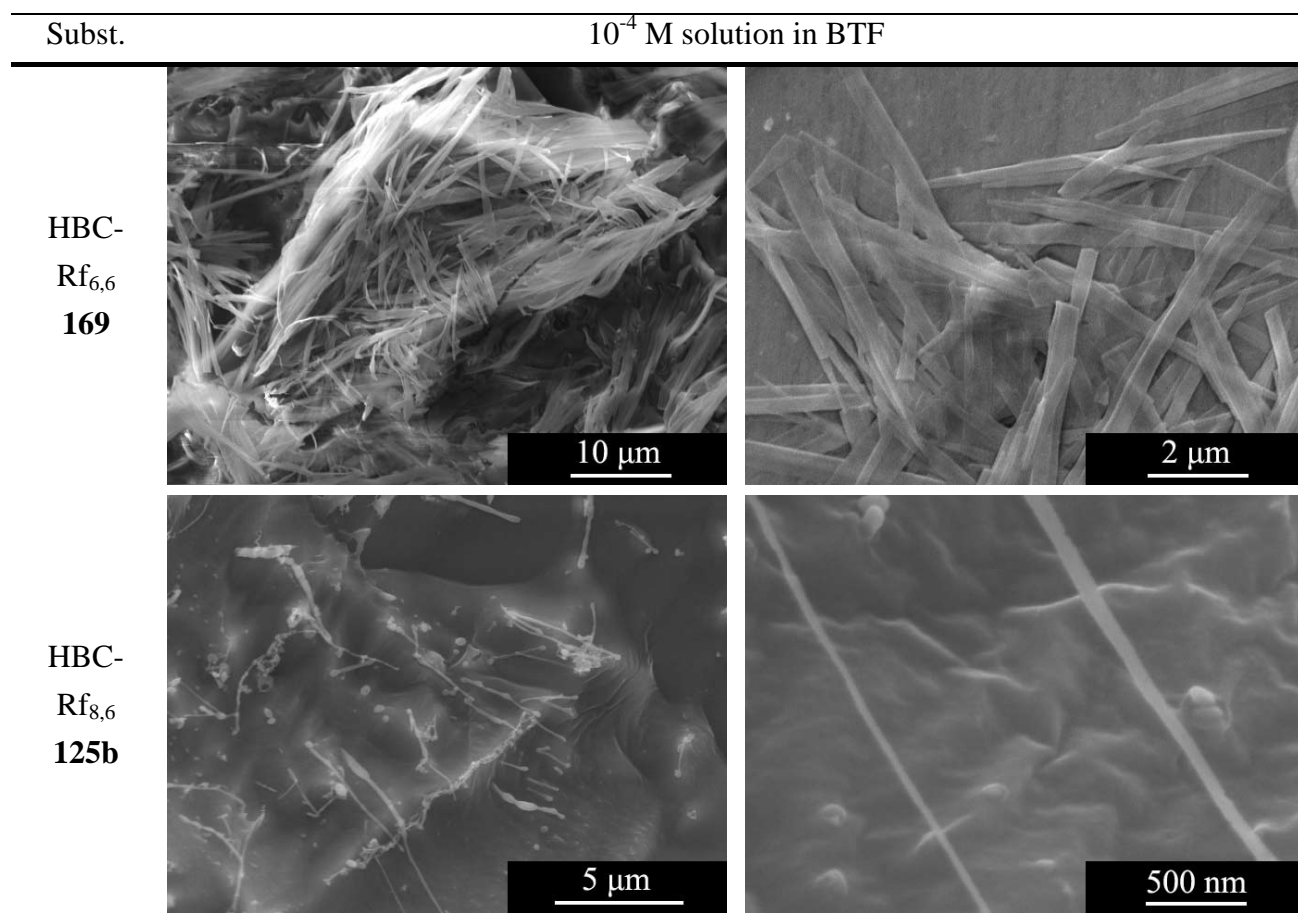
The structures of HBC-Rf<sub>4,6</sub> (**94b**) extend over several tens of  $\mu\text{m}$  whereas their diameter varies strongly between 100 and 2000 nm. Furthermore the structures are branched which taper off quite rapidly and are organized rather in sheets than in round architectures compared to HBC-Rf<sub>3,6</sub> (**82a**).

HBC-Rf<sub>5,6</sub> (**106a**) forms very linear and uniform structures extending over almost 0.1 mm consisting of no branching at all. Their uniform rectangular cross-section lies in the range of about 1  $\mu\text{m}$ . Moreover the structures end in a breaking like manner without any tapering off effect.

HBC-Rf<sub>6,6</sub> (**169**) exists again in a large variety of different geometries. Short structures are about 5  $\mu\text{m}$  long whereas others extend over several tens of  $\mu\text{m}$ . The cross-section is anisotropic too as flat sheet like structures are observed, similar to HBC-Rf<sub>4,6</sub> (**94b**) but even more pronounced. One dimension of the sheets lies in the  $\mu\text{m}$  range whereas the second dimension lies in the nm range as the structures are so thin that the underlying structure is nearly observed with the electron beam.

HBC-Rf<sub>8,6</sub> (**125b**) has a completely different behaviour as already indicated with the fluorescence experiments. The number of structures is drastically reduced compared to the other samples. The observed structures are more or less linear but contain mostly thick swollen parts. Furthermore their end parts do not taper off at all but form rather thick round endings. Together with this completely round and oval structures are found. Nevertheless some linear monostranded stacks were found even at this fairly high concentration.

Subst.	$10^{-4}$ M solution in BTF	
HBC- Rf <sub>2,6</sub> <b>63a</b>	 <p>SEM image showing a surface with large, irregular, and somewhat rounded features. A scale bar indicates 200 μm.</p>	 <p>SEM image showing a surface with a network of fine, branching structures. A scale bar indicates 50 μm.</p>
	 <p>SEM image showing a surface with a dense, granular texture. A scale bar indicates 50 μm.</p>	 <p>SEM image showing a curved, layered structure. A scale bar indicates 1 μm.</p>
HBC- Rf <sub>3,6</sub> <b>82a</b>	 <p>SEM image showing a surface with a dense, granular texture. A scale bar indicates 50 μm.</p>	 <p>SEM image showing a curved, layered structure. A scale bar indicates 1 μm.</p>
	 <p>SEM image showing a surface with a dense, granular texture. A scale bar indicates 10 μm.</p>	 <p>SEM image showing a curved, layered structure. A scale bar indicates 1 μm.</p>
HBC- Rf <sub>4,6</sub> <b>94b</b>	 <p>SEM image showing a surface with a dense, granular texture. A scale bar indicates 10 μm.</p>	 <p>SEM image showing a curved, layered structure. A scale bar indicates 1 μm.</p>
	 <p>SEM image showing a surface with a dense, granular texture. A scale bar indicates 20 μm.</p>	 <p>SEM image showing a curved, layered structure. A scale bar indicates 1 μm.</p>
HBC- Rf <sub>5,6</sub> <b>106a</b>	 <p>SEM image showing a surface with a dense, granular texture. A scale bar indicates 20 μm.</p>	 <p>SEM image showing a curved, layered structure. A scale bar indicates 1 μm.</p>
	 <p>SEM image showing a surface with a dense, granular texture. A scale bar indicates 20 μm.</p>	 <p>SEM image showing a curved, layered structure. A scale bar indicates 1 μm.</p>



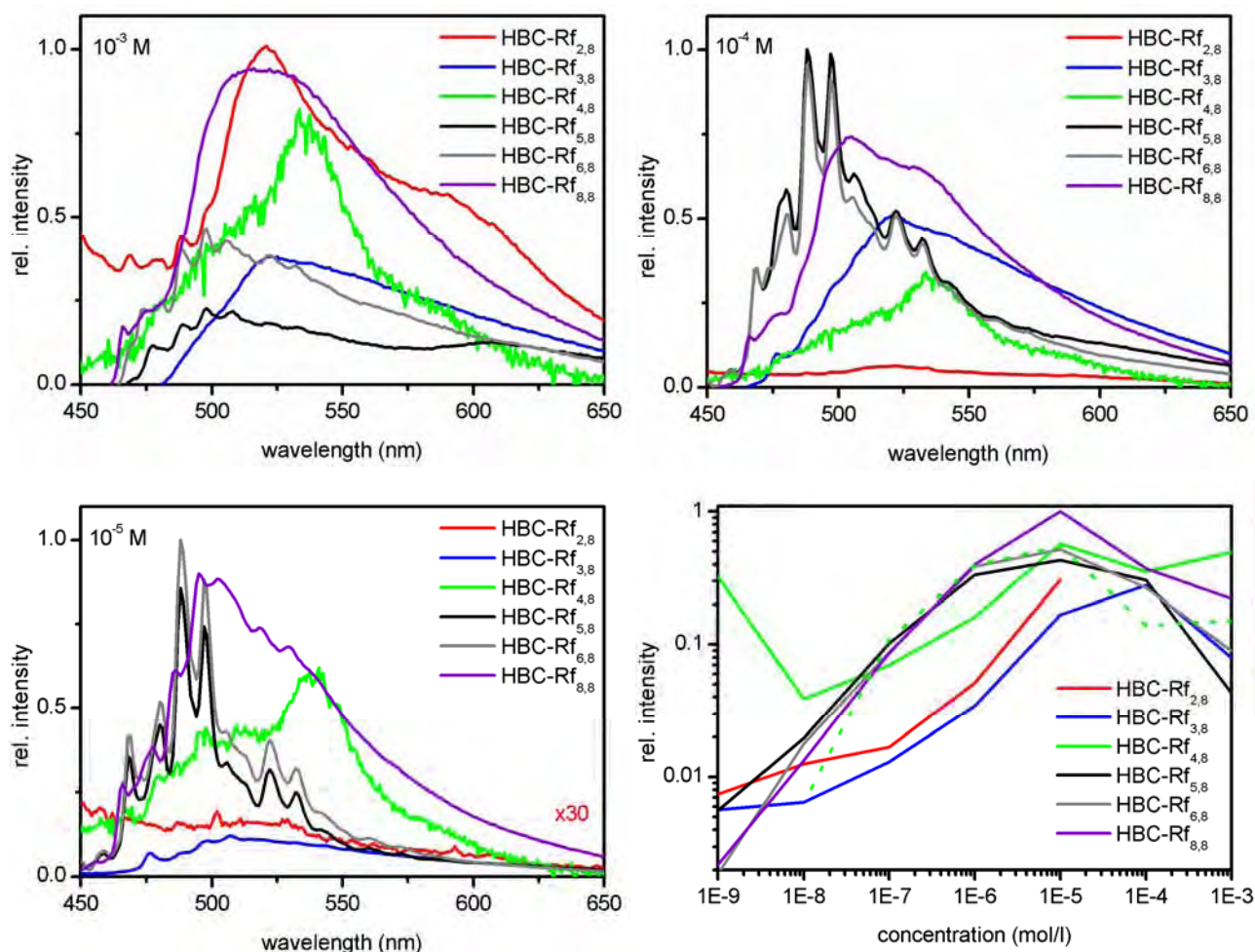
**Figure 15.9** – Cryo-SEM micrographs of  $10^{-4}$  M BTF solutions of HBC derivatives bearing linear perfluoroalkylated side chains with six perfluorinated carbon tails.

Figure 15.10 is the corresponding illustration of the fluorescence data of all HBC derivatives carrying an eight carbon perfluorinated end part in the lateral chain. As already anticipated the elongation of the perfluorinated part of the side chain provokes a decrease of the solubility and enhances with this inherently the lateral aggregation of the formed HBC stacks. The collected spectra of  $10^{-3}$  M BTF solutions illustrate these findings very clearly. All measured derivatives show a pronounced aggregation in their fluorescence. As observed earlier, the only two compounds revealing clear monomer features are HBC-Rf<sub>5,8</sub> (**114**) and HBC-Rf<sub>6,8</sub> (**106b**), where HBC **114** with its five carbon alkyl spacer has again a minimal lateral aggregation.

By decreasing the concentration to  $10^{-4}$  M the situation is not changed at all. The only derivatives indicating monomeric HBC are HBC-Rf<sub>5,8</sub> (**114**) and HBC-Rf<sub>6,8</sub> (**106b**) having nearly identical emission patterns. Surprisingly this is even not altered by decreasing the concentration ten times more to  $10^{-5}$  M. HBC-Rf<sub>5,8</sub> (**114**) and HBC-Rf<sub>6,8</sub> (**106b**) reveal only monomeric HBC features whereas HBC-Rf<sub>8,8</sub> (**125c**) starts to show fine structured bands, indicating the presence of monomers.



By integrating the overall emission of each HBC derivative, the most intense fluorescence spectrum was for each derivative at  $10^{-5}$  M with the only exception being HBC-Rf<sub>3,8</sub> (**82b**) having its maximum at  $10^{-4}$  M. Surprisingly the only derivative indicating a re-increase at high concentrations is HBC-Rf<sub>4,8</sub> (**94c**), even though the fluorescence spectra in BTF do not look promising.



**Figure 15.10** – Emission spectra ( $\lambda_{\text{ex}} = 360$  nm) of BTF solutions of HBCs differing by the number of  $\text{CH}_2$ 's of the lateral chain having all eight perfluorinated carbon atoms; **upper left:**  $10^{-3}$  M; **upper right:**  $10^{-4}$  M; **lower left:**  $10^{-5}$  M; **lower right:** integration of the emission in between 400 and 700 nm, solid lines (BTF solutions), dashed lines (HFB solutions); all spectra are arbitrarily scaled without varying the relative intensities

The morphology in solution of these HBC derivatives was investigated by cryo-SEM measurements and is summarized in Figure 15.11. HBC-Rf<sub>2,8</sub> (**63b**) showed no traces of the desired linear architectures. Moreover nearly no material was observed, indicating only short range order of this HBC derivative. Fluorescence measurements revealed large amounts of aggregated structures indicating a quite similar behaviour as HBC-Rf<sub>2,6</sub> (**63a**). The short range order in combination with the fact that no filamentous structures are observed indicates that this HBC derivative has no tendency to form big, well defined aggregates but forms rather small undefined aggregates.

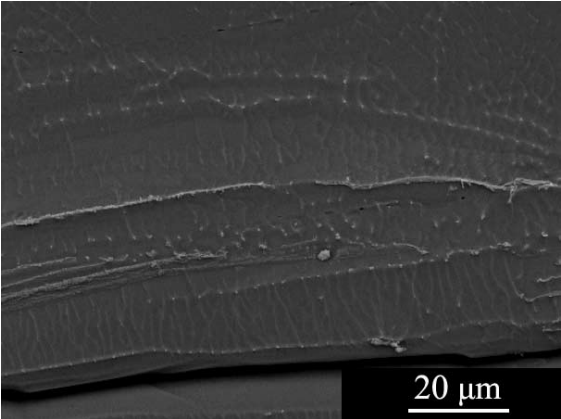
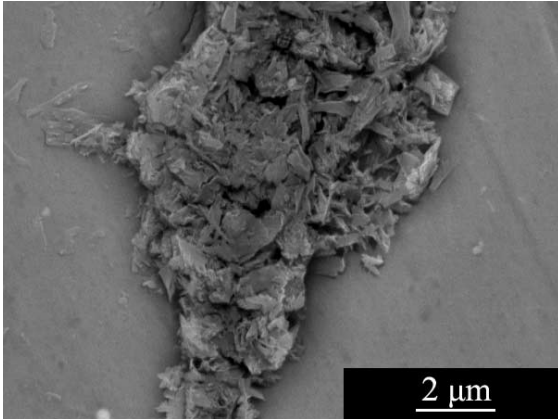
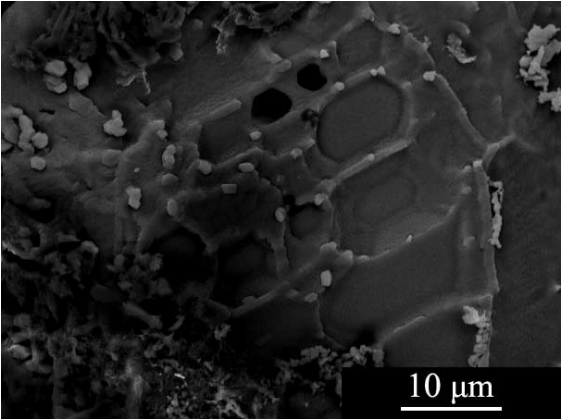
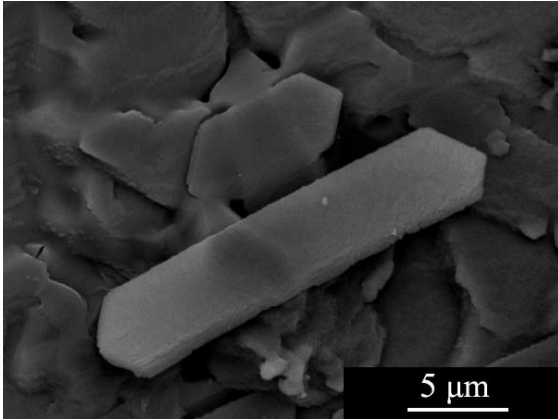
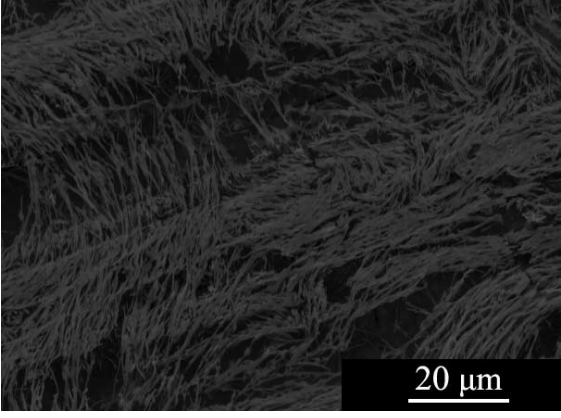
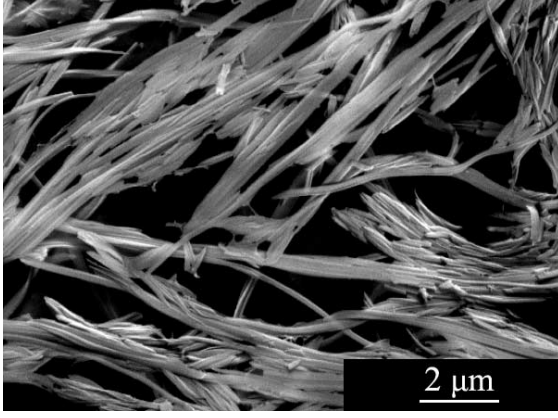
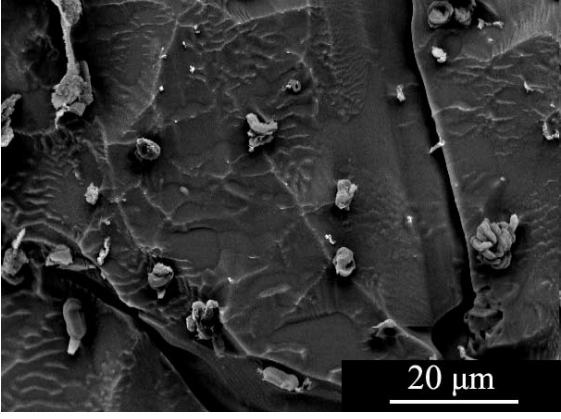
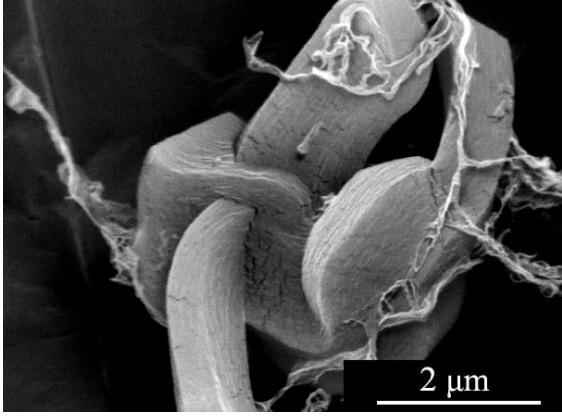
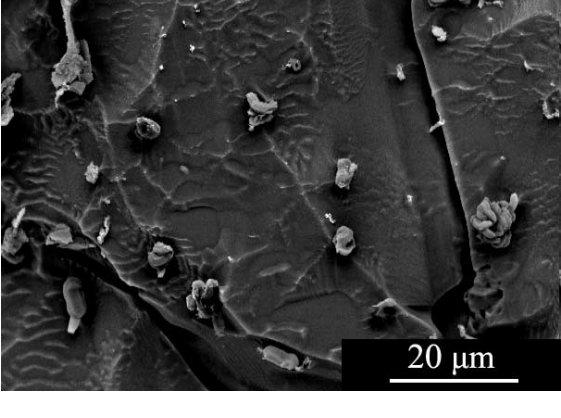
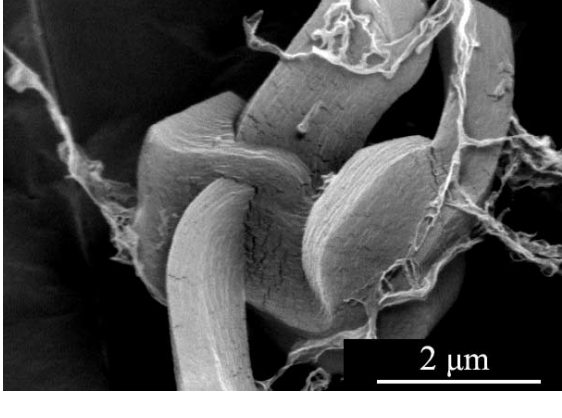


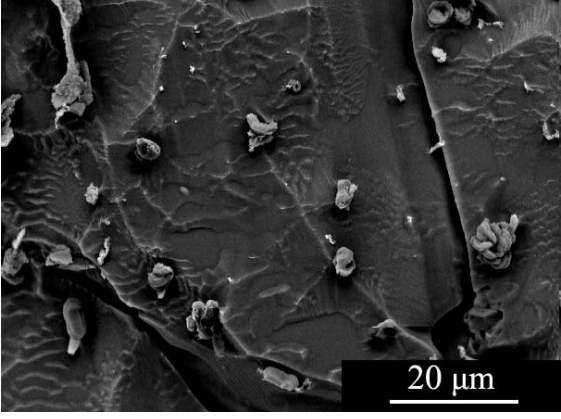
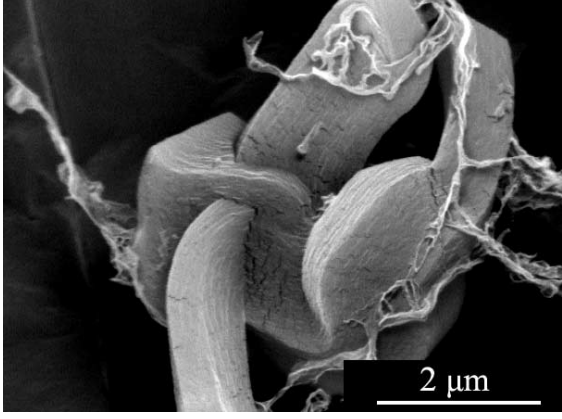


HBC-Rf<sub>3,8</sub> (**82b**) consisted of a special morphology never observed for perfluoroalkylated HBC derivatives so far. Linear structures were observed with a typical length around 10  $\mu\text{m}$ . The cross-section was of rectangular shape with one dimension being about two times larger than the other. The tails tapered off in an arrow shape rendering the whole structure like an elongated hexagon.

HBC-Rf<sub>4,8</sub> (**94c**) is the only derivatives of this series forming well defined linear structures with thin cross-sections around 100 nm with a typical length of several  $\mu\text{m}$ . The amount of material assembled on top of the frozen solvent is considerably high underlining the well pronounced tendency of this HBC to self-assemble into ordered architectures (indicated too by the fluorescence measurements presented in this section). The material seems to consist of thin and narrow sheets made of single monostranded stacks which are loosely bound together laterally, as the structures showed several branching points and fractures.

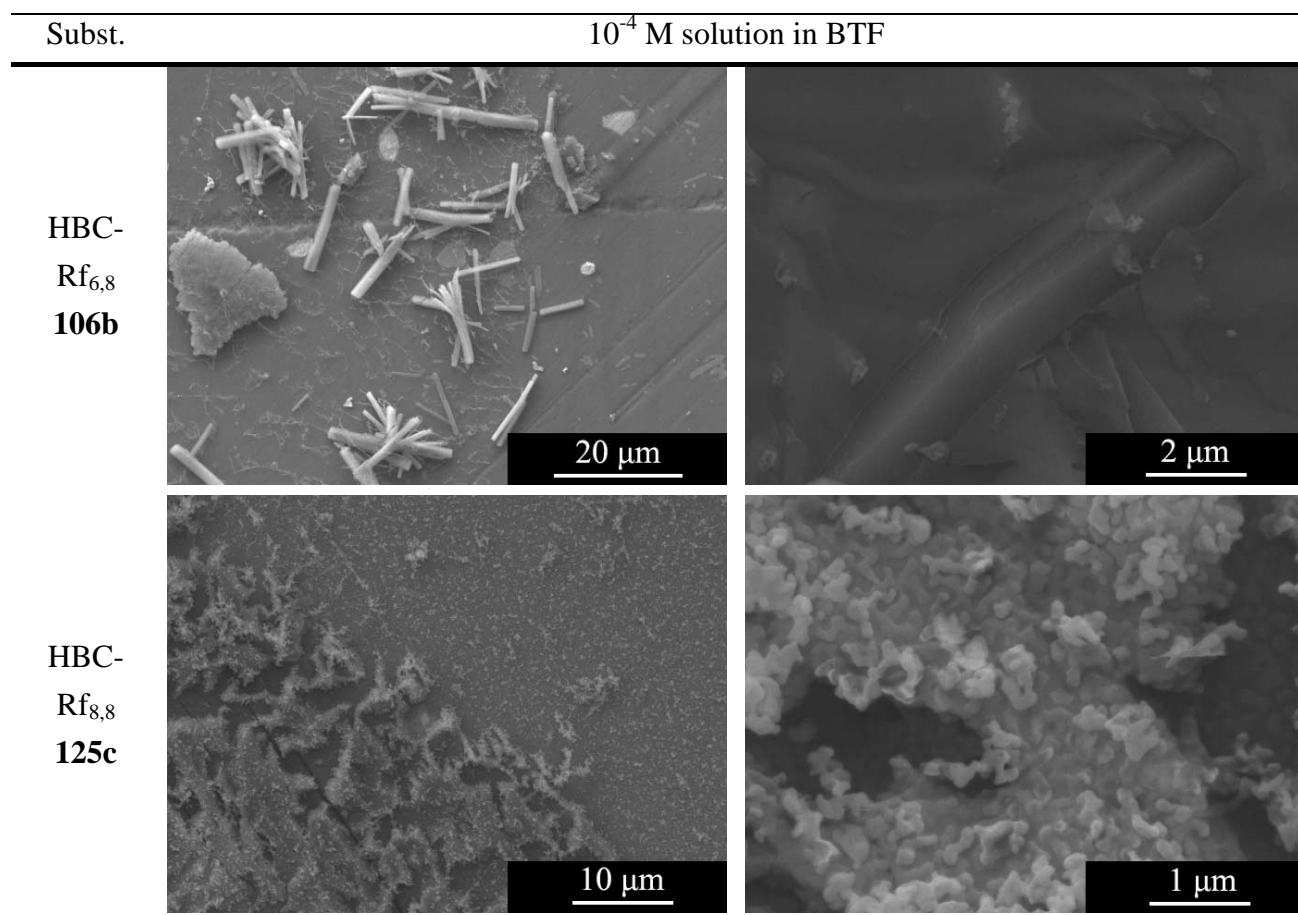
HBC-Rf<sub>5,8</sub> (**114**) in contrary formed very large rectangular structures with cross-sections of 1  $\mu\text{m}$  to 5  $\mu\text{m}$  and a length of several tens of  $\mu\text{m}$ . Furthermore all linear rectangular strands are curled around each other to form a large variety of different architectures. On top of that a braking of the structures may be induced under the focus of the electron beam indicating a tension in the formed strands.

HBC-Rf<sub>6,8</sub> (**106b**) formed again very linear and rectangular objects of a fairly uniform length of about 10  $\mu\text{m}$  and a varying cross-section of about 1  $\mu\text{m}$ . These rectangular blocks are most probably made of finer sheets indicated by the observed splitting at the tail into a lamellar architecture. Nearly all observed structures ended abruptly without any tendency to taper off smoothly.

HBC-Rf<sub>8,8</sub> (**125c**) showed a completely different behaviour which was already indicated by the fluorescence measurements of this section. This HBC derivative formed no linear structures at all but organized itself into drop like oval small structures, comparable with micrographs obtained from block polymers.<sup>[254]</sup> The thickness of individual branches of this network are around 100 nm with linear parts of maximally 500 nm.

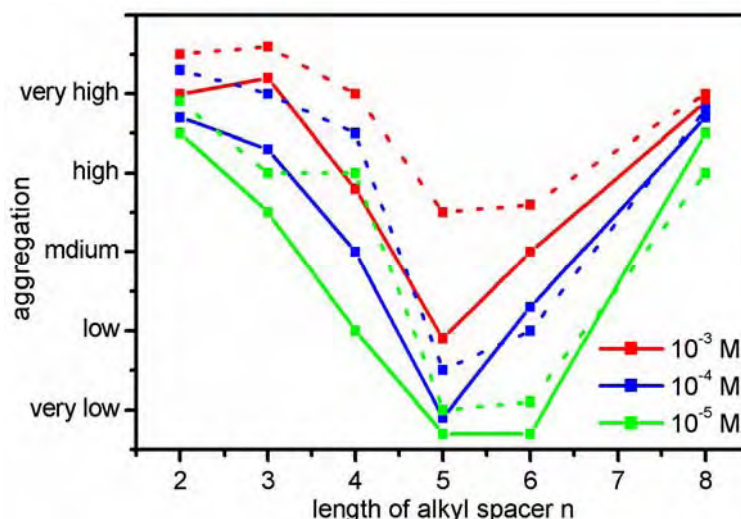
Subst.	$10^{-4}$ M solution in BTF	
HBC- Rf <sub>2,8</sub> <b>63b</b>		
		
HBC- Rf <sub>3,8</sub> <b>82b</b>		
		
HBC- Rf <sub>4,8</sub> <b>94c</b>		
		
HBC- Rf <sub>5,8</sub> <b>114</b>		
		





**Figure 15.11** – Cryo-SEM micrographs of  $10^{-4}$  M BTF solutions of HBC derivatives carrying eight perfluorinated carbon tails

In summary the variation of the alkyl spacers influences the self-aggregation of HBC derivatives tremendously. Fluorescence experiments indicated the lateral aggregation to be rather big by using short alkyl spacers (two or three  $\text{CH}_2$ ). The derivatives thereafter bearing slightly longer alkyl parts (four, five or six  $\text{CH}_2$ ) reveal a dynamic equilibrium in between monomers and aggregated structures in the observed concentration range. By increasing the alkyl spacer even more (eight  $\text{CH}_2$ ) the lateral aggregation is dominating again. A graphical illustration of these findings is given in Figure 15.12 where all HBC-Rf<sub>n,6</sub> and HBC-Rf<sub>n,8</sub> derivatives are reported in three concentrations with respect to their lateral aggregation tendency. Figure 15.12 illustrates very nicely the gap of derivatives carrying four, five or six  $\text{CH}_2$  having the least amount of lateral aggregation. The difference between Rf<sub>6</sub> and Rf<sub>8</sub> derivatives consists of the narrower gap for Rf<sub>8</sub> compounds. But in principle their behaviour is quite comparable. These findings are underlined by cryo-SEM investigations revealing large amounts of linear but mostly aggregated structures for HBC-Rf<sub>4,6</sub> (**94b**), HBC-Rf<sub>5,6</sub> (**106a**), HBC-Rf<sub>6,6</sub> (**169**) as well as HBC-Rf<sub>4,8</sub> (**94c**).



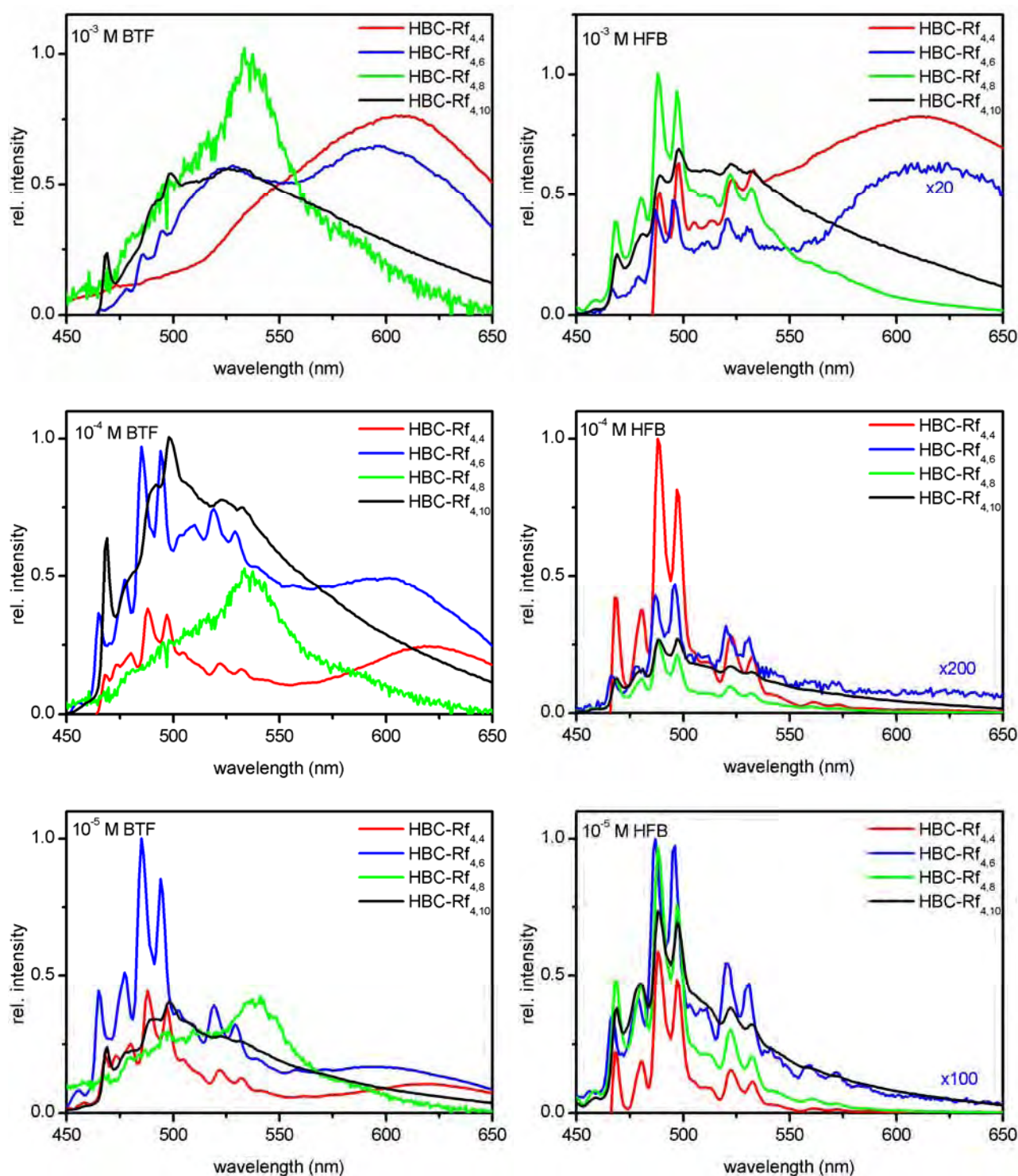
**Figure 15.12** – Lateral aggregation as function of the alkyl spacer for two type of compounds: HBC-Rf<sub>n,6</sub> (solid lines) and HBC-Rf<sub>n,8</sub> (dashed lines). The aggregation was determined in BTF solution from the fluorescence data presented in this section.

### 15.2.2 Variation of the perfluoro spacer m of linear chains in HBC-Rf<sub>n,m</sub>

Figure 15.13 summarized the fluorescence data obtained from all HBC derivatives carrying a four carbon alkyl spacer in combination with a four, six, eight or ten perfluoro-carbon tail in order to investigate the role of the length of the fluorine part of the lateral chain. For a better understanding, the measurements were carried out in BTF as well as in HFB. At  $10^{-3}$  M in BTF all four samples showed a pronounced tendency for lateral aggregation indicated by the large unresolved bands in the region between 500 and 650 nm. In HFB the monomer emission is, as expected, better developed but has nevertheless features of aggregated structures. Surprisingly, only HBC-Rf<sub>4,8</sub> (**94c**) reveals no lateral aggregation at all, which could not be explained.

By decreasing the concentration to  $10^{-4}$  M the monomer features start to gain importance in the BTF solutions too. HBC-Rf<sub>4,4</sub> (**94a**) and HBC-Rf<sub>4,6</sub> (**94b**) have nearly the same fluorescence pattern, differing only in the intensity, whereas HBC-Rf<sub>4,8</sub> (**94c**) and HBC-Rf<sub>4,10</sub> (**94d**) contain still mostly large unresolved bands. In HFB the situation is quite different as now all derivatives show exclusively the features of monomer emission, differing only in the intensity which is most probably influenced by the amount of “dark” monostranded stacks present.

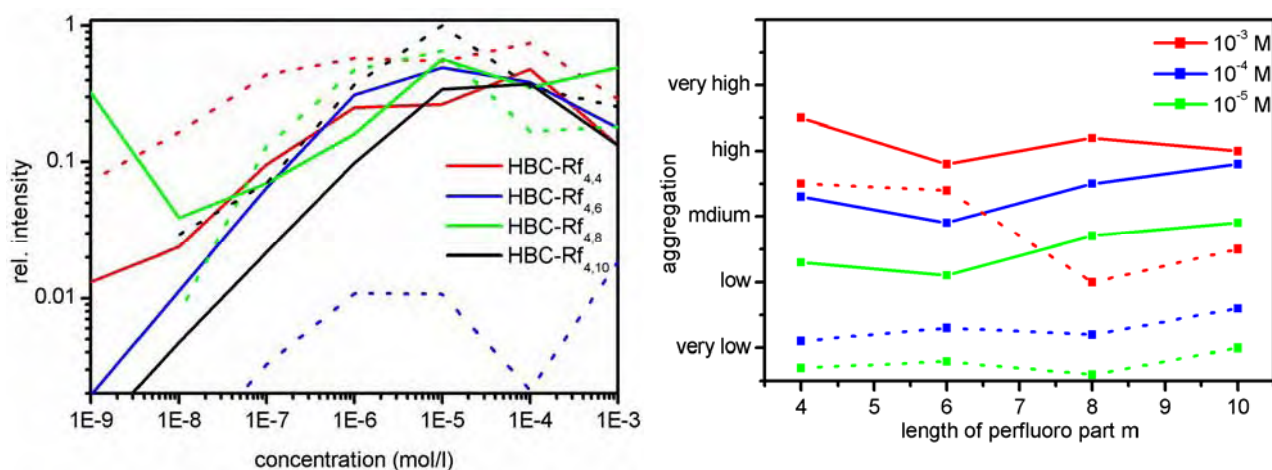
At  $10^{-5}$  M the situation is quite similar for the BTF solution, only that the lateral aggregation is vanishing slowly. For the HFB solution only the ranking of the intensities shifted due to a varying amount of monostranded stacks present in the different solutions.



**Figure 15.13** – Emission spectra ( $\lambda_{\text{ex}} = 360$  nm) of BTf (left) and HFB (right) solutions of HBCs differing by the number of  $\text{CF}_2$  of the lateral chain having all a four alkyl carbon spacer; **upper left:**  $10^{-3}$  M BTf; **upper right:**  $10^{-3}$  M HFB; **middle left:**  $10^{-4}$  M BTf; **middle right:**  $10^{-4}$  M HFB; **lower left:**  $10^{-5}$  M BTf; **lower right:**  $10^{-5}$  M HFB

By integrating the overall emission of these derivatives in between 400 and 700 nm the curves depicted in Figure 15.14 are obtained. The intensity of the luminescence is increasing steadily for all derivatives by increasing the concentration, with the only exception being HBC-Rf<sub>4,8</sub> (**94c**) at  $10^{-9}$  M which is most probably due to artefacts. All compounds reach their maximal intensities between  $10^{-5}$  and  $10^{-4}$  M and decrease thereafter. For the BTF solutions (solid lines) only HBC **94c** re-increases the intensity indicating the presence of monostranded HBC stacks. Whereas in HFB (dashed lines) all compounds with exception of HBC-Rf<sub>4,4</sub> (**94a**) show a re-increasing intensity, illustrating clearly the importance of the choice of solvent.

The monitoring of the lateral aggregation as a function of concentration and the length of the perfluoro part is shown on the right hand side of Figure 15.14. The illustration indicates that a four perfluorinated carbon atoms are not ideal concerning the lateral aggregation as HBC **94a** has a rather strong tendency for side-on interactions. HBC **94b** carrying six perfluorinated carbons seem to be the ideal choice in BTF whereas in HFB also HBC **94a** - **c** behave favourably, above all at concentrations lower than  $10^{-4}$  M. Surprisingly the effect of the number of perfluorinated carbon atoms was not found to be very pronounced in this HBC series which was not at all observed in the previous chapter (see chapter 15.2.2), where the aggregation was strongly influenced by increasing the perfluorinated part. Moreover, the solubility of the four compounds in HFB is decreasing from very soluble (HBC **94a**) to almost insoluble (HBC **94d**).



**Figure 15.14** – Left: integration of the emission in between 400 and 700 nm, solid lines (BTF solutions), dashed lines (HFB solutions); all spectra are arbitrarily scaled without varying the relative intensities; right: lateral aggregation as function of the perfluorinated part  $m$  with a constant four carbon alkyl spacer; BTF solutions (solid lines) and HBC solutions (dashed lines).

An overview of all performed cryo-SEM experiments is given in Figure 15.15. HBC-Rf<sub>4,4</sub> (**94a**) formed similar structures in both solvents consisting of large, nearly round architectures with a typical length of 20  $\mu\text{m}$  and a diameter of about 1  $\mu\text{m}$ . In both systems, the obtained HBC structures tapered off rapidly at the tail. In BTF an additional feature was observed, namely smaller HBC

sheets, typically 200 nm broad. Most probably such sheet form previously and aggregate then further into the larger structures. The fluorescence data discussed at the beginning of this section indicated a much higher aggregation in BTF solutions which was also confirmed by cryo-SEM as in BTF much more aggregated structures were detected than in HFB.

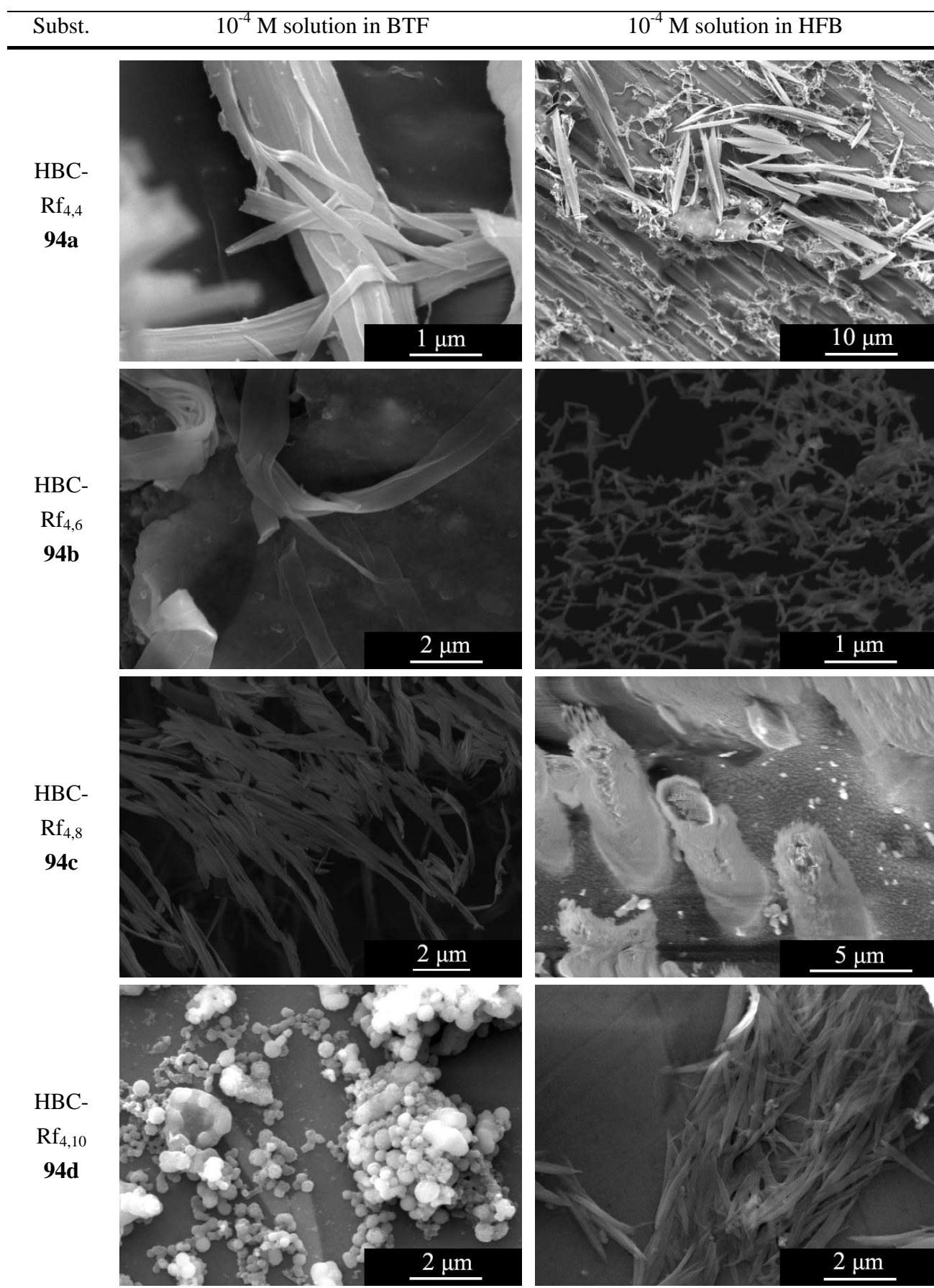
HBC-Rf<sub>4,6</sub> (**94b**) formed large aggregated sheets and bundles in BTF whereas in HFB no lateral aggregated architectures were found but only monostranded HBC stacks. This is the first example of a HBC sample which formed at a specific concentration large amounts of monostranded stack without any sign of lateral aggregation.

HBC-Rf<sub>4,8</sub> (**94c**) formed surprisingly in BTF much finer structures than the other derivatives bearing four aliphatic carbons in the side chain. The obtained fibres were found to have various lengths between 1 and 30  $\mu\text{m}$  together with a more uniform cross-section of roughly 200 nm. The filamentous linear structures were found to cover all the surface of the frozen solvent indicating that the equilibrium was shifted highly towards these structures. In HFB the situation was completely different as no aggregated structures were found, already indicated by the fluorescence measurements. The frozen surface contained a variety of rectangular and tubular objects, formed most probably during the sublimation process. Due to the high concentration it is possible that very short monostranded stacks assembled during the sublimation and hindered this on specific places. This phenomenon is often observed in winter times when snow sublimates.

HBC-Rf<sub>4,10</sub> (**94d**) was the only derivative of this series unable to form linear structures. Instead of this, regular round balls with a diameter between 200 and 800 nm were formed. Probably BTF was in this case not able to completely solubilize this derivative which provoked agglomeration of material into round shaped objects. By using HFB with its high solubilizing capacity, the typical structures were observed again. The observed architectures are of rectangular shape with a length of maximally 10  $\mu\text{m}$ . The cross-section is about 200 nm width whereas the thickness seems to vary stronger. This is most probably due to the fact that first sheet like structures are formed which aggregate further into staples.

In summary, the most promising results are obtained with six or maximally eight perfluorinated carbons. Furthermore HBC-Rf<sub>4,6</sub> (**94b**) showed excellent results at  $10^{-4}$  M in HFB where only monostranded HBC stacks were observed. Moreover six and eight perfluorinated tails showed also the most promising results with other aliphatic carbon spacers.





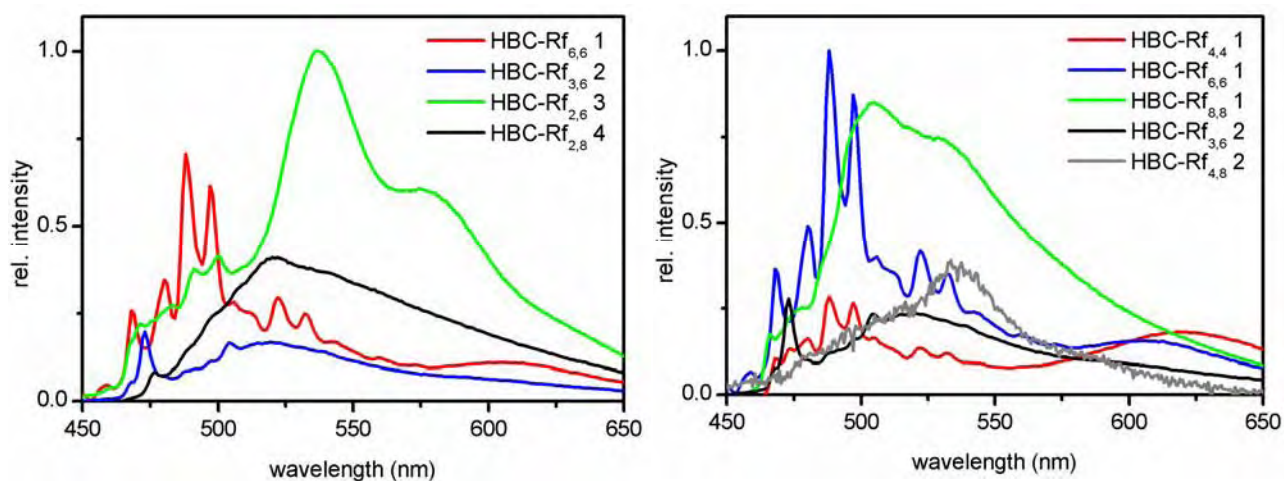
**Figure 15.15** – Cryo-SEM micrographs from  $10^{-4}$  M BTF and HFB solutions of perfluoroalkylated HBC derivatives carrying a four aliphatic carbon spacer

## 15.2.3 Comparing the perfluoro / alkyl ratio

Next in importance to the absolute length of the alkyl spacer and the perfluorinated part is the ratio of the two chemically strongly different parts of the side chain. On the left of Figure 15.16 the luminescence of four HBC derivatives differing strongly in the perfluoro / alkyl ratio is sketched. HBC-Rf<sub>6,6</sub> (**169**) with a 1 to 1 ratio consists of a well developed monomer fluorescence together with a small amount of aggregate. HBC-Rf<sub>3,6</sub> (**82a**) reveals already a large aggregated part with a 2 to 1 ratio in favour of the fluorines. Increasing the ratio then to 3 to 1 for HBC-Rf<sub>2,6</sub> (**63a**) or even to 4 to 1 (HBC-Rf<sub>2,8</sub> **63b**) shifts the emission completely to the red. This indicates that the perfluoro / alkyl ratio should preferentially not be higher than 2 as else the stiffness of the perfluorinated part provokes the lateral aggregation instead of preventing this unfavourable interaction.

Comparison of the chain length is illustrated on the left side of Figure 15.16, where different HBC with the same perfluoro / alkyl ratio are shown. HBCs with an equal number of perfluorinated and hydrogenated carbon atoms are HBC-Rf<sub>4,4</sub> (**94a**), HBC-Rf<sub>6,6</sub> (**169**) and HBC-Rf<sub>8,8</sub> (**125c**). HBC **94a** carrying an eight carbon chain seems to be a bit too short to prevent the lateral aggregation effectively where as for HBC **169** with a twelve carbon side chain the aggregate emission is well reduced. By increasing the total lateral chain to sixteen carbon atoms (HBC **125c**) the lateral aggregation is favoured again. Similar findings for the length are drawn with compounds having a 2 to 1 perfluoro / alkyl ratio. HBC **82a** bearing a nine carbon side chain was never found to have well developed fluorescence whereas HBC **94c** with its twelve carbon side chain showed a very promising emission in HFB solutions.

In summary the ratio of perfluoro / alkyl is preferentially in the range of 1 and 2 in combination with a total length around twelve carbon atoms.

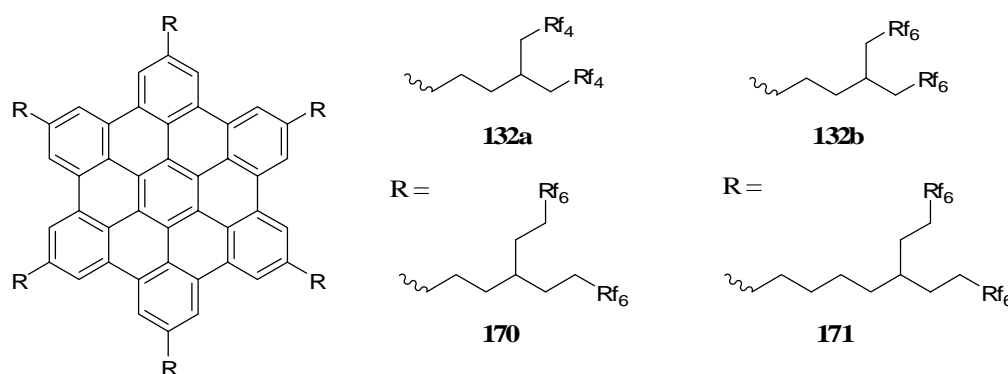


**Figure 15.16** – **Left:** luminescence spectra ( $\lambda_{\text{ex}} = 360$  nm) of  $10^{-4}$  M BTF solutions of HBCs with different perfluoro / alkyl ratios of the lateral side chain; **right:** illustration of HBCs having identical perfluoro / alkyl ratios but differ in the length of the side chain

### 15.2.4 Branched perfluoroalkyl chains

The ideal length of the perfluorinated part of the lateral chain was found to be six or maximally eight carbon atoms, as discussed in the previous section (chapters 15.2.1, 15.2.2 and 15.2.3). Unfortunately the solubility is already seriously hampered with eight carbon atoms. The only way to increase the density of the fluorine coating around the HBC core is to take branched perfluoroalkylated side chains instead of linear ones.

The first derivative (HBC-Rf<sub>3,3,6,6</sub> **132b**) is decorated with six branched chains carrying each two perfluorinated hexyl end groups as shown in Figure 15.17. Modelling of the geometry of this chain revealed a T-shaped arrangement of the perfluorinated end part with respect to the alkyl spacer before the branching point. This geometry inherently imposes a large sterical hindrance for the  $\pi$ - $\pi$  stacking. Because of this other derivatives were prepared as shown in Figure 15.17. The first one carrying two perfluorobutyl groups instead of perfluorohexyl (HBC-Rf<sub>3,3,4,4</sub> **132a**), the second one was endowed with a longer alkyl spacer after the branching point (HBC **170**)<sup>g</sup> whereas the third derivative has an elongated alkyl spacer before and after the branching point (HBC **171**)<sup>g</sup>. To reduce the sterical hindrance even more effectively the last derivative was provided with only three lateral chains (HBC-(Rf<sub>3,3,6,6</sub>)<sub>3</sub> **148**).



**Figure 15.17** – Prepared HBC derivatives carrying different branched perfluorinated side chains<sup>[255]</sup>

The fluorescence data of the HBC derivatives carrying branched perfluorinated side chains is shown in Figure 15.18. All used derivatives displayed a very high solubility in BTF (clear solutions up to  $10^{-2}$  M) which altered the collection of excitation and luminescence data most probably due to the inner filter effect. The excitation spectra at  $10^{-3}$  M reveal artefacts for all derivatives as the principal band at 360 nm has completely vanished for two derivatives. This induces then a reduced quality for the luminescence data as the excitation was carried out around 360 nm. Because of that, it was impossible to collect luminescence data for HBC **148**, HBC **170** and HBC **171** at  $10^{-3}$  M by exciting at 359 nm. The other two derivatives showed nevertheless characteristic data. It has to be pointed

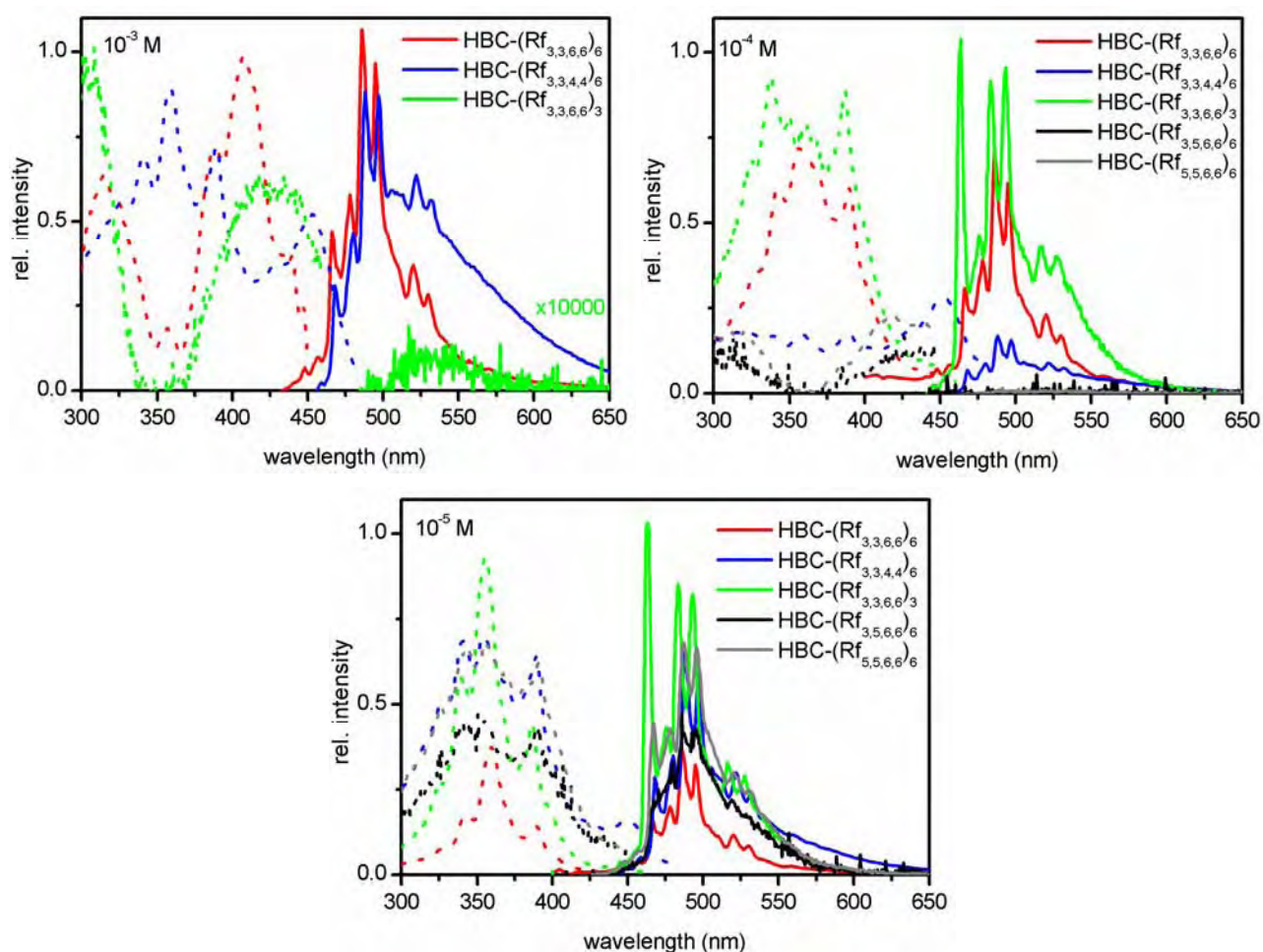
<sup>g</sup> The synthesis is reported in detail in the Master thesis of David Muñoz<sup>[255]</sup>



out that HBC **132b** does not show any sign of lateral aggregation even at this fairly high concentration, indicating that the introduction of branched chains does prevent this type of aggregation properly. Nevertheless the influence on the one dimensional stacking has not yet been thoroughly investigated. HBC **132a** carrying the shorter branched chains revealed slight lateral aggregation at this concentration displaying the reduction of the sterical hindrance around the aromatic core.

Lowering the concentration to  $10^{-4}$  M reduces the inner filter effect for HBC **148**, which allowed the collection of the luminescence for this derivative. Still a high inner filter effect was obtained for HBC **170** and **171**. The reason for this strong effect even at  $10^{-4}$  M could not be explained. The lateral aggregation is found to be reduced even for HBC **132a** indicating that all derivatives exist in solution at  $10^{-4}$  M as monomers or one dimensional aggregated structure. The intense band at 463 nm for HBC **148** may be due to the reduced symmetry from  $D_{6h}$  to  $D_{3h}$ . Even though the symmetry of the HBC core, the chromophore for the fluorescence, is not altered, the unequal lateral decoration may alter the fluorescence behaviour slightly. Probably there are also other reasons for the large intensity increase of the 463 nm band as other authors reported identical emission spectra for HBCs with a varying number of identical substituents.<sup>[256]</sup>

By diluting the solution to  $10^{-5}$  M exactly the same emission spectra are obtained. Only the intensity of the luminescence and excitation spectra of HBC **132a** and **b** are inversed which is most probably due to the still impure excitation spectra. Even the luminescence spectra of HBC **170** and **171** were obtained at this concentration, where HBC **171** showed a usual fluorescence whereas HBC **170** yielded unresolved signals.



**Figure 15.18** – Emission spectra ( $\lambda_{\text{ex}} = 360$  nm) of BTF solutions of HBCs carrying branched perfluoroalkylated side chains; **upper left:**  $10^{-3}$  M, the spectra of HBC **170** and **171** are omitted for clarity as no signal was obtained due to the inner filter effect; **upper right:**  $10^{-4}$  M; **lower left:**  $10^{-5}$  M

Figure 15.19 summarizes the performed cryo-SEM experiments. HBC- $\text{Rf}_{3,3,4,4}$  (**132a**) carrying the smaller lateral chain formed long regular structures of several  $\mu\text{m}$  length and a typical diameter of 80 nm. Next to the regular structure, sheet-like architectures were found which could probably be made either of monostranded stacks or of monomers which assembled during the cryogenation process into an ultra fine skin on top of the solvent. All free standing tails of the observed structures consisted of round balls as if the substance coiled together.

HBC- $\text{Rf}_{3,3,6,6}$  (**132b**) with its bulkier side chains formed some linear monostranded structures too but only very few of them. Most probably a large part of the material exists as monomer at this concentration. The lateral chain of this derivative seems to be sterically too bulky in order to form large amounts of monostranded stacks.

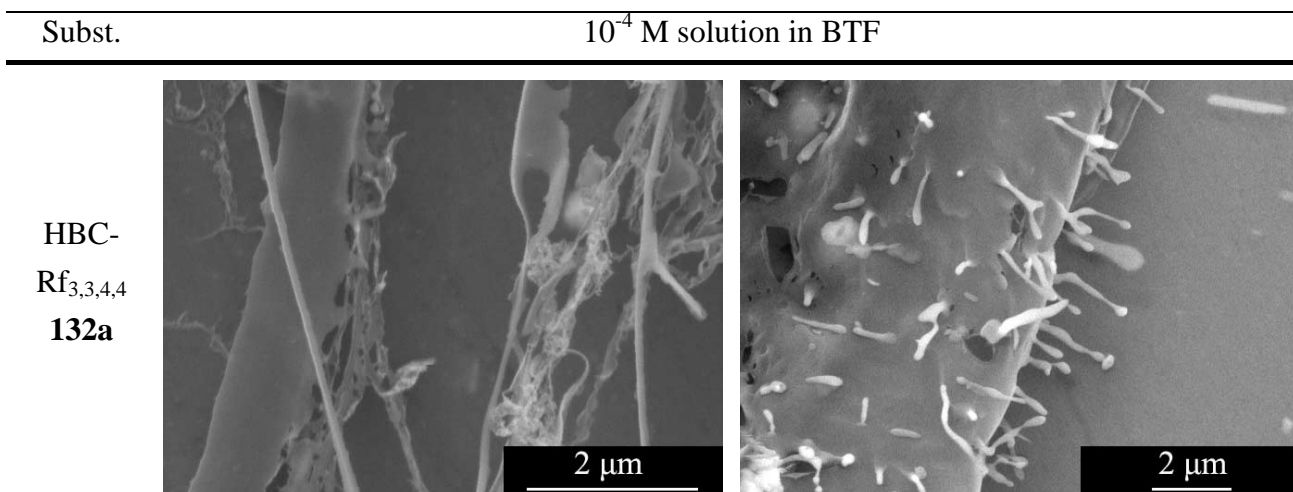
HBC- $(\text{Rf}_{3,3,6,6})_3$  (**148**) which was endowed with only three bulky lateral chains would be an ideal model compound to form a monostranded stack by rotating each disk by  $60^\circ$  from its neighbour. Unfortunately the cryo-SEM investigation did not reveal such monostranded stacks but indicated

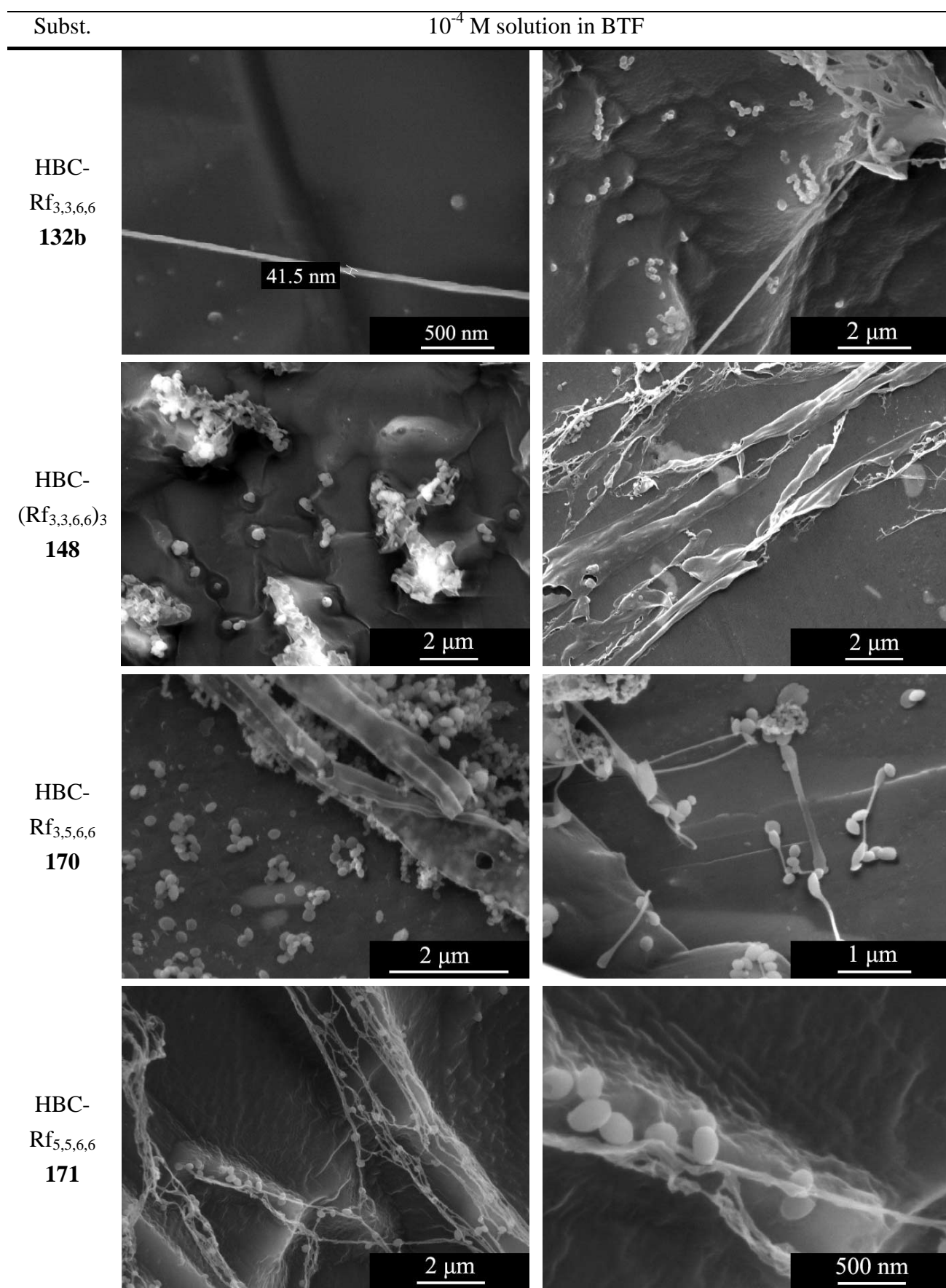
the formation of small aggregated architecture without formation of a unique direction of growth. Moreover large amounts of substance were found which formed skin like thin structures. This phenomenon occurred probably during the cryogenation process by the formation of a monomeric film on top of the solvent. Another possibility for the missing columns could be the presence of the two regio-isomers of HBC **148**. The desired isomer **148a** has a regular spacing of the lateral chains allowing for the formation of monostranded stacks. On the contrary isomer **148b** could also form a monostranded stack but only with its own isomers. Unfortunately it could not be determined if the observed architectures are “isomerically pure” or not.

HBC-Rf<sub>3,5,6,6</sub> (**170**) carries branched perfluorinated side chains made of an ethyl spacer between the branching point and the perfluorinated carbons compared to a methyl spacer for HBC **132b**. This increased spacer endows the molecule with an additional flexibility and reduces the T-shape geometry of the lateral chain. This should as consequence facilitate the formation of monostranded stacks without decreasing the fluorine coating around the formed stack. This was partially observed: monostranded fine structures were found which consisted of ball shape round tails where the round ending was found to be more pronounced than for HBC **132a**. Furthermore small round and oval architectures were found as if monostranded stacks were formed and curled together to form droplet like aggregates.

HBC-Rf<sub>5,5,6,6</sub> (**171**) was bestowed with an additional flexibility as the branching point was separated from the aromatic core by a pentyl spacer instead an propyl one as for all other branched derivatives. The observed effect was then rather small as similar structures were observed than for HBC **170**: small linear filaments together with many oval shaped balls.

In summary afforded only HBC **132a** promising results in the formation of monostranded stacks. All other derivatives with branched side chains formed either droplet like structures in the cryo-SEM or the collection of fluorescence data was hampered due to the inner filter effect.





**Figure 15.19** – Cryo-SEM micrographs of  $10^{-4}$  M BTF solutions of HBC derivatives bearing branched perfluoroalkylated side chains

## 16 Morphology of HBC derivatives

### 16.1 DSC and TGA investigations

The thermal behaviour of all synthesized HBC derivatives was analyzed by DSC, TGA and XRD<sup>h</sup> with a heating and cooling rate of 20 °C / min. The products started to decompose in air above 250 °C before clearing in the isotropic liquid, the temperature of which could not be determined or most derivatives. Most derivatives are found to exhibit a liquid-crystalline mesophase, often after several crystal-to-crystal phase transitions, most probably due to small rearrangements of the lateral chains. Figure 16.1 shows as one example the obtained data from the DSC analysis for HBC **94b** where the following thermal sequence for the DSC trace could be determined: Cr<sub>1</sub>, 103.2 °C Cr<sub>2</sub>, 155.9 °C Cr<sub>3</sub>, 194.1 °C Col<sub>h</sub>. An overview and comparison with the DSC data of all investigated compounds is given in Figure 16.2 and later in Table 16.1.

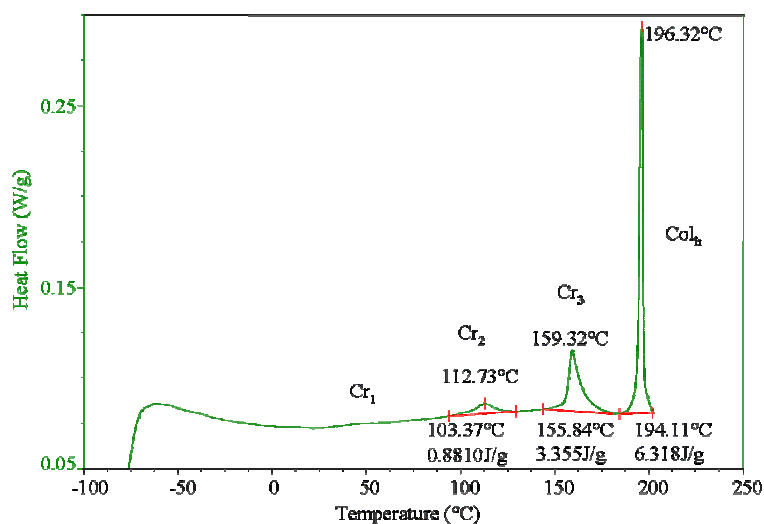


Figure 16.1 – DSC trace of HBC **94b** (second heating)

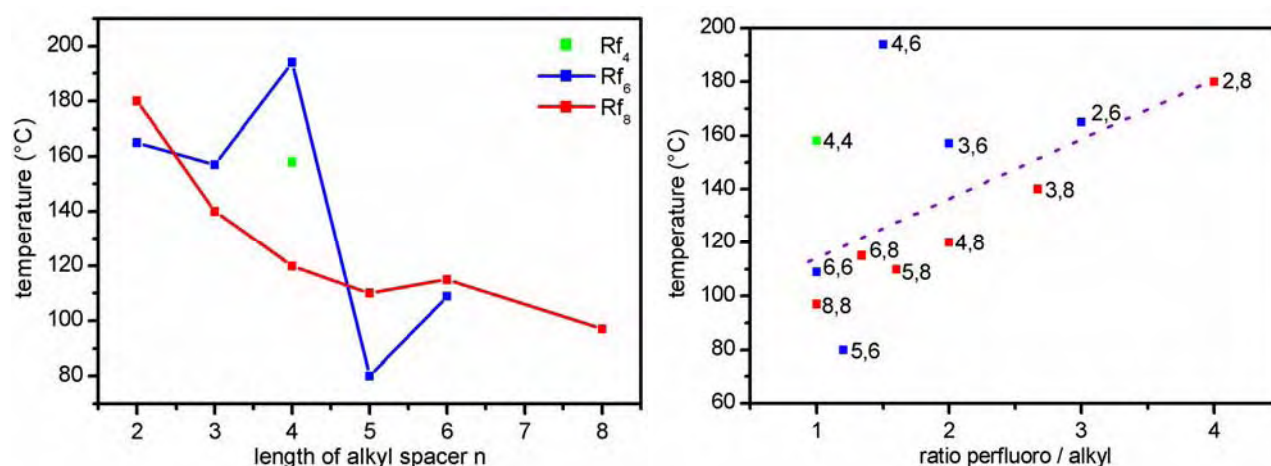
All mesomorphic HBCs have transition temperatures which were found to be strongly influenced by the structure of the mesogen, *i.e.* the nature and the length of the side chain. All transition temperatures to the mesophase are represented graphically in Figure 16.2 in two different ways. On the left hand side the derivatives are presented with respect to their alkyl spacer whereas on the right hand side the perfluoro / alkyl ratio was the key parameter. HBC-Rf<sub>4,4</sub> (**94a**) was the only derivative bearing a perfluorobutyl part which showed a mesomorphic behaviour (it has to be noted that only two perfluorobutyl derivatives were prepared). For the HBC series bearing perfluorohexyl end parts only HBC-Rf<sub>8,6</sub> (**125b**) is not mesomorph whereas all derivatives carrying perfluorooctyl parts are

<sup>h</sup> DSC, TGA and XRD experiments were performed by Dr. Bertrand Donnio, group of Prof. Guillon, IPCMS, Strasbourg

mesomorph. The left part of Figure 16.2 indicates clearly a decrease of the transition temperature towards the mesophase by increasing the alkyl spacer of the side chain as general trend. In the case of the Rf<sub>6</sub> series there are two interesting exceptions, HBC-Rf<sub>4,6</sub> (**94b**) being much too high (194.1 °C) and HBC-Rf<sub>5,6</sub> (**106a**) being too low (80.0 °C). A possible reason for the high transition temperature of HBC **94b** might be a higher stability due to an ideal packing of the lateral chains which is no longer possible for HBC **106a**.

By drawing the transition temperatures against the perfluoro / alkyl ratio only HBC **94b** diverges clearly. A trend line through all transition temperatures indicates that the larger the difference of alkyl spacer and perfluorinated part, the higher the transition temperature. A high perfluoro / alkyl ratio inherently implies a long perfluorinated end part, which bestows the side chain with a pronounced stiffness, hindering their melting. Therefore an increased transition temperature is reasonable for derivatives having large perfluoro / alkyl ratios.

It has to be noted that all measured HBC derivatives start to decompose above 250°C as shown by TGA analysis.

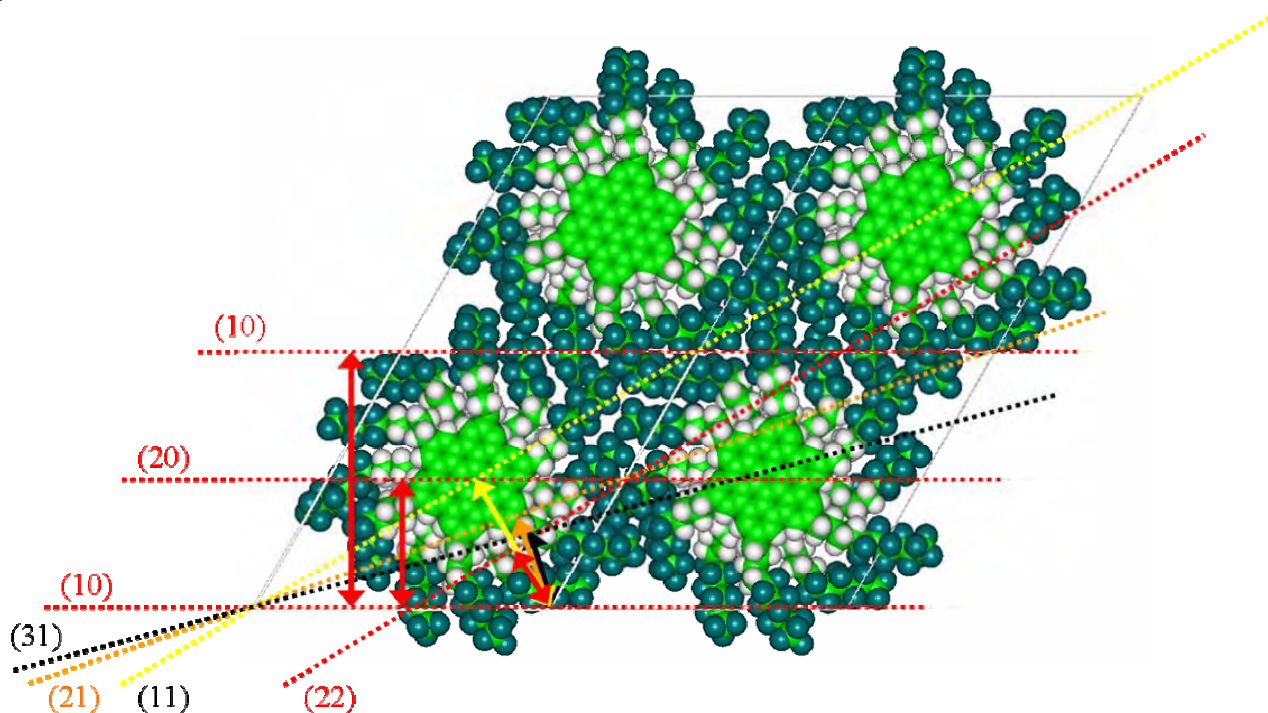


**Figure 16.2** – Graphical illustration of DSC transition temperatures towards the mesophase. **Left:** transition temperature vs. the length of the alkyl spacer n; **right:** transition temperature vs. the perfluoro / alkyl ratio, the numbering refers to the numbers of alkylated and perfluoroalkylated carbon atoms



## 16.2 X-ray investigations

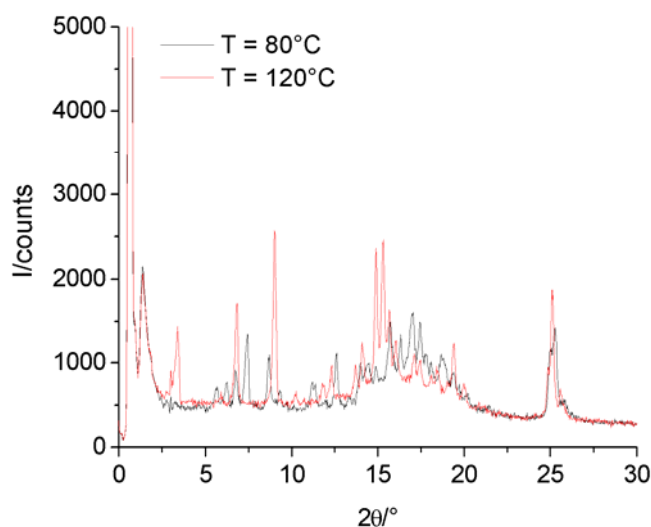
In order to guarantee a deeper understanding of the X-ray data, Figure 16.3 illustrates a drawing of the different used Miller indices together with the distances obtained from the XRD pattern. The (10) index is illustrated for example by the red line, whereas the corresponding distances is given by the red arrow in between the (10) index and the origin. This distance is then shown in the diffraction pattern.



**Figure 16.3** – Projections on the hexagonal lattice of HBC-Rf<sub>4,6</sub> **94b** with their respective Miller indices. The arrows indicate the corresponding distances  $d$  shown in the XRD diffraction

### 16.2.1 Temperature dependence of X-ray

As shown by the DSC micrographs (Figure 16.1) there are several crystal-to-crystal phase transitions before the mesophase is reached. In order to elucidate the adopted structure of the different crystalline phases, XRD data were collected at different temperatures as shown in Figure 16.4. The black curve, obtained at 80 °C (Cr<sub>1</sub>), showed already several diffractions which indicate a periodic arrangement of the material. By heating the sample to 120 °C (Cr<sub>2</sub>) the diffraction pattern is clearly changed, underlining the DSC data, which indicated the formation of a second crystalline phase. Unfortunately it was up to now not possible to assign a geometry to the different obtained XRD patterns. Because of that all further presented XRD data were collected at 200 °C as at this temperature all mesomorphic HBC derivatives already reached the liquid crystalline phase, as presented later in Table 16.1.



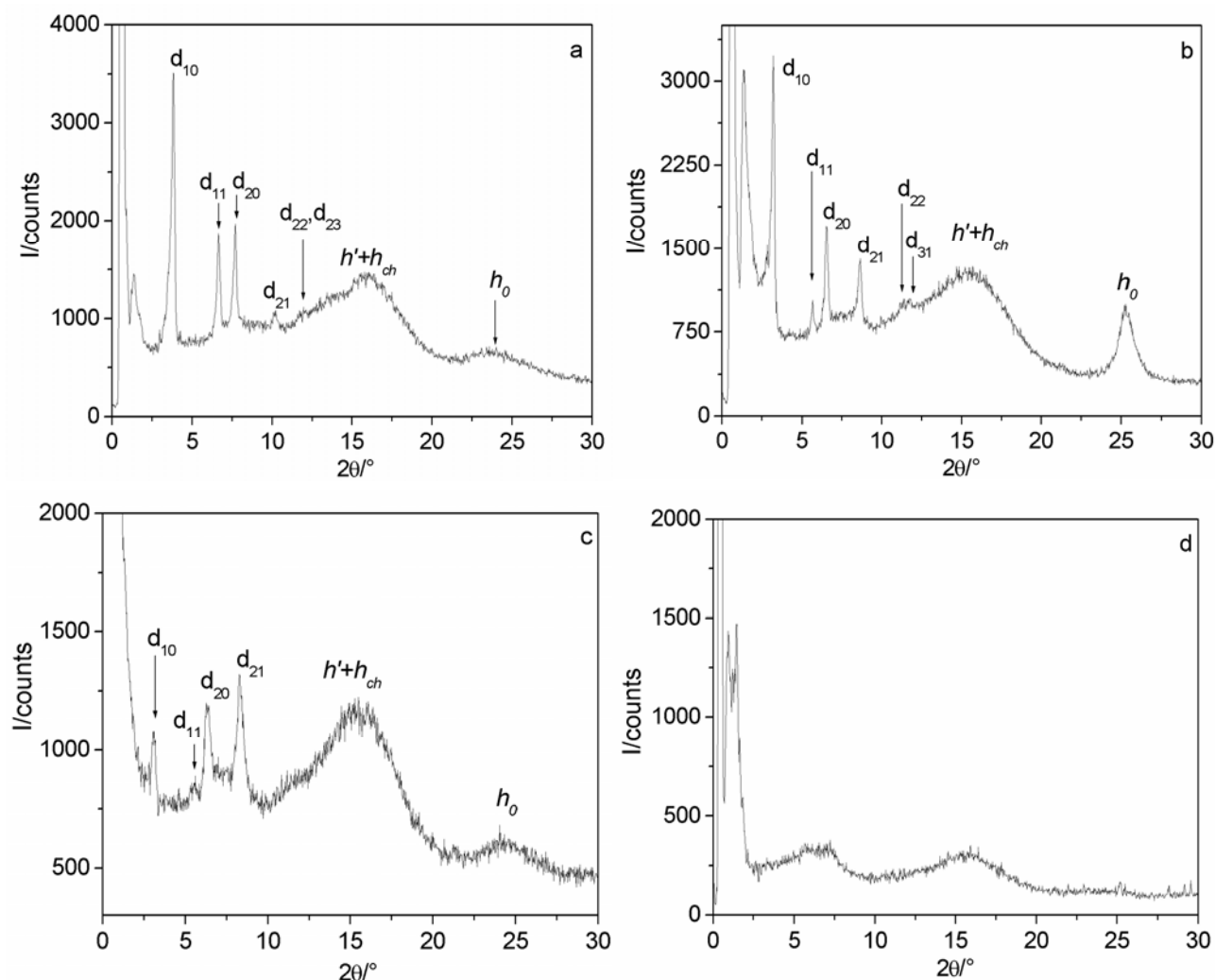
**Figure 16.4** – Temperature depended XRD pattern of HBC-Rf<sub>4.6</sub> (**94b**)

### 16.2.2 X-ray investigation at high temperatures

The XRD patterns are shown in Figure 16.5 for all HBC derivatives bearing a four alkyl carbon spacer in the lateral chain. HBC **94b**, showing the clearest diffraction pattern, is analysed in detail in order to indicate the process of evaluation of these XRD patterns.

At 200 °C, the XRD pattern of HBC **94b** exhibits several sharp and small-angle reflections, with the spacings being in the ratio  $1:\sqrt{3}:\sqrt{4}:\sqrt{7}:\sqrt{12}:\sqrt{13}$ , respectively (see Figure 16.5). These reflections are readily assigned as the (10), (11), (20), (21), (22), and (31) indices of a hexagonal 2D lattice, illustrated in Figure 16.3, with a parameter  $a = 31.4 \text{ \AA}$  (at  $T = 200 \text{ °C}$ , see Table 16.1). A broad halo ( $h_{ch}$ ) and another sharp signal ( $h_0$ ) are observed in the wide angle part, at 5.65 and 3.5 Å, corresponding to the liquid-like order of the molten fluorinated chains, and the stacking of the flat molecular cores in the third dimension, respectively.

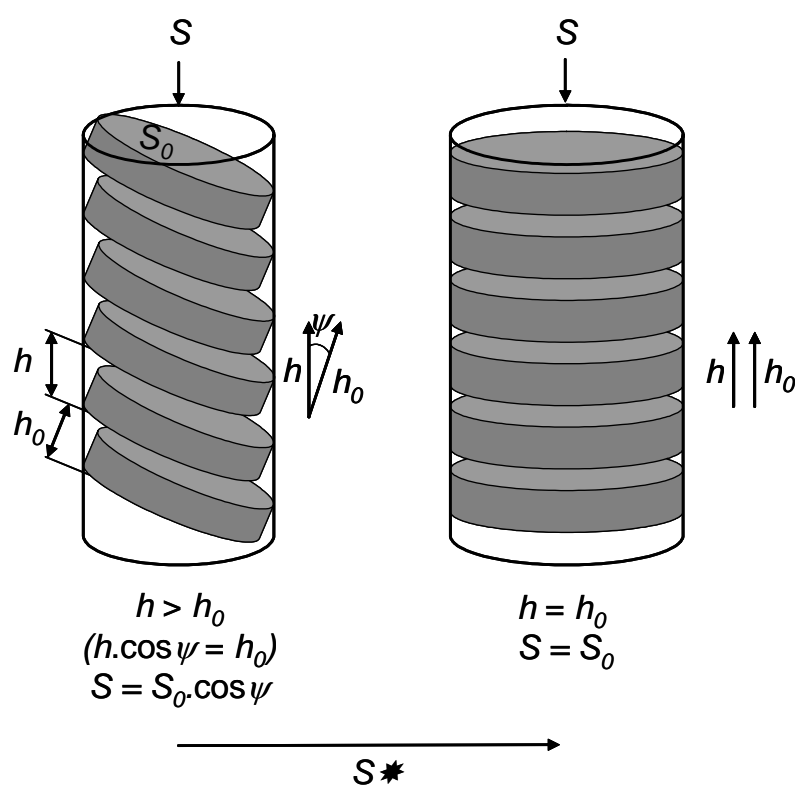




**Figure 16.5** – Illustration of four different XRD patterns, measured all at 200°C; a HBC-Rf<sub>4,4</sub> **94a**; b HBC-Rf<sub>4,6</sub> **94b**; c HBC-Rf<sub>4,8</sub> **94c**; d HBC-Rf<sub>4,10</sub> **94d**

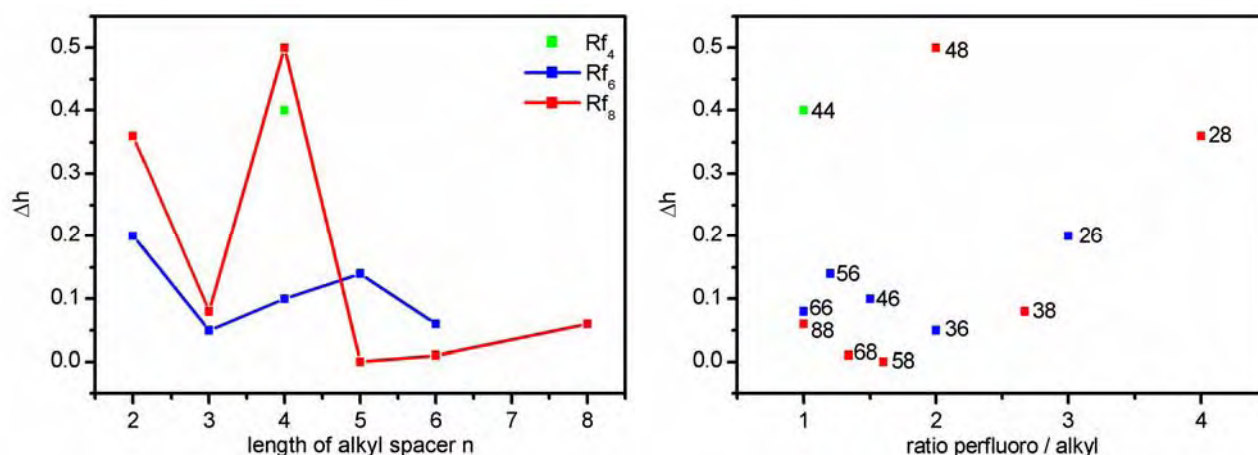
The knowledge of the columnar cross section ( $S$ , c.f. caption of Table 16.1) and the stacking periodicity ( $h_0$ ) along the molecular disc normal permits to understand the molecular packing inside the columns.<sup>[257]</sup> For instance, one can deduce the intra-columnar repeating periodicity along the columnar axis,  $h$ , from the columnar cross section,  $S$ , obtained directly from the X-ray diffraction data (see Table 16.1), and the molecular volume ( $V_{mol}$ ), which are analytically linked through the relation  $h \cdot S = N \cdot V_{mol}$ , where  $N$  is the number of molecules (aggregation number) within this fraction of column;<sup>[257a]</sup> in this case,  $N$  is chosen equal to 1 as the molecule is disc-like.

The comparison of  $h$  and  $h_0$  is very informative as it can tell us about the various possible organizations of the disc-like molecules within the columns. Thus, for  $N = 1$ , an intramolecular stacking of 3.6 Å was determined ( $h = V_{mol}/S$ ), nearly identical to the stacking periodicity within the column ( $h_0 = 3.5$  Å) measured by XRD, indicating that the molecules are (almost) stacked perpendicular (not tilted) with respect to the columnar axis as illustrated in Figure 16.6.



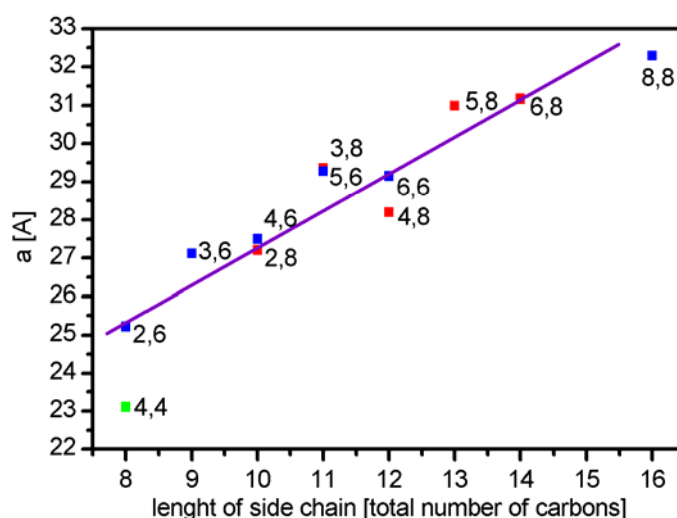
**Figure 16.6** – Representation of two types of stacking of discs within the column and the different parameters  $h$ ,  $h_0$ ,  $S$  and  $S_0$  (obtained from X-ray diffraction and dilatometry) allowing for their discrimination.  $\psi$  is the angle between the columnar axis and the molecular disc normal

The difference ( $\Delta h$ ) between the measured molecular stacking distance  $h_0$  and the calculated stacking distance  $h$  gives an indication of the distortion (order of magnitude of  $\psi$ ) of the self-aggregated strand. The length of the alkyl spacer was related with  $\Delta h$  which allowed the preparation of Figure 16.7. Short alkyl spacers (two  $\text{CH}_2$ ) yielded materials with a large  $\Delta h$  indicating a considerably tilted structure. For all longer alkyl spacers  $\Delta h$  decreases smoothly to level out inbetween 0 and 0.1. As only exception HBC-Rf<sub>4,8</sub> (**94c**) may be cited exhibiting an unusual large  $\Delta h$ . The reason for this odd behaviour is far from clear. Unusual large  $\Delta h$  values are obtained for HBC-Rf<sub>2,6</sub> (**63a**), HBC-Rf<sub>2,8</sub> (**63b**), HBC-Rf<sub>4,4</sub> (**94a**) and HBC-Rf<sub>4,8</sub> (**94c**) carrying all pair numbers of alkyl carbons in their lateral chain. Furthermore, low  $\Delta h$  values are observed for HBC-Rf<sub>3,6</sub> (**82a**), HBC-Rf<sub>3,8</sub> (**82b**) and all derivatives bearing longer chains than HBC-Rf<sub>5,8</sub> (**114**). Probably the fluctuation of  $\Delta h$  is provoked by an odd or even number of alkyl carbons in the lateral chain as a similar behaviour is observed for the melting point of alkanes. The correlation of  $\Delta h$  with the perfluoro / alkyl ratio reaches a local minimum for  $\Delta h$  for ratios between 1 and 2.5. In this representation no systematic dependence on the length of the perfluorinated part is found.



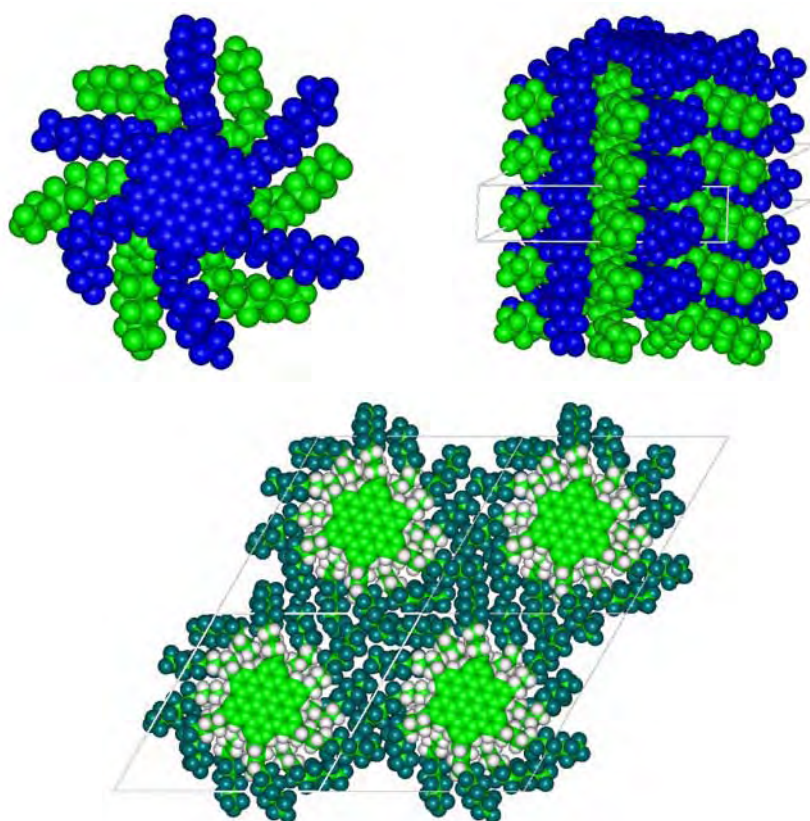
**Figure 16.7** – Left: illustration of the  $\Delta h$  being the difference between  $h_0$  (molecular stacking distance) and  $h$  (calculated stacking distance) vs. the length of the alkyl spacer; right:  $\Delta h$  is shown vs. the perfluoro / alkyl ratio

Another parameter worth to be mentioned is the dimension of the unit cell, expressed by the  $d_{10}$  reflection. Figure 16.8 illustrates the variation of the dimension of the unit cell by increasing the lengths of the perfluoroalkyl chain. The smallest  $d_{10}$  value (23.1 Å) was found for HBC- $Rf_{4,4}$  (**94a**) which was surprisingly even smaller (25.2 Å) than for HBC- $Rf_{2,6}$  (**63a**). The other three pairs of derivatives (HBC- $Rf_{2,8}$  (**63b**) and HBC- $Rf_{4,6}$  (**94b**), HBC- $Rf_{3,8}$  (**82b**) and HBC- $Rf_{5,6}$  (**106a**); HBC- $Rf_{4,8}$  (**94c**) and HBC- $Rf_{6,6}$  (**169**)), which exhibit the same number of carbon atoms in the lateral chain, have more comparable  $d_{10}$  values. This indicates only that the perfluoro / alkyl ratio exerts only a minor influence on the dimensions of the unit cell. This is a rather surprising finding as perfluorinated alkyl chains are much stiffer and bulkier than normal alkyl chains. Therefore one intuitively thinks that the unit cell of HBC derivatives bearing more perfluorinated carbon atoms should inherently be bigger. As in our case most of the variations are limited to two perfluorinated carbons this may not be large enough to provoke a significant difference.



**Figure 16.8** – Correlation of the measured diffraction spacing ( $a$ ) with the length of the side chain

In order to accommodate the cross-sections ( $\sim 5.6$  Å) of the fluorinated side chains, which largely exceeds the thickness of the core ( $\sim 3.6$  Å), the molecules are likely to stack in a staggered fashion (rotation of approx.  $30^\circ$ ), the flexible aliphatic spacer allowing the bulky fluorinated chains to expand out of the center to fill the available volume. This dense packing model of the HBCs into columns is supported by molecular dynamics simulations<sup>i</sup>. For this experiment, a periodic molecular model was built from experimental X-ray data, where a tetramer with a slice thickness of  $14.0$  Å ( $4 \times 3.5$  Å, corresponding to four stacked molecules) was taken as repeating unit. The result of these calculations evidenced a good space filling of the available volume as well as the enhancement of the micro segregation (separation of the three non miscible parts (aromatic, alkyl and perfluoroalkyl) of the molecule in the mesophase), contributing to the cohesion of the columnar structure. The surface area of the discs stacked in a flat conformation is fully compatible with the cross-section of the hexagonal lattice.



**Figure 16.9** – **Top left:** view of the stacking of neighbouring molecules (top view); **top right:** view of the stacking within the column (side view); **bottom:** Snapshot showing the molecular self-assembly of HBC-Rf<sub>4,6</sub> **94b** into the hexagonal lattice of the Col<sub>h</sub> phases central core in green, aliphatic spacers in grey, fluorinated segments in dark green

This model of the packing of HBC **94b** can be used to explain the absence of mesomorphism in the case of HBC **132b** and HBC **170** as the branched chains are too bulky to be accommodated with the cross-sections of the HBC cores, clearly indicating that both, a strong disc-disc interaction and effi-

<sup>i</sup> The modelling was performed by Dr. Cyril Bourgoigne and Dr. Benoit Heinrich, University Louis Pasteur, France

cient micro-segregation is needed for mesomorphism to occur. In line with this argument HBC **94d**, carrying ten perfluorinated carbon atoms in each side chain, shows an amorphous behaviour too. Most probably the length and the stiffness of the perfluorinated part hinder the formation of mesomorphic structures in this case. For HBC **125a** the main reason for the absence of mesomorphism may be the incorporation of chlorine into the HBC core, hindering the  $\pi$ - $\pi$ -stacking. Only for HBC **125b** no reason could be found for the amorphous behaviour of this compound. MALDI-TOF measurements revealed that no chlorine insertion occurred. Probably the conformations of the side chain prevented any micro-segregation. For HBC **148**, carrying only three branched chains, the absence of mesomorphism is only hardly explained as theoretically enough space is available to accommodate the lateral chains. Probably the presence of the two regio-isomers prevent the formation of the mesophase.

Table 16.1 gives a summary of the thermal and liquid-crystalline properties of all prepared HBC derivatives bearing perfluoroalkylated side chains.

**Table 16.1** – Overview of the thermal and liquid-crystalline properties of perfluoroalkylated HBC derivatives

HBC	$d_{\text{exp}}$ [Å] <sup>a</sup>	[hkl] <sup>b</sup>	Intensity <sup>c</sup>	$d_{\text{theo}}$ [Å] <sup>a,d</sup>	Parameters at T = 200°C <sup>d,e</sup>
<b>HBC-Rf<sub>2,6</sub></b>	25.22	10	VS (sh)	24.9	PCr <sub>1</sub> 128.7 PCr <sub>2</sub> 156.25 PCr <sub>3</sub>
<b>63a</b>	12.35	20	S (sh)	12.45	165.0 Col <sub>h</sub>
	9.37	21	S (sh)	9.4	$T_{\text{dec.}} \sim 250^\circ\text{C}$
	5.6	$h' + h_{\text{ch}}$	VS (br)	F-chains	$a = 28.75 \text{ Å}$
	3.6	$h_0$	W (br)	stacking	$S = 716.15 \text{ Å}^2$
					$V_{\text{mol}} = 2725 \text{ Å}^3$
					$h = 3.8 \text{ Å}$
<b>HBC-Rf<sub>2,8</sub></b>	27.2	20/11	M (sh)	27.2	Cr <sub>1</sub> 122.0 Cr <sub>2</sub> 138.0 Cr <sub>3</sub>
<b>63b</b>	15.7	31	M (sh)	15.7	180.0 Col <sub>hr</sub>
	12.3	41	M (sh)	12.5	$T_{\text{dec.}} \sim 250^\circ\text{C}$
	10.3	42/51/13	W (sh)	10.3	$a = 54.4, b = 31.4$
	5.8	$h_{\text{ch}}$	VS (br)	F-chains	$(a = 31.4)$
	3.5	$h_0$	S (sh)	stacking	$V_{\text{mol}} = 3300 \text{ Å}^3$
					$h = 3.86 \text{ Å}$

HBC	$d_{\text{exp}}$ [Å] <sup>a</sup>	[hkl] <sup>b</sup>	Intensity <sup>c</sup>	$d_{\text{theo}}$ [Å] <sup>a,d</sup>	Parameters at T = 200°C <sup>d,e</sup>
<b>HBC-Rf<sub>3,6</sub></b>	27.12	10	VS (sh)	26.85	PCr <sub>1</sub> 90.35 PCr <sub>2</sub> 135.75 PCr <sub>3</sub> 157.0 Col <sub>h</sub>
<b>82a</b>	13.43	20	S (sh)	13.45	$T_{\text{dec.}} \sim 250^\circ\text{C}$
	10.12	21	S (sh)	10.15	$a = 31.0 \text{ Å}$
	7.72	22	S (sh)	7.75	$S = 830.0 \text{ Å}^2$
	7.43	31	S (sh)	7.45	$V_{\text{mol}} = 2910 \text{ Å}^3$
	5.7	$h' + h_{ch}$	VS (br)	F-chains	$h = 3.5 \text{ Å}$
	3.55	$h_0$	S (sh)	stacking	
<b>HBC-Rf<sub>3,8</sub></b>	29.36	10	S (sh)	29.2	Cr 140 Col <sub>h</sub>
<b>82b</b>	14.6	20	S (sh)	14.6	$T_{\text{dec.}} \sim 250^\circ\text{C}$
	10.96	21	VS (sh)	11.05	$a = 33.7 \text{ Å}$
	5.65	$h' + h_{ch}$	VS (br)	F-chains	$S = 998.0 \text{ Å}^2$
	3.56	$h_0$	S (sh)	stacking	$V_{\text{mol}} = 3480 \text{ Å}^3$
					$h = 3.48 \text{ Å}$
<b>HBC-Rf<sub>4,4</sub></b>	23.1	10	VS (sh)	23.05	Cr <sub>1</sub> 108.85 Cr <sub>2</sub> 143.0 Cr <sub>3</sub>
<b>94a</b>	13.38	11	S (sh)	13.3	157.8 Col <sub>h</sub>
	11.48	20	S (sh)	11.5	$T_{\text{dec.}} \sim 200^\circ\text{C}$
	8.67	21	S (sh)	8.7	$a = 26.6 \text{ Å}$
	5.5	$h' + h_{ch}$	VS (br)	F-chains	$S = 615.5 \text{ Å}^2$
	3.7	$h_0$	W (br)	stacking	$V_{\text{mol}} = 2525 \text{ Å}^3$
					$h = 4.1 \text{ Å}$
<b>HBC-Rf<sub>4,6</sub></b>	27.25	10	VS (sh)	27.2	Cr <sub>1</sub> 103.35 Cr <sub>2</sub> 155.85 Cr <sub>3</sub>
<b>94b</b>	15.75	11	S (sh)	15.7	194.1 Col <sub>h</sub>
	13.55	20	VS (sh)	13.6	$T_{\text{dec.}} \sim 250^\circ\text{C}$
	10.3	21	S (sh)	10.3	$a = 31.4 \text{ Å}$
	7.85	22	M (sh)	7.85	$S = 854.3 \text{ Å}^2$
	7.55	31	M (sh)	7.55	$V_{\text{mol}} = 3100 \text{ Å}^3$
	5.65	$h' + h_{ch}$	VS (br)	F-chains	$h = 3.6 \text{ Å}$
	3.5	$h_0$	S (sh)	stacking	
<b>HBC-Rf<sub>4,8</sub></b>	28.2	10	M (sh)	28.1	Cr <sub>1</sub> 82.0 Cr <sub>2</sub> 120.0 Col <sub>h</sub>
<b>94c</b>	16.2	11	W (sh)	16.2	$T_{\text{dec.}} \sim 220^\circ\text{C}$
	14.0	20	M (sh)	14.05	$a = 32.45 \text{ Å}$
	10.6	21	M (sh)	10.6	$S = 911.9 \text{ Å}^2$
	5.8	$h' + h_{ch}$	VS (br)	F-chains	$V_{\text{mol}} = 3660 \text{ Å}^3$
	3.5	$h_0$	M (br)	stacking	$h = 4.0 \text{ Å}$

HBC	$d_{\text{exp}}$ [Å] <sup>a</sup>	[hkl] <sup>b</sup>	Intensity <sup>c</sup>	$d_{\text{theo}}$ [Å] <sup>a,d</sup>	Parameters at T = 200°C <sup>d,e</sup>
<b>HBC-Rf<sub>4,10</sub></b>	13.7		S (br)		amorphous solid
<b>94d</b>	5.6	$h'+h_{ch}$	S (br)	F-chains	$T_{\text{dec.}} \sim 200^\circ\text{C}$
	3.6	$h_0$	VW (br)	stacking	$V_{\text{mol}} = 4230 \text{ Å}^3$
<b>HBC-Rf<sub>5,6</sub></b>	29.28	10	VS (sh)	29.1	Cr 80 Col <sub>h</sub>
<b>106a</b>	16.75	11	S (sh)	16.8	$T_{\text{dec.}} \sim 200^\circ\text{C}$
	14.5	20	VS (sh)	14.55	$a = 33.6 \text{ Å}$
	10.98	21	S (sh)	11.0	$S = 977.8 \text{ Å}^2$
	5.56	$h'+h_{ch}$	VS (br)	F-chains	$V_{\text{mol}} = 3275 \text{ Å}^3$
	3.49	$h_0$	S (sh)	stacking	$h = 3.35 \text{ Å}$
<b>HBC-Rf<sub>5,8</sub></b>	31.0	10	VW (sh)	30.85	Cr 110 Col <sub>h</sub>
<b>114</b>	17.84	11	S (sh)	17.8	$T_{\text{dec.}} \sim 220^\circ\text{C}$
	15.42	20	VS (sh)	15.4	$a = 35.6 \text{ Å}$
	11.59	21	S (sh)	11.65	$S = 1098.9 \text{ Å}^2$
	5.61	$h'+h_{ch}$	VS (br)	F-chains	$V_{\text{mol}} = 3845 \text{ Å}^3$
	3.5	$h_0$	S (br)	stacking	$h = 3.5 \text{ Å}$
<b>HBC-Rf<sub>6,6</sub></b>	29.15	10	S (sh)	29.0	Cr <sub>1</sub> 50.0 Cr <sub>2</sub> 109.0 Col <sub>h</sub>
<b>169</b>	16.65	11	S (sh)	16.75	$T_{\text{dec.}} \sim 200^\circ\text{C}$
	14.5	20	S (sh)	14.5	$a = 33.5 \text{ Å}$
	10.95	21	M (sh)	11.0	$S = 971.9 \text{ Å}^2$
	5.8	$h'+h_{ch}$	VS (br)	F-chains	$V_{\text{mol}} = 3460 \text{ Å}^3$
	3.5	$h_0$	S (sh)	stacking	$h = 3.56 \text{ Å}$
<b>HBC-Rf<sub>6,8</sub></b>	31.17	10	VW (sh)	31.05	Cr <sub>1</sub> 77.0 Cr <sub>2</sub> 96.0 Cr <sub>3</sub> 115 Col <sub>h</sub>
<b>106b</b>	17.95	11	M (sh)	17.9	$T_{\text{dec.}} \sim 200^\circ\text{C}$
	15.52	20	VS (sh)	15.5	$a = 35.85 \text{ Å}$
	11.66	21	M (sh)	11.75	$S = 1113.2 \text{ Å}^2$
	5.58	$h'+h_{ch}$	VS (br)	F-chains	$V_{\text{mol}} = 4030 \text{ Å}^3$
	3.59	$h_0$	W (br)	stacking	$h = 3.6 \text{ Å}$
<b>HBCRf<sub>8,4</sub></b>	29.0		VS (br)		amorphous solid
<b>125a</b>	14.9		S (br)		$T_{\text{dec.}} \sim 200^\circ\text{C}$
	5.5	$h'+h_{ch}$	VS (br)	F-chains	$V_{\text{mol}} = 3260 \text{ Å}^3$
	3.55	$h_0$	W (br)	stacking	
<b>HBC-Rf<sub>8,6</sub></b>	15.6		S (br)		amorphous solid
<b>125b</b>	5.5	$h'+h_{ch}$	VS (br)	F-chains	$T_{\text{dec.}} \sim 200^\circ\text{C}$
	3.6	$h_0$	W (br)	stacking	$V_{\text{mol}} = 3830 \text{ Å}^3$

HBC	$d_{exp}$ [Å] <sup>a</sup>	[hkl] <sup>b</sup>	Intensity <sup>c</sup>	$d_{theo}$ [Å] <sup>a,d</sup>	Parameters at T = 200 °C <sup>d,e</sup>
<b>HBC-Rf<sub>8,8</sub></b>	32.3	10	M (sh)	32.25	Cr 97.0 Col <sub>h</sub>
<b>125c</b>	18.6	11	S (sh)	18.6	$T_{dec.} \sim 220^\circ\text{C}$
	16.11	20	S (sh)	16.1	$a = 37.25 \text{ Å}$
	5.5	$h' + h_{ch}$	VS (br)	F-chains	$S = 1201.3 \text{ Å}^2$
	3.6	$h_0$	VW (br)	stacking	$V_{mol} = 4400 \text{ Å}^3$
					$h = 3.66 \text{ Å}$
<b>HBC-Rf<sub>3,3,4,4</sub></b>	27.65	10	M (sh)	27.7	Cr 178.2 Col <sub>h</sub>
<b>132a</b>	15.96	20	S (sh)	15.91	
	5.5	$h' + h_{ch}$	VS (br)	F-chains	
<b>HBC-Rf<sub>3,3,6,6</sub></b>					amorphous solid
<b>132</b>					
<b>HBC-(Rf<sub>3,3,6,6</sub>)<sub>3</sub></b>					amorphous solid
<b>148</b>					
<b>HBC-Rf<sub>3,5,6,6</sub></b>					amorphous solid
<b>170</b>					
<b>HBC-Rf<sub>5,5,6,6</sub></b>	29.47	10	S (sh)	29.45	Col <sub>h</sub> 120.0
<b>171</b>	17.08	11	M (sh)	17.8	
	14.6	20	S (sh)	14.57	
	11.11	21	S (br)	F-chains	
	3.6	$h_0$	VW (br)	stacking	

<sup>a</sup> $d_{exp}$  and  $d_{theo}$  are the experimentally measured and calculated diffraction spacings. The distances are given in Å. <sup>b</sup>[hk] refer to the indexation of the reflections, and  $h_0$ ,  $h'$  and  $h_{ch}$  are the various short range periodicities determined by XRD corresponding to the molecular stacking distance ( $h_0$ ) and to the liquid-like order of the molten chains ( $h_{ch}$ ); the double periodicity  $h' = 2 \cdot h_0$  is observed, although not measurable as hidden under the large diffuse scattering. <sup>c</sup>Intensity of the reflections: VS: very strong, S: strong, M: medium, W: weak; br and sh stand for broad and sharp reflections, respectively. <sup>d</sup> $d_{theor}$  and the lattice parameter  $a$  is deduced from the following mathematical expressions:  $\langle d_{10} \rangle = 1/N_{hk} [\sum_{hk} d_{hk} \cdot (h^2 + k^2 + hk)^{1/2}]$  where  $N_{hk}$  is the number of  $hk$  reflections and  $a = 2 \langle d_{10} \rangle / \sqrt{3}$ . <sup>e</sup> Col<sub>h</sub>: hexagonal columnar phase, Cr<sub>i</sub>: crystalline solids, PCr<sub>i</sub>: partially crystalline solids, I: isotropic liquid.  $S$  is the lattice area (i.e.) columnar cross-section:  $S = a^2 \sqrt{3}/2$ .  $V_{mol}$  is the molecular volume:  $V_{mol} = V_{HBC} + 6(nV_{CH_2} + mV_{CF_2})$ , where  $V_{HBC} = 650 \text{ Å}^3$ ,  $V_{CH_2} = 26.5616 + 0.02023T$  ( $30.6076 \text{ Å}^3$  at  $200^\circ\text{C}$ ), and  $V_{CF_2} = 40.815 + 0.03318T$  ( $47.451 \text{ Å}^3$  at  $200^\circ\text{C}$ );  $h$  is the intracolumnar repeating distance, deduced directly from the measured molecular volume and the columnar cross-section according to  $h = V_{mol}/S$ ;



## 17 Alternative techniques for the detection of self-aggregated stacks

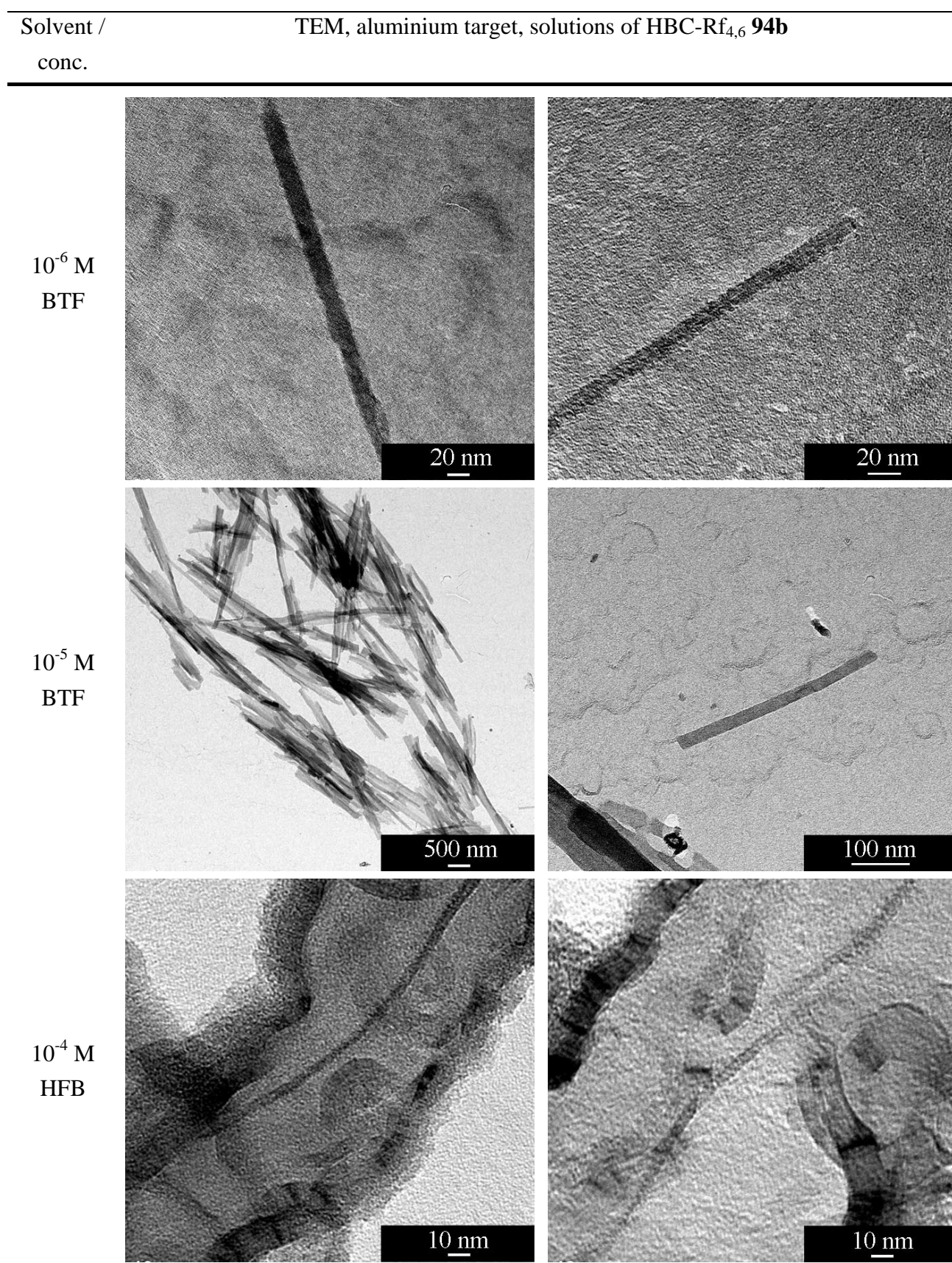
### 17.1 TEM investigations

The observation of the self-aggregation in solution by cryo-SEM has the main disadvantage that the sampled needs to be sputtered with platinum in order to permit the observation. This prevents the determination of the exact diameter of the obtained structures. Because of that, the most promising BTF and HFB solutions of HBC-Rf<sub>4,6</sub> (**94b**) were investigated by TEM, with does not need any treatment previous to the measurement.

Figure 17.1 summarizes the performed measurements. Diluted BTF ( $10^{-6}$  M) solutions revealed straight rectangular structures of several hundred nanometres length and a diameter of about 20 nm. This implies that at around fifty monostranded stack are aggregated laterally. Unfortunately no thinner filaments were found, despite the fact they were observed previously by using the cryo-SEM technique. This discrepancy may arise from the differences in sample preparation. For TEM observation the solution is filtered through an ultra fine grid (300 mesh covered with a “transparent” (for TEM) carbon film) on which the self-assembled fibbers should be retained. Most probably the fine structures are broken by this procedure and are not retained on the grid. Because of that only thicker, aggregated structures may be observed.

The same observation was made by using a more concentrated solution ( $10^{-5}$  M), where several rectangular structures of a typical length of several  $\mu\text{m}$  and a diameter of about 100 nm occurred, which is consistent with the observations performed by cryo-SEM (see section 15.1.2). Again, no thinner architectures were found supporting the statement that thin HBC fibres may not be observable by TEM by applying this sample preparation.

By using a  $10^{-4}$  M HFB solution, in which during the cryo-SEM measurements a large amount of monostranded stacks were found, no isolated structures were revealed. The only observed architectures where large objects containing fine filaments in the inner part. The dimensions (3 nm x 100 nm) of these additional structures would correspond to the observations of the cryo-SEM measurements. Unfortunately no freestanding structures were observed hence the observed linear structures are probably contaminated with impurities stabilizing the formed monostranded stacks.



**Figure 17.1** – TEM micrographs obtained from BTF of HBF solutions of HBC-Rf<sub>4,6</sub> **94b**

## 17.2 THz investigations

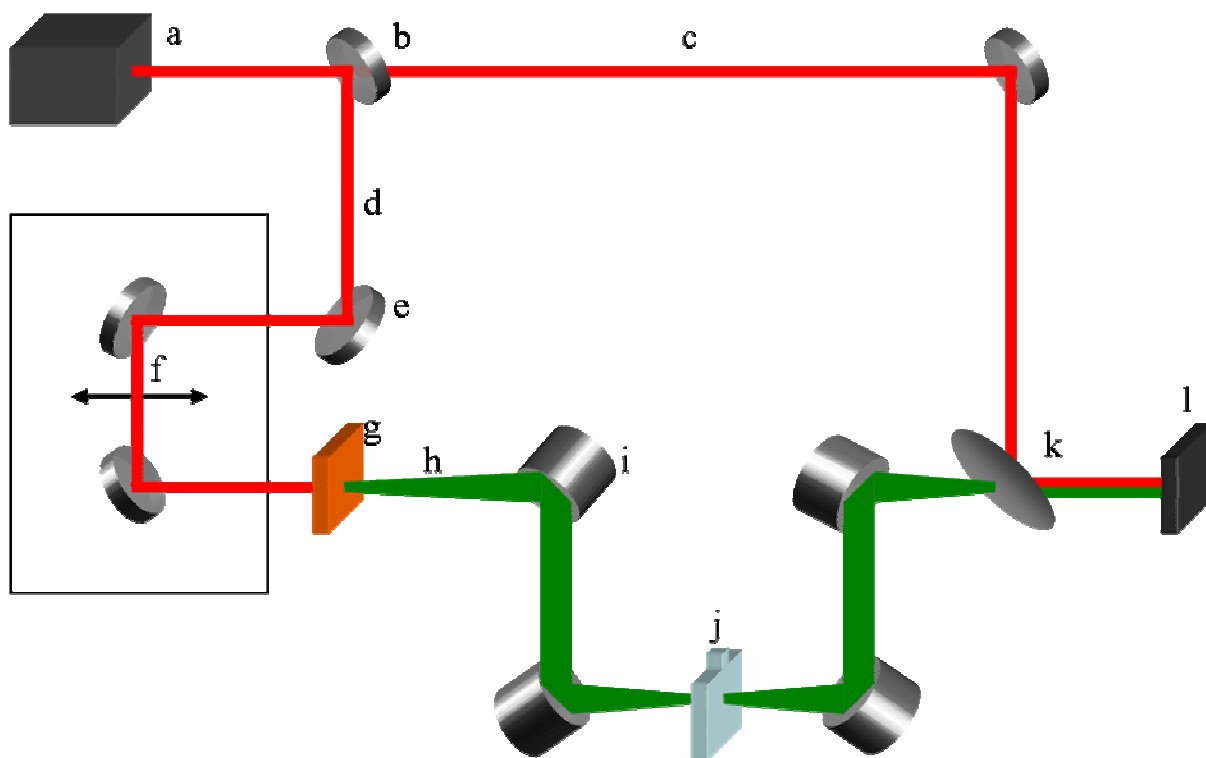
### 17.2.1 General considerations

Terahertz (THz) radiation, laying between infrared and microwave radiation, was over a long time not accessible due to technical problems in generation and detection. Recent technological innovations made this radiation range available for studying a variety of phenomena, including systems able to transport charges.<sup>[258]</sup> To our knowledge THz has up to now never been used to investigate PAH columns.

### 17.2.2 Generation of THz pulses and set up of the measurement

Broadband THz pulses may be generated by several techniques, using femtosecond laser pulses and nonlinear optical crystals. Organic nonlinear optical materials offer several advantages for THz application, namely their high nonlinear optical susceptibilities as one example. Out of these derivatives, DAST (4-*N,N*-dimethylamino-4'-*N'*-methyl stilbazolium tosylate) crystals are among the most promising ones. A frequently used technique for the detection of THz pulses is electro-optic sampling, a process that is based on the interaction of an optical pulse with the THz wave in a nonlinear material.<sup>[259]</sup>

Figure 17.2 shows an experimental set-up for the generation and detection of THz pulses.<sup>[260]</sup> The femtosecond laser beam (a) is splitted at a beam splitter (b) into probe (c) and pump (d) beams. The pump beam is incidented on the DAST crystal used as THz emitter (g) to generate THz pulses (h) after being sent through a delay stage (f). Then the THz pulse is collimated and focused on the target using parabolic mirrors (i). After transmission through the sample (j), the THz pulse is collimated and re-focused on the THz detector (k and l). The optical probe beam is used to gate the detector and measure the instantaneous THz electric field. A delay stage (f) is used to offset the pump and probe beams and allow the THz temporal profile to be iteratively sampled.



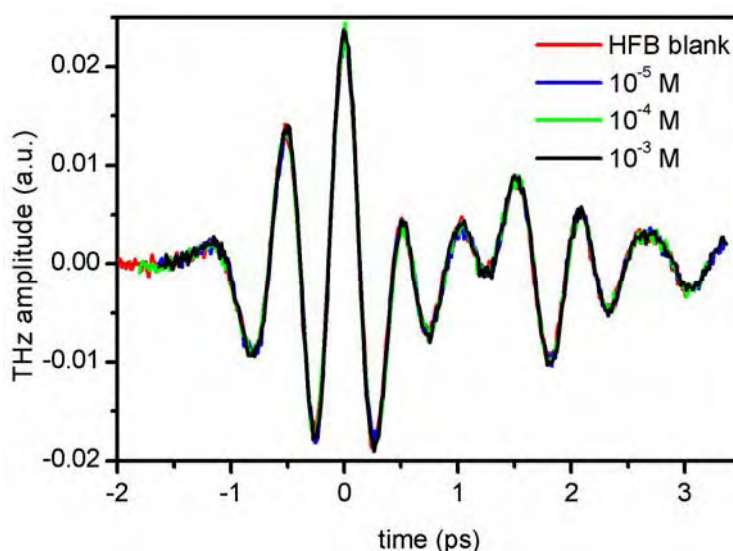
**Figure 17.2** – Illustration of a THz set up: a femtosecond laser; b beam splitter; c detection pulse (probe beam); d excitation pulse (pump beam); e mirror; f delay line; g THz emitter (DAST crystal); h THz beam; i parabolic mirror; j sample; k pellicle (transmits THz pulse and reflects optical pulse partially); l detection crystal (DAST)<sup>[260]</sup>

THz radiation is generated in a second-order non-linear process and can thus only take place in media that lack inversion symmetry such as DAST crystals for example. Optical rectification in such a non-absorbing medium is a process in which a laser pulse creates a time-dependent polarization that follows the envelope of the pulse. It is called rectification because the rapid oscillations of the electric field of the laser pulse are "rectified" and only the envelope of the oscillations remains. This polarisation then emits an electric field, namely the THz pulse.

As THz radiation is absorbed by different metals and other materials, able to transport charges one expects that monostranded HBC stacks may absorb THz radiation as well, whereas monomers and laterally aggregated structures are transparent for this type of radiation. By investigating HBC solutions of different concentrations the ideal domain for linear self-aggregated HBC filaments is intended to be found.

### 17.2.3 THz experiment on HBC derivatives

To our knowledge there are no literature reports concerning the absorption of THz radiation by conducting self-assembled supramolecular structures. The investigation<sup>j</sup> was again performed with BTF and HFB solutions of HBC-Rf<sub>4,6</sub> (**94b**) at various concentrations. Figure 17.3 summarizes the results from the HFB solutions. Unfortunately no difference in the absorption signal of the THz radiation was observed between pure HFB and solutions containing HBC. Even at 10<sup>-3</sup> M, where in cryo-SEM large amounts of aggregated structures were observed, no effects were observed, despite the fact, that this solution was no longer fully transparent. This indicates that either the used THz set up was not sensitive enough to reveal any absorption of the dissolved HBC or other so far unknown parameters prevented an absorption, since the high conductivity of stacked HBCs had been proven by several other techniques.<sup>[32a]</sup>



**Figure 17.3** – THz amplitude of HFB solutions of HBC-Rf<sub>4,6</sub> **94b** of various concentrations<sup>j</sup>

<sup>j</sup> The THz measurements were performed by Dr. Arno Schneider, ETHZ



## 18 Deposition attempts of primer HBCs

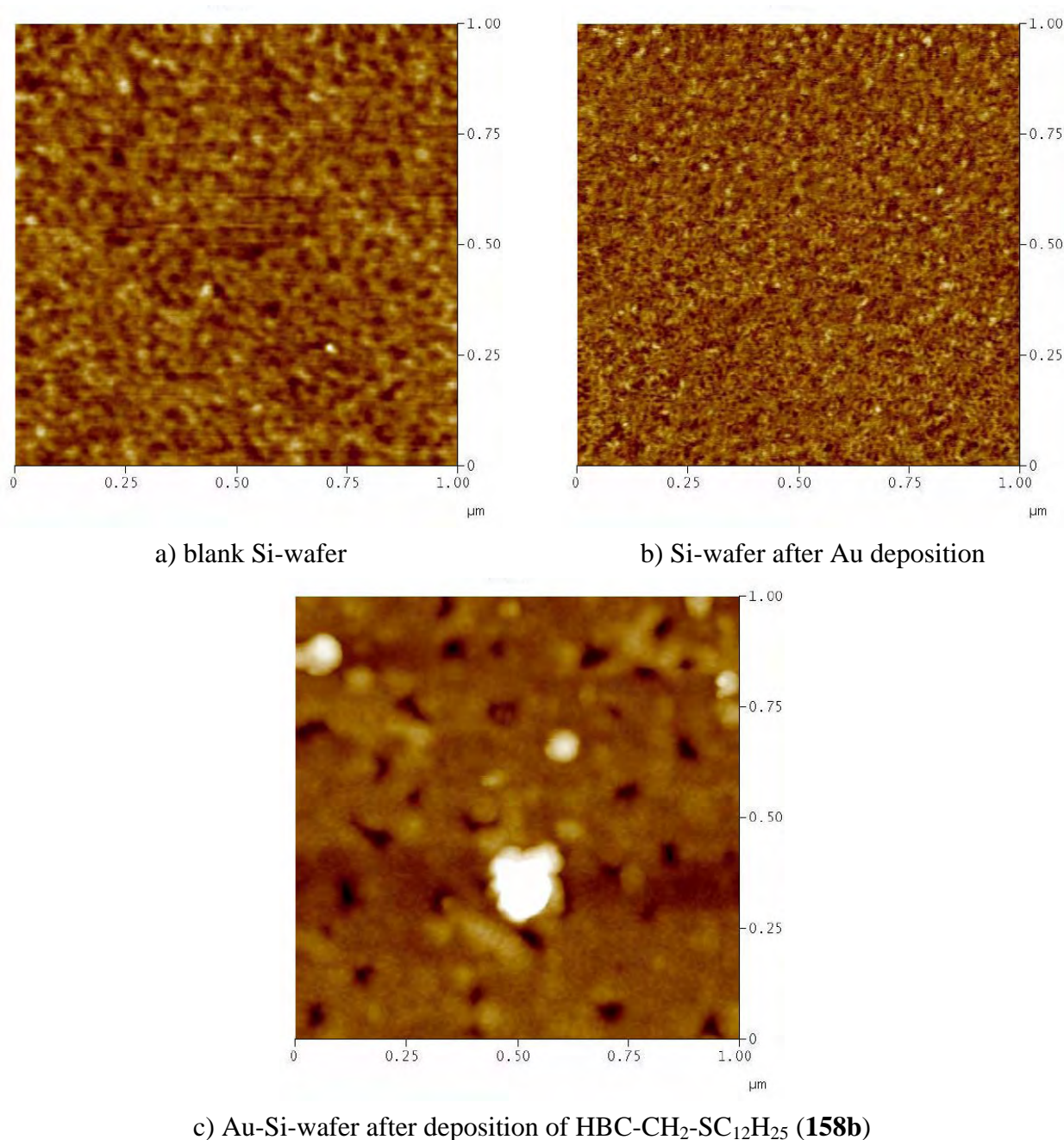
### 18.1 Solution deposition on a gold-silicon wafer

The deposition of a primer HBC has been attempted by two different methods. In a first, preliminary attempt a Si-wafer was taken onto which a thin gold film was deposited by sputtering. Onto this gold-Si wafer the primer HBC molecules were deposited out of solution in the following way: to a  $10^{-5}$  M solution of HBC-CH<sub>2</sub>-SC<sub>12</sub>H<sub>25</sub> (**158b**) in toluene 10 equivalents of TFA were added. The obtained solution was stirred at room temperature for 6 hours, before the gold-Si wafer was immersed for 2 hours in the solution. Afterwards the wafer was cleaned by acetone followed by drying under vacuum.

Three AFM pictures are shown in Figure 18.1: One of the blank Si-wafer (a), one of the gold-Si-wafer (b) and the last one after the deposition of HBC **158b**. By assuming a diameter of the HBC primer of about 2 nm with a thickness of 0.3 nm it is obvious that already the naked Si-wafer has a too rough surface. The “hills and valleys” of the surface have a depth up to 1 nm and a cross-section up to 50 nm. It is evident that no conclusion may be drawn from such an experiment as the starting surface is much too uneven to observe the deposition of the desired HBC derivative.

Nevertheless a picture of the wafer after the gold sputtering was taken with the result that the irregularity of the surface kept the same cross-section in combination with an increased depth of up to 4 nm. After the deposition of the desired molecule it was clear that on top of the not ideal surface the way of deposition is far of being perfect as large humps of 60 nm height were found on the substrate. Due to this negative result, other deposition attempts were performed in collaboration with the EMPA who has already gained much experience in the technique of the deposition of PAH on flat substrates.





**Figure 18.1** – AFM pictures of: a Si-wafer; b Au-Si-wafer; c Au-Si-wafer after deposition of HBC **158b**

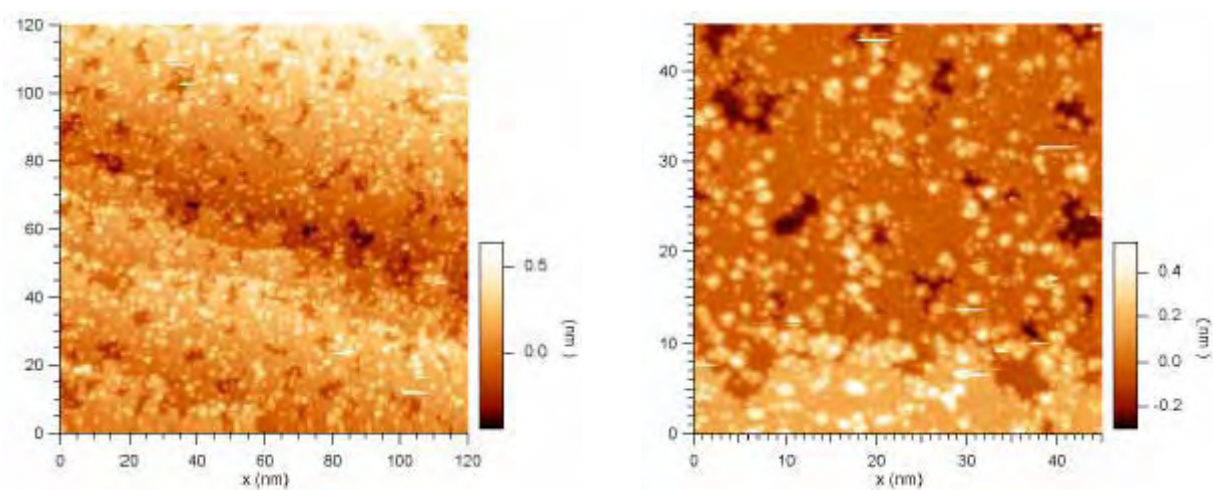
## 18.2 Sublimation on a gold wafer

Previous investigations of the self-assembly of PAHs revealed well ordered structures on different substrates, indicating a rather strong interaction with the surface atom layer, as shown by STM investigations.<sup>[261]</sup> Because of that, derivatives as **158a**, carrying six protected sulfur atoms in the lateral chain are ideal candidate to be irreversibly deposited onto a copper or gold surface. In contrast to the “pedestrian-AFM” attempts shown in the previous section, the STM investigations were performed by sublimation of the target molecule (**158a**) on a highly uniform Au (111) surface.



The micrographs obtained are depicted in Figure 18.2<sup>k</sup>. The deposited material looks rather inhomogeneous and it is impossible to determine a single type of molecules. The reason why HBC **158a** does not behave like the “naked” HBC, forming a highly ordered monolayer<sup>[261]</sup> may be the followings: *i*) the derivative may be too fragile to sublime correctly and fragmentise during the deposition attempt; *ii*) as the derivative is nearly insoluble, remaining impurities could hamper the deposition; *iii*) six lateral groups bearing heteroatoms may be too much for the deposition as up to now no report on the deposition of sulfur containing PAH was made in literature; *iv*) the *t*-Bu protecting group of the sulfur may be cleaved off by the first contact on the gold surface. By this irreversible deposition it would be impossible to grow a homogeneous monolayer.

In conclusion new deposition attempt are planed using HBC derivatives with a reduced number of lateral chains, such as derivatives **161** or **168**.



**Figure 18.2** – STM micrographs obtained from the deposition of HBC-CH<sub>2</sub>-SiBu **158a** onto a Au(111) surface

<sup>k</sup> The AFM investigations were performed by Dr. Pascal Ruffieux, group of Prof. Gröning, EMPA



## **IV Conclusion and outlook**



## 19 Conclusion and outlook

The synthesis of thirteen, systematically different HBC derivatives, carrying long perfluoroalkylated side chains was successfully performed. The variation of the alkyl spacer as well as the perfluorinated tail of the side chain proved to crucially influence the solubility and therefore the self-assembly properties of these new derivatives as well. The elaboration of the synthetic pathways towards the new derivatives has been inspired by the available publication on purely alkylated derivatives but needed more than just adaptation due to the incorporation of the fluorines. The most delicate transformations, which needed major improvements, were the Sonogashira cross-coupling to form the tolane derivatives as well as the final cyclodehydrogenation. The reason was the low solubility of the perfluoroalkylated derivatives, which hampered these reactions as well as their purification.

Additionally four HBC derivatives carrying branched perfluoroalkylated side chains were prepared in order to increase the fluorine content and hence to decrease the tendency for lateral aggregation. The self-assembly properties of these HBC derivatives proved to be even more sensitive to the composition of the side chain as minor changes had showed a tremendous influence.

Finally one HBC derivative was prepared bearing only three branched side chains in order to decrease the sterical hindrance around the aromatic core. Unfortunately all synthetic attempts leading to the pure derivatives did not succeed. The derivative was hence prepared as a mixture of two regio-isomers.

Investigation of the self-aggregation behaviour of these HBC derivatives in solution was performed with fluorescence and cryo-SEM experiments. The fluorescence spectrum of HBC derivatives is well known in the literature and was interpreted differently by several authors. As many of the published interpretations are misleading several investigations and discussions were needed in order to understand the spectra. Second, the fluorescence of HBCs in highly fluorinated solvents is very sensitive to the state of aggregation. Monomers as well as laterally aggregated HBC strands have a specific luminescence where as monostranded HBC stacks behave as “dark material”. Together with cryo-SEM investigations of these solutions a deeper insight into the self-aggregation of HBC derivatives was obtained. Medium alkyl spacer (4 or 5 CH<sub>2</sub>) in combination with six or eight perfluorinated carbon atoms (HBC-Rf<sub>4,6</sub> **94b** and HBC-Rf<sub>4,8</sub> **94c**, HBC-Rf<sub>5,6</sub> (**106a**)) showed the most promising results for the preparation of monostranded HBC stacks. Branched derivatives did in general not reveal an enhanced tendency to form monostranded stacks but formed more often nano-scaled droplets (typical diameter 200 nm), which is an unusual but very interesting behaviour. The cryo-SEM technique was preferred over the normal SEM analysis as the fragile self-aggregated structures are much better preserved on the recoiling surface of the frozen solvent than by solvent evaporation, spin coating or other deposition techniques.

DSC analysis indicated that most of the prepared HBC derivatives carrying linear perfluoroalkylated side chains have a mesomorphic phase at elevated temperatures after several crystal to crystal transformations. Mesomorphism was unfortunately only observed for the HBC moiety with the shortest branched perfluorinated tail (HBC-Rf<sub>3,3,4,4</sub> **132a**) and the longest tail (HBC-Rf<sub>5,5,6,6</sub> **171**) whereas all other branched HBCs remained amorphous until the decomposition started around 250°C. Even the derivative with reduced sterical hindrance, bearing only three lateral branched chains, was amorphous. Nevertheless, HBC-Rf<sub>3,3,6,6</sub> (**132b**) showed a very interesting behaviour as it was the only HBC derivative with perfluorinated side chains, which was a highly viscous liquid.

X-Ray analysis showed that all mesomorphic HBCs existed in a hexagonal columnar arrangement. The XRD pattern allowed further the determination of the aryl-aryl distance (3.6 Å), an ideal distance for  $\pi$ - $\pi$  interaction. The halo of the lateral perfluorinated chains corresponds to a diameter of around 5.7 Å. These data allowed for molecular modelling, which indicated that the formation of monostranded stacks is very likely to occur by twisting the molecules by 30°C with respect to each other. Moreover only HBC-Rf<sub>4,8</sub> (**94c**) was found to have the HBC disks tilted in the monostranded stacks as all other derivatives were found to stack perpendicular one to each other.

Several primer derivatives, intended to be used as “docking stations” for perfluorinated HBCs on a gold surface, carrying sulfur in the lateral chain were synthesized too. First HBC-SCF<sub>3</sub> (**152**) was prepared, where the sulfur atom is directly connected to the HBC core. This derivative was unfortunately found to insert chlorine during the final oxidation under the chosen reaction conditions. Furthermore it is very much possible that the sulfur is cleaved off during this reaction step as many unidentified products were found after the reaction. Because of that all other derivatives were fitted with an additional CH<sub>2</sub> between the aromatic core and the sulfur substituent. One derivative bearing a dodecyl protecting group together with three other *tert*-butyl protected HBCs were synthesized. Preliminary attempts to deposit these HBCs on a gold surface did not yet yield satisfactory results.

In order to construct a device based on self-assembled perfluorinated HBC derivatives several additional tasks have to be solved: *i*) the conditions affording monostranded HBC structures had to be refined in order to prevent the lateral aggregation completely; *ii*) the deposition of such monostranded stacks onto a surface with the aid of HBC primers has to be continued as only preliminary experiments were done; *iii*) more collaboration is needed, before all for different experiments such as the determination of the charge carrier mobility and furthermore for testing the new derivatives in order to produce any type of application.

The result of this PhD thesis has been published in three papers out of which one manuscript had been accepted as cover article. Furthermore two additional publications on the latest results are in preparation.

O. F. Aebischer, P. Tondo, B. Alameddine, T. A. Jenny, *Synthesis*, **2006**, 17, 2891-2896.

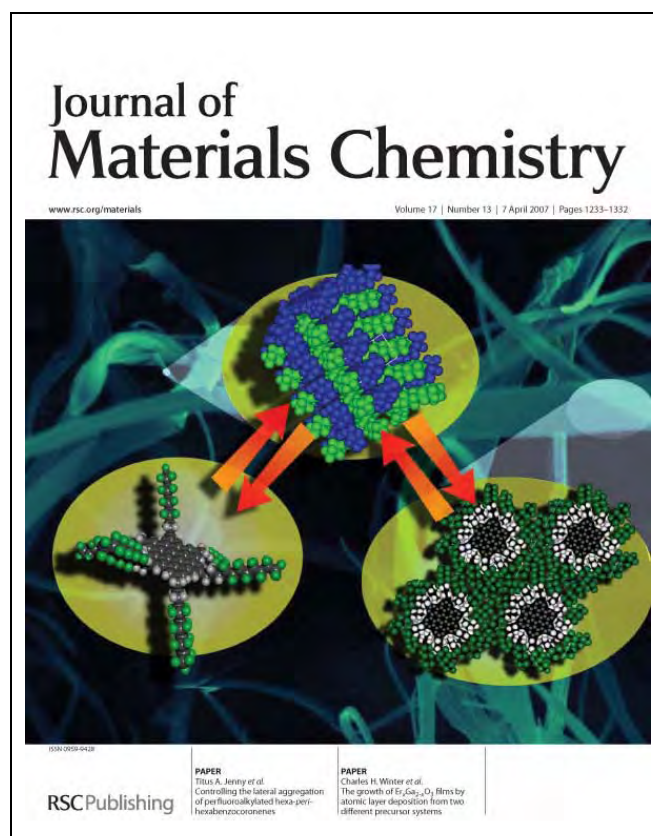
“Synthesis of Novel Fluorinated Hexa-peri-hexabenzocoronenes”

O. F. Aebischer, A. Aebischer, P. Tondo, B. Alameddine, M. Dadras, H.-U. Güdel, T. A. Jenny, *Chem. Comm.*, **2007**, 2, 4221-4223.

“Self-aggregated perfluoroalkylated hexa-peri-hexabenzocoronenes fibres observed by cryo-SEM and fluorescence spectroscopy”

O. F. Aebischer, A. Aebischer, B. Donnio, B. Alameddine, M. Dadras, H.-U. Güdel, D. Guillon, T. A. Jenny, *J. Mater. Chem.*, **2007**, 17, 1262-1267.

“Controlling the lateral aggregation of perfluoroalkylated hexa-peri-hexabenzocoronenes”







## **V Experimental Part**



## 20 General considerations

All used chemicals were purchased from Fluka, Acros, Aldrich, Merck, Strem, ABCR, Riedel-de Haën and Fluorochem and were used without further purification if not stated otherwise. Cross-coupling reaction and other sensitive reactions were performed under inert atmosphere using dry nitrogen (45) or dry argon (48) purchased from Carbagas. Solvents (THF, ether, pentane, dichloromethane and toluene) were dried and deoxygenated by passing them over activated alox using a similar system than the one proposed by Grubbs.<sup>[262]</sup> Benzene was distilled over potassium, further was the first fraction discarded. DMSO and dioxane were dried by adding molecular sieves. All solvents were saturated with argon (5-30 minutes) prior to use.

**Thin layer chromatography (TLC)** was performed using aluminium sheets coated with silica gel 60 F<sub>254</sub> and visualized by a KMnO<sub>4</sub> solution.

**Column chromatography** purification were performed either with Merck silica gel 60 (0.04-0.063 mm, 230-400 mesh) or with basic aluminium oxide, Brockmann activity I, Fluka.

**NMR** spectra were recorded on a Bruker Advance DRX 500 (<sup>1</sup>H: 500 MHz; <sup>13</sup>C: 125.77 MHz) and a Bruker Advance DPX 360 (<sup>1</sup>H: 360 MHz; <sup>13</sup>C: 90.55 MHz) spectrometer using CDCl<sub>3</sub>, DMSO-*d*<sub>6</sub> and HFB as solvents. Chemical shifts (δ) are reported in ppm, coupling constants (*J*) are given in Hz whereas the chemical shifts are referred to tetramethylsilane (TMS). Chemical shift assignments are based on APT, DEPT 90, DEPT 135, COSY, HETCOR, COLOC and NOESY experiments.

**Solid state NMR** was performed on a Bruker Advance DPX 400 (<sup>1</sup>H 400 MHz; <sup>13</sup>C 100.62 MHz), together with a SB-MAS probe head. Magic angle adjustments were performed using oxalic acid-*d*<sub>6</sub>, following a known procedure.<sup>[242]</sup> All needed parameters were optimized prior to each measurement using the *paropt* function.

**Mass spectra** were recorded on the following spectrometers: EI ionization was recorded on a HP 5988A Quadrupol spectrometer; FAB ionization was measured on a Vacuum Generators Micro-mass VG70/70 spectrometer; ESI techniques were performed on a Bruker HCT Esquire ion trap spectrometer in the negative and positive mode. Samples were direct injected at a flow rate of 250 µl/h; MALDI-ICR spectra were performed on a FT/ICR mass spectrometer Bruker 4.7 T BioApex II; MALDI-TOF spectra were either collected on a Bruker Reflex or a Bruker Ultraflex II spectrometer. All MALDI techniques used DCTB or TCNQ as matrices in combination with a 337 nm nitrogen laser; Volatile compounds were measured on a GC/MS ThermoQuest TraceGC 2000/Voyager spectrometer.

**Absorption** spectra were recorded on a Cary 6000i (Varian) spectrophotometer in  $\alpha,\alpha,\alpha$ -trifluorobenzene.

**Luminescence and excitation** spectra were measured on a Spex-Fluorolog-3-system in 1,2,4-trichlorobenzene,  $\alpha,\alpha,\alpha$ -trifluorobenzene or hexafluorobenzene.

**Time-resolved fluorescence** measurements were carried out with the time-correlated single photon counting (TCSPC) technique. Excitation was performed at a repetition rate of 40 MHz which  $>90$  ps pulses generated by a laser diode ( $\lambda_{\text{exc}} = 395$  nm). Fluorescence was collected at  $90^\circ$  at magic angle with respect to the polarization of the pump pulses.

**Cryo-SEM** micrographs were taken on a Gatan ALTO 2500 installed on a Philips XL30 ESEM FEG microscope using 1,2,4-trichlorobenzene,  $\alpha,\alpha,\alpha$ -trifluorobenzene or hexafluorobenzene solutions. The samples were rendered conducting by sputtering 20 nm of platinum.

**TEM** micrographs were collected on a TEM Philips CM200, working under 200 kV.

**AFM** measurements were taken either on a AFM DI 3100 for solution deposition. Sublimation depositions were performed in an ultrahigh-vacuum chamber with a low-temperature scanning tunnelling microscope (STM) from Omicron Nanotechnology GmbH. Monolayer systems were prepared by vacuum sublimation from heated quartz crucibles (Kentax, TCE-BSC) with the sample kept at room temperature. A quartz microbalance was used for thickness calibration. Subsequently, the sample was cooled to 77 K directly in the STM. The Au(111) surface was prepared by several cycles of  $\text{Ar}^+$  ion sputtering and subsequent annealing to 800 K.

**XRD** patterns were obtained with two different experimental set-ups. In all cases, a linear monochromatic  $\text{CuK}\alpha_1$  beam ( $\lambda = 1.5404$  Å) was obtained using a sealed-tube generator (90 W) equipped with a bent quartz monochromator. In the first set, the transmission Guinier geometry was used, whereas a Debye-Scherrer-like geometry was used in the second experimental set-up. In all cases, the crude powder was filled in Lindemann capillaries of 1 mm diameter and 10  $\mu\text{m}$  thickness. An initial set of diffraction patterns was recorded in an image plate; periodicities up to 80 Å can be measured, and the sample temperature controlled to within  $\pm 0.3$  °C from 20 to 350 °C. The second set of diffraction patterns was recorded with a curved Inel CPS 120 counter gas-filled detector linked to a data acquisition computer; periodicities up to 60 Å can be measured, and the sample temperature controlled to within  $\pm 0.05$  °C from 20 to 200 °C. In each case, exposure times were varied from 1 to 24 hours.

**Molecular modelling calculations** were performed on a SGI Origin 200 4 CPU computer and on a SGI Octane2 workstation using the DISCOVERY 3 molecular mechanics package from Accelry with the pcff force field.

**Electronic transitions** were calculated using the TDDFT method in combination with a B3LYP/6-31G\* basis set.

**DSC** measurements were done with a TA Instruments DSC-Q1000 instrument operated at a scanning rate of 2 to 10 °C min<sup>-1</sup> on heating and on cooling. The apparatus was calibrated with indium (156.6 °C; 28.4 Jg<sup>-1</sup>) and gallium (29.8 °C) as the standards.

**TGA** measurements were carried out on a SDTQ 600 apparatus using always a scanning rate of 10 °C min<sup>-1</sup>.

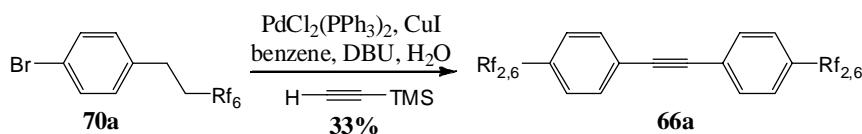
**THz measurement** were done in the following way: As laser source an amplified Clark-MXR, CPA 2001 Ti:Sapphire laser (pulse duration 160 ns at FWHM, repetition rate 1 kHz) was used. The tunability of the wavelength was achieved by means of an optical parametric generator-amplifier (Quatronix, TO-PAS). The detection DAST crystal was oriented such that both THz and probe pulses were polarized along the crystals *a* axis.



## 21 Synthesis of HBCs bearing linear alkyl / perfluoroalkyl side chains

### 21.1 Synthesis of HBC-(Rf<sub>2,6</sub>)<sub>6</sub>

#### 21.1.1 1-(3,3,4,4,5,5,6,6,7,7,8,8,8-tridecafluorooctyl)-4-{[4-(3,3,4,4,5,5,6,6,7,7,8,8,8-tridecafluorooctyl)phenyl]ethynyl}benzene



#### Method A

CuI (18.9 mg, 99.4  $\mu\text{mol}$ ) and  $\text{PdCl}_2(\text{PPh}_3)_2$  (41.8 mg, 59.6  $\mu\text{mol}$ ) were loaded in an oven dried Schlenk reaction vessel under inert atmosphere and suspended in benzene (10 mL). Compound **70a** (0.5 g, 0.94 mmol) was degassed separately and dissolved in benzene (10 mL) before being added into the reaction vessel. Degassed DBU (0.95 mL, 5.96 mmol) was added via syringe into the Schlenk, before the reaction medium was purged with argon.  $\text{H}_2\text{O}$  (7  $\mu\text{L}$ , 0.40 mmol) and cooled (4  $^\circ\text{C}$ ) TMSA (72  $\mu\text{L}$ , 0.50 mmol) were added simultaneously with two syringes. The Schlenk was then covered with an aluminium foil and heated to 75  $^\circ\text{C}$ . After 29 hours of reaction the black mixture was allowed to cool to room temperature before ether (50 mL) was added. The crude mixture was washed with  $\text{H}_2\text{O}$  (2 x 100 mL), 10% HCl (50 mL), brine (50 mL) and  $\text{H}_2\text{O}$  (50 mL). The combined organic fractions were dried over  $\text{Na}_2\text{SO}_4$  and all volatiles were removed yielding a brown solid which was purified by column chromatography over silica gel using pentane as eluent. All product fractions were combined and all volatiles were removed under reduced pressure yielding the desired tolane **66a** as white solid (143 mg, 33%).

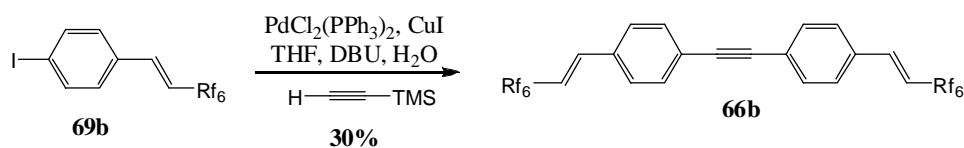
**TLC:**  $R_f$  = 0.46 (silica gel, pentane,  $\text{KMnO}_4$ ).

**$^1\text{H-NMR}$ :** (360 MHz,  $\text{CDCl}_3$ ):  $\delta$  7.49 (*d*, 4H,  $^3J_{\text{HH}}$  = 8.1 Hz, Ph), 7.20 (*d*, 4H,  $^3J_{\text{HH}}$  = 8.1 Hz, Ph), 2.93 (*m*, 4H,  $^3J_{\text{HH}}$  = 8.4 Hz,  $\text{CH}_2\text{CH}_2\text{Rf}_6$ ), 2.23-2.44 (*m*, 4H,  $\text{CH}_2\text{CH}_2\text{Rf}_6$ ).

**$^{13}\text{C-NMR}$ :** (90.55 MHz,  $\text{CDCl}_3$ ):  $\delta$  139.38 (Ph), 131.98 (Ph), 128.35 (Ph), 121.73 (Ph), 108.38-119.99 ( $\text{Rf}_6$ ), 89.07 (acetylene), 32.68 (*t*,  $^3J_{\text{CF}}$  = 22.1 Hz,  $\text{CH}_2\text{CH}_2\text{Rf}_6$ ), 26.40 ( $\text{CH}_2\text{CH}_2\text{Rf}_6$ ).

**EI-MS:**  $m/z$  (% int.): 870.1 ( $\text{M}^{+\bullet}$ , 100%), 481.3 (20%).

21.1.2 1-(3,3,4,4,5,5,6,6,7,7,8,8,8-Tridecafluorooct-1-enyl)-4-{[4-(3,3,4,4,5,5,6,6,7,7,8,8,8-tridecafluorooct-1-enyl)phenyl]ethynyl}benzene



The synthesis was carried out following **method A** using compound **69b** (4.99 g, 10 mmol) as precursor, together with  $\text{PdCl}_2(\text{PPh}_3)_2$  (421 mg, 0.4 mmol), CuI (190.4 mg, 1.0 mmol), DBU (9.0 mL, 60.0 mmol),  $\text{H}_2\text{O}$  (72  $\mu\text{L}$ , 4.0 mmol) TMSA (0.73 mL, 5.0 mmol) in THF (50 mL). After 24 hours of reaction at room temperature, the mixture was quenched by the addition of methanol (30 mL). All volatiles were removed under reduced pressure and the remaining dark solid was dissolved in pentane and filtered over a plug of silica gel under reduced pressure. After removing the solvent, tolane **66b** was afforded as yellow solid which was recrystallized from ether – ethanol, to yield colourless crystals (0.64 g, 30 %).

**TLC:**  $R_f$  = 0.62 (silica gel, pentane,  $\text{KMnO}_4$ ).

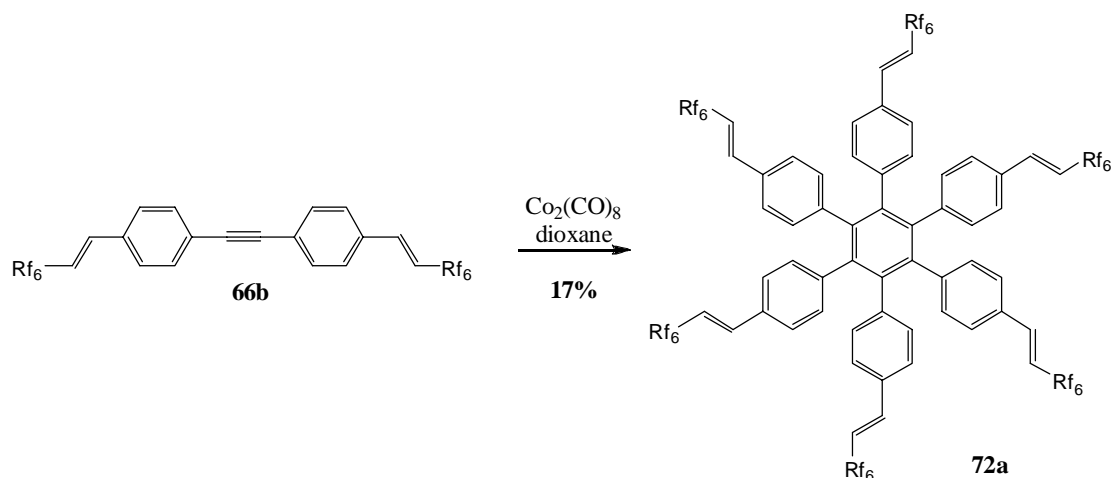
**$^1\text{H-NMR}$ :** (360 MHz,  $\text{CDCl}_3$ ):  $\delta$  7.57 (*d*, 4H,  $^3J_{\text{HH}}$  = 8.2 Hz, Ph), 7.49 (*d*, 4H,  $^3J_{\text{HH}}$  = 8.2 Hz, Ph), 7.18 (*d*, 2H,  $^3J_{\text{HH}}$  = 16.4 Hz,  $\text{CH}=\text{CHRf}_6$ ), 6.24 (*dt*, 2H,  $^3J_{\text{HH}}$  = 16.4 Hz,  $^3J_{\text{HF}}$  = 12.0 Hz,  $\text{CH}=\text{CHRf}_6$ ).

**$^{13}\text{C-NMR}$ :** (125.77 MHz,  $\text{CDCl}_3$ ):  $\delta$  138.88 (*t*,  $^3J_{\text{CF}}$  = 9.6 Hz,  $\text{CH}=\text{CHRf}_6$ ), 133.53 (Ph), 132.17 (Ph), 127.67 (Ph), 124.77 (Ph), 108.43-119.86 ( $\text{Rf}_6$ ), 115.24 (*t*,  $^2J_{\text{CF}}$  = 23.0 Hz,  $\text{CH}=\text{CHRf}_6$ ), 90.85 (acetylene).

**MALDI-ICR-MS (DCTB):**  $m/z$  (% int.): 1732.11 ( $[\text{2M}]^{*+}$ , 100%), 1117.20 ( $[\text{M}+\text{DCTB}]^{*+}$ , 52%), 866.05 ( $\text{M}^{*+}$ , 15%).



## 21.1.3 Hexakis[4-(3,3,4,4,5,5,6,6,7,7,8,8,8-tridecafluorooct-1-enyl)phenyl]benzene

**Method B**

A 50 ml two necked round bottomed flask was charged with tolane **66b** (0.5 g, 0.58 mmol) under inert atmosphere. Addition of deoxygenated dioxane (20 mL) followed by  $\text{Co}_2(\text{CO})_8$  (15.8 mg, 46.0  $\mu\text{mol}$ ) under a positive pressure of argon, afforded a dark brown solution which was refluxed for 48 hours. Removing the solvent under reduced pressure yielded the crude compound **72a** as grey solid, which was dissolved in ether (50 mL). Extraction with HCl 15 % (2 x 25 mL) was done. The organic phase was filtered over a plug of silica gel under reduced pressure using ether as eluent and afforded a yellow solid after removing the solvent. The obtained solid was suspended in pentane and collected by suction filtration over Millipore<sup>®</sup> and afforded the desired trimer **72a** as off-white solid in low yield (58 mg, 17 %).

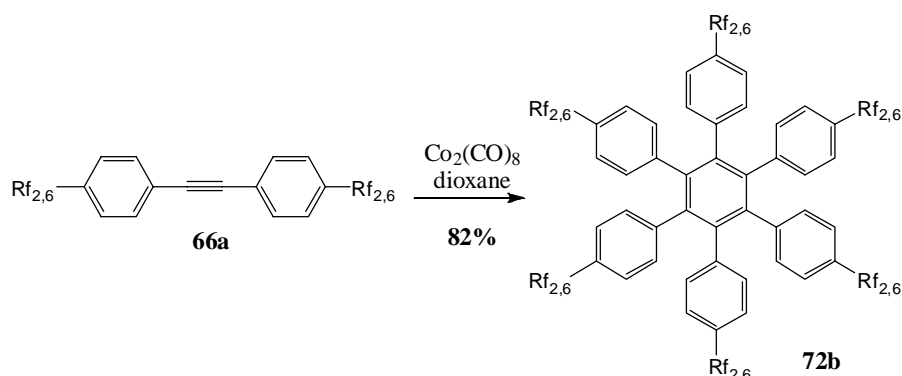
**TLC:**  $R_f$  = 0.05 (silica gel, pentane – ether (9:1),  $\text{KMnO}_4$ ).

**$^1\text{H-NMR}$ :** (360 MHz,  $\text{CDCl}_3$ ):  $\delta$  7.04 (*d*, 12H,  $^3J_{\text{HH}}$  = 8.2 Hz, Ph), 6.85 (*d*, 12H,  $^3J_{\text{HH}}$  = 8.2 Hz, Ph), 6.94 (*d*, 6H,  $^3J_{\text{HH}}$  = 16.4 Hz,  $\text{CH=CHRf}_6$ ), 6.01 (*dt*, 6H,  $^3J_{\text{HH}}$  = 16.4 Hz,  $^3J_{\text{HF}}$  = 12.0 Hz  $\text{CH=CHRf}_6$ ).

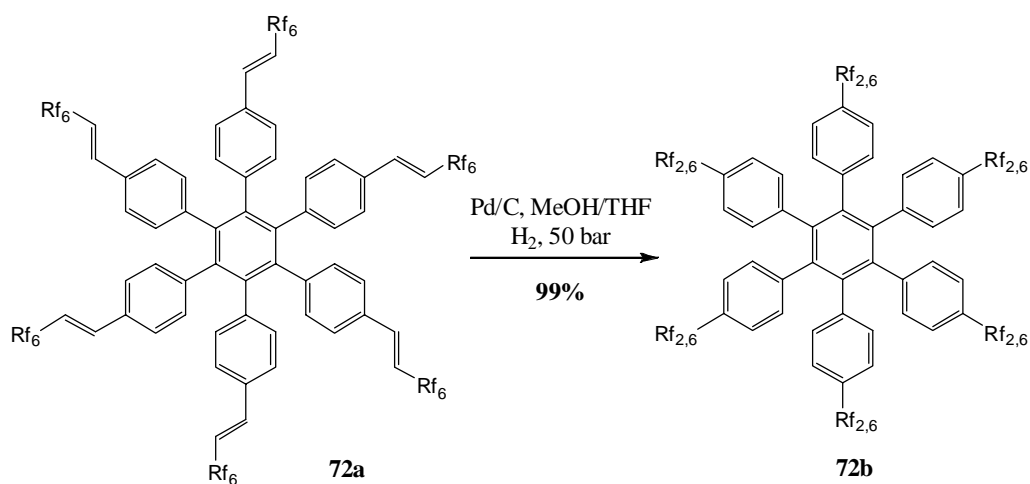
**$^{13}\text{C-NMR}$ :** (90.55 MHz,  $\text{CDCl}_3$ ):  $\delta$  141.66 (Ph), 139.86 (Ph), 139.16 (*t*,  $^3J_{\text{CF}}$  = 8.7 Hz,  $\text{CH=CHRf}_6$ ), 131.62 (Ph), 131.02 (Ph), 126.56 (Ph), 113.96 (*t*,  $^2J_{\text{CF}}$  = 22.5 Hz,  $\text{CH=CHRf}_6$ ), 108.01-118.55 ( $\text{Rf}_6$ ).

**MALDI-ICR-MS (DCTB):**  $m/z$  (% int.): 2598.12 ( $\text{M}^{+}$ , 35%), 2201.10 (25%), 642.63 (100%).

## 21.1.4 Hexakis[4-(3,3,4,4,5,5,6,6,7,7,8,8,8-tridecafluorooctyl)phenyl]benzene

a) Trimerization of tolane **66a**

The synthesis was done using **method B** starting with the tolane **66a** (0.1 g, 115  $\mu\text{mol}$ ) as precursor,  $\text{Co}_2(\text{CO})_8$  (2.4 mg, 6.9  $\mu\text{mol}$ ) as catalyst and dioxane (20 mL) as solvent. After 48 hours of reaction, all volatiles were removed yielding a brown solid. All traces of the catalyst were removed by filtration over a plug of silica gel using ether as solvent. The obtained yellow solid was recrystallized from ether – ethanol yielding the title HPB **72b** as a white solid in good yield (82 mg, 82 %).

b) Hydrogenation of trimer **72a**

HPB **72a** (30 mg, 11.5  $\mu\text{mol}$ ) was charged together with Pd/C (20 mg) in an oven dried Schlenk before being suspended in THF (0.7 mL) and methanol (0.7 mL). The reaction mixture was stirred under 3 bar of hydrogen for 6 hours before the crude mixture was filtered over a plug of silica gel under reduced pressure. All solvents were evaporated yielding the desired hydrogenated HPB **72b** in quantitative yield (29.9 mg, 99 %).

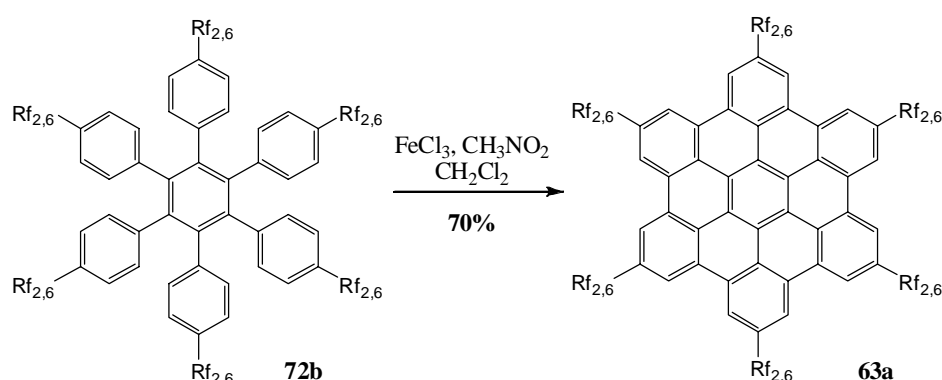
**TLC:**  $R_f = 0.85$  (silica gel, pentane – ethyl acetate (9:1),  $\text{KMnO}_4$ ).

**$^1\text{H-NMR}$ :** (360 MHz,  $\text{CDCl}_3$ ):  $\delta$  6.73 (*d*, 12H,  $^3J_{\text{HH}} = 8.1$  Hz, Ph), 6.70 (*d*, 12H,  $^3J_{\text{HH}} = 8.1$  Hz, Ph), 2.68 (*t*, 12H,  $^3J_{\text{HH}} = 7.9$  Hz,  $\text{CH}_2\text{CH}_2\text{Rf}_6$ ), 2.07-2.21 (*m*, 12H,  $\text{CH}_2\text{CH}_2\text{Rf}_6$ ).

**$^{13}\text{C-NMR}$ :** (90.55 MHz,  $\text{CDCl}_3$ ):  $\delta$  140.06 (Ph), 138.90 (Ph), 135.98 (Ph), 131.65 (Ph), 126.52 (Ph), 109.25-120.15 ( $\text{Rf}_6$ ), 32.54 (*t*,  $^2J_{\text{CF}} = 22.1$  Hz,  $\text{CH}_2\text{CH}_2\text{Rf}_6$ ), 25.88 (*t*,  $^3J_{\text{CF}} = 4.0$  Hz,  $\text{CH}_2\text{CH}_2\text{Rf}_6$ ).

**MALDI-ICR-MS (DCTB):**  $m/z$  (% int.): 2610.22 ( $\text{M}^{*+}$ , 100%), 2264.29 (15%).

#### 21.1.5 2,5,8,11,14,17-Hexakis(3,3,4,4,5,5,6,6,7,7,8,8,8-tridecafluorooctyl)hexabenzocoronene



#### Method C

HPB **72b** (0.2 g, 76.6  $\mu\text{mol}$ ) was dissolved in dry  $\text{CH}_2\text{Cl}_2$  (10 mL) under inert atmosphere in a three necked flask. At the same time a solution of  $\text{FeCl}_3$  (0.75 g, 4.59 mmol, 5 eq. / H to be removed) was prepared in  $\text{CH}_3\text{NO}_2$  (4 mL). The  $\text{FeCl}_3$  solution was added to the reaction mixture at 45 °C drop by drop with a syringe. Argon was bubbled through the reaction mixture by a Teflon capillary during all the reaction time. After 6 h of reaction the mixture was quenched by the addition of methanol (20 mL). The black precipitate was collected by suction filtration over Millipore<sup>®</sup> and was suspended in different common organic solvents (dichloromethane, methanol, ether and pentane). The formed suspensions were each time treated in an ultrasonic bath for 30 minutes followed by refluxing for 1 h. After 2 h of cooling in the refrigerator the suspensions were filtrated over Millipore<sup>®</sup>. The obtained powder was reprecipitated first from BTF and finally three times from HFB, yielding the title HBC **63a** as a yellow powder in good yield (139 mg, 70%).

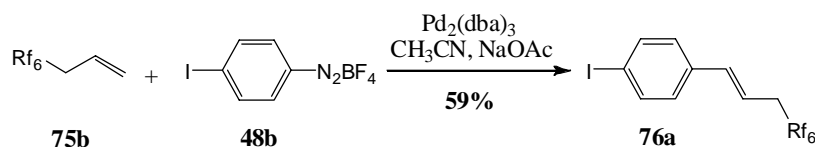
**$^1\text{H-NMR}$ :** (500 MHz, HFB,  $\text{CDCl}_3$ ):  $\delta$  8.82 (br. *s*, 12H, Ph), 3.63 (br. *s*, 12H,  $\text{CH}_2\text{CH}_2\text{Rf}_6$ ), 3.02 (*m*, 12H,  $\text{CH}_2\text{CH}_2\text{Rf}_6$ ).

**MALDI-ICR-MS (DCTB):**  $m/z$  (% int.): 2598.17 ( $\text{M}^{*+}$ , 100%; calcd. for  $\text{C}_{90}\text{H}_{36}\text{F}_{78}$  2598.16), 2265.16 ( $[\text{M-Rf}_{1,6}]^{*+}$ , 15%), 1932.17 ( $[\text{M}-2 \times \text{Rf}_{1,6}]^{*+}$ , 5%).

**UV/VIS:** (BTF,  $10^{-6}$  M,  $\epsilon = 5.4 \cdot 10^4$ ),  $\lambda_{\text{max}} = 341, 362, 391, 411$  nm.

## 21.2 Synthesis of HBC-(Rf<sub>3,6</sub>)<sub>6</sub>

### 21.2.1 1-(4,4,5,5,6,6,7,7,8,8,9,9,9-Tridecafluoronon-1-enyl)-4-iodobenzene



#### Method D

Diazonium salt **48b** (9.7 g, 30.5 mmol), Pd<sub>2</sub>(dba)<sub>3</sub> (508 mg, 0.56 mmol) and NaOAc (7.9 g, 97.0 mmol) were added to a two necked round bottomed flask equipped with a reflux condenser under inert atmosphere. Degassed acetonitrile (100 mL) was added. Compound **75b** (10 g, 27.8 mmol) was degassed in a separate flask and was diluted with CH<sub>3</sub>CN (40 mL) and syringed into the reaction vessel. The inert gas entry was changed against a bubble counter. The reaction mixture was stirred at room temperature for 4 hours until the formation of nitrogen stopped. All volatiles were removed under reduced pressure yielding a dark brown solid which was dissolved in pentane (400 mL) and filtered over a plug of silica gel under reduced pressure using pentane as eluent. After removing all volatiles, compound **76a** was recovered as slightly yellow solid which was further purified by column chromatography using pentane as eluent. Evaporating all volatiles from the desired fractions yielded compound **76a** as white solid in moderate yield (10.14 g, 59%).

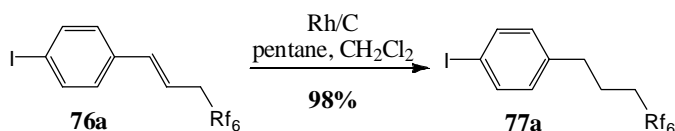
**TLC:** R<sub>f</sub> = 0.66 (silica gel, pentane, KMnO<sub>4</sub>).

**<sup>1</sup>H-NMR:** (360 MHz, CDCl<sub>3</sub>): δ 7.66 (*d*, 2H, <sup>3</sup>J<sub>HH</sub> = 8.2 Hz, Ph), 7.12 (*d*, 2H, <sup>3</sup>J<sub>HH</sub> = 8.2 Hz, Ph), 6.55 (*d*, 1H, <sup>3</sup>J<sub>HH</sub> = 15.4 Hz, CHCHCH<sub>2</sub>Rf<sub>6</sub>), 6.15 (*dt*, 1H, <sup>3</sup>J<sub>HH</sub> = 15.4 Hz, <sup>3</sup>J<sub>HH</sub> = 7.5 Hz, CHCHCH<sub>2</sub>Rf<sub>6</sub>), 3.00 (*dt*, 2H, <sup>3</sup>J<sub>FH</sub> = 17.9 Hz, <sup>3</sup>J<sub>HH</sub> = 7.5 Hz, CHCHCH<sub>2</sub>Rf<sub>6</sub>).

**<sup>13</sup>C-NMR:** (90.55 MHz, CDCl<sub>3</sub>): δ 137.75 (Ph), 136.22 (CHCHCH<sub>2</sub>Rf<sub>6</sub>), 135.66 (Ph), 128.17 (Ph), 117.00 (*t*, <sup>3</sup>J<sub>CF</sub> = 4.6 Hz, CHCHCH<sub>2</sub>Rf<sub>6</sub>), 105.70-120.02 (Rf<sub>6</sub>), 93.57 (Ph), 35.14 (*t*, <sup>2</sup>J<sub>CF</sub> = 22.8 Hz, CHCHCH<sub>2</sub>Rf<sub>6</sub>).

**EI-MS:** *m/z* (% int.): 562.8 (M<sup>+</sup>, 7%), 535.5 ([M-I]<sup>+</sup>, 1%), 116.0 (100%).

### 21.2.2 1-(4,4,5,5,6,6,7,7,8,8,9,9,9-Tridecafluorononyl)-4-iodobenzene



#### Method E

Iodoaryl **76a** (6.4 g, 11.4 mmol) was dissolved in CH<sub>2</sub>Cl<sub>2</sub> (15 mL) and added into a 200 mL autoclave. After the addition of pentane (50 mL), an argon bubbling of the reaction mixture was performed for 10 minutes before Rh/C (5% Rh, 929 mg, 0.456 mmol) was added. The autoclave was

then tightly closed and purged with hydrogen (3 x 50 bar). The reaction mixture was afterwards stirred at room temperature under 60 bar of hydrogen for 28 hours before the suspension was filtered over a plug of silica gel with pentane as eluent. After removal of all volatiles compound **77a** was afforded as white solid in quantitative yield (6.3 g, 98%).

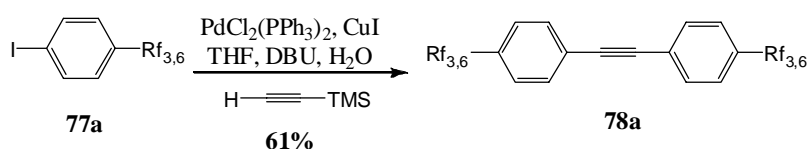
**TLC:**  $R_f = 0.66$  (silica gel, pentane,  $\text{KMnO}_4$ ).

**$^1\text{H-NMR}$ :** (360 MHz,  $\text{CDCl}_3$ ):  $\delta$  7.64 (*d*, 2H,  $^3J_{\text{HH}} = 8.2$  Hz, Ph), 6.96 (*d*, 2H,  $^3J_{\text{HH}} = 8.2$  Hz, Ph), 2.67 (*t*, 2H,  $^3J_{\text{HH}} = 7.5$  Hz,  $\text{CH}_2\text{CH}_2\text{CH}_2\text{Rf}_6$ ), 2.00-2.18 (*m*, 2H,  $\text{CH}_2\text{CH}_2\text{CH}_2\text{Rf}_6$ ), 1.93 (*quint*, 2H,  $^3J_{\text{HH}} = 7.5$  Hz,  $\text{CH}_2\text{CH}_2\text{CH}_2\text{Rf}_6$ ).

**$^{13}\text{C-NMR}$ :** (90.55 MHz,  $\text{CDCl}_3$ ):  $\delta$  140.20 (Ph), 137.65 (Ph), 130.40 (Ph), 107.69-121.51 ( $\text{Rf}_6$ ), 91.41 (Ph), 34.49 ( $\text{CH}_2\text{CH}_2\text{CH}_2\text{Rf}_6$ ), 30.20 (*t*,  $^2J_{\text{CF}} = 22.5$  Hz,  $\text{CH}_2\text{CH}_2\text{CH}_2\text{Rf}_6$ ), 21.66 (*t*,  $^3J_{\text{CF}} = 3.3$  Hz,  $\text{CH}_2\text{CH}_2\text{CH}_2\text{Rf}_6$ ).

**EI-MS:**  $m/z$  (% int.): 564.8 ( $\text{M}^{+\bullet}$ , 42%), 437.5 ( $[\text{M-I}]^{+\bullet}$ , 1%), 217.0 ( $[\text{M-Rf}_{2,6}]^{+\bullet}$ , 100%).

### 21.2.3 1-(4,4,5,5,6,6,7,7,8,8,9,9,9-Tridecafluorononyl)-4-[[4-(4,4,5,5,6,6,7,7,8,8,9,9,9-tridecafluorononyl)phenyl]ethynyl]benzene



The synthesis was performed following **method A**, using compound **77a** (6.2 g, 11,0 mmol) as starting material in the presence of  $\text{PdCl}_2(\text{PPh}_3)_2$  (463 mg, 0.66 mmol),  $\text{CuI}$  (209 mg, 1.1 mmol), DBU (9.9 mL, 65.9 mmol), THF (60 mL),  $\text{H}_2\text{O}$  (79  $\mu\text{L}$ , 4.4 mmol) and TMSA (0.8 mL, 5.5 mmol). The desired tolane **78a** was afforded after 28 hours of reaction at  $65^\circ\text{C}$  as brown powder which was purified by several recrystallizations from ether – pentane and ether – ethanol. Each time the tolane **78a** was collected by suction filtration over Millipore<sup>®</sup> yielding finally a white solid (3.0 g, 61%).

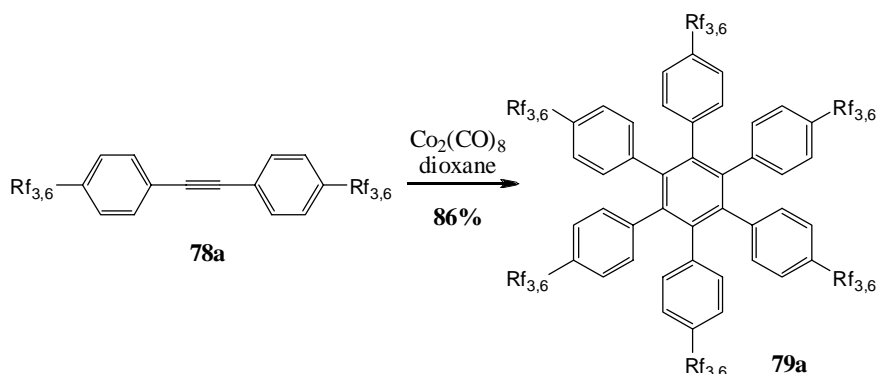
**TLC:**  $R_f = 0.42$  (silica gel, pentane,  $\text{KMnO}_4$ ).

**$^1\text{H-NMR}$ :** (360 MHz,  $\text{CDCl}_3$ ):  $\delta$  7.47 (*d*, 4H,  $^3J_{\text{HH}} = 8.2$  Hz, Ph), 7.17 (*d*, 4H,  $^3J_{\text{HH}} = 8.2$  Hz, Ph), 2.73 (*t*, 4H,  $^3J_{\text{HH}} = 7.3$  Hz,  $\text{CH}_2\text{CH}_2\text{CH}_2\text{Rf}_6$ ), 1.91-2.17 (*m*, 8H,  $\text{CH}_2\text{CH}_2\text{CH}_2\text{Rf}_6$ ).

**$^{13}\text{C-NMR}$ :** (90.55 MHz,  $\text{CDCl}_3$ ):  $\delta$  140.88 (Ph), 131.81 (Ph), 128.39 (Ph), 121.32 (Ph), 105.69-120.49 ( $\text{Rf}_6$ ), 89.01 (acetylene), 34.90 ( $\text{CH}_2\text{CH}_2\text{CH}_2\text{Rf}_6$ ), 30.23 (*t*,  $^2J_{\text{CF}} = 22.5$  Hz,  $\text{CH}_2\text{CH}_2\text{CH}_2\text{Rf}_6$ ), 21.63 (*t*,  $^3J_{\text{CF}} = 3.3$  Hz,  $\text{CH}_2\text{CH}_2\text{CH}_2\text{Rf}_6$ ).

**EI-MS:**  $m/z$  (% int.): 900.0 ( $\text{M}^{+\bullet}$ , 11%), 551.9 ( $[\text{M-Rf}_{2,6}]^{+\bullet}$ , 100%).

## 21.2.4 Hexakis[4-(4,4,5,5,6,6,7,7,8,8,9,9,9-tridecafluorononyl)phenyl]benzene



The synthesis was performed following **method B** starting with tolane **78a** (2.8 g, 3.1 mmol) as precursor together with Co<sub>2</sub>(CO)<sub>8</sub> (64 mg, 0.19 mmol) in dioxane (180 mL). After 60 hours of reaction at 110 °C, the solvent was removed and the crude HPB **79a** was suspended in pentane and agitated in an ultrasonic bath for 2 hours. Collection of the solid by suction filtration over Millipore<sup>®</sup> afforded the desired compound **79a** in good yield (2.4 g, 86%) as white solid.

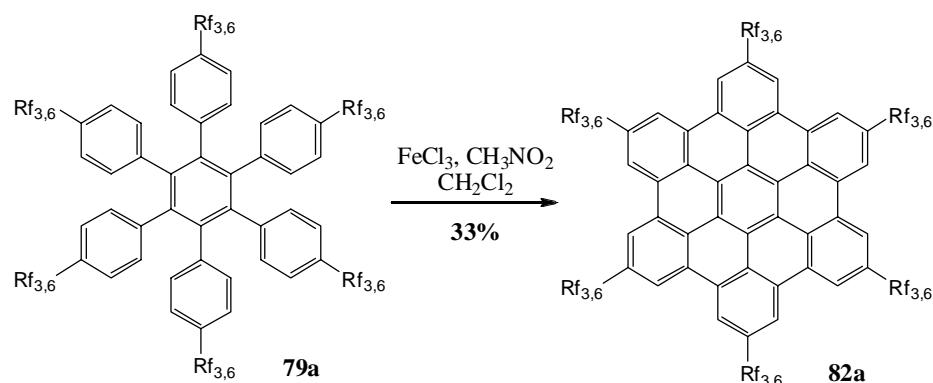
**TLC:** Rf = 0.95 (silica gel, pentane – ether (9:1), KMnO<sub>4</sub>).

**<sup>1</sup>H-NMR:** (360 MHz, CDCl<sub>3</sub>): δ 6.70 (*d*, 12H, <sup>3</sup>J<sub>HH</sub> = 7.7 Hz, Ph), 6.63 (*d*, 12H, <sup>3</sup>J<sub>HH</sub> = 7.7 Hz, Ph), 2.43 (*t*, 12H, <sup>3</sup>J<sub>HH</sub> = 6.8 Hz, CH<sub>2</sub>CH<sub>2</sub>CH<sub>2</sub>Rf<sub>6</sub>), 1.71-1.83 (*m*, 24H, CH<sub>2</sub>CH<sub>2</sub>CH<sub>2</sub>Rf<sub>6</sub>).

**<sup>13</sup>C-NMR:** (90.55 MHz, CDCl<sub>3</sub>): δ 140.10 (Ph), 138.75 (Ph), 137.11 (Ph), 131.65 (Ph), 126.53 (Ph), 104.19-120.29 (Rf<sub>6</sub>), 34.13 (CH<sub>2</sub>CH<sub>2</sub>CH<sub>2</sub>Rf<sub>6</sub>), 29.71 (*t*, <sup>2</sup>J<sub>CF</sub> = 22.5 Hz, CH<sub>2</sub>CH<sub>2</sub>CH<sub>2</sub>Rf<sub>6</sub>), 21.45 (CH<sub>2</sub>CH<sub>2</sub>CH<sub>2</sub>Rf<sub>6</sub>).

**MALDI-ICR-MS (DCTB):** m/z (% int.): 2695.34 (M<sup>+</sup>, 100%).

21.2.5 2,5,8,11,14,17-Hexakis(4,4,5,5,6,6,7,7,8,8,9,9,9-tridecafluorononyl)hexabenzocoronene  
[bc,ef,hi,kl,no,qr]coronene



The synthesis was carried out following **method C** using HPB **79a** (0.2 g, 74  $\mu\text{mol}$ ) as precursor together with  $\text{FeCl}_3$  (433 mg, 2.67 mmol, 3 eq / H to be removed),  $\text{CH}_2\text{Cl}_2$  (15 mL) and  $\text{CH}_3\text{NO}_2$  (5 mL). After 9 hours of reaction at 45  $^\circ\text{C}$  the mixture was quenched by the addition of methanol (50 mL). The black precipitate was collected by suction filtration over Millipore<sup>®</sup> and was suspended in different common organic solvents (dichloromethane, methanol, ether and pentane). The formed suspensions were each time treated in an ultrasonic bath for 30 minutes followed by refluxing for 1 h. After 2 h of cooling in the refrigerator the suspensions were filtrated over Millipore<sup>®</sup> yielding HBC **82a** as bright yellow powder in moderate yield (62 mg, 33%).

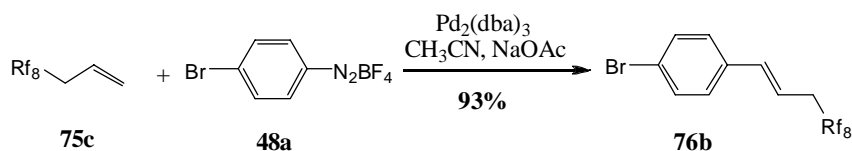
**$^1\text{H-NMR}$ :** (500 MHz, HFB,  $\text{CDCl}_3$ ):  $\delta$  8.69 (br. s, 12H, Ph), 3.55 (br. s, 12H,  $\text{CH}_2\text{CH}_2\text{CH}_2\text{Rf}_6$ ), 2.74 (m, 24H,  $\text{CH}_2\text{CH}_2\text{CH}_2\text{Rf}_6$ ).

**MALDI-ICR-MS (DCTB):** m/z (% int.): 2682.22 ( $\text{M}^{++}$ , 100%; calcd. for  $\text{C}_{96}\text{H}_{48}\text{F}_{78}$  2682.25), 2336.20 ( $[\text{M-Rf}_{2,6}]^{++}$ , 20%).

**UV/VIS:** (BTF,  $10^{-5}$  M,  $\epsilon = 5.6 \cdot 10^3$ ),  $\lambda_{\text{max}} = 344, 361, 386, 412$  nm.

### 21.3 Synthesis of HBC-(Rf<sub>3,8</sub>)<sub>6</sub>

#### 21.3.1 1-(4,4,5,5,6,6,7,7,8,8,9,9,10,10,11,11,11-Heptadecafluoroundec-1-enyl)-4-bromobenzene



This synthesis was carried out following **method D** using compound **75c** (13.0 g, 28.25 mmol), diazonium salt **48a** (8.4 g, 31.08 mmol), Pd<sub>2</sub>(dba)<sub>3</sub> (440 mg, 0.42 mmol), NaOAc (8.1 g, 9.89 mmol) and acetonitrile (140 mL). The reaction mixture was stirred at room temperature under argon for 3 hours. All volatiles of the brown suspension were evaporated and the dark residue was suspended in pentane (250 mL) and filtrated over a plug of silica gel under vacuum. After evaporation of the pentane a green-yellow solid was recovered and further purified by column chromatography using pentane as eluent yielding the desired compound **76b** as white solid (16.2 g, 93%).

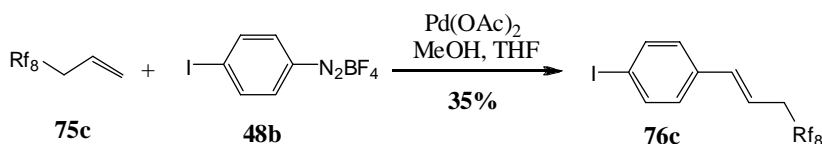
**TLC:** R<sub>f</sub> = 0.54 (silica gel, pentane, KMnO<sub>4</sub>).

**<sup>1</sup>H-NMR:** (360 MHz, CDCl<sub>3</sub>): δ 7.46 (*d*, 2H, <sup>3</sup>J<sub>HH</sub> = 8.2 Hz, Ph), 7.25 (*d*, 2H, <sup>3</sup>J<sub>HH</sub> = 8.2 Hz, Ph), 6.56 (*d*, 1H, <sup>3</sup>J<sub>HH</sub> = 15.4 Hz, CHCHCH<sub>2</sub>Rf<sub>8</sub>), 6.13 (*dt*, 1H, <sup>3</sup>J<sub>HH</sub> = 15.4 Hz, <sup>3</sup>J<sub>HH</sub> = 7.5 Hz, CHCHCH<sub>2</sub>Rf<sub>8</sub>), 3.00 (*dt*, 2H, <sup>3</sup>J<sub>FH</sub> = 17.7 Hz, <sup>3</sup>J<sub>HH</sub> = 7.5 Hz, CHCHCH<sub>2</sub>Rf<sub>8</sub>).

**<sup>13</sup>C-NMR:** (90.55 MHz, CDCl<sub>3</sub>): δ 136.09 (CHCHCH<sub>2</sub>Rf<sub>8</sub>), 135.09 (Ph), 131.78 (Ph), 127.96 (Ph), 122.02 (Ph), 116.89 (*t*, <sup>3</sup>J<sub>CF</sub> = 4.3 Hz, CHCHCH<sub>2</sub>Rf<sub>8</sub>), 105.70-120.02 (Rf<sub>8</sub>), 35.14 (*t*, <sup>2</sup>J<sub>CF</sub> = 22.8 Hz, CHCHCH<sub>2</sub>Rf<sub>8</sub>).

**EI-MS:** m/z (% int.): 615.0 (M<sup>+</sup>, 7%), 535.8 ([M-Br]<sup>+</sup>, 1%), 168.9 (100%).

#### 21.3.2 1-(4,4,5,5,6,6,7,7,8,8,9,9,10,10,11,11,11-Heptadecafluoroundec-1-enyl)-4-iodobenzene



Iodoaryl **76c** was formed according to **method D**, using allyl **75c** (6.0 g, 13.04 mmol) diazonium salt **48b** (4.14 g, 13.04 mmol), and Pd(OAc)<sub>2</sub> (58 mg, 0.26 mmol), methanol (20 mL) and THF (5 mL) which were reacted for 18 hours at 40 °C before all volatiles of the brown suspension were removed under vacuum. The dark residue was suspended in pentane (350 mL) and filtrated over a plug of silica gel under vacuum. After evaporation of the pentane the title compound **76c** was collected as white, but impure solid. Final purification was performed by silica gel chromatography using pentane as eluent yielding pure **76c** as white solid (3.0 g, 35%).



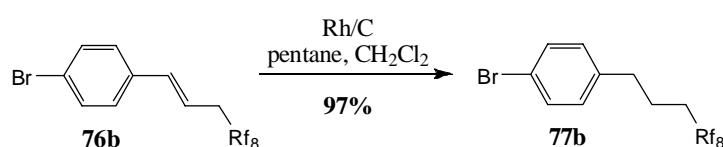
**TLC:**  $R_f = 0.54$  (silica gel, pentane,  $\text{KMnO}_4$ ).

**$^1\text{H-NMR}$ :** (360 MHz,  $\text{CDCl}_3$ ):  $\delta$  7.66 (*d*, 2H,  $^3J_{\text{HH}} = 8.4$  Hz, Ph), 7.12 (*d*, 2H,  $^3J_{\text{HH}} = 8.4$  Hz, Ph), 6.55 (*d*, 1H,  $^3J_{\text{HH}} = 15.4$  Hz,  $\text{CHCHCH}_2\text{Rf}_8$ ), 6.15 (*dt*, 1H,  $^3J_{\text{HH}} = 15.4$  Hz,  $^3J_{\text{HH}} = 7.5$  Hz,  $\text{CHCHCH}_2\text{Rf}_8$ ), 3.00 (*dt*, 2H,  $^3J_{\text{FH}} = 17.7$  Hz,  $^3J_{\text{HH}} = 7.5$  Hz,  $\text{CHCHCH}_2\text{Rf}_8$ ).

**$^{13}\text{C-NMR}$ :** (90.55 MHz,  $\text{CDCl}_3$ ):  $\delta$  137.76 (Ph), 136.22 ( $\text{CHCHCH}_2\text{Rf}_8$ ), 135.67 (Ph), 128.17 (Ph), 117.03 (*t*,  $^3J_{\text{CF}} = 4.3$  Hz,  $\text{CHCHCH}_2\text{Rf}_8$ ), 105.70-120.02 ( $\text{Rf}_8$ ), 93.56 (Ph), 35.16 (*t*,  $^2J_{\text{CF}} = 22.8$  Hz,  $\text{CHCHCH}_2\text{Rf}_8$ ).

**EI-MS:**  $m/z$  (% int.): 663.1 ( $\text{M}^{*+}$ , 7%), 535.8 ( $[\text{M-I}]^{*+}$ , 1%), 115.7 (100%).

### 21.3.3 1-(4,4,5,5,6,6,7,7,8,8,9,9,10,10,11,11,11-Heptafluoroundecyl)-4-bromobenzene



The hydrogenation was performed using **method E**: Compound **76b** (14.0 g, 23.0 mmol), rhodium on carbon (702 mg, 3.4  $\mu\text{mol}$ ), pentane (60 mL) and  $\text{CH}_2\text{Cl}_2$  (20 mL) were reacted in a 200 mL autoclave at room temperature under 50 bar hydrogen for 24 hours. Afterward the crude reaction mixture was filtered through a plug of silica gel under reduced pressure using pentane as eluent. Evaporation of the solvents afforded compound **77b** as a colourless oil (13.9 g, 97%), which crystallized slowly at room temperature.

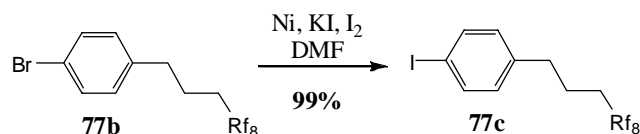
**TLC:**  $R_f = 0.54$  (silica gel, pentane,  $\text{KMnO}_4$ ).

**$^1\text{H-NMR}$ :** (360 MHz,  $\text{CDCl}_3$ ):  $\delta$  7.43 (*d*, 2H,  $^3J_{\text{HH}} = 8.2$  Hz, Ph), 7.06 (*d*, 2H,  $^3J_{\text{HH}} = 8.2$  Hz, Ph), 2.67 (*t*, 2H,  $^3J_{\text{HH}} = 7.5$  Hz,  $\text{CH}_2\text{CH}_2\text{CH}_2\text{Rf}_8$ ), 2.0-2.14 (*m*, 2H,  $\text{CH}_2\text{CH}_2\text{CH}_2\text{Rf}_8$ ), 1.92 (*quint*, 2H,  $^3J_{\text{HH}} = 7.5$  Hz,  $\text{CH}_2\text{CH}_2\text{CH}_2\text{Rf}_8$ ).

**$^{13}\text{C-NMR}$ :** (90.55 MHz,  $\text{CDCl}_3$ ):  $\delta$  139.55 (Ph), 131.68 (Ph), 130.06 (Ph), 120.13 (Ph), 107.78-122.29 ( $\text{Rf}_8$ ), 34.41 ( $\text{CH}_2\text{CH}_2\text{CH}_2\text{Rf}_8$ ), 30.21 (*t*,  $^2J_{\text{CF}} = 22.5$  Hz,  $\text{CH}_2\text{CH}_2\text{CH}_2\text{Rf}_8$ ), 21.71 (*t*,  $^3J_{\text{CF}} = 3.3$  Hz,  $\text{CH}_2\text{CH}_2\text{CH}_2\text{Rf}_8$ ).

**EI-MS:**  $m/z$  (% int.): 617.0 ( $\text{M}^{*+}$ , 15%), 537.8 ( $[\text{M-Br}]^{*+}$ , 1%), 170.8 ( $[\text{M-Rf}_{2,8}]^{*+}$ , 100%).

## 21.3.4 1-(4,4,5,5,6,6,7,7,8,8,9,9,10,10,11,11,11-Heptafluoroundecyl)-4-iodobenzene

**Method F**

Ni (6.2 g, 10.6 mmol), KI (7.0 g, 42.2 mmol) and I<sub>2</sub> (268 mg, 1.1 mmol) were charged into a Schlenk reaction vessel and suspended in DMF (30 mL) under inert atmosphere. Compound **77b** (13.0 g, 21.0 mmol) was degassed in a separate flask, diluted with DMF (30 mL) and added to the reaction mixture which was heated afterwards to 150 °C for 27 hours. The dark brown mixture was, after cooling to room temperature, decanted off from the nickel residue. The crude product was then extracted with pentane (3 x 100 mL), before the combined organic fractions were washed with water (100 mL), HCl 3%, (50 mL) and water (100 mL), dried over Na<sub>2</sub>SO<sub>4</sub>. After removal of all volatiles compound **77c** was afforded as a yellow crystalline solid. Purification was completed by filtration over a plug of silica gel under reduced pressure using pentane as eluent yielding a white crystalline solid **77c** in excellent yield (13.7 g, 99%).

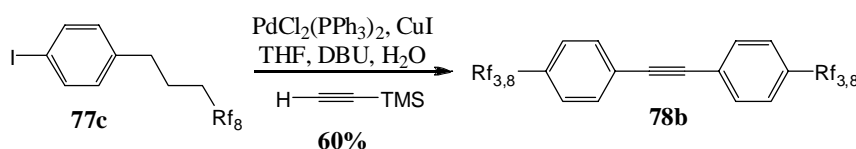
**TLC:** R<sub>f</sub> = 0.54 (silica gel, pentane, KMnO<sub>4</sub>).

**<sup>1</sup>H-NMR:** (360 MHz, CDCl<sub>3</sub>): δ 7.63 (*d*, 2H, <sup>3</sup>J<sub>HH</sub> = 8.2 Hz, Ph), 6.94 (*d*, 2H, <sup>3</sup>J<sub>HH</sub> = 8.2 Hz, Ph), 2.65 (*t*, 2H, <sup>3</sup>J<sub>HH</sub> = 7.5 Hz, CH<sub>2</sub>CH<sub>2</sub>CH<sub>2</sub>Rf<sub>8</sub>), 1.95-2.14 (*m*, 2H, CH<sub>2</sub>CH<sub>2</sub>CH<sub>2</sub>Rf<sub>8</sub>), 1.91 (*quint*, 2H, <sup>3</sup>J<sub>HH</sub> = 7.5 Hz, CH<sub>2</sub>CH<sub>2</sub>CH<sub>2</sub>Rf<sub>8</sub>).

**<sup>13</sup>C-NMR:** (90.55 MHz, CDCl<sub>3</sub>): δ 140.22 (Ph), 137.66 (Ph), 130.40 (Ph), 107.74-120.13 (Rf<sub>8</sub>), 91.41 (Ph), 34.51 (CH<sub>2</sub>CH<sub>2</sub>CH<sub>2</sub>Rf<sub>8</sub>), 30.21 (*t*, <sup>2</sup>J<sub>CF</sub> = 22.5 Hz, CH<sub>2</sub>CH<sub>2</sub>CH<sub>2</sub>Rf<sub>8</sub>), 21.68 (*t*, <sup>3</sup>J<sub>CF</sub> = 3.3 Hz, CH<sub>2</sub>CH<sub>2</sub>CH<sub>2</sub>Rf<sub>8</sub>).

**EI-MS:** m/z (% int.): 665.1 (M<sup>+</sup>, 15%), 537.8 ([M-I]<sup>+</sup>, 1%), 217.0 ([M-Rf<sub>2,8</sub>]<sup>+</sup>, 100%).

## 21.3.5 1-(4,4,5,5,6,6,7,7,8,8,9,9,10,10,11,11,11-Heptafluoroundecyl)-4-{[4-(4,4,5,5,6,6,7,7,8,8,9,9,10,10,11,11,11-heptafluoroundecyl)phenyl]ethynyl}benzene



The synthesis was performed using **method A**, starting with iodoaryl **77c** (5.0 g, 7.7 mmol) together with PdCl<sub>2</sub>(PPh<sub>3</sub>)<sub>2</sub> (530 mg, 0.46 mmol), CuI (146 mg, 0.77 mmol), DBU (6.9 mL, 45.2 mmol), THF (40 mL), H<sub>2</sub>O (55 μL, 3.1 mmol) and TMSA (0.56 mL, 3.8 mmol). The reaction was heated to 50 °C for 15 hours, then to 75 °C for 6 hours before the crude reaction mixture was diluted with ether (500 mL) and extracted with 10% HCl (100 mL), water (100 mL), NaCl sat. (100 mL) and

water (100 mL). The combined organic fractions were dried over  $\text{Na}_2\text{SO}_4$  and all volatiles were removed. The obtained dark brown solid was dissolved in ether – pentane (300 mL, 1:9) and filtered over a plug of basic Alox under reduced pressure, yielding after removal of the eluents the desired compound **78b** as dark yellow solid. Several crystallisations from ether – pentane – ethanol afforded tolane **78b** as off-white solid in good yield (2.71 g, 60%).

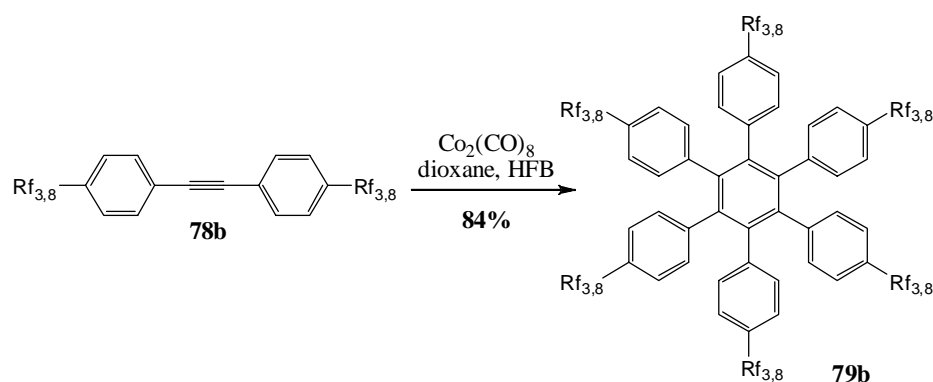
**TLC:**  $R_f = 0.90$  (silica gel, pentane – ether (9:1),  $\text{KMnO}_4$ ).

**$^1\text{H-NMR}$ :** (360 MHz,  $\text{CDCl}_3$ ):  $\delta$  7.47 (*d*, 4H,  $^3J_{\text{HH}} = 8.2$  Hz, Ph), 7.17 (*d*, 4H,  $^3J_{\text{HH}} = 8.2$  Hz, Ph), 2.73 (*t*, 4H,  $^3J_{\text{HH}} = 7.5$  Hz,  $\text{CH}_2\text{CH}_2\text{CH}_2\text{Rf}_8$ ), 1.95-2.14 (*m*, 8H,  $\text{CH}_2\text{CH}_2\text{CH}_2\text{Rf}_8$ ).

**$^{13}\text{C-NMR}$ :** (90.55 MHz,  $\text{CDCl}_3$ ):  $\delta$  140.87 (Ph), 131.80 (Ph), 128.39 (Ph), 121.30 (Ph), 107.74-120.13 ( $\text{Rf}_8$ ), 89.01 (acetylene), 34.89 ( $\text{CH}_2\text{CH}_2\text{CH}_2\text{Rf}_8$ ), 30.23 (*t*,  $^2J_{\text{CF}} = 22.5$  Hz,  $\text{CH}_2\text{CH}_2\text{CH}_2\text{Rf}_8$ ), 21.63 (*t*,  $^3J_{\text{CF}} = 3.3$  Hz,  $\text{CH}_2\text{CH}_2\text{CH}_2\text{Rf}_8$ ).

**MALDI-ICR-MS (DCTB):**  $m/z$  (% int.): 1349.27 ( $[\text{M}+\text{DCTB}]^{*+}$ , 80 %), 1089.10 ( $\text{M}^{*+}$ , 100 %).

#### 21.3.6 Hexakis[4-(4,4,5,5,6,6,7,7,8,8,9,9,10,10,11,11,11-heptafluoroundecyl)phenyl]-benzene



The HPB formation was performed following **method B** using tolane **78b** (0.5 g, 0.45 mmol),  $\text{Co}_2(\text{CO})_8$  (12.4 mg, 36.4  $\mu\text{mol}$ ), dioxane (50 mL) and HFB (10mL). The dark mixture was refluxed for 2 days before all volatiles were removed under reduced pressure. The brown solid was dissolved in dichloromethane and suction filtrated over Millipore<sup>®</sup> to remove the insoluble catalyst. The filtrate was reduced to the maximum and dissolved in BTF. The obtained brown solution was hot (65 °C) filtrated over a very short plug of silica gel under normal pressure. The plug was exhaustively washed with hot BTF before all volatiles of the filtrate were removed affording the HPB derivative **79b** as white solid in good yield (0.42 g, 84%).

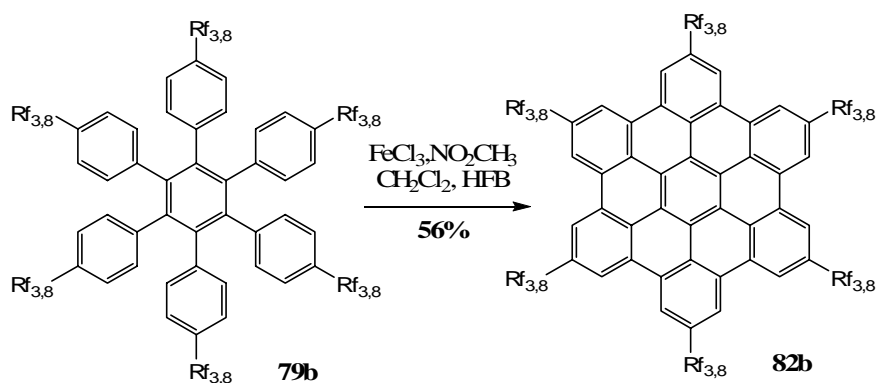
**TLC:**  $R_f = 0.43$  (silica gel, pentane – ether 1:1,  $\text{KMnO}_4$ ).

**$^1\text{H-NMR}$ :** (500 MHz,  $\text{CDCl}_3$ ):  $\delta$  6.74 (*d*, 12H,  $^3J_{\text{HH}} = 8.2$  Hz, Ph), 6.66 (*d*, 12H,  $^3J_{\text{HH}} = 8.2$  Hz, Ph), 2.45 (*t*, 12H,  $^3J_{\text{HH}} = 7.3$  Hz,  $\text{CH}_2\text{CH}_2\text{CH}_2\text{Rf}_8$ ), 1.81-1.91 (*m*, 12H,  $\text{CH}_2\text{CH}_2\text{CH}_2\text{Rf}_8$ ), 1.70-1.77 (*m*, 12H,  $\text{CH}_2\text{CH}_2\text{CH}_2\text{Rf}_8$ ).

**$^{13}\text{C-NMR}$ :** (125.77 MHz,  $\text{CDCl}_3$ ):  $\delta$  140.30 (Ph), 138.99 (Ph), 137.32 (Ph), 131.83 (Ph), 126.65 (Ph), 105.32-120.11 ( $\text{Rf}_8$ ), 34.32 ( $\text{CH}_2\text{CH}_2\text{CH}_2\text{Rf}_8$ ), 30.14 (*t*,  $^2J_{\text{CF}} = 22.1$  Hz,  $\text{CH}_2\text{CH}_2\text{CH}_2\text{Rf}_8$ ), 21.63 ( $\text{CH}_2\text{CH}_2\text{CH}_2\text{Rf}_8$ ).

**MALDI-ICR-MS (DCTB):**  $m/z$  (% int.): 3294.22 ( $\text{M}^{*+}$ , 100%), 2858.20 ( $[\text{M-Rf}_{2,8}]^{*+}$ , 10%).

21.3.7 2,5,8,11,14,17-Hexakis(4,4,5,5,6,6,7,7,8,8,9,9,10,10,11,11,11-heptafluoroundecyl)-hexabenzo[bc,ef,hi,kl,no,qr]coronene



The HBC formation was achieved by using **method C** taking HPB **79b** (50 mg, 15  $\mu\text{mol}$ ) as precursor, together with  $\text{FeCl}_3$  (220 mg, 1.36 mmol, 7.5 eq / H to be removed),  $\text{CH}_2\text{Cl}_2$  (5 mL),  $\text{CH}_3\text{NO}_2$  (4 mL) and HFB (5 mL). The dark mixture was stirred at 45 °C under a constant stream of argon for 8 hours before methanol (30 mL) was added to precipitate the desired HBC **82b**, which was collected by suction filtration over Millipore<sup>®</sup>. The brown solid was successively suspended in common organic solvents such as ether, dichloromethane, nitromethane and BTF, sonicated, completely precipitated in the fridge and suction filtrated over Millipore<sup>®</sup> to yield the title HBC **82b** as bright yellow solid (28 mg, 56%).

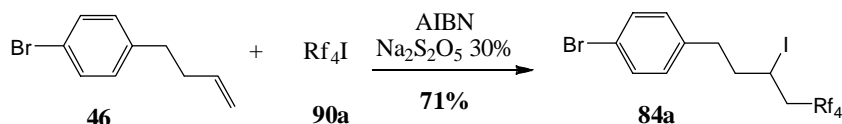
**$^1\text{H-NMR}$ :** (500 MHz, HFB,  $\text{CDCl}_3$ ):  $\delta$  8.95 (*s*, 12H, Ph), 3.61 (br. *s*, 12H,  $\text{CH}_2\text{CH}_2\text{CH}_2\text{Rf}_8$ ), 2.73 (br. *s*, 24H,  $\text{CH}_2\text{CH}_2\text{CH}_2\text{Rf}_8$ ).

**MALDI-ICR-MS (DCTB):**  $m/z$  (% int.): 3282.21 ( $\text{M}^{*+}$ , 100%; calcd. for  $\text{C}_{108}\text{H}_{48}\text{F}_{102}$  3282.21), 2836.20 ( $[\text{M-Rf}_{2,8}]^{*+}$ , 30%).

**UV/VIS:** (BTF,  $10^{-6}$  M,  $\epsilon = 1.5 \cdot 10^5$ ),  $\lambda_{\text{max}} = 352, 369, 396$  nm.

21.4 Synthesis of HBC-(Rf<sub>4,4</sub>)<sub>6</sub>

## 21.4.1 1-Bromo-4-(5,5,6,6,7,7,8,8,8-nonafluoro-3-iodooctyl)benzene

**Method G**

Bromo aryl **46** (17 g, 80.53 mmol) was added to a round bottomed flask and heated to 50°C before a 30% aq. solution of Na<sub>2</sub>S<sub>2</sub>O<sub>5</sub> (7.6 mL) and Rf<sub>4</sub>I **90a** (27 g, 78.45 mmol) was added. Under a positive stream of argon AIBN (230 mg, 1.39 mmol) was added and the reaction mixture was heated to 80 °C for 2 hours. The mixture was allowed to reach room temperature before water (50 mL) was added. The obtained suspension was extracted with ether (3 x 100 mL). The combined organic phases were washed with water (50 mL), dried over Na<sub>2</sub>SO<sub>4</sub> and all volatiles were removed under reduced pressure yielding the desired compound **84a** as colourless oil in good yield (31.1 g, 71%).

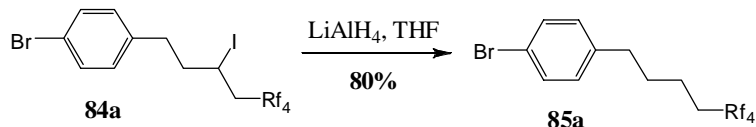
**TLC:** Rf = 0.85 (silica gel, pentane, KMnO<sub>4</sub>).

**<sup>1</sup>H-NMR:** (360 MHz, CDCl<sub>3</sub>): δ 7.38 (*d*, 2H, <sup>3</sup>J<sub>HH</sub> = 8.6 Hz, Ph), 7.09 (*d*, 2H, <sup>3</sup>J<sub>HH</sub> = 8.6 Hz, Ph), 4.23 (*tt*, 1H, <sup>3</sup>J<sub>HH</sub> = 8.2 Hz, <sup>3</sup>J<sub>HH</sub> = 5.0 Hz, CH<sub>2</sub>CH<sub>2</sub>CHICH<sub>2</sub>Rf<sub>4</sub>), 2.67-3.02 (*m*, 2H, CH<sub>2</sub>CH<sub>2</sub>CHICH<sub>2</sub>Rf<sub>4</sub>), 2.66 (*t*, 2H, <sup>3</sup>J<sub>HH</sub> = 8.2 Hz, CH<sub>2</sub>CH<sub>2</sub>CHICH<sub>2</sub>Rf<sub>4</sub>), 2.02-2.16 (*m*, 2H, CH<sub>2</sub>CH<sub>2</sub>CHICH<sub>2</sub>Rf<sub>4</sub>).

**<sup>13</sup>C-NMR:** (90.55 MHz, CDCl<sub>3</sub>): 138.76 (Ph), 131.68 (Ph), 130.22 (Ph), 120.21 (Ph), 108.40-122.40 (Rf<sub>4</sub>), 41.57 (*t*, <sup>2</sup>J<sub>CF</sub> = 22.5 Hz, CH<sub>2</sub>CH<sub>2</sub>CHICH<sub>2</sub>Rf<sub>4</sub>), 41.38 (CH<sub>2</sub>CH<sub>2</sub>CHICH<sub>2</sub>Rf<sub>4</sub>), 35.12 (CH<sub>2</sub>CH<sub>2</sub>CHICH<sub>2</sub>Rf<sub>4</sub>), 19.65 (*t*, <sup>3</sup>J<sub>CF</sub> = 2.5 Hz, CH<sub>2</sub>CH<sub>2</sub>CHICH<sub>2</sub>Rf<sub>4</sub>).

**EI-MS:** m/z (% int.): 556.7 (M<sup>+</sup>, 8 %), 429.5 ([M-I]<sup>+</sup>, 12 %), 168.9 ([M-Rf<sub>3,4</sub>]<sup>+</sup>, 100 %).

## 21.4.2 1-Bromo-4-(5,5,6,6,7,7,8,8,8-nonafluorooctyl)benzene

**Method H**

LiAlH<sub>4</sub> (1.8 g, 47.4 mmol) was placed in a 500 mL three necked flask under inert atmosphere and THF (60 mL) was syringed in. Compound **84a** (22 g, 39.5 mmol) was dissolved in THF (40 mL) and was carefully added to the LiAlH<sub>4</sub> slurry in such a rate to maintain the reaction medium at a gentle reflux. After 6 hours of reaction at room temperature the mixture was quenched by the addition of H<sub>2</sub>O (5 mL), 15 % NaOH (5 mL) and H<sub>2</sub>O (15 mL). The crude reaction product was extracted with ether (3 x 200 mL). The combined organic phases were filtrated over Büchner and the

filtrate was washed with water (50 mL), dried over Na<sub>2</sub>SO<sub>4</sub> and all volatiles were removed under reduced pressure yielding the title compound (**85a**) as a colourless oil in good yield (13.6 g, 80%).

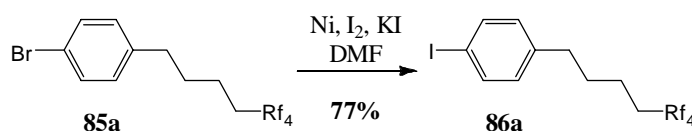
**TLC:** R<sub>f</sub> = 0.85 (silica gel, pentane, KMnO<sub>4</sub>).

**<sup>1</sup>H-NMR:** (360 MHz, CDCl<sub>3</sub>): δ 7.37 (*d*, 2H, <sup>3</sup>J<sub>HH</sub> = 8.6 Hz, Ph), 7.04 (*d*, 2H, <sup>3</sup>J<sub>HH</sub> = 8.6 Hz, Ph), 2.58 (*t*, 2H, <sup>3</sup>J<sub>HH</sub> = 6.8 Hz, CH<sub>2</sub>(CH<sub>2</sub>)<sub>3</sub>Rf<sub>4</sub>), 2.00-2.13 (*m*, 2H, (CH<sub>2</sub>)<sub>3</sub>CH<sub>2</sub>Rf<sub>4</sub>), 1.58-1.69 (*m*, 4H, CH<sub>2</sub>CH<sub>2</sub>CH<sub>2</sub>CH<sub>2</sub>Rf<sub>4</sub>).

**<sup>13</sup>C-NMR:** (90.55 MHz, CDCl<sub>3</sub>): 140.53 (Ph), 131.46 (Ph), 130.05 (Ph), 119.7 (Ph), 107.19-121.07 (Rf<sub>4</sub>), 35.11 (CH<sub>2</sub>(CH<sub>2</sub>)<sub>3</sub>Rf<sub>4</sub>), 30.64 (CH<sub>2</sub>CH<sub>2</sub>CH<sub>2</sub>CH<sub>2</sub>Rf<sub>4</sub>), 30.54 (*t*, <sup>2</sup>J<sub>CF</sub> = 22.5 Hz, (CH<sub>2</sub>)<sub>3</sub>CH<sub>2</sub>Rf<sub>4</sub>), 19.69 (*t*, <sup>3</sup>J<sub>CF</sub> = 3.3 Hz, CH<sub>2</sub>CH<sub>2</sub>CH<sub>2</sub>CH<sub>2</sub>Rf<sub>4</sub>).

**EI-MS:** m/z (% int.): 430.5 (M<sup>•+</sup>, 12 %), 168.9 ([M-Rf<sub>3,4</sub>]<sup>•+</sup>, 100 %).

#### 21.4.3 1-Iodo-4-(5,5,6,6,7,7,8,8,8-nonafluorooctyl)benzene



The synthesis was performed using **method F** starting with compound **85a** (5.5 g, 12.75 mmol) as precursor in combination with Ni (3.74 g, 63.78 mmol), KI (4.23 g, 25.51 mmol), I<sub>2</sub> (160 mg, 0.63 mmol) and DMF (35 mL). The reaction mixture was heated to 150°C for 14 hours, then cooled to room temperature and extracted with pentane (3 x 50 mL). The combined pentane fractions were washed with water (100 mL), dried over Na<sub>2</sub>SO<sub>4</sub> and all volatiles were evaporated. The obtained brown oil was dissolved in pentane and filtrated over a silica gel plug under reduced pressure, yielding, after removal of all volatiles, the desired iodoaryl **86a** as colourless oil (4.71 g, 77 %).

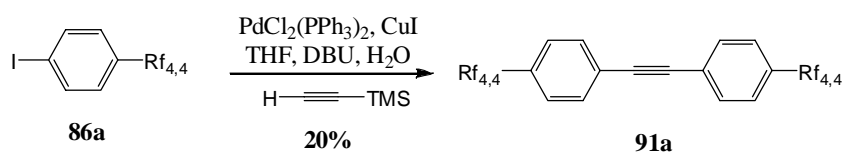
**TLC:** R<sub>f</sub> = 0.85 (silica gel, pentane, KMnO<sub>4</sub>).

**<sup>1</sup>H-NMR:** (360 MHz, CDCl<sub>3</sub>): δ 7.60 (*d*, 2H, <sup>3</sup>J<sub>HH</sub> = 8.2 Hz, Ph), 7.04 (*d*, 2H, <sup>3</sup>J<sub>HH</sub> = 8.2 Hz, Ph), 2.59 (*t*, 2H, <sup>3</sup>J<sub>HH</sub> = 7.3 Hz, CH<sub>2</sub>(CH<sub>2</sub>)<sub>3</sub>Rf<sub>4</sub>), 1.99-2.16 (*m*, 2H, (CH<sub>2</sub>)<sub>3</sub>CH<sub>2</sub>Rf<sub>4</sub>), 1.62-1.67 (*m*, 4H, CH<sub>2</sub>CH<sub>2</sub>CH<sub>2</sub>CH<sub>2</sub>Rf<sub>4</sub>).

**<sup>13</sup>C-NMR:** (90.55 MHz, CDCl<sub>3</sub>): 141.24 (Ph), 137.47 (Ph), 130.44 (Ph), 108.55-122.20 (Rf<sub>4</sub>), 90.98 (Ph), 35.03 (CH<sub>2</sub>(CH<sub>2</sub>)<sub>3</sub>Rf<sub>4</sub>), 30.58 (*t*, <sup>2</sup>J<sub>CF</sub> = 22.5 Hz, (CH<sub>2</sub>)<sub>3</sub>CH<sub>2</sub>Rf<sub>4</sub>), 30.06 (CH<sub>2</sub>CH<sub>2</sub>CH<sub>2</sub>CH<sub>2</sub>Rf<sub>4</sub>), 19.72 (*t*, <sup>3</sup>J<sub>CF</sub> = 3.3 Hz, CH<sub>2</sub>CH<sub>2</sub>CH<sub>2</sub>CH<sub>2</sub>Rf<sub>4</sub>).

**EI-MS:** m/z (% int.): 478.6 (M<sup>•+</sup>, 45 %), 217.0 ([M-Rf<sub>3,4</sub>]<sup>•+</sup>, 100 %).

## 21.4.4 1-(5,5,6,6,7,7,8,8,8-Nonafluorooctyl)-4-{[4-(5,5,6,6,7,7,8,8,8-nonafluorooctyl)phenyl]-ethynyl}benzene



The synthesis was carried out following **method A** using compound **86a** (11.2 g, 26.0 mmol) as starting material. In addition  $\text{PdCl}_2(\text{PPh}_3)_2$  (1.09 g, 1.56 mmol), CuI (496 mg, 2.6 mmol), DBU (23.3 mL, 156.2 mmol), THF (125 mL),  $\text{H}_2\text{O}$  (190  $\mu\text{L}$ , 10.4 mmol) and TMSA (1.9 mL, 13.0 mmol) was used. The mixture was stirred at 80 °C for 43 hours before an extraction with ether (3 x 200 mL) was done. The combined organic phases were washed with water (3 x 50 mL), 10% HCl (50 mL) and sat. NaCl (100 mL), dried over  $\text{Na}_2\text{SO}_4$  and all volatiles were removed. Filtration over a plug of basic alox using pentane (500 mL) as eluent afforded the desired tolane **91a** as yellow solid which was recrystallized from pentane – methanol in order to obtain a white powder (1.9 g, 20%).

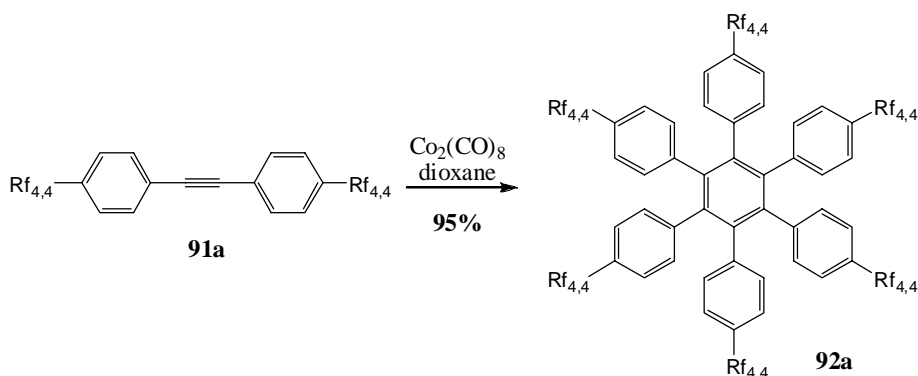
**TLC:**  $R_f = 0.82$  (silica gel, pentane – ether 9:1,  $\text{KMnO}_4$ ).

**$^1\text{H-NMR}$ :** (360 MHz,  $\text{CDCl}_3$ ):  $\delta$  7.45 (*d*, 4H,  $^3J_{\text{HH}} = 8.2$  Hz, Ph), 7.15 (*d*, 4H,  $^3J_{\text{HH}} = 8.2$  Hz, Ph), 2.67 (*t*, 4H,  $^3J_{\text{HH}} = 7.3$  Hz,  $\text{CH}_2(\text{CH}_2)_3\text{Rf}_4$ ), 2.01-2.17 (*m*, 4H,  $(\text{CH}_2)_3\text{CH}_2\text{Rf}_4$ ), 1.62-1.76 (*m*, 8H,  $\text{CH}_2\text{CH}_2\text{CH}_2\text{CH}_2\text{Rf}_4$ ).

**$^{13}\text{C-NMR}$ :** (90.55 MHz,  $\text{CDCl}_3$ ): 141.89 (Ph), 131.64 (Ph), 128.38 (Ph), 110.50-125.52 ( $\text{Rf}_4$ ), 120.94 (Ph), 88.96 (acetylene), 35.44 ( $\text{CH}_2(\text{CH}_2)_3\text{Rf}_4$ ), 30.62 ( $\text{CH}_2\text{CH}_2\text{CH}_2\text{CH}_2\text{Rf}_4$ ), 30.62 (*t*,  $^2J_{\text{CF}} = 22.5$  Hz,  $(\text{CH}_2)_3\text{CH}_2\text{Rf}_4$ ), 19.75 (*t*,  $^3J_{\text{CF}} = 3.3$  Hz,  $\text{CH}_2\text{CH}_2\text{CH}_2\text{CH}_2\text{Rf}_4$ ).

**EI-MS:**  $m/z$  (% int.): 727.5 ( $\text{M}^+$ , 20 %), 465.7 ( $[\text{M-Rf}_{3,4}]^+$ , 100 %).

## 21.4.5 Hexakis[4-(5,5,6,6,7,7,8,8,8-nonafluorooctyl)phenyl]benzene



The synthesis was done with respect to **method B** using tolane **91a** (1.8 g, 2.48 mmol) as starting material in presence of Co<sub>2</sub>(CO)<sub>8</sub> (51 mg, 0.15 mmol) and dioxane (150 mL). The reaction mixture was refluxed for 21 hours before a cooling to room temperature was allowed. The purification was achieved by filtration over a plug of silica gel under reduced pressure using ether as eluent. The brown product was suspended in methanol. After 2 hours in the ultrasonic bath and one night in the refrigerator HPB **92a** was collected by suction filtration over Millipore<sup>®</sup> as white solid in quantitative yield (1.7 g, 95%).

**TLC:** R<sub>f</sub> = 0.92 (silica gel, pentane – ether (9:1), KMnO<sub>4</sub>).

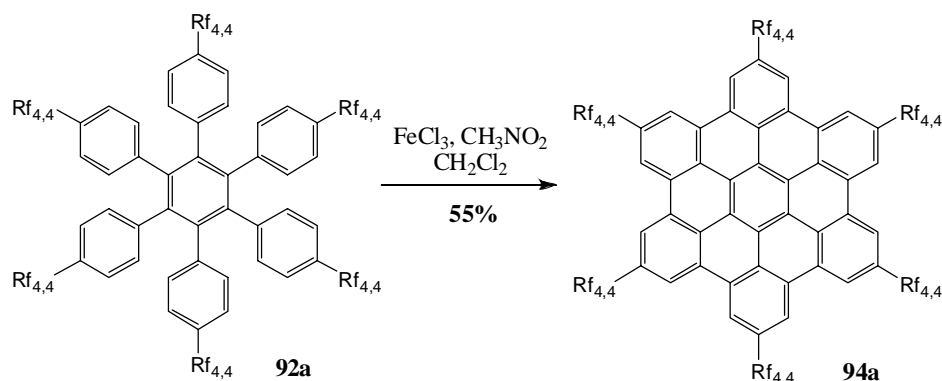
**<sup>1</sup>H-NMR:** (360 MHz, CDCl<sub>3</sub>): δ 6.68 (*d*, 12H, <sup>3</sup>J<sub>HH</sub> = 8.2 Hz, Ph), 6.62 (*d*, 12H, <sup>3</sup>J<sub>HH</sub> = 8.2 Hz, Ph), 2.39 (*t*, 12H, <sup>3</sup>J<sub>HH</sub> = 6.8 Hz, CH<sub>2</sub>(CH<sub>2</sub>)<sub>3</sub>Rf<sub>4</sub>), 1.90-2.03 (*m*, 12H, (CH<sub>2</sub>)<sub>3</sub>CH<sub>2</sub>Rf<sub>4</sub>), 1.35-1.55 (*m*, 24H, CH<sub>2</sub>CH<sub>2</sub>CH<sub>2</sub>CH<sub>2</sub>Rf<sub>4</sub>).

**<sup>13</sup>C-NMR:** (90.55 MHz, CDCl<sub>3</sub>): 140.19 (Ph), 138.52 (Ph), 137.85 (Ph), 131.58 (Ph), 126.44 (Ph), 105.63-121.06 (Rf<sub>4</sub>), 34.61 (CH<sub>2</sub>(CH<sub>2</sub>)<sub>3</sub>Rf<sub>4</sub>), 30.45 (*t*, <sup>2</sup>J<sub>CF</sub> = 22.5 Hz, (CH<sub>2</sub>)<sub>3</sub>CH<sub>2</sub>Rf<sub>4</sub>), 30.35 (CH<sub>2</sub>CH<sub>2</sub>CH<sub>2</sub>CH<sub>2</sub>Rf<sub>4</sub>), 18.94 (CH<sub>2</sub>CH<sub>2</sub>CH<sub>2</sub>CH<sub>2</sub>Rf<sub>4</sub>).

**MALDI-ICR-MS (DCTB):** m/z (% int.): 2179.48 (M<sup>+</sup>, 100%).



## 21.4.6 2,5,8,11,14,17-Hexakis(5,5,6,6,7,7,8,8,8-nonafluorooctyl)hexabenzob[bc,ef,hi,kl,no,qr]-coronene



The synthesis was carried out following **method C** using HPB **92a** (0.2 g, 92  $\mu\text{mol}$ ) as precursor together with  $\text{FeCl}_3$  (535 mg, 3.3 mmol, 3 eq / H to be removed) in  $\text{CH}_3\text{NO}_2$  (5 mL) and  $\text{CH}_2\text{Cl}_2$  (15 mL). The mixture was continuously purged with argon through a Teflon capillary while being stirred at 45 °C for 9 hours. The dark mixture was then quenched at 45 °C by the addition of methanol (20 mL) which provoked a red precipitate which was collected by suction filtration over Millipore<sup>®</sup>. The red solid was suspended in pentane and ether, treated in an ultrasonic bath for 30 minutes, cooled in the fridge for 1 hour and suction filtrated over Millipore<sup>®</sup> yielding HBC **94a** as a bright yellow solid (110 mg, 55%).

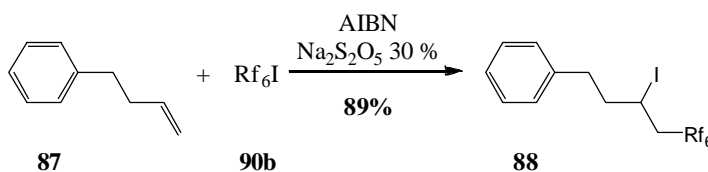
**<sup>1</sup>H-NMR:** (500 MHz, HFB,  $\text{CDCl}_3$ ):  $\delta$  9.06 (s, 12H, Ph), 3.57 (t, 12H,  $^3J_{\text{HH}} = 7.8$  Hz,  $\text{CH}_2(\text{CH}_2)_3\text{Rf}_4$ ), 2.59-2.63 (m, 24H,  $\text{CH}_2\text{CH}_2\text{CH}_2\text{CH}_2\text{Rf}_4$ ), 2.30 (quint, 12H,  $^3J_{\text{HH}} = 7.8$  Hz,  $\text{CH}_2\text{CH}_2\text{CH}_2\text{CH}_2\text{Rf}_4$ ).

**MALDI-ICR-MS (DCTB):** m/z (% int.): 2166.36 ( $\text{M}^{+}$ , 100%; calcd. for  $\text{C}_{90}\text{H}_{60}\text{F}_{54}$  2166.38), 1906.34 ( $[\text{M}-\text{Rf}_{3,4}]$ , 20%), 1644.28 ( $[\text{M}-2 \times \text{Rf}_{3,4}]$ , 10%), 1384.27 ( $[\text{M}-3 \times \text{Rf}_{3,4}]$ , 5%).

**UV/VIS:** (BTF,  $10^{-6}$  M,  $\epsilon = 1.2 \cdot 10^5$ ),  $\lambda_{\text{max}} = 343, 360, 391$  nm.

21.5 Synthesis of HBC-(Rf<sub>4,6</sub>)<sub>6</sub>

## 21.5.1 (5,5,6,6,7,7,8,8,9,9,10,10,10-Tridecafluoro-3-iododecyl)benzene



The synthesis was achieved using **method G**. Perfluoroheptyliodide **90b** (4.5 g, 10 mmol), 30 % Na<sub>2</sub>S<sub>2</sub>O<sub>5</sub> solution (2 mL), AIBN (33 mg, 0.2 mmol) and compound **87** (1.5 mL, 10.3 mmol) were used. The reaction mixture was heated to 80 °C for 4 hours. Addition of water (20 mL) and extraction of the reaction mixture with CH<sub>2</sub>Cl<sub>2</sub> (3 x 50 mL) was performed. The combined organic phases were washed with water (3 x 50 mL), dried over Na<sub>2</sub>SO<sub>4</sub> and all volatiles were evaporated under reduced pressure yielding the desired compound **88** as a colourless oil (5.14 g, 89 %).

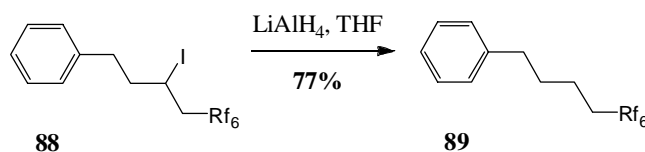
**TLC:** R<sub>f</sub> = 0.63 (silica gel, pentane, KMnO<sub>4</sub>).

**<sup>1</sup>H-NMR:** (360 MHz, CDCl<sub>3</sub>): δ 7.19-7.33 (*m*, 5H, Ph), 4.27 (*tt*, 1H, <sup>3</sup>J<sub>HH</sub> = 8.2 Hz, <sup>3</sup>J<sub>HH</sub> = 5.0 Hz, CH<sub>2</sub>CH<sub>2</sub>CHICH<sub>2</sub>Rf<sub>6</sub>), 2.68-3.03 (*m*, 4H, CH<sub>2</sub>CH<sub>2</sub>CHICH<sub>2</sub>Rf<sub>6</sub>), 2.12 (*m*, 2H, CH<sub>2</sub>CH<sub>2</sub>CHICH<sub>2</sub>Rf<sub>6</sub>).

**<sup>13</sup>C-NMR:** (90.55 MHz, CDCl<sub>3</sub>): δ 139.90 (Ph), 128.62 (Ph), 128.50 (Ph), 126.41 (Ph), 105.69-121.98 (Rf<sub>6</sub>), 41.80 (CH<sub>2</sub>CH<sub>2</sub>CHICH<sub>2</sub>Rf<sub>6</sub>), 41.73 (*t*, <sup>2</sup>J<sub>CF</sub> = 20.8 Hz, CH<sub>2</sub>CH<sub>2</sub>CHICH<sub>2</sub>Rf<sub>6</sub>), 35.70 (CH<sub>2</sub>CH<sub>2</sub>CHICH<sub>2</sub>Rf<sub>6</sub>), 20.04 (CH<sub>2</sub>CH<sub>2</sub>CHICH<sub>2</sub>Rf<sub>6</sub>).

**EI-MS:** *m/z* (% int.): 578.8 (M<sup>+</sup>, 5 %), 451.6 ([M-I]<sup>+</sup>, 22 %), 116.9 (44 %), 90.9 ([M-C<sub>3</sub>H<sub>5</sub>IRf<sub>6</sub>]<sup>+</sup>, 100 %).

## 21.5.2 (5,5,6,6,7,7,8,8,9,9,10,10,10-Tridecafluorodecyl)benzene



The synthesis was performed following **method H** using compound **88** (6.5 g, 11.2 mmol) as starting material, together with LiAlH<sub>4</sub> (0.85 g, 22.5 mmol) in THF (15 mL). The grey slurry was stirred at room temperature for 6 days before the mixture was quenched by the addition of H<sub>2</sub>O (2 mL), 0.2 M NaOH (2 mL) and H<sub>2</sub>O (6 mL) forming a white suspension which was Büchner filtrated and washed exhaustively with ether. The filtrate was washed with water (100 mL), dried over Na<sub>2</sub>SO<sub>4</sub> and all volatiles were removed. Filtration over a silica gel plug under reduced pressure using pen-

tane as eluent afforded a colourless oil with was further purified by bulb to bulb distillation (50 mbar, 150 °C) yielding the desired compound **89** as colourless oil in good yield (3.01 g, 77 %).

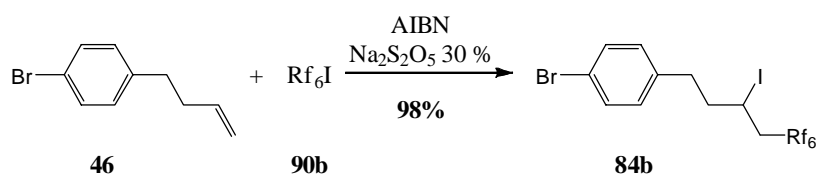
**TLC:**  $R_f$  = 0.95 (silica gel, pentane,  $\text{KMnO}_4$ ).

**$^1\text{H-NMR}$ :** (360 MHz,  $\text{CDCl}_3$ ):  $\delta$  7.16-7.31 (*m*, 5H, Ph), 2.66 (*t*, 2H,  $^3J_{\text{HH}} = 7.0$  Hz,  $\text{CH}_2(\text{CH}_2)_3\text{Rf}_6$ ), 2.01-2.17 (*m*, 2H,  $(\text{CH}_2)_3\text{CH}_2\text{Rf}_6$ ), 1.61-1.76 (*m*, 4H,  $\text{CH}_2\text{CH}_2\text{CH}_2\text{CH}_2\text{Rf}_6$ ).

**$^{13}\text{C-NMR}$ :** (90.55 MHz,  $\text{CDCl}_3$ ):  $\delta$  141.64 (Ph), 128.42 (Ph), 128.34 (Ph), 125.97 (Ph), 107.32 – 119.24 ( $\text{Rf}_6$ ), 35.54 ( $\text{CH}_2(\text{CH}_2)_3\text{Rf}_6$ ), 30.88 ( $\text{CH}_2\text{CH}_2\text{CH}_2\text{CH}_2\text{Rf}_6$ ), 30.73 (*t*,  $^2J_{\text{CF}} = 22.1$  Hz,  $(\text{CH}_2)_3\text{CH}_2\text{Rf}_6$ ), 19.82 (*t*,  $^3J_{\text{CF}} = 3.6$  Hz,  $\text{CH}_2\text{CH}_2\text{CH}_2\text{CH}_2\text{Rf}_6$ ).

**EI-MS:**  $m/z$  (% int.): 552.8 ( $\text{M}^{*+}$ , 20 %), 90.8 ( $[\text{M-Rf}_{3,6}]^{*+}$ , 100 %).

### 21.5.3 1-Bromo-4-(5,5,6,6,7,7,8,8,9,9,10,10,10-tridecafluoro-3-iododecyl)benzene



The synthesis was carried out following **method G** using compound **46** (1.2 g, 5.7 mmol), **90b** (2.6 g, 5.9 mmol), aq. 30%  $\text{Na}_2\text{S}_2\text{O}_5$  (1 mL) and AIBN (19 mg, 0.11 mmol). The reaction was stirred at 80 °C for 4 hours before a quenching with water (10 mL) was done. The formed emulsion was extracted with  $\text{CH}_2\text{Cl}_2$  (3 x 25 mL). The combined organic fractions were dried over  $\text{Na}_2\text{SO}_4$  and all volatiles were removed yielding compound **84b** as colourless oil in quantitative yield (3.67 g, 98 %).

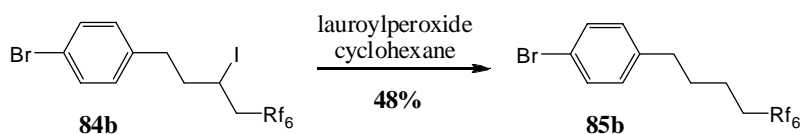
**TLC:**  $R_f$  = 0.81 (silica gel, pentane,  $\text{KMnO}_4$ ).

**$^1\text{H-NMR}$ :** (360 MHz,  $\text{CDCl}_3$ ):  $\delta$  7.41 (*d*, 2H,  $^3J_{\text{HH}} = 8.2$  Hz, Ph), 7.09 (*d*, 2H,  $^3J_{\text{HH}} = 8.2$  Hz, Ph), 4.23 (*tt*, 1H,  $^3J_{\text{HH}} = 8.9$  Hz,  $^3J_{\text{HH}} = 4.5$  Hz,  $\text{CH}_2\text{CH}_2\text{CHICH}_2\text{Rf}_6$ ), 2.64-3.04 (*m*, 4H,  $\text{CH}_2\text{CH}_2\text{CHICH}_2\text{Rf}_6$ ), 2.04-2.12 (*m*, 2H,  $\text{CH}_2\text{CH}_2\text{CHICH}_2\text{Rf}_6$ ).

**$^{13}\text{C-NMR}$ :** (90.55 MHz,  $\text{CDCl}_3$ ):  $\delta$  138.78 (Ph), 131.70 (Ph), 130.24 (Ph), 120.21 (Ph), 107.56-121.07 ( $\text{Rf}_6$ ), 41.69 (*t*,  $^2J_{\text{CF}} = 21.1$  Hz,  $\text{CH}_2\text{CH}_2\text{CHICH}_2\text{Rf}_6$ ), 41.42 ( $\text{CH}_2\text{CH}_2\text{CHICH}_2\text{Rf}_6$ ), 35.13 ( $\text{CH}_2\text{CH}_2\text{CHICH}_2\text{Rf}_6$ ), 19.71 ( $\text{CH}_2\text{CH}_2\text{CHICH}_2\text{Rf}_6$ ).

**EI-MS:**  $m/z$  (% int.): 656.9 ( $\text{M}^{*+}$ , 4 %), 529.6 ( $[\text{M-I}]^{*+}$ , 12 %), 130.9 ( $[\text{M-C}_3\text{H}_5\text{IRf}_6]^{*+}$ , 100 %), 91.0 ( $[\text{M-C}_3\text{H}_5\text{IRf}_6\text{-Br}]^{*+}$ , 72 %).

## 21.5.4 1-Bromo-4-(5,5,6,6,7,7,8,8,9,9,10,10,10-tridecafluorodecyl)benzene



A two necked round bottomed flask was fitted with a reflux condenser, septum and precautions for inert atmosphere were taken. Compound **84b** (1.0 g, 1.5 mmol) was deoxygenated separately, diluted with cyclohexane (15 mL) and syringed into the prepared two necked flask. This solution was heated for 20 minutes at 50 °C before lauroylperoxide (102 mg, 0.26 mmol) was added. The reaction mixture was stirred at 85 °C for 24 hours. All volatiles were removed under reduce pressure yielding a crude oil. Column chromatography purification over silica gel using pentane as eluent afforded the desired compound **85b** as colourless oil in moderate yield (390 mg, 48 %).

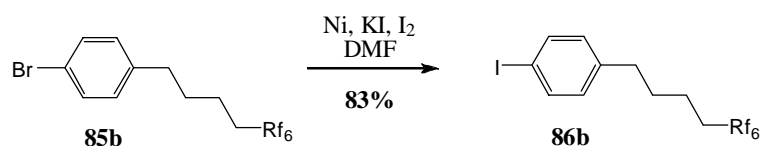
**TLC:** R<sub>f</sub> = 0.63 (silica gel, pentane, KMnO<sub>4</sub>).

**<sup>1</sup>H-NMR:** (360 MHz, CDCl<sub>3</sub>): δ 7.41 (*d*, 2H, <sup>3</sup>J<sub>HH</sub> = 8.2 Hz, Ph), 7.05 (*d*, 2H, <sup>3</sup>J<sub>HH</sub> = 8.2 Hz, Ph), 2.61 (*t*, 2H, <sup>3</sup>J<sub>HH</sub> = 7.0 Hz, CH<sub>2</sub>(CH<sub>2</sub>)<sub>3</sub>Rf<sub>6</sub>), 2.01-2.15 (*m*, 2H, (CH<sub>2</sub>)<sub>3</sub>CH<sub>2</sub>Rf<sub>6</sub>), 1.61-1.73 (*m*, 4H, CH<sub>2</sub>CH<sub>2</sub>CH<sub>2</sub>CH<sub>2</sub>Rf<sub>6</sub>).

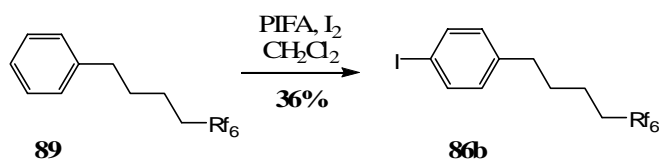
**<sup>13</sup>C-NMR:** (90.55 MHz, CDCl<sub>3</sub>): δ 140.55 (Ph), 131.49 (Ph), 130.08 (Ph), 119.73 (Ph), 108.04-121.99 (Rf<sub>6</sub>), 34.94 (CH<sub>2</sub>(CH<sub>2</sub>)<sub>3</sub>Rf<sub>6</sub>), 30.69 (CH<sub>2</sub>CH<sub>2</sub>CH<sub>2</sub>CH<sub>2</sub>Rf<sub>6</sub>), 30.69 (*t*, <sup>2</sup>J<sub>CF</sub> = 22.5 Hz, (CH<sub>2</sub>)<sub>3</sub>CH<sub>2</sub>Rf<sub>6</sub>), 19.75 (*t*, <sup>3</sup>J<sub>CF</sub> = 3.6 Hz, CH<sub>2</sub>CH<sub>2</sub>CH<sub>2</sub>CH<sub>2</sub>Rf<sub>6</sub>).

**EI-MS:** m/z (% int.): 530.7 (M<sup>+</sup>, 28 %), 168.9 ([M-Rf<sub>3,6</sub>]<sup>+</sup>, 100 %), 91.0 ([M-Br-Rf<sub>3,6</sub>]<sup>+</sup>, 68 %).

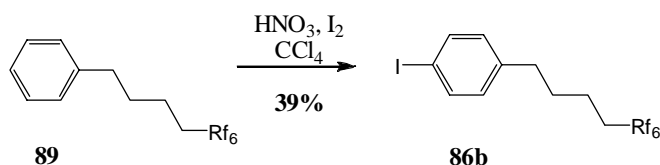
## 21.5.5 1-Iodo-4-(5,5,6,6,7,7,8,8,9,9,10,10,10-tridecafluorodecyl)benzene

a) Halogen exchange of bromoaryl **85b**

The halogen exchange was performed following **method F** using compound **85b** (0.1 g, 0.19 mmol), Ni (54.8 mg, 0.94 mmol), KI (62 mg, 0.38 mmol), iodine (2.3 mg, 9.34 μmol), DMF (0.5 mL). The suspension was heated for 27 hours at 150 °C before the crude mixture was extracted with pentane (3 x 20 mL). The combined organic fractions were washed with 10% HCl (10 mL) and H<sub>2</sub>O (10 mL), dried over Na<sub>2</sub>SO<sub>4</sub> and all volatiles were removed. The obtained brown oil was filtered over a silica gel plug under reduced pressure using pentane as eluent affording the desired compound **86b** in good yield (90 mg, 83 %).

b) Iodination of aryl **89** $\alpha$ ) using PIFA

An oven dried Schlenk tube was charged under inert atmosphere with  $I_2$  (120 mg, 0.5 mmol) and [bis(trifluoroacetoxy)iodo]benzene (PIFA, 240 mg, 0.55 mmol). The starting compound **89** (452 mg, 1 mmol) was separately deoxygenated, diluted with  $CH_2Cl_2$  (7 mL) and syringed in the Schlenk reaction vessel. The Schlenk tube was covered with aluminium foil as light protection and the solution was stirred at room temperature for 24 hours. The crude reaction mixture was diluted with  $CH_2Cl_2$  (50 mL) and extracted with a saturated solution of  $Na_2S_2O_3$  (3 x 30 mL), washed with water (3 x 30 mL) and dried over  $Na_2SO_4$ . Evaporation of the volatiles under reduced pressure yielded a slightly violet waxy solid, which was purified by column chromatography over silica gel using pentane as eluent yielding the desired compound **86b** in moderate yield (208 mg, 36%)

 $\beta$ ) using  $HNO_3$ **Method L**

A two necked flask was fitted with a reflux condenser, a septum and a dropping funnel and was set under inert atmosphere.  $I_2$  (6.7 g, 26.5 mmol) was added under a positive pressure of nitrogen and was dissolved by the addition of  $CCl_4$  (50 mL). Compound **89** (20 g, 44.2 mmol) was separately deoxygenated, diluted with  $CCl_4$  (20 mL) and syringed to the iodine solution. The inert gas inlet was replaced with a bubbler counter. The reaction mixture was heated to 50 °C before fuming  $HNO_3$  (4.0 mL, 97.26 mmol) was syringed in, and was then stirred at 90 °C for 18 hours until a second portion of  $I_2$  (1.3 g, 5.1 mmol) and fuming  $HNO_3$  (2 mL, 48.63 mmol) was added. Stirring at 90 °C was continued for 6 hours. The reaction mixture was allowed returning to room temperature and was diluted with  $CH_2Cl_2$  (100 mL). Extraction with a saturated solution of  $Na_2S_2O_3$  (3 x 50 mL), washing with water (3 x 50 mL) and drying of the organic phase over  $Na_2SO_4$  afforded after evaporation of all volatiles a dark yellow oil. Column chromatography purification on silica gel using pentane as eluent was performed and repeated 7 times to yield finally the desired pure compound **86b** as slightly violet oil (9.9 g 39%).

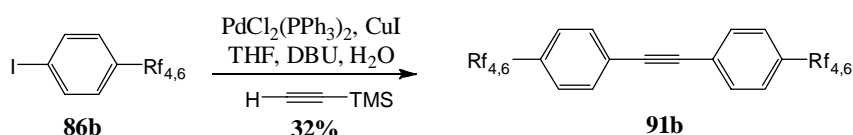
**TLC:** Rf = 0.65 (silica gel, pentane, KMnO<sub>4</sub>).

**<sup>1</sup>H-NMR:** (360 MHz, CDCl<sub>3</sub>): δ 7.61 (*d*, 2H, <sup>3</sup>J<sub>HH</sub> = 8.2 Hz, Ph), 6.93 (*d*, 2H, <sup>3</sup>J<sub>HH</sub> = 8.2 Hz, Ph), 2.60 (*t*, 2H, <sup>3</sup>J<sub>HH</sub> = 7.04 Hz, CH<sub>2</sub>(CH<sub>2</sub>)<sub>3</sub>Rf<sub>6</sub>), 2.00-2.15 (*m*, 2H, (CH<sub>2</sub>)<sub>3</sub>CH<sub>2</sub>Rf<sub>6</sub>), 1.61-1.71 (*m*, 4H, CH<sub>2</sub>CH<sub>2</sub>CH<sub>2</sub>CH<sub>2</sub>Rf<sub>6</sub>).

**<sup>13</sup>C-NMR:** (90.55 MHz, CDCl<sub>3</sub>): δ 141.22 (Ph), 137.47 (Ph), 130.44 (Ph), 107.65-121.84 (Rf<sub>6</sub>), 90.98 (Ph), 35.03 (CH<sub>2</sub>(CH<sub>2</sub>)<sub>3</sub>Rf<sub>6</sub>), 30.68 (*t*, <sup>2</sup>J<sub>CF</sub> = 22.5 Hz, (CH<sub>2</sub>)<sub>3</sub>CH<sub>2</sub>Rf<sub>6</sub>), 30.65 (CH<sub>2</sub>CH<sub>2</sub>CH<sub>2</sub>CH<sub>2</sub>Rf<sub>6</sub>), 19.76 (*t*, <sup>3</sup>J<sub>CF</sub> = 3.6 Hz, CH<sub>2</sub>CH<sub>2</sub>CH<sub>2</sub>CH<sub>2</sub>Rf<sub>6</sub>).

**EI-MS:** m/z (% int.): 578.8 (M<sup>+</sup>, 46 %), 216.9 ([M-Rf<sub>3,6</sub>]<sup>+</sup>, 100 %), 89.9 ([M-I-Rf<sub>3,6</sub>]<sup>+</sup>, 82 %).

21.5.6 1-(5,5,6,6,7,7,8,8,9,9,10,10,10-Tridecafluorodecyl)-4-[[4-(5,5,6,6,7,7,8,8,9,9,10,10,10-tridecafluorodecyl)phenyl]ethynyl]benzene



The synthesis was performed accordingly to **method A**. Compound **86b** (9.9 g, 17.12 mmol), CuI (326 mg, 1.71 mmol), PdCl<sub>2</sub>(PPh<sub>3</sub>)<sub>2</sub> (721 mg, 1.03 mmol), DBU (15.35 mL, 103 mmol), H<sub>2</sub>O (123 μL, 6.85 mmol), TMSA (1.32 mL, 9.08 mmol) and THF (80 mL) were used as reagents. After 28 hours of reaction at 65 °C the black reaction mixture was allowed to cool to room temperature before ether (400 mL) was added. The crude suspension was then washed with H<sub>2</sub>O (2x 300 mL), 10% HCl (100 mL), brine (100 mL) and H<sub>2</sub>O (100 mL). The combined organic fractions were dried over Na<sub>2</sub>SO<sub>4</sub> and all volatiles were removed yielding a brown solid which was dissolved in ether – pentane 9:1 (400 mL) and filtered over a plug of basic alox under reduced pressure. After evaporation of all volatiles a yellow solid was obtained which was further purified by recrystallization from pentane – ether – ethanol yielding the title compound **91b** as an off-white solid in moderate yield (3.5 g, 32%).

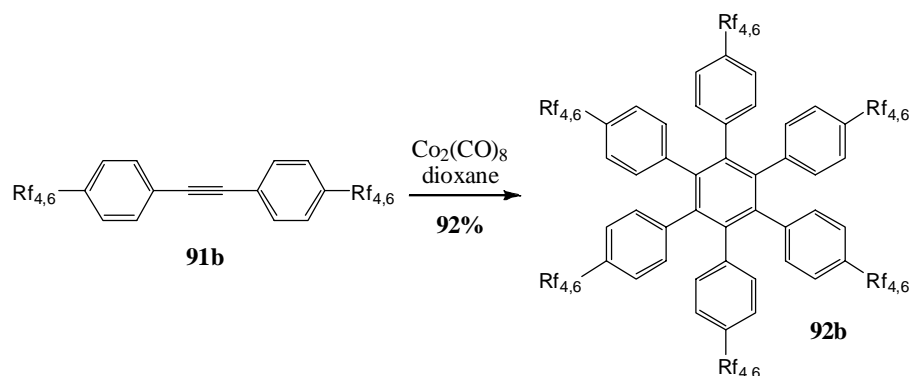
**TLC:** Rf = 0.95 (silica gel, pentane – ethyl acetate (4:1), KMnO<sub>4</sub>).

**<sup>1</sup>H-NMR:** (500 MHz, CDCl<sub>3</sub>): δ 7.45 (*d*, 4H, <sup>3</sup>J<sub>HH</sub> = 8.1 Hz, Ph), 7.15 (*d*, 4H, <sup>3</sup>J<sub>HH</sub> = 8.1 Hz, Ph), 2.67 (*t*, 4H, <sup>3</sup>J<sub>HH</sub> = 7.5 Hz, CH<sub>2</sub>(CH<sub>2</sub>)<sub>3</sub>Rf<sub>6</sub>), 2.05–2.14 (*m*, 4H, (CH<sub>2</sub>)<sub>3</sub>CH<sub>2</sub>Rf<sub>6</sub>), 1.68-1.76 (*m*, 8H, CH<sub>2</sub>CH<sub>2</sub>CH<sub>2</sub>CH<sub>2</sub>Rf<sub>6</sub>).

**<sup>13</sup>C-NMR:** (125 MHz, CDCl<sub>3</sub>): 141.89 (Ph), 131.65 (Ph), 128.37 (Ph), 121.00 (Ph), 105.63-121.06 (Rf<sub>6</sub>), 88.96 (acetylene), 35.45 (CH<sub>2</sub>(CH<sub>2</sub>)<sub>3</sub>Rf<sub>6</sub>), 30.72 (*t*, <sup>2</sup>J<sub>CF</sub> = 22.1 Hz, (CH<sub>2</sub>)<sub>3</sub>CH<sub>2</sub>Rf<sub>6</sub>), 30.62 (CH<sub>2</sub>CH<sub>2</sub>CH<sub>2</sub>CH<sub>2</sub>Rf<sub>6</sub>), 19.79 (CH<sub>2</sub>CH<sub>2</sub>CH<sub>2</sub>CH<sub>2</sub>Rf<sub>6</sub>).

**EI-MS:** m/z (% int.): 928.0 (M<sup>+</sup>, 20 %), 565.9 ([M-Rf<sub>3,6</sub>]<sup>+</sup>, 100 %).

## 21.5.7 Hexakis[4-(5,5,6,6,7,7,8,8,9,9,10,10,10-tridecafluorodecyl)phenyl]benzene



The synthesis was performed following **method B**. Tolane **91b** (2.8 g, 3.02 mmol) and  $\text{Co}_2(\text{CO})_8$  (62.16 mg, 0.18 mmol) were used as reagents in dioxane (180 mL). The reaction mixture was heated to 110 °C for 60 hours before the mixture was cooled down to room temperature and all volatiles were removed yielding a brown solid. Filtration through a plug of silica gel under reduced pressure using ether as solvent removed all traces of the catalyst and yielded a yellow solid which was recrystallized from ether – ethanol. The obtained slightly yellow compound **92b** was suspended in pentane using an ultrasonic bath and suction filtration over Millipore<sup>®</sup> afforded the HPB derivative **92b** as white solid in very good yield (2.57 g, 92%).

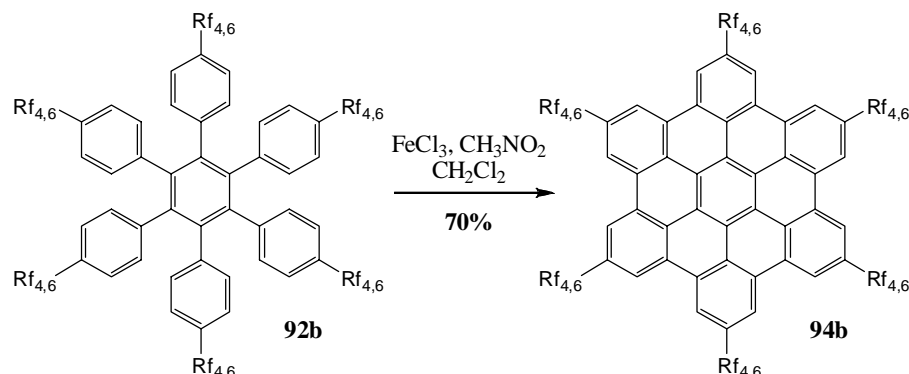
**TLC:**  $R_f$  = 0.19 (silica gel, pentane – ethyl acetate (9:1),  $\text{KMnO}_4$ ).

**<sup>1</sup>H-NMR:** (500 MHz,  $\text{CDCl}_3$ ):  $\delta$  = 6.68 (*d*, 12H,  $^3J_{\text{HH}}$  = 7.9 Hz, Ph), 6.62 (*d*, 12H,  $^3J_{\text{HH}}$  = 7.9 Hz, Ph), 2.39 (*t*, 12H,  $^3J_{\text{HH}}$  = 7.0 Hz,  $\text{CH}_2(\text{CH}_2)_3\text{Rf}_6$ ), 1.89-2.04 (*m*, 12H,  $(\text{CH}_2)_3\text{CH}_2\text{Rf}_6$ ), 1.46-1.53 (*m*, 12H,  $\text{CH}_2\text{CH}_2\text{CH}_2\text{CH}_2\text{Rf}_6$ ), 1.34-1.45 (*m*, 12H,  $\text{CH}_2\text{CH}_2\text{CH}_2\text{CH}_2\text{Rf}_6$ ).

**<sup>13</sup>C-NMR:** (125 MHz,  $\text{CDCl}_3$ ): 140.19 (Ph), 138.53 (Ph), 137.85 (Ph), 131.58 (Ph), 126.45 (Ph), 108.07-121.19 ( $\text{Rf}_6$ ), 34.62 ( $\text{CH}_2(\text{CH}_2)_3\text{Rf}_6$ ), 30.55 (*t*,  $^2J_{\text{CF}}$  = 22.5 Hz,  $(\text{CH}_2)_3\text{CH}_2\text{Rf}_6$ ), 30.38 ( $\text{CH}_2\text{CH}_2\text{CH}_2\text{CH}_2\text{Rf}_6$ ), 18.96 ( $\text{CH}_2\text{CH}_2\text{CH}_2\text{CH}_2\text{Rf}_6$ ).

**MALDI-ICR-MS (DCTB):**  $m/z$  (% int.): 2779.45 ( $\text{M}^{+}$ , 100%).

21.5.8 2,5,8,11,14,17-Hexakis(5,5,6,6,7,7,8,8,9,9,10,10,10-tridecafluorodecyl)hexabenzocoronene  
[bc,ef,hi,kl,no,q]coronene



The synthesis was performed following **method C** taking HPB **92b** (1.0 g, 0.36 mmol), FeCl<sub>3</sub> (1.40 g, 8.63 mmol, 2 eq / H to be removed), CH<sub>3</sub>NO<sub>2</sub> (20 mL) and CH<sub>2</sub>Cl<sub>2</sub> (50 mL) as starting materials. After 22 hours of reaction the mixture was quenched with methanol (50 mL). The dark precipitate was collected by suction filtration over Millipore<sup>®</sup> and was suspended successively in common organic solvents (methanol, nitromethane, ether, and trifluorobenzene), treated in an ultrasonic bath for 30 minutes and passed over Millipore<sup>®</sup> yielding a brown solid. Reprecipitation from hexafluorobenzene (3 mL / 100 mg) with methanol and ether afforded after suction filtration over Millipore<sup>®</sup> HBC **94b** as bright yellow solid in very good yield (697 mg, 70%).

**<sup>1</sup>H-NMR:** (360 MHz, CDCl<sub>3</sub>): 8.73 (br. s, 12H, Ph), 3.38 (br. s, 12H, CH<sub>2</sub>(CH<sub>2</sub>)<sub>3</sub>Rf<sub>6</sub>), 2.52 (br. s, 12H, (CH<sub>2</sub>)<sub>3</sub>CH<sub>2</sub>Rf<sub>6</sub>), 2.37 (br. s, 12H, CH<sub>2</sub>CH<sub>2</sub>CH<sub>2</sub>CH<sub>2</sub>Rf<sub>6</sub>), 2.22 (br. s, 12H, CH<sub>2</sub>CH<sub>2</sub>CH<sub>2</sub>CH<sub>2</sub>Rf<sub>6</sub>).

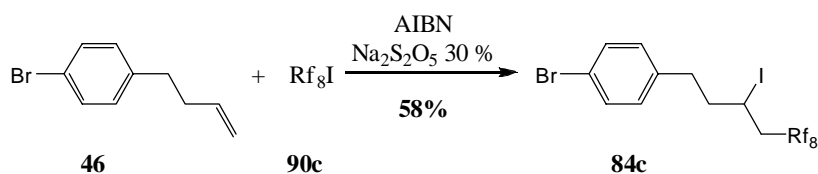
**MALDI-ICR-MS (DCTB):** m/z (% int.): 2766.33 (M<sup>•+</sup>, 100%; calcd. for C<sub>102</sub>H<sub>60</sub>F<sub>78</sub> 2766.34), 2406.29 ([M-Rf<sub>3,6</sub>]<sup>•+</sup>, 10%), 2045.32 ([M-2 x Rf<sub>3,6</sub>]<sup>•+</sup>, 5%), 1684.27 ([M-3 x Rf<sub>3,6</sub>]<sup>•+</sup>, 4%), 1322.24 ([M-4 x Rf<sub>3,6</sub>]<sup>•+</sup>, 3%), 961.21 ([M-5 x Rf<sub>3,6</sub>]<sup>•+</sup>, 2%).

**UV/VIS:** (BTF, 10<sup>-6</sup> M, ε = 1.4 · 10<sup>5</sup>), λ<sub>max</sub> = 344, 360, 390 nm.



21.6 Synthesis of HBC-(Rf<sub>4,8</sub>)<sub>6</sub>

## 21.6.1 1-Bromo-4-(5,5,6,6,7,7,8,8,9,9,10,10,11,11,12,12,12-heptafluoro-3-iodododecyl)-benzene



The synthesis was carried out using **method G**. Bromoaryl **46** (6.02 g, 35.34 mmol), Rf<sub>8</sub>I (**90c**, 18.83 g, 34.48 mmol), AIBN (230 mg, 1.39 mmol) and a 30% aq. sol. of Na<sub>2</sub>S<sub>2</sub>O<sub>5</sub> (2.3 mL) were used. The obtained emulsion was stirred at 80 °C for 2 hours before water (50 mL) was added. The cold reaction mixture was extracted with ether (3 x 150 mL), dried over Na<sub>2</sub>SO<sub>4</sub> and all volatiles were removed under reduced pressure yielding compound **84c** as colourless oil (15.14 g, 58%).

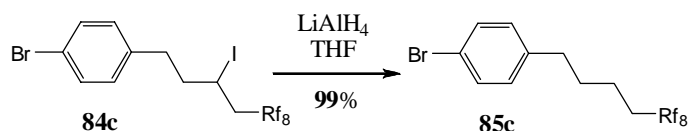
**TLC:** R<sub>f</sub> = 0.95 (silica gel, pentane, KMnO<sub>4</sub>).

**<sup>1</sup>H-NMR:** (360 MHz, CDCl<sub>3</sub>): δ = 7.42 (*d*, 2H, <sup>3</sup>J<sub>HH</sub> = 8.2 Hz, Ph), 7.08 (*d*, 2H, <sup>3</sup>J<sub>HH</sub> = 8.2 Hz, Ph), 4.23 (*tt*, 1H, <sup>3</sup>J<sub>HH</sub> = 8.2 Hz, <sup>3</sup>J<sub>HH</sub> = 5.0 Hz, CH<sub>2</sub>CH<sub>2</sub>CHICH<sub>2</sub>Rf<sub>8</sub>), 2.67-3.02 (*m*, 2H, CH<sub>2</sub>CH<sub>2</sub>CHICH<sub>2</sub>Rf<sub>8</sub>), 2.66 (*t*, 2H, <sup>3</sup>J<sub>HH</sub> = 8.2 Hz, CH<sub>2</sub>CH<sub>2</sub>CHICH<sub>2</sub>Rf<sub>8</sub>), 2.04-2.12 (*m*, 2H, CH<sub>2</sub>CH<sub>2</sub>CHICH<sub>2</sub>Rf<sub>8</sub>).

**<sup>13</sup>C-NMR:** (90.55 MHz, CDCl<sub>3</sub>): 138.80 (Ph), 131.70 (Ph), 130.24 (Ph), 120.23 (Ph), 107.21-119.55 (Rf<sub>8</sub>), 41.72 (*t*, <sup>2</sup>J<sub>CF</sub> = 22.5 Hz, CH<sub>2</sub>CH<sub>2</sub>CHICH<sub>2</sub>Rf<sub>8</sub>), 41.44 (CH<sub>2</sub>CH<sub>2</sub>CHICH<sub>2</sub>Rf<sub>8</sub>), 35.15 (CH<sub>2</sub>CH<sub>2</sub>CHICH<sub>2</sub>Rf<sub>8</sub>), 19.72 (*t*, <sup>3</sup>J<sub>CF</sub> = 2.5 Hz, CH<sub>2</sub>CH<sub>2</sub>CHICH<sub>2</sub>Rf<sub>8</sub>).

**EI-MS:** *m/z* (% int.): 756.6 (M<sup>+</sup>, 2 %), 629.5 ([M-I]<sup>+</sup>, 6 %), 169.1 ([M-Rf<sub>3,8</sub>-I]<sup>+</sup>, 6 %).

## 21.6.2 1-Bromo-4-(5,5,6,6,7,7,8,8,9,9,10,10,11,11,12,12,12-heptafluorodecyl)benzene



The synthesis was performed accordingly to **method H** taking arylbromide **84c** (34.29 g, 45.3 mmol) and LiAlH<sub>4</sub> (2.06 g, 54.4 mmol) in THF (100 mL). The grey slurry was stirred for 15 hours at room temperature before a quenching with water (7 mL), 0.2 M NaOH (7 mL) and water (21 mL) was done. The obtained suspension was Büchner filtrated. The white precipitate was exhaustively washed with ether, before the filtrate was washed with water (30 mL), dried over Na<sub>2</sub>SO<sub>4</sub> and reduced in a rotary evaporator. The obtained slightly yellow oil was filtered over a silica gel plug under reduced pressure using pentane as eluent yielding **85c** as colourless oil (28.38 g, 99%).

**TLC:** R<sub>f</sub> = 0.59 (silica gel, pentane, KMnO<sub>4</sub>).

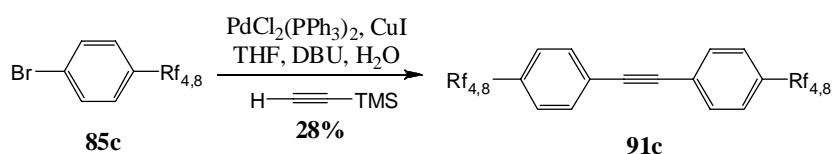
**<sup>1</sup>H-NMR:** (360 MHz, CDCl<sub>3</sub>): δ 7.37 (*d*, 2H, <sup>3</sup>J<sub>HH</sub> = 8.2 Hz, Ph), 7.02 (*d*, 2H, <sup>3</sup>J<sub>HH</sub> = 8.2 Hz, Ph), 2.63 (*t*, 2H, <sup>3</sup>J<sub>HH</sub> = 7.0 Hz, CH<sub>2</sub>(CH<sub>2</sub>)<sub>3</sub>Rf<sub>8</sub>), 2.01-2.15 (*m*, 2H, (CH<sub>2</sub>)<sub>3</sub>CH<sub>2</sub>Rf<sub>8</sub>), 1.61-1.73 (*m*, 4H, CH<sub>2</sub>CH<sub>2</sub>CH<sub>2</sub>CH<sub>2</sub>Rf<sub>8</sub>).

**<sup>13</sup>C-NMR:** (90.55 MHz, CDCl<sub>3</sub>): δ 140.54 (Ph), 131.47 (Ph), 130.04 (Ph), 119.72 (Ph), 107.08-121.97 (Rf<sub>8</sub>), 34.92 (CH<sub>2</sub>(CH<sub>2</sub>)<sub>3</sub>Rf<sub>8</sub>), 30.67 (CH<sub>2</sub>CH<sub>2</sub>CH<sub>2</sub>CH<sub>2</sub>Rf<sub>8</sub>), 30.67 (*t*, <sup>2</sup>J<sub>CF</sub> = 22.5 Hz, (CH<sub>2</sub>)<sub>3</sub>CH<sub>2</sub>Rf<sub>8</sub>), 19.75 (*t*, <sup>3</sup>J<sub>CF</sub> = 3.6 Hz, CH<sub>2</sub>CH<sub>2</sub>CH<sub>2</sub>CH<sub>2</sub>Rf<sub>8</sub>).

**EI-MS:** m/z (% int.): 631.1 (M<sup>+</sup>, 100 %).

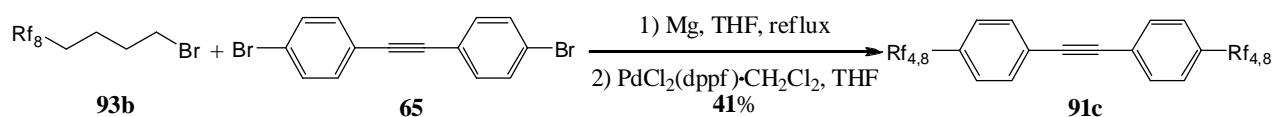
21.6.3 1-(5,5,6,6,7,7,8,8,9,9,10,10,11,11,12,12,12-Heptafluorododecyl)-4-{[4-(5,5,6,6,7,7,8,8,9,9,10,10,11,11,12,12,12-heptafluorododecyl)phenyl]ethynyl}benzene

a) Sonogashira cross-coupling of bromoaryl **85c**



The tolane formation was performed following **method A**. Compound **85c** (12.0 g, 19.2 mmol), PdCl<sub>2</sub>(PPh<sub>3</sub>)<sub>2</sub> (0.8 g, 1.14 mmol), CuI (362 mg, 1.92 mmol), DBU (17.06 mL, 0.114 mol), THF (120 mL), TMSA (1.38 mL, 9.5 mmol) and H<sub>2</sub>O (0.14 mL, 7.6 mmol) were used. The mixture was stirred at 80 °C for 35 hours before the mixture was quenched by the addition of methanol (40 mL). The mixture was extracted with CH<sub>2</sub>Cl<sub>2</sub> (4 x 300 mL). The combined organic fractions were concentrated up to 100 mL in a rotary evaporator. The obtained solution was diluted with pentane (800 mL) and filtered over basic alox. Evaporation of the filtrate yielded tolane **91c** as yellow solid. Precipitation out of ether – methanol afforded **91c** as off-white solid in moderate yield (3.0 g, 28%)

b) Kumada cross-coupling



## Method I

An oven dried Schlenk tube was charged with freshly activated magnesium turnings (0.26 g, 10.8 mmol) under inert atmosphere. The magnesium was stirred under vacuum for 1 hour and heated three times with a heat gun. As soon as the reaction vessel reached room temperature THF (5 mL) was syringed in under argon. Compound **93b** (5.0 g, 9.0 mmol), dissolved in THF (5 mL) was syringed onto the magnesium suspension. The sealed Schlenk tube was heated to 75 °C for 24 hours.

In a second oven dried Schlenk tube  $\text{PdCl}_2(\text{dppf})\cdot\text{CH}_2\text{Cl}_2$  (260 mg, 33.8  $\mu\text{mol}$ ) and 4,4'-dibromotolane **65** (760 mg, 2.25 mmol) were suspended under inert atmosphere in THF (5 mL). The previously freshly prepared brownish Grignard solution of **93b** was diluted with THF (5 mL) and syringed in. The Schlenk tube was sealed and heated to 75 °C for 6 days. The dark brown reaction mixture was quenched by the injection of methanol (20 mL). The obtained suspension was diluted with the addition of  $\text{CH}_2\text{Cl}_2$  (200 mL), extracted with a saturated  $\text{NH}_4\text{Cl}$  solution (50 mL) and washed with  $\text{H}_2\text{O}$  (50 mL). All volatiles were removed yielding a brown solid which was suspended in  $\text{CH}_2\text{Cl}_2$  (10 mL). Suction filtration over Millipore<sup>®</sup> afforded after several repetitions the desired compound **91c** as off-white solid in moderate yield (1.04 g, 41 %).

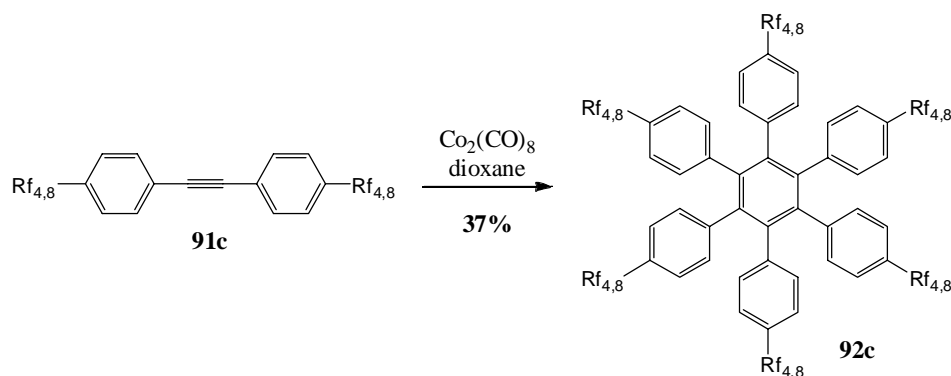
**TLC:**  $R_f = 0.05$  (silica gel, pentane – ether (9:1),  $\text{KMnO}_4$ ).

**$^1\text{H-NMR}$ :** (360 MHz,  $\text{CDCl}_3$ ):  $\delta$  7.45 (*d*, 4H,  $^3J_{\text{HH}} = 7.7$  Hz, Ph), 7.15 (*d*, 4H,  $^3J_{\text{HH}} = 7.7$  Hz, Ph), 2.67 (*t*, 4H,  $^3J_{\text{HH}} = 7.0$  Hz,  $\text{CH}_2(\text{CH}_2)_3\text{Rf}_8$ ), 2.0-2.16 (*m*, 4H,  $(\text{CH}_2)_3\text{CH}_2\text{Rf}_8$ ), 1.63-1.77 (*m*, 8H,  $\text{CH}_2\text{CH}_2\text{CH}_2\text{CH}_2\text{Rf}_8$ ).

**$^{13}\text{C-NMR}$ :** (125.77 MHz,  $\text{CDCl}_3$ ):  $\delta$  141.89 (Ph), 131.62 (Ph), 128.37 (Ph), 120.94 (Ph), 106.54-119.46 ( $\text{Rf}_8$ ), 88.93 (acetylene), 35.44 ( $\text{CH}_2(\text{CH}_2)_3\text{Rf}_8$ ), 30.95 (*t*,  $^3J_{\text{CF}} = 21.9$  Hz,  $(\text{CH}_2)_3\text{CH}_2\text{Rf}_8$ ), 30.62 ( $\text{CH}_2\text{CH}_2\text{CH}_2\text{CH}_2\text{Rf}_8$ ), 19.77 ( $\text{CH}_2\text{CH}_2\text{CH}_2\text{CH}_2\text{Rf}_8$ ).

**MALDI-ICR-MS (DCTB):**  $m/z$  (% int.): 1377.35 ( $[\text{M}+\text{DCTB}]^{*+}$ , 35%), 1126.20 ( $\text{M}^{*+}$ , 100%).

#### 21.6.4 Hexakis[4-(5,5,6,6,7,7,8,8,9,9,10,10,11,11,12,12,12-heptafluorododecyl)phenyl]-benzene



The cyclotrimerisation was performed using **method B**. Tolane **91c** (0.2 g, 0.178  $\mu\text{mol}$ ),  $\text{Co}_2(\text{CO})_8$  (7 mg, 20  $\mu\text{mol}$ ) and dioxane (25 mL) were taken. The obtained dark brown solution was refluxed under argon for 48 hours. Removing the solvent under reduced pressure yielded the crude HPB **92c** as grey solid, which was dissolved in ether (50 mL) and extracted with HCl 15 % (2 x 25 mL). The organic phase was filtrated over a plug of silica gel under reduced pressure using ether as eluent and afforded a yellow solid after removing the solvent. Suspending the crude HPB **92c** in pentane and suction filtration over Millipore<sup>®</sup> afforded the desired HPB **92c** as off-white solid (73 mg, 37 %).

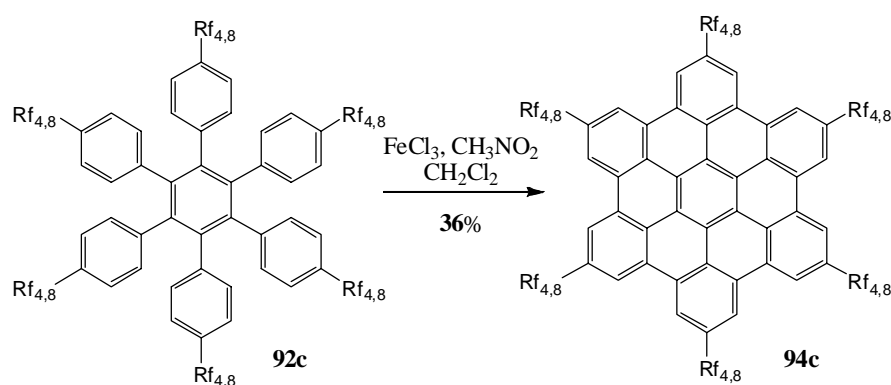
**TLC:** Rf = 95 (silica gel, pentane – ether (9:1), KMnO<sub>4</sub>).

**<sup>1</sup>H-NMR:** (360 MHz, CDCl<sub>3</sub>): δ 6.68 (br. *d*, 12H, <sup>3</sup>J<sub>HH</sub> = 8.2 Hz, Ph), 6.62 (*br d*, 12H, <sup>3</sup>J<sub>HH</sub> = 8.2 Hz, Ph), 2.39 (*t*, 12H, <sup>3</sup>J<sub>HH</sub> = 6.8 Hz, CH<sub>2</sub>(CH<sub>2</sub>)<sub>3</sub>Rf<sub>8</sub>), 1.91-2.04 (*m*, 12H, (CH<sub>2</sub>)<sub>3</sub>CH<sub>2</sub>Rf<sub>8</sub>), 1.38-1.54 (*m*, 24H, CH<sub>2</sub>CH<sub>2</sub>CH<sub>2</sub>CH<sub>2</sub>Rf<sub>8</sub>).

**<sup>13</sup>C-NMR:** (125.77 MHz, CDCl<sub>3</sub>): δ 140.16 (Ph), 138.51 (Ph), 137.84 (Ph), 131.56 (Ph), 126.44 (Ph), 106.46-119.32 (Rf<sub>8</sub>), 34.62 (CH<sub>2</sub>(CH<sub>2</sub>)<sub>3</sub>Rf<sub>8</sub>), 30.94 (CH<sub>2</sub>CH<sub>2</sub>CH<sub>2</sub>CH<sub>2</sub>Rf<sub>8</sub>), 30.52 (*t*, <sup>3</sup>J<sub>CF</sub> = 22.0 Hz, (CH<sub>2</sub>)<sub>3</sub>CH<sub>2</sub>Rf<sub>8</sub>), 20.01 (CH<sub>2</sub>CH<sub>2</sub>CH<sub>2</sub>CH<sub>2</sub>Rf<sub>8</sub>).

**MALDI-ICR-MS (DCTB):** m/z (% int.): 3378.40 (M<sup>+</sup>, 100%), 2904.23 ([M-Rf<sub>4,8</sub>]<sup>+</sup>, 15%), 2381.31 (30%), 1689.16 (71%).

21.6.5 2,5,8,11,14,17-Hexakis(5,5,6,6,7,7,8,8,9,9,10,10,11,11,12,12,12-heptafluorododecyl)-hexabenzo[bc,ef,hi,kl,no,qr]coronene



The oxidation was carried out following **method C** using HPB **92c** (50 mg, 14.8 μmol), FeCl<sub>3</sub> (216 mg, 1.33 mmol, 7.5 eq / H to be removed), CH<sub>3</sub>NO<sub>2</sub> (2 mL) and CH<sub>2</sub>Cl<sub>2</sub> (8 mL). The dark mixture was stirred at 45 °C for 16 hours under a constant bubbling of argon before a quenching with methanol (20 mL) was performed. The precipitated dark solid was collected by suction filtration over Millipore<sup>®</sup> and was then suspended successively in different solvents (methanol, ether, pentane, toluene), treated in a ultrasonic bath and collected over Millipore<sup>®</sup> yielding HBC **94c** as yellow solid in moderate yield (18 mg, 36%).

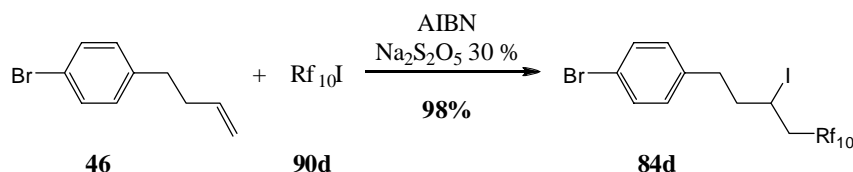
**<sup>1</sup>H-NMR:** (360 MHz, CDCl<sub>3</sub>): 9.27 (br. *s*, 12H, Ph), 3.70 (br. *s*, 12H, CH<sub>2</sub>(CH<sub>2</sub>)<sub>3</sub>Rf<sub>8</sub>), 2.60 (br. *s*, 24H, CH<sub>2</sub>CH<sub>2</sub>CH<sub>2</sub>CH<sub>2</sub>Rf<sub>8</sub>), 2.38 (br. *s*, 12H, CH<sub>2</sub>CH<sub>2</sub>CH<sub>2</sub>CH<sub>2</sub>Rf<sub>8</sub>).

**MALDI-ICR-MS (DCTB):** m/z (% int.): 3366.40 (M<sup>+</sup>, 100%; calcd. for C<sub>114</sub>H<sub>60</sub>F<sub>102</sub> 3366.31), 2906.46 ([M-Rf<sub>3,8</sub>]<sup>+</sup>, 46 %), 2445.39 ([M-2 x Rf<sub>3,8</sub>]<sup>+</sup>, 12 %), 1984.28 ([M-3 x Rf<sub>3,8</sub>]<sup>+</sup>, 4 %).

**UV/VIS:** (BTF, 10<sup>-5</sup> M, ε = 4.3 · 10<sup>4</sup>), λ<sub>max</sub> = 356, 409 nm.

21.7 Synthesis of HBC-(Rf<sub>4,10</sub>)<sub>6</sub>

## 21.7.1 1-Bromo-4-(5,5,6,6,7,7,8,8,9,9,10,10,11,11,12,12,13,13,14,14,14-henicosafluoro-3-iodotetradecyl)benzene



The synthesis was performed according to **method G**, using **46** (4.45 g, 21.1 mmol), **90d** (15 g, 23.2 mmol), AIBN (70 mg, 0.42 mmol) and 30% Na<sub>2</sub>S<sub>2</sub>O<sub>5</sub> (5 mL). The mixture was stirred for 8 hours at 90 °C before an extraction with ether was performed. The combined organic fractions were dried over Na<sub>2</sub>SO<sub>4</sub> and all volatiles were removed yielding **84d** as white solid (18.9 g, 98%).

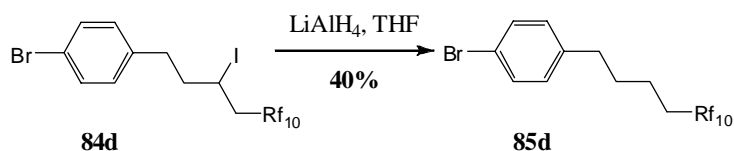
**TLC:** R<sub>f</sub> = 0.91 (silica gel, pentane, KMnO<sub>4</sub>).

**<sup>1</sup>H-NMR:** (360 MHz, CDCl<sub>3</sub>): δ 7.43 (*d*, 2H, <sup>3</sup>J<sub>HH</sub> = 8.2 Hz, Ph), 7.09 (*d*, 2H, <sup>3</sup>J<sub>HH</sub> = 8.2 Hz, Ph), 4.23 (*tt*, 1H, <sup>3</sup>J<sub>HH</sub> = 8.6 Hz, <sup>3</sup>J<sub>HH</sub> = 5.0 Hz, CH<sub>2</sub>CH<sub>2</sub>CHICH<sub>2</sub>Rf<sub>10</sub>), 2.65-3.04 (*m*, 2H, CH<sub>2</sub>CH<sub>2</sub>CHICH<sub>2</sub>Rf<sub>10</sub>), 2.65-2.73 (*m*, 2H, CH<sub>2</sub>CH<sub>2</sub>CHICH<sub>2</sub>Rf<sub>10</sub>), 2.05-2.12 (*m*, 2H, CH<sub>2</sub>CH<sub>2</sub>CHICH<sub>2</sub>Rf<sub>10</sub>).

**<sup>13</sup>C-NMR:** (90.55 MHz, CDCl<sub>3</sub>): 138.78 (Ph), 131.70 (Ph), 130.24 (Ph), 120.21 (Ph), 108.37-121.10 (Rf<sub>10</sub>), 41.71 (*t*, <sup>2</sup>J<sub>CF</sub> = 21.1 Hz, CH<sub>2</sub>CH<sub>2</sub>CHICH<sub>2</sub>Rf<sub>10</sub>), 41.42 (CH<sub>2</sub>CH<sub>2</sub>CHICH<sub>2</sub>Rf<sub>10</sub>), 35.14 (CH<sub>2</sub>CH<sub>2</sub>CHICH<sub>2</sub>Rf<sub>10</sub>), 19.74 (CH<sub>2</sub>CH<sub>2</sub>CHICH<sub>2</sub>Rf<sub>10</sub>).

**EI-MS:** m/z (% int.): 857.5 (M<sup>+</sup>, 1 %), 730.3 ([M-I]<sup>+</sup>, 4 %), 168.9 ([M-Rf<sub>3,10</sub>]<sup>+</sup>, 100 %).

## 21.7.2 1-Bromo-4-(5,5,6,6,7,7,8,8,9,9,10,10,11,11,12,12,13,13,14,14,14-henicosafluorotetradecyl)benzene



The elimination of the iodine was performed by applying **method H**, using compound **84d** (18.0 g, 21 mmol), LiAlH<sub>4</sub> (797 mg, 21 mmol) and THF (50 mL). The grey emulsion was stirred at room temperature for 25 hours before water (6 mL), 0.2 M NaOH (6 mL) and water (18 mL) were added slowly. The precipitate was filtered off and washed exhaustively with ether before the filtrate was washed with water (50 mL), dried over Na<sub>2</sub>SO<sub>4</sub> and reduced maximally. Column chromatography on silica gel using pentane as eluent afforded compound **85d** as white solid (6.2 g, 40%).

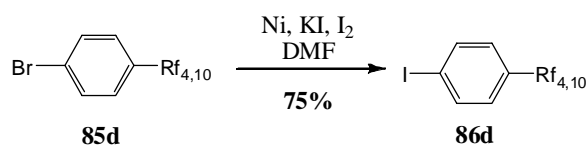
**TLC:**  $R_f$  = 0.80 (silica gel, pentane,  $\text{KMnO}_4$ ).

**$^1\text{H-NMR}$ :** (360 MHz,  $\text{CDCl}_3$ ):  $\delta$  7.41 (*d*, 2H,  $^3J_{\text{HH}}$  = 8.2 Hz, Ph), 7.04 (*d*, 2H,  $^3J_{\text{HH}}$  = 8.2 Hz, Ph), 2.61 (*t*, 2H,  $^3J_{\text{HH}}$  = 6.8 Hz,  $\text{CH}_2(\text{CH}_2)_3\text{Rf}_{10}$ ), 2.00-2.17 (*m*, 2H,  $(\text{CH}_2)_3\text{CH}_2\text{Rf}_{10}$ ), 1.63-1.76 (*m*, 4H,  $\text{CH}_2\text{CH}_2\text{CH}_2\text{CH}_2\text{Rf}_{10}$ ).

**$^{13}\text{C-NMR}$ :** (90.55 MHz,  $\text{CDCl}_3$ ): 140.54 (Ph), 131.48 (Ph), 130.08 (Ph), 119.72 (Ph), 107.77-121.88 ( $\text{Rf}_{10}$ ), 34.94 ( $\text{CH}_2(\text{CH}_2)_3\text{Rf}_{10}$ ), 30.69 ( $\text{CH}_2\text{CH}_2\text{CH}_2\text{CH}_2\text{Rf}_{10}$ ), 30.69 (*t*,  $^2J_{\text{CF}}$  = 21.1 Hz,  $(\text{CH}_2)_3\text{CH}_2\text{Rf}_{10}$ ), 19.75 (*t*,  $^3J_{\text{CF}}$  = 4.0 Hz,  $\text{CH}_2\text{CH}_2\text{CH}_2\text{CH}_2\text{Rf}_{10}$ ).

**EI-MS:**  $m/z$  (% int.): 731.8 ( $\text{M}^{++}$ , 80 %), 170.9 ( $[\text{M-Rf}_{3,10}]^{++}$ , 100 %).

### 21.7.3 1-Iodo-4-(5,5,6,6,7,7,8,8,9,9,10,10,11,11,12,12,13,13,14,14,14-henicosafuorotetradecyl)-benzene



The halogen exchange was done according to **method F**, taking compound **85d** (6.0 g, 8.2 mmol), Ni (2.4 g, 41 mmol), KI (2.7 g, 16.4 mmol), iodine (104 mg, 0.4 mmol) and DMF (25 mL). The mixture was heated to 150 °C for 24 hours. The crude reaction mixture was extracted with pentane (3 x 100 mL). The combined pentane fractions were washed with water (60 mL) and 10% HCl (100 mL). The organic fraction was filtered over a plug of silica gel under reduced pressure using pentane as eluent yielding the iodinated compound **86d** in good yield (6.2 g, 75 %).

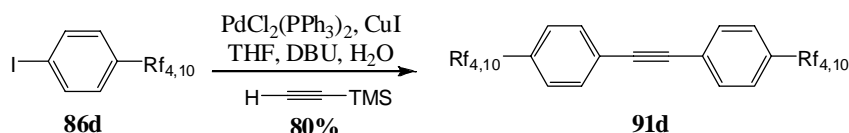
**TLC:**  $R_f$  = 0.90 (silica gel, pentane,  $\text{KMnO}_4$ ).

**$^1\text{H-NMR}$ :** (360 MHz,  $\text{CDCl}_3$ ):  $\delta$  7.60 (*d*, 2H,  $^3J_{\text{HH}}$  = 8.2 Hz, Ph), 6.92 (*d*, 2H,  $^3J_{\text{HH}}$  = 8.2 Hz, Ph), 2.59 (*t*, 2H,  $^3J_{\text{HH}}$  = 6.8 Hz,  $\text{CH}_2\text{CH}_2\text{CH}_2\text{CH}_2\text{Rf}_{10}$ ), 2.01-2.16 (*m*, 2H,  $(\text{CH}_2)_3\text{CH}_2\text{Rf}_{10}$ ), 1.64-1.75 (*m*, 4H,  $\text{CH}_2\text{CH}_2\text{CH}_2\text{CH}_2\text{Rf}_{10}$ ).

**$^{13}\text{C-NMR}$ :** (90.55 MHz,  $\text{CDCl}_3$ ): 141.26 (Ph), 137.50 (Ph), 130.44 (Ph), 107.79-121.91 ( $\text{Rf}_{10}$ ), 90.98 (Ph), 35.05 ( $\text{CH}_2(\text{CH}_2)_3\text{Rf}_{10}$ ), 30.67 ( $\text{CH}_2\text{CH}_2\text{CH}_2\text{CH}_2\text{Rf}_{10}$ ), 30.67 (*t*,  $^2J_{\text{CF}}$  = 21.8 Hz,  $(\text{CH}_2)_3\text{CH}_2\text{Rf}_{10}$ ), 19.77 (*t*,  $^3J_{\text{CF}}$  = 3.5 Hz,  $\text{CH}_2\text{CH}_2\text{CH}_2\text{CH}_2\text{Rf}_{10}$ ).

**EI-MS:**  $m/z$  (% int.): 777.9 ( $\text{M}^{++}$ , 95 %), 216.9 ( $[\text{M-Rf}_{3,10}]^{++}$ , 100 %).

21.7.4 1-(5,5,6,6,7,7,8,8,9,9,10,10,11,11,12,12,13,13,14,14,14-Henicosafuorotetradecyl)-4-{[4-(5,5,6,6,7,7,8,8,9,9,10,10,11,11,12,12,13,13,14,14,14-henicosafuorotetradecyl)phenyl]ethynyl}benzene



The synthesis was carried out following **method A** by reacting **86d** (3.76 g, 4.8 mmol),  $\text{PdCl}_2(\text{PPh}_3)_2$  (203 mg, 0.29 mmol), CuI (92 mg, 0.48 mmol), DBU (4.3 mL, 29.0 mmol), TMSA (0.35 mL, 2.4 mmol) and water (35  $\mu\text{L}$ , 1.9 mmol) in THF (40 mL) at room temperature for 2 days. The formed yellow precipitate was filtered off and reprecipitated five times in ether to afford the desired tolane **91d** as white solid in excellent yield (80%).

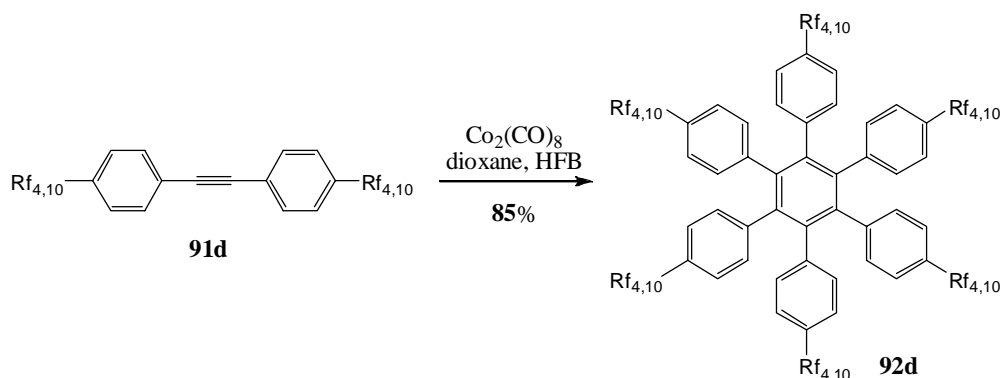
**TLC:**  $R_f = 0.60$  (silica gel, pentane – ether 1:1,  $\text{KMnO}_4$ ).

**$^1\text{H-NMR}$ :** (360 MHz,  $\text{CDCl}_3$ ):  $\delta$  7.45 (*d*, 4H,  $^3J_{\text{HH}} = 7.7$  Hz, Ph), 7.15 (*d*, 4H,  $^3J_{\text{HH}} = 7.7$  Hz, Ph), 2.67 (*t*, 4H,  $^3J_{\text{HH}} = 6.8$  Hz,  $\text{CH}_2(\text{CH}_2)_3\text{Rf}_{10}$ ), 2.01-2.16 (*m*, 4H,  $(\text{CH}_2)_3\text{CH}_2\text{Rf}_{10}$ ), 1.64-1.75 (*m*, 8H,  $\text{CH}_2\text{CH}_2\text{CH}_2\text{CH}_2\text{Rf}_{10}$ ).

**$^{13}\text{C-NMR}$ :** (125.77 MHz,  $\text{CDCl}_3$ ): 141.89 (Ph), 131.73 (Ph), 128.37 (Ph), 121.28 (Ph), 107.79-121.91 ( $\text{Rf}_{10}$ ), 89.08 (acetylene), 35.47 ( $\text{CH}_2(\text{CH}_2)_3\text{Rf}_{10}$ ), 30.97 (*t*,  $^2J_{\text{CF}} = 22.1$  Hz,  $(\text{CH}_2)_3\text{CH}_2\text{Rf}_{10}$ ), 30.59 ( $\text{CH}_2\text{CH}_2\text{CH}_2\text{CH}_2\text{Rf}_{10}$ ), 19.93 ( $\text{CH}_2\text{CH}_2\text{CH}_2\text{CH}_2\text{Rf}_{10}$ ).

**MALDI-ICR-MS (DCTB):**  $m/z$  (% int.): 1577.27 ( $[\text{M}+\text{DCTB}]^+$ , 85 %), 1326.12 ( $\text{M}^{*+}$ , 100 %).

21.7.5 Hexakis[4-(5,5,6,6,7,7,8,8,9,9,10,10,11,11,12,12,13,13,14,14,14-henicosafuorotetradecyl)phenyl]benzene



The cyclotrimerisation was carried out using **method B** taking tolane **91d** (0.2 g, 0.15 mmol),  $\text{Co}_2(\text{CO})_8$  (4.1 mg, 12  $\mu\text{mol}$ ), dioxane (10 mL) and hexafluorobenzene (10 mL). The mixture was

refluxed for 3 days before all volatiles were removed. The brown solid was filtered over a small plug of silica gel using BTF (65 °C) as solvent, yielding HPB **92d** as white solid (164 mg, 85%).

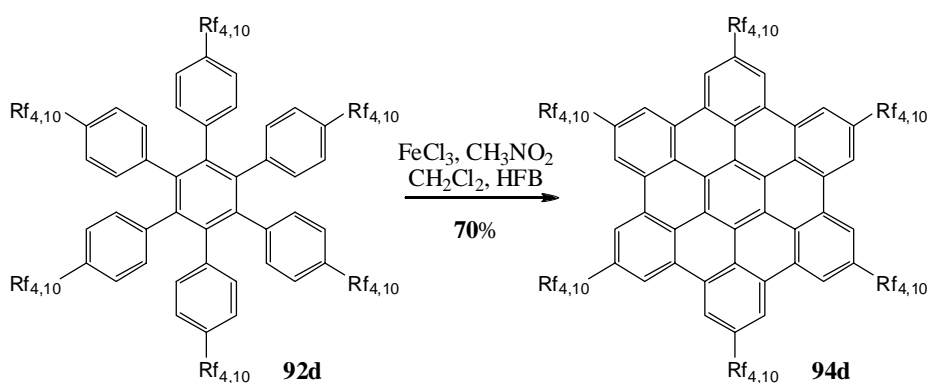
**TLC:** R<sub>f</sub> = 0.85 (silica gel, BTF, KMnO<sub>4</sub>).

**<sup>1</sup>H-NMR:** (500 MHz, CDCl<sub>3</sub>): δ 6.66 (br *d*, 12H, <sup>3</sup>J<sub>HH</sub> = 8.2 Hz, Ph), 6.60 (br *d*, 12H, <sup>3</sup>J<sub>HH</sub> = 8.2 Hz, Ph), 2.33 (*t*, 12H, <sup>3</sup>J<sub>HH</sub> = 6.8 Hz, CH<sub>2</sub>(CH<sub>2</sub>)<sub>3</sub>Rf<sub>10</sub>), 1.97-2.08 (*m*, 12H, (CH<sub>2</sub>)<sub>3</sub>CH<sub>2</sub>Rf<sub>10</sub>), 1.54-1.60 (*m*, 12H, CH<sub>2</sub>CH<sub>2</sub>CH<sub>2</sub>CH<sub>2</sub>Rf<sub>10</sub>), 1.36-1.42 (*m*, 12H, CH<sub>2</sub>CH<sub>2</sub>CH<sub>2</sub>CH<sub>2</sub>Rf<sub>10</sub>).

**<sup>13</sup>C-NMR:** (125.77 MHz, CDCl<sub>3</sub>): δ 140.33 (Ph), 138.89 (Ph), 138.44 (Ph), 131.48 (Ph), 126.43 (Ph), 108.68-120.94 (Rf<sub>10</sub>), 35.32 (CH<sub>2</sub>(CH<sub>2</sub>)<sub>3</sub>Rf<sub>10</sub>), 31.12 (CH<sub>2</sub>CH<sub>2</sub>CH<sub>2</sub>CH<sub>2</sub>Rf<sub>10</sub>), 30.83 (*t*, <sup>3</sup>J<sub>CF</sub> = 22.0 Hz, (CH<sub>2</sub>)<sub>3</sub>CH<sub>2</sub>Rf<sub>10</sub>), 20.17 (CH<sub>2</sub>CH<sub>2</sub>CH<sub>2</sub>CH<sub>2</sub>Rf<sub>10</sub>).

**MALDI-ICR-MS (DCTB):** m/z (% int.): 3978.41 (M<sup>+</sup>, 100 %).

#### 21.7.6 2,5,8,11,14,17-Hexakis[4-(5,5,6,6,7,7,8,8,9,9,10,10,11,11,12,12,13,13,14,14,14-henicosafuorotetradecyl)hexabenzob[bc,ef,hi,kl,no,qr]coronene



The synthesis was carried out similar to **method C**, taking HPB **92d** (0.1 g, 25.0 μmol), FeCl<sub>3</sub> (366 mg, 2.26 mmol, 7.5 eq / H to be removed), CH<sub>3</sub>NO<sub>2</sub> (8 mL), CH<sub>2</sub>Cl<sub>2</sub> (10 mL) and hexafluorobenzene (10 mL). The reaction mixture was heated to 37 °C and stirred under argon bubbling for 6 hours before methanol (40 mL) was added. The formed precipitate was collected by suction filtration over Millipore<sup>®</sup> and was suspended in different organic solvents (methanol, pentane, ether, dichloromethane, toluene and trifluorotoluene), shaken in an ultrasonic bath and suction filtrated over Millipore<sup>®</sup> yielding the title HBC **94d** as dark yellow solid (70 mg, 70%).

**<sup>1</sup>H-NMR:** (500 MHz, CDCl<sub>3</sub>): 9.12 (br. *s*, 12H, Ph), 3.58 (br. *s*, 12H, CH<sub>2</sub>(CH<sub>2</sub>)<sub>3</sub>Rf<sub>10</sub>), 2.52 (br. *s*, 24H, CH<sub>2</sub>CH<sub>2</sub>CH<sub>2</sub>CH<sub>2</sub>Rf<sub>10</sub>), 2.37 (br. *s*, 12H, CH<sub>2</sub>CH<sub>2</sub>CH<sub>2</sub>CH<sub>2</sub>Rf<sub>10</sub>).

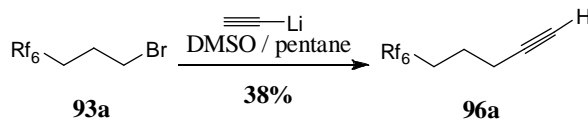
**MALDI-ICR-MS (DCTB):** m/z (% int.): 3966.22 (M<sup>+</sup>, 100%; calcd. for C<sub>126</sub>H<sub>60</sub>F<sub>126</sub> 3966.27), 3405.01 ([M-Rf<sub>3,10</sub>]<sup>+</sup>, 43 %).

**UV/VIS:** (BTF, 10<sup>-5</sup> M, ε = 4.2 · 10<sup>4</sup>), λ<sub>max</sub> = 364 nm.



21.8 Synthesis of HBC-(Rf<sub>5,6</sub>)<sub>6</sub>

## 21.8.1 6,6,7,7,8,8,9,9,10,10,11,11,11-Tridecafluoroundec-1-yne

**Method J**

Lithium acetylide ethylenediamine complex (18.2 g, 0.20 mol) was suspended in DMSO (90 mL) in a round bottomed flask under inert atmosphere. To the brown coloured suspension the brominated compound **93a** (29 g, 65.7 mmol) was added, dissolved in pentane (10 mL), at 8°C. Afterwards the black suspension was stirred at room temperature for 17 hours before the mixture was quenched by the addition of water (30 mL). The resulting suspension was diluted with CH<sub>2</sub>Cl<sub>2</sub> (100 mL), Büchner filtrated and extracted with CH<sub>2</sub>Cl<sub>2</sub> (3 x 100 mL). The combined organic phases were dried over Na<sub>2</sub>SO<sub>4</sub> and all volatiles were removed under reduced pressure. The resulting black oily liquid was filtered over a plug of silica gel under reduced pressure using pentane as eluent. After removal of pentane compound **96a** was obtained as colourless oil (9.64 g, 38%).

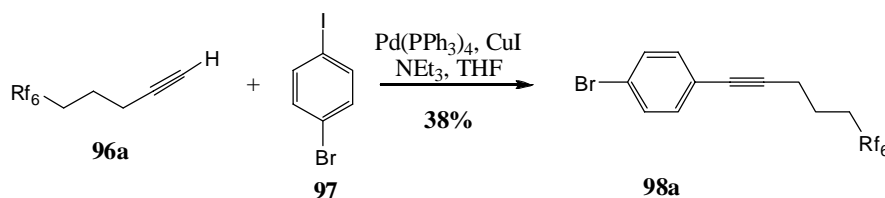
**TLC:** R<sub>f</sub> = 0.95 (silica gel, pentane, KMnO<sub>4</sub>).

**<sup>1</sup>H-NMR:** (360 MHz, CDCl<sub>3</sub>): δ 2.33 (*td*, 2H, <sup>3</sup>J<sub>HH</sub> = 6.8 Hz, <sup>4</sup>J<sub>HH</sub> = 2.7 Hz, HC≡CCH<sub>2</sub>CH<sub>2</sub>CH<sub>2</sub>Rf<sub>6</sub>), 2.16-2.28 (*m*, 2H, HC≡CCH<sub>2</sub>CH<sub>2</sub>CH<sub>2</sub>Rf<sub>6</sub>), 2.02 (*t*, 1H, <sup>4</sup>J<sub>HH</sub> = 2.7 Hz, HC≡C(CH<sub>2</sub>)<sub>3</sub>Rf<sub>6</sub>), 1.78-1.89 (*m*, 2H, HC≡CCH<sub>2</sub>CH<sub>2</sub>CH<sub>2</sub>Rf<sub>6</sub>).

**<sup>13</sup>C-NMR:** (90.55 MHz, CDCl<sub>3</sub>): δ 108.10-121.18 (Rf<sub>6</sub>), 82.27 (C≡C(CH<sub>2</sub>)<sub>3</sub>Rf<sub>6</sub>), 79.72 (C≡C(CH<sub>2</sub>)<sub>3</sub>Rf<sub>6</sub>), 29.83 (*t*, <sup>2</sup>J<sub>CF</sub> = 22.5 Hz, C≡CCH<sub>2</sub>CH<sub>2</sub>CH<sub>2</sub>Rf<sub>6</sub>), 19.34 (*t*, <sup>3</sup>J<sub>CF</sub> = 3.3 Hz, C≡CCH<sub>2</sub>CH<sub>2</sub>CH<sub>2</sub>Rf<sub>6</sub>), 17.91 (C≡CCH<sub>2</sub>CH<sub>2</sub>CH<sub>2</sub>Rf<sub>6</sub>).

**EI-MS:** m/z (% int.): 117.0 ([M-Rf<sub>5</sub>]<sup>+</sup>, 15%), 66.9 ([M-Rf<sub>6</sub>]<sup>+</sup>, 100%).

## 21.8.2 1-Bromo-4-(6,6,7,7,8,8,9,9,10,10,11,11,11-tridecafluoroundec-1-ynyl)benzene

**Method K**

Pd(PPh<sub>3</sub>)<sub>4</sub> (1.65 g, 1.43 mmol), CuI (453 mg, 2.38 mmol) and 1-bromo-4-iodobenzene (**97**, 6.74 g, 23.8 mmol) were dissolved in THF (110 mL) in a Schlenk reaction vessel under inert atmosphere. Compound **96a** (9.2 g, 23.8 mmol) was degassed in a separate flask, diluted with THF (20 mL) and added into the Schlenk flask, before NEt<sub>3</sub> (20.0 mL, 143 mmol) was syringed in. The Schlenk tube

was sealed and heated to 80 °C for 6 days. The cold reaction mixture was then quenched by the addition of water (100 mL) and extracted with ether (3 x 100 mL). The combined organic fractions were washed with HCl 10% (150 mL) and water (100 mL), dried over Na<sub>2</sub>SO<sub>4</sub> and all volatiles were removed yielding a brown oil. Several filtrations over silica gel under reduced pressure using first pentane – ether 9:1 as eluent, followed by pentane for the succeeding filtrations were performed, yielding the desired compound **98a** as colourless oil (4.91 g, 38%).

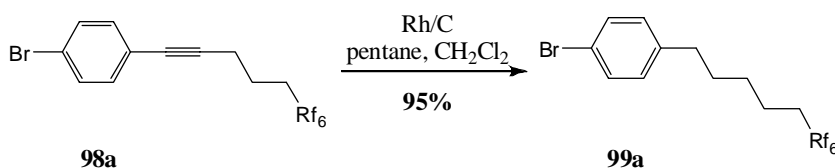
**TLC:** R<sub>f</sub> = 0.78 (silica gel, pentane, KMnO<sub>4</sub>).

**<sup>1</sup>H-NMR:** (360 MHz, CDCl<sub>3</sub>): δ 7.42 (*d*, 2H, <sup>3</sup>J<sub>HH</sub> = 8.2 Hz, Ph), 7.25 (*d*, 2H, <sup>3</sup>J<sub>HH</sub> = 8.2 Hz, Ph), 2.53 (*t*, 2H, <sup>3</sup>J<sub>HH</sub> = 6.8 Hz, C≡CCH<sub>2</sub>CH<sub>2</sub>CH<sub>2</sub>Rf<sub>6</sub>), 2.20-2.34 (*m*, 2H, C≡CCH<sub>2</sub>CH<sub>2</sub>CH<sub>2</sub>Rf<sub>6</sub>), 1.88-1.96 (*m*, 2H, C≡CCH<sub>2</sub>CH<sub>2</sub>CH<sub>2</sub>Rf<sub>6</sub>).

**<sup>13</sup>C-NMR:** (90.55 MHz, CDCl<sub>3</sub>): δ 133.01 (Ph), 131.51 (Ph), 122.35 (Ph), 122.06 (Ph), 107.70-118.79 (Rf<sub>6</sub>), 89.06 (C≡C(CH<sub>2</sub>)<sub>3</sub>Rf<sub>6</sub>), 81.00 (C≡C(CH<sub>2</sub>)<sub>3</sub>Rf<sub>6</sub>), 30.06 (*t*, <sup>2</sup>J<sub>CF</sub> = 22.5 Hz, C≡CCH<sub>2</sub>CH<sub>2</sub>CH<sub>2</sub>Rf<sub>6</sub>), 19.58 (*t*, <sup>3</sup>J<sub>CF</sub> = 3.3 Hz, C≡CCH<sub>2</sub>CH<sub>2</sub>CH<sub>2</sub>Rf<sub>6</sub>), 18.94 (C≡CCH<sub>2</sub>CH<sub>2</sub>CH<sub>2</sub>Rf<sub>6</sub>).

**EI-MS:** m/z (% int.): 540.9 (M<sup>+</sup>, 32%), 461.7 ([M-Br]<sup>+</sup>, 8%), 223.1 ([M-Rf<sub>5</sub>]<sup>+</sup>, 17%), 192.9 ([M-Rf<sub>2,6</sub>]<sup>+</sup>, 100%), 172.0 (45%), 142 (63%), 128.0 (63%).

### 21.8.3 1-Bromo-4-(6,6,7,7,8,8,9,9,10,10,11,11,11-tridecafluoroundecyl)benzene



The hydrogenation of compound **98a** (4.8 g, 8.9 mmol) was carried out following **method E** using Rh/C (300 mg) as catalyst and a mixture of pentane – CH<sub>2</sub>Cl<sub>2</sub> (60 mL 3:1) as solvents. The reaction was stirred for 15 hours at room temperature under 60 atmospheres of hydrogen before the catalyst was removed by filtration over silica gel. All volatiles of the filtrate were removed yielding compound **99a** as pure colourless oil (4.61 g, 95%).

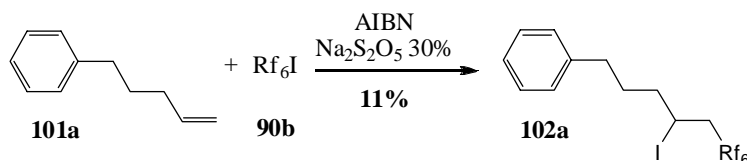
**TLC:** R<sub>f</sub> = 0.85 (silica gel, pentane, KMnO<sub>4</sub>).

**<sup>1</sup>H-NMR:** (360 MHz, CDCl<sub>3</sub>): δ 7.40 (*d*, 2H, <sup>3</sup>J<sub>HH</sub> = 8.2 Hz, Ph), 7.04 (*d*, 2H, <sup>3</sup>J<sub>HH</sub> = 8.2 Hz, Ph), 2.58 (*t*, 2H, <sup>3</sup>J<sub>HH</sub> = 7.7 Hz, CH<sub>2</sub>(CH<sub>2</sub>)<sub>4</sub>Rf<sub>6</sub>), 1.97-2.11 (*m*, 2H, (CH<sub>2</sub>)<sub>4</sub>CH<sub>2</sub>Rf<sub>6</sub>), 1.60-1.68 (*m*, 4H, CH<sub>2</sub>CH<sub>2</sub>CH<sub>2</sub>CH<sub>2</sub>CH<sub>2</sub>Rf<sub>6</sub>), 1.36-1.43 (*m*, 2H, CH<sub>2</sub>CH<sub>2</sub>CH<sub>2</sub>CH<sub>2</sub>CH<sub>2</sub>Rf<sub>6</sub>).

**<sup>13</sup>C-NMR:** (90.55 MHz, CDCl<sub>3</sub>): δ 141.06 (Ph), 131.39 (Ph), 130.12 (Ph), 119.53 (Ph), 105.33-118.80 (Rf<sub>6</sub>), 35.01 (CH<sub>2</sub>(CH<sub>2</sub>)<sub>4</sub>Rf<sub>6</sub>), 30.86 (CH<sub>2</sub>CH<sub>2</sub>(CH<sub>2</sub>)<sub>3</sub>Rf<sub>6</sub>), 30.79 (*t*, <sup>2</sup>J<sub>CF</sub> = 22.5 Hz, (CH<sub>2</sub>)<sub>4</sub>CH<sub>2</sub>Rf<sub>6</sub>), 28.54 (CH<sub>2</sub>CH<sub>2</sub>CH<sub>2</sub>CH<sub>2</sub>CH<sub>2</sub>Rf<sub>6</sub>), 19.99 (*t*, <sup>3</sup>J<sub>CF</sub> = 3.3 Hz, (CH<sub>2</sub>)<sub>3</sub>CH<sub>2</sub>CH<sub>2</sub>Rf<sub>6</sub>).

**EI-MS:** m/z (% int.): 544.9 (M<sup>+</sup>, 8%), 168.9 ([M-Rf<sub>4,6</sub>]<sup>+</sup>, 100%), 91.0 ([M-Rf<sub>4,6</sub>-Br]<sup>+</sup>, 27%).

## 21.8.4 (6,6,7,7,8,8,9,9,10,10,11,11,11-Tridecafluoro-4-iodoundecyl)benzene



The synthesis was carried out following **method G** using pent-4-enylbenzene **101a** (7.0 g, 47.86 mmol) as precursor together with **90b** (21.7 g, 49.12 mmol), AIBN (140 mg, 0.85 mmol) and a 30% aqueous solution of  $\text{Na}_2\text{S}_2\text{O}_5$  (4.7 mL). The reaction was heated to  $80^\circ\text{C}$  where after AIBN was added periodically every two hours (three addition of 140 mg, 0.085 mmol). The crude product was then extracted with ether and purified by column chromatography on silica gel using pentane as eluent affording the desired compound **102a** as colourless oil in low yield (3.14 g, 11%).

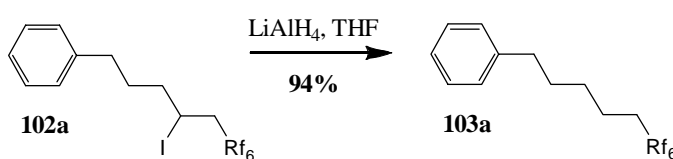
**TLC:**  $R_f = 0.73$  (silica gel, pentane,  $\text{KMnO}_4$ ).

**$^1\text{H-NMR}$ :** (360 MHz,  $\text{CDCl}_3$ ):  $\delta$  7.28-7.32 (*m*, 2H, Ph), 7.18-7.22 (*m*, 3H, Ph), 4.34 (*tt*, 1H,  $^3J_{\text{HH}} = 8.2$  Hz,  $^3J_{\text{HH}} = 5.0$  Hz,  $(\text{CH}_2)_3\text{CHICH}_2\text{Rf}_6$ ), 2.74-2.98 (*m*, 2H,  $(\text{CH}_2)_3\text{CHICH}_2\text{Rf}_6$ ), 2.58-2.74 (*m*, 2H,  $\text{CH}_2\text{CH}_2\text{CH}_2\text{CHICH}_2\text{Rf}_6$ ), 1.73-1.93 (*m*, 4H,  $\text{CH}_2\text{CH}_2\text{CH}_2\text{CHICH}_2\text{Rf}_6$ ).

**$^{13}\text{C-NMR}$ :** (90.55 MHz,  $\text{CDCl}_3$ ):  $\delta$  141.40 (Ph), 128.43 (Ph), 128.35 (Ph), 126.03 (Ph), 107.21-120.69 ( $\text{Rf}_6$ ), 41.61 (*t*,  $^2J_{\text{CF}} = 22.5$  Hz,  $(\text{CH}_2)_3\text{CHICH}_2\text{Rf}_6$ ), 39.79 ( $\text{CH}_2\text{CH}_2\text{CH}_2\text{CHICH}_2\text{Rf}_6$ ), 34.69 ( $\text{CH}_2\text{CH}_2\text{CH}_2\text{CHICH}_2\text{Rf}_6$ ), 31.32 ( $\text{CH}_2\text{CH}_2\text{CH}_2\text{CHICH}_2\text{Rf}_6$ ), 20.22 ( $(\text{CH}_2)_3\text{CHICH}_2\text{Rf}_6$ ).

**EI-MS:**  $m/z$  (% int.): 465.8 ( $[\text{M-I}]^+$ , 14%), 90.9 ( $[\text{M-Rf}_{4,6}\text{-I}]^+$ , 100%).

## 21.8.5 (6,6,7,7,8,8,9,9,10,10,11,11,11-Tridecafluoroundecyl)benzene



Dehalogenation of **102a** (10.0 g, 16.88 mmol) was carried out following **method H** using  $\text{LiAlH}_4$  (2.56 g, 67.54 mmol) in THF (40 mL). After one night of reaction at room temperature the grey slurry was quenched by the addition of water (7.5 mL), 0.2 M  $\text{NaOH}$  (7.5 mL) and water (7.5 mL). The obtained suspension was Büchner filtrated, exhaustively washed with ether before the organic phase was separated from the filtrate. After drying over  $\text{Na}_2\text{SO}_4$  and evaporation of all volatiles compound **103a** was obtained as colourless oil in excellent yield (7.4 g, 94%).

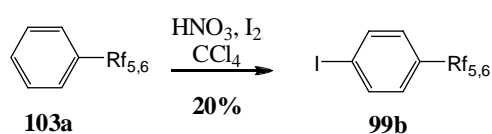
**TLC:** Rf = 0.92 (silica gel, pentane, KMnO<sub>4</sub>).

**<sup>1</sup>H-NMR:** (360 MHz, CDCl<sub>3</sub>): δ 7.27-7.31 (*m*, 2H, Ph), 7.17-7.21 (*m*, 3H, Ph), 2.63 (*t*, 2H, <sup>3</sup>J<sub>HH</sub> = 7.7 Hz, CH<sub>2</sub>(CH<sub>2</sub>)<sub>4</sub>Rf<sub>6</sub>), 1.96-2.12 (*m*, 2H, (CH<sub>2</sub>)<sub>4</sub>CH<sub>2</sub>Rf<sub>6</sub>), 1.59-1.71 (*m*, 4H, CH<sub>2</sub>CH<sub>2</sub>CH<sub>2</sub>CH<sub>2</sub>CH<sub>2</sub>Rf<sub>6</sub>), 1.38-1.46 (*m*, 2H, CH<sub>2</sub>CH<sub>2</sub>CH<sub>2</sub>CH<sub>2</sub>CH<sub>2</sub>Rf<sub>6</sub>).

**<sup>13</sup>C-NMR:** (90.55 MHz, CDCl<sub>3</sub>): δ 142.19 (Ph), 128.37 (Ph), 128.34 (Ph), 125.80 (Ph), 108.11-119.18 (Rf<sub>6</sub>), 35.65 (CH<sub>2</sub>(CH<sub>2</sub>)<sub>4</sub>Rf<sub>6</sub>), 31.04 (CH<sub>2</sub>CH<sub>2</sub>(CH<sub>2</sub>)<sub>3</sub>Rf<sub>6</sub>), 30.82 (*t*, <sup>2</sup>J<sub>CF</sub> = 22.5 Hz, (CH<sub>2</sub>)<sub>4</sub>CH<sub>2</sub>Rf<sub>6</sub>), 28.66 (CH<sub>2</sub>CH<sub>2</sub>CH<sub>2</sub>CH<sub>2</sub>CH<sub>2</sub>Rf<sub>6</sub>), 20.01 (*t*, <sup>3</sup>J<sub>CF</sub> = 3.3 Hz, (CH<sub>2</sub>)<sub>3</sub>CH<sub>2</sub>CH<sub>2</sub>Rf<sub>6</sub>).

**EI-MS:** m/z (% int.): 466.4 (M<sup>+</sup>, 18%), 91.1 ([M-Rf<sub>4,6</sub>]<sup>+</sup>, 100%).

#### 21.8.6 1-Iodo-4-(6,6,7,7,8,8,9,9,10,10,11,11,11-tridecafluoroundecyl)benzene



The iodination of the aryl derivative **103a** (6.8 g, 14.6 mmol) was performed accordingly to **method L** using HNO<sub>3</sub> (2.0 mL, 49.1 mmol) and I<sub>2</sub> (2.96 g, 11.67 mmol), which were added portion wise in CCl<sub>4</sub> (30 mL). After 36 hours of reaction at 90 °C, the mixture was cooled to room temperature and extracted with ether (3 x 150 mL). The organic phase was washed with water (50 mL), brine (100 mL) and 0.5 M NaOH (200 mL), dried over Na<sub>2</sub>SO<sub>4</sub> and all volatiles were removed yielding a yellow oil which was purified by three subsequent column chromatographies over silica gel using pentane as eluent, yielding finally **99b** as colourless oil in moderate yield (1.7 g, 20 %).

**TLC:** Rf = 0.95 (silica gel, pentane, KMnO<sub>4</sub>).

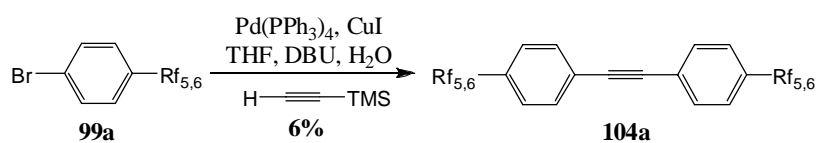
**<sup>1</sup>H-NMR:** (360 MHz, CDCl<sub>3</sub>): δ 7.57 (*d*, 2H, <sup>3</sup>J<sub>HH</sub> = 8.2 Hz, Ph), 6.92 (*d*, 2H, <sup>3</sup>J<sub>HH</sub> = 8.2 Hz, Ph), 2.57 (*t*, 2H, <sup>3</sup>J<sub>HH</sub> = 7.7 Hz, CH<sub>2</sub>(CH<sub>2</sub>)<sub>4</sub>Rf<sub>6</sub>), 1.96-2.11 (*m*, 2H, (CH<sub>2</sub>)<sub>4</sub>CH<sub>2</sub>Rf<sub>6</sub>), 1.60-1.68 (*m*, 4H, CH<sub>2</sub>CH<sub>2</sub>CH<sub>2</sub>CH<sub>2</sub>CH<sub>2</sub>Rf<sub>6</sub>), 1.35-1.44 (*m*, 2H, CH<sub>2</sub>CH<sub>2</sub>CH<sub>2</sub>CH<sub>2</sub>CH<sub>2</sub>Rf<sub>6</sub>).

**<sup>13</sup>C-NMR:** (90.55 MHz, CDCl<sub>3</sub>): δ 141.76 (Ph), 137.37 (Ph), 130.49 (Ph), 107.21-121.18 (Rf<sub>6</sub>), 90.78 (Ph), 35.11 (CH<sub>2</sub>(CH<sub>2</sub>)<sub>4</sub>Rf<sub>6</sub>), 30.83 (CH<sub>2</sub>CH<sub>2</sub>(CH<sub>2</sub>)<sub>3</sub>Rf<sub>6</sub>), 30.78 (*t*, <sup>2</sup>J<sub>CF</sub> = 22.5 Hz, (CH<sub>2</sub>)<sub>4</sub>CH<sub>2</sub>Rf<sub>6</sub>), 28.54 (CH<sub>2</sub>CH<sub>2</sub>CH<sub>2</sub>CH<sub>2</sub>CH<sub>2</sub>Rf<sub>6</sub>), 19.99 (*t*, <sup>3</sup>J<sub>CF</sub> = 3.3 Hz, (CH<sub>2</sub>)<sub>3</sub>CH<sub>2</sub>CH<sub>2</sub>Rf<sub>6</sub>).

**EI-MS:** m/z (% int.): 593.0 (M<sup>+</sup>, 18%), 217.0 ([M-Rf<sub>4,6</sub>]<sup>+</sup>, 100%), 90.9 ([M-Rf<sub>4,6</sub>-I]<sup>+</sup>, 24%).

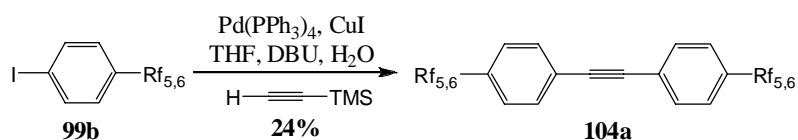
21.8.7 1-(6,6,7,7,8,8,9,9,10,10,11,11,11-Tridecafluoroundecyl)-4-{{[4-(6,6,7,7,8,8,9,9,10,10,11,11,11-tridecafluoroundecyl)phenyl]ethynyl}benzene

a) using the brominated aryl derivative **99a**



This Sonogashira reaction was carried out accordingly to **method A** using compound **99a** (4.6 g, 8.4 mmol), PdCl<sub>2</sub>(PPh<sub>3</sub>)<sub>2</sub> (585 g, 0.5 mmol), CuI (161 mg, 0.84 mmol), DBU (7.6 mL, 50.6 mmol), TMSA (0.735 mL, 5.06 mmol), water (60 µL, 3.38 mmol) and THF (50 mL). The mixture was stirred at 80 °C for 2 days before being cooled to room temperature and diluted with ether (300 mL). The obtained dark suspension was washed with water (100 mL), 10% HCl (100 mL) and water (100 mL), dried over Na<sub>2</sub>SO<sub>4</sub> and all volatiles were removed under reduced pressure. The obtained dark solid was dissolved in ether and filtrated over a plug of basic Alox taking pentane – ether (9:1) as eluent. The filtrate was reduced maximally and the brown solid was recrystallized from pentane – methanol yielding the desired tolane **104a** as off-white solid in very poor yield (225 mg, 6%).

b) using the iodinated aryl derivative **99b**



This Sonogashira coupling was performed similar to **method A** using compound **99b** (1.54 g, 2.6 mmol), PdCl<sub>2</sub>(PPh<sub>3</sub>)<sub>2</sub> (180 mg, 0.17 mmol), CuI (50 mg, 0.26 mmol), DBU (2.2 mL, 15.6 mmol), TMSA (0.2 mL, 1.43 mmol), water (19 µL, 1.04 mmol) and THF (20 mL). After 29 hours at 40°C the black reaction mixture was extracted with ether (3 x 200 mL). The combined organic fractions were washed with water (100 mL), 10% HCl (100 mL) and water (50 mL), dried over Na<sub>2</sub>SO<sub>4</sub> and reduced. The obtained solid was dissolved in ether – pentane (9:1) and filtered over a plug of basic alox. The filtrate was again reduced and the obtained solid was recrystallized from pentane – ethanol to afford tolane **104a** as off-white solid (297 mg, 24%).

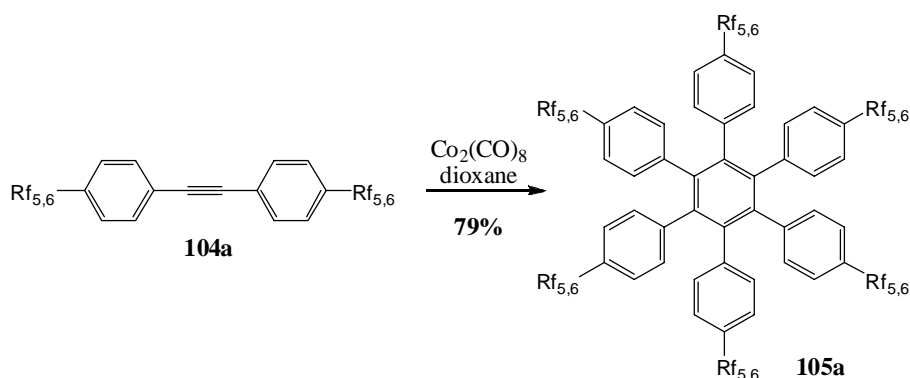
**TLC:** R<sub>f</sub> = 0.95 (silica gel, pentane – ether 9:1, KMnO<sub>4</sub>).

**<sup>1</sup>H-NMR:** (360 MHz, CDCl<sub>3</sub>): δ 7.37 (*d*, 4H, <sup>3</sup>J<sub>HH</sub> = 8.2 Hz, Ph), 7.08 (*d*, 4H, <sup>3</sup>J<sub>HH</sub> = 8.2 Hz, Ph), 2.57 (*t*, 4H, <sup>3</sup>J<sub>HH</sub> = 7.3 Hz, CH<sub>2</sub>(CH<sub>2</sub>)<sub>4</sub>Rf<sub>6</sub>), 1.90-2.09 (*m*, 4H, (CH<sub>2</sub>)<sub>4</sub>CH<sub>2</sub>Rf<sub>6</sub>), 1.56-1.64 (*m*, 8H, CH<sub>2</sub>CH<sub>2</sub>CH<sub>2</sub>CH<sub>2</sub>CH<sub>2</sub>CH<sub>2</sub>Rf<sub>6</sub>), 1.30-1.38 (*m*, 4H, CH<sub>2</sub>CH<sub>2</sub>CH<sub>2</sub>CH<sub>2</sub>CH<sub>2</sub>CH<sub>2</sub>Rf<sub>6</sub>).

**$^{13}\text{C}$ -NMR:** (90.55 MHz,  $\text{CDCl}_3$ ):  $\delta$  142.45 (Ph), 131.56 (Ph), 128.40 (Ph), 120.83 (Ph), 108.10-118.79 ( $\text{Rf}_6$ ), 88.93 (acetylene), 35.55 ( $\text{CH}_2(\text{CH}_2)_4\text{Rf}_6$ ), 30.79 ( $\text{CH}_2\text{CH}_2(\text{CH}_2)_3\text{Rf}_6$ ), 30.79 (*t*,  $^2J_{\text{CF}} = 22.5$  Hz,  $(\text{CH}_2)_4\text{CH}_2\text{Rf}_6$ ), 28.59 ( $\text{CH}_2\text{CH}_2\text{CH}_2\text{CH}_2\text{CH}_2\text{Rf}_6$ ), 20.00 (*t*,  $^3J_{\text{CF}} = 3.3$  Hz,  $(\text{CH}_2)_3\text{CH}_2\text{CH}_2\text{Rf}_6$ ).

**MALDI-ICR-MS (DCTB):**  $m/z$  (% int.): 1205.34 ( $[\text{M}+\text{DCTB}]^{*+}$ , 90 %), 954.18 ( $\text{M}^{*+}$ , 100 %).

#### 21.8.8 Hexakis[4-(6,6,7,7,8,8,9,9,10,10,11,11,11-tridecafluoroundecyl)phenyl]benzene



The cyclotrimerisation was performed following **method B** using tolane **104a** (0.3 g, 0.31 mmol),  $\text{Co}_2(\text{CO})_8$  (8.6 mg, 25  $\mu\text{mol}$ ) and dioxane (20 mL). The dark reaction mixture was refluxed for 5 days, cooled to room temperature and reduced. The obtained brown solid was filtrated over a plug of silica gel using ether as eluent. The filtrate was again reduced and the obtained red solid was re-crystallized from pentane – ether yielding the title HPB **105a** as white solid (238 mg, 79%).

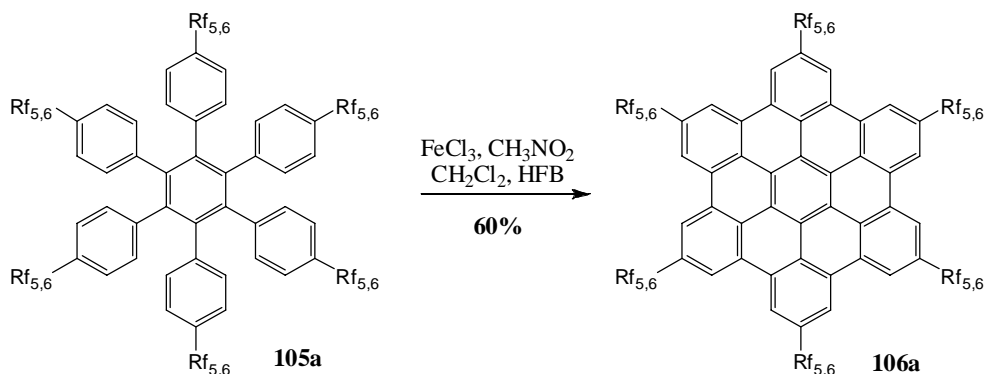
**TLC:**  $R_f = 0.95$  (silica gel, pentane – ether 9:1,  $\text{KMnO}_4$ ).

**$^1\text{H}$ -NMR:** (360 MHz,  $\text{CDCl}_3$ ):  $\delta$  6.68 (*d*, 12H,  $^3J_{\text{HH}} = 8.2$  Hz, Ph), 6.61 (*d*, 12H,  $^3J_{\text{HH}} = 8.2$  Hz, Ph), 2.36 (*t*, 12H,  $^3J_{\text{HH}} = 7.3$  Hz,  $\text{CH}_2(\text{CH}_2)_4\text{Rf}_6$ ), 1.90-2.04 (*m*, 12H,  $(\text{CH}_2)_4\text{CH}_2\text{Rf}_6$ ), 1.47-1.55 (*m*, 12H,  $\text{CH}_2\text{CH}_2(\text{CH}_2)_3\text{Rf}_6$ ), 1.41-1.45 (*m*, 12H,  $(\text{CH}_2)_3\text{CH}_2\text{CH}_2\text{Rf}_6$ ), 1.17-1.21 (*m*, 12H,  $\text{CH}_2\text{CH}_2\text{CH}_2\text{CH}_2\text{CH}_2\text{Rf}_6$ ).

**$^{13}\text{C}$ -NMR:** (90.55 MHz,  $\text{CDCl}_3$ ):  $\delta$  140.20 (Ph), 138.43 (Ph), 138.39 (Ph), 131.45 (Ph), 126.42 (Ph), 110.39-118.72 ( $\text{Rf}_6$ ), 34.94 ( $\text{CH}_2(\text{CH}_2)_4\text{Rf}_6$ ), 30.79 ( $\text{CH}_2\text{CH}_2(\text{CH}_2)_3\text{Rf}_6$ ), 30.79 (*t*,  $^2J_{\text{CF}} = 22.5$  Hz,  $(\text{CH}_2)_4\text{CH}_2\text{Rf}_6$ ), 28.07 ( $\text{CH}_2\text{CH}_2\text{CH}_2\text{CH}_2\text{CH}_2\text{Rf}_6$ ), 19.87 (*t*,  $^3J_{\text{CF}} = 3.3$  Hz,  $(\text{CH}_2)_3\text{CH}_2\text{CH}_2\text{Rf}_6$ ).

**MALDI-ICR-MS (DCTB):**  $m/z$  (% int.): 2862.51 ( $\text{M}^{*+}$ , 100%).

## 21.8.9 2,5,8,11,14,17-Hexakis-(6,6,7,7,8,8,9,9,10,10,11,11,11-tridecafluoroundecyl)hexabenzobenzene [bc,ef,hi,kl,no,q]coronene



The cyclodehydrogenation was performed similarly to **method C** taking HPB **105a** (100 mg, 35.0  $\mu\text{mol}$ ) as precursor together with  $\text{FeCl}_3$  (340 mg, 2.1 mmol, 5 eq / H to be removed),  $\text{CH}_3\text{NO}_2$  (8 mL) and  $\text{CH}_2\text{Cl}_2$  (20 mL). The reaction mixture was stirred at 45 °C under constant argon bubbling for 8 hours, before being quenched by methanol (20 mL). The formed brown precipitate was collected by suction filtration over Millipore<sup>®</sup>, and was purified by suspending in ether, dichloromethane, ethanol, methanol and nitromethane, treated each time in an ultrasonic bath and collected by Millipore<sup>®</sup> filtration. Final purification was achieved by precipitation out of BTF by the addition of ethanol and ether. The title HBC **106a** was afforded as yellow solid (60 mg, 60%).

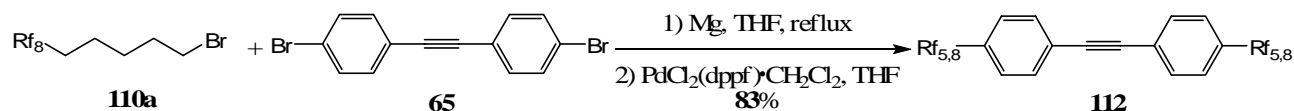
**<sup>1</sup>H-NMR:** (360 MHz, HFB,  $\text{CDCl}_3$ ):  $\delta$  8.99 (br. s, 12H, Ph), 3.55 (br. s, 12H,  $\text{CH}_2(\text{CH}_2)_4\text{Rf}_6$ ), 2.50 (br. s, 24H,  $\text{CH}_2\text{CH}_2\text{CH}_2\text{CH}_2\text{CH}_2\text{Rf}_6$ ), 2.15 (br. s, 24H,  $\text{CH}_2\text{CH}_2\text{CH}_2\text{CH}_2\text{CH}_2\text{Rf}_6$ ).

**MALDI-ICR-MS (DCTB):** m/z (% int.): 2850.44 ( $\text{M}^{+}$ , 100%; calcd. for  $\text{C}_{108}\text{H}_{72}\text{F}_{78}$  2850.44), 2476.40 ( $[\text{M}-\text{Rf}_{4,6}]^{+}$ , 50%), 2101.36 ( $[\text{M}-2 \times \text{Rf}_{4,6}]^{+}$ , 15%), 1725.33 ( $[\text{M}-3 \times \text{Rf}_{4,6}]^{+}$ , 10%).

**UV/VIS:** (BTF,  $10^{-6}$  M,  $\epsilon = 2.8 \cdot 10^5$ ),  $\lambda_{\text{max}} = 346, 360, 391$  nm.

21.9 Synthesis of HBC-(Rf<sub>5,8</sub>)<sub>6</sub>

## 21.9.1 1-(6,6,7,7,8,8,9,9,10,10,11,11,12,12,13,13,13-Heptafluorotridecyl)-4-{[4-(6,6,7,7,8,8,9,9,10,10,11,11,12,12,13,13,13-heptafluorotridecyl)phenyl]ethynyl}benzene



The synthesis was carried out similarly to **method I**. The Grignard reagent was prepared from the bromoalkyl derivative **110a** (1.71 g, 3.0 mmol) and magnesium turnings (87.5 mg, 3.6 mmol) in THF (2 mL) by refluxing under argon for 12 hours. The Kumada coupling was achieved by using the freshly formed Grignard derivative together with 4,4'-dibromotoluene **65** (252 mg, 0.74 mmol), PdCl<sub>2</sub>(dppf)·CH<sub>2</sub>Cl<sub>2</sub> (61.5 mg, 75 μmol) and THF (6 mL). The suspension was refluxed for 7 days before the mixture was quenched by the addition of methanol (20 mL). The formed precipitate was Büchner filtered and washed with methanol and pentane yielding the desired tolane **112** as off-white solid in excellent yield (720 mg, 83%).

**TLC:** R<sub>f</sub> = 0.77 (silica gel, dichloromethane – cyclohexane (3:7), KMnO<sub>4</sub>).

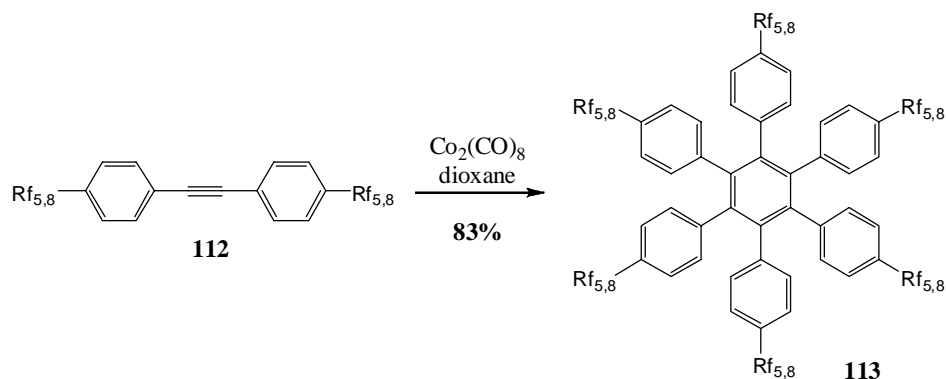
**<sup>1</sup>H-NMR:** (360 MHz, CDCl<sub>3</sub>): δ 7.45 (*d*, 4H, <sup>3</sup>J<sub>HH</sub> = 8.2 Hz, Ph), 7.15 (*d*, 4H, <sup>3</sup>J<sub>HH</sub> = 8.2 Hz, Ph), 2.64 (*t*, 4H, <sup>3</sup>J<sub>HH</sub> = 7.7 Hz, CH<sub>2</sub>(CH<sub>2</sub>)<sub>4</sub>Rf<sub>8</sub>), 1.97-2.13 (*m*, 4H, (CH<sub>2</sub>)<sub>4</sub>CH<sub>2</sub>Rf<sub>8</sub>), 1.61-1.71 (*m*, 8H, CH<sub>2</sub>CH<sub>2</sub>CH<sub>2</sub>CH<sub>2</sub>CH<sub>2</sub>Rf<sub>8</sub>), 1.37-1.46 (*m*, 4H, CH<sub>2</sub>CH<sub>2</sub>CH<sub>2</sub>CH<sub>2</sub>CH<sub>2</sub>Rf<sub>8</sub>).

**<sup>13</sup>C-NMR:** (125.77 MHz, CDCl<sub>3</sub>): δ 142.44 (Ph), 131.54 (Ph), 128.40 (Ph), 120.80 (Ph), 107.21-121.24 (Rf<sub>8</sub>), 88.91 (acetylene), 35.53 (CH<sub>2</sub>(CH<sub>2</sub>)<sub>4</sub>Rf<sub>8</sub>), 30.78 (*t*, <sup>2</sup>J<sub>CF</sub> = 22.1 Hz, (CH<sub>2</sub>)<sub>4</sub>CH<sub>2</sub>Rf<sub>8</sub>), 30.78 (CH<sub>2</sub>CH<sub>2</sub>(CH<sub>2</sub>)<sub>3</sub>Rf<sub>8</sub>), 28.58 (CH<sub>2</sub>CH<sub>2</sub>CH<sub>2</sub>CH<sub>2</sub>CH<sub>2</sub>Rf<sub>8</sub>), 19.99 ((CH<sub>2</sub>)<sub>3</sub>CH<sub>2</sub>CH<sub>2</sub>Rf<sub>8</sub>).

**EI-MS:** *m/z* (% int.): 1154.14 (M<sup>+</sup>, 10%), 679.08 ([M-Rf<sub>4,8</sub>]<sup>+</sup>, 100%), 204.07 ([M-2 x Rf<sub>4,8</sub>]<sup>+</sup>, 70%).



## 21.9.2 Hexakis[4-(6,6,7,7,8,8,9,9,10,10,11,11,12,12,13,13,13-heptafluorotridecyl)phenyl]-benzene



The synthesis was performed following **method B** using toluene **112** (231 mg, 0.2 mmol) as starting material, together with Co<sub>2</sub>(CO)<sub>8</sub> (10.7 mg, 31.2 μmol) and dioxane (75 mL). The mixture was refluxed for 3 days before all volatiles were removed. The obtained solid was dissolved in ether (10 mL) and filtered over a plug of silica gel using a mixture of pentane – ether (9:1) as eluent. After removal of all volatiles from the filtrate under reduced pressure, HPB **113** was afforded as white powder (191 mg, 83 %).

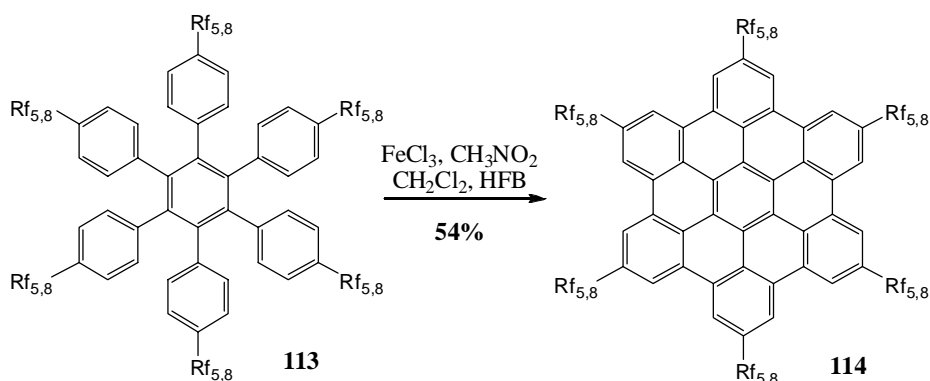
**TLC:** R<sub>f</sub> = 0.95 (silica gel, pentane – ether (5:1), KMnO<sub>4</sub>).

**<sup>1</sup>H-NMR:** (360 MHz, CDCl<sub>3</sub>): δ 6.69 (*d*, 12H, <sup>3</sup>J<sub>HH</sub> = 8.2 Hz, Ph), 6.61 (*d*, 12H, <sup>3</sup>J<sub>HH</sub> = 8.2 Hz, Ph), 2.36 (*t*, 12H, <sup>3</sup>J<sub>HH</sub> = 7.3 Hz, CH<sub>2</sub>(CH<sub>2</sub>)<sub>4</sub>Rf<sub>8</sub>), 1.88-2.04 (*m*, 12H, (CH<sub>2</sub>)<sub>4</sub>CH<sub>2</sub>Rf<sub>8</sub>), 1.47-1.55 (*m*, 12H, CH<sub>2</sub>CH<sub>2</sub>(CH<sub>2</sub>)<sub>3</sub>Rf<sub>8</sub>), 1.36-1.45 (*m*, 12H, (CH<sub>2</sub>)<sub>3</sub>CH<sub>2</sub>CH<sub>2</sub>Rf<sub>8</sub>), 1.14-1.21 (*m*, 12H, CH<sub>2</sub>CH<sub>2</sub>CH<sub>2</sub>CH<sub>2</sub>CH<sub>2</sub>Rf<sub>8</sub>).

**<sup>13</sup>C-NMR:** (125.77 MHz, CDCl<sub>3</sub>): δ 140.29 (Ph), 138.55 (Ph), 138.45 (Ph), 131.54 (Ph), 126.43 (Ph), 108.67-120.49 (Rf<sub>8</sub>), 34.97 (CH<sub>2</sub>(CH<sub>2</sub>)<sub>4</sub>Rf<sub>8</sub>), 30.92 (*t*, <sup>2</sup>J<sub>CF</sub> = 22.1 Hz, (CH<sub>2</sub>)<sub>4</sub>CH<sub>2</sub>Rf<sub>8</sub>), 30.78 (CH<sub>2</sub>CH<sub>2</sub>(CH<sub>2</sub>)<sub>3</sub>Rf<sub>8</sub>), 28.13 (CH<sub>2</sub>CH<sub>2</sub>CH<sub>2</sub>CH<sub>2</sub>CH<sub>2</sub>Rf<sub>8</sub>), 19.96 ((CH<sub>2</sub>)<sub>3</sub>CH<sub>2</sub>CH<sub>2</sub>Rf<sub>8</sub>).

**MALDI-ICR-MS (DCTB):** m/z (% int.): 3462.41 (M<sup>+</sup>, 100%), 2973.41 ([M-Rf<sub>5,8</sub>]<sup>+</sup>, 10%).

21.9.3 2,5,8,11,14,17-Hexakis(6,6,7,7,8,8,9,9,10,10,11,11,12,12,13,13,13-heptafluorotri-  
decyl)hexabenzob[bc,ef,hi,kl,no,qr]coronene



The oxidation was performed following **method C** using HPB **113** (0.1 g, 28.0  $\mu\text{mol}$ ) as precursor together with  $\text{FeCl}_3$  (423 mg, 2.6 mmol, 7.5 eq / H to be removed),  $\text{CH}_2\text{Cl}_2$  (10 mL),  $\text{CH}_3\text{NO}_2$  (8 mL) and HFB (10 mL). The mixture was heated to 45  $^\circ\text{C}$  for 8 hours under a constant bubbling of argon before methanol (40 mL) was added. The formed precipitate was collected by suction filtration over Millipore<sup>®</sup> and was suspended in the following organic solvents (ether, dichloromethane, nitromethane and BTF), sonicated, stored in the fridge for 2 hours and suction filtered over Millipore<sup>®</sup>. Further purification was achieved by precipitation from HFB – ether to yield the desired HBC **114** as yellow solid in moderate yield (54 mg, 54%).

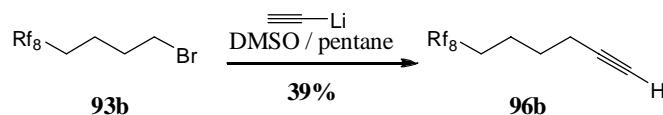
**$^1\text{H-NMR}$ :** (360 MHz,  $\text{CDCl}_3$ ): 9.06 (br. s, 12H, Ph), 3.60 (br. s, 12H,  $\text{CH}_2(\text{CH}_2)_4\text{Rf}_8$ ), 2.65 (br. s, 24H,  $\text{CH}_2\text{CH}_2\text{CH}_2\text{CH}_2\text{CH}_2\text{Rf}_8$ ), 2.20 (br. s, 24H,  $\text{CH}_2\text{CH}_2\text{CH}_2\text{CH}_2\text{CH}_2\text{Rf}_8$ ).

**MALDI-ICR-MS (DCTB):** m/z (% int.): 3450.50 ( $\text{M}^{*+}$ , 100%; calcd. for  $\text{C}_{120}\text{H}_{78}\text{F}_{102}$  3450.40), 2976.34 ( $[\text{M-Rf}_{4,8}]^{*+}$ , 10%).

**UV/VIS:** (BTF,  $10^{-6}$  M,  $\epsilon = 1.9 \cdot 10^5$ ),  $\lambda_{\text{max}} = 345, 360, 391$  nm.

21.10 Synthesis of HBC-(Rf<sub>6,8</sub>)<sub>6</sub>

## 21.10.1 7,7,8,8,9,9,10,10,11,11,12,12,13,13,14,14,14-Heptafluorotetradec-1-yne



The synthesis was performed accordingly to **method J** using compound **93b** (15 g, 25.2 mmol), lithium acetylide ethylenediamine complex (7.0 g, 75.6 mmol), DMSO (30 mL) and pentane (15 mL). The black suspension was stirred at room temperature for 15 hours before the mixture was quenched by the addition of water (20 mL). The resulting suspension was diluted with CH<sub>2</sub>Cl<sub>2</sub> (100 mL) and Büchner filtrated. The filtrate was extracted with CH<sub>2</sub>Cl<sub>2</sub> (3 x 100 mL). The combined organic phases were dried over Na<sub>2</sub>SO<sub>4</sub> and all volatiles were removed under reduced pressure. The resulting black oily liquid was filtered over a plug of silica gel using pentane as eluent. After removal of pentane compound **96b** was obtained as colourless oil (4.94 g, 39%).

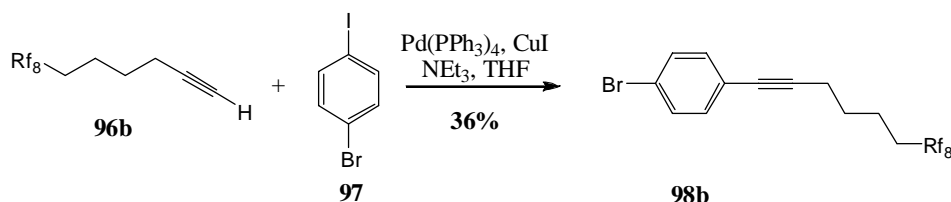
**TLC:** Rf = 0.90 (silica gel, pentane, KMnO<sub>4</sub>).

**<sup>1</sup>H-NMR:** (360 MHz, CDCl<sub>3</sub>): δ 2.25 (*td*, 2H, <sup>3</sup>J<sub>HH</sub> = 6.8 Hz, <sup>4</sup>J<sub>HH</sub> = 2.7 Hz, HC≡CCH<sub>2</sub>(CH<sub>2</sub>)<sub>3</sub>Rf<sub>8</sub>), 2.02-2.17 (*m*, 2H, HC≡C(CH<sub>2</sub>)<sub>3</sub>CH<sub>2</sub>Rf<sub>8</sub>), 1.98 (*t*, 1H, <sup>4</sup>J<sub>HH</sub> = 2.7 Hz, HC≡C(CH<sub>2</sub>)<sub>4</sub>Rf<sub>8</sub>), 1.71-1.80 (*m*, 2H, HC≡CCH<sub>2</sub>CH<sub>2</sub>CH<sub>2</sub>CH<sub>2</sub>Rf<sub>8</sub>), 1.59-1.67 (*m*, 2H, HC≡CCH<sub>2</sub>CH<sub>2</sub>CH<sub>2</sub>CH<sub>2</sub>Rf<sub>8</sub>).

**<sup>13</sup>C-NMR:** (90.55 MHz, CDCl<sub>3</sub>): δ 107.43-121.94 (Rf<sub>8</sub>), 83.27 (C≡C(CH<sub>2</sub>)<sub>4</sub>Rf<sub>8</sub>), 68.94 (C≡C(CH<sub>2</sub>)<sub>4</sub>Rf<sub>8</sub>), 30.44 (*t*, <sup>2</sup>J<sub>CF</sub> = 22.5 Hz, C≡C(CH<sub>2</sub>)<sub>3</sub>CH<sub>2</sub>Rf<sub>8</sub>), 27.76 (C≡CCH<sub>2</sub>CH<sub>2</sub>CH<sub>2</sub>CH<sub>2</sub>Rf<sub>8</sub>), 19.34 (*t*, <sup>3</sup>J<sub>CF</sub> = 3.3 Hz, C≡CCH<sub>2</sub>CH<sub>2</sub>CH<sub>2</sub>CH<sub>2</sub>Rf<sub>8</sub>), 18.13 (C≡CCH<sub>2</sub>(CH<sub>2</sub>)<sub>3</sub>Rf<sub>8</sub>).

**EI-MS:** m/z (% int.): 500.8 (M<sup>+</sup>, 2 %), 131.0 ([M-Rf<sub>7</sub>]<sup>+</sup>, 42 %), 81.0 ([M-Rf<sub>8</sub>]<sup>+</sup>, 100 %).

## 21.10.2 1-Bromo-4-(7,7,8,8,9,9,10,10,11,11,12,12,13,13,14,14,14-heptafluorotetradec-1-ynyl)benzene



The Sonogashira cross coupling was performed following **method K** taking compound **96b** (4.8 g, 9.6 mmol), Pd(PPh<sub>3</sub>)<sub>4</sub> (670 mg, 0.57 mmol), CuI (183 mg, 0.96 mmol), 1-bromo-4-iodobenzene (**97**, 2.7 g, 9.6 mmol), NEt<sub>3</sub> (8.0 mL, 57.6 mmol) and THF (50 mL). The Schlenk tube was sealed and heated to 80 °C for 3 days. The cold reaction mixture was quenched by the addition of water

(50 mL) and extracted with ether (2 x 100 mL). The combined organic fractions were washed with HCl 10% (100 mL) and water (50 mL), dried over Na<sub>2</sub>SO<sub>4</sub> and all volatiles were removed. Several filtrations over silica gel under reduced pressure using first pentane – ether 9:1 as eluent, followed by pentane were performed, yielding compound **98b** as colourless oil (2.27 g, 36%).

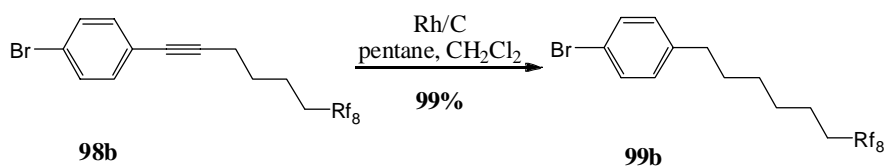
**TLC:** R<sub>f</sub> = 0.62 (silica gel, pentane, KMnO<sub>4</sub>).

**<sup>1</sup>H-NMR:** (360 MHz, CDCl<sub>3</sub>): δ 7.41 (*d*, 2H, <sup>3</sup>J<sub>HH</sub> = 8.2 Hz, Ph), 7.24 (*d*, 2H, <sup>3</sup>J<sub>HH</sub> = 8.2 Hz, Ph), 2.46 (*t*, 2H, <sup>3</sup>J<sub>HH</sub> = 6.8 Hz, C≡CCH<sub>2</sub>(CH<sub>2</sub>)<sub>3</sub>Rf<sub>8</sub>), 2.06-2.20 (*m*, 2H, C≡C(CH<sub>2</sub>)<sub>3</sub>CH<sub>2</sub>CH<sub>2</sub>Rf<sub>8</sub>), 1.75-1.84 (*m*, 2H, C≡CCH<sub>2</sub>CH<sub>2</sub>CH<sub>2</sub>CH<sub>2</sub>Rf<sub>8</sub>), 1.66-1.74 (*m*, 2H, C≡CCH<sub>2</sub>CH<sub>2</sub>CH<sub>2</sub>CH<sub>2</sub>Rf<sub>6</sub>).

**<sup>13</sup>C-NMR:** (90.55 MHz, CDCl<sub>3</sub>): δ 132.99 (Ph), 131.46 (Ph), 122.65 (Ph), 121.82 (Ph), 107.74-119.07 (Rf<sub>8</sub>), 90.16 (C≡C(CH<sub>2</sub>)<sub>4</sub>Rf<sub>8</sub>), 80.36 (C≡C(CH<sub>2</sub>)<sub>4</sub>Rf<sub>8</sub>), 30.45 (*t*, <sup>2</sup>J<sub>CF</sub> = 22.5 Hz, C≡C(CH<sub>2</sub>)<sub>3</sub>CH<sub>2</sub>Rf<sub>8</sub>), 27.89 (C≡CCH<sub>2</sub>CH<sub>2</sub>CH<sub>2</sub>CH<sub>2</sub>Rf<sub>8</sub>), 19.50 (*t*, <sup>3</sup>J<sub>CF</sub> = 3.3 Hz, C≡CCH<sub>2</sub>CH<sub>2</sub>CH<sub>2</sub>CH<sub>2</sub>Rf<sub>8</sub>), 19.13 (C≡CCH<sub>2</sub>(CH<sub>2</sub>)<sub>3</sub>Rf<sub>8</sub>).

**EI-MS:** m/z (% int.): 655.2 (M<sup>+</sup>, 12%), 576.1 ([M-Br]<sup>+</sup>, 16%), 221.0 ([M-Rf<sub>2,8</sub>]<sup>+</sup>, 27%), 192.9 ([M-Rf<sub>3,8</sub>]<sup>+</sup>, 90%), 142 (100%), 128.0 (83%).

#### 21.10.3 1-Bromo-4-(7,7,8,8,9,9,10,10,11,11,12,12,13,13,14,14,14-heptafluorotetradecyl)-benzene



The hydrogenation of compound **98b** (2.0 g, 3.1 mmol) was carried out following **method E** using Rh/C (100 mg) as catalyst and a mixture of pentane (18 mL) and CH<sub>2</sub>Cl<sub>2</sub> (6 mL) as solvents. The reaction was stirred for 17 hours at room temperature under 60 atmospheres of hydrogen before the catalyst was removed by filtration over silica gel. All volatiles of the filtrate were removed yielding compound **99b** as colourless oil (2.0 g, 99%).

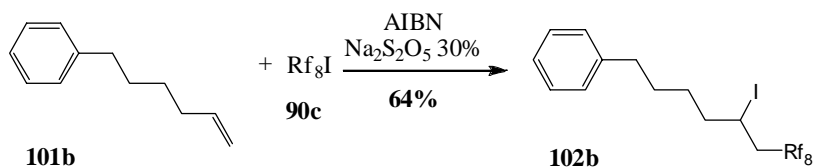
**TLC:** R<sub>f</sub> = 0.65 (silica gel, pentane, KMnO<sub>4</sub>).

**<sup>1</sup>H-NMR:** (360 MHz, CDCl<sub>3</sub>): δ 7.39 (*d*, 2H, <sup>3</sup>J<sub>HH</sub> = 8.2 Hz, Ph), 7.04 (*d*, 2H, <sup>3</sup>J<sub>HH</sub> = 8.2 Hz, Ph), 2.56 (*t*, 2H, <sup>3</sup>J<sub>HH</sub> = 7.7 Hz, CH<sub>2</sub>(CH<sub>2</sub>)<sub>5</sub>Rf<sub>8</sub>), 1.96-2.11 (*m*, 2H, (CH<sub>2</sub>)<sub>5</sub>CH<sub>2</sub>Rf<sub>8</sub>), 1.56-1.65 (*m*, 4H, CH<sub>2</sub>CH<sub>2</sub>CH<sub>2</sub>CH<sub>2</sub>CH<sub>2</sub>CH<sub>2</sub>CH<sub>2</sub>Rf<sub>8</sub>), 1.34-1.42 (*m*, 4H, CH<sub>2</sub>CH<sub>2</sub>CH<sub>2</sub>CH<sub>2</sub>CH<sub>2</sub>CH<sub>2</sub>Rf<sub>8</sub>).

**<sup>13</sup>C-NMR:** (90.55 MHz, CDCl<sub>3</sub>): δ 141.39 (Ph), 131.32 (Ph), 130.12 (Ph), 119.40 (Ph), 107.69-118.71 (Rf<sub>8</sub>), 35.19 (CH<sub>2</sub>(CH<sub>2</sub>)<sub>5</sub>Rf<sub>8</sub>), 30.99 (CH<sub>2</sub>CH<sub>2</sub>(CH<sub>2</sub>)<sub>4</sub>Rf<sub>8</sub>), 30.83 (*t*, <sup>2</sup>J<sub>CF</sub> = 22.5 Hz, (CH<sub>2</sub>)<sub>5</sub>CH<sub>2</sub>Rf<sub>8</sub>), 28.92-28.72 (2C, CH<sub>2</sub>CH<sub>2</sub>CH<sub>2</sub>CH<sub>2</sub>CH<sub>2</sub>CH<sub>2</sub>Rf<sub>8</sub>), 20.03 (*t*, <sup>3</sup>J<sub>CF</sub> = 3.3 Hz, (CH<sub>2</sub>)<sub>4</sub>CH<sub>2</sub>CH<sub>2</sub>Rf<sub>8</sub>).

**EI-MS:** m/z (% int.): 659.3 (M<sup>+</sup>, 6%), 168.9 ([M-Rf<sub>5,8</sub>]<sup>+</sup>, 100%), 91.0 ([M-Rf<sub>5,8</sub>-Br]<sup>+</sup>, 24%).

## 21.10.4 (7,7,8,8,9,9,10,10,11,11,12,12,13,13,14,14,14-Heptaecafluoro-5-iodotetradecyl)benzene



The synthesis was carried out following **method G** using hex-5-enylbenzene **101b** (3.1 g, 19.34 mmol) as precursor together with  $\text{Rf}_8\text{I}$  (10.83 g, 19.85 mmol), AIBN (50 mg, 0.33 mmol) and a 30% aqueous solution of  $\text{Na}_2\text{S}_2\text{O}_5$  (1.9 mL). The reaction was heated to 85°C over night. The crude product was then extracted with ether and purified by column chromatography on silica gel using pentane as eluent affording the desired compound **102b** as colourless oil in moderate yield (8.75 g, 64%).

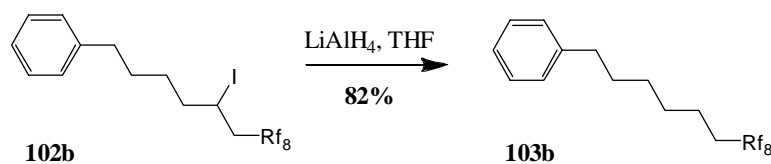
**TLC:**  $R_f = 0.76$  (silica gel, pentane,  $\text{KMnO}_4$ ).

**$^1\text{H-NMR}$ :** (360 MHz,  $\text{CDCl}_3$ ):  $\delta$  7.28-7.32 (*m*, 2H, Ph), 7.18-7.22 (*m*, 3H, Ph), 4.34 (*tt*, 1H,  $^3J_{\text{HH}} = 8.2$  Hz,  $^3J_{\text{HH}} = 5.0$  Hz,  $(\text{CH}_2)_4\text{CHICH}_2\text{Rf}_8$ ), 2.74-3.00 (*m*, 2H,  $(\text{CH}_2)_4\text{CHICH}_2\text{Rf}_8$ ), 2.62 (*t*, 2H,  $\text{CH}_2(\text{CH}_2)_3\text{CHICH}_2\text{Rf}_8$ ), 1.78-1.90 (*m*, 2H,  $\text{CH}_2\text{CH}_2\text{CH}_2\text{CH}_2\text{CHICH}_2\text{Rf}_8$ ), 1.59-1.74 (*m*, 4H,  $\text{CH}_2\text{CH}_2\text{CH}_2\text{CH}_2\text{CHICH}_2\text{Rf}_8$ ).

**$^{13}\text{C-NMR}$ :** (90.55 MHz,  $\text{CDCl}_3$ ):  $\delta$  142.10 (Ph), 128.35 (Ph), 128.34 (Ph), 125.82 (Ph), 107.21-120.76 ( $\text{Rf}_8$ ), 41.70 (*t*,  $^2J_{\text{CF}} = 22.5$  Hz,  $(\text{CH}_2)_4\text{CHICH}_2\text{Rf}_8$ ), 40.14 ( $\text{CH}_2(\text{CH}_2)_3\text{CHICH}_2\text{Rf}_8$ ), 35.64 ( $\text{CH}_2\text{CH}_2\text{CH}_2\text{CH}_2\text{CHICH}_2\text{Rf}_8$ ), 30.31 ( $\text{CH}_2\text{CH}_2\text{CH}_2\text{CH}_2\text{CHICH}_2\text{Rf}_8$ ), 30.31 ( $(\text{CH}_2)_3\text{CH}_2\text{CHICH}_2\text{Rf}_8$ ), 20.53 ( $(\text{CH}_2)_4\text{CHICH}_2\text{Rf}_8$ ).

**EI-MS:**  $m/z$  (% int.): 580.1 ( $[\text{M-I}]^+$ , 100%).

## 21.10.5 (7,7,8,8,9,9,10,10,11,11,12,12,13,13,14,14,14-Heptaecafluorotetradecyl)benzene



Dehalogenation of **102b** (12.3 g, 17.41 mmol) was carried out following **method H** using  $\text{LiAlH}_4$  (2.64 g, 69.66 mmol) in THF (40 mL). After one night of reaction at room temperature the grey slurry was quenched by the addition of water (7.5 mL), 0.2 M NaOH (7.5 mL) and water (7.5 mL). The obtained suspension was Büchner filtrated, exhaustively washed with ether before the organic phase was separated from the filtrate. After drying over  $\text{Na}_2\text{SO}_4$  and evaporation of all volatiles compound **103b** was obtained as colourless oil in good yield (8.34 g, 82%).

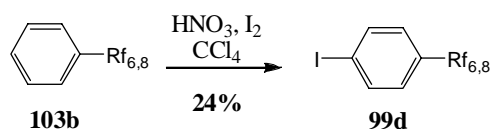
**TLC:**  $R_f = 0.78$  (silica gel, pentane,  $\text{KMnO}_4$ ).

**$^1\text{H-NMR}$ :** (360 MHz,  $\text{CDCl}_3$ ):  $\delta$  7.26-7.30 (*m*, 2H, Ph), 7.16-7.20 (*m*, 3H, Ph), 2.61 (*t*, 2H,  $^3J_{\text{HH}} = 7.7$  Hz,  $\text{CH}_2(\text{CH}_2)_5\text{Rf}_8$ ), 1.96-2.09 (*m*, 2H,  $(\text{CH}_2)_5\text{CH}_2\text{Rf}_8$ ), 1.58-1.68 (*m*, 4H,  $\text{CH}_2\text{CH}_2\text{CH}_2\text{CH}_2\text{CH}_2\text{CH}_2\text{Rf}_8$ ), 1.36-1.45 (*m*, 4H,  $\text{CH}_2\text{CH}_2\text{CH}_2\text{CH}_2\text{CH}_2\text{CH}_2\text{Rf}_8$ ).

**$^{13}\text{C-NMR}$ :** (90.55 MHz,  $\text{CDCl}_3$ ):  $\delta$  142.49 (Ph), 128.36 (Ph), 128.28 (Ph), 125.69 (Ph), 108.17-118.74 ( $\text{Rf}_8$ ), 35.81 ( $\text{CH}_2(\text{CH}_2)_5\text{Rf}_8$ ), 31.18 ( $\text{CH}_2\text{CH}_2(\text{CH}_2)_4\text{Rf}_8$ ), 30.82 (*t*,  $^2J_{\text{CF}} = 22.5$  Hz,  $(\text{CH}_2)_5\text{CH}_2\text{Rf}_8$ ), 28.97 ( $\text{CH}_2\text{CH}_2\text{CH}_2\text{CH}_2\text{CH}_2\text{CH}_2\text{Rf}_8$ ), 28.83 ( $\text{CH}_2\text{CH}_2\text{CH}_2\text{CH}_2\text{CH}_2\text{CH}_2\text{Rf}_8$ ), 20.03 (*t*,  $^3J_{\text{CF}} = 3.3$  Hz,  $(\text{CH}_2)_4\text{CH}_2\text{CH}_2\text{Rf}_8$ ).

**EI-MS:**  $m/z$  (% int.): 581.1 ( $\text{M}^{*+}$ , 12%), 91.1 ( $[\text{M-Rf}_{5,8}]^{*+}$ , 100%).

#### 21.10.6 1-Iodo-4-(7,7,8,8,9,9,10,10,11,11,12,12,13,13,14,14,14-heptafluorotetradecyl)-benzene



The iodination of the aryl derivative **103b** (7.48 g, 12.89 mmol) was performed accordingly to **method L** using  $\text{HNO}_3$  (1.97 mL, 47.7 mmol) and  $\text{I}_2$  (2.56 g, 10.2 mmol), which were added portion wise in  $\text{CCl}_4$  (25 mL). After 12 hours of reaction at 90 °C, the mixture was cooled to room temperature and extracted with ether (3 x 150 mL). The organic phase was washed with water (50 mL), brine (100 mL) and 0.5 M NaOH (200 mL), dried over  $\text{Na}_2\text{SO}_4$  and all volatiles were removed yielding an yellow oil which was purified by five subsequent column chromatographies over silica gel using pentane as eluent, yielding finally **99d** as colourless oil in moderate yield (2.2 g, 24 %).

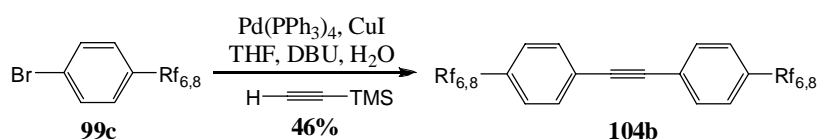
**TLC:**  $R_f = 0.85$  (silica gel, pentane,  $\text{KMnO}_4$ ).

**$^1\text{H-NMR}$ :** (360 MHz,  $\text{CDCl}_3$ ):  $\delta$  7.57 (*d*, 2H,  $^3J_{\text{HH}} = 8.2$  Hz, Ph), 6.92 (*d*, 2H,  $^3J_{\text{HH}} = 8.2$  Hz, Ph), 2.57 (*t*, 2H,  $^3J_{\text{HH}} = 7.7$  Hz,  $\text{CH}_2(\text{CH}_2)_5\text{Rf}_8$ ), 1.99-2.11 (*m*, 2H,  $(\text{CH}_2)_5\text{CH}_2\text{Rf}_8$ ), 1.56-1.62 (*m*, 4H,  $\text{CH}_2\text{CH}_2\text{CH}_2\text{CH}_2\text{CH}_2\text{CH}_2\text{Rf}_8$ ), 1.37-1.44 (*m*, 4H,  $\text{CH}_2\text{CH}_2\text{CH}_2\text{CH}_2\text{CH}_2\text{CH}_2\text{Rf}_8$ ).

**$^{13}\text{C-NMR}$ :** (90.55 MHz,  $\text{CDCl}_3$ ):  $\delta$  142.07 (Ph), 137.30 (Ph), 130.48 (Ph), 107.21-121.18 ( $\text{Rf}_8$ ), 90.65 (Ph), 35.28 ( $\text{CH}_2(\text{CH}_2)_5\text{Rf}_8$ ), 30.96 ( $\text{CH}_2\text{CH}_2(\text{CH}_2)_4\text{Rf}_8$ ), 30.81 (*t*,  $^2J_{\text{CF}} = 22.5$  Hz,  $(\text{CH}_2)_5\text{CH}_2\text{Rf}_8$ ), 28.90 ( $\text{CH}_2\text{CH}_2\text{CH}_2(\text{CH}_2)_3\text{Rf}_8$ ), 28.72 ( $(\text{CH}_2)_3\text{CH}_2\text{CH}_2\text{CH}_2\text{Rf}_8$ ), 20.01 (*t*,  $^3J_{\text{CF}} = 3.3$  Hz,  $(\text{CH}_2)_4\text{CH}_2\text{CH}_2\text{Rf}_8$ ).

**EI-MS:**  $m/z$  (% int.): 707.4 ( $\text{M}^{*+}$ , 6%), 217.0 ( $[\text{M-Rf}_{5,8}]^{*+}$ , 100%).

21.10.7 1-(7,7,8,8,9,9,10,10,11,11,12,12,13,13,14,14,14-heptafluorotetradecyl)-4-{[4-(7,7,8,8,9,9,10,10,11,11,12,12,13,13,14,14,14-heptafluorotetradecyl)phenyl]ethynyl}benzene



This Sonogashira reaction was carried out accordingly to **method A** using compound **99c** (3.0 g, 4.6 mmol), Pd(PPh<sub>3</sub>)<sub>4</sub> (316 g, 0.27 mmol), CuI (87 mg, 0.46 mmol), DBU (4.08 mL, 27.3 mmol), TMSA (0.33 mL, 2.27 mmol), water (32  $\mu$ L, 1.8 mmol) and THF (25 mL). The mixture was stirred at 77 °C for 3 days before being cooled to room temperature and diluted with ether (400 mL). The obtained dark suspension was washed with water (100 mL), 10% HCl (100 mL) and water (100 mL), dried over Na<sub>2</sub>SO<sub>4</sub> and all volatiles were removed under reduced pressure. The obtained dark solid was dissolved in ether and filtered over a plug of basic Alox taking pentane – ether (5:1) as eluent. The filtrate was reduced maximally and the brown solid was recrystallized first from ether – pentane – ethanol and second from dichloromethane – ethanol yielding the desired tolane **104b** as white solid in moderate yield (1.2 g, 46%).

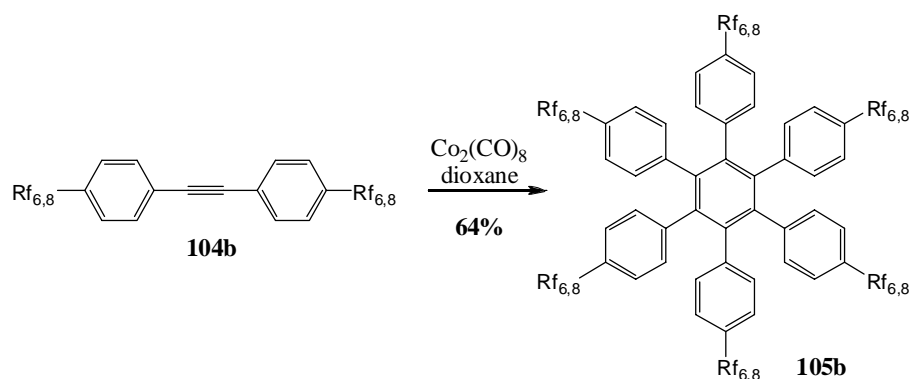
**TLC:** R<sub>f</sub> = 0.95 (silica gel, pentane – ether (9:1), KMnO<sub>4</sub>).

**<sup>1</sup>H-NMR:** (500 MHz, CDCl<sub>3</sub>):  $\delta$  7.42 (*d*, 4H, <sup>3</sup>J<sub>HH</sub> = 8.2 Hz, Ph), 7.13 (*d*, 4H, <sup>3</sup>J<sub>HH</sub> = 8.2 Hz, Ph), 2.62 (*t*, 4H, <sup>3</sup>J<sub>HH</sub> = 7.7 Hz, CH<sub>2</sub>(CH<sub>2</sub>)<sub>5</sub>Rf<sub>8</sub>), 1.99-2.10 (*m*, 4H, (CH<sub>2</sub>)<sub>5</sub>CH<sub>2</sub>Rf<sub>8</sub>), 1.57-1.67 (*m*, 8H, CH<sub>2</sub>CH<sub>2</sub>CH<sub>2</sub>CH<sub>2</sub>CH<sub>2</sub>CH<sub>2</sub>Rf<sub>8</sub>), 1.36-1.40 (*m*, 8H, CH<sub>2</sub>CH<sub>2</sub>CH<sub>2</sub>CH<sub>2</sub>CH<sub>2</sub>CH<sub>2</sub>Rf<sub>8</sub>).

**<sup>13</sup>C-NMR:** (125.77 MHz, CDCl<sub>3</sub>):  $\delta$  142.76 (Ph), 131.57 (Ph), 128.40 (Ph), 120.92 (Ph), 109.13-121.02 (Rf<sub>8</sub>), 89.00 (acetylene), 35.75 (CH<sub>2</sub>(CH<sub>2</sub>)<sub>5</sub>Rf<sub>8</sub>), 31.00 (*t*, <sup>2</sup>J<sub>CF</sub> = 22.5 Hz, (CH<sub>2</sub>)<sub>5</sub>CH<sub>2</sub>Rf<sub>8</sub>), 30.88 (CH<sub>2</sub>CH<sub>2</sub>(CH<sub>2</sub>)<sub>4</sub>Rf<sub>8</sub>), 28.99 ((CH<sub>2</sub>)<sub>3</sub>CH<sub>2</sub>CH<sub>2</sub>CH<sub>2</sub>Rf<sub>8</sub>), 28.78 (CH<sub>2</sub>CH<sub>2</sub>CH<sub>2</sub>(CH<sub>2</sub>)<sub>3</sub>Rf<sub>8</sub>), 20.13 (*t*, <sup>3</sup>J<sub>CF</sub> = 3.3 Hz, (CH<sub>2</sub>)<sub>4</sub>CH<sub>2</sub>CH<sub>2</sub>Rf<sub>8</sub>).

**MALDI-ICR-MS (DCTB):** m/z (% int.): 1433.35 ([M+DCTB]<sup>+</sup>, 45%), 1182.20 (M<sup>+</sup>, 100%).

## 21.10.8 Hexakis[4-(7,7,8,8,9,9,10,10,11,11,12,12,13,13,14,14,14-heptafluorotetradecyl)-phenyl]benzene



The cyclotrimerisation was performed following **method B** using tolane **104b** (1.0 g, 0.85 mmol), Co<sub>2</sub>(CO)<sub>8</sub> (17.4 mg, 51 μmol) and dioxane (75 mL). The dark reaction mixture was refluxed for 2 days and was then cooled to room temperature and reduced. The obtained brown solid was filtered over a plug of silica gel using ether as eluent. The filtrate was again reduced and the obtained brown solid was suspended in pentane, sonicated and collected by suction filtration over Millipore®. Re-crystallization from dichloromethane – pentane, followed by BTF – pentane yielded the title HPB **105b** as white solid (642 mg, 64%).

**TLC:** R<sub>f</sub> = 0.98 (silica gel, pentane – ether (9:1), KMnO<sub>4</sub>).

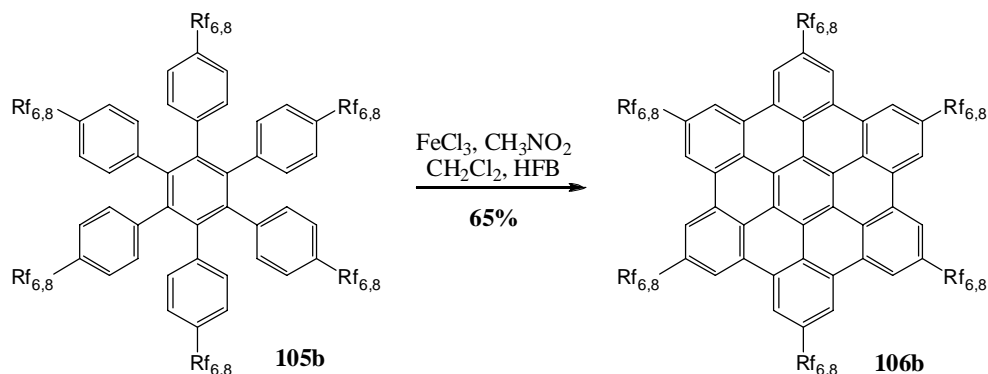
**<sup>1</sup>H-NMR:** (500 MHz, CDCl<sub>3</sub>): δ 6.67 (*d*, 12H, <sup>3</sup>J<sub>HH</sub> = 8.2 Hz, Ph), 6.60 (*d*, 12H, <sup>3</sup>J<sub>HH</sub> = 8.2 Hz, Ph), 2.34 (*t*, 12H, <sup>3</sup>J<sub>HH</sub> = 7.3 Hz, CH<sub>2</sub>(CH<sub>2</sub>)<sub>5</sub>Rf<sub>8</sub>), 1.95-2.06 (*m*, 12H, (CH<sub>2</sub>)<sub>5</sub>CH<sub>2</sub>Rf<sub>8</sub>), 1.49-1.56 (*m*, 12H, CH<sub>2</sub>CH<sub>2</sub>(CH<sub>2</sub>)<sub>4</sub>Rf<sub>8</sub>), 1.38-1.45 (*m*, 12H, CH<sub>2</sub>CH<sub>2</sub>CH<sub>2</sub>(CH<sub>2</sub>)<sub>3</sub>Rf<sub>8</sub>), 1.27-1.33 (*m*, 12H, (CH<sub>2</sub>)<sub>4</sub>CH<sub>2</sub>CH<sub>2</sub>Rf<sub>8</sub>), 1.11-1.17 (*m*, 12H, (CH<sub>2</sub>)<sub>3</sub>CH<sub>2</sub>CH<sub>2</sub>CH<sub>2</sub>Rf<sub>8</sub>).

**<sup>13</sup>C-NMR:** (125.77 MHz, CDCl<sub>3</sub>): δ 140.31 (Ph), 138.67 (Ph), 138.48 (Ph), 131.50 (Ph), 126.43 (Ph), 108.71-120.53 (Rf<sub>8</sub>), 35.12 (CH<sub>2</sub>(CH<sub>2</sub>)<sub>5</sub>Rf<sub>8</sub>), 30.98 (*t*, <sup>2</sup>J<sub>CF</sub> = 22.5 Hz, (CH<sub>2</sub>)<sub>5</sub>CH<sub>2</sub>Rf<sub>8</sub>), 30.85 (CH<sub>2</sub>CH<sub>2</sub>(CH<sub>2</sub>)<sub>4</sub>Rf<sub>8</sub>), 29.01 (CH<sub>2</sub>CH<sub>2</sub>CH<sub>2</sub>(CH<sub>2</sub>)<sub>3</sub>Rf<sub>8</sub>), 28.34 ((CH<sub>2</sub>)<sub>3</sub>CH<sub>2</sub>CH<sub>2</sub>CH<sub>2</sub>Rf<sub>8</sub>), 20.14 (*t*, <sup>3</sup>J<sub>CF</sub> = 3.3 Hz, (CH<sub>2</sub>)<sub>4</sub>CH<sub>2</sub>CH<sub>2</sub>Rf<sub>8</sub>).

**MALDI-ICR-MS (DCTB):** m/z (% int.): 3546.64 (M<sup>+</sup>, 100%).



## 21.10.9 2,5,8,11,14,17-Hexakis-(7,7,8,8,9,9,10,10,11,11,12,12,13,13,14,14,14-heptafluoro-tetradecyl)hexabenzob[bc,ef,hi,kl,no,q]coronene



The cyclodehydrogenation was performed similarly to **method C** taking HPB **105b** (200 mg, 56.0  $\mu\text{mol}$ ) as precursor together with  $\text{FeCl}_3$  (820 mg, 5.0 mmol, 7.5 eq / H to be removed),  $\text{CH}_3\text{NO}_2$  (12 mL),  $\text{CH}_2\text{Cl}_2$  (15 mL), HFB (15 mL). The reaction mixture was stirred at 35 °C under constant argon bubbling for 8 hours, before being quenched by the addition of methanol (50 mL). The formed brown precipitate was collected by suction filtration over Millipore<sup>®</sup>, and was purified by suspending in ether, dichloromethane, ethanol, methanol and nitromethane, treated each time in an ultrasonic bath and collected by Millipore<sup>®</sup> filtration. Final purification was achieved by precipitation out of BTF by the addition of ethanol and ether. The title HBC **106b** was afforded as yellow solid (130 mg, 65%).

**<sup>1</sup>H-NMR:** (360 MHz, HFB,  $\text{CDCl}_3$ ):  $\delta$  8.83 (br. s, 12H, Ph), 3.48 (br. s, 12H,  $\text{CH}_2(\text{CH}_2)_5\text{Rf}_8$ ), 2.46 (br. s, 24H,  $\text{CH}_2\text{CH}_2\text{CH}_2\text{CH}_2\text{CH}_2\text{CH}_2\text{Rf}_8$ ), 2.10 (br. s, 36H,  $\text{CH}_2\text{CH}_2\text{CH}_2\text{CH}_2\text{CH}_2\text{CH}_2\text{Rf}_8$ ).

**MALDI-ICR-MS (DCTB):**  $m/z$  (% int.): 3534.55 ( $\text{M}^{+}$ , 100%; calcd. for  $\text{C}_{126}\text{H}_{84}\text{F}_{102}$  3534.49), 3046.68 ( $[\text{M}-\text{Rf}_{5,8}]^{+}$ , 24%).

**UV/VIS:** (BTF,  $10^{-6}$  M,  $\epsilon = 2.5 \cdot 10^5$ ),  $\lambda_{\text{max}} = 346, 360, 391$  nm.



mmol),  $\text{NEt}_3$  (25.6 mL, 0.18 mol) and THF (120 mL). The Schlenk tube was sealed and heated to 75 °C for 22 hours. The cold reaction mixture was then quenched by the addition of water (100 mL) and extracted with ether (3 x 100 mL). The combined organic fractions were washed with HCl 10% (150 mL) and water (100 mL), dried over  $\text{Na}_2\text{SO}_4$  and all volatiles were removed yielding a brown oil. Several filtrations over silica gel under reduced pressure using first pentane – ether (9:1) as eluent, followed by pentane for the succeeding filtrations were performed, yielding the desired compound **120a** as colourless oil (11.6 g, 78%).

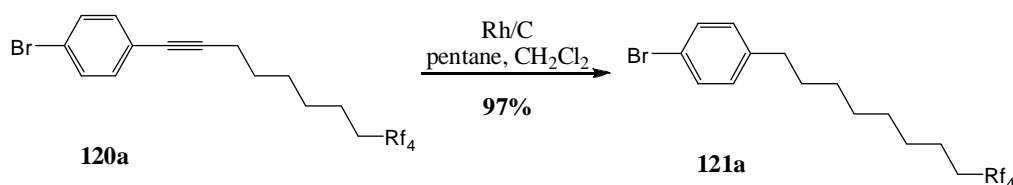
**TLC:**  $R_f$  = 0.81 (silica gel, pentane,  $\text{KMnO}_4$ ).

**$^1\text{H}$ -NMR:** (360 MHz,  $\text{CDCl}_3$ ):  $\delta$  7.42 (*d*, 2H,  $^3J_{\text{HH}}$  = 8.2 Hz, Ph), 7.26 (*d*, 2H,  $^3J_{\text{HH}}$  = 8.2 Hz, Ph), 2.42 (*t*, 2H,  $^3J_{\text{HH}}$  = 6.8 Hz,  $\text{C}\equiv\text{CCH}_2(\text{CH}_2)_5\text{Rf}_4$ ), 2.01-2.16 (*m*, 2H,  $\text{C}\equiv\text{C}(\text{CH}_2)_5\text{CH}_2\text{Rf}_4$ ), 1.59-1.69 (*m*, 4H,  $\text{C}\equiv\text{CCH}_2\text{CH}_2\text{CH}_2\text{CH}_2\text{CH}_2\text{CH}_2\text{Rf}_4$ ), 1.45-1.53 (*m*, 4H,  $\text{C}\equiv\text{CCH}_2\text{CH}_2\text{CH}_2\text{CH}_2\text{CH}_2\text{CH}_2\text{Rf}_4$ ).

**$^{13}\text{C}$ -NMR:** (90.55 MHz,  $\text{CDCl}_3$ ):  $\delta$  132.99 (Ph), 131.42 (Ph), 122.90 (Ph), 121.64 (Ph), 108.54-121.07 ( $\text{Rf}_4$ ), 91.23 ( $\text{C}\equiv\text{C}(\text{CH}_2)_6\text{Rf}_4$ ), 79.82 ( $\text{C}\equiv\text{C}(\text{CH}_2)_6\text{Rf}_4$ ), 30.72 (*t*,  $^2J_{\text{CF}}$  = 22.5 Hz,  $\text{C}\equiv\text{C}(\text{CH}_2)_5\text{CH}_2\text{Rf}_4$ ), 28.61 ( $\text{C}\equiv\text{CCH}_2\text{CH}_2(\text{CH}_2)_4\text{Rf}_4$ ), 28.45 ( $\text{C}\equiv\text{CCH}_2\text{CH}_2\text{CH}_2(\text{CH}_2)_3\text{Rf}_4$ ), 28.27 ( $\text{C}\equiv\text{C}(\text{CH}_2)_3\text{CH}_2\text{CH}_2\text{CH}_2\text{Rf}_4$ ), 20.00 (*t*,  $^3J_{\text{CF}}$  = 3.3 Hz,  $\text{C}\equiv\text{C}(\text{CH}_2)_4\text{CH}_2\text{CH}_2\text{Rf}_4$ ), 19.31 ( $\text{C}\equiv\text{CCH}_2(\text{CH}_2)_5\text{Rf}_4$ ).

**EI-MS:**  $m/z$  (% int.): 484.7 ( $\text{M}^{+}$ , 9%), 237.1 ( $[\text{M}-\text{Rf}_{2,4}]^{+}$ , 8%), 223.1 ( $[\text{M}-\text{Rf}_{3,4}]^{+}$ , 22%), 209.0 ( $[\text{M}-\text{Rf}_{4,4}]^{+}$ , 6%), 194.9 ( $[\text{M}-\text{Rf}_{5,4}]^{+}$ , 65%), 181.8 ( $[\text{M}-\text{Rf}_{6,4}]^{+}$ , 12%), 168.9 ( $[\text{M}-\text{CRf}_{6,4}]^{+}$ , 8%), 142 (100%).

### 21.11.3 1-Bromo-4-(9,9,10,10,11,11,12,12,12-nonafluorododecyl)benzene



The hydrogenation of compound **120a** (2.4 g, 4.96 mmol) was carried out following **method E** using Rh/C (150 mg) as catalyst and a mixture of pentane (18 mL) and  $\text{CH}_2\text{Cl}_2$  (6 mL) as solvent. The reaction was stirred for 18 hours at room temperature under 60 atmospheres of hydrogen before the catalyst was removed by filtration over silica gel. All volatiles of the filtrate were removed yielding compound **121a** as pure colourless oil (2.34 g, 97%).

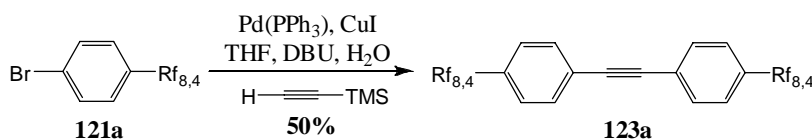
**TLC:**  $R_f$  = 0.91 (silica gel, pentane,  $\text{KMnO}_4$ ).

**$^1\text{H}$ -NMR:** (360 MHz,  $\text{CDCl}_3$ ):  $\delta$  7.39 (*d*, 2H,  $^3J_{\text{HH}}$  = 8.2 Hz, Ph), 7.05 (*d*, 2H,  $^3J_{\text{HH}}$  = 8.2 Hz, Ph), 2.56 (*t*, 2H,  $^3J_{\text{HH}}$  = 7.7 Hz,  $\text{CH}_2(\text{CH}_2)_7\text{Rf}_4$ ), 1.97-2.12 (*m*, 2H,  $(\text{CH}_2)_7\text{CH}_2\text{Rf}_4$ ), 1.54-1.60 (*m*, 4H,  $\text{CH}_2\text{CH}_2(\text{CH}_2)_4\text{CH}_2\text{CH}_2\text{Rf}_4$ ), 1.28-1.39 (*m*, 8H,  $\text{CH}_2\text{CH}_2(\text{CH}_2)_4\text{CH}_2\text{CH}_2\text{Rf}_4$ ).

**$^{13}\text{C}$ -NMR:** (90.55 MHz,  $\text{CDCl}_3$ ):  $\delta$  141.67 (Ph), 131.26 (Ph), 130.15 (Ph), 119.29 (Ph), 105.35-120.77 ( $\text{Rf}_4$ ), 35.29 ( $\text{CH}_2(\text{CH}_2)_7\text{Rf}_4$ ), 31.26 ( $\text{CH}_2\text{CH}_2(\text{CH}_2)_6\text{Rf}_4$ ), 30.75 ( $t$ ,  $^2J_{\text{CF}} = 22.5$  Hz,  $(\text{CH}_2)_7\text{CH}_2\text{Rf}_4$ ), 29.02-29.17 ( $4\text{C}$   $\text{CH}_2\text{CH}_2(\text{CH}_2)_4\text{CH}_2\text{CH}_2\text{Rf}_4$ ), 20.03 ( $t$ ,  $^3J_{\text{CF}} = 3.3$  Hz,  $(\text{CH}_2)_6\text{CH}_2\text{CH}_2\text{Rf}_4$ ).

**EI-MS:**  $m/z$  (% int.): 488.7 ( $\text{M}^{+\bullet}$ , 13%), 168.9 ( $[\text{M}-\text{Rf}_{7,4}]^{+\bullet}$ , 100%), 91.0 ( $[\text{M}-\text{Rf}_{7,4}-\text{Br}]^{+\bullet}$ , 41%).

21.11.4 1-(9,9,10,10,11,11,12,12,12-Nonafluorododecyl)-4-{{[4-(9,9,10,10,11,11,12,12,12-nonafluorododecyl)phenyl]ethynyl}benzene



This Sonogashira reaction was carried out accordingly to **method A** using compound **121a** (11.4 g, 23.4 mmol),  $\text{Pd(PPh}_3)_4$  (1.62 g, 1.4 mmol),  $\text{CuI}$  (446 mg, 2.3 mmol), DBU (20.9 mL, 0.14 mol), TMSA (1.29 mL, 13.0 mmol), water (0.15 mL, 9.4 mmol) and THF (120 mL). The mixture was stirred at 80 °C for 3 days before being cooled to room temperature and being diluted with ether (500 mL). The obtained dark suspension was washed with water (100 mL), 10% HCl (200 mL) and water (100 mL), dried over  $\text{Na}_2\text{SO}_4$  and all volatiles were removed under reduced pressure. The obtained dark solid was dissolved in ether and filtered over a plug of basic alox taking pentane – ether (9:1) as eluent. The filtrate was reduced maximally and the orange solid was recrystallized from pentane – methanol yielding the desired tolane **123a** as white solid in good yield (4.8 g, 50%).

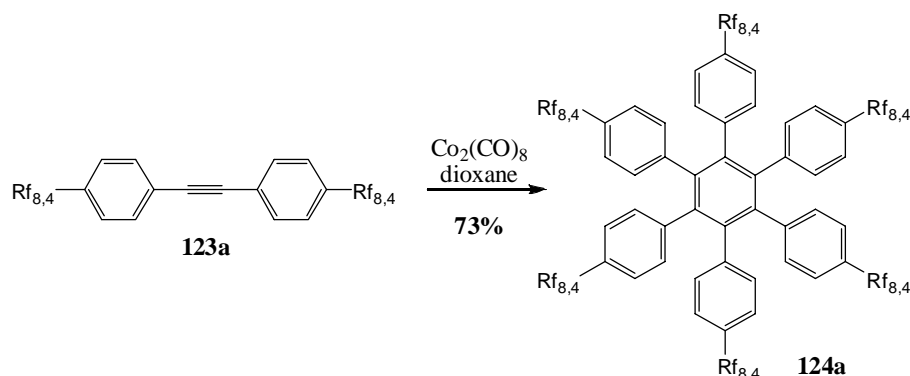
**TLC:**  $R_f = 0.52$  (silica gel, pentane,  $\text{KMnO}_4$ ).

**$^1\text{H}$ -NMR:** (360 MHz,  $\text{CDCl}_3$ ):  $\delta$  7.43 ( $d$ , 4H,  $^3J_{\text{HH}} = 8.2$  Hz, Ph), 7.15 ( $d$ , 4H,  $^3J_{\text{HH}} = 8.2$  Hz, Ph), 2.61 ( $t$ , 4H,  $^3J_{\text{HH}} = 7.3$  Hz,  $\text{CH}_2(\text{CH}_2)_7\text{Rf}_4$ ), 1.97-2.12 ( $m$ , 4H,  $(\text{CH}_2)_7\text{CH}_2\text{Rf}_4$ ), 1.55-1.63 ( $m$ , 8H,  $\text{CH}_2\text{CH}_2(\text{CH}_2)_4\text{CH}_2\text{CH}_2\text{Rf}_4$ ), 1.28-1.39 ( $m$ , 16H,  $\text{CH}_2\text{CH}_2(\text{CH}_2)_4\text{CH}_2\text{CH}_2\text{Rf}_4$ ).

**$^{13}\text{C}$ -NMR:** (90.55 MHz,  $\text{CDCl}_3$ ):  $\delta$  143.06 (Ph), 131.48 (Ph), 128.44 (Ph), 120.65 (Ph), 105.25-119.03 ( $\text{Rf}_4$ ), 88.92 (acetylene), 35.85 ( $\text{CH}_2(\text{CH}_2)_7\text{Rf}_4$ ), 31.19 ( $\text{CH}_2\text{CH}_2(\text{CH}_2)_6\text{Rf}_4$ ), 30.77 ( $t$ ,  $^2J_{\text{CF}} = 22.5$  Hz,  $(\text{CH}_2)_7\text{CH}_2\text{Rf}_4$ ), 29.06-29.22 ( $8\text{C}$   $\text{CH}_2\text{CH}_2(\text{CH}_2)_4\text{CH}_2\text{CH}_2\text{Rf}_4$ ), 20.06 ( $t$ ,  $^3J_{\text{CF}} = 3.3$  Hz,  $(\text{CH}_2)_6\text{CH}_2\text{CH}_2\text{Rf}_4$ ).

**MALDI-ICR-MS (DCTB):**  $m/z$  (% int.): 1089.44 ( $[\text{M}+\text{DCTB}]^{+\bullet}$ , 100%), 838.29 ( $\text{M}^{+\bullet}$ , 63%).

## 21.11.5 Hexakis[4-(9,9,10,10,11,11,12,12,12-nonafluorododecyl)phenyl]benzene



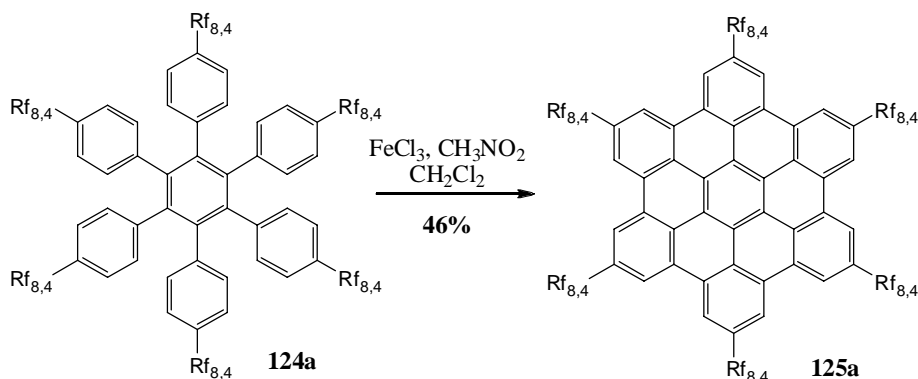
The cyclotrimerisation was performed taking **method B** using tolane **123a** (2.5 g, 2.98 mmol),  $\text{Co}_2(\text{CO})_8$  (61 mg, 0.179 mmol) and dioxane (120 mL). The dark reaction mixture was refluxed for 23 hours, cooled to room temperature and reduced. The obtained brown oil was filtered over a plug of silica gel using first pentane followed by ether. The pentane fraction was discarded whereas all volatiles of the ether fraction were removed yielding the HPB derivative **124a** as slightly violet oil in good yield (1.82 g, 73%).

**TLC:**  $R_f = 0.97$  (silica gel, pentane – ether (9:1),  $\text{KMnO}_4$ ).

**$^1\text{H-NMR}$ :** (360 MHz,  $\text{CDCl}_3$ ):  $\delta$  6.67 (*d*, 12H,  $^3J_{\text{HH}} = 8.2$  Hz, Ph), 6.61 (*d*, 12H,  $^3J_{\text{HH}} = 8.2$  Hz, Ph), 2.34 (*t*, 12H,  $^3J_{\text{HH}} = 7.3$  Hz,  $\text{CH}_2(\text{CH}_2)_7\text{Rf}_4$ ), 1.95-2.10 (*m*, 12H,  $(\text{CH}_2)_7\text{CH}_2\text{Rf}_4$ ), 1.50-1.61 (*m*, 24H,  $\text{CH}_2\text{CH}_2(\text{CH}_2)_4\text{CH}_2\text{CH}_2\text{Rf}_4$ ), 1.25-1.39 (*m*, 48H,  $\text{CH}_2\text{CH}_2(\text{CH}_2)_4\text{CH}_2\text{CH}_2\text{Rf}_4$ ).

**$^{13}\text{C-NMR}$ :** (90.55 MHz,  $\text{CDCl}_3$ ):  $\delta$  140.27 (Ph), 138.85 (Ph), 138.33 (Ph), 131.42 (Ph), 126.43 (Ph), 107.63-122.18 ( $\text{Rf}_4$ ), 35.29 ( $\text{CH}_2(\text{CH}_2)_7\text{Rf}_4$ ), 31.13 ( $\text{CH}_2\text{CH}_2(\text{CH}_2)_6\text{Rf}_4$ ), 30.77 (*t*,  $^2J_{\text{CF}} = 22.5$  Hz,  $(\text{CH}_2)_7\text{CH}_2\text{Rf}_4$ ), 28.70-29.24 (24C  $\text{CH}_2\text{CH}_2(\text{CH}_2)_4\text{CH}_2\text{CH}_2\text{Rf}_4$ ), 20.07 (*t*,  $^3J_{\text{CF}} = 3.3$  Hz,  $(\text{CH}_2)_6\text{CH}_2\text{CH}_2\text{Rf}_4$ ).

**MALDI-ICR-MS (DCTB):**  $m/z$  (% int.): 2514.85 ( $\text{M}^+$ , 100%).

21.11.6 2,5,8,11,14,17-Hexakis-(9,9,10,10,11,11,12,12,12-nonafluorododecyl)hexabenzocoronene  
 [bc,ef,hi,kl,no,qr]coronene


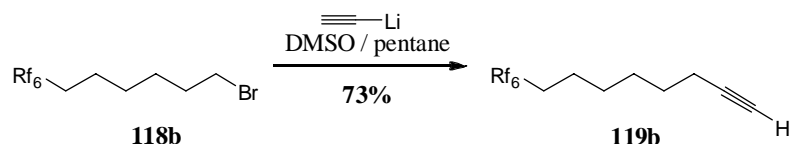
The planarization was performed following **method C** using HPB **124a** (1.0 g, 0.4 mmol) as precursor together with  $\text{FeCl}_3$  (5.8 g, 36 mmol, 7.5 eq / H to be removed),  $\text{CH}_3\text{NO}_2$  (20 mL) and  $\text{CH}_2\text{Cl}_2$  (80 mL). The reaction mixture was heated at 45 °C for 7 hours under constant argon bubbling before a reductive workup was performed by the addition of methanol (100 mL). The crude product was suction filtered over Millipore<sup>®</sup> and obtained as black “crystalline” product. Precipitation out of BTF and HFB yielded at best a dark brown powder in moderate yield (0.46 g, 46%).

**MALDI-ICR-MS (DCTB):**  $m/z$  (% int.): 2502.1 ( $\text{M}^{*+}$ , 100%; calcd. for  $\text{C}_{114}\text{H}_{108}\text{F}_{54}$  2502.76), 2536.1 ( $[\text{M}-\text{H}+\text{Cl}]^{*+}$ , 25%), 2570.0 ( $[\text{M}-2 \times \text{H} + 2 \times \text{Cl}]^{*+}$ , 16%), 2604.0 ( $[\text{M}-3 \times \text{H} + 3 \times \text{Cl}]^{*+}$ , 5%), 2637.9 ( $[\text{M}-4 \times \text{H} + 4 \times \text{Cl}]^{*+}$ , 2%).

**UV/VIS:** (BTF,  $10^{-6}$  M,  $\epsilon = 5.2 \cdot 10^5$ ),  $\lambda_{\text{max}} = 323, 372, 451$  nm.

21.12 Synthesis of HBC-(Rf<sub>8,6</sub>)<sub>6</sub>

## 21.12.1 9,9,10,10,11,11,12,12,13,13,14,14,14-Tridecafluorotetradec-1-yne



Compound **118b** (12.0 g, 24.8 mmol) was reacted accordingly to **method J** with lithium acetylide ethylenediamine complex (16.9 g, 74.5 mmol) in a mixture of pentane (20 mL) and DMSO (30 mL). The dark suspension was stirred at room temperature for 19 hours, before water (20 mL) was added to quench the reaction. The resulting black suspension was Büchner filtrated and washed exhaustively with dichloromethane. The filtrate was washed with water (2 x 100 mL), dried over Na<sub>2</sub>SO<sub>4</sub> and all volatiles were removed. Filtration over a short plug of silica gel under reduced pressure using pentane as eluent afforded after evaporation of pentane the desired alkyne **119b** as colourless oil (7.72 g, 73%).

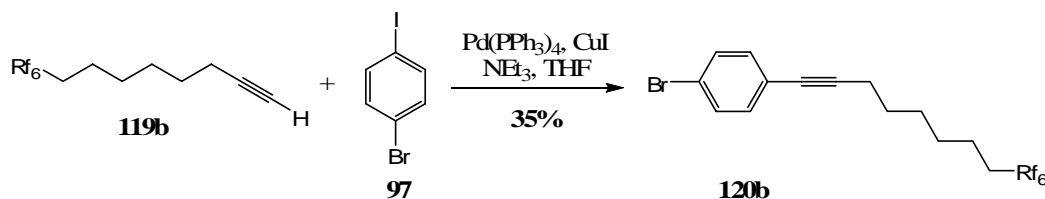
**TLC:** R<sub>f</sub> = 0.84 (silica gel, pentane, KMnO<sub>4</sub>).

**<sup>1</sup>H-NMR:** (360 MHz, CDCl<sub>3</sub>): δ 2.21 (*td*, 2H, <sup>3</sup>J<sub>HH</sub> = 7.0 Hz, <sup>4</sup>J<sub>HH</sub> = 2.7 Hz, HC≡CCH<sub>2</sub>(CH<sub>2</sub>)<sub>5</sub>Rf<sub>6</sub>), 2.00-2.15 (*m*, 2H, HC≡C(CH<sub>2</sub>)<sub>5</sub>CH<sub>2</sub>Rf<sub>6</sub>), 1.96 (*t*, 1H, <sup>4</sup>J<sub>HH</sub> = 2.7 Hz, HC≡C(CH<sub>2</sub>)<sub>6</sub>Rf<sub>6</sub>), 1.59-1.67 (*m*, 2H, HC≡C(CH<sub>2</sub>)<sub>4</sub>CH<sub>2</sub>CH<sub>2</sub>Rf<sub>6</sub>), 1.52-1.59 (*m*, 2H, Hz, HC≡C(CH<sub>2</sub>)<sub>3</sub>CH<sub>2</sub>CH<sub>2</sub>CH<sub>2</sub>Rf<sub>6</sub>), 1.39-1.52 (*m*, 4H, HC≡CCH<sub>2</sub>CH<sub>2</sub>CH<sub>2</sub>(CH<sub>2</sub>)<sub>3</sub>Rf<sub>6</sub>).

**<sup>13</sup>C-NMR:** (90.55 MHz, CDCl<sub>3</sub>): δ 103.61-121.66 (Rf<sub>6</sub>), 84.30 (HC≡C(CH<sub>2</sub>)<sub>6</sub>Rf<sub>6</sub>), 68.34 (HC≡C(CH<sub>2</sub>)<sub>6</sub>Rf<sub>6</sub>), 30.81 (*t*, <sup>2</sup>J<sub>CF</sub> = 22.5 Hz, HC≡C(CH<sub>2</sub>)<sub>5</sub>CH<sub>2</sub>Rf<sub>6</sub>), 28.56 (HC≡C(CH<sub>2</sub>)<sub>3</sub>CH<sub>2</sub>CH<sub>2</sub>CH<sub>2</sub>Rf<sub>6</sub>), 28.24 (HC≡CCH<sub>2</sub>CH<sub>2</sub>CH<sub>2</sub>(CH<sub>2</sub>)<sub>3</sub>Rf<sub>6</sub>), 28.11 (HC≡CCH<sub>2</sub>CH<sub>2</sub>(CH<sub>2</sub>)<sub>4</sub>Rf<sub>6</sub>), 20.00 (*t*, <sup>3</sup>J<sub>CF</sub> = 3.3 Hz, HC≡C(CH<sub>2</sub>)<sub>4</sub>CH<sub>2</sub>CH<sub>2</sub>Rf<sub>6</sub>), 18.28 (HC≡CCH<sub>2</sub>(CH<sub>2</sub>)<sub>5</sub>Rf<sub>6</sub>).

**EI-MS:** m/z (% int.): 95.1 ([M-Rf<sub>2,6</sub>]<sup>+</sup>, 33%), 81.1 ([M-Rf<sub>3,6</sub>]<sup>+</sup>, 100%), 67.1 ([M-Rf<sub>4,6</sub>]<sup>+</sup>, 36%).

## 21.12.2 1-Bromo-4-(9,9,10,10,11,11,12,12,13,13,14,14,14-tridecafluorotetradec-1-ynyl)benzene



This synthesis was carried out following **method K**. Compound **119b** (5.5 g, 12.8 mmol) was reacted with 1-bromo-4-iodobenzene (3.6 g, 12.8 mmol) using  $\text{Pd(PPh}_3)_4$  (0.89 g, 0.77 mmol) as catalyst and  $\text{CuI}$  (245 mg, 1.28 mmol) and  $\text{NEt}_3$  (10.75 mL, 77.0 mmol) as addend and THF (65 mL) as solvent. After six days of reaction the crude mixture was extracted with ether (5 x 100 mL). The combined organic phases were washed with HCl 10% (100 mL) and water (100 mL), dried over  $\text{Na}_2\text{SO}_4$  and all solvents were evaporated. The resulting dark oil was filtered over silica gel with a mixture of pentane – ether (9:1) first and pentane second to yield the desired compound **120b** as a colourless oil (2.63 g, 35%).

**TLC:**  $R_f$  = 0.86 (silica gel, pentane,  $\text{KMnO}_4$ ).

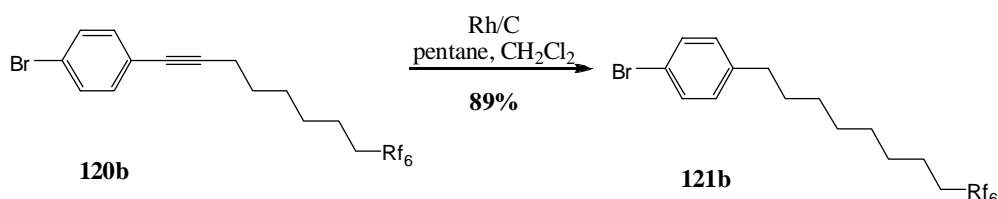
**$^1\text{H-NMR}$ :** (360 MHz,  $\text{CDCl}_3$ ):  $\delta$  7.42 (*d*, 2H,  $^3J_{\text{HH}}$  = 8.2 Hz, Ph), 7.26 (*d*, 2H,  $^3J_{\text{HH}}$  = 8.2 Hz, Ph), 2.42 (*t*, 2H,  $^3J_{\text{HH}}$  = 6.8 Hz,  $\text{C}\equiv\text{CCH}_2(\text{CH}_2)_5\text{Rf}_6$ ), 2.01-2.16 (*m*, 2H,  $\text{C}\equiv\text{C}(\text{CH}_2)_5\text{CH}_2\text{Rf}_6$ ), 1.59-1.70 (*m*, 4H,  $\text{C}\equiv\text{CCH}_2\text{CH}_2\text{CH}_2\text{CH}_2\text{CH}_2\text{CH}_2\text{Rf}_6$ ), 1.45-1.55 (*m*, 4H,  $\text{C}\equiv\text{CCH}_2\text{CH}_2\text{CH}_2\text{CH}_2\text{CH}_2\text{CH}_2\text{Rf}_6$ ).

**$^{13}\text{C-NMR}$ :** (90.55 MHz,  $\text{CDCl}_3$ ):  $\delta$  132.99 (Ph), 131.42 (Ph), 122.90 (Ph), 121.64 (Ph), 107.22-119.17 ( $\text{Rf}_6$ ), 91.23 ( $\text{C}\equiv\text{C}(\text{CH}_2)_6\text{Rf}_6$ ), 79.83 ( $\text{C}\equiv\text{C}(\text{CH}_2)_6\text{Rf}_6$ ), 30.83 (*t*,  $^2J_{\text{CF}}$  = 22.5 Hz,  $\text{C}\equiv\text{C}(\text{CH}_2)_5\text{CH}_2\text{Rf}_6$ ), 28.62 ( $\text{C}\equiv\text{CCH}_2\text{CH}_2(\text{CH}_2)_4\text{Rf}_6$ ), 28.45 ( $\text{C}\equiv\text{CCH}_2\text{CH}_2\text{CH}_2(\text{CH}_2)_3\text{Rf}_6$ ), 28.29 ( $\text{C}\equiv\text{C}(\text{CH}_2)_3\text{CH}_2\text{CH}_2\text{CH}_2\text{Rf}_6$ ), 20.03 (*t*,  $^3J_{\text{CF}}$  = 3.3 Hz,  $\text{C}\equiv\text{C}(\text{CH}_2)_4\text{CH}_2\text{CH}_2\text{Rf}_6$ ), 19.32 ( $\text{C}\equiv\text{CCH}_2(\text{CH}_2)_5\text{Rf}_6$ ).

**EI-MS:**  $m/z$  (% int.): 584.9 ( $\text{M}^+$ , 7%), 237.1 ( $[\text{M-Rf}_{2,6}]^+$ , 8%), 223.1 ( $[\text{M-Rf}_{3,6}]^+$ , 35%), 209.0 ( $[\text{M-Rf}_{4,6}]^+$ , 6%), 194.9 ( $[\text{M-Rf}_{5,6}]^+$ , 84%), 181.8 ( $[\text{M-Rf}_{6,6}]^+$ , 12%), 168.9 ( $[\text{M-CRf}_{6,6}]^+$ , 18%), 142 (100%).



## 21.12.3 1-Bromo-4-(9,9,10,10,11,11,12,12,13,13,14,14,14-tridecafluorotetradecyl)benzene



The hydrogenation of compound **120b** (2.5 g, 4.3 mmol) was carried out following **method E** using Rh/C (130 mg) as catalyst and a mixture of pentane (24 mL) and CH<sub>2</sub>Cl<sub>2</sub> (7 mL) as solvents. The reaction was stirred for 24 hours at room temperature under 60 atmospheres of hydrogen before the catalyst was removed by filtration over silica gel. All volatiles of the filtrate were removed yielding compound **121b** as pure colourless oil (2.24 g, 89%).

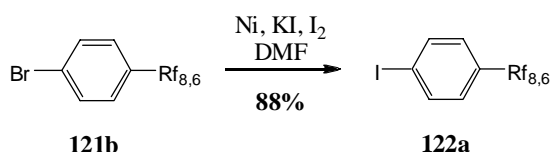
**TLC:** R<sub>f</sub> = 0.90 (silica gel, pentane, KMnO<sub>4</sub>).

**<sup>1</sup>H-NMR:** (360 MHz, CDCl<sub>3</sub>): δ 7.39 (*d*, 2H, <sup>3</sup>J<sub>HH</sub> = 8.2 Hz, Ph), 7.05 (*d*, 2H, <sup>3</sup>J<sub>HH</sub> = 8.2 Hz, Ph), 2.56 (*t*, 2H, <sup>3</sup>J<sub>HH</sub> = 7.7 Hz, CH<sub>2</sub>(CH<sub>2</sub>)<sub>7</sub>Rf<sub>6</sub>), 1.98-2.13 (*m*, 2H, Ph-(CH<sub>2</sub>)<sub>7</sub>CH<sub>2</sub>Rf<sub>6</sub>), 1.56-1.60 (*m*, 4H, CH<sub>2</sub>CH<sub>2</sub>(CH<sub>2</sub>)<sub>4</sub>CH<sub>2</sub>CH<sub>2</sub>Rf<sub>6</sub>), 1.27-1.38 (*m*, 8H, CH<sub>2</sub>CH<sub>2</sub>(CH<sub>2</sub>)<sub>4</sub>CH<sub>2</sub>CH<sub>2</sub>Rf<sub>6</sub>).

**<sup>13</sup>C-NMR:** (90.55 MHz, CDCl<sub>3</sub>): δ 141.67 (Ph), 131.27 (Ph), 130.15 (Ph), 119.29 (Ph), 105.35-120.77 (Rf<sub>6</sub>), 35.30 (CH<sub>2</sub>(CH<sub>2</sub>)<sub>7</sub>Rf<sub>6</sub>), 31.23 (CH<sub>2</sub>CH<sub>2</sub>(CH<sub>2</sub>)<sub>6</sub>Rf<sub>6</sub>), 30.85 (*t*, <sup>2</sup>J<sub>CF</sub> = 22.5 Hz, (CH<sub>2</sub>)<sub>7</sub>CH<sub>2</sub>Rf<sub>6</sub>), 29.05-29.11 (4C, CH<sub>2</sub>CH<sub>2</sub>(CH<sub>2</sub>)<sub>4</sub>CH<sub>2</sub>CH<sub>2</sub>Rf<sub>6</sub>), 20.07 (*t*, <sup>3</sup>J<sub>CF</sub> = 3.3 Hz, (CH<sub>2</sub>)<sub>6</sub>CH<sub>2</sub>CH<sub>2</sub>Rf<sub>6</sub>).

**EI-MS:** m/z (% int.): 589.7 (M<sup>+</sup>, 9%), 170.9 ([M-Rf<sub>7,6</sub>]<sup>+</sup>, 100%), 90.9 ([M-Rf<sub>7,6</sub>-Br]<sup>+</sup>, 33%).

## 21.12.4 1-Iodo-4-(9,9,10,10,11,11,12,12,13,13,14,14,14-tridecafluorotetradecyl)benzene



The halogen exchange was performed as described in **method F** by reacting compound **121b** (2.1 g, 3.6 mmol) with KI (1.2 g, 7.15 mmol) in the presence of Ni (1.05 g, 17.9 mmol), I<sub>2</sub> (45 mg, 0.18 mmol) and DMF (15 mL). The dark reaction mixture was stirred at 150 °C for 24 hours before the crude product was extracted with pentane (3 x 50 mL). The combined organic phases were washed with water (100 mL), 10% HCl (100 mL) and water (50 mL), dried over Na<sub>2</sub>SO<sub>4</sub> and all volatiles were removed. Silica gel plug filtration under reduced pressure using pentane yielded the desired compound **122a** as colourless oil (2.0 g, 88%).

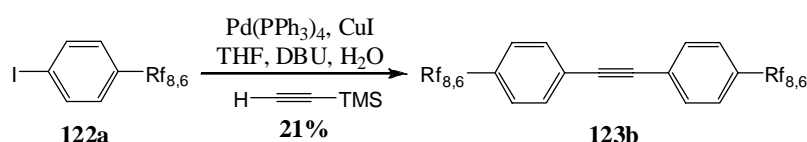
**TLC:**  $R_f$  = 0.90 (silica gel, pentane,  $\text{KMnO}_4$ ).

**$^1\text{H-NMR}$ :** (360 MHz,  $\text{CDCl}_3$ ):  $\delta$  7.58 (*d*, 2H,  $^3J_{\text{HH}} = 8.2$  Hz, Ph), 6.92 (*d*, 2H,  $^3J_{\text{HH}} = 8.2$  Hz, Ph), 2.54 (*t*, 2H,  $^3J_{\text{HH}} = 7.3$  Hz,  $\text{CH}_2(\text{CH}_2)_7\text{Rf}_6$ ), 1.96-2.11 (*m*, 2H,  $(\text{CH}_2)_7\text{CH}_2\text{Rf}_6$ ), 1.54-1.60 (*m*, 4H,  $\text{CH}_2\text{CH}_2(\text{CH}_2)_4\text{CH}_2\text{CH}_2\text{Rf}_6$ ), 1.28-1.39 (*m*, 8H,  $\text{CH}_2\text{CH}_2(\text{CH}_2)_4\text{CH}_2\text{CH}_2\text{Rf}_6$ ).

**$^{13}\text{C-NMR}$ :** (90.55 MHz,  $\text{CDCl}_3$ ):  $\delta$  142.78 (Ph), 137.67 (Ph), 130.94 (Ph), 90.94 (Ph), 105.79-119.70 ( $\text{Rf}_6$ ), 35.79 ( $\text{CH}_2(\text{CH}_2)_7\text{Rf}_6$ ), 31.60 ( $\text{CH}_2\text{CH}_2(\text{CH}_2)_6\text{Rf}_6$ ), 31.26 (*t*,  $^2J_{\text{CF}} = 22.5$  Hz,  $(\text{CH}_2)_7\text{CH}_2\text{Rf}_6$ ), 29.45-29.52 (4C,  $\text{CH}_2\text{CH}_2(\text{CH}_2)_4\text{CH}_2\text{CH}_2\text{Rf}_6$ ), 20.47 (*t*,  $^3J_{\text{CF}} = 3.3$  Hz,  $(\text{CH}_2)_6\text{CH}_2\text{CH}_2\text{Rf}_6$ ).

**EI-MS:**  $m/z$  (% int.): 635.2 ( $\text{M}^{*+}$ , 16%), 217.0 ( $[\text{M-Rf}_{7,6}]^{*+}$ , 100%), 90.9 ( $[\text{M-Rf}_{7,6}-\text{I}]^{*+}$ , 29%).

21.12.5 1-(9,9,10,10,11,11,12,12,13,13,14,14,14-Tridecafluorotetradecyl)-4-{[4-(9,9,10,10,11,11,12,12,13,13,14,14,14-tridecafluorotetradecyl)phenyl]ethynyl}benzene



The tolane formation was achieved using **method A**. Iodoaryl **122a** (2.0 g, 3.15 mmol) was reacted with  $\text{Pd(PPh}_3)_4$  (219 mg, 0.19 mmol),  $\text{CuI}$  (60 mg, 0.32 mmol), DBU (2.8 mL, 18.9 mmol), TMSA (0.23 mL, 1.57 mmol),  $\text{H}_2\text{O}$  (23  $\mu\text{L}$ , 1.26 mmol) and THF (20 mL) for 6 hours at 40 °C followed by 75 °C for 3 days. The reaction mixture was quenched by the addition of a saturated solution of  $\text{NH}_4\text{Cl}$  (50 mL). The formed emulsion was extracted with water (50 mL) and HCl 10% (100 mL). The combined organic fractions were dried over  $\text{Na}_2\text{SO}_4$  and all volatiles were removed under reduced pressure. The obtained brown solid was dissolved in pentane – ether (9:1) and filtrated over basic alox under reduced pressure. After removal of the solvent a yellow solid was obtained which was recrystallized in pentane – ethanol. Suction filtration over Millipore<sup>®</sup> yielded the desired tolane **123b** as white powder (346 mg, 21 %).

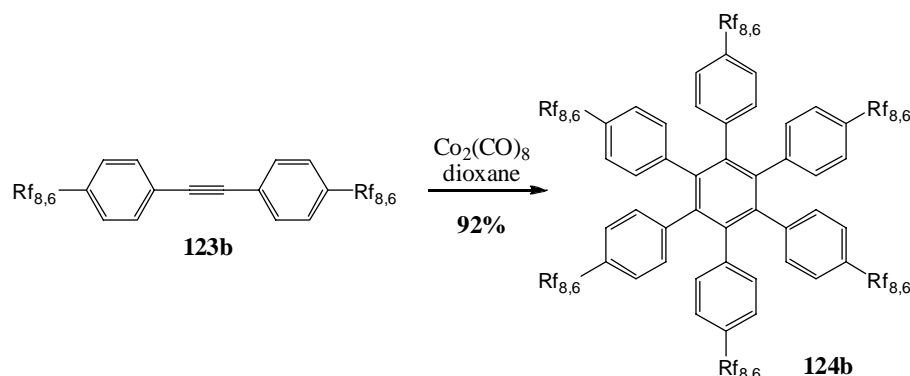
**TLC:**  $R_f$  = 0.95 (silica gel, pentane – ether 9:1,  $\text{KMnO}_4$ ).

**$^1\text{H-NMR}$ :** (360 MHz,  $\text{CDCl}_3$ ):  $\delta$  7.43 (*d*, 4H,  $^3J_{\text{HH}} = 8.2$  Hz, Ph), 7.15 (*d*, 4H,  $^3J_{\text{HH}} = 8.2$  Hz, Ph), 2.61 (*t*, 4H,  $^3J_{\text{HH}} = 7.7$  Hz,  $\text{CH}_2(\text{CH}_2)_7\text{Rf}_6$ ), 1.97-2.12 (*m*, 4H,  $(\text{CH}_2)_7\text{CH}_2\text{Rf}_6$ ), 1.55-1.61 (*m*, 8H,  $\text{CH}_2\text{CH}_2(\text{CH}_2)_4\text{CH}_2\text{CH}_2\text{Rf}_6$ ), 1.28-1.39 (*m*, 16H,  $\text{CH}_2\text{CH}_2(\text{CH}_2)_4\text{CH}_2\text{CH}_2\text{Rf}_6$ ).

**$^{13}\text{C-NMR}$ :** (90.55 MHz,  $\text{CDCl}_3$ ):  $\delta$  143.45 (Ph), 131.87 (Ph), 128.83 (Ph), 121.05 (Ph), 104.64-122.38 ( $\text{Rf}_6$ ), 89.31 (acetylene), 36.25 ( $\text{CH}_2(\text{CH}_2)_7\text{Rf}_6$ ), 31.57 ( $\text{CH}_2\text{CH}_2(\text{CH}_2)_6\text{Rf}_6$ ), 31.26 (*t*,  $^2J_{\text{CF}} = 22.5$  Hz,  $(\text{CH}_2)_7\text{CH}_2\text{Rf}_6$ ), 29.46-29.54 (8C  $\text{CH}_2\text{CH}_2(\text{CH}_2)_4\text{CH}_2\text{CH}_2\text{Rf}_6$ ), 20.47 (*t*,  $^3J_{\text{CF}} = 3.3$  Hz,  $(\text{CH}_2)_6\text{CH}_2\text{CH}_2\text{Rf}_6$ ).

**MALDI-ICR-MS (DCTB):**  $m/z$  (% int.): 1289.43 ( $[\text{M+DCTB}]^{*+}$ , 100%), 1038.27 ( $\text{M}^{*+}$ , 91%).

## 21.12.6 Hexakis[4-(9,9,10,10,11,11,12,12,13,13,14,14,14-tridecafluorotetradecyl)phenyl]benzene



This cyclotrimerisation was carried out following **method B** using tolane **123b** (0.3 g, 0.29 mmol) and  $\text{Co}_2(\text{CO})_8$  (5.9 mg, 17  $\mu\text{mol}$ ) in dioxane (25 mL). The mixture was refluxed for 18 hours, reduced and filtered over a plug of silica gel using ether as eluent. After removal of all volatiles the HPB derivative **124b** was afforded as slightly brown oil. Column purification using pentane – ether (99 : 1) afforded **124b** as faint yellow oil in good yield (275 mg, 92%).

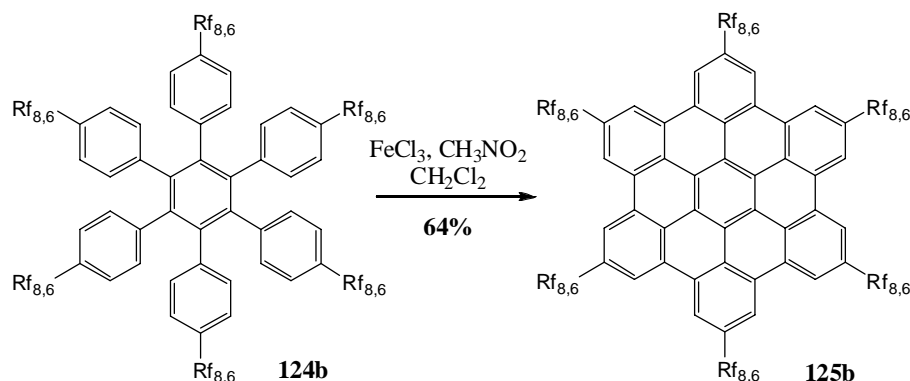
**TLC:**  $R_f$  = 0.95 (silica gel, pentane – ether 9:1,  $\text{KMnO}_4$ ).

**$^1\text{H-NMR}$ :** (360 MHz,  $\text{CDCl}_3$ ):  $\delta$  6.67 (*d*, 12H,  $^3J_{\text{HH}}$  = 8.2 Hz, Ph), 6.61 (*d*, 12H,  $^3J_{\text{HH}}$  = 8.2 Hz, Ph), 2.34 (*t*, 12H,  $^3J_{\text{HH}}$  = 7.3 Hz,  $\text{CH}_2(\text{CH}_2)_7\text{Rf}_6$ ), 1.95-2.10 (*m*, 12H,  $(\text{CH}_2)_7\text{CH}_2\text{Rf}_6$ ), 1.50-1.61 (*m*, 24H,  $\text{CH}_2\text{CH}_2(\text{CH}_2)_4\text{CH}_2\text{CH}_2\text{Rf}_6$ ), 1.21-1.41 (*m*, 48H,  $\text{CH}_2\text{CH}_2(\text{CH}_2)_4\text{CH}_2\text{CH}_2\text{Rf}_6$ ).

**$^{13}\text{C-NMR}$ :** (90.55 MHz,  $\text{CDCl}_3$ ):  $\delta$  140.27 (Ph), 138.86 (Ph), 138.33 (Ph), 131.42 (Ph), 126.44 (Ph), 105.03-119.65 ( $\text{Rf}_6$ ), 35.31 ( $\text{CH}_2(\text{CH}_2)_7\text{Rf}_6$ ), 31.15 ( $\text{CH}_2\text{CH}_2(\text{CH}_2)_6\text{Rf}_6$ ), 30.77 (*t*,  $^2J_{\text{CF}}$  = 22.5 Hz,  $(\text{CH}_2)_7\text{CH}_2\text{Rf}_6$ ), 28.70-29.27 (24C  $\text{CH}_2\text{CH}_2(\text{CH}_2)_4\text{CH}_2\text{CH}_2\text{Rf}_6$ ), 20.10 (*t*,  $^3J_{\text{CF}}$  = 3.3 Hz,  $(\text{CH}_2)_6\text{CH}_2\text{CH}_2\text{Rf}_6$ ).

**MALDI-ICR-MS (DCTB):**  $m/z$  (% int.): 3114.82 ( $\text{M}^+$ , 100%).

21.12.7 2,5,8,11,14,17-Hexakis-(9,9,10,10,11,11,12,12,13,13,14,14,14-tridecafluorotetradecyl)-hexabenzob[bc,ef,hi,kl,no,qr]coronene



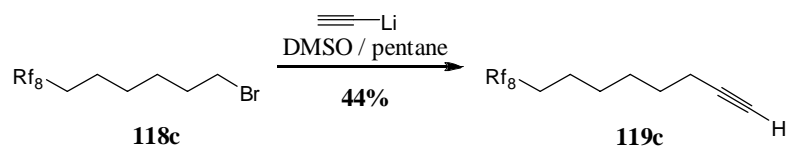
The synthesis was carried out accordingly to **method C** using HPB **124b** (0.1 g, 32  $\mu\text{mol}$ ),  $\text{FeCl}_3$  (468 mg, 2.9 mmol, 7.5 eq / H to be removed),  $\text{CH}_3\text{NO}_2$  (18 mL) and  $\text{CH}_2\text{Cl}_2$  (4 mL). After 9 hours of reaction at 45 °C under constant argon bubbling, methanol (20 mL) was added to quench the mixture. The formed dark precipitate was collected by suction filtration over Millipore<sup>®</sup>. Purification was performed by repetitive refluxing in a mixture of ether, dichloromethane and BTF. Filtration over Millipore<sup>®</sup> yielded finally HBC **125b** as brown solid in moderate yield (64 mg, 64%).

**MALDI-TOF-MS (DCTB):**  $m/z$  (% int.): 3103.4 ( $\text{M}^{*+}$ , 35%; calcd. for  $\text{C}_{126}\text{H}_{108}\text{F}_{78}$  3102.72), 1001.6 (100%).

**UV/VIS:** (BTF,  $10^{-6}$  M,  $\epsilon = 9.2 \cdot 10^5$ ),  $\lambda_{\text{max}} = 371$  nm.

21.13 Synthesis of HBC-(Rf<sub>8,8</sub>)<sub>6</sub>

## 21.13.1 9,9,10,10,11,11,12,12,13,13,14,14,15,15,16,16,16-Heptadecafluorohexadec-1-yne



Compound **118c** (14.1 g, 24.2 mmol) was reacted according to **method J** with lithium acetylide ethyldiamine complex (6.7 g, 72.6 mmol) in a mixture of pentane (30 mL) and DMSO (40 mL). The black suspension was stirred at room temperature for 4 days. Water (50 mL) was added to quench the reaction. The resulting suspension was Büchner filtrated and washed exhaustively with dichloromethane. The filtrate was washed with water (2 x 100 mL), dried over Na<sub>2</sub>SO<sub>4</sub> and all volatiles were removed. Filtration over a short plug of silica gel under reduced pressure using pentane as eluent afforded after evaporation of pentane the desired alkyne derivative **119c** as colourless oil (5.6 g, 44%).

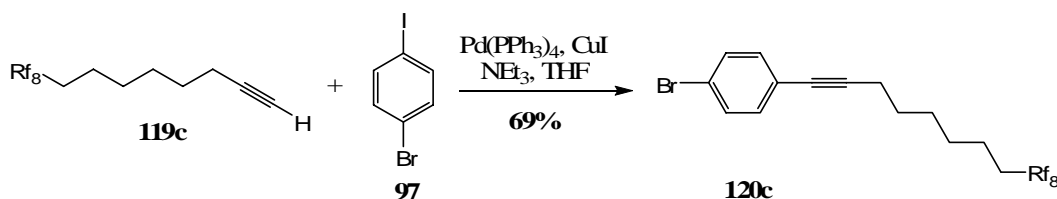
**TLC:** R<sub>f</sub> = 0.80 (silica gel, pentane, KMnO<sub>4</sub>).

**<sup>1</sup>H-NMR:** (360 MHz, CDCl<sub>3</sub>): δ 2.21 (*td*, 2H, <sup>3</sup>J<sub>HH</sub> = 7.0 Hz, <sup>4</sup>J<sub>HH</sub> = 2.7 Hz, HC≡CCH<sub>2</sub>(CH<sub>2</sub>)<sub>5</sub>Rf<sub>8</sub>), 2.00-2.15 (*m*, 2H, HC≡C(CH<sub>2</sub>)<sub>5</sub>CH<sub>2</sub>Rf<sub>8</sub>), 1.95 (*t*, 1H, <sup>4</sup>J<sub>HH</sub> = 2.7 Hz, HC≡C(CH<sub>2</sub>)<sub>6</sub>Rf<sub>8</sub>), 1.59-1.67 (*m*, 2H, HC≡C(CH<sub>2</sub>)<sub>4</sub>CH<sub>2</sub>CH<sub>2</sub>Rf<sub>8</sub>), 1.52-1.59 (*m*, 2H, Hz, HC≡C(CH<sub>2</sub>)<sub>3</sub>CH<sub>2</sub>CH<sub>2</sub>CH<sub>2</sub>Rf<sub>8</sub>), 1.40-1.52 (*m*, 4H, HC≡CCH<sub>2</sub>CH<sub>2</sub>CH<sub>2</sub>(CH<sub>2</sub>)<sub>3</sub>Rf<sub>8</sub>).

**<sup>13</sup>C-NMR:** (90.55 MHz, CDCl<sub>3</sub>): δ 107.80-118.72 (Rf<sub>8</sub>), 84.30 (HC≡C(CH<sub>2</sub>)<sub>6</sub>Rf<sub>8</sub>), 68.34 (HC≡C(CH<sub>2</sub>)<sub>6</sub>Rf<sub>8</sub>), 30.82 (*t*, <sup>2</sup>J<sub>CF</sub> = 22.5 Hz, HC≡C(CH<sub>2</sub>)<sub>5</sub>CH<sub>2</sub>Rf<sub>8</sub>), 28.56 (HC≡C(CH<sub>2</sub>)<sub>3</sub>CH<sub>2</sub>CH<sub>2</sub>CH<sub>2</sub>Rf<sub>8</sub>), 28.24 (HC≡CCH<sub>2</sub>CH<sub>2</sub>CH<sub>2</sub>(CH<sub>2</sub>)<sub>3</sub>Rf<sub>8</sub>), 28.11 (HC≡CCH<sub>2</sub>CH<sub>2</sub>(CH<sub>2</sub>)<sub>4</sub>Rf<sub>8</sub>), 20.00 (*t*, <sup>3</sup>J<sub>CF</sub> = 3.3 Hz, HC≡C(CH<sub>2</sub>)<sub>4</sub>CH<sub>2</sub>CH<sub>2</sub>Rf<sub>8</sub>), 18.28 (HC≡CCH<sub>2</sub>(CH<sub>2</sub>)<sub>5</sub>Rf<sub>8</sub>).

**EI-MS:** m/z (% int.): 131.0 (43%), 81.0 ([M-Rf<sub>3,8</sub>]<sup>•+</sup>, 100%), 67.0 ([M-Rf<sub>4,8</sub>]<sup>•+</sup>, 30%).

## 21.13.2 1-Bromo-4-(9,9,10,10,11,11,12,12,13,13,14,14,15,15,16,16,16-heptafluorohexadec-1-ynyl)benzene



This synthesis was carried out following **method K**. Compound **119c** (5.5 g, 10.4 mmol) was reacted with 1-bromo-4-iodobenzene (2.9 g, 10.4 mmol) using  $\text{Pd(PPh}_3)_4$  (0.72 g, 0.62 mmol) as catalyst and  $\text{CuI}$  (198 mg, 1.04 mmol) and  $\text{NEt}_3$  (8.7 mL, 62.5 mmol) as addend and THF (70 mL) as solvent. After seven days of reaction the crude mixture was extracted with ether (5 x 100 mL). The combined organic phases were washed with HCl 10% (100 mL) and water (100 mL), dried over  $\text{Na}_2\text{SO}_4$  and all solvents were evaporated. The resulting dark oil was filtered over silica gel with a mixture of pentane – ether (9:1) first and plenty of pentane second to yield the desired compound **120c** as colourless oil (2.46 g, 69%).

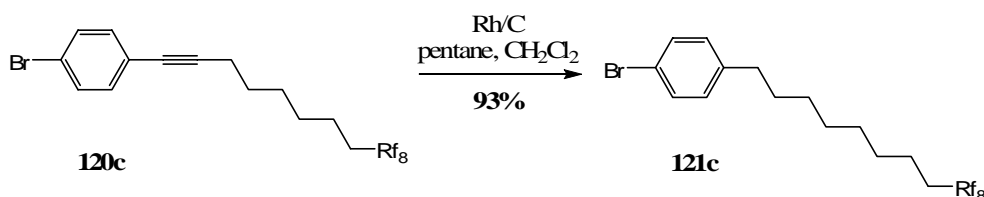
**TLC:**  $R_f = 0.79$  (silica gel, pentane,  $\text{KMnO}_4$ ).

**$^1\text{H-NMR}$ :** (360 MHz,  $\text{CDCl}_3$ ):  $\delta$  7.42 (*d*, 2H,  $^3J_{\text{HH}} = 8.2$  Hz, Ph), 7.25 (*d*, 2H,  $^3J_{\text{HH}} = 8.2$  Hz, Ph), 2.41 (*t*, 2H,  $^3J_{\text{HH}} = 6.8$  Hz,  $\text{C}\equiv\text{CCH}_2(\text{CH}_2)_5\text{Rf}_8$ ), 2.00-2.15 (*m*, 2H,  $\text{C}\equiv\text{C}(\text{CH}_2)_5\text{CH}_2\text{Rf}_8$ ), 1.59-1.69 (*m*, 4H,  $\text{C}\equiv\text{CCH}_2\text{CH}_2\text{CH}_2\text{CH}_2\text{CH}_2\text{CH}_2\text{Rf}_8$ ), 1.45-1.55 (*m*, 4H,  $\text{C}\equiv\text{CCH}_2\text{CH}_2\text{CH}_2\text{CH}_2\text{CH}_2\text{CH}_2\text{Rf}_8$ ).

**$^{13}\text{C-NMR}$ :** (90.55 MHz,  $\text{CDCl}_3$ ):  $\delta$  132.99 (Ph), 131.42 (Ph), 122.89 (Ph), 121.64 (Ph), 108.17-118.36 ( $\text{Rf}_8$ ), 91.23 ( $\text{C}\equiv\text{C}(\text{CH}_2)_6\text{Rf}_8$ ), 79.82 ( $\text{C}\equiv\text{C}(\text{CH}_2)_6\text{Rf}_8$ ), 30.82 (*t*,  $^2J_{\text{CF}} = 22.5$  Hz,  $\text{C}\equiv\text{C}(\text{CH}_2)_5\text{CH}_2\text{Rf}_8$ ), 28.62 ( $\text{C}\equiv\text{CCH}_2\text{CH}_2(\text{CH}_2)_4\text{Rf}_8$ ), 28.45 ( $\text{C}\equiv\text{CCH}_2\text{CH}_2\text{CH}_2(\text{CH}_2)_3\text{Rf}_8$ ), 28.27 ( $\text{C}\equiv\text{C}(\text{CH}_2)_3\text{CH}_2\text{CH}_2\text{CH}_2\text{Rf}_8$ ), 20.03 (*t*,  $^3J_{\text{CF}} = 3.3$  Hz,  $\text{C}\equiv\text{C}(\text{CH}_2)_4\text{CH}_2\text{CH}_2\text{Rf}_8$ ), 19.31 ( $\text{C}\equiv\text{CCH}_2(\text{CH}_2)_5\text{Rf}_8$ ).

**EI-MS:**  $m/z$  (% int.): 685.2 ( $\text{M}^+$ , 7%), 237.1 ( $[\text{M-Rf}_{2,8}]^+$ , 8%), 223.1 ( $[\text{M-Rf}_{3,8}]^+$ , 34%), 209.0 ( $[\text{M-Rf}_{4,8}]^+$ , 9%), 194.9 ( $[\text{M-Rf}_{5,8}]^+$ , 82%), 181.8 ( $[\text{M-Rf}_{6,8}]^+$ , 15%), 168.9 ( $[\text{M-CRf}_{6,8}]^+$ , 18%), 142 (100%).

## 21.13.3 1-Bromo-4-(9,9,10,10,11,11,12,12,13,13,14,14,15,15,16,16,16-heptafluorohexadecyl)benzene



The hydrogenation of compound **120c** (4.5 g, 6.6 mmol) was carried out following **method E** using Rh/C (200 mg) as catalyst and a mixture of pentane (21 mL) and CH<sub>2</sub>Cl<sub>2</sub> (7 mL) as solvents. The reaction was stirred for 18 hours at room temperature under 60 atmospheres of hydrogen before the catalyst was removed by filtration over silica gel. All volatiles of the filtrate were removed yielding compound **121c** as pure, colourless oil (4.21 g, 93%).

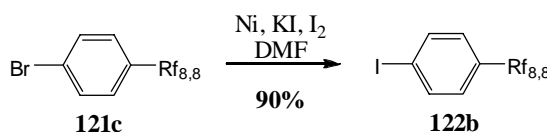
**TLC:** R<sub>f</sub> = 0.85 (silica gel, pentane, KMnO<sub>4</sub>).

**<sup>1</sup>H-NMR:** (360 MHz, CDCl<sub>3</sub>): δ 7.39 (*d*, 2H, <sup>3</sup>J<sub>HH</sub> = 8.2 Hz, Ph), 7.05 (*d*, 2H, <sup>3</sup>J<sub>HH</sub> = 8.2 Hz, Ph), 2.56 (*t*, 2H, <sup>3</sup>J<sub>HH</sub> = 7.7 Hz, CH<sub>2</sub>(CH<sub>2</sub>)<sub>7</sub>Rf<sub>8</sub>), 1.98-2.13 (*m*, 2H, (CH<sub>2</sub>)<sub>7</sub>CH<sub>2</sub>Rf<sub>8</sub>), 1.56-1.60 (*m*, 4H, CH<sub>2</sub>CH<sub>2</sub>(CH<sub>2</sub>)<sub>4</sub>CH<sub>2</sub>CH<sub>2</sub>Rf<sub>8</sub>), 1.27-1.39 (*m*, 8H, CH<sub>2</sub>CH<sub>2</sub>(CH<sub>2</sub>)<sub>4</sub>CH<sub>2</sub>CH<sub>2</sub>Rf<sub>8</sub>).

**<sup>13</sup>C-NMR:** (90.55 MHz, CDCl<sub>3</sub>): δ 142.08 (Ph), 131.67 (Ph), 130.55 (Ph), 119.70 (Ph), 106.40-118.86 (Rf<sub>8</sub>), 35.70 (CH<sub>2</sub>(CH<sub>2</sub>)<sub>7</sub>Rf<sub>8</sub>), 31.64 (CH<sub>2</sub>CH<sub>2</sub>(CH<sub>2</sub>)<sub>6</sub>Rf<sub>8</sub>), 31.26 (*t*, <sup>2</sup>J<sub>CF</sub> = 22.5 Hz, CH<sub>2</sub>)<sub>7</sub>CH<sub>2</sub>Rf<sub>8</sub>), 29.45-29.58 (4C, CH<sub>2</sub>CH<sub>2</sub>(CH<sub>2</sub>)<sub>4</sub>CH<sub>2</sub>CH<sub>2</sub>Rf<sub>8</sub>), 20.47 (*t*, <sup>3</sup>J<sub>CF</sub> = 3.3 Hz, (CH<sub>2</sub>)<sub>6</sub>CH<sub>2</sub>CH<sub>2</sub>Rf<sub>8</sub>).

**EI-MS:** m/z (% int.): 689.3 (M<sup>+</sup>, 9%), 170.8 ([M-Rf<sub>7,8</sub>]<sup>+</sup>, 100%), 90.9 ([M-Rf<sub>7,8</sub>-Br]<sup>+</sup>, 33%).

## 21.13.4 1-Iodo-4-(9,9,10,10,11,11,12,12,13,13,14,14,15,15,16,16,16-heptafluorohexadecyl)benzene



The halogen exchange was performed as described in **method F** by reacting compound **121c** (4.1 g, 5.9 mmol) with KI (2.0 g, 11.9 mmol) in the presence of Ni (1.75 g, 29.8 mmol), I<sub>2</sub> (76 mg, 0.30 mmol) and DMF (20 mL). The dark reaction mixture was stirred at 150 °C for 3 days before the crude product was extracted with pentane (3 x 50 mL). The combined organic phases were washed with water (100 mL), 10% HCl (100 mL) and water (50 mL), dried over Na<sub>2</sub>SO<sub>4</sub> and all volatiles were removed. Silica gel plug filtration under reduced pressure using pentane as eluent yielded the desired compound **122b** as colourless oil (3.96 g, 90%).

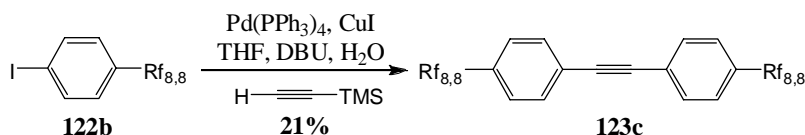
**TLC:**  $R_f$  = 0.85 (silica gel, pentane,  $\text{KMnO}_4$ ).

**$^1\text{H-NMR}$ :** (360 MHz,  $\text{CDCl}_3$ ):  $\delta$  7.58 (*d*, 2H,  $^3J_{\text{HH}}$  = 8.2 Hz, Ph), 6.92 (*d*, 2H,  $^3J_{\text{HH}}$  = 8.2 Hz, Ph), 2.54 (*t*, 2H,  $^3J_{\text{HH}}$  = 7.3 Hz,  $\text{CH}_2(\text{CH}_2)_7\text{Rf}_8$ ), 1.96-2.09 (*m*, 2H,  $(\text{CH}_2)_7\text{CH}_2\text{Rf}_8$ ), 1.54-1.59 (*m*, 4H,  $\text{CH}_2\text{CH}_2(\text{CH}_2)_4\text{CH}_2\text{CH}_2\text{Rf}_8$ ), 1.28-1.39 (*m*, 8H,  $\text{CH}_2\text{CH}_2(\text{CH}_2)_4\text{CH}_2\text{CH}_2\text{Rf}_8$ ).

**$^{13}\text{C-NMR}$ :** (90.55 MHz,  $\text{CDCl}_3$ ):  $\delta$  142.78 (Ph), 137.67 (Ph), 130.94 (Ph), 105.79-119.70 ( $\text{Rf}_8$ ), 90.94 (Ph), 35.79 ( $\text{CH}_2(\text{CH}_2)_7\text{Rf}_8$ ), 31.61 ( $\text{CH}_2\text{CH}_2(\text{CH}_2)_6\text{Rf}_8$ ), 31.26 (*t*,  $^2J_{\text{CF}}$  = 22.5 Hz,  $\text{CH}_2)_7\text{CH}_2\text{Rf}_8$ ), 29.45-29.52 (4C,  $\text{CH}_2\text{CH}_2(\text{CH}_2)_4\text{CH}_2\text{CH}_2\text{Rf}_8$ ), 20.47 (*t*,  $^3J_{\text{CF}}$  = 3.3 Hz,  $(\text{CH}_2)_6\text{CH}_2\text{CH}_2\text{Rf}_8$ ).

**EI-MS:**  $m/z$  (% int.): 735.4 ( $\text{M}^{++}$ , 8%), 217.0 ( $[\text{M-Rf}_{7,8}]^{++}$ , 100%), 91.0 ( $[\text{M-Rf}_{7,8} - \text{I}]^{++}$ , 24%).

21.13.5 1-(9,9,10,10,11,11,12,12,13,13,14,14,15,15,16,16,16-Heptafluorohexadecyl)-4-{[4-(9,9,10,10,11,11,12,12,13,13,14,14,15,15,16,16,16-heptafluorohexadecyl)phenyl]-ethynyl}benzene



The tolane formation was achieved using **method A**. Iodoaryl **122b** (3.8 g, 5.2 mmol) was reacted with  $\text{Pd}(\text{PPh}_3)_4$  (360 mg, 0.31 mmol),  $\text{CuI}$  (98.5 mg, 0.52 mmol), DBU (4.6 mL, 31.05 mmol), TMSA (0.38 mL, 2.6 mmol),  $\text{H}_2\text{O}$  (30  $\mu\text{L}$ , 2.07 mmol) and THF (30 mL) for 2 days at 75  $^\circ\text{C}$ . The reaction mixture was diluted with ether (300 mL) and extracted with water (50 mL). The combined organic fractions were dried over  $\text{Na}_2\text{SO}_4$  and all volatiles were removed under reduced pressure. The obtained brown solid was dissolved in pentane / ether 1:1 and filtrated over basic alox under reduced pressure. After removal of the solvent a yellow solid was obtained which was recrystallized in pentane / ethanol. Suction filtration over Millipore<sup>®</sup> yielded the desired tolane **123c** as white powder (680 mg, 21 %).

**TLC:**  $R_f$  = 0.95 (silica gel, pentane – ether 9:1,  $\text{KMnO}_4$ ).

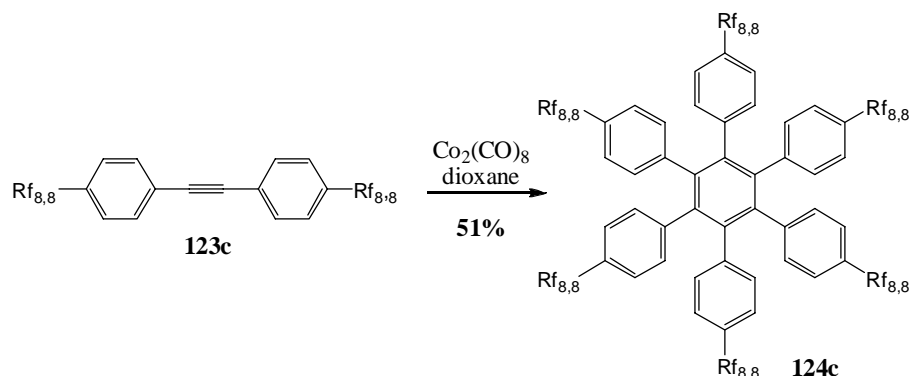
**$^1\text{H-NMR}$ :** (360 MHz,  $\text{CDCl}_3$ ):  $\delta$  7.43 (*d*, 4H,  $^3J_{\text{HH}}$  = 8.2 Hz, Ph), 7.15 (*d*, 4H,  $^3J_{\text{HH}}$  = 8.2 Hz, Ph), 2.61 (*t*, 4H,  $^3J_{\text{HH}}$  = 7.7 Hz,  $\text{CH}_2(\text{CH}_2)_7\text{Rf}_8$ ), 1.99-2.14 (*m*, 4H,  $(\text{CH}_2)_7\text{CH}_2\text{Rf}_8$ ), 1.56-1.61 (*m*, 8H,  $\text{CH}_2\text{CH}_2(\text{CH}_2)_4\text{CH}_2\text{CH}_2\text{Rf}_8$ ), 1.28-1.39 (*m*, 16H,  $\text{CH}_2\text{CH}_2(\text{CH}_2)_4\text{CH}_2\text{CH}_2\text{Rf}_8$ ).

**$^{13}\text{C-NMR}$ :** (90.55 MHz,  $\text{CDCl}_3$ ):  $\delta$  143.05 (Ph), 131.46 (Ph), 128.43 (Ph), 120.64 (Ph), 105.02-118.85 ( $\text{Rf}_8$ ), 89.90 (acetylene), 35.84 ( $\text{CH}_2(\text{CH}_2)_7\text{Rf}_8$ ), 31.17 ( $\text{CH}_2\text{CH}_2(\text{CH}_2)_6\text{Rf}_8$ ), 30.86 (*t*,  $^2J_{\text{CF}}$  = 22.5 Hz,  $(\text{CH}_2)_7\text{CH}_2\text{Rf}_8$ ), 29.05 (4C  $\text{CH}_2\text{CH}_2(\text{CH}_2)_4\text{CH}_2\text{CH}_2\text{Rf}_8$ ), 20.07 (*t*,  $^3J_{\text{CF}}$  = 3.3 Hz,  $(\text{CH}_2)_6\text{CH}_2\text{CH}_2\text{Rf}_8$ ).

**MALDI-ICR-MS (DCTB):**  $m/z$  (% int.): 1489.41 ( $[\text{M}+\text{DCTB}]^{++}$ , 22%), 1238.26 ( $[\text{M}]^{++}$ , 100%).



## 21.13.6 Hexakis[4-(9,9,10,10,11,11,12,12,13,13,14,14,15,15,16,16,16-heptafluorohexadecyl)-phenyl]benzene



The cyclotrimerisation was achieved using **method B** taking tolane **123c** (659 mg, 0.53 mmol), Co<sub>2</sub>(CO)<sub>8</sub> (10.8 mg, 31.6 μmol) and dioxane (50 mL). The dark mixture was refluxed for 7 days before a cooling to room temperature was allowed and all volatiles were removed under reduced pressure. The obtained dark solid was dissolved in ether and filtrated over a silica gel pad. The filtrate was reduced and the obtained yellow solid was suspended in pentane, sonicated and suction filtrated over Millipore<sup>®</sup> which yielded the title compound **124c** as a white solid (329 mg, 51%).

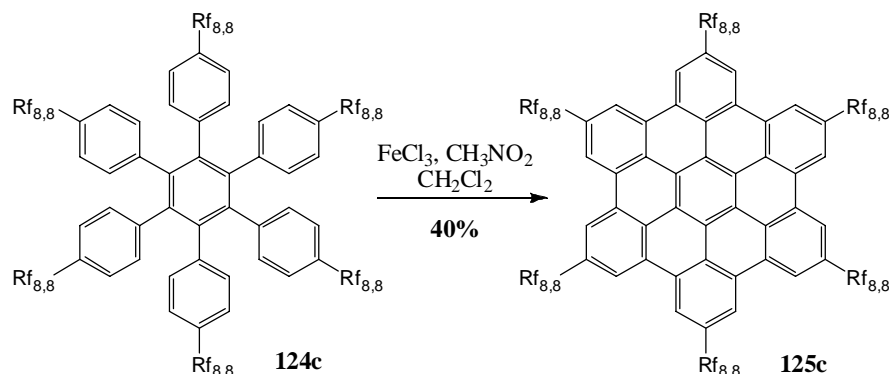
**TLC:** Rf = 0.95 (silica gel, pentane – ether 9:1, KMnO<sub>4</sub>).

**<sup>1</sup>H-NMR:** (500 MHz, CDCl<sub>3</sub>): δ 6.66 (*d*, 12H, <sup>3</sup>J<sub>HH</sub> = 8.2 Hz, Ph), 6.60 (*d*, 12H, <sup>3</sup>J<sub>HH</sub> = 8.2 Hz, Ph), 2.33 (*t*, 12H, <sup>3</sup>J<sub>HH</sub> = 7.3 Hz, CH<sub>2</sub>(CH<sub>2</sub>)<sub>7</sub>Rf<sub>8</sub>), 1.97-2.08 (*m*, 12H, (CH<sub>2</sub>)<sub>7</sub>CH<sub>2</sub>Rf<sub>8</sub>), 1.54-1.60 (*m*, 12H, CH<sub>2</sub>CH<sub>2</sub>(CH<sub>2</sub>)<sub>6</sub>Rf<sub>8</sub>), 1.35-1.42 (*m*, 12H, CH<sub>2</sub>CH<sub>2</sub>CH<sub>2</sub>(CH<sub>2</sub>)<sub>5</sub>Rf<sub>8</sub>), 1.30-1.35 (*m*, 12H, (CH<sub>2</sub>)<sub>6</sub>CH<sub>2</sub>CH<sub>2</sub>Rf<sub>8</sub>), 1.09-1.28 (*m*, 36H, (CH<sub>2</sub>)<sub>3</sub>(CH<sub>2</sub>)<sub>3</sub>CH<sub>2</sub>CH<sub>2</sub>Rf<sub>8</sub>).

**<sup>13</sup>C-NMR:** (125.77 MHz, CDCl<sub>3</sub>): δ 140.33 (Ph), 138.89 (Ph), 138.44 (Ph), 131.48 (Ph), 126.43 (Ph), 108.68-120.94 (Rf<sub>8</sub>), 35.32 (CH<sub>2</sub>(CH<sub>2</sub>)<sub>7</sub>Rf<sub>8</sub>), 31.12 (CH<sub>2</sub>CH<sub>2</sub>(CH<sub>2</sub>)<sub>6</sub>Rf<sub>8</sub>), 31.01 (*t*, <sup>2</sup>J<sub>CF</sub> = 22.5 Hz, (CH<sub>2</sub>)<sub>7</sub>CH<sub>2</sub>Rf<sub>8</sub>), 28.72-29.24 (24C CH<sub>2</sub>CH<sub>2</sub>(CH<sub>2</sub>)<sub>4</sub>CH<sub>2</sub>CH<sub>2</sub>Rf<sub>8</sub>), 20.17 (*t*, <sup>3</sup>J<sub>CF</sub> = 3.3 Hz, (CH<sub>2</sub>)<sub>6</sub>CH<sub>2</sub>CH<sub>2</sub>Rf<sub>8</sub>).

**MALDI-ICR-MS (DCTB):** m/z (% int.): 3714.72 (M<sup>+</sup>, 100%).

21.13.7 2,5,8,11,14,17-Hexakis-(9,9,10,10,11,11,12,12,13,13,14,14,15,15,16,16,16-heptafluorohexadecyl)hexabenzob[bc,ef,hi,kl,no,q]coronene



The oxidation was performed following **method C** taking HPB **124c** (200 mg, 54  $\mu\text{mol}$ ),  $\text{FeCl}_3$  (523 mg, 3.2 mmol, 5 eq / H to be removed),  $\text{CH}_3\text{NO}_2$  (12 mL),  $\text{CH}_2\text{Cl}_2$  (30 mL) and HFB (10 mL). The mixture was gently refluxed under a constant bubbling of argon for 7 hours before methanol (40 mL) was added. The formed precipitate was collected by suction filtration over Millipore<sup>®</sup>. The obtained black solid was suspended in common organic solvents (dichloromethane, ether, pentane and ethanol) sonicated and collected by suction filtration over Millipore<sup>®</sup>. Final purification was achieved by precipitation out of 1,2,4-TCB after refluxing. The slightly brown solid was collected by Millipore<sup>®</sup> filtration and was obtained in moderate yield (80 mg, 40%).

**<sup>1</sup>H-NMR:** (360 MHz, HFB,  $\text{CDCl}_3$ ):  $\delta$  9.00 (br. s, 12H, Ph), 3.51 (br. s, 12H,  $\text{CH}_2(\text{CH}_2)_8\text{Rf}_8$ ), 2.34 (br. s, 24H,  $\text{CH}_2\text{CH}_2(\text{CH}_2)_5\text{CH}_2\text{Rf}_8$ ), 1.88 (br. s, 60H,  $\text{CH}_2\text{CH}_2(\text{CH}_2)_5\text{CH}_2\text{Rf}_8$ ).

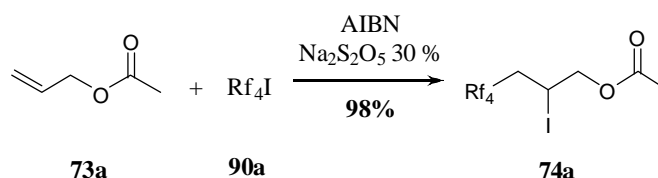
**MALDI-ICR-MS (DCTB):** m/z (% int.): 3702.71 ( $\text{M}^{+}$ , 100%; calcd. for  $\text{C}_{138}\text{H}_{108}\text{F}_{102}$  3702.68), 3186.87 ( $[\text{M}-\text{Rf}_{7,8}]^{+}$ , 17%), 2656.42 ( $[\text{M}-2 \times \text{Rf}_{7,8}]^{+}$ , 12%), 2139.37 ( $[\text{M}-3 \times \text{Rf}_{7,8}]^{+}$ , 8%).

**UV/VIS:** (BTF,  $10^{-6}$  M,  $\epsilon = 1.5 \cdot 10^5$ ),  $\lambda_{\text{max}} = 345, 360, 391$  nm.

## 22 Synthesis of HBCs carrying branched perfluorinated side chains

### 22.1 Synthesis of HBC-(Rf<sub>3,3,4,4</sub>)<sub>6</sub>

#### 22.1.1 4,4,5,5,6,6,7,7,7-Nonafluoro-2-iodoheptyl acetate



This transformation was carried out accordingly to **method G** using allylacetate **73a** (14.05 g, 0.141 mol), Rf<sub>4</sub>I **90a** (50.0 g, 0.144 mol), AIBN (350 mg, 2.35 mmol) and a 30% aq. sol. of Na<sub>2</sub>S<sub>2</sub>O<sub>5</sub> (14 mL). The mixture was heated to 85°C for 3 hours before water (100 mL) was added. The formed slurry was extracted with dichloromethane (3 x 300 mL), dried over Na<sub>2</sub>SO<sub>4</sub> and all volatiles were removed yielding the title compound **74a** as colourless oil (61.68 g, 98%).

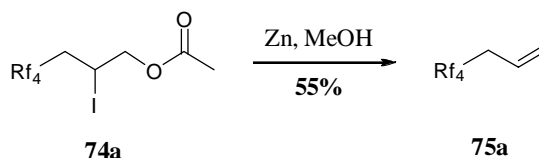
**TLC:** Rf = 0.25 (silica gel, pentane, KMnO<sub>4</sub>).

**<sup>1</sup>H-NMR:** (360 MHz, CDCl<sub>3</sub>): δ 4.27-4.46 (*m*, 3H, CH<sub>2</sub>CHICH<sub>2</sub>Rf<sub>4</sub>), 2.71-3.01 (*m*, 2H, CH<sub>2</sub>CHICH<sub>2</sub>Rf<sub>4</sub>), 2.13 (*s*, 3H, CH<sub>3</sub>).

**<sup>13</sup>C-NMR:** (90.55 MHz, CDCl<sub>3</sub>): δ 170.03 (C=O), 68.40 (CH<sub>2</sub>CHICH<sub>2</sub>Rf<sub>4</sub>), 38.06 (*t*, <sup>3</sup>J<sub>CF</sub> = 21.1 Hz, CH<sub>2</sub>CHICH<sub>2</sub>Rf<sub>4</sub>), 20.65 (CH<sub>3</sub>), 11.78 (CH<sub>2</sub>CHICH<sub>2</sub>Rf<sub>4</sub>).

**EI-MS:** m/z (% int.): 386.2 ([M-OAc]<sup>+</sup>, 25%), 319.3 ([M-I]<sup>+</sup>, 100%).

#### 22.1.2 4,4,5,5,6,6,7,7,7-Nonafluorohept-1-ene



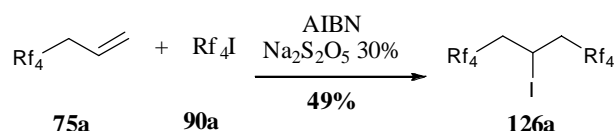
Freshly activated zinc powder (15.82 g, 0.242 mol) was added into a round bottomed flask, suspended in methanol (60 mL) and heated to 65° under inert atmosphere. Compound **74a** (60.64 g, 0.136 mol) was heated separately to 65°C and was added portion wise over a period of 2 hours. The mixture was stirred for 3 more hours at this temperature before the title compound was fractionated over a short vigreux column directly out of the crude reaction mixture yielding **75a** as colourless oil (19.4 g, 55%).

**TLC:** Rf = 0.98 (silica gel, pentane, KMnO<sub>4</sub>).

**<sup>1</sup>H-NMR:** (360 MHz, CDCl<sub>3</sub>): δ 5.81 (*ddt*, 1H, <sup>3</sup>J<sub>HH</sub> = 16.8 Hz, <sup>3</sup>J<sub>HH</sub> = 10.4 Hz, <sup>2</sup>J<sub>HH</sub> = 7.3 Hz, CH<sub>2</sub>CHCH<sub>2</sub>Rf<sub>4</sub>), 5.35 (*d*, 1H, <sup>3</sup>J<sub>HH</sub> = 16.8 Hz, CH<sub>2</sub>CHCH<sub>2</sub>Rf<sub>4</sub>), 5.33 (*d*, 1H, <sup>3</sup>J<sub>HH</sub> = 10.4 Hz, CH<sub>2</sub>CHCH<sub>2</sub>Rf<sub>4</sub>), 2.86 (*dt*, 2H, <sup>3</sup>J<sub>HH</sub> = 7.3 Hz, <sup>3</sup>J<sub>HF</sub> = 18.4 Hz, CH<sub>2</sub>CHCH<sub>2</sub>Rf<sub>4</sub>).

**<sup>13</sup>C-NMR:** (90.55 MHz, CDCl<sub>3</sub>): δ 124.97 (*t*, <sup>3</sup>J<sub>CF</sub> = 4.0 Hz, CH<sub>2</sub>CHCH<sub>2</sub>Rf<sub>4</sub>), 122.54 (CH<sub>2</sub>CHCH<sub>2</sub>Rf<sub>4</sub>), 108.03-119.26 (Rf<sub>4</sub>), 35.65 (*t*, <sup>2</sup>J<sub>CF</sub> = 22.5 Hz, CH<sub>2</sub>CHCH<sub>2</sub>Rf<sub>4</sub>).

### 22.1.3 1,1,1,2,2,3,3,4,4,8,8,9,9,10,10,11,11,11-Octadecafluoro-6-iodoundecane



The synthesis was carried out following **method G** taking perfluoroallyl **75a** (5.5 g, 21.14 mmol), Rf<sub>4</sub>I **90a** (7.67 g, 22.18 mmol), AIBN (170 mg, 1.05 mmol) and a 30% aq. sol. Na<sub>2</sub>S<sub>2</sub>O<sub>5</sub> (3.5 mL). The mixture was heated for 3 hours at 85°C, quenched by the addition of water (35 mL), extracted with CH<sub>2</sub>Cl<sub>2</sub> (3 x 50 mL), dried over Na<sub>2</sub>SO<sub>4</sub> and reduced maximally. The desired product **126a** was obtained as colourless oil in moderate yield (6.36 g, 49%).

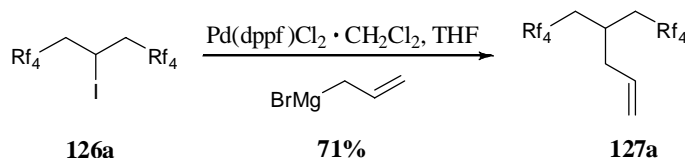
**TLC:** Rf = 0.95 (silica gel, pentane, KMnO<sub>4</sub>).

**<sup>1</sup>H-NMR:** (360 MHz, CDCl<sub>3</sub>): δ 4.52 (*quint*, 1H, <sup>3</sup>J<sub>HH</sub> = 6.8 Hz, Rf<sub>4</sub>CH<sub>2</sub>CHCH<sub>2</sub>Rf<sub>4</sub>), 2.89-3.02 (*m*, 4H, Rf<sub>4</sub>CH<sub>2</sub>CHCH<sub>2</sub>Rf<sub>4</sub>).

**<sup>13</sup>C-NMR:** (90.55 MHz, CDCl<sub>3</sub>): δ 106.21-119.36 (Rf<sub>4</sub>), 41.97 (*t*, <sup>3</sup>J<sub>CF</sub> = 21.1 Hz, Rf<sub>4</sub>CH<sub>2</sub>CHCH<sub>2</sub>Rf<sub>4</sub>), 0.00 (Rf<sub>4</sub>CH<sub>2</sub>CHCH<sub>2</sub>Rf<sub>4</sub>).

**EI-MS:** m/z (% int.): 806.4 (M<sup>+</sup>, 5%), 479.4 ([M-I]<sup>+</sup>, 30%), 459.4 (41%), 245.2 ([M-I-Rf<sub>2,4</sub>]<sup>+</sup>, 69%), 195.1 (95%), 69.0 (100%).

### 22.1.4 6,6,7,7,8,8,9,9,9-Nonafluoro-4-(2,2,3,3,4,4,5,5,5-nonafluoropentyl)non-1-ene



#### Method L

An oven dried Schlenk tube was charged with Pd(dppf)Cl<sub>2</sub> · CH<sub>2</sub>Cl<sub>2</sub> (250 mg, 0.30 mmol) under inert atmosphere. Compound **126a** (6.3 g, 10.4 mmol) was separately deoxygenated, diluted with THF (16 mL) and syringed into the Schlenk tube. The reaction mixture was then cooled to 0 °C in an ice / NaCl bath. Afterwards allylmagnesium bromide (1 M in ether, 14.6 mL, 14.6 mmol) was syringed in slowly (2 h), yielding a yellow solution. The ice bath was removed after the addition

was completed and the reaction mixture (turning green) was stirred for 16 h at room temperature before being quenched with methanol (8 mL). All volatiles were removed under reduced pressure yielding a brown suspension which was filtered over a silica gel plug under reduced pressure using pentane as solvent. After evaporation of pentane the title compound **127a** (3.86 g, 71 %) was obtained as colourless oil.

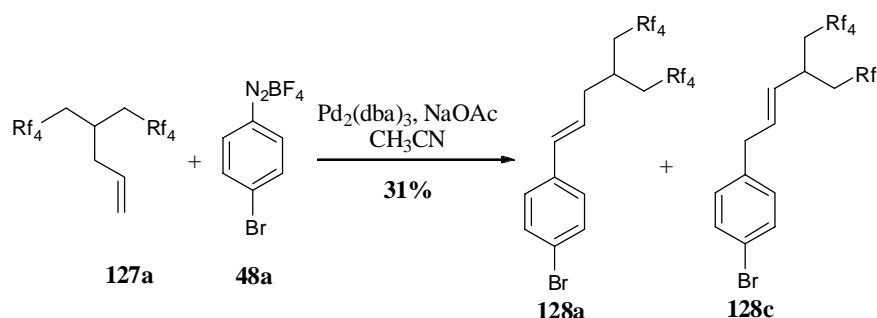
**TLC:**  $R_f = 0.95$  (silica gel, pentane,  $\text{KMnO}_4$ ).

**$^1\text{H-NMR}$ :** (360 MHz,  $\text{CDCl}_3$ ):  $\delta$  5.72 (*ddt*, 1H,  $^3J_{\text{HH}} = 17.0$  Hz,  $^3J_{\text{HH}} = 10.0$  Hz,  $^2J_{\text{HH}} = 6.8$  Hz,  $\text{CH}_2\text{CHCH}_2\text{CH}$ ), 5.19 (*d*, 1H,  $^3J_{\text{HH}} = 17.0$  Hz,  $\text{CH}_2\text{CHCH}_2\text{CH}$ ), 5.14 (*d*,  $^3J_{\text{HH}} = 10.0$  Hz,  $\text{CH}_2\text{CHCH}_2\text{CH}$ ), 2.54 (*septet*, 1H,  $^3J_{\text{HH}} = 6.8$  Hz,  $\text{Rf}_4\text{CH}_2\text{CHCH}_2\text{Rf}_4$ ), 2.33 (*t*, 2H,  $^3J_{\text{HH}} = 6.8$  Hz,  $\text{CH}_2\text{CHCH}_2\text{CH}$ ), 2.12-2.27 (*m*, 4H,  $\text{Rf}_4\text{CH}_2\text{CHCH}_2\text{Rf}_4$ ).

**$^{13}\text{C-NMR}$ :** (90.55 MHz,  $\text{CDCl}_3$ ):  $\delta$  133.5 ( $\text{CH}_2\text{CHCH}_2\text{CH}$ ), 119.40 ( $\text{CH}_2\text{CHCH}_2\text{CH}$ ), 108.86-118.89 ( $\text{Rf}_4$ ), 38.78 ( $\text{CH}_2\text{CHCH}_2\text{CH}$ ), 33.53 (*t*,  $^3J_{\text{CF}} = 21.1$  Hz,  $\text{Rf}_4\text{CH}_2\text{CHCH}_2\text{Rf}_4$ ), 24.91 ( $\text{Rf}_4\text{CH}_2\text{CHCH}_2\text{Rf}_4$ ).

**EI-MS:**  $m/z$  (% int.): 520.5 ( $\text{M}^{+}$ , 7%), 287.3 ( $[\text{M-Rf}_{2,4}]^{+}$ , 100%).

#### 22.1.5 1-Bromo-4-[6,6,7,7,8,8,9,9,9-nonafluoro-4-(2,2,3,3,4,4,5,5,5-nonafluoropentyl)non-1-enyl]benzene



The synthesis was carried out following **method D** using **127a** (0.52 g, 1.0 mmol), **48a** (0.3 g, 1.1 mmol),  $\text{Pd}_2(\text{dba})_3$  (15.5 mg, 15  $\mu\text{mol}$ ), NaOAc (287 mg, 3.5 mmol) and  $\text{CH}_3\text{CN}$  (5 mL). The mixture was heated to 40  $^\circ\text{C}$  for 3 hours until the evolution of nitrogen eased followed by 11 hours at 70  $^\circ\text{C}$ . After cooling to room temperature all volatiles were removed under reduced pressure and the crude black product was filtered over a silica gel plug using pentane – ether 4:1 as eluent. Final purification was achieved by column chromatography on silica gel together with pentane as eluent yielding the title compound **128a** as colourless oil in an inseparable mixture together with compound **128c** in an 4:1 ratio (209 mg, 31%).

**TLC:** R<sub>f</sub> = 0.71 (silica gel, pentane, KMnO<sub>4</sub>).

**<sup>1</sup>H-NMR:** (360 MHz, CDCl<sub>3</sub>): δ 7.44 (*d*, 2H, <sup>3</sup>J<sub>HH</sub> = 8.2 Hz, Ph), 7.22 (*d*, 2H, <sup>3</sup>J<sub>HH</sub> = 8.2 Hz, Ph), 6.42 (*d*, 1H, <sup>3</sup>J<sub>HH</sub> = 15.8 Hz, CHCHCH<sub>2</sub>CH), 6.06 (*dt*, 1H, <sup>3</sup>J<sub>HH</sub> = 15.8 Hz, <sup>3</sup>J<sub>HH</sub> = 7.3 Hz, CHCHCH<sub>2</sub>CH), 2.63 (*septept*, 1H, <sup>3</sup>J<sub>HH</sub> = 6.4 Hz, Rf<sub>4</sub>CH<sub>2</sub>CHCH<sub>2</sub>Rf<sub>4</sub>), 2.48 (*t*, 2H, <sup>3</sup>J<sub>HH</sub> = 7.3 Hz, CHCHCH<sub>2</sub>CH), 2.18-2.30 (*m*, 4H, Rf<sub>4</sub>CH<sub>2</sub>CHCH<sub>2</sub>Rf<sub>4</sub>).

**<sup>13</sup>C-NMR:** (90.55 MHz, CDCl<sub>3</sub>): δ 135.63 (Ph), 133.31 (CHCHCH<sub>2</sub>CH), 131.75 (Ph), 127.70 (Ph), 125.65 (CHCHCH<sub>2</sub>CH), 121.45 (Ph), 109.82-120.05 (Rf<sub>4</sub>), 37.95 (CHCHCH<sub>2</sub>CH), 33.69 (*t*, <sup>2</sup>J<sub>CF</sub> = 21.1 Hz, Rf<sub>4</sub>CH<sub>2</sub>CHCH<sub>2</sub>Rf<sub>4</sub>), 25.46 (Rf<sub>4</sub>CH<sub>2</sub>CHCH<sub>2</sub>Rf<sub>4</sub>).

**EI-MS:** m/z (% int.): 674.6 ( $M^{+}$ , 2%), 197.1 ( $[M-Rf_4CH_2CHCH_2Rf_4]^{+}$ , 30%), 116.0 ( $[M-Rf_4CH_2CHCH_2Rf_4-Br]^{+}$ , 100%).

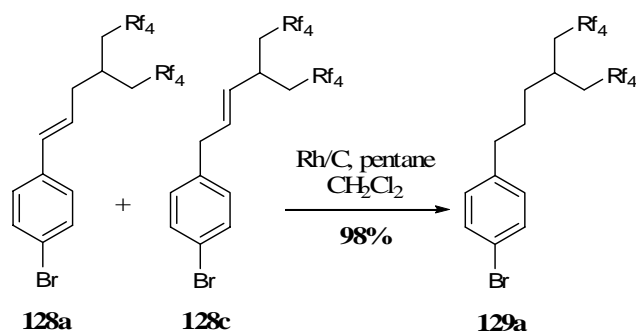
**TLC:** R<sub>f</sub> = 0.65 (silica gel, pentane, KMnO<sub>4</sub>).

**<sup>1</sup>H-NMR:** (360 MHz, CDCl<sub>3</sub>): δ 7.41 (*d*, 2H, <sup>3</sup>J<sub>HH</sub> = 8.2 Hz, Ph), 7.02 (*d*, 2H, <sup>3</sup>J<sub>HH</sub> = 8.2 Hz, Ph), 5.74 (*dt*, 1H, <sup>3</sup>J<sub>HH</sub> = 15.4 Hz, <sup>3</sup>J<sub>HH</sub> = 6.4 Hz, CH<sub>2</sub>CHCHCH), 5.39 (*dd*, 1H, <sup>3</sup>J<sub>HH</sub> = 15.4 Hz, <sup>3</sup>J<sub>HH</sub> = 9.1 Hz, CH<sub>2</sub>CHCHCH), 3.31 (*d*, 2H, <sup>3</sup>J<sub>HH</sub> = 6.4 Hz, CH<sub>2</sub>CHCHCH), 3.12 (*m*, 1H, Rf<sub>4</sub>CH<sub>2</sub>CHCH<sub>2</sub>Rf<sub>4</sub>), 2.18-2.30 (*m*, 4H, Rf<sub>4</sub>CH<sub>2</sub>CHCH<sub>2</sub>Rf<sub>4</sub>).

**<sup>13</sup>C-NMR:** (90.55 MHz, CDCl<sub>3</sub>): δ 138.49 (Ph), 131.84 (CH<sub>2</sub>CHCHCH), 131.51 (Ph), 131.14 (CH<sub>2</sub>CHCHCH), 130.31 (Ph), 121.45 (Ph), 107.81-118.87 (Rf<sub>4</sub>), 37.96 (CH<sub>2</sub>CHCHCH), 35.61 (*t*, <sup>2</sup>J<sub>CF</sub> = 21.1 Hz, Rf<sub>4</sub>CH<sub>2</sub>CHCH<sub>2</sub>Rf<sub>4</sub>), 29.75 (Rf<sub>4</sub>CH<sub>2</sub>CHCH<sub>2</sub>Rf<sub>4</sub>).

**EI-MS:** m/z (% int.): 674.6 ( $M^{*+}$ , 2%), 197.1 ( $[M-Rf_4CH_2CHCH_2Rf_4]^{*+}$ , 30%), 116.0 ( $[M-Rf_4CH_2CHCH_2Rf_4-Br]^{*+}$ , 100%).

22.1.6 1-Bromo-4-[6,6,7,7,8,8,9,9,9-nonafluoro-4-(2,2,3,3,4,4,5,5,6,6,6-nonafluoropentyl)nonyl]-benzene



The synthesis was performed using **method E** taking a mixture of compound **128a** and **128 c** (1.75 g, 2.6 mmol), Rh/C (100 mg), pentane (20 mL) and CH<sub>2</sub>Cl<sub>2</sub> (10 mL). The reaction was stirred at room temperature under 60 bar of hydrogen for 18 hours before the mixture was filtered over a sil-

ica gel pad using pentane. After removing all volatiles, compound **129a** (1.75 g, 98%) was obtained as colourless oil.

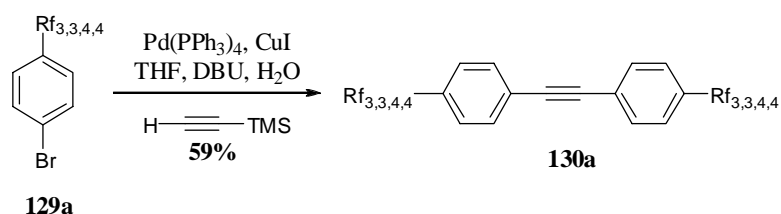
**TLC:**  $R_f = 0.81$  (silica gel, pentane,  $\text{KMnO}_4$ ).

**$^1\text{H-NMR}$ :** (360 MHz,  $\text{CDCl}_3$ ):  $\delta$  7.41 (*d*, 2H,  $^3J_{\text{HH}} = 8.2$  Hz, Ph), 7.04 (*d*, 2H,  $^3J_{\text{HH}} = 8.2$  Hz, Ph), 2.59 (*t*, 2H,  $^3J_{\text{HH}} = 7.0$  Hz,  $\text{CH}_2\text{CH}_2\text{CH}_2\text{CH}$ ), 2.44 (*septet*, 1H,  $^3J_{\text{HH}} = 5.9$  Hz,  $\text{Rf}_4\text{CH}_2\text{CHCH}_2\text{Rf}_4$ ), 2.09-2.24 (*m*, 4H,  $\text{Rf}_4\text{CH}_2\text{CHCH}_2\text{Rf}_4$ ), 1.58-1.66 (*m*, 4H,  $\text{CH}_2\text{CH}_2\text{CH}_2\text{CH}$ ).

**$^{13}\text{C-NMR}$ :** (90.55 MHz,  $\text{CDCl}_3$ ):  $\delta$  140.48 (Ph), 131.50 (Ph), 130.05 (Ph), 119.78 (Ph), 108.52-121.21 ( $\text{Rf}_4$ ), 35.01 ( $\text{CH}_2\text{CH}_2\text{CH}_2\text{CH}$ ), 34.24 ( $\text{CH}_2\text{CH}_2\text{CH}_2\text{CH}$ ), 34.13 (*t*,  $^2J_{\text{CF}} = 21.1$  Hz,  $\text{Rf}_4\text{CH}_2\text{CHCH}_2\text{Rf}_4$ ), 27.76 ( $\text{CH}_2\text{CH}_2\text{CH}_2\text{CH}$ ), 25.34 ( $\text{Rf}_4\text{CH}_2\text{CHCH}_2\text{Rf}_4$ ).

**EI-MS:**  $m/z$  (% int.): 676.6 ( $\text{M}^{+}$ , 6 %), 171.0 ( $[\text{M}-\text{CH}_2\text{CH}_2\text{CH}(\text{CH}_2\text{Rf}_4)_2]^{+}$ , 100%).

22.1.7 1-[6,6,7,7,8,8,9,9,-Nonafluoro-4-(2,2,3,3,4,4,5,5,5-nonafluoropentyl)nonyl]-4-({4-[6,6,7,7,8,8,9,9,-nonafluoro-4-(2,2,3,3,4,4,5,5,5-nonafluoropentyl)nonyl]phenyl}-ethynyl)benzene



The synthesis was performed following **method A** using bromoaryl **129a** (1.0 g, 1.48 mmol),  $\text{Pd(PPh}_3)_4$  (103 mg, 89  $\mu\text{mol}$ ),  $\text{CuI}$  (28 mg, 0.15 mmol), DBU (1.32 mL, 8.9 mmol), TMSA (0.11 mL, 0.74 mmol),  $\text{H}_2\text{O}$  (10  $\mu\text{L}$ , 0.59 mmol) and THF (10 mL). The reaction mixture was stirred at 80  $^\circ\text{C}$  in the sealed Schlenk reaction vessel for 3 days before the mixture was cooled to room temperature. Dilution with ether (200 mL) and washing with water (100 mL), 10%  $\text{HCl}$  (150 mL) were done before the organic fraction was dried over  $\text{Na}_2\text{SO}_4$ . Final purification was achieved by column chromatography over silica gel using pentane as eluent. Combination of all product fractions and evaporation of pentane afforded the desired tolane **130a** as slightly yellow oil (530 mg, 59 %).

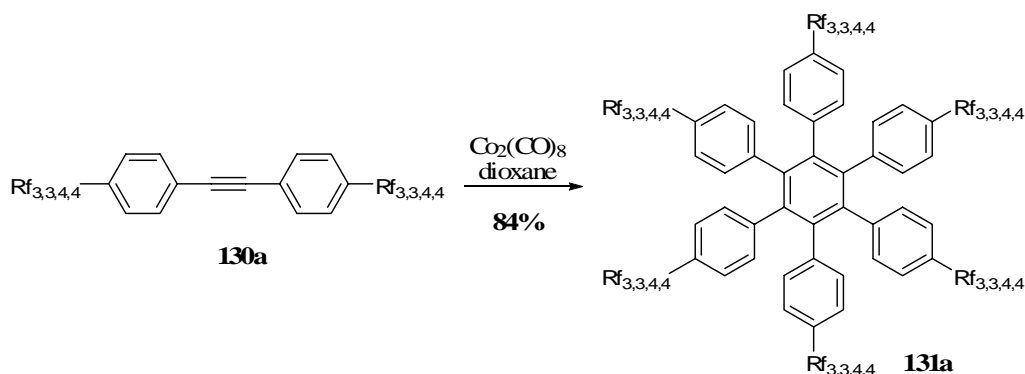
**TLC:**  $R_f = 0.15$  (silica gel, pentane,  $\text{KMnO}_4$ ).

**$^1\text{H-NMR}$ :** (360 MHz,  $\text{CDCl}_3$ ):  $\delta$  7.45 (*d*, 4H,  $^3J_{\text{HH}} = 8.2$  Hz, Ph), 7.15 (*d*, 4H,  $^3J_{\text{HH}} = 8.2$  Hz, Ph), 2.65 (*t*, 4H,  $^3J_{\text{HH}} = 7.1$  Hz,  $\text{CH}_2\text{CH}_2\text{CH}_2\text{CH}$ ), 2.45 (*septet*, 2H,  $^3J_{\text{HH}} = 6.0$  Hz,  $\text{Rf}_4\text{CH}_2\text{CHCH}_2\text{Rf}_4$ ), 2.05-2.26 (*m*, 8H,  $\text{Rf}_4\text{CH}_2\text{CHCH}_2\text{Rf}_4$ ), 1.61-1.69 (*m*, 8H,  $\text{CH}_2\text{CH}_2\text{CH}_2\text{CH}$ ).

**$^{13}\text{C-NMR}$ :** (125.77 MHz,  $\text{CDCl}_3$ ):  $\delta$  141.83 (Ph), 131.66 (Ph), 128.34 (Ph), 121.06 (Ph), 108.10 – 120.69 ( $\text{Rf}_6$ ), 88.95 (acetylene), 35.52 ( $\text{CH}_2\text{CH}_2\text{CH}_2\text{CH}$ ), 34.31 ( $\text{CH}_2\text{CH}_2\text{CH}_2\text{CH}$ ), 34.16 (*t*,  $^3J_{\text{CF}} = 21.1$  Hz,  $\text{Rf}_4\text{CH}_2\text{CHCH}_2\text{Rf}_4$ ), 27.66 ( $\text{CH}_2\text{CH}_2\text{CH}_2\text{CH}$ ), 25.37 ( $\text{Rf}_4\text{CH}_2\text{CHCH}_2\text{Rf}_4$ ).

**MALDI-ICR-MS (DCTB):**  $m/z$  (% int.): 1469.33 ( $[\text{M}+\text{DCTB}]^{+}$ , 99 %), 1218.18 ( $\text{M}^{+}$ , 100 %).

22.1.8 Hexakis[4-(2,2,3,3,4,4,5,5,5-nonafluoro-4-{2,2,3,3,4,4,5,5,5-nonafluoropentyl}undecyl)-phenyl]benzene



The synthesis was carried out following **method B** using tolane **130a** (0.5 g, 0.41 mmol) as precursor together with Co<sub>2</sub>(CO)<sub>8</sub> (11.2 mg, 33 μmol) and dioxane (50 mL). The dark mixture was refluxed for 17 hours before all volatiles were removed under reduced pressure. The obtained oil was filtered over a silica gel plug using ether as eluent, yielding the desired HPB **131a** as brown oil which was further purified by column chromatography on silica gel using pentane – ether (99:1) as eluent yielding compound **131a** as faint yellow oil (0.42 g, 84 %).

**TLC:** R<sub>f</sub> = 0.21 (silica gel, pentane – ether (99:1), KMnO<sub>4</sub>).

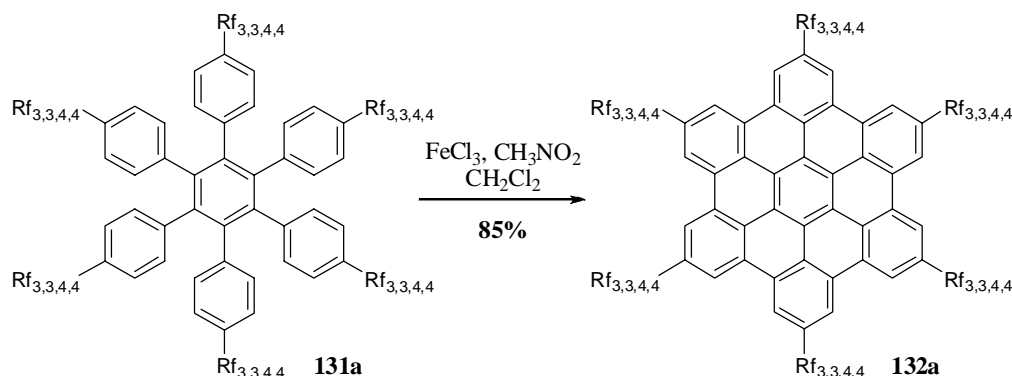
**<sup>1</sup>H-NMR:** (500 MHz, CDCl<sub>3</sub>): δ 6.70 (*d*, 12H, <sup>3</sup>J<sub>HH</sub> = 8.2 Hz, Ph), 6.61 (*d*, 12H, <sup>3</sup>J<sub>HH</sub> = 8.2 Hz, Ph), 2.36 (*m*, 6H, Rf<sub>4</sub>CH<sub>2</sub>CHCH<sub>2</sub>Rf<sub>4</sub>), 2.01-2.20 (*m*, 24H, Rf<sub>4</sub>CH<sub>2</sub>CHCH<sub>2</sub>Rf<sub>4</sub>), 1.35-1.45 (*m*, 24H, CH<sub>2</sub>CH<sub>2</sub>CH<sub>2</sub>CH).

**<sup>13</sup>C-NMR:** (125 MHz, CDCl<sub>3</sub>): δ 140.18 (Ph), 138.60 (Ph), 137.81 (Ph), 131.57 (Ph), 126.33 (Ph), 106.14-120.41 (Rf<sub>4</sub>), 34.74 (CH<sub>2</sub>CH<sub>2</sub>CH<sub>2</sub>CH), 34.05 (*t*, <sup>3</sup>J<sub>CF</sub> = 21.1 Hz, Rf<sub>4</sub>CH<sub>2</sub>CHCH<sub>2</sub>Rf<sub>4</sub>), 33.81 (CH<sub>2</sub>CH<sub>2</sub>CH<sub>2</sub>CH), 27.36 (CH<sub>2</sub>CH<sub>2</sub>CH<sub>2</sub>CH), 25.15 (Rf<sub>4</sub>CH<sub>2</sub>CHCH<sub>2</sub>Rf<sub>4</sub>).

**MALDI-ICR-MS (DCTB):** m/z (% int.): 3655.50 (M<sup>+</sup>, 100 %).



## 22.1.9 2,5,8,11,14,17-Hexakis[4-(2,2,3,3,4,4,5,5,5-nonafluoro-4-{2,2,3,3,4,4,5,5,5-nonafluoropentyl}undecyl)]hexabenz[bc,ef,hi,kl,no,q]coronene



The synthesis was performed following **method C** using HPB **131a** (0.2 g, 55  $\mu\text{mol}$ ) as precursor together with  $\text{FeCl}_3$  (800 mg, 4.9 mmol, 7.5 eq / H to be removed),  $\text{CH}_3\text{NO}_2$  (16 mL) and  $\text{CH}_2\text{Cl}_2$  (40 mL). The reaction was stirred at 37 °C under constant argon bubbling for 7 hours before methanol (40 mL) was added to quench the mixture which initiated the precipitation of dark oil, which assembled at the bottom of the flasks and solidified gently. The crude mixture was stored one night in the fridge before the crude black solid was suction filtrated over Millipore<sup>®</sup>. The crude HBC was suspended in ether – pentane and filtrated over Millipore<sup>®</sup> yielding a brown solid which was dissolved in a minimum amount of hot BTF and precipitated by the addition of ether and methanol. Suction filtration over Millipore<sup>®</sup> afforded finally HBC **132a** as yellow powder in excellent yield (170 mg, 84 %).

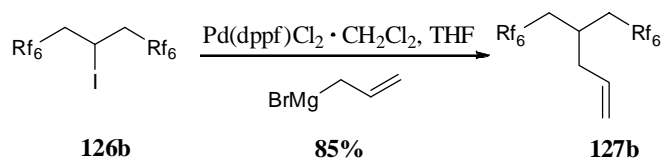
**<sup>1</sup>H-NMR:** (360 MHz,  $\text{CDCl}_3$ ): 9.29 (br. s, 12H, Ph), 3.67 (br. s, 12H,  $\text{CH}_2\text{CH}_2\text{CH}_2\text{CH}$ ), 2.99 (br. s, 6H,  $\text{Rf}_4\text{CH}_2\text{CHCH}_2\text{Rf}_4$ ), 2.44-2.71 (m, 36H,  $\text{CH}_2\text{CH}_2\text{CH}_2(\text{CHCH}_2\text{Rf}_4)_2$ ), 2.54 (m, 12H,  $\text{CH}_2\text{CH}_2\text{CH}_2\text{CH}$ ).

**MALDI-ICR-MS (DCTB):** m/z (% int.): 3642.43 ( $\text{M}^{+}$ , 100%; calcd. for  $\text{C}_{126}\text{H}_{78}\text{F}_{108}$  3642.44).

**UV/VIS:** (BTF,  $10^{-6}$  M,  $\varepsilon = 2.4 \cdot 10^5$ ),  $\lambda_{\text{max}} = 346, 361, 391$  nm.

22.2 Synthesis of HBC-(Rf<sub>3,3,6,6</sub>)<sub>6</sub>

## 22.2.1 6,6,7,7,8,8,9,9,10,10,11,11,11-Tridecafluoro-4-(2,2,3,3,4,4,5,5,6,6,7,7,7-tridecafluoroheptyl)undec-1-ene



The Kumada cross-coupling was performed following **method L**. An oven dried Schlenk tube was charged with Pd(dppf)Cl<sub>2</sub> · CH<sub>2</sub>Cl<sub>2</sub> (253 mg, 0.31 mmol), compound **126b** (5 g, 6.2 mmol), THF (20 mL) and allylmagnesium bromide (1 M in ether, 9.3 mL, 9.3 mmol) which was syringed in slowly during 2 h at 0°C. The ice bath was removed after the addition was completed and the reaction mixture was stirred for 12 h at room temperature before being quenched with methanol (10 mL). All volatiles were removed under reduced pressure yielding a brown suspension which was filtered over a silica gel plug under reduced pressure using pentane as solvent. After evaporation of pentane the title compound **127b** (3.79 g, 85 %) was obtained as colourless oil.

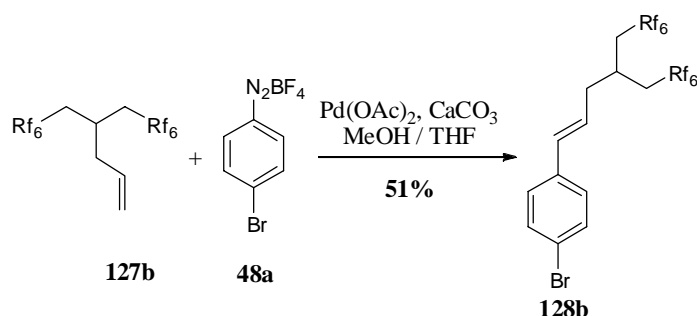
**TLC:** R<sub>f</sub> = 0.86 (silica gel, pentane – ether (4:1), KMnO<sub>4</sub>).

**<sup>1</sup>H-NMR:** (360 MHz, CDCl<sub>3</sub>): δ 5.72 (*ddt*, 1H, <sup>3</sup>J<sub>HH</sub> = 17.3 Hz, <sup>3</sup>J<sub>HH</sub> = 10.0 Hz, <sup>2</sup>J<sub>HH</sub> = 6.8 Hz, CH<sub>2</sub>CHCH<sub>2</sub>CH), 5.20 (*d*, 1H, <sup>3</sup>J<sub>HH</sub> = 17.3 Hz, CH<sub>2</sub>CHCH<sub>2</sub>CH), 5.15 (*d*, 1H, <sup>3</sup>J<sub>HH</sub> = 10.0 Hz, CH<sub>2</sub>CHCH<sub>2</sub>CH), 2.55 (*septept*, 1H, <sup>3</sup>J<sub>HH</sub> = 6.8 Hz, Rf<sub>6</sub>CH<sub>2</sub>CHCH<sub>2</sub>Rf<sub>6</sub>), 2.34 (*t*, 2H, <sup>3</sup>J<sub>HH</sub> = 6.8 Hz, CH<sub>2</sub>CHCH<sub>2</sub>CH), 2.13-2.27 (*m*, 4H, Rf<sub>6</sub>CH<sub>2</sub>CHCH<sub>2</sub>Rf<sub>6</sub>).

**<sup>13</sup>C-NMR:** (90.55 MHz, CDCl<sub>3</sub>): δ 133.5 (CH<sub>2</sub>CHCH<sub>2</sub>CH), 119.32 (CH<sub>2</sub>CHCH<sub>2</sub>CH), 105.25-122.33 (Rf<sub>6</sub>), 38.80 (CH<sub>2</sub>CHCH<sub>2</sub>CH), 33.60 (*t*, <sup>3</sup>J<sub>CF</sub> = 21.1 Hz, Rf<sub>6</sub>CH<sub>2</sub>CHCH<sub>2</sub>Rf<sub>6</sub>), 24.94 (Rf<sub>6</sub>CH<sub>2</sub>CHCH<sub>2</sub>Rf<sub>6</sub>).

**EI-MS:** m/z (% int.): 721.2 (M<sup>•+</sup>, 2%), 387.3 ([M-Rf<sub>2,6</sub>]<sup>•+</sup>, 100%).

## 22.2.2 1-Bromo-4-[6,6,7,7,8,8,9,9,10,10,11,11,11-tridecafluoro-4-(2,2,3,3,4,4,5,5,6,6,7,7,7-tridecafluoroheptyl)undec-1-enyl]benzene



To a suspension of 4-bromobenzenediazonium tetrafluoroborate **48a** (5.4 g, 20 mmol),  $\text{Pd}(\text{OAc})_2$  (90 mg, 0.4 mmol) and  $\text{CaCO}_3$  (2 g, 20 mmol) in methanol (12 mL) compound **127b** (14.4 g, 20.0 mmol) in THF (36 mL) was added. The reaction mixture was heated to 50 °C and stirred for 44 h. Afterwards all volatiles were removed yielding a crude brown solid, which was suspended in pentane and filtered over a plug of silica gel under reduced pressure using pentane as eluent. Evaporation of the pentane afforded the crude reaction product, which was purified by silica gel column chromatography with pentane as eluent. The combined fractions yielded after evaporation of pentane the title compound **128b** (8.98 g, 51 %) as colourless oil.

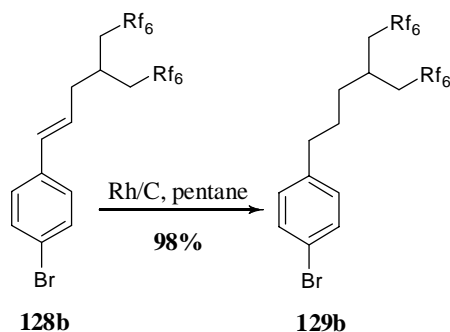
**TLC:**  $R_f$  = 0.55 (silica gel, pentane,  $\text{KMnO}_4$ ).

**$^1\text{H}$ -NMR:** (360 MHz,  $\text{CDCl}_3$ ):  $\delta$  7.45 (*d*, 2H,  $^3J_{\text{HH}}$  = 8.2 Hz, Ph), 7.22 (*d*, 2H,  $^3J_{\text{HH}}$  = 8.2 Hz, Ph), 6.43 (*d*, 1H,  $^3J_{\text{HH}}$  = 15.9 Hz,  $\text{CHCHCH}_2\text{CH}$ ), 6.06 (*dt*, 1H,  $^3J_{\text{HH}}$  = 15.9 Hz,  $^3J_{\text{HH}}$  = 7.3 Hz,  $\text{CHCHCH}_2\text{CH}$ ), 2.63 (*septept*, 1H,  $^3J_{\text{HH}}$  = 5.9 Hz,  $\text{Rf}_6\text{CH}_2\text{CHCH}_2\text{Rf}_6$ ), 2.49 (*t*, 2H,  $^3J_{\text{HH}}$  = 7.3 Hz,  $\text{CHCHCH}_2\text{CH}$ ), 2.17-2.30 (*m*, 4H,  $\text{Rf}_6\text{CH}_2\text{CHCH}_2\text{Rf}_6$ ).

**$^{13}\text{C}$ -NMR:** (90.55 MHz,  $\text{CDCl}_3$ ):  $\delta$  135.61 (Ph), 133.29 ( $\text{CHCHCH}_2\text{CH}$ ), 131.73 (Ph), 127.69 (Ph), 125.65 ( $\text{CHCHCH}_2\text{CH}$ ), 121.45 (Ph), 107.81-118.87 ( $\text{Rf}_6$ ), 37.96 ( $\text{CHCHCH}_2\text{CH}$ ), 33.76 (*t*,  $^2J_{\text{CF}}$  = 20.8 Hz,  $\text{Rf}_6\text{CH}_2\text{CHCH}_2\text{Rf}_6$ ), 25.46 ( $\text{Rf}_6\text{CH}_2\text{CHCH}_2\text{Rf}_6$ ).

**EI-MS:**  $m/z$  (% int.): 873.98 ( $\text{M}^{+\bullet}$ , 85 %), 461.04 (12 %), 198.03 ( $[\text{M}-\text{Rf}_6\text{CH}_2\text{CHCH}_2\text{Rf}_6]^{+\bullet}$ , 100 %).

22.2.3 1-Bromo-4-[6,6,7,7,8,8,9,9,10,10,11,11,11-tridecafluoro-4-(2,2,3,3,4,4,5,5,6,6,7,7,7-tridecafluoroheptyl)undecyl]benzene



The synthesis was performed using **method E** taking compound **128b** (9.6 g, 11.0 mmol), Rh/C (450 mg) and pentane (90 mL). The reaction was stirred at room temperature under 60 bar of hydrogen for 22 hours before the catalyst was removed by filtration over a silica gel pad using pentane as eluent. After removing of all volatiles, compound **129b** (9.0 g, 95%) was obtained as colourless oil in nearly quantitative yield.

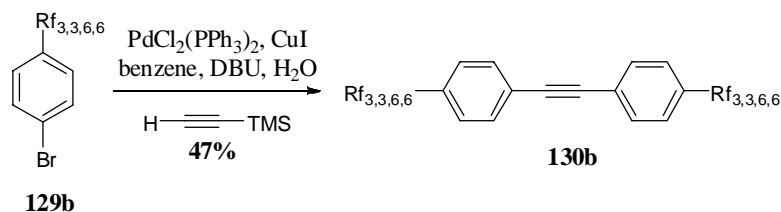
**TLC:**  $R_f = 0.70$  (silica gel, pentane,  $\text{KMnO}_4$ ).

**$^1\text{H-NMR}$ :** (360 MHz,  $\text{CDCl}_3$ ):  $\delta$  7.41 (*d*, 2H,  $^3J_{\text{HH}} = 8.2$  Hz, Ph), 7.05 (*d*, 2H,  $^3J_{\text{HH}} = 8.2$  Hz, Ph), 2.59 (*t*, 2H,  $^3J_{\text{HH}} = 6.5$  Hz,  $\text{CH}_2\text{CH}_2\text{CH}_2\text{CH}$ ), 2.44 (*septet*, 1H,  $^3J_{\text{HH}} = 5.5$  Hz,  $\text{Rf}_6\text{CH}_2\text{CHCH}_2\text{Rf}_6$ ), 2.07-2.24 (*m*, 4H,  $\text{Rf}_6\text{CH}_2\text{CHCH}_2\text{Rf}_6$ ), 1.58-1.65 (*m*, 4H,  $\text{CH}_2\text{CH}_2\text{CH}_2\text{CH}$ ).

**$^{13}\text{C-NMR}$ :** (90.55 MHz,  $\text{CDCl}_3$ ):  $\delta$  140.52 (Ph), 131.51 (Ph), 130.05 (Ph), 119.80 (Ph), 108.36-119.75 ( $\text{Rf}_6$ ), 35.02 ( $\text{CH}_2\text{CH}_2\text{CH}_2\text{CH}$ ), 34.27 ( $\text{CH}_2\text{CH}_2\text{CH}_2\text{CH}$ ), 34.22 (*t*,  $^2J_{\text{CF}} = 21.1$  Hz,  $\text{Rf}_6\text{CH}_2\text{CHCH}_2\text{Rf}_6$ ), 27.78 ( $\text{CH}_2\text{CH}_2\text{CH}_2\text{CH}$ ), 25.40 ( $\text{Rf}_6\text{CH}_2\text{CHCH}_2\text{Rf}_6$ ).

**EI-MS:**  $m/z$  (% int.): 875.99 ( $\text{M}^{+\bullet}$ , 100 %).

22.2.4 1-[6,6,7,7,8,8,9,9,10,10,11,11,11-Tridecafluoro-4-(2,2,3,3,4,4,5,5,6,6,7,7,7-tridecafluoroheptyl)undecyl]-4-({4-[6,6,7,7,8,8,9,9,10,10,11,11,11-tridecafluoro-4-(2,2,3,3,4,4,5,5,6,6,7,7,7-tridecafluoroheptyl)undecyl]phenyl}ethynyl)benzene



The synthesis was performed following **method A** using bromoaryl **129b** (2.8 g, 3.2 mmol),  $\text{PdCl}_2(\text{PPh}_3)_2$  (134 mg, 0.19 mmol), CuI (60.8 mg, 0.32 mmol), DBU (2.7 mL, 19 mmol), TMSA (0.22 mL, 1.5 mmol),  $\text{H}_2\text{O}$  (23  $\mu\text{L}$ , 1.3 mmol) and benzene (15 mL). The reaction mixture was

stirred at 80 °C in the sealed Schlenk reaction vessel for 2 days before the mixture was cooled to room temperature. Dilution with ether (200 mL) and washing with water (100 mL), 10% HCl (50 mL) were done before the organic fraction was dried over Na<sub>2</sub>SO<sub>4</sub>. Final purification was achieved by column chromatography over silica gel using pentane as eluent. Combination of all product fractions and evaporation of pentane afforded the desired tolane **130b** as faint brown oil (1.2 g, 47 %).

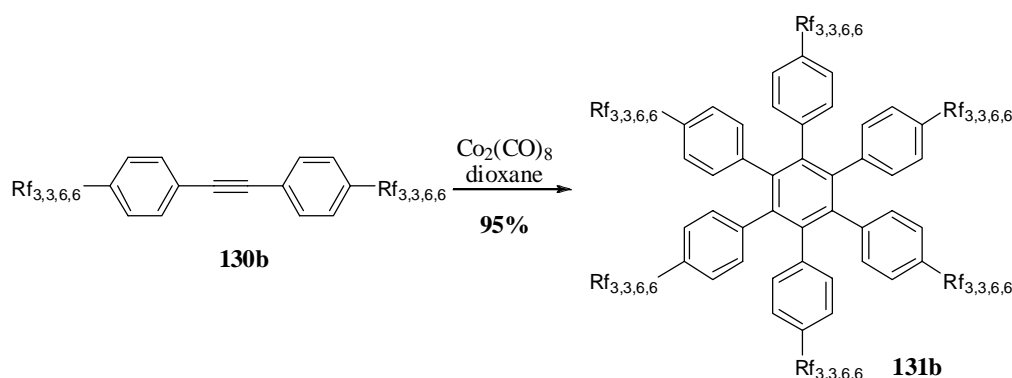
**TLC:** R<sub>f</sub> = 0.15 (silica gel, pentane, KMnO<sub>4</sub>).

**<sup>1</sup>H-NMR:** (360 MHz, CDCl<sub>3</sub>): δ 7.46 (*d*, 4H, <sup>3</sup>J<sub>HH</sub> = 8.2 Hz, Ph), 7.15 (*d*, 4H, <sup>3</sup>J<sub>HH</sub> = 8.2 Hz, Ph), 2.65 (*t*, 4H, <sup>3</sup>J<sub>HH</sub> = 6.8 Hz, CH<sub>2</sub>CH<sub>2</sub>CH<sub>2</sub>CH), 2.45 (*septept*, 2H, <sup>3</sup>J<sub>HH</sub> = 5.9 Hz, Rf<sub>6</sub>CH<sub>2</sub>CHCH<sub>2</sub>Rf<sub>6</sub>), 2.07-2.24 (*m*, 8H, Rf<sub>6</sub>CH<sub>2</sub>CHCH<sub>2</sub>Rf<sub>6</sub>), 1.58-1.65 (*m*, 8H, CH<sub>2</sub>CH<sub>2</sub>CH<sub>2</sub>CH).

**<sup>13</sup>C-NMR:** (125.77 MHz, CDCl<sub>3</sub>): δ 141.83 (Ph), 131.66 (Ph), 128.35 (Ph), 121.06 (Ph), 108.05 – 120.83 (Rf<sub>6</sub>), 88.95 (acetylene), 35.52 (CH<sub>2</sub>CH<sub>2</sub>CH<sub>2</sub>CH), 34.30 (CH<sub>2</sub>CH<sub>2</sub>CH<sub>2</sub>CH), 34.24 (*t*, <sup>3</sup>J<sub>CF</sub> = 21.1 Hz, Rf<sub>6</sub>CH<sub>2</sub>CHCH<sub>2</sub>Rf<sub>6</sub>), 27.66 (CH<sub>2</sub>CH<sub>2</sub>CH<sub>2</sub>CH), 25.40 (Rf<sub>6</sub>CH<sub>2</sub>CHCH<sub>2</sub>Rf<sub>6</sub>).

**MALDI-ICR-MS (DCTB):** m/z (% int.): 1618.15 (M<sup>+</sup>, 100 %), 1387.08 (18 %), 989.12 (18 %), 911.10 (15 %).

#### 22.2.5 Hexakis[4-(6,6,7,7,8,8,9,9,10,10,11,11,11-tridecafluoro-4-{2,2,3,3,4,4,5,5,6,6,7,7,7-tridecafluoroheptyl}undecyl)phenyl]benzene



The synthesis was carried out following **method B** using tolane **130b** (1.1 g, 0.67 mmol) as precursor together with Co<sub>2</sub>(CO)<sub>8</sub> (18.6 mg, 54 μmol) and dioxane (20 mL). The dark mixture was refluxed for 25 hours before all volatiles were removed under reduced pressure. The obtained oil was filtered over a silica gel plug using ether as eluent, yielding the desired HPB **131b** as slightly brown oil (1.05 g, 95 %).

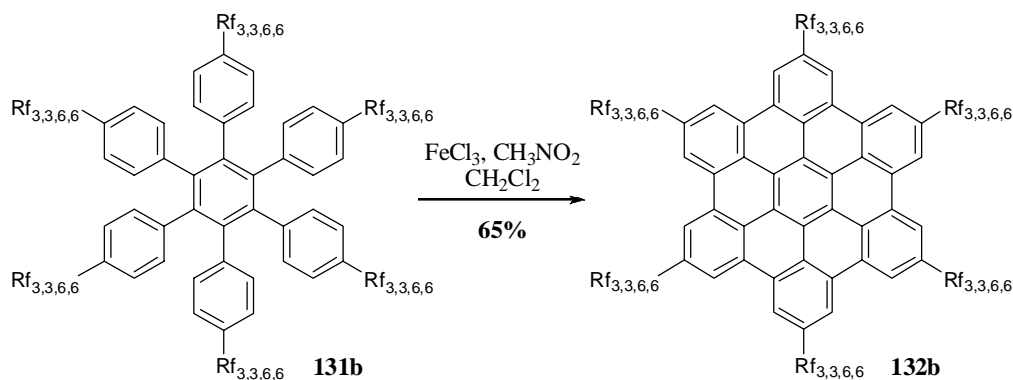
**TLC:** R<sub>f</sub> = 0.90 (silica gel, ether, KMnO<sub>4</sub>).

**<sup>1</sup>H-NMR:** (360 MHz, CDCl<sub>3</sub>): δ 6.69 (*d*, 12H, <sup>3</sup>J<sub>HH</sub> = 8.2 Hz, Ph), 6.60 (*d*, 12H, <sup>3</sup>J<sub>HH</sub> = 8.2 Hz, Ph), 2.35 (*m*, 6H, Rf<sub>6</sub>CH<sub>2</sub>CHCH<sub>2</sub>Rf<sub>6</sub>), 2.34 (*m*, 12H, CH<sub>2</sub>CH<sub>2</sub>CH<sub>2</sub>CH), 1.99-2.19 (*m*, 24H, Rf<sub>6</sub>CH<sub>2</sub>CHCH<sub>2</sub>Rf<sub>6</sub>), 1.35-1.46 (*m*, 24H, CH<sub>2</sub>CH<sub>2</sub>CH<sub>2</sub>CH).

**$^{13}\text{C}$ -NMR:** (125.77 MHz,  $\text{CDCl}_3$ ):  $\delta$  140.16 (Ph), 138.59 (Ph), 137.81 (Ph), 131.55 (Ph), 126.33 (Ph), 110.56-120.60 ( $\text{Rf}_6$ ), 34.73 ( $\text{CH}_2\text{CH}_2\text{CH}_2\text{CH}$ ), 34.11 ( $t$ ,  $^3J_{\text{CF}} = 21.1$  Hz,  $\text{Rf}_6\text{CH}_2\text{CHCH}_2\text{Rf}_6$ ), 33.78 ( $\text{CH}_2\text{CH}_2\text{CH}_2\text{CH}$ ), 27.36 ( $\text{CH}_2\text{CH}_2\text{CH}_2\text{CH}$ ), 25.19 ( $\text{Rf}_6\text{CH}_2\text{CHCH}_2\text{Rf}_6$ ).

**MALDI-ICR-MS (DCTB):**  $m/z$  (% int.): 4854.45 ( $\text{M}^{*+}$ , 100 %).

22.2.6 2,5,8,11,14,17-Hexakis[4-(6,6,7,7,8,8,9,9,10,10,11,11,11-tridecafluoro-4-{2,2,3,3,4,4,5,5,6,6,7,7,7-tridecafluoroheptyl}undecyl)]hexabenzob[bc,ef,hi,kl,no,qr]coronene



The synthesis was performed following **method C** using HPB **131b** (1.0 g, 0.2 mmol) as precursor together with  $\text{FeCl}_3$  (600 mg, 3.6 mmol, 1.5 eq / H to be removed),  $\text{CH}_3\text{NO}_2$  (80 mL) and  $\text{CH}_2\text{Cl}_2$  (80 mL). The reaction was stirred at 45 °C under constant argon bubbling for 22 hours before methanol (80 mL) was added to quench the mixture which initiated the precipitation of dark oil, which assembled at the bottom of the flasks. The supernatant was removed by cannula filtration. This procedure was repeated using different solvents (dichloromethane, ethanol and ether) yielding finally the desired HBC **132b** as dark oily solid (650 mg, 65 %).

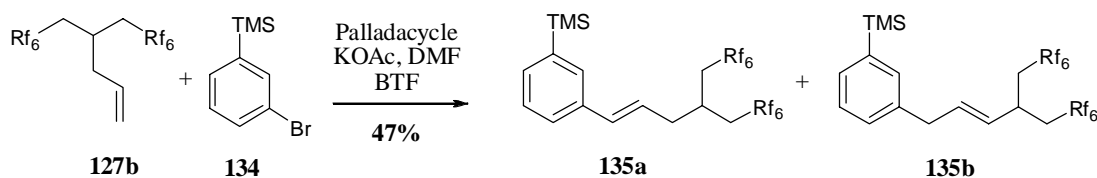
**$^1\text{H}$ -NMR:** (360 MHz,  $\text{CDCl}_3$ ): 9.19 (br. *s*, 12H, Ph), 3.55 (br. *s*, 12H,  $\text{CH}_2\text{CH}_2\text{CH}_2\text{CH}$ ), 2.87 (br. *s*, 6H,  $\text{Rf}_6\text{CH}_2\text{CHCH}_2\text{Rf}_6$ ), 2.58-2.34 (*m*, 48H,  $\text{CH}_2\text{CH}_2\text{CH}_2(\text{CHCH}_2\text{Rf}_6)_2$ ).

**MALDI-ICR-MS (DCTB):**  $m/z$  (% int.): 4282.39 ( $\text{M}^{*+}$ , 100%; calcd. for  $\text{C}_{150}\text{H}_{78}\text{F}_{156}$  4842.36).

**UV/VIS:** (BTF,  $10^{-5}$  M,  $\epsilon = 4.5 \cdot 10^4$ ),  $\lambda_{\text{max}} = 346, 363, 391$  nm.

## 22.3 Synthesis HBC-(Rf<sub>3,3,6,6</sub>)<sub>3</sub>

### 22.3.1 Trimethyl{3-[6,6,7,7,8,8,9,9,10,10,11,11,11-tridecafluoro-4-(2,2,3,3,4,4,5,5,6,6,7,7,7-tridecafluoroheptyl)undec-1-enyl]phenyl}silane



#### Method M

Palladacycle (242 mg, 0.26 mmol) and KOAc (1.65 g, 16.7 mmol) were added into an oven dried Schlenk under inert atmosphere. Compound **127b** (9.3 g, 12.9 mmol) and **134** (2.96 g, 12.9 mmol) were degassed and dissolved separately in BTF (5 mL each) and syringed into the Schlenk vessel. After the addition of DMF (20 mL) the mixture was heated to 125 °C for 27 hours. After the mixture reached room temperature the crude product was extracted with ether. The combined organic fractions were washed with water, dried over Na<sub>2</sub>SO<sub>4</sub> before all volatiles were removed under slightly reduced pressure. The crude product was purified by column chromatography using pentane as eluent yielding a mixture of **135a** and **b** (5.3 g, 47%).

#### Compound **135a**

**TLC:** R<sub>f</sub> = 0.64 (silica gel, pentane, KMnO<sub>4</sub>).

**<sup>1</sup>H-NMR:** (360 MHz, CDCl<sub>3</sub>): δ 7.46 (br. *s*, 1H, Ph), 7.42 (*d*, 1H, <sup>3</sup>J<sub>HH</sub> = 6.8 Hz, Ph), 7.36 (*d*, 1H, <sup>3</sup>J<sub>HH</sub> = 7.7 Hz, Ph), 7.32 (*dd*, 1H, <sup>3</sup>J<sub>HH</sub> = 7.7 Hz, <sup>3</sup>J<sub>HH</sub> = 6.8 Hz, Ph), 6.51 (*d*, 1H, <sup>3</sup>J<sub>HH</sub> = 15.9 Hz, CHCHCH<sub>2</sub>CH), 6.10 (*dt*, 1H, <sup>3</sup>J<sub>HH</sub> = 15.9 Hz, <sup>3</sup>J<sub>HH</sub> = 7.3 Hz, CHCHCH<sub>2</sub>CH), 2.64 (*septet*, 1H, <sup>3</sup>J<sub>HH</sub> = 5.9 Hz, Rf<sub>6</sub>CH<sub>2</sub>CHCH<sub>2</sub>Rf<sub>6</sub>), 2.50 (*t*, 2H, <sup>3</sup>J<sub>HH</sub> = 7.3 Hz, CHCHCH<sub>2</sub>CH), 2.14-2.37 (*m*, 4H, Rf<sub>6</sub>CH<sub>2</sub>CHCH<sub>2</sub>Rf<sub>6</sub>), 0.28 (*s*, 9H, TMS).

**<sup>13</sup>C-NMR:** (90.55 MHz, CDCl<sub>3</sub>): δ 140.94 (Ph), 135.93 (Ph), 134.71 (Ph), 132.70 (Ph), 131.38 (CHCHCH<sub>2</sub>CH), 128.02 (Ph), 126.33 (Ph), 124.71 (CHCHCH<sub>2</sub>CH), 106.31-118.92 (Rf<sub>6</sub>), 38.09 (CHCHCH<sub>2</sub>CH), 33.75 (*t*, <sup>2</sup>J<sub>CF</sub> = 20.8 Hz, Rf<sub>6</sub>CH<sub>2</sub>CHCH<sub>2</sub>Rf<sub>6</sub>), 25.57 (Rf<sub>6</sub>CH<sub>2</sub>CHCH<sub>2</sub>Rf<sub>6</sub>), -1.24 (TMS).

**EI-MS:** m/z (% int.): 869.0 (M<sup>+</sup>, 5 %), 167.1 (100 %).

#### Compound **135b**

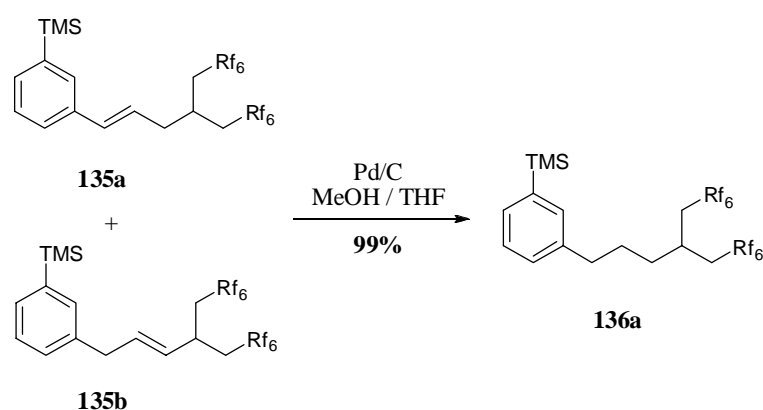
**TLC:** R<sub>f</sub> = 0.64 (silica gel, pentane, KMnO<sub>4</sub>).

**<sup>1</sup>H-NMR:** (360 MHz, CDCl<sub>3</sub>): δ 7.53 (*d*, 1H, <sup>3</sup>J<sub>HH</sub> = 6.8 Hz, Ph), 7.47 (br. *s*, 1H, Ph), 7.35 (*dd*, 1H, <sup>3</sup>J<sub>HH</sub> = 7.7 Hz, <sup>3</sup>J<sub>HH</sub> = 6.8 Hz, Ph), 7.22 (*d*, 1H, <sup>3</sup>J<sub>HH</sub> = 7.7 Hz, Ph), 5.36 (br. *s*, 1H, CH<sub>2</sub>CHCHCH), 5.13 (br. *s*, 1H, CH<sub>2</sub>CHCHCH), 2.79 (*d*, 2H, <sup>3</sup>J<sub>HH</sub> = 7.3 Hz, CH<sub>2</sub>CHCHCH), 2.43 (*septet*, 1H, <sup>3</sup>J<sub>HH</sub> = 5.9 Hz, Rf<sub>6</sub>CH<sub>2</sub>CHCH<sub>2</sub>Rf<sub>6</sub>), 2.14-2.37 (*m*, 4H, Rf<sub>6</sub>CH<sub>2</sub>CHCH<sub>2</sub>Rf<sub>6</sub>), 0.27 (*s*, 9H, TMS).

**$^{13}\text{C}$ -NMR:** (90.55 MHz,  $\text{CDCl}_3$ ):  $\delta$  143.26 (Ph), 135.91 (Ph), 133.43 (Ph), 132.68 (Ph), 131.83 ( $\text{CH}_2\text{CHCHCH}$ ), 131.10 ( $\text{CH}_2\text{CHCHCH}$ ), 129.32 (Ph), 127.33 (Ph), 106.31-118.92 ( $\text{Rf}_6$ ), 37.92 ( $\text{CH}_2\text{CHCHCH}$ ), 35.75 ( $t$ ,  $^2J_{\text{CF}} = 21.1$  Hz,  $\text{Rf}_6\text{CH}_2\text{CHCH}_2\text{Rf}_6$ ), 25.68 ( $\text{Rf}_6\text{CH}_2\text{CHCH}_2\text{Rf}_6$ ), -1.26 (TMS).

**EI-MS:**  $m/z$  (% int.): 869.0 ( $\text{M}^{+\bullet}$ , 5 %), 167.1 (100 %).

### 22.3.2 Trimethyl{3-[6,6,7,7,8,8,9,9,10,10,11,11,11-tridecafluoro-4-(2,2,3,3,4,4,5,5,6,6,7,7,7-tridecafluoroheptyl)undecyl]phenyl}silane



A mixture of **135a** and **b** (0.5 g, 0.57 mmol) was dissolved in THF (5 mL) and added together with Pd/C (60 mg, 10%) into a Schlenk reaction vessel. After the addition of MeOH (5 mL) the tube was purged three times with hydrogen before being stirred under 1.5 bar of  $\text{H}_2$  for 15 minutes at room temperature. Afterwards, the reaction mixture was filtered over a plug of silica gel using pentane as solvent to remove the catalyst. All volatiles of the filtrate were removed yielding **136a** as colourless oil in quantitative yield (0.5 g, 99%).

**TLC:**  $R_f = 0.91$  (silica gel, pentane,  $\text{KMnO}_4$ ).

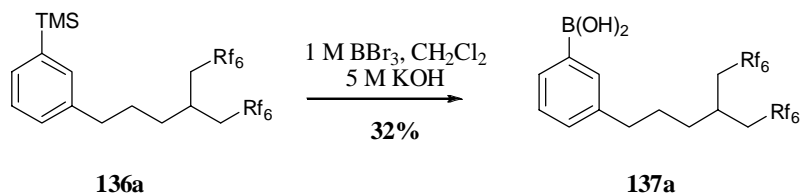
**$^1\text{H}$ -NMR:** (360 MHz,  $\text{CDCl}_3$ ):  $\delta$  7.37 ( $d$ , 1H,  $^3J_{\text{HH}} = 7.2$  Hz, Ph), 7.31 (br.  $s$ , 1H, Ph), 7.29 ( $t$ , 1H,  $^3J_{\text{HH}} = 7.2$  Hz, Ph), 7.17 ( $d$ , 1H,  $^3J_{\text{HH}} = 7.2$  Hz, Ph), 2.64 ( $t$ , 2H,  $^3J_{\text{HH}} = 6.8$  Hz,  $\text{CH}_2\text{CH}_2\text{CH}_2\text{CH}$ ), 2.46 ( $\text{septet}$ , 1H,  $^3J_{\text{HH}} = 5.9$  Hz,  $\text{Rf}_6\text{CH}_2\text{CHCH}_2\text{Rf}_6$ ), 2.06-2.27 ( $m$ , 4H,  $\text{Rf}_6\text{CH}_2\text{CHCH}_2\text{Rf}_6$ ), 1.57-1.69 ( $m$ , 4H,  $\text{CH}_2\text{CH}_2\text{CH}_2\text{CH}$ ), 0.26 ( $s$ , 9H, TMS).

**$^{13}\text{C}$ -NMR:** (90.55 MHz,  $\text{CDCl}_3$ ):  $\delta$  140.75 (Ph), 140.70 (Ph), 133.23 (Ph), 131.05 (Ph), 128.78 (Ph), 127.83 (Ph), 108.03-121.40 ( $\text{Rf}_6$ ), 35.71 ( $\text{CH}_2\text{CH}_2\text{CH}_2\text{CH}$ ), 34.81 ( $\text{CH}_2\text{CH}_2\text{CH}_2\text{CH}$ ), 34.19 ( $t$ ,  $^2J_{\text{CF}} = 20.8$  Hz,  $\text{Rf}_6\text{CH}_2\text{CHCH}_2\text{Rf}_6$ ), 28.04 ( $\text{CH}_2\text{CH}_2\text{CH}_2\text{CH}$ ), 25.38 ( $\text{Rf}_6\text{CH}_2\text{CHCH}_2\text{Rf}_6$ ), -1.22 (TMS).

**EI-MS:**  $m/z$  (% int.): 870.1 ( $\text{M}^{+\bullet}$ , 100 %), 798.0 (45 %), 758.9 (52%), 463.0 (64%), 445.1 (95%).



## 22.3.3 3-[6,6,7,7,8,8,9,9,10,10,11,11,11-Tridecafluoro-4-(2,2,3,3,4,4,5,5,6,6,7,7,7-tridecafluoroheptyl)undecyl]phenylboronic acid



Compound **136a** (0.5 g, 0.57 mmol) was dissolved in  $\text{CH}_2\text{Cl}_2$  (4 mL) and added into a Schlenk tube which was cooled to  $-78^\circ\text{C}$  before a 1M solution of  $\text{BBr}_3$  (0.9 mL, 0.9 mmol) was slowly syringed in. The mixture was stirred for 1 hour at  $-78^\circ\text{C}$  and was then slowly allowed to reach room temperature. The reaction was completed by over night refluxing. The addition of an aqueous 5 M solution of  $\text{KOH}$  (2 mL) was performed again at  $-78^\circ\text{C}$ . At room temperature, the aqueous layer was decanted off and diluted by the addition of ether (10 mL) and 2 M  $\text{HCl}$  (10 mL). The obtained emulsion was vigorously stirred for 2 hours before the aqueous layer was discarded. The organic phase was dried over  $\text{Na}_2\text{SO}_4$  and all volatiles were removed yielding the boronic acid **137a** (158 mg, 32%).

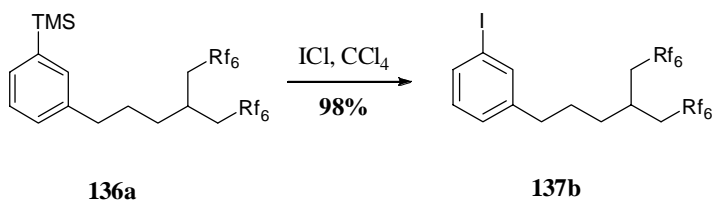
**TLC:**  $R_f = 0.53$  (silica gel, pentane – ether (9:1),  $\text{KMnO}_4$ ).

**$^1\text{H-NMR}$ :** (360 MHz,  $\text{CDCl}_3$ ):  $\delta$  7.17-7.22 (*m*, 2H, Ph), 7.07-7.11 (*m*, 2H, Ph), 2.54 (br. *s*, 2H,  $\text{CH}_2\text{CH}_2\text{CH}_2\text{CH}$ ), 2.35 (br. *m*, 1H,  $\text{Rf}_6\text{CH}_2\text{CHCH}_2\text{Rf}_6$ ), 2.02-2.12 (*m*, 4H,  $\text{Rf}_6\text{CH}_2\text{CHCH}_2\text{Rf}_6$ ), 1.53 (br. *s*, 4H,  $\text{CH}_2\text{CH}_2\text{CH}_2\text{CH}$ ).

**$^{13}\text{C-NMR}$ :** (90.55 MHz,  $\text{CDCl}_3$ ):  $\delta$  141.60 (Ph), 129.15 (*q*,  $^2J_{\text{CB}} = 89.2$  Hz, Ph), 128.44 (Ph), 128.41 (Ph), 128.30 (Ph), 126.03 (Ph), 108.21-121.39 ( $\text{Rf}_6$ ), 35.63 ( $\text{CH}_2\text{CH}_2\text{CH}_2\text{CH}$ ), 34.39 ( $\text{CH}_2\text{CH}_2\text{CH}_2\text{CH}$ ), 34.19 (*t*,  $^2J_{\text{CF}} = 20.8$  Hz,  $\text{Rf}_6\text{CH}_2\text{CHCH}_2\text{Rf}_6$ ), 27.93 ( $\text{CH}_2\text{CH}_2\text{CH}_2\text{CH}$ ), 25.39 ( $\text{Rf}_6\text{CH}_2\text{CHCH}_2\text{Rf}_6$ ).

**EI-MS:**  $m/z$  (% int.): 799.0 ( $[\text{M-B(OH)}_2]^+$ , 100 %), 409.4 (20 %), 387.4 ( $[\text{C}_5\text{H}_9\text{Rf}_6]^+$ , 70 %).

## 22.3.4 1-Iodo-3-[6,6,7,7,8,8,9,9,10,10,11,11,11-tridecafluoro-4-(2,2,3,3,4,4,5,5,6,6,7,7,7-tridecafluoroheptyl)undecyl]benzene



To a solution of compound **136a** (0.5 g, 0.57 mmol) in  $\text{CCl}_4$  (4 mL) was added drop wise a solution of  $\text{ICl}$  (97.9 mg, 0.60 mmol) in  $\text{CCl}_4$  (1 mL) at  $0^\circ\text{C}$ . The reaction was stirred at this temperature for 3 hours before the mixture was quenched by the addition of an aqueous solution of thiosulfate. The

obtained emulsion was extracted with  $\text{CH}_2\text{Cl}_2$ . The combined organic layers were dried over  $\text{Na}_2\text{SO}_4$  and all volatiles were removed affording **137b** (520 mg, 98%) as colourless oil.

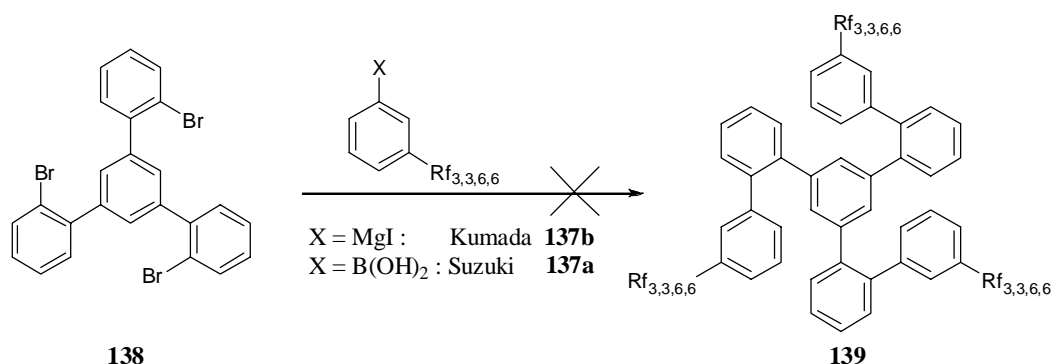
**TLC:**  $R_f = 0.94$  (silica gel, pentane,  $\text{KMnO}_4$ ).

**$^1\text{H-NMR}$ :** (360 MHz,  $\text{CDCl}_3$ ):  $\delta$  7.55 (br. s, 2H, Ph), 7.14 (d, 1H,  $^3J_{\text{HH}} = 7.7$  Hz, Ph), 7.04 (t, 1H,  $^3J_{\text{HH}} = 7.7$  Hz, Ph), 2.58 (t, 2H,  $^3J_{\text{HH}} = 6.8$  Hz,  $\text{CH}_2\text{CH}_2\text{CH}_2\text{CH}$ ), 2.46 (septet, 1H,  $^3J_{\text{HH}} = 5.9$  Hz,  $\text{Rf}_6\text{CH}_2\text{CHCH}_2\text{Rf}_6$ ), 2.11-2.25 (m, 4H,  $\text{Rf}_6\text{CH}_2\text{CHCH}_2\text{Rf}_6$ ), 1.60-1.64 (m, 4H,  $\text{CH}_2\text{CH}_2\text{CH}_2\text{CH}$ ).

**$^{13}\text{C-NMR}$ :** (90.55 MHz,  $\text{CDCl}_3$ ):  $\delta$  143.99 (Ph), 137.34 (Ph), 135.15 (Ph), 130.17 (Ph), 127.57 (Ph), 108.82-120.46 ( $\text{Rf}_6$ ), 94.51 (Ph), 35.15 ( $\text{CH}_2\text{CH}_2\text{CH}_2\text{CH}$ ), 34.28 ( $\text{CH}_2\text{CH}_2\text{CH}_2\text{CH}$ ), 34.18 (t,  $^2J_{\text{CF}} = 20.8$  Hz,  $\text{Rf}_6\text{CH}_2\text{CHCH}_2\text{Rf}_6$ ), 27.70 ( $\text{CH}_2\text{CH}_2\text{CH}_2\text{CH}$ ), 25.36 ( $\text{Rf}_6\text{CH}_2\text{CHCH}_2\text{Rf}_6$ ).

**EI-MS:**  $m/z$  (% int.): 926.0 ( $\text{M}^{++}$ , 100 %).

### 22.3.5 1,3,5-Tri(3''-{3'''-[6,6,7,7,8,8,9,10,10,11,11,11-tridecafluoro-4''']-(2,2,3,3,4,4,5,5,6,6,7,7,7-tridecafluoroheptyl)undecyl}}-2'-biphenyl)benzene



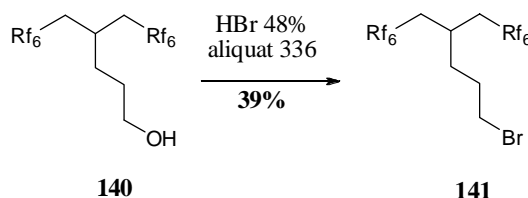
#### a) Kumada cross-coupling

The Kumada cross-coupling was performed following **method I** using **137b** (0.5 g, 0.54 mmol), Mg (26.3 mg, 1.08 mmol) and THF (2 mL) for the Grignard formation and **138** (48.9 mg, 90  $\mu\text{mol}$ )  $\text{PdCl}_2(\text{dppf}) \cdot \text{CH}_3\text{Cl}$  (11 mg, 13  $\mu\text{mol}$ ) and THF (2 mL) for the cross-coupling. The reaction was refluxed for 5 days before methanol was added to quench the mixture. Extraction with ether was performed three times. The combined organic fractions were reduced maximally and analyzed by  $^1\text{H-NMR}$  which indicated only the presence of the starting materials.

#### b) Suzuki cross-coupling

Compound **138** (11 mg, 19.7  $\mu\text{mol}$ ), **137a** (100 mg, 0.12 mmol),  $\text{Pd(PPh}_3)_4$  (4 mg, 3.0  $\mu\text{mol}$ ) were charged in an oven dried Schlenk vessel and dissolved by the addition of toluene (2 mL). After the addition of an aqueous 1 M solution of  $\text{K}_2\text{CO}_3$  the mixture was refluxed for 5 days. The crude mixture was extracted with ether. The combined organic layers were then reduced maximally and analyzed by  $^1\text{H-NMR}$  which indicated only the presence of **138** and deboronated **137a**.

22.3.7 8-(3-Bromopropyl)-1,1,1,2,2,3,3,4,4,5,5,6,6,10,10,11,11,12,12,13,13,14,14,15,15,15-hexacosafuoropentadecane

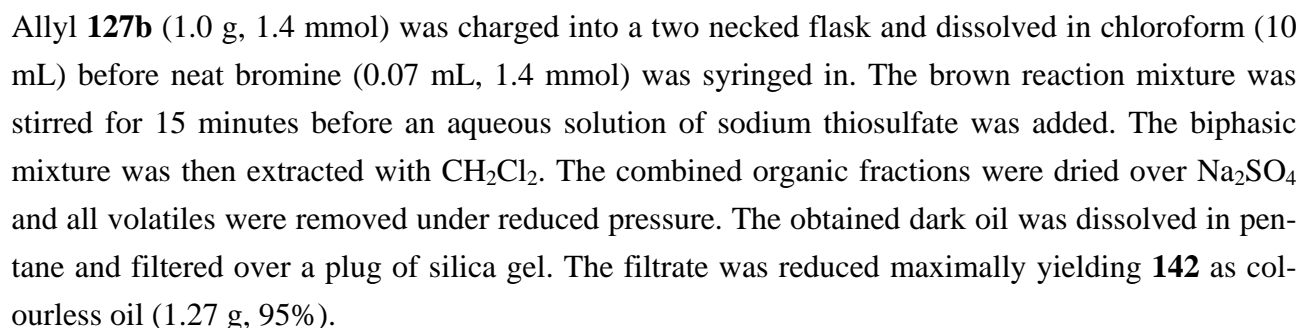


The alcohol **140** (400 mg, 0.54 mmol) was mixed with HBr 48 % (0.22 mL, 1.95 mmol) and aliquat 336 (0.01 mL) in a round bottomed flask and refluxed over night. The crude product was extracted with ether. The combined organic phases were dried over Na<sub>2</sub>SO<sub>4</sub> and all volatiles were removed

**TLC:** R<sub>f</sub> = 0.76 (silica gel, pentane, KMnO<sub>4</sub>).

**<sup>13</sup>C-NMR:** (90.55 MHz, CDCl<sub>3</sub>): δ 106.31-122.13 (Rf<sub>6</sub>), 33.34 (BrCH<sub>2</sub>CH<sub>2</sub>CH<sub>2</sub>CH), 34.28 (*t*, <sup>3</sup>J<sub>CF</sub> = 21.1 Hz, Rf<sub>6</sub>CH<sub>2</sub>CHCH<sub>2</sub>Rf<sub>6</sub>), 32.56 (BrCH<sub>2</sub>CH<sub>2</sub>CH<sub>2</sub>CH), 29.27 (BrCH<sub>2</sub>CH<sub>2</sub>CH<sub>2</sub>CH), 25.08 (Rf<sub>6</sub>CH<sub>2</sub>CHCH<sub>2</sub>Rf<sub>6</sub>).

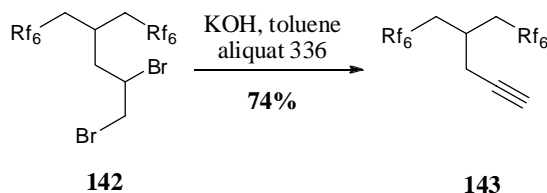
22.3.8 8-(2,3-Dibromopropyl)-1,1,1,2,2,3,3,4,4,5,5,6,6,10,10,11,11,12,12,13,13,14,14,15,15,15-hexacosafuoropentadecane



**<sup>1</sup>H-NMR:** (360 MHz, CDCl<sub>3</sub>): δ 4.07-4.13 (*m*, 1H, BrCH<sub>2</sub>CHBrCH<sub>2</sub>CH), 3.92 (*dd*, 1H, <sup>3</sup>J<sub>HH</sub> = 10.5 Hz, <sup>3</sup>J<sub>HH</sub> = 4.09 Hz, BrCH<sub>2</sub>CHBrCH<sub>2</sub>CH), 3.61 (*t*, 1H, <sup>3</sup>J<sub>HH</sub> = 10.5 Hz, BrCH<sub>2</sub>CHBrCH<sub>2</sub>CH), 2.81-2.86 (*m*, 1H, Rf<sub>6</sub>CH<sub>2</sub>CHCH<sub>2</sub>Rf<sub>6</sub>), 2.42-2.48 (*m*, 2H, BrCH<sub>2</sub>CHBrCH<sub>2</sub>CH), 2.18-2.33 (*m*, 4H, Rf<sub>6</sub>CH<sub>2</sub>CHCH<sub>2</sub>Rf<sub>6</sub>).

**EI-MS:** m/z (% int.): 799.7 ([M-Br]<sup>•+</sup>, 8%), 729.7 ([M-2 x Br]<sup>•+</sup>, 52%), 465.3 ([M-Rf<sub>1.6</sub>]<sup>•+</sup>, 12%), 405.4 (51%), 387.3 ([M-2 x Br-Rf<sub>1.6</sub>]<sup>•+</sup>, 90%), 119.0 (100%).

## 22.3.9 6,6,7,7,8,8,9,9,10,10,11,11,11-Tridecafluoro-4-(2,2,3,3,4,4,5,5,6,6,7,7,7-tridecafluoroheptyl)undec-1-yne



Well pulverized KOH (223 mg, 3.9 mmol) was added into an oven dried Schlenk vessel and heated three times with a heat gun under vacuum. Compound **142** (0.5 g, 0.57 mmol) was degassed separately, dissolved in toluene (5 mL) and added to the KOH. Aliquat 336 (0.2 mL) was syringed in before the mixture was refluxed for 19 hours. The crude product was extracted with ether. All combined organic fractions were then dried over  $\text{Na}_2\text{SO}_4$  and all volatiles were removed. The obtained product was purified by filtration over a silica gel pad using pentane as eluent. After removal of all volatiles alkyne **143** was afforded as colourless oil (300 mg, 74 %).

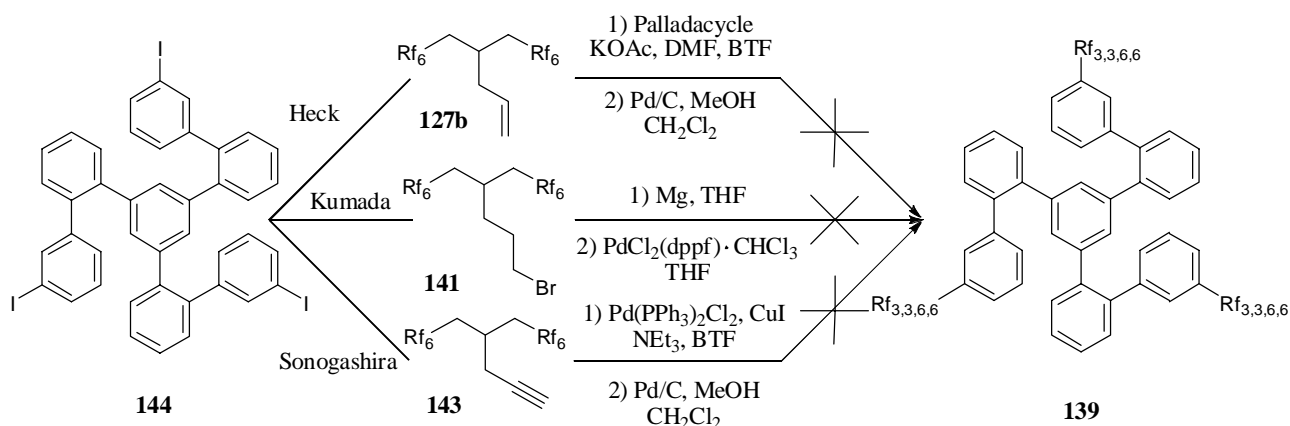
**TLC:**  $R_f = 0.99$  (silica gel, pentane,  $\text{KMnO}_4$ ).

**$^1\text{H-NMR}$ :** (360 MHz,  $\text{CDCl}_3$ ):  $\delta$  2.55-2.61 (*m*, 1H,  $\text{Rf}_6\text{CH}_2\text{CHCH}_2\text{Rf}_6$ ), 2.45-2.46 (*m*, 2H,  $\text{CH}\equiv\text{CCH}_2\text{CH}$ ), 2.05-2.19 (*m*, 4H,  $\text{Rf}_6\text{CH}_2\text{CHCH}_2\text{Rf}_6$ ), 2.02 (*t*, 1H,  $^4J_{\text{HH}} = 1.7$  Hz,  $\text{CH}\equiv\text{CCH}_2\text{CH}$ ).

**$^{13}\text{C-NMR}$ :** (90.55 MHz,  $\text{CDCl}_3$ ):  $\delta$  105.62-118.77 ( $\text{Rf}_6$ ), 92.51 ( $\text{CH}\equiv\text{CCH}_2\text{CH}$ ), 71.97 ( $\text{CH}\equiv\text{CCH}_2\text{CH}$ ), 30.15 (*t*,  $^3J_{\text{CF}} = 21.1$  Hz,  $\text{Rf}_6\text{CH}_2\text{CHCH}_2\text{Rf}_6$ ), 24.39 ( $\text{Rf}_6\text{CH}_2\text{CHCH}_2\text{Rf}_6$ ), 24.24 ( $\text{CH}\equiv\text{CCH}_2\text{CH}$ ).

**EI-MS:**  $m/z$  (% int.): 718.8 ( $\text{M}^+$ , 2 %), 449.5 (13%), 429.4 (11%), 404.4 (27%), 399.4 ( $[\text{M}-\text{Rf}_6]^+$ , 30 %), 385.4 ( $[\text{M}-\text{Rf}_{1,6}]^+$ , 8 %), 69.1 (100%).

## 22.3.10 1,3,5-Tri(3''-{3'''-[6,6,7,7,8,8,9,9,10,10,11,11,11-tridecafluoro-4'''-(2,2,3,3,4,4,5,5,6,6,7,7,7-trideca-fluoroheptyl)undecyl]}-2'-biphenyl)benzene



The Heck cross-coupling was performed following **method M** using **144** (56.3 mg, 61.7  $\mu$ mol), **127b** (0.2 g, 0.28 mmol), Palladacycle (1.7 mg, 1.86  $\mu$ mol), KOAc (23.6 mg, 0.24 mmol), BTF (0.5 mL) and DMF (1 mL). The mixture was refluxed for 3 days before all volatiles of the black mixture were removed. The residue was dissolved in ether and extracted with water and an aqueous sol. of  $\text{NH}_4\text{Cl}$ . The combined organic fractions were dried over  $\text{Na}_2\text{SO}_4$ , reduced and filtered over a plug of silica gel using pentane – ether (19:1) as eluent. The obtained oily substance was only composed of both starting materials **144** and **127b**.

The Kumada cross-coupling was performed like **method I** using **144** (22 mg, 32.5  $\mu$ mol), **141** (150 mg, 0.19 mmol), magnesium turnings (7 mg, 0.28 mmol), PdCl<sub>2</sub>(dppf)·CH<sub>2</sub>Cl<sub>2</sub> (4.6 mg, 5.6  $\mu$ mol) and THF (4 mL). The Grignard solution was refluxed for 1 day whereas the cross-coupling was refluxed for 6 days. The crude mixture was quenched by the addition of methanol (5 mL) before all volatiles were removed. Filtration over a silica gel plug using pentane – ether (19:1) as solvent afforded a colourless oil which did not contain any desired product **139**.

The Sonogashira cross-coupling was reattempted accordingly to **method K** using **144** (170 mg, 0.19 mmol), **143** (1.0 g, 1.4 mmol), PdCl<sub>2</sub>(PPh<sub>3</sub>)<sub>2</sub> (23.45 mg, 33.5 μmol), CuI (10.6 mg, 50.7 μmol), NEt<sub>3</sub> (10 mL) and BTF (10 mL). The reaction mixture was refluxed for 21 hours before the remaining NEt<sub>3</sub> was distilled off the reaction medium under slightly reduced pressure. The crude brown solid was dissolved in ether and washed with 10% HCl and water. The organic phase was then dried over Na<sub>2</sub>SO<sub>4</sub> before all volatiles were removed. The crude obtained product was analyzed by <sup>1</sup>H-NMR revealing the presence of the starting materials only.

Compound **120b** (1.0 g, 1.14 mmol), PdCl<sub>2</sub>(PPh<sub>3</sub>)<sub>2</sub> (40 mg, 57 μmol) and CuI (5 mg, 28.5 μmol) were added in a Schlenk reaction vessel under inert atmosphere. Phenylacetylene **145** (110 mg, 1.14 mmol) and triethylamine (8 mL) were then injected in and the reaction mixture was heated to 65 °C

for 13 hours. The triethylamine was then distilled directly out of the reaction mixture (85°C, 400 mbar). The crude obtained solid was dissolved in ether and washed with 10% HCl and water. The combined organic phases were dried over Na<sub>2</sub>SO<sub>4</sub> and all volatiles were removed. Filtration over a plug of silica gel using pentane – ether 1:1 afforded the desired compound **146** as orange oil. Final purification was then achieved by column chromatography on silica gel using pentane as eluent which afforded compound **146** as colourless oil in moderate yield (350 mg, 34%).

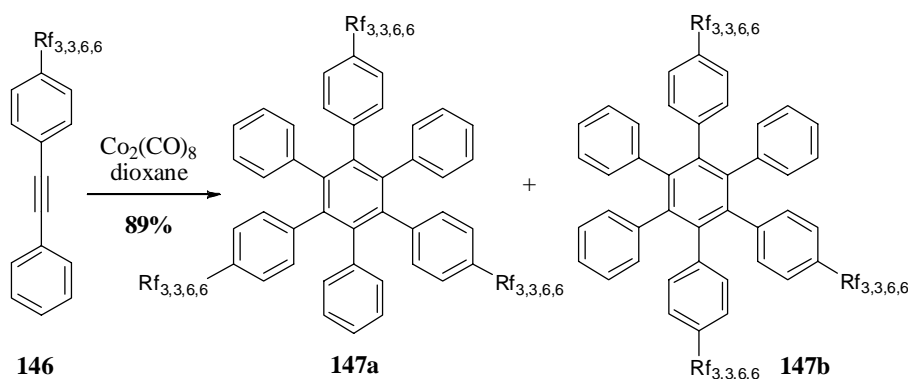
**TLC:** R<sub>f</sub> = 0.53 (silica gel, pentane, KMnO<sub>4</sub>).

**<sup>1</sup>H-NMR:** (360 MHz, CDCl<sub>3</sub>): δ 7.55-7.52 (*m*, 2H, Ph), 7.47 (*d*, 2H, <sup>3</sup>J<sub>HH</sub> = 8.2 Hz, Ph), 7.34-7.37 (*m*, 3H, Ph), 7.17 (*d*, 2H, <sup>3</sup>J<sub>HH</sub> = 8.2 Hz, Ph), 2.66 (*t*, 2H, <sup>3</sup>J<sub>HH</sub> = 6.8 Hz, CH<sub>2</sub>CH<sub>2</sub>CH<sub>2</sub>CH), 2.46 (*septept*, 1H, <sup>3</sup>J<sub>HH</sub> = 5.9 Hz, Rf<sub>6</sub>CH<sub>2</sub>CHCH<sub>2</sub>Rf<sub>6</sub>), 2.11-2.25 (*m*, 4H, Rf<sub>6</sub>CH<sub>2</sub>CHCH<sub>2</sub>Rf<sub>6</sub>), 1.60-1.73 (*m*, 4H, CH<sub>2</sub>CH<sub>2</sub>CH<sub>2</sub>CH).

**<sup>13</sup>C-NMR:** (90.55 MHz, CDCl<sub>3</sub>): δ 141.94 (Ph), 131.69 (Ph), 131.5 (Ph), 128.36 (Ph), 128.32 (Ph), 120.93 (Ph), 89.30 (acetylene), 88.98 (acetylene), 35.53 (CH<sub>2</sub>CH<sub>2</sub>CH<sub>2</sub>CH), 34.33 (CH<sub>2</sub>CH<sub>2</sub>CH<sub>2</sub>CH), 34.21 (*t*, <sup>2</sup>J<sub>CF</sub> = 20.8 Hz, Rf<sub>6</sub>CH<sub>2</sub>CHCH<sub>2</sub>Rf<sub>6</sub>), 27.67 (CH<sub>2</sub>CH<sub>2</sub>CH<sub>2</sub>CH), 25.38 (Rf<sub>6</sub>CH<sub>2</sub>CHCH<sub>2</sub>Rf<sub>6</sub>).

**EI-MS:** m/z (% int.): 898.0 (M<sup>+</sup>, 100 %), 190.8 ([M-Rf<sub>2,3,6,6</sub>]<sup>+</sup>, 33 %).

#### 22.3.12 1,3,5-Tris-[4-(6,6,7,7,8,8,9,9,10,10,11,11,11-tridecafluoro-4-{2,2,3,3,4,4,5,5,6,6,7,7,7-tridecafluoroheptyl}undecyl)phenyl]-2,4,6-trisphenylbenzene



The cyclotrimerization was performed following **method B** using tolane **146** (0.30 g, 0.33 mmol) together with Co<sub>2</sub>(CO)<sub>8</sub> (9.1 mg, 0.1 μmol) and dioxane (50 mL). The mixture was refluxed for 5 days before all volatiles were removed. The crude black product was filtrated over a silica gel plug using ether as eluent. The obtained violet product was purified by column chromatography over silica gel using pentane – ether (49:1) as eluent affording the desired HPB **147a** and **147b** as colourless oil in an inseparable mixture (267 mg, 89%).

compounds **147a** and **b**

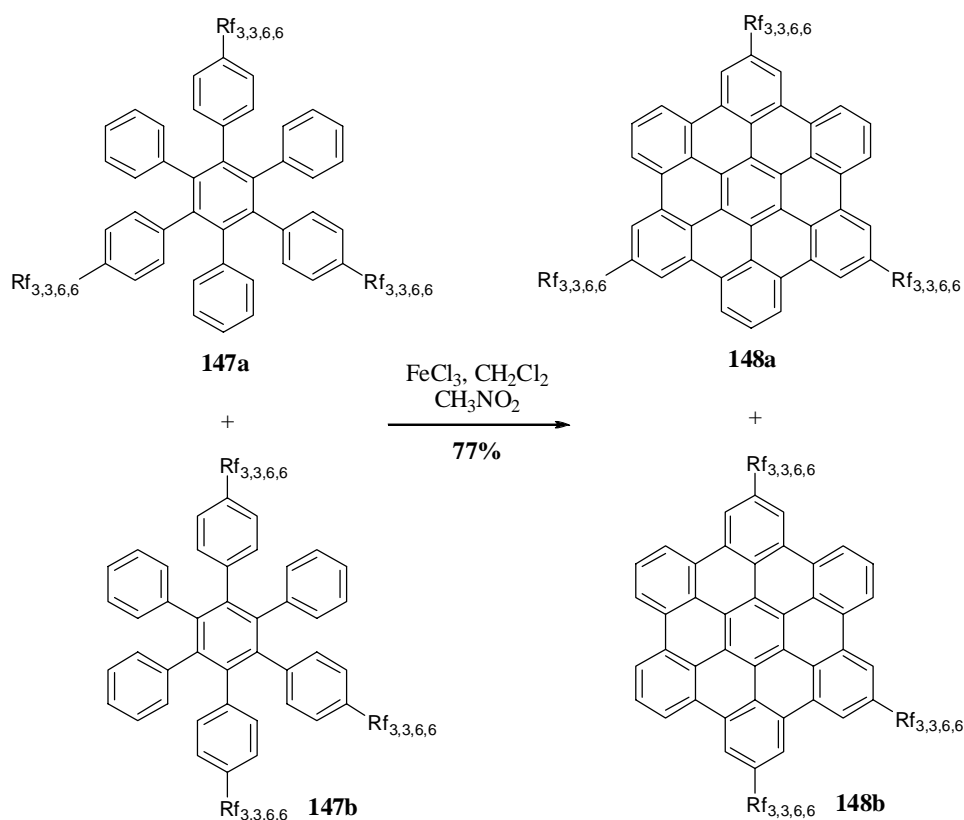
**TLC:** Rf = 0.29 (silica gel, pentane – ether (49:1), KMnO<sub>4</sub>).

**<sup>1</sup>H-NMR:** (500 MHz, CDCl<sub>3</sub>): δ 6.76-6.86 (*m*, 15H, Ph), 6.74-6.72 (*m*, 6H, Ph), 6.65-6.62 (*m*, 6H, Ph), 2.41-2.33 (*m*, 9H, CH<sub>2</sub>CH<sub>2</sub>CH<sub>2</sub>CH), 2.18-2.03 (*m*, 12H, Rf<sub>6</sub>CH<sub>2</sub>CHCH<sub>2</sub>Rf<sub>6</sub>), 1.48-1.42 (*m*, 6H, CH<sub>2</sub>CH<sub>2</sub>CH<sub>2</sub>CH), 1.38-1.27 (*m*, 6H, CH<sub>2</sub>CH<sub>2</sub>CH<sub>2</sub>CH).

**<sup>13</sup>C-NMR:** (125.77 MHz, CDCl<sub>3</sub>): δ 140.90 (Ph), 140.85 (Ph), 140.77 (Ph), 140.74 (Ph), 140.44 (Ph), 140.32 (Ph), 140.25 (Ph), 140.21 (Ph), 140.16 (Ph), 140.12 (Ph), 138.44 (Ph), 138.42 (Ph), 138.35 (Ph), 138.01 (Ph), 137.95 (Ph), 137.93 (Ph), 131.46 (Ph), 131.41 (Ph), 126.59 (Ph), 126.47 (Ph), 126.36 (Ph), 126.33 (Ph), 124.89 (Ph), 124.78 (Ph), 124.73 (Ph), 34.84 (CH<sub>2</sub>CH<sub>2</sub>CH<sub>2</sub>CH), 34.16 (*t*, <sup>2</sup>J<sub>CF</sub> = 20.8 Hz, Rf<sub>6</sub>CH<sub>2</sub>CHCH<sub>2</sub>Rf<sub>6</sub>), 33.86 (CH<sub>2</sub>CH<sub>2</sub>CH<sub>2</sub>CH), 27.36 (CH<sub>2</sub>CH<sub>2</sub>CH<sub>2</sub>CH), 25.33 (Rf<sub>6</sub>CH<sub>2</sub>CHCH<sub>2</sub>Rf<sub>6</sub>).

**MALDI-TOF-MS (DCTB):** m/z (% int.): 2694.3 (M<sup>+</sup>, 100%).

22.3.13 2,8,14-Tris[6,6,7,7,8,8,9,9,10,10,11,11,11-tridecafluoro-4-{2,2,3,3,4,4,5,5,6,6,7,7,7-tridecafluoroheptyl}]hexabenz[bc,ef,hi,kl,no,q]coronene



The synthesis was carried out following **method C** using a mixture of HPB **147a** and **b** (0.1 g, 37 μmol) as precursor together with FeCl<sub>3</sub> (361 mg, 2.2 mmol, 5 eq / H to be removed), CH<sub>2</sub>Cl<sub>2</sub> (10 mL) and CH<sub>3</sub>NO<sub>2</sub> (4 mL). After 6 hours of reaction at 37 °C the mixture was quenched by the addition of methanol (40 mL). The black precipitate was collected by suction filtration over Millipore<sup>®</sup> and was suspended in different common organic solvents (dichloromethane, methanol, ether and



pentane). The formed suspensions were each time treated in an ultrasonic bath for 30 minutes followed by refluxing for 1 h. After 2 h of cooling in the refrigerator the suspensions were filtrated over Millipore® yielding an inseparable mixture of HBC **148a** and **b** as bright yellow powder in fair yield (77 mg, 77%).

**<sup>1</sup>H-NMR:** (360 MHz, CDCl<sub>3</sub>): δ 8.99-8.75 (*m*, 12H, Ph), 8.04-7.93 (*m*, 3H, Ph), 3.48-3.37 (*m*, 6H, CH<sub>2</sub>CH<sub>2</sub>CH<sub>2</sub>CH), 2.90-2.86 (*m*, 3H, CH<sub>2</sub>CH<sub>2</sub>CH<sub>2</sub>CH), 2.64-2.41 (*m*, 12H, Rf<sub>6</sub>CH<sub>2</sub>CHCH<sub>2</sub>Rf), 2.40-2.23 (*m*, 6H, CH<sub>2</sub>CH<sub>2</sub>CH<sub>2</sub>CH), 2.22-2.10 (*m*, 6H, CH<sub>2</sub>CH<sub>2</sub>CH<sub>2</sub>CH).

**MALDI-TOF-MS (DCTB):** *m/z* (% int.): 2681.7 (M<sup>•+</sup>, 100%; calcd. for C<sub>96</sub>H<sub>48</sub>F<sub>78</sub> 2682.25), 5374.6 ([M + **147**]<sup>•+</sup>, 8%).

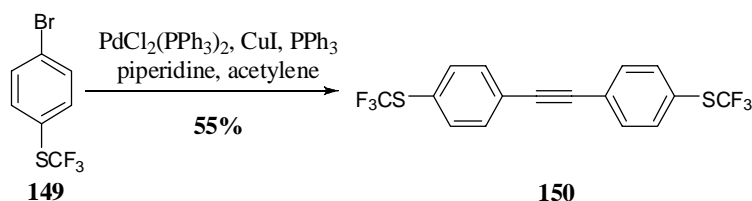
**UV/VIS:** (BTF, 10<sup>-6</sup> M, ε = 2.9 · 10<sup>5</sup>), λ<sub>max</sub> = 343, 357, 387 nm.



## 23 Synthesis of HBC primers

### 23.1 Synthesis of HBC-(SCF<sub>3</sub>)<sub>6</sub>

#### 23.1.1 1-[(Trifluoromethyl)thio]-4-(4-[trifluoromethyl]thio)phenyl)ethynyl)benzene



A 100 ml three necked flask was fitted under inert atmosphere with a reflux condenser and a gas inlet. Compound **149** (2.5 g 9.7 mmol), PdCl<sub>2</sub>(PPh<sub>3</sub>)<sub>2</sub> (140 mg, 0.2 mmol), CuI (60 mg, 0.31 mmol) and PPh<sub>3</sub> (70 mg, 0.26 mmol) were charged in the flask and dissolved in deoxygenated piperidine (32 mL). The reaction mixture was heated to 80 °C and continuously bubbled with acetylene for 6 hours at this temperature. After 6 hours the acetylene addition was stopped and the dark brown reaction mixture was stirred at 80 °C under argon for further 12 hours. The reaction mixture was cooled to room temperature and a saturated solution of NH<sub>4</sub>Cl (50 mL) was added. The resulting mixture was extracted with CH<sub>2</sub>Cl<sub>2</sub> (3 x 100 mL) and the combined organic phases were washed with water (3 x 50 mL). The resulting solution was dried over Na<sub>2</sub>SO<sub>4</sub> and all volatiles were evaporated under reduced pressure yielding a brown oil which was filtrated over a plug of silica gel under reduced pressure using pentane as solvent. Removing the pentane under reduced pressure afforded the desired tolane **150** as white solid in moderate yield (1.0 g, 55 %).

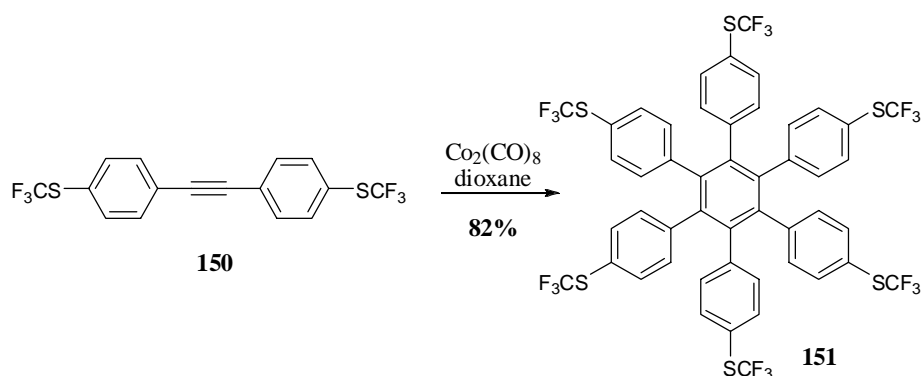
**TLC:** R<sub>f</sub> = 0.57 (silica gel, pentane, KMnO<sub>4</sub>).

**<sup>1</sup>H-NMR:** (360 MHz, CDCl<sub>3</sub>): δ 7.64 (*d*, 4H, <sup>3</sup>J<sub>HH</sub> = 8.2 Hz, Ph), 6.57 (*d*, 4H, <sup>3</sup>J<sub>HH</sub> = 8.2 Hz, Ph).

**<sup>13</sup>C-NMR:** (90.55 MHz, CDCl<sub>3</sub>): δ 136.09 (Ph), 132.51 (Ph), 129.38 (*q*, <sup>1</sup>J<sub>CF</sub> = 308 Hz, SCF<sub>3</sub>), 125.47 (Ph), 125.89 (Ph), 90.52 (acetylene).

**EI-MS:** *m/z* (% int.): 377.95 (M<sup>+</sup>, 87%), 309.10 ([M-CF<sub>3</sub>]<sup>+</sup>, 100%), 240.40 ([M-2 x CF<sub>3</sub>]<sup>+</sup>, 81%), 208.45 ([M-CF<sub>3</sub>-SCF<sub>3</sub>]<sup>+</sup>, 39%).

## 23.1.2 Hexakis{4-[(trifluoromethyl)thio]phenyl}benzene



The synthesis was carried out employing **method B** using tolane **150** (0.9 g, 2.4 mmol) as starting material together with  $\text{Co}_2(\text{CO})_8$  (40.7 mg, 0.12 mmol) in dioxane (45). The mixture was refluxed for 2 days before all volatiles were removed under reduced pressure. The desired trimer **151** was obtained as white powder after several recrystallizations in pentane in good yield (0.74 g, 82 %).

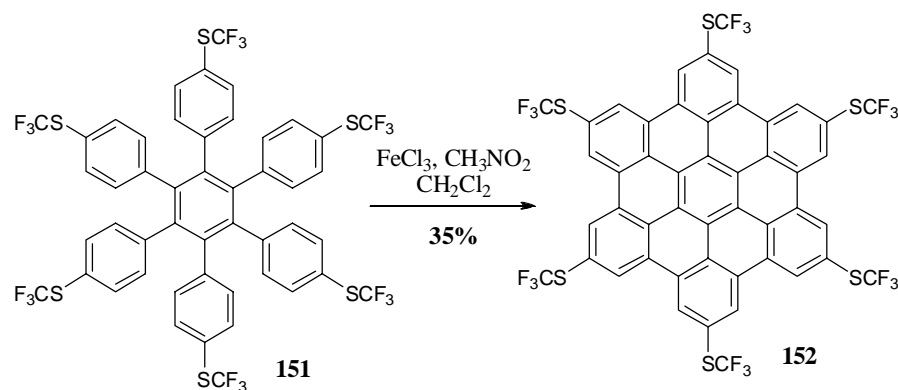
**TLC:**  $R_f = 0.63$  (silica gel, pentane,  $\text{KMnO}_4$ ).

**$^1\text{H-NMR}$ :** (360 MHz,  $\text{CDCl}_3$ ):  $\delta$  7.20 (*d*, 12H,  $^3J_{\text{HH}} = 8.2$  Hz, Ph), 6.83 (*d*, 12H,  $^3J_{\text{HH}} = 8.2$  Hz, Ph).

**$^{13}\text{C-NMR}$ :** (90.55 MHz,  $\text{CDCl}_3$ ):  $\delta$  141.76 (Ph), 139.58 (Ph), 135.18 (Ph), 131.86 (Ph), 129.22 (*q*,  $^1J_{\text{CF}} = 308$  Hz,  $\text{SCF}_3$ ), 122.71 (Ph).

**EI-MS:**  $m/z$  (% int.): 1133.98 ( $\text{M}^+$ , 100%), 932.06 ( $[\text{M}-2 \times \text{SCF}_3]^+$ , 10%), 831.08 ( $[\text{M}-3 \times \text{SCF}_3]^+$ , 8%), 730.12 ( $[\text{M}-4 \times \text{SCF}_3]^+$ , 6%).

## 23.1.3 2,5,8,11,14,17-Hexakis[(trifluoromethyl)thio]hexabenzobc,ef,hi,kl,no,qr]coronene

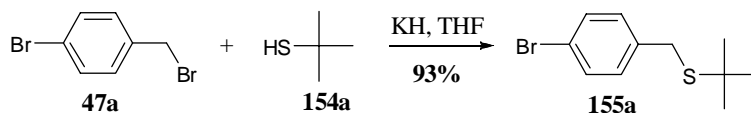


The oxidation of precursor **151** (0.3 g, 0.26 mmol) was carried out following **method C** using  $\text{FeCl}_3$  (2.06 g, 12.7 mmol, 4 eq / H to be removed),  $\text{CH}_3\text{NO}_2$  (35 mL) and  $\text{CH}_2\text{Cl}_2$  (200 mL). The obtained solution was purged with argon for 30 minutes before the iron(III)chloride solution was syringed in portion wise over 6 hours at 45°C. The reaction mixture was stirred at this temperature for 4 days under a continuous purging of argon. Afterwards the reaction mixture was quenched by the addition of methanol (200 ml) and the precipitate was collected by suction filtration over Millipore<sup>®</sup> and was continuously washed with ether, dichloromethane and methanol to afford a dark yellow powder (107 mg, 35%).

**UV/VIS:** (TCB,  $10^{-5}$  M,  $\epsilon = 8.0 \cdot 10^4$ ),  $\lambda_{\text{max}} = 347, 388, 418$  nm.

## 23.2 Synthesis of HBC-(CH<sub>2</sub>S-*t*-butyl)<sub>6</sub>

### 23.2.1 1-Bromo-4-[(*tert*-butylthio)methyl]benzene



#### Method O

KH (2.3 g, 20 mmol, 35% in mineral oil) was added to a Schlenk vessel and suspended in THF (80 mL). Degassed *tert*-butylmercaptan **154a** (2.5 mL, 22.2 mmol) in THF (20 mL) was added slowly at 0°C after which the stirring was continued for 90 minutes. 4-Bromobenzylbromide **47a** (5.0 g, 20 mmol) in THF (20 mL) was syringed onto the KH suspension at 0°C. The mixture was allowed to reach room temperature and was stirred for 16 hours. The resulting green mixture was quenched by the addition of NH<sub>4</sub>Cl (100 mL) and extracted with ether (3 x 50 mL). The combined organic fractions were dried over Na<sub>2</sub>SO<sub>4</sub> and all volatiles were removed. Filtration over a plug of silica gel using pentane – ethyl acetate 99:1 as eluent afforded compound **155a** as colourless oil (5.8 g, 93%).

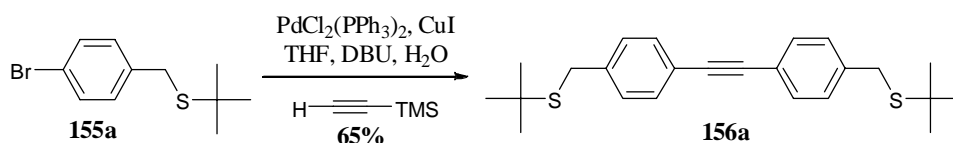
**TLC:** R<sub>f</sub> = 0.48 (silica gel, pentane, KMnO<sub>4</sub>).

**<sup>1</sup>H-NMR:** (360 MHz, CDCl<sub>3</sub>): δ 7.41 (*d*, 2H, <sup>3</sup>J<sub>HH</sub> = 8.6 Hz, Ph), 7.22 (*d*, 2H, <sup>3</sup>J<sub>HH</sub> = 8.6 Hz, Ph), 3.70 (*s*, 2H, CH<sub>2</sub>), 1.33 (*s*, 9H, C(CH<sub>3</sub>)<sub>3</sub>).

**<sup>13</sup>C-NMR:** (90.55 MHz, CDCl<sub>3</sub>): δ 138.17 (Ph), 131.93 (Ph), 131.07 (Ph), 120.97 (Ph), 43.92 (C(CH<sub>3</sub>)<sub>3</sub>), 33.24 (CH<sub>2</sub>), 31.32 (C(CH<sub>3</sub>)<sub>3</sub>).

**EI-MS:** *m/z* (% int.): 258.2 (M<sup>+</sup>, 30%), 202.0 ([M-*t*Bu]<sup>+</sup>, 26%), 169.1 ([M-S*t*Bu]<sup>+</sup>, 53%), 121.0 ([M-*t*Bu-Br]<sup>+</sup>, 11%), 89.0 ([M-S*t*Bu-Br]<sup>+</sup>, 6%), 57.1 ([*t*Bu]<sup>+</sup>, 100%).

### 23.2.2 4-[(*tert*-Butylthio)methyl]-4-({4-[(*tert*-butylthio)methyl]phenyl}ethynyl)-benzene



The tolane formation was achieved using **method A**. Bromoaryl **155a** (1.0 g, 3.8 mmol) was reacted with Pd(PPh<sub>3</sub>)<sub>4</sub> (267 mg, 0.23 mmol), CuI (73 mg, 0.38 mmol), DBU (3.5 mL, 23.0 mmol), TMSA (0.28 mL, 1.9 mmol), H<sub>2</sub>O (30 μL, 1.5 mmol) and THF (20 mL) for 22 hours at 75 °C. The reaction mixture was quenched by the addition of a saturated solution of NH<sub>4</sub>Cl (50 mL). The formed emulsion was extracted with water (50 mL) and HCl 10% (100 mL). The combined organic fractions were dried over Na<sub>2</sub>SO<sub>4</sub> and all volatiles were removed. The brown solid was suspended in pentane and treated in an ultrasonic bath for 15 minutes before being suction filtrated over Millipore<sup>®</sup> yielding tolane **156a** as slightly beige powder (485 mg, 65 %).

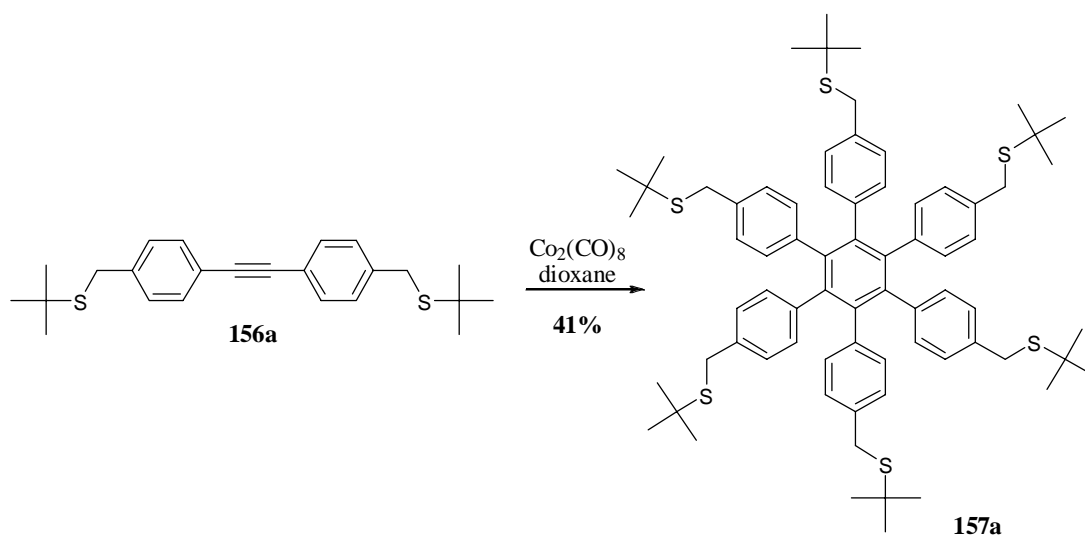
**TLC:**  $R_f = 0.82$  (silica gel, pentane – ether 9:1,  $\text{KMnO}_4$ ).

**$^1\text{H-NMR}$ :** (360 MHz,  $\text{CDCl}_3$ ):  $\delta$  7.45 (*d*, 4H,  $^3J_{\text{HH}} = 8.2$  Hz, Ph), 7.33 (*d*, 4H,  $^3J_{\text{HH}} = 8.2$  Hz, Ph), 3.77 (*s*, 4H,  $\text{CH}_2$ ), 1.35 (*s*, 18H,  $\text{C}(\text{CH}_3)_3$ ).

**$^{13}\text{C-NMR}$ :** (90.55 MHz,  $\text{CDCl}_3$ ):  $\delta$  139.40 (Ph), 132.07 (Ph), 129.41 (Ph), 122.10 (Ph), 89.65 (acetylene), 43.53 ( $\text{C}(\text{CH}_3)_3$ ), 33.81 ( $\text{CH}_2$ ), 31.33 ( $\text{C}(\text{CH}_3)_3$ ).

**EI-MS:**  $m/z$  (% int.): 382.1 ( $\text{M}^{+}$ , 27%), 293.2 ( $[\text{M-S}t\text{Bu}]^{+}$ , 100%), 237.1 ( $[\text{M-S}t\text{Bu-}t\text{Bu}]^{+}$ , 39%), 204.0 ( $[\text{M-2 x S}t\text{Bu}]^{+}$ , 88%).

### 23.2.3 Hexakis[4- $\{(\text{tert-butylthio})\text{methyl}\}$ phenyl]benzene



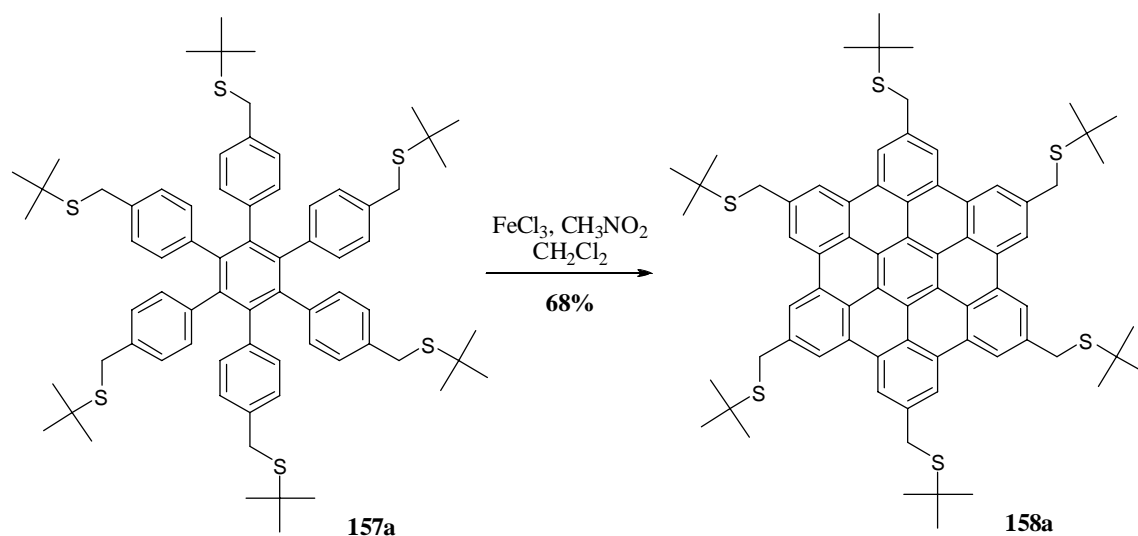
The trimerization of tolane **156a** was carried out according to **method B** using tolane **156a** (0.2 g, 0.52 mmol) as starting material in dioxane (30 mL). The reaction was catalyzed by  $\text{Co}_2(\text{CO})_8$  (10.7 mg, 31.5  $\mu\text{mol}$ ). After 25 hours of reaction all volatiles were removed and the dark brown solid was dissolved in dichloromethane and filtered over a plug of silica gel under reduced pressure. After removal of the eluent the slightly brown solid was suspended in pentane (10 mL), treated in an ultrasonic bath for 20 minutes and suction filtrated over Millipore<sup>®</sup> which yielded the desired HPB **157a** as white solid (82 mg, 41 %).

**TLC:**  $R_f = 0.57$  (silica gel, pentane –  $\text{CH}_2\text{Cl}_2$  7:3,  $\text{KMnO}_4$ ).

**$^1\text{H-NMR}$ :** (360 MHz,  $\text{CDCl}_3$ ):  $\delta$  6.78 (*d*, 12H,  $^3J_{\text{HH}} = 8.3$  Hz, Ph), 6.66 (*d*, 12H,  $^3J_{\text{HH}} = 8.3$  Hz, Ph), 3.49 (*s*, 12H,  $\text{CH}_2$ ), 1.16 (*s*, 54H,  $\text{C}(\text{CH}_3)_3$ ).

**$^{13}\text{C-NMR}$ :** (90.55 MHz,  $\text{CDCl}_3$ ):  $\delta$  140.96 (Ph), 139.92 (Ph), 136.63 (Ph), 132.19 (Ph), 128.16 (Ph), 43.59 ( $\text{C}(\text{CH}_3)_3$ ), 34.24 ( $\text{CH}_2$ ), 31.95 ( $\text{C}(\text{CH}_3)_3$ ).

**MALDI-ICR-MS (DCTB / KCl):**  $m/z$  (% int.): 1185.50 ( $[\text{M}+\text{K}]^{+}$ , 100%).

23.2.4 2,5,8,11,14,17-Hexakis[(*tert*-buthylthio)methyl]hexabenz[bc,ef,hi,kl,no,qr]coronene

The synthesis of HBC **157a** was carried out similarly to **method C**. The hexaphenylbenzene derivative **157a** (50 mg, 43.6  $\mu\text{mol}$ ) was dissolved in dichloromethane (10 mL) and slowly (2 hours) treated with  $\text{FeCl}_3$  (159 mg, 0.98 mmol, 2 eq. / H) in  $\text{CH}_3\text{NO}_2$  (1 mL) at 45°C. The stirring was continued at 45 °C for 3 hours. In addition was the reaction mixture constantly purged with a stream of argon through a Teflon capillary. The warm reaction mixture was quenched under argon by the addition of methanol (10 mL) which provoked the formation of a brownish solid which was collected by suction filtration over Millipore<sup>®</sup>. The obtained solid was repetitively suspended in common organic solvents (methanol, nitromethane, dichloromethane and ether), treated for 15 minutes in an ultrasonic bath and suction filtrated over Millipore<sup>®</sup>, yielding finally the desired HBC **158a** as yellow solid (34 mg, 68 %).

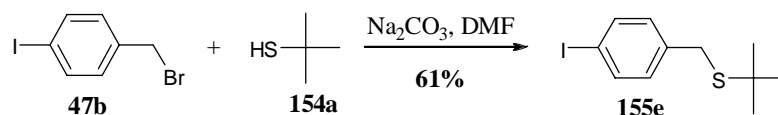
**MALDI-TOF-MS (DCTB):**  $m/z$  (% int.): 607.1 ( $[\text{M}-4 \times \text{CH}_2\text{StBu}]^{*+}$ , 100%).

**UV/VIS:** (toluene,  $10^{-4}$  M,  $\epsilon = 3.2 \cdot 10^3$ ),  $\lambda_{\text{max}} = 353, 386, 429$  nm.



### 23.3 Synthesis of HBC-(CH<sub>2</sub>S-*t*-butyl)<sub>3</sub>

#### 23.3.1 1-Iodo-4-[(*tert*-butylthio)methyl]benzene



The synthesis was performed following **method O** using compound **47b** (5.0 g, 16.84 mmol), **154a** (1.97 g, 21.89 mmol) and Na<sub>2</sub>CO<sub>3</sub> (4.64 g, 43.78 mmol) in DMF. The mixture was stirred for 3 hours at room temperature before sat. NH<sub>4</sub>Cl (5 mL) was added to quench the reaction which was extracted with ether (3 x 50 mL). The combined organic fractions were dried over Na<sub>2</sub>SO<sub>4</sub> and all volatiles were removed. Filtration over a plug of silica gel under reduced pressure using pentane – ethyl acetate 99:1 as eluent afforded the desired compound **155e** as colourless oil (3.14 g, 61%).

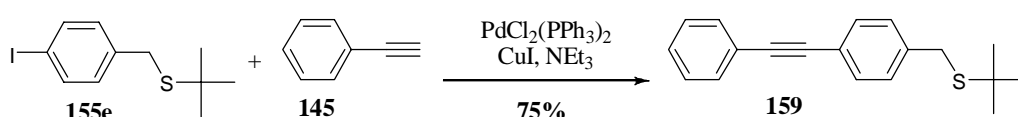
**TLC:** R<sub>f</sub> = 0.68 (silica gel, pentane, KMnO<sub>4</sub>).

**<sup>1</sup>H-NMR:** (360 MHz, CDCl<sub>3</sub>): δ 7.61 (*d*, 2H, <sup>3</sup>J<sub>HH</sub> = 8.2 Hz, Ph), 7.10 (*d*, 2H, <sup>3</sup>J<sub>HH</sub> = 8.2 Hz, Ph), 3.69 (*s*, 2H, CH<sub>2</sub>), 1.34 (*s*, 9H, C(CH<sub>3</sub>)<sub>3</sub>).

**<sup>13</sup>C-NMR:** (90.55 MHz, CDCl<sub>3</sub>): δ 138.40 (Ph), 137.46 (Ph), 130.92 (Ph), 91.97 (Ph), 43.05 (C(CH<sub>3</sub>)<sub>3</sub>), 32.89 (CH<sub>2</sub>), 30.87 (C(CH<sub>3</sub>)<sub>3</sub>).

**EI-MS:** *m/z* (% int.): 306.2 (M<sup>+</sup>, 22%), 250.1 ([M-*t*Bu]<sup>+</sup>, 43%), 217.1 ([M-S-*t*Bu]<sup>+</sup>, 47%), 57.1 ([*t*Bu]<sup>+</sup>, 100%).

#### 23.3.2 *Tert*-butyl 4-(phenylethynyl)benzyl sulfide



The transformation was carried out accordingly to **method N** using iodoaryl **155e** (1.0 g, 3.3 mmol), PdCl<sub>2</sub>(PPh<sub>3</sub>)<sub>2</sub> (115 mg, 0.16 mmol), CuI (15.5 mg, 81.6 μmol) and NEt<sub>3</sub> (35 mL). The reaction mixture was stirred at room temperature for 24 hours before the triethylamine was distilled out under slightly reduced pressure at 70 °C. The resulting dark solid was dissolved in ether and extracted with water and 10% HCl. The combined organic fractions were dried over Na<sub>2</sub>SO<sub>4</sub> and reduced under vacuum. Column chromatography on silica gel, using pentane – ether (1:19) as eluent, afforded the desired tolane **159** as beige solid (690 mg, 75%).

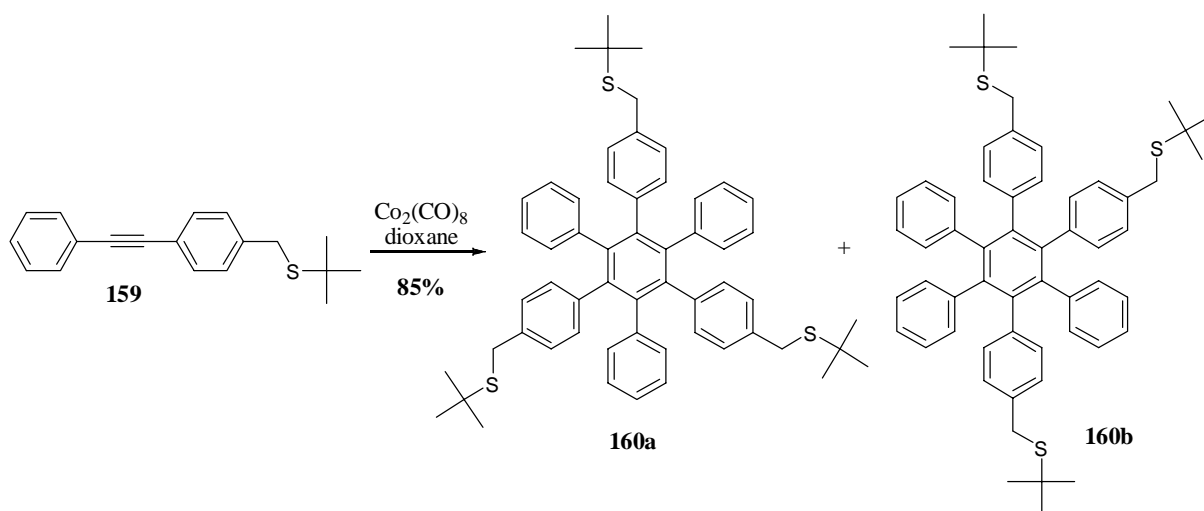
**TLC:** R<sub>f</sub> = 0.39 (silica gel, pentane, KMnO<sub>4</sub>).

**<sup>1</sup>H-NMR:** (360 MHz, CDCl<sub>3</sub>): δ 7.55-7.52 (*m*, 2H, Ph), 7.48 (*d*, 2H, <sup>3</sup>J<sub>HH</sub> = 8.2 Hz, Ph), 7.35 (*d*, 2H, <sup>3</sup>J<sub>HH</sub> = 8.2 Hz, Ph), 7.36-7.34 (*m*, 3H, Ph), 3.78 (*s*, 2H, CH<sub>2</sub>), 1.36 (*s*, 9H, C(CH<sub>3</sub>)<sub>3</sub>).

**<sup>13</sup>C-NMR:** (90.55 MHz, CDCl<sub>3</sub>): δ 139.07 (Ph), 131.68 (Ph), 131.57 (Ph), 128.99 (Ph), 128.32 (Ph), 128.19 (Ph), 123.28 (Ph), 121.63 (Ph), 89.28 (acetylene), 43.05 (C(CH<sub>3</sub>)<sub>3</sub>), 33.35 (CH<sub>2</sub>), 30.91 (C(CH<sub>3</sub>)<sub>3</sub>).

**EI-MS:** m/z (% int.): 280.3 (M<sup>•+</sup>, 33%), 191.2 ([M-S-*t*Bu]<sup>•+</sup>, 100%).

### 23.3.3 1,3,5-Tris-[4-{( *tert*-butylthio)methyl}phenyl]-2,4,6-trisphenylbenzene



The cyclotrimerisation was performed similar to **method B** using tolane **159** (0.3 g, 1.07 mmol),  $\text{Co}_2(\text{CO})_8$  (29.2 mg, 85.5  $\mu\text{mol}$ ) and dioxane (50 mL). The dark mixture was refluxed for 2 days before all volatiles were removed yielding a brown oil which was purified by column chromatography over silica gel using pentane – ether (49:1) as eluent. The desired HPB derivative **160a** was afforded as slightly beige solid together with its isomer **160b** in an inseparable one to one mixture (256 mg, 85%)

#### Compound **160a**

**TLC:** R<sub>f</sub> = 0.89 (silica gel, pentane – ether (49:1), KMnO<sub>4</sub>).

**<sup>1</sup>H-NMR:** (360 MHz, CDCl<sub>3</sub>): δ 6.87-6.83 (*m*, 6H, Ph), 6.83-6.79 (*m*, 15H, Ph), 6.75-6.73 (*m*, 6H, Ph), 3.54 (*s*, 6H, CH<sub>2</sub>), 1.19 (*s*, 27H, C(CH<sub>3</sub>)<sub>3</sub>).

**<sup>13</sup>C-NMR:** (90.55 MHz, CDCl<sub>3</sub>): δ 140.53 (Ph), 140.46 (Ph), 140.06 (Ph), 139.06 (Ph), 135.8 (Ph), 131.33 (Ph), 127.24 (Ph), 126.54 (Ph), 125.09 (Ph), 42.67 (C(CH<sub>3</sub>)<sub>3</sub>), 33.37 (CH<sub>2</sub>), 31.05 (C(CH<sub>3</sub>)<sub>3</sub>).

**EI-MS:** m/z (% int.): 841.3 ([M+H]<sup>•+</sup>, 84%), 751.0 ([M-S-*t*Bu]<sup>•+</sup>, 100%), 671.1 (57%), 605 (34%), 527.8 (25%).

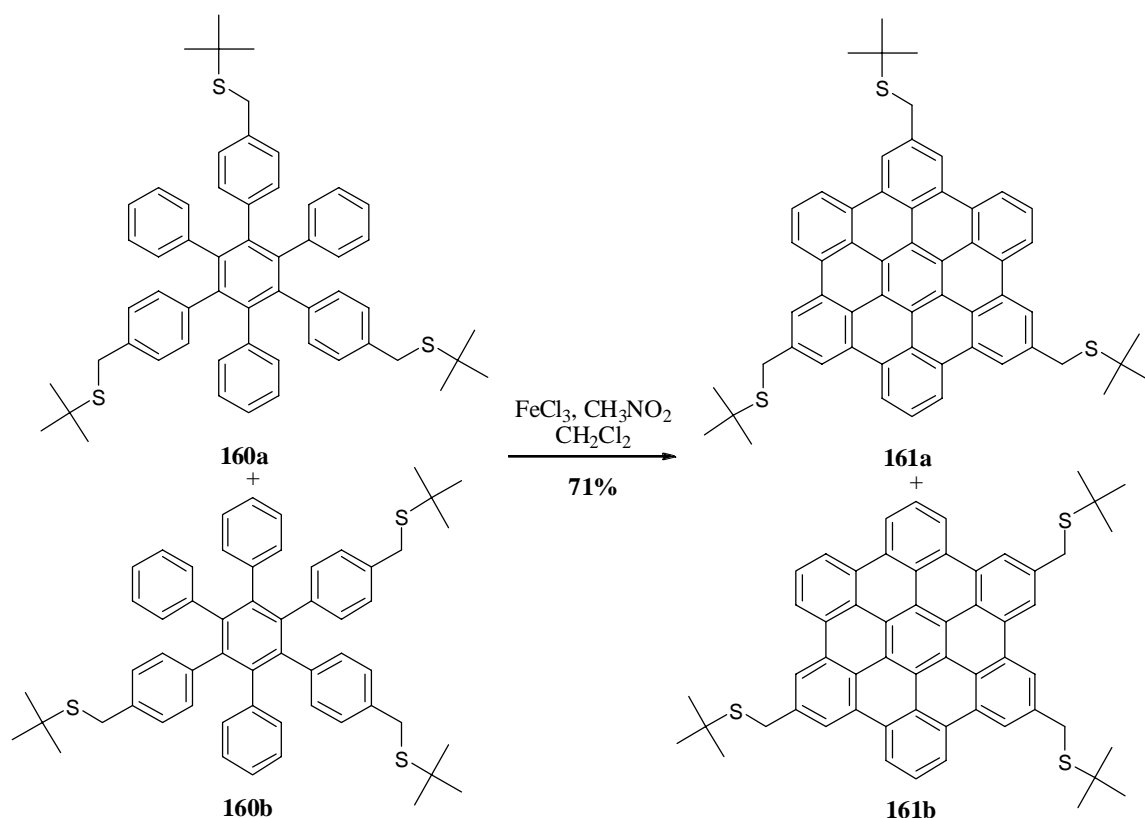
Compound **160b**

**TLC:** R<sub>f</sub> = 0.89 (silica gel, pentane – ether (49:1), KMnO<sub>4</sub>).

**<sup>1</sup>H-NMR:** (360 MHz, CDCl<sub>3</sub>): δ 6.87-6.83 (*m*, 6H, Ph), 6.83-6.79 (*m*, 15H, Ph), 6.75-6.73 (*m*, 6H, Ph), 3.54 (*s*, 6H, CH<sub>2</sub>), 1.19 (*s*, 27H, C(CH<sub>3</sub>)<sub>3</sub>).

**<sup>13</sup>C-NMR:** (90.55 MHz, CDCl<sub>3</sub>): δ 140.37 (Ph), 140.30 (Ph), 139.98 (Ph), 139.11 (Ph), 135.80 (Ph), 131.33 (Ph), 127.20 (Ph), 126.59 (Ph), 125.09 (Ph), 42.67 (C(CH<sub>3</sub>)<sub>3</sub>), 33.37 (CH<sub>2</sub>), 31.05 (C(CH<sub>3</sub>)<sub>3</sub>).

**EI-MS:** m/z (% int.): 841.3 ([M+H]<sup>+</sup>, 84%), 751.0 ([M-S-*t*Bu]<sup>+</sup>, 100%), 671.1 (57%), 605 (34%), 527.8 (25%).

23.3.4 2,8,14-Tris[(*tert*-buthylthio)methyl]hexabenzob[bc,ef,hi,kl,no,q]coronene

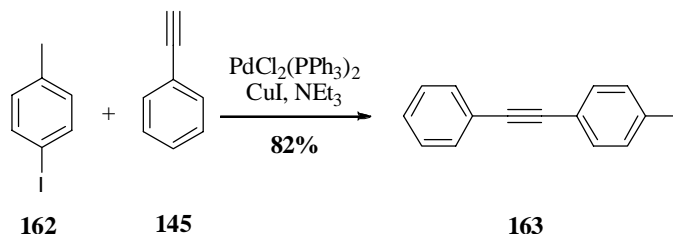
The oxidation was performed following **method C** using a mixture of **160a** and **b** (0.1 g, 0.12 mmol), FeCl<sub>3</sub> (1.7 g, 10.7 mmol, 7.5 eq. / H), CH<sub>3</sub>NO<sub>2</sub> (8 mL) and CH<sub>2</sub>Cl<sub>2</sub> (20 mL). The mixture was heated to 37°C for 3 hours under constant purging of argon. After this methanol (30 mL) was added to the warm mixture. The brown precipitate was collected by suction filtration over Millipore<sup>®</sup> and was purified by treatment in methanol, ether and dichloromethane, sonication and Millipore<sup>®</sup> filtration affording HBC **161** as slightly brown isomeric mixture of **161a** and **b** (71 mg, 71%).

**MALDI-TOF-MS (DCTB):** m/z (% int.): 829.0 (M<sup>+</sup>, 100%; calcd. for C<sub>57</sub>H<sub>49</sub>S<sub>3</sub> 829.29).

**UV/VIS:** (toluene, 10<sup>-4</sup> M, ε = 4.6 · 10<sup>3</sup>), λ<sub>max</sub> = 387, 450 nm.

23.4 Synthesis of HBC-(CH<sub>2</sub>S-*t*-butyl)<sub>1</sub>

## 23.4.1 1-Methyl-4-(phenylethynyl)benzene



The synthesis was carried out accordingly to **method N** using 4-iodotoluene **162** (1 g, 4.58 mmol), phenylacetylene (**145**, 0.47 g, 4.58 mmol), PdCl<sub>2</sub>(PPh<sub>3</sub>)<sub>2</sub> (160 mg, 0.23 mmol), CuI (21 mg, 0.11 mmol) and NEt<sub>3</sub> (35 mL) as reagents. The mixture was stirred at room temperature for one night before NEt<sub>3</sub> was removed by distillation at 70°C under slightly reduced pressure (400 mbar). The resulting solid was dissolved in ether and washed with 10% HCl. The organic phase was dried over Na<sub>2</sub>SO<sub>4</sub> and reduced maximally affording a brown solid which was dissolved in pentane and filtrated over a plug of silica gel. Removal of all volatiles yielded tolane **163** as slightly yellow solid (0.72 g, 82%)

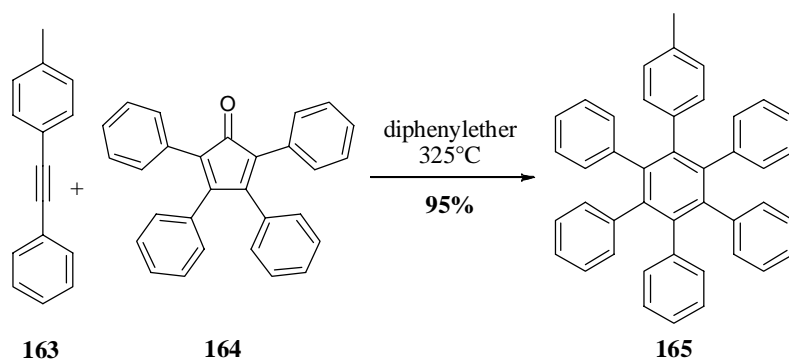
**TLC:** R<sub>f</sub> = 0.95 (silica gel, pentane – ether (9:1), KMnO<sub>4</sub>).

**<sup>1</sup>H-NMR:** (360 MHz, CDCl<sub>3</sub>): δ 7.55-7.53 (*m*, 2H, Ph), 7.45 (*d*, 2H, <sup>3</sup>J<sub>HH</sub> = 8.2 Hz, Ph), 7.38-7.33 (*m*, 3H, Ph), 7.17 (*d*, 2H, <sup>3</sup>J<sub>HH</sub> = 8.2 Hz, Ph), 2.39 (*s*, 3H, CH<sub>3</sub>).

**<sup>13</sup>C-NMR:** (90.55 MHz, CDCl<sub>3</sub>): δ 138.37 (Ph), 131.52 (Ph), 131.48 (Ph), 129.10 (Ph), 128.30 (Ph), 128.05 (Ph), 123.43 (Ph), 120.14 (Ph), 89.52 (acetylene), 88.69 (acetylene), 21.50 (CH<sub>3</sub>).

**EI-MS:** *m/z* (% int.): 192.0 (M<sup>•+</sup>, 100%), 165.1 (18%).

## 23.4.2 1-(4-Methylhexaphenyl)-2,3,4,5,6-pentakisphenylbenzene



Tolane **163** (0.3 g, 1.56 mmol) and tetraphenylcyclopentadienone **164** (0.6 g, 1.56 mmol) was dissolved in diphenylether (5 mL) in a sealed Schlenk tube which was afterwards heated at 325 °C for

3 days in a graphite bath. After cooling to room temperature the diphenylether was removed by distillation (180 °C, 50 mbar). The remaining solid was dissolved in  $\text{CH}_2\text{Cl}_2$  and crystallized by the addition of ethanol. The crystallization was repeated twice which afforded **165** as beige crystals in high yield (810 mg, 95%).

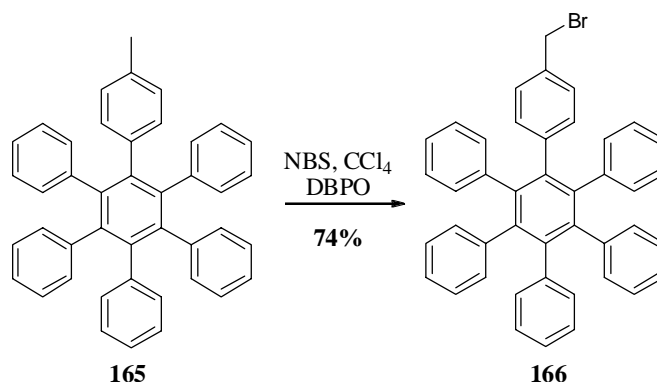
**TLC:**  $R_f = 0.71$  (silica gel, pentane – ether (9:1),  $\text{KMnO}_4$ ).

**$^1\text{H}$ -NMR:** (360 MHz,  $\text{CDCl}_3$ ):  $\delta$  6.86–6.85 (*m*, 25H, Ph), 6.71 (*d*, 2H,  $^3J_{\text{HH}} = 7.7$  Hz, Ph), 6.66 (*d*, 2H,  $^3J_{\text{HH}} = 7.7$  Hz, Ph), 2.09 (*s*, 3H,  $\text{CH}_3$ ).

**$^{13}\text{C}$ -NMR:** (90.55 MHz,  $\text{CDCl}_3$ ):  $\delta$  140.73 (Ph), 140.67 (Ph), 140.37 (Ph), 140.26 (Ph), 137.41 (Ph), 134.42 (Ph), 131.40 (Ph), 131.21 (Ph), 127.27 (Ph), 126.52 (Ph), 125.09 (Ph), 125.03 (Ph), 21.01 ( $\text{CH}_3$ ).

**EI-MS:**  $m/z$  (% int.): 548.2 ( $\text{M}^{+\bullet}$ , 100%).

#### 23.4.3 1-(4-Bromomethylphenyl)-2,3,4,5,6-pentakisphenylbenzene



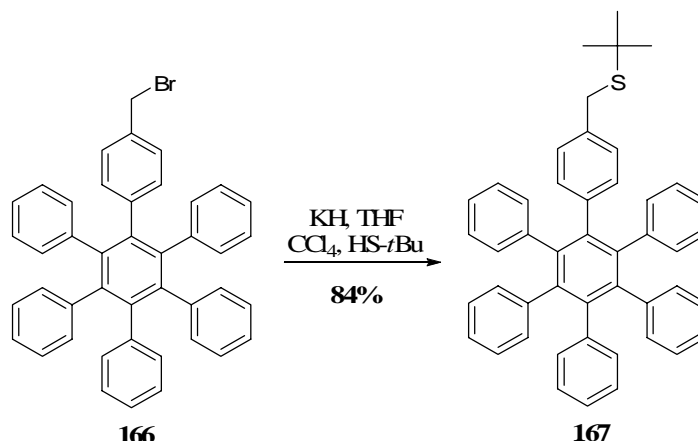
Hexaphenylbenzene **165** (0.5 g, 0.91 mmol), NBS (178 mg, 1.0 mmol) and DBPO (7.7 mg, 3.2  $\mu\text{mol}$ ) were dissolved in  $\text{CCl}_4$  (20 mL) and refluxed for one night before all volatiles were removed under reduced pressure. The obtained brown solid was dissolved in  $\text{CH}_2\text{Cl}_2$  and precipitated by the addition of ethanol which afforded **166** as slightly yellow solid (416 mg, 74%).

**TLC:**  $R_f = 0.57$  (silica gel, pentane – ether (9:1),  $\text{KMnO}_4$ ).

**$^1\text{H}$ -NMR:** (360 MHz,  $\text{CDCl}_3$ ):  $\delta$  6.90–6.78 (*m*, 29H, Ph), 4.27 (*s*, 2H,  $\text{CH}_2\text{Br}$ ).

**$^{13}\text{C}$ -NMR:** (90.55 MHz,  $\text{CDCl}_3$ ):  $\delta$  140.99 (Ph), 140.46 (Ph), 140.35 (Ph), 140.22 (Ph), 134.50 (Ph), 131.72 (Ph), 131.36 (Ph), 127.36 (Ph), 126.65 (Ph), 126.57 (Ph), 125.29 (Ph), 125.21 (Ph), 33.77 ( $\text{CH}_2\text{Br}$ ).

**EI-MS:**  $m/z$  (% int.): 628.3 ( $\text{M}^{+\bullet}$ , 96%), 547.3 ( $[\text{M}-\text{Br}]^{+\bullet}$ , 100%).

23.4.4 1-(4-[(*tert*-Butylthio)methylphenyl]-2,3,4,5,6-pentakisphenylbenzene

The transformation was performed following **method O** using **166** (0.3 g, 0.48 mmol), *tert*-butylmercaptan (0.06 ml, 0.52 mmol), KH (55 mg, 0.48 mmol) dissolved in a mixture of THF (10 mL) and CCl<sub>4</sub> (5 mL). After one night of reaction the mixture was quenched by the addition of a sat. solution of NH<sub>4</sub>Cl. The crude product was then extracted with ether, dried over Na<sub>2</sub>SO<sub>4</sub> and all volatiles were removed. Recrystallization from CH<sub>2</sub>Cl<sub>2</sub> – pentane – ethanol afforded **167** as slightly yellow crystals (255 mg, 84 %).

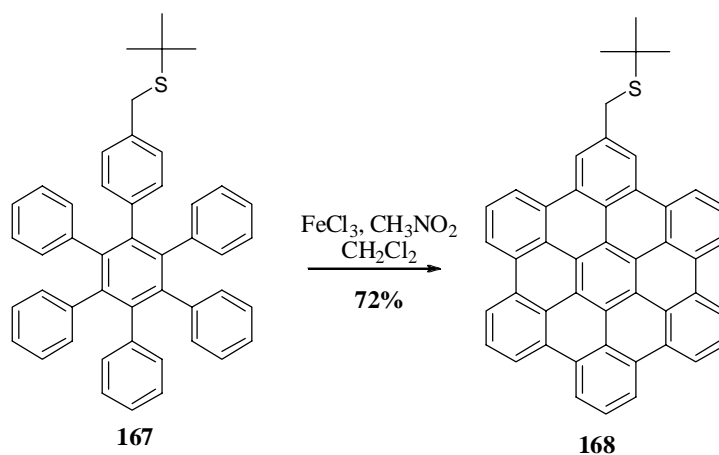
**TLC:** R<sub>f</sub> = 0.51 (silica gel, pentane – ether (9:1), KMnO<sub>4</sub>).

**<sup>1</sup>H-NMR:** (360 MHz, CDCl<sub>3</sub>): δ 6.88-6.83 (*m*, 27H, Ph), 6.76 (*d*, 2H, <sup>3</sup>J<sub>HH</sub> = 8.2 Hz, Ph), 3.54 (*s*, 2H, CH<sub>2</sub>), 1.17 (*s*, 9H, C(CH<sub>3</sub>)<sub>3</sub>).

**<sup>13</sup>C-NMR:** (90.55 MHz, CDCl<sub>3</sub>): δ 140.59 (Ph), 140.52 (Ph), 140.33 (Ph), 140.24 (Ph), 139.09 (Ph), 139.03 (Ph), 135.84 (Ph), 131.38 (Ph), 127.24 (Ph), 126.82 (Ph), 126.57 (Ph), 125.14 (Ph), 42.63 (C(CH<sub>3</sub>)<sub>3</sub>), 33.38 (CH<sub>2</sub>), 31.04 (C(CH<sub>3</sub>)<sub>3</sub>).

**EI-MS:** m/z (% int.): 636.3 ([M]<sup>+</sup>, 78%), 580.3 ([M-*t*Bu]<sup>+</sup>, 87%), 547.3 ([M-S-*t*Bu]<sup>+</sup>, 100%).

## 23.4.5 2-[(tert-butylthio)methyl]hexabenzob[bc,ef,hi,kl,no,q]coronene



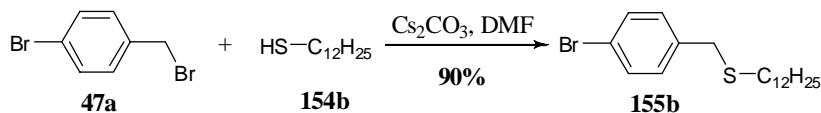
The oxidation was performed using **method C** together with HPB **167** (0.1 g, 0.16 mmol),  $\text{FeCl}_3$  (2.3 g, 14 mmol 7.5 eq. / H),  $\text{CH}_3\text{NO}_2$  (8 mL),  $\text{CH}_2\text{Cl}_2$  (20 mL). The reaction mixture was stirred for 6 hours under a constant bubbling of argon before methanol was added to quench the reaction. Suction filtration over Millipore<sup>®</sup> afforded the crude HBC as black powder. Treatment in toluene, ether, THF and TCB afforded finally HBC **168** as brown solid (72 mg, 72%).

**MALDI-TOF-MS (DCTB):**  $m/z$  (% int.): 625.1 ( $[\text{M}+\text{H}]^{*+}$ , 1%; calcd. for  $\text{C}_{47}\text{H}_{29}\text{S}$  625.20), 607.1 (100%).

**UV/VIS:** (toluene,  $10^{-4}$  M,  $\epsilon = 6.2 \cdot 10^3$ ),  $\lambda_{\text{max}} = 344, 361, 392, 420$  nm.

23.5 Synthesis of HBC-(CH<sub>2</sub>S-dodecyl)<sub>6</sub>

## 23.5.1 1-Bromo-4-[(dodecylthio)methyl]benzene



4-Bromobenzyl bromide **47a** (2.5 g, 10.0 mmol) and Cs<sub>2</sub>CO<sub>3</sub> (8.5 g, 26 mmol) were added to a round bottomed flask and suspended in DMF (20 mL). The formed suspension was cooled to 0°C in an ice-water bath before the thiol **154b** (3.1 mL, 13 mmol) was syringed in. The reaction mixture was allowed to reach room temperature and the stirring was continued for 3 hours. A sat. solution of NH<sub>4</sub>Cl (20 mL) was added and the formed emulsion was extracted three times with pentane (50 mL). The combined organic phases were dried over Na<sub>2</sub>SO<sub>4</sub> and all volatiles were removed under reduced pressure. Filtration over a plug of silica gel under reduced pressure using pentane as eluent afforded after removal of the solvent the desired compound **155b** as colourless oil (3.3 g, 90%).

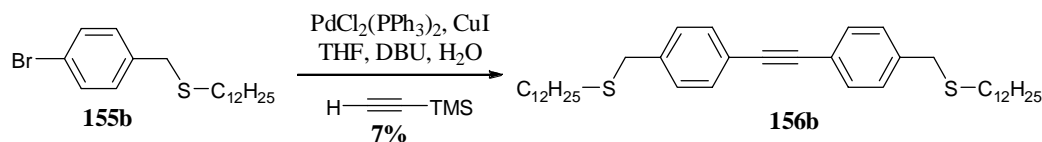
**TLC:** R<sub>f</sub> = 0.68 (silica gel, pentane, KMnO<sub>4</sub>).

**<sup>1</sup>H-NMR:** (360 MHz, CDCl<sub>3</sub>): δ 7.42 (*d*, 2H, <sup>3</sup>J<sub>HH</sub> = 8.2 Hz, Ph), 7.19 (*d*, 2H, <sup>3</sup>J<sub>HH</sub> = 8.2 Hz, Ph), 3.64 (*s*, 2H, Ph-CH<sub>2</sub>), 2.38 (*t*, 2H, <sup>3</sup>J<sub>HH</sub> = 7.5 Hz, CH<sub>2</sub>(CH<sub>2</sub>)<sub>10</sub>CH<sub>3</sub>), 1.53 (*quint*, 2H, <sup>3</sup>J<sub>HH</sub> = 6.8 Hz, (CH<sub>2</sub>)<sub>10</sub>CH<sub>2</sub>CH<sub>3</sub>), 1.25 (*br. s*, 18H, CH<sub>2</sub>-(CH<sub>2</sub>)<sub>9</sub>-CH<sub>2</sub>CH<sub>3</sub>), 0.88 (*t*, 2H, <sup>3</sup>J<sub>HH</sub> = 6.8 Hz, (CH<sub>2</sub>)<sub>11</sub>CH<sub>3</sub>).

**<sup>13</sup>C-NMR:** (90.55 MHz, CDCl<sub>3</sub>): δ 138.17 (Ph), 131.93 (Ph), 130.92 (Ph), 121.07 (Ph), 36.07 (Ph-CH<sub>2</sub>), 32.33 (CH<sub>2</sub>(CH<sub>2</sub>)<sub>10</sub>CH<sub>3</sub>), 31.78 ((CH<sub>2</sub>)<sub>9</sub>CH<sub>2</sub>CH<sub>2</sub>CH<sub>3</sub>), 30.07-29.26 (8C, CH<sub>2</sub>(CH<sub>2</sub>)<sub>8</sub>CH<sub>2</sub>CH<sub>2</sub>CH<sub>3</sub>), 23.11 ((CH<sub>2</sub>)<sub>10</sub>CH<sub>2</sub>CH<sub>3</sub>), 14.54 ((CH<sub>2</sub>)<sub>11</sub>CH<sub>3</sub>).

**EI-MS:** *m/z* (% int.): 372.5 (M<sup>+</sup>, 4%), 201.1 ([M-(CH<sub>2</sub>)<sub>11</sub>CH<sub>3</sub>]<sup>+</sup>, 90%), 170.8 ([M-S(CH<sub>2</sub>)<sub>11</sub>CH<sub>3</sub>]<sup>+</sup>, 100%).

## 23.5.2 4-[(dodecylthio)methyl]-4-({4-[(dodecylthio)methyl]phenyl}-ethynyl)benzene



The tolane formation was performed following **method A** using bromoaryl **155b** (3.0 g, 8.1 mmol), PdCl<sub>2</sub>(PPh<sub>3</sub>)<sub>2</sub> (560 mg, 0.48 mmol), CuI (153 mg, 0.81 mmol), THF (40 mL), DBU (7.2 mL, 48.0 mmol), H<sub>2</sub>O (60 μL, 4.9 mmol) and TMSA (0.7 mL, 4.9 mmol) as reagents. The mixture was stirred at 80 °C for 2 days before a cooling to room temperature was allowed. The extraction of the crude mixture with ether (3 x 100 mL) followed a washing of the organic fraction with water (100 mL) and 10% HCl (50 mL) and a drying over Na<sub>2</sub>SO<sub>4</sub>. After removal of all volatiles under reduced pres-



sure, the product was dissolved in ether – pentane 1:1 and filtrated over a plug of silica gel. The obtained yellow powder was further purified by column chromatography using pentane – dichloromethane 4:1 as eluents. Combining of all product fractions yielded after removal of all volatiles the desired tolane **156b** in very poor yield as white solid (174 mg, 7%).

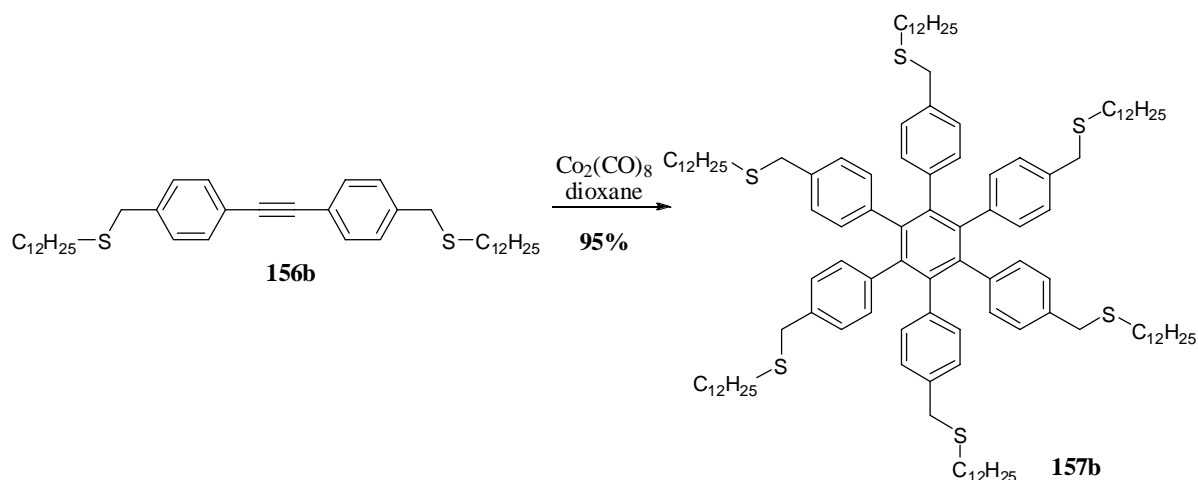
**TLC:**  $R_f$  = 0.68 (silica gel, pentane – dichloromethane 4:1,  $\text{KMnO}_4$ ).

**$^1\text{H-NMR}$ :** (360 MHz,  $\text{CDCl}_3$ ):  $\delta$  7.47 (*d*, 4H,  $^3J_{\text{HH}}$  = 8.2 Hz, Ph), 7.29 (*d*, 4H,  $^3J_{\text{HH}}$  = 8.2 Hz, Ph), 3.70 (*s*, 4H, Ph- $\text{CH}_2$ ), 2.39 (*t*, 4H,  $^3J_{\text{HH}}$  = 7.3 Hz,  $\text{CH}_2(\text{CH}_2)_{10}\text{CH}_3$ ), 1.54 (*tt*, 4H,  $^3J_{\text{HH}}$  = 7.3 Hz,  $^3J_{\text{HH}}$  = 6.8 Hz,  $(\text{CH}_2)_{10}\text{CH}_2\text{CH}_3$ ), 1.25 (*s*, 36H,  $\text{CH}_2-(\text{CH}_2)_9-\text{CH}_2\text{CH}_3$ ), 0.88 (*t*, 4H,  $^3J_{\text{HH}}$  = 6.8 Hz,  $(\text{CH}_2)_{11}\text{CH}_3$ ).

**$^{13}\text{C-NMR}$ :** (90.55 MHz,  $\text{CDCl}_3$ ):  $\delta$  139.01 (Ph), 131.64 (Ph), 128.86 (Ph), 121.75 (Ph), 89.25 (acetylene), 36.11 (Ph- $\text{CH}_2$ ), 31.91 ( $\text{CH}_2(\text{CH}_2)_{10}\text{CH}_3$ ), 31.33 ( $(\text{CH}_2)_9\text{CH}_2\text{CH}_2\text{CH}_3$ ), 29.64-28.85 (16C,  $\text{CH}_2(\text{CH}_2)_8\text{CH}_2\text{CH}_2\text{CH}_3$ ), 22.68 ( $(\text{CH}_2)_{10}\text{CH}_2\text{CH}_3$ ), 14.11 ( $(\text{CH}_2)_{11}\text{CH}_3$ ).

**MALDI-ICR-MS (DCTB / AgCl):**  $m/z$  (% int.): 715.33 ( $[\text{M}+\text{Ag}]^{++}$ , 50%), 667.35 (100%), 649.08 (55%), 633.09 (35%).

### 23.5.3 Hexakis[4-[(dodecylthio)methyl]phenyl]benzene



The tolane trimerization was performed following **method B** using tolane **156b** (150 mg, 0.25 mmol),  $\text{Co}_2(\text{CO})_8$  (6.8 mg, 20  $\mu\text{mol}$ ) and dioxane (25 mL) as precursors. The mixture was refluxed for 19 hours before all volatiles were removed. Filtration over a plug of silica gel using pentane – ether 4:1 as eluent afforded the title HPB derivative **157b** as slightly brown oil in excellent yield (143 mg, 95%).

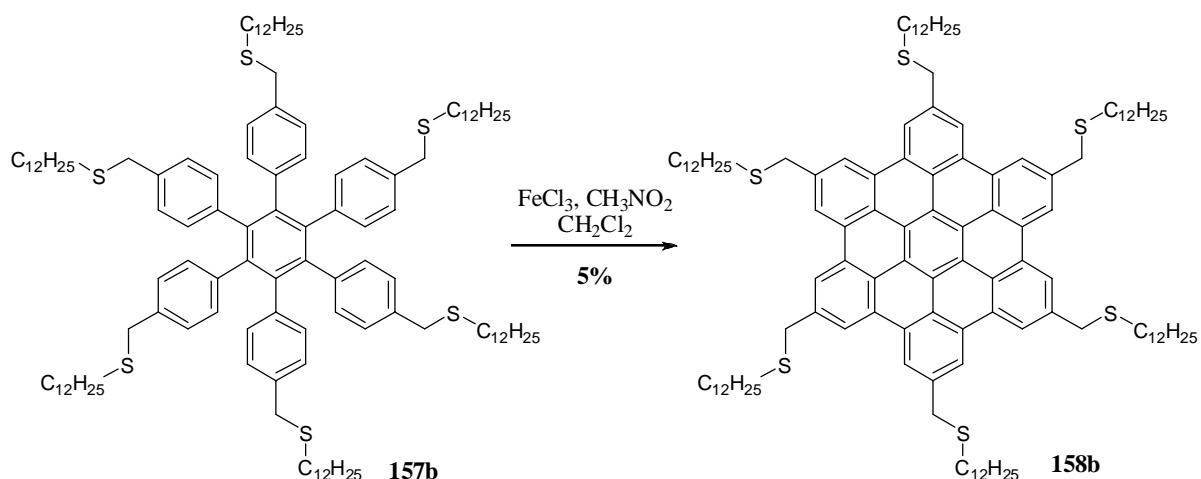
**TLC:**  $R_f$  = 0.78 (silica gel, pentane,  $\text{KMnO}_4$ ).

**$^1\text{H-NMR}$ :** (360 MHz,  $\text{CDCl}_3$ ):  $\delta$  6.73 (*d*, 12H,  $^3J_{\text{HH}}$  = 8.2 Hz, Ph), 6.71 (*d*, 12H,  $^3J_{\text{HH}}$  = 8.2 Hz, Ph), 3.44 (*s*, 12H, Ph- $\text{CH}_2$ ), 2.11 (*t*, 12H,  $^3J_{\text{HH}}$  = 7.3 Hz,  $\text{CH}_2(\text{CH}_2)_{10}\text{CH}_3$ ), 1.43 (*m*, 12H,  $(\text{CH}_2)_{10}\text{CH}_2\text{CH}_3$ ), 1.26 (*s*, 108H,  $\text{CH}_2-(\text{CH}_2)_9-\text{CH}_2\text{CH}_3$ ), 0.88 (*t*, 12H,  $^3J_{\text{HH}}$  = 6.8 Hz,  $(\text{CH}_2)_{11}\text{CH}_3$ ).

**$^{13}\text{C}$ -NMR:** (90.55 MHz,  $\text{CDCl}_3$ ):  $\delta$  140.08 (Ph), 139.18 (Ph), 135.01 (Ph), 131.45 (Ph), 127.27 (Ph), 35.58 (Ph- $\text{CH}_2$ ), 31.92 ( $\text{CH}_2(\text{CH}_2)_{10}\text{CH}_3$ ), 30.51 ( $(\text{CH}_2)_9\text{CH}_2\text{CH}_2\text{CH}_3$ ), 29.70-28.94 (48C,  $\text{CH}_2(\text{CH}_2)_8\text{CH}_2\text{CH}_2\text{CH}_3$ ), 22.69 ( $(\text{CH}_2)_{10}\text{CH}_2\text{CH}_3$ ), 14.12 ( $(\text{CH}_2)_{11}\text{CH}_3$ ).

**MALDI-TOF-MS (DCTB):**  $m/z$  (% int.): 1925.9 ( $[\text{M}+\text{Ag}]^{*+}$ , 100%; calcd. for  $\text{C}_{120}\text{H}_{168}\text{AgS}_6$  1926.19).

#### 23.5.4 2,5,8,11,14,17-Hexakis[(dodecylthio)methyl]hexabenzob[bc,ef,hi,kl,no,qr]coronene



The planarization was performed using **method C**, taking HPB **124b** (0.1 g, 55  $\mu\text{mol}$ ) together with  $\text{FeCl}_3$  (530 mg, 3.3 mmol, 5 eq. / H) in  $\text{CH}_3\text{NO}_2$  (8 mL) and  $\text{CH}_2\text{Cl}_2$  (20 mL). The mixture was heated to 45  $^\circ\text{C}$  under a constant bubbling of argon through a Teflon capillary for 6 hours before methanol (40 mL) was added to quench the mixture. The obtained precipitated was collected by suction filtration over Millipore<sup>®</sup>, suspended in common organic solvents (toluene – methanol, ether – methanol), sonicated and collected by suction filtration over Millipore<sup>®</sup> yielding the desired HBC **158b** as slightly brown solid (5 mg, 5%).

**UV/VIS:** (toluene,  $10^{-5}$  M,  $\epsilon = 4.1 \cdot 10^4$ ),  $\lambda_{\text{max}} = 356, 374, 402$  nm.

## **VI Annexes**



## 24 Index of main compounds

number	structure
63a	HBC-Rf <sub>2,6</sub>
63b	HBC-Rf <sub>2,8</sub>
82a	HBC-Rf <sub>3,6</sub>
82b	HBC-Rf <sub>3,8</sub>
94a	HBC-Rf <sub>4,4</sub>
94b	HBC-Rf <sub>4,6</sub>
94c	HBC-Rf <sub>4,8</sub>
94d	HBC-Rf <sub>4,10</sub>
106a	HBC-Rf <sub>5,6</sub>
106b	HBC-Rf <sub>6,8</sub>
114	HBC-Rf <sub>5,8</sub>
125a	HBC-Rf <sub>8,4</sub>
125b	HBC-Rf <sub>8,6</sub>
125c	HBC-Rf <sub>8,8</sub>
131a	HBC-Rf <sub>3,3,4,4</sub>
131b	HBC-Rf <sub>3,3,6,6</sub>
148	HBC-(Rf <sub>3,3,6,6</sub> ) <sub>3</sub>
152	SCF <sub>3</sub>
158a	CH <sub>2</sub> -S- <i>t</i> Bu
158b	CH <sub>2</sub> -S-C <sub>12</sub> H <sub>25</sub>
161a	HBC-(CH <sub>2</sub> - <i>t</i> Bu) <sub>3</sub>
168	HBC-(CH <sub>2</sub> - <i>t</i> Bu) <sub>1</sub>
169	HBC-Rf <sub>6,6</sub>
170	HBC-Rf <sub>3,5,6,6</sub>
171	HBC-Rf <sub>5,5,6,6</sub>



## **VII. Curriculum Vitae**





**Olivier Aebischer**

Panoramastrasse 24, 1712 Tavers  
 +4179 714 37 08  
 olivier.aebischer2@unifr.ch

**Personal details**

Name: Aebischer  
 First Name: Olivier Frédéric  
 Date of Birth: 17<sup>th</sup> May 1978  
 Native Place: Schmitten  
 Marital status: unmarried

**Education**

01. 2004 - present **Dissertation in chemistry**, University of Fribourg  
*„Controlling the supramolecular assembly of perfluorinated polycondensed aromatic hydrocarbons by side chain engineering “*  
 supervised by Prof. Dr. Titus A. Jenny
10. 1999 - 12. 2003 **4 years Diploma in chemistry**, University of Fribourg,  
 Diploma thesis in organic chemistry: *„Investigation of a new hexa-peri-hexaphenylbenzocoronene bearing perfluorinated chains“*  
 and physical chemistry, *„Investigation of a C<sub>12</sub>H<sub>14</sub> bird-cage hydrocarbon under ionization and photolysis“*
05. - 07. 1999 **Language stay in Brighton**, England, level 8 of 10
- 1994 - 1998 **Swiss High School in Fribourg.**  
 Area of specialisation: natural science

**Professional experience**

- 2005 - present **Teaching (professional baccalaureat classes), final year, chemistry**  
 GIBS (Gewerbliche und Industrielle Berufsschule, industrial and commercial vocational school), Fribourg
15. and 21. 03. 2006 **Development and execution of an advanced training course for laboratory employees**  
 in co-operation with the Weiterbildungs- und Informatikzentrum WIZ (Centre for continuing education and computer science), Fribourg  
*„Spectroscopie de résonance magnétique nucléaire (RMN)“*
01. 2005 - present **Structure and maintenance of a LC-MS/MS service**  
 Organisation of various master practical courses and discharge of the MS-service of the University of Fribourg  
 Structuring of the LC-MS/MS services of the University of Fribourg

05. 2004 - present	<b>Structure and operation/handling of a Solid State MAS-NMR Service</b> Organisation of various practical courses in co-operation with the Universities of Berne and Neuchâtel. Structuring of the Solid State NMR Service of the University of Fribourg
10. 2004 - 06. 2005	<b>Supervision of students' practical courses</b> First year, University of Fribourg
02. - 05. 2003	<b>Private lessons in chemistry</b> Study circle, Murten
	<b>Language skills</b>  German: Mother tongue  French: very good written and spoken knowledge  English: very good written and spoken knowledge
	<b>IT-skills</b>  Standard Software: Microsoft Office, Acrobat Writer, Photoshop, Corel Draw  Scientific Software: Chem Draw, Top Spin, Origin
	<b>Military education</b>
06. - 09. 2001	Swiss Military Academy in Birmenstorf, training as a heavy mortar lieutenant of infantry
2006 - 2007	Formation to NBC officer, centre of competence, Spiez and AAL, Luzern
	<b>Extracurricular activities</b>
2005 - present	<b>Extended executive board of the <i>Floorball Association Saane-Fribourg</i></b> Section finances
2000 - 2003	<b>President of the <i>Gambach Open</i> floorball tournament</b> Largest floorball tournament of Europe in the event centre „Forum Fribourg“ with over 350 participating teams
	<b>Hobbies</b>  Long-distance run, cycling, floorball, reading, piano, hiking

## **VIII. References**



- 
- [1] (a) J. S. Weissmann, P. S. Kim, *Science*, **1991**, 253, 1386-1393. (b) T. E. Creighton, *Biochem. J.*, **1990**, 270, 1-16.
- [2] (a) J.-M. Lehn, *Science*, **2002**, 295, 2401-2402. (b) D. N. Reinhoudt, M. Crego-Calama, *Science*, **2002**, 295, 2403-2407. (c) C. Tschierske, *Annu. Rep. Prog. Chem. Sect. C*, **2001**, 97, 191-267. (d) O. Ikkala, G. ten Brinke, *Science*, **2002**, 295, 2407-2409.
- [3] G. M. Whitesides, J. P. Mathias, C. T. Seto, *Science*, **1991**, 254, 1312-1319.
- [4] (a) M. S. Cubberley, B. L. Iverson, *J. Am. Chem. Soc.*, **2001**, 123, 7560-7563. (b) C. G. Claessens, J. F. Stoddart, *J. Phys. Org. Chem.*, **1997**, 10, 254-272.
- [5] (a) T. Dewa, K. Endo, Y. Aoyama, *J. Am. Chem. Soc.*, **1998**, 120, 8933-8940. (b) L. J. Prins, D. N. Reinhoudt, P. Timmerman, *Angew. Chem. Int. Ed.*, **2001**, 40, 2382-2426. (c) R. I. Gearba, M. Lehmann, J. Levin, D. A. Ivanov, M. H. J. Koch, J. Barbera, M. G. Debije, J. Parris, Y. H. Geerts, *Adv. Mater.*, **2003**, 15, 1614-1618.
- [6] S. V. Kolotuchin, S. C. Zimmerman, *J. Am. Chem. Soc.*, **1998**, 120, 9092-9093.
- [7] C. Gorman, *Adv. Mater.*, **1998**, 10, 295-309.
- [8] (a) S. Chandrasekhar, B. K. Sadashiva, K. A. Suresh, *Pramana*, **1977**, 9, 471-480. (b) C. Tschierske, *J. Mater. Chem.* **2001**, 11, 2647-2671.
- [9] (a) S. Förster, T. Plantenberg, *Angew. Chem. Int. Ed.*, **2002**, 41, 688-714. (b) S. Förster, M. Antonietti, *Adv. Mater.*, **1998**, 10, 195-217.
- [10] (a) L. Brunsveld, B. J. B. Folmer, E. W. Meijer, R. P. Sijbesma, *Chem. Rev.*, **2001**, 101, 4071-4097. (b) F. Zeng, S. C. Zimmerman, *Chem. Rev.*, **1997**, 97, 1681-1712.
- [11] (a) Y. Cui, S. J. Lee, W. Lin, *J. Am. Chem. Soc.*, **2003**, 125, 6014-6015. (b) C. Kaes, M. W. Hosseini, C. E. F. Rickard, B. W. Skelton, A. H. White, *Angew. Chem. Int. Ed.*, **1998**, 37, 920-922. (c) T. L. Hennigar, D. C. MacQuarrie, P. Losier, R. D. Rogers, M. J. Zaworotko, *Angew. Chem. Int. Ed.*, **1997**, 36, 972-973.
- [12] (a) E. Clar, *Polycyclic Hydrocarbons*, volume 1 and 2, **1964**, Academic Press, London. (b) E. Clar, *The Aromatic Sextet*, **1972**, Wiley, London. (c) E. Clar, C. T. Ironside, M. Zander, *J. Chem. Soc.*, **1959**, 142-147.
- [13] J. C. Fetzer, *Large ( $C \geq 24$ ) Polycyclic Aromatic Hydrocarbons: Chemistry and Analysis*, **1976**, Wiley, New York.
- [14] M. Zander, *Polycyclische Aromaten*, **1995**, B. G. Teubner, Stuttgart
- [15] R. L. Jaffe, G. D. Smith, *J. Chem. Phys.*, **1996**, 105, 2780-2788.
- [16] D. B. Smithrud, F. Diederich, *J. Am. Chem. Soc.*, **1990**, 112, 339-343.
- [17] A. S. Shetty, J. Zhang, J. S. Moore, *J. Am. Chem. Soc.*, **1996**, 118, 1019-1027.
- [18] C. A. Hunter, J. K. M. Sanders, *J. Am. Chem. Soc.*, **1990**, 112, 5525-5534.
- [19] G. R. Desiraju, A. Gavezzotti, *J. Chem. Soc., Chem. Commun.*, **1989**, 621-623.
- [20] C. Giessner-Prettre, B. Pullman, P. N. Borer, L.-S. Kan, P. O. P. Ts'O, *Biopolymers*, **1976**, 15, 2277-2286.

- [21] J. B. Birks, *Photophysics of Aromatic Molecules*, **1970**, Wiley, London.
- [22] D. Zhao, J. S. Moore, *Chem. Comm.*, **2003**, 7, 807-818.
- [23] (a) R. B. Martin, *Chem. Rev.*, **1996**, 96, 3034-3064. (b) W. Wang, J. J. Han, L.-Q. Wang, L.-S. Li, J. Shaw, A. D. Q. Li, *Nano Lett.*, **2003**, 3, 455-458.
- [24] P. G. Schouten, J. M. Warman, M. P. de Haas, J. F. van der Pol, J. W. Zwikker, *J. Am. Chem. Soc.*, **1992**, 114, 9028-9034.
- [25] (a) E. Muller-Horsche, D. Haarer, H. Scher, *Phys. Rev. B*, **1987**, 35, 1273-1280. (b) M. Redecker, H. Bässler, H. H. Hörhold, *J. Phys. Chem. B*, **1997**, 101, 7398-7403.
- [26] X. Ai, M. C. Beard, K. P. Knutsen, S. E. Shaheen, G. Rumbles, R. J. Ellingson, *J. Phys. Chem. B*, **2006**, 110, 25462-25471.
- [27] A. N. van de Craats, L. D. A. Siebbeles, I. Bleyl, D. Haarer, Y. A. Berlin, A. A. Zharikov, J. M. Warman, *J. Phys. Chem. B*, **1998**, 102, 9625-9634.
- [28] (a) S. Alexander, J. Bernasconi, W. R. Schneider, R. Orbach, *Rev. of Modern Phys.*, **1981**, 53, 175-198. (b) N. Boden, R. J. Bushby, J. Clements, *J. Chem. Phys.*, **1993**, 98, 5920-5931. (c) Y. Harima, X. Jiang, Y. Kunugi, K. Yamashita, A. Naka, K. K. Lee, M. Ishikawa, *J. Mater. Chem.*, **2003**, 13, 1298-1305. (d) A. N. van de Craats, J. M. Warman, P. Schlichting, U. Rohr, Y. Geerts, K. Müllen, *Synth. Met.*, **1999**, 102, 1550-1551. (e) A. N. van de Craats, M. P. de Haas, J. M. Warman, *Synth. Met.*, **1997**, 86, 2125-2126.
- [29] J. Simmerer, B. Glösen, W. Paulus, A. Kettner, P. Schumacher, D. Adam, K.-H. Etzbach, K. Siemensmeyer, J. H. Wendorff, H. Ringsdorf, D. Haarer, *Adv. Mater.*, **1996**, 8, 815-819.
- [30] (a) N. Boden, R. J. Bushby, J. Clements, B. Movaghar, *Phys. Rev. B*, **1995**, 52, 13274-13280. (b) D. Adam, P. Schumacher, J. Simmerer, L. Häussling, K. Siemensmeyer, K.-H. Etzbach, H. Ringsdorf, D. Haarer, *Nature*, **1994**, 371, 141-143. (c) D. Adam, F. Closs, T. Frey, D. Funhoff, D. Haarer, H. Ringsdorf, P. Schumacher, K. Siemensmeyer, *Phys. Rev. Lett.*, **1993**, 70, 457-460. (d) M. G. Debije, J. Piris, M. P. de Haas, J. M. Warman, Z. Tomovic, D. Simpson, M. D. Watson, K. Müllen, *J. Am. Chem. Soc.*, **2004**, 126, 4641-4645. (e) M. A. Rampi et al., *Adv. Mater.*, **2006**, 18, 329-333.
- [31] (a) A. Soncini, E. Steiner, P. W. Fowler, R. W. A. Havenith, L. W. Jenneskens, *Chem. Eur. J.*, **2003**, 9, 2974-2981. (b) Y. Ruiz-Morales, *J. Phys. Chem. A*, **2002**, 106, 11283-11308.
- [32] (a) W. Pisula, M. Kastler, D. Wasserfallen, M. Mondeshki, J. Piris, I. Schnell, K. Müllen, *Chem. Mater.*, **2006**, 18, 3634-3640. (b) M. D. Curtis, J. Cao, J. W. Kampf, *J. Am. Chem. Soc.*, **2004**, 126, 4318-4328.
- [33] X. Jiang, R. Patil, Y. Harima, J. Ohshita, A. Kunai, *J. Phys. Chem. B*, **2005**, 109, 221-229.
- [34] N. Boden, R. J. Bushby, J. Clements, B. Movaghar, *J. Mater. Chem.*, **1999**, 9, 2081-2086.
- [35] G. Binning, H. Rohrer, Ch. Gerber, E. Weibel, *Phys. Rev. Lett.*, **1982**, 49, 57-61.
- [36] R. P. Feynman, *Engineering and Science*, **1960**, (<http://www.zyvex.com/nanotech/feynman.html>, downloaded: 05. 02. 2007).
- [37] P. Gröning, *Adv. Engineering Mater.*, **2005**, 7, 279-291.

- [38] C. Pannemann, T. Diekmann, U. Hilleringmann, *Microelectronic Engineering*, **2003**, 67-68, 845-852.
- [39] (a) D. J. Gundlach, Y. Y. Lin, T. N. Jackson, S. F. Nelson, D. G. Schlom, *IEEE Electron Dev. Lett.*, **1997**, 18, 87-89. (b) Y. Y. Lin, D. J. Gundlach, S. F. Nelson, T. N. Jackson, *IEEE Electron Dev. Lett.*, **1997**, 18, 606-608.
- [40] A. R. Brown, A. Pomp, C. M. Hart, D. M. de Leeuw, *Science*, **1995**, 270, 972-974.
- [41] (a) C. Pannemann, T. Diekmann, U. Hilleringmann, *J. Mater. Res.*, **2004**, 19, 1999-2002. (b) P. von Ragué Schleyer, M. Manoharan, H. Jiao, F. Stahl, *Org. Lett.*, **2001**, 3, 3643-3646.
- [42] (a) J. H. Burroughes, D. D. C. Bradley, A. R. Brown, R. N. Marks, K. Mackay, R. H. Friend, P. L. Burns, A. B. Holmes, *Nature*, **1990**, 347, 539-541. (b) C. W. Tang, S. A. Van Slyke, *Appl. Phys. Lett.*, **1987**, 51, 913-915.
- [43] P. Avouris, *Acc. Chem. Res.*, **2002**, 35, 1026-1034.
- [44] C. D. Dimitrakopoulos, P. R. L. Malenfant, *Adv. Mater.*, **2002**, 14, 99-117.
- [45] T. Mori, H. Takeuchi, H. Fujikawa, *J. Appl. Phys.*, **2005**, 97, 066102/1-066102/3.
- [46] (a) M. A. Wolak, J. Delcamp, C. A. Landis, P. A. Lane, J. Anthony, Z. Kafafi, *Adv. Funct. Mater.*, **2006**, 16, 1943-1949. (b) B. W. D'Andrade, S. R. Forrest, *Adv. Mater.*, **2004**, 16, 1585-1595. (c) L. Schmidt-Mende, A. Fechtenkötter, K. Müllen, E. Moons, R. H. Friend, J. D. MacKenzie, *Science*, **2001**, 293, 1119-1122. (d) B. Geffroy, P. le Roy, C. Prat, *Polym. Int.*, **2006**, 55, 572-582.
- [47] M. O'Neill, S. M. Kelly, *Adv. Mater.*, **2003**, 15, 1135-1146.
- [48] E. L. Williams, K. Haavisto, J. Li, G. E. Jabbour, *Adv. Mater.*, **2007**, 19, 197-202.
- [49] M. C. Gather, A. Köhnen, A. Falcou, H. Becker, K. Meerholz, *Adv. Funct. Mater.*, **2007**, 17, 19-200.
- [50] H. A. Al Attar, A. P. Monkman, *Adv. Funct. Mater.*, **2006**, 16, 2231-2242.
- [51] K. Bullis, *Technology Review*, **2006**, 1-3.
- [52] <http://de.wikipedia.org/wiki/Kathodenstrahlr%C3%B6hrenbildschirm>, downloaded: 21. 12. 2006.
- [53] (a) R. H. Fowler, L. Nordheim, *Roy. Soc. Proc. A*, **1928**, 119, 173-181. (b) L. W. Nordheim, *Roy. Soc. Proc. A*, **1928**, 119, 626-639.
- [54] (a) P. Gröning, *Introduction to Carbon Nanotubes*, **2006**, Swiss Foundation for Research in Microtechnology, Neuchâtel, 08. 12. 2006. (b) O. Gröning, O. M. Küttel, C. Emmenegger, P. Gröning, L. Schlappbach, *J. Vac. Sci. Technol. B*, **2000**, 18, 665-678. (c) G. N. Fursey, *App. Sur. Sc.*, **2003**, 215, 113-134.
- [55] R. D. Young, *Phys. Rev.*, **1959**, 113, 110-114.
- [56] (a) L. Nilsson, O. Gröning, O. M. Küttel, P. Gröning, L. Schlappbach, *J. Vac. Sci. Technol. B*, **2002**, 20, 326-337. (b) L. Nilsson, O. Gröning, P. Gröning, O. M. Küttel, L. Schlappbach, *Thin Solid Films*, **2001**, 383, 78-80.

- [57] P. Gröning, P. Ruffieux, L. Schlappbach, O. Gröning, *Adv. Engineering Mater.*, **2003**, 5, 541-550.
- [58] B. C. Dzubua, N. N. Chubun, *IEEE Trans. Electron. Dev.*, **1991**, 38, 2314-2316.
- [59] R. G. Forbes, *Solid-state electronics*, **2001**, 45, 779-808.
- [60] P. R. Schwoebel, I. Brodie, *J. Vac. Sci. Technol. B*, **1995**, 13, 1391-1410.
- [61] A. A. Talin, K. A. Dean, J. E. Jaskie, *Solid-state electronics*, **2001**, 45, 963-976.
- [62] J. B. Cui, J. Ristein, L. Ley, *Phys. Rev. B*, **1999**, 60, 16135-16142.
- [63] S. Iijima, *Nature*, **1991**, 354, 56-58.
- [64] W. I. Milne, K. B. K. Teo, G. A. J. Amaratunga, P. Legagneux, L. Gangloff, J.-P. Schnell, V. Semet, V. T. Binh, O. Gröning, *J. Mater. Chem.*, **2004**, 14, 933-943.
- [65] A. Thess et al., *Science*, **1996**, 273, 483-487.
- [66] M. Su, B. Zheng, J. Liu, *Chem. Phys. Lett.*, **2000**, 322, 321-326.
- [67] O. Zhou, H. Shimoda, B. Gao, S. Oh, L. Fleming, G. Yue, *Acc. Chem. Res.*, **2002**, 35, 1045-1053.
- [68] (a) R. H. Baughman, A. A. Zakhidov, W. A. de Heer, *Science*, **2002**, 297, 787-792. (b) M. Ouyang, J.-L. Huang, C. M. Lieber, *Acc. Chem. Res.*, **2002**, 35, 1018-1025.
- [69] (a) D.-S. Chung et al., *Appl. Phys. Lett.*, **2002**, 80, 4045-4047. (b) J. Dijon et al., *J. Soc. Inf. Display*, **2004**, 12, 373-378.
- [70] H. Dai, *Acc. Chem. Res.*, **2002**, 35, 1035-1044.
- [71] T. Utsumi, *IEEE Trans. Electron. Dev.*, **1991**, 38, 2276-2283.
- [72] S. T. Purcell, P. Vincent, M. Rodriguez, C. Journet, S. Vignoli, D. Guillot, A. Ayari, *Chem. Vap. Deposition*, **2006**, 12, 331-344.
- [73] L. Nilsson, O., Gröning, P. Gröning, L. Schlappbach, *Appl. Phys. Lett.*, **2001**, 79, 1036-1038.
- [74] P. Gröning, L. Nilsson, P. Ruffieux, O. Gröning, *Encyclopedia of Nanoscience and Nanotechnology*, H. S. Nalwa, ed., **2004**, 1, 547-579.
- [75] Z. F. Ren, Z. P. Huang, J. W. Xu, J. H. Wang, P. Bush, M. P. Siegal, P. N. Provencio, *Science*, **1998**, 282, 1105-1107.
- [76] M. Chhowalla, K. B. K. Teo, C. Ducati, N. L. Rupesinghe, G. A. J. Amaratunga, A. C. Ferrari, D. Roy, J. Robertson, W. I. Milne, *J. Appl. Phys.*, **2001**, 90, 5308-5417.
- [77] (a) O. Gröning, R. Clergereaux, L. Nilsson, P. Ruffieux, P. Gröning, L. Schlappbach, *Chimia*, **2002**, 56, 553-561. (b) J.-M. Bonard, N. Weiss, H. Kind, T. Stöckli, L. Forro, K. Kern, A. Châtelain, *Adv. Mater.*, **2001**, 13, 184-188.
- [78] (a) E. Minoux et al., *Nano Lett.*, **2005**, 5, 2135-2138. (b) K. B. K. Theo et al., *Nanotechnology*, **2003**, 14, 204-211.
- [79] W. I. Milne et al., *Diamond Relat. Mater.*, **2003**, 12, 422-428.
- [80] (a) A. P. Ramirez, *Bell Labs Tech. J.*, **2005**, 10, 171-185. (b) N. S. Lee et al., *Diamond Relat. Mater.*, **2001**, 10, 265-270. (c) Y. Satio, S. Uemura, *Carbon*, **2000**, 38, 169-182. (d) W.



- B. Choi et al., *Appl. Phys. Lett.*, **1999**, 75, 3129-3131. (e) W. A. de Heer, A. Châtelain, D. Ugarte, *Science*, **1995**, 270, 1179-1180. (f) Y. Yoshida, A. Ishizuka, H. Makishima, *Mat. Chem. Phys.*, **1995**, 40, 267-272.
- [81] D. Chattopadhyay, I. Galeska, F. Papadimitrakopoulos, *J. Am. Chem. Soc.*, **2003**, 125, 3370-3375.
- [82] C. D. Simpson, J. Wu, M. D. Watson, K. Müllen, *J. Mater. Chem.*, **2004**, 14, 494-504.
- [83] (a) A. M. van de Craats, N. Stutzmann, O. Bunk, M. M. Nielsen, M. Watson, K. Müllen, H. D. Chanzy, H. Sirringhaus, R. H. Friend, *Adv. Mater.*, **2003**, 15, 495-499. (b) P. C. M. Christianen et al., *J. Am. Chem. Soc.*, **2005**, 127, 16233-16237.
- [84] S. J. Tans, A. R. M. Verschueren, C. Dekker, *Nature*, **1998**, 393, 49-52.
- [85] W. Pisula, A. Menon, M. Stepputat, I. Lieberwirth, U. Kolb, A. Tracz, H. Sirringhaus, T. Pakula, K. Müllen, *Adv. Mater.*, **2005**, 17, 684-688.
- [86] R. Tran, B. Alameddine, T. A. Jenny, T. A. Wesolowski, *J. Phys. Chem. A*, **2004**, 108, 9155-9160.
- [87] G. Zucchi, B. Donni, Y. H. Geerts, *Chem. Mater.*, **2005**, 17, 4273-4277.
- [88] U. Rohr, P. Schlichting, A. Böhm, M. Gross, K. Meerholz, C. Bräuchle, K. Müllen, *Angew. Chem. Int. Ed.*, **1998**, 37, 1434-1437.
- [89] J. S. Moore, *Acc. Chem. Res.*, **1997**, 30, 402-414.
- [90] F. Dötz, J. D. Brand, S. Ito, L. Gherghel, K. Müllen, *J. Am. Chem. Soc.*, **2000**, 122, 7707-7717.
- [91] A. M. van de Craats, J. M. Warman, *Adv. Mater.*, **2001**, 13, 130-133.
- [92] S. Kumar, *Liq. Cryst.*, **2005**, 32, 1089-1113.
- [93] A. M. van de Craats, J. M. Warman, A. Fechtenkötter, J. D. Brand, M. A. Harbison, K. Müllen, *Adv. Mater.*, **1999**, 11, 1469-1472.
- [94] W. Pisula, Z. Tomovic, C. Simpson, M. Kastler, T. Papula, K. Müllen, *Chem. Mater.*, **2005**, 17, 4296-4303.
- [95] Robertson, Trotter, *J. Chem. Soc.*, **1961**, 1280-1284.
- [96] R. Goddard, M. W. Heanel, W. C. Herndon, C. Krüger, M. Zander, *J. Am. Chem. Soc.*, **1995**, 117, 30-41.
- [97] P. Herwig, C. W. Kayser, K. Müllen, G. W. Spiess, *Adv. Mater.*, **1996**, 8, 510-513.
- [98] M. Kastler, W. Pisula, D. Wasserfallen, R. Pakula, K. Müllen, *J. Am. Chem. Soc.*, **2005**, 127, 4286-4296.
- [99] M. Müller, C. Kübel, K. Müllen, *Chem. Eur. J.*, **1998**, 11, 2099-2108.
- [100] A. Fechtenkötter, N. Tchebotareva, M. Watson, K. Müllen, *Tetrahedron*, **2001**, 57, 3769-3783.
- [101] C.-Y. Liu, A. Fechtenkötter, M. D. Watson, K. Müllen, A. J. Bard, *Chem. Mater.*, **2003**, 15, 124-130.

- [102] D. W. Breiby, F. Hansteen, W. Pisula, O. Bunk, U. Kolb, J. W. Andreasen, K. Müllen, M. M. Nielsen, *J. Phys. Chem. B*, **2005**, 109, 22319-22325.
- [103] W. Pisula, M. Kastler, D. Wasserfallen, T. Pakula, K. Müllen, *J. Am. Chem. Soc.*, **2004**, 126, 8074-8075.
- [104] J. Wu, A. Fechtenkötter, J. Gauss, M. D. Watson, M. Kastler, C. Fechtenkötter, M. Wagner, K. Müllen, *J. Am. Chem. Soc.*, **2004**, 126, 11311-11321.
- [105] L. Piot, A. Marchenko, J. Wu, K. Müllen, D. Fichou, *J. Am. Chem. Soc.*, **2005**, 127, 16245-16250.
- [106] (a) D. W. Breiby et al., *J. Am. Chem. Soc.*, **2005**, 127, 11288-11293. (b) O. Bunk, M. M. Nielsen, T. I. Solling, A. M. van de Craats, N. Stutzmann, *J. Am. Chem. Soc.*, **2003**, 125, 2252-2258. (c) S. P. Brown, I. Schnell, J. D. Brand, K. Müllen, H. W. Spiess, *J. Am. Chem. Soc.*, **1999**, 121, 6712-6718.
- [107] J. M. Warman, J. Piris, W. Pisula, M. Kastler, D. Wasserfallen, K. Müllen, *J. Am. Chem. Soc.*, **2005**, 127, 14257-14262.
- [108] A. Fechtenkötter, K. Saalwächter, M. A. Herbison, K. Müllen, H. W. Spiess, *Angew. Chem. Int. Ed.*, **1999**, 38, 3039-3042.
- [109] N. Reitzel et al., *Chem. Eur. J.*, **2001**, 7, 4894-4901.
- [110] J. Wu, M. D. Watson, L. Zhang, Z. Wang, K. Müllen, *J. Am. Chem. Soc.*, **2004**, 126, 177-186.
- [111] K. Müllen et al., *Adv. Funct. Mater.*, **2005**, 15, 1585-1594.
- [112] S. Ito, M. Wehmeier, J. D. Brand, C. Kübel, R. Epsch, J. P. Rabe, K. Müllen, *Chem. Eur. J.*, **2000**, 6, 4327-4342.
- [113] W. Pisula, Z. Tomovic, B. El Hamaoui, M. D. Watson, T. Pakula, K. Müllen, *Adv. Funct. Mater.*, **2005**, 15, 893-904.
- [114] I. Fischbach, T. Pakula, P. Minkin, A. Fechtenkötter, K. Müllen, H. W. Spiess, K. Saalwächter, *J. Phys. Chem. B*, **2002**, 106, 6408-6418.
- [115] J. Piris, M. G. debyie, N. Stutzmann, A. M. van de Craats, M. D. Watson, K. Müllen, J. M. Warman, *Adv. Mater.*, **2003**, 15, 1736-1740.
- [116] J. Wu, M. D. Watson, K. Müllen, *Angew. Chem. Int. Ed.*, **2003**, 42, 5329-5333.
- [117] D. Wasserfallen, I. Fischbach, N. Chebotareva, M. Kastler, W. Pisula, F. Jäckel, M. D. Watson, I. Schnell, J. P. Rabe, H. W. Spiess, K. Müllen, *Adv. Funct. Mater.*, **2005**, 15, 1585-1594.
- [118] T. Yamamoto, T. Fukushima, Y. Yamamoto, A. Kosaka, W. Jin, N. Ishii, T. Aida, *J. Am. Chem. Soc.*, **2006**, 128, 14337-14340.
- [119] P. Samori, A. Fechtenkötter, E. Reuther, M. D. Watson, N. Severin, K. Müllen, S. P. Rabe, *Adv. Mater.*, **2006**, 18, 1317-1321.
- [120] J. Wu, M. Baumgarten, M. G. Debyie, J. M. Warman, K. Müllen, *Angew. Chem. Int. Ed.*, **2004**, 43, 5331-5335.

- [121] W. Jin, T. Fukushima, A. Kosaka, M. Niki, N. Ishii, T. Aida, *J. Am. Chem. Soc.*, **2005**, 127, 8284-8285.
- [122] T. Aida et al., *Adv. Mater.*, **2006**, 18, 1297-1300.
- [123] E. J. R. Sudhölter et al., *J. Am. Chem. Soc.*, **2000**, 122, 11057-11066.
- [124] D. F. Eaton, B. E. Smart, *J. Am. Chem. Soc.*, **1990**, 112, 2821-2823.
- [125] A. Kohlmeier, D. Janietz, *Chem. Mater.*, **2006**, 18, 59-68.
- [126] M. D'Amore, G. Talarico, V. Barone, *J. Am. Chem. Soc.*, **2006**, 128, 1099-1108.
- [127] J. G. Riess, *Tetrahedron*, **2002**, 58, 4113-4131.
- [128] B. Alameddine, O. F. Aebischer, W. Amrein, B. Donnio, R. Deschenaux, D. Guillon, C. Savary, D. Scanu, O. Scheidegger, T. A. Jenny, *Chem. Mater.*, **2005**, 17, 4798-4807.
- [129] F. Guittard, E. T. de Givenchy, S. Geribaldi, A. Cambon, *J. Fluorine Chem.*, **1999**, 100, 85-96.
- [130] B. Alameddine, *Synthesis and Investigation of New Large Self-Assembled Supramolecules as Potential Electron Emitters*, **2004**, Thesis No. 1440, University of Fribourg.
- [131] (a) O. F. Aebischer, A. Aebischer, B. Donnio, B. Alameddine, M. Dadras, H.-U. Güdel, D. Guillon, T. A. Jenny, *J. Mater. Chem.*, **2007**, 17, 1262-1267. (b) O. F. Aebischer, A. Aebischer, P. Tondo, B. Alameddine, M. Dadras, H.-U. Güdel, T. A. Jenny, *Chem. Comm.*, **2006**, 2, 4221-4223.
- [132] (a) M. Broniatowski, P. Dynarowicz-Latka, W. Witko, *J. Fluorine Chem.*, **2005**, 126, 79-86. (b) X. Cheng, M. Prehm, M. K. Das, J. Kain, U. Baumeister, S. Diele, D. Leine, A. Blume, C. Tschierske, *J. Am. Chem. Soc.*, **2003**, 125, 10977-10996.
- [133] A. Halleux, R. H. Martin, G. S. D. King, *Helv. Chim. Acta*, **1958**, 41, 1177-1183.
- [134] R. Scholl, J. Mansfeld, *Ber. der deutsch. chem. Gesellschaft*, **1910**, Part 2, 1734-1747.
- [135] P. Kovacic, M. B. Jones, *Chem. Rev.*, **1987**, 87, 357-379.
- [136] P. Kovacic, R. M. Lange, *J. Org. Chem.*, **1962**, 28, 968-972.
- [137] P. Kovacic, A. Kyriakis, *J. Am. Chem. Soc.*, **1963**, 85, 454-458.
- [138] X. Feng, J. Wu, V. Enkelmann, K. Müllen, *Org. Lett.*, **2006**, 8, 1145-1148.
- [139] (a) A. G. Brown, P. D. Edwards, *Tetrahedron Lett.*, **1990**, 45, 6581-6584. (b) M. A. Schwartz, P. T. K. Pham, *J. Org. Chem.*, **1988**, 53, 2318-2322. (c) P. Magnus, J. Schultz, T. Gallagher, *J. Am. Chem. Soc.*, **1985**, 107, 4984-4988. (d) S. M. Kupchan, O. P. Dhingra, C.-K. Kim, *J. Org. Chem.*, **1978**, 43, 4076-4081. (e) S. Kumar, S. K. Varshney, *Synthesis*, **2001**, 2, 305-311.
- [140] E. C. Taylor, J. G. Andrade, G. J. H. Rall, A. McKillop, *J. Am. Chem. Soc.*, **1980**, 102, 6513-6519.
- [141] (a) L. Liu, B. Yang, T. J. Katz, M. K. Poindexter, *J. Org. Chem.*, **1991**, 56, 3769-3775. (b) R. J. Bushby, C. Hardy, *J. Chem. Soc., Perkin Trans. I*, **1986**, 721-723.
- [142] W. Jaworek, F. Vögtle, *Chem. Ber.*, **1991**, 124, 347-352.
- [143] P. G. Copeland, R. E. Dean, D. McNeil, *J. Chem. Soc.*, **1960**, 1689-1691.

- [144] (a) M. Müller, V. S. Iyer, C. Kübel, V. Enkelmann, K. Müllen, *Angew. Chem. Int. Ed.*, **1997**, 36, 1607-1610. (b) M. Müller, J. Petersen, R. Strohmaier, C. Günther, N. Karl, K. Müllen, *Angew. Chem. Int. Ed.*, **1996**, 35, 886-888. (c) P. Kovacic, J. Oziomek, *J. Org. Chem.*, **1964**, 29, 100-104.
- [145] P. Rempala, J. Kroulik, B. T. King, *J. Am. Chem. Soc.*, **2004**, 126, 15002-15003.
- [146] M. Tanaka, H. Nakashima, M. Fujiwara, H. Ando, Y. Souma, *J. Org. Chem.*, **1996**, 61, 788-792.
- [147] (a) J. M. T. B. Varejão et al., *Org. Biomol. Chem.*, **2003**, 1, 565-574. (b) E. S. Kryachko, M. T. Nguyen, *J. Phys. Chem. A*, **2001**, 105, 153-155.
- [148] M. Randic, X. Guo, *New. J. Chem.*, **1999**, 251-260.
- [149] P. Kovacic, R. W. Koch, *J. Org. Chem.*, **1963**, 28, 1864-1867.
- [150] M. Di Stefano, F. Negri, C. Carbone, K. Müllen, *Chem. Phys.*, **2005**, 314, 85-99.
- [151] V. Mamane, A. Gref, F. Lefloch, O. Riant, *J. Organometal. Chem.*, **2001**, 637-639, 84-88.
- [152] M. Berthelot, *Acad. Sci.*, **1866**, 62, 905-907.
- [153] W. Reppe, O. Schlichting, K. Klager, T. Toepel, *Annalen der Chemie*, **1948**, Band 560, 1-6.
- [154] (a) S. Saito, T. Kawasaki, N. Tsuboya, Y. Yamamoto, *J. Org. Chem.*, **2001**, 66, 796-802. (b) A. J. Chalk, R. A. Jerussi, *Tetrahedron Lett.*, **1972**, 61-62.
- [155] (a) J. Yang, J. G. Verkade, *Organometallics*, **2000**, 19, 893-900. (b) J. Yang, J. G. Verkade, *J. Am. Chem. Soc.*, **1998**, 120, 6834-6835.
- [156] (a) K. P. Vollhardt, *Angew. Chem. Int. Ed.*, **1984**, 23, 539-556. (b) K. P. Vollhardt, *Acc. Chem. Res.*, **1977**, 10, 1-8. (c) U. Krüerke, W. Hübel, *Anorganisch-Chemisches Laboratorium der European Research Associates Brüssel*, **1961**, 2829-2856. (d) L. S. Hegedus, *Transition Metals in the Synthesis of Complex Organic Molecules*, 2<sup>nd</sup> ed., **1999**, Univesity Science Books, (e) R. L. Funk, K. P. Vollhardt, *J. Am. Chem. Soc.*, **1980**, 102, 5253-5261.
- [157] D. R. McAlister, J. E. Bercaw, R. G. Bergman, *J. Am. Chem. Soc.*, **1977**, 99, 1666-1668.
- [158] (a) S. A. R. Knox, R. F. D. Stansfield, F. G. A. Stone, M. J. Winter, P. Woodward, *J. Chem. Soc., Chem. Comm.*, **1978**, 221-223. (b) R. S. Dickson, P. J. Fraser, B. M. Gatehouse, *J. Chem. Soc., Dalton Trans.*, **1972**, 2278-2282.
- [159] R. J. Kaufman, R. S. Sidhu, *J. Org. Chem.*, **1982**, 47, 4941-4947.
- [160] M. A. Bennett, P. B. Donaldson, *Inorg. Chem.*, **1978**, 17, 1995-2000.
- [161] J. A. Hyatt, *OPPI Briefs*, **1991**, 23, 460-463.
- [162] R. Rathore, C. L. Burns, I. A. Guzei, *J. Org. Chem.*, **2004**, 69, 1524-1530.
- [163] K. Kobayashi, N. Kobayashi, M. Ikuta, B. Therrien, S. Sakamoto, K. Yamaguchi, *J. Org. Chem.*, **2005**, 70, 749-752.
- [164] M. J. Mio, L. C. Kopel, J. B. Braun, R. L. Gadzikwa, K. L. Hull, R. G. Brisbois, C. J. Markworth, P. A. Grieco, *Org. Lett.*, **2002**, 4, 3199-3202.
- [165] Z. Novak, P. Nemes, A. Kotschy, *Org. Lett.*, **2004**, 6, 4917-4920.

- [166] (a) U. B. Vasconcelos, E. Dalmolin, A., A. Merlo, *Org. Lett.*, **2005**, 7, 1027-1030. (b) R. M. Harrison, R. Brotin, B. C. Noll, J. Michl, *Organometallics*, **1997**, 16, 3401-3412. (c) M. A. Fox, J. A. K. Howard, J. A. H. MacBride, A. Mackinnon, K. Wade, *J. Organometal. Chem.*, **2003**, 680, 155-164. (d) A. Bader, D. Arlt, *US Patent*, **1993**, US005185454A; 5,185,454. (e) C.-J. Li, D.-L. Chen, C. W. Costello, *Org. Proc. Res. Develop.*, **1997**, 1, 325-327.
- [167] (a) A. S. Hay, *J. Org. Chem.*, **1962**, 27, 3320-3321. (b) A. S. Hay, *J. Org. Chem.*, **1960**, 25, 1275-1276.
- [168] P. Siemsen, R. C. Livingston, F. Diederich, *Angew. Chem. Int. Ed.*, **2002**, 39, 2632-2657.
- [169] (a) H.-F. Chow, C.-W. Wan, K.-H. Low, Y.-Y. Yeung, *J. Org. Chem.*, **2001**, 66, 1910-1013. (b) J. M. Kehoe, J. H. Kiley, J. J. English, C. a. Johnson, R. C. Petersen, M. M. Haley, *Org. Lett.*, **2000**, 2, 969-972. (c) O. Mongin, A. Gossauer, *Tetrahedron*, **1997**, 53, 6835-6846.
- [170] (a) J. G. Rodriguez, J. Esquivias, A. Lafuente, C. Diaz, *J. Org. Chem.*, **2003**, 68, 8120-8128. (b) M. Kimura, A. Sakaguchi, K. Ohta, K. Hanabusa, H. Shirai, N. Kobayashi, *Inorg. Chem.*, **2003**, 42, 2821-2823.
- [171] C. J. Cooksey, J. L. Courtneidge, A. G. Davies, P. S. Gregory, J. E. Evans, C. C. Rowlands, *J. Chem. Soc., Perkin Trans. II*, **1988**, 807-813.
- [172] (a) S. Darses, M. Pucheault, J.-P. Genêt, *Eur. J. Org. Chem.*, **2001**, 66, 1121-1128. (b) S. Darses, G. Michaud, J.-P. Genêt, *Eur. J. Org. Chem.*, **1999**, 64, 1875-1883.
- [173] (a) P. Mazerolles, P. Boussaguet, V. Huc, *Org. Synthesis*, **1999**, 76, 221-224. (b) M. Tamura, J. Kochi, *J. Am. Chem. Soc.*, **1971**, 93, 1485-1487.
- [174] H. Yoshino, N. Toda, M. Kobata, K. Ukai, K. Oshima, K. Utimoto, S. Matsubara, *Chem. Eur. J.*, **2006**, 12, 721-726.
- [175] A. C. Grimsdale et al., *Synthesis*, **2002**, 9, 1229-1238.
- [176] A. C. Grimsdale, K. Müllen, *Chem. Record*, **2001**, 1, 243-257.
- [177] H. des Abbayes, J.-C. Clément, P. Laurent, G. Tanguy, N. Thilmont, *Organometallics*, **1988**, 2293-2299.
- [178] M. S. Yusybov, V. D. Filimonov, *Synthesis*, **1991**, 131-132.
- [179] J. Hassan, M. Sévignon, C. Gozzi, E. Schulz, M. Lemaire, *Chem. Rev.*, **2002**, 102, 1359-1469.
- [180] A. F. Littke, G. C. Fu, *Angew. Chem. Int. Ed.*, **2002**, 41, 4176-4211.
- [181] (a) N. Miyaura, A. Suzuki, *Chem. Rev.*, **1995**, 95, 2457-2483. (b) N. Miyaura, A. Suzuki, *J. Chem. Soc., Chem. Comm.*, **1979**, 866-867.
- [182] (a) V. Bonnet, F. Mongin, F. Trécourt, G. Quéquiner, P. Knochel, *Tetrahedron Lett.*, **2001**, 42, 5717-5719. (b) K. Tamao, K. Sumitani, Y. Kiso, M. Zembayashi, A. Fujioka, S. Kodama, I. Nakajima, A. Minato, K. Kumada, *Bull. Chem. Soc. Jpn.*, **1976**, 49, 1958-1969. (c) K. Tamao, K. Sumitani, M. Kumada, *J. Am. Chem. Soc.*, **1972**, 94, 4374-4376.
- [183] U. Christmann, R. Vilar, *Angew. Chem. Int. Ed.*, **2005**, 44, 366-374.
- [184] M. W. Hooper, M. Utsunomiya, J. F. Hartwig, *J. Org. Chem.*, **2003**, 68, 2861-2873.

- [185] L.-M. Yang, L.-F. Huang, T.-Y. Luh, *Org. Lett.* **2004**, 6, 1461-1463.
- [186] T. J. Colacot, H. A. Shea, *Org. Lett.*, **2004**, 6, 3731-3734.
- [187] R. Martin, A. Fürstner, *Angew. Chem. Int. Ed.*, **2004**, 43, 3955-3957.
- [188] M. Kumada, K. Tamao, K. Sumitani, *Org. Synthesis*, **1978**, 58, 407-410.
- [189] M. S. Viciu, R. M. Kissling, E. D. Stevens, S. P. Nolan, *Org. Lett.*, **2002**, 4, 2229-2232.
- [190] C. Amatore, E. Carré, A. Jutand, M. A. M'Barki, G. Meyer, *Organometallics*, **1995**, 14, 5605-5614.
- [191] (a) I. P. Beletskaya, A. V. Cheprakov, *Chem. Rev.*, **2000**, 100, 3009-3066. (b) S. Bräse, A. de Meijere, *Palladium-Catalyzed Coupling of Organyl Halides to Alkenes – The Heck Reaction*, **1997**, Wiley, Weinheim.
- [192] C. Amatore, F. Pflüger, *Organometallics*, **1990**, 9, 2276-2282.
- [193] G. K. Friestad, B. P. Branchaud, *Tetrahedron Lett.*, **1995**, 36, 7047-7050.
- [194] R. F. Heck, *Acc. Chem. Res.*, **1979**, 12, 146-151.
- [195] S. Lemaire-Audoire, M. Savignac, C. Dupuis, J.-P. Genêt, *Tetrahedron Lett.*, **1996**, 37, 2003-2006.
- [196] S. Laschat, F. Narjes, L. E. Overman, *Tetrahedron*, **1994**, 50, 347-358.
- [197] J. M. Schkeryantz, S. J. Danishefsky, *J. Am. Chem. Soc.*, **1995**, 117, 4722-4723.
- [198] Q.-Y. Chen, Z.-Y. Yang, *Tetrahedron Lett.*, **1986**, 27, 1171-1174.
- [199] E. Negishi, L. Anastasia, *Chem. Rev.*, **2003**, 103, 1979-2017.
- [200] R. D. Stephens, C. E. Castro, *J. Am. Chem. Soc.*, **1963**, 85, 3313-3315.
- [201] (a) S. Takahashi, Y. Kuroyama, K. Sonogashira, N. Hagihara, *Synthesis*, **1980**, 627-628. (b) Y. Tohda, K. Sonogashira, N. Hagihara, *Synthesis*, **1977**, 777-778. (c) K. Sonogashira, T. Yatake, Y. Thoda, S. Takahashi, N. Hagihara, *J. Chem. Soc., Chem. Comm.*, **1977**, 291-292.
- [202] K. Sonogashira, Y. Tohda, N. Hagihara, *Tetrahedron Lett.*, **1975**, 50, 4467-4470.
- [203] A. C. Hillier, G. A. Grasa, M. S. Viciu, H. M. Lee, C. Yang, S. P. Nolan, *J. Organometal. Chem.*, **2002**, 653, 69-82.
- [204] R. R. Tykwinski, *Angew. Chem. Int. Ed.*, **2003**, 42, 1566-1568.
- [205] O. F. Aebischer, P. Tondo, B. Alameddine, T. A. Jenny, *Synthesis*, **2006**, 17, 2891-2896.
- [206] (a) D. P. Curran, S. Hadida, *J. Am. Chem. Soc.*, **1996**, 118, 2531-2532. (b) C. Tamborski, G. J. Moore, *J. Organometal. Chem.*, **1971**, 26, 153-156.
- [207] B. Schmidt, *Chem. Comm.*, **2003**, 14, 1656-1657.
- [208] C. Yang, S. P. Nolan, *Organometallics*, **2002**, 21, 1020-1022.
- [209] I. Kaljurand, R. Rodima, I. Leito, I. A. Koppel, R. Schwesinger, *J. Org. Chem.*, **2000**, 65, 6202-6208.
- [210] (a) O. Geis, H.-G. Schmalz, *Angew. Chem. Int. Ed.*, **1998**, 37, 911-914. (b) R. L. Funk, K. P. C. Vollhardt, *J. Am. Chem. Soc.*, **1976**, 98, 6755-6757.
- [211] (a) J.-L. Débieux, *Synthèse de nouveaux hexabenzocoronènes portant de longues chaînes perfluorées*, **2004**, Diploma work, University of Fribourg. (b) P. Tondo, *Synthesis of Hexa-*

- benzo[bc,ef,hi,kl,no,qr]coronenes carrying Perfluorinated Side Chains*, **2005**, Diploma work, University of Fribourg.
- [212] (a) G. Gambaretto, L. Conte, G. Fornasieri, C. Zarantonello, D. Tonei, A. Sassi, R. Bertani, *J. Fluorine Chem.*, **2003**, 121, 57-63. (b) B. Améduri, B. Boutevin, M. Nouiri, M. Talbi, *J. Fluorine Chem.*, **1995**, 74, 191-197.
- [213] G. Johansson, V. Percec, U. Ungar, J. P. Zhou, *Macromolecules*, **1996**, 29, 646-660.
- [214] N. O. Brace, *J. Fluorine Chem.*, **1999**, 93, 1-25.
- [215] S. Rubio, H. Blancou, A. Commeyras, *J. Fluorine Chem.*, **1999**, 99, 171-175.
- [216] S. H. Yang, C. S. Li, C. H. Cheng, *J. Org. Chem.*, **1987**, 52, 691-694.
- [217] B. Nicholls, M. C. Whiting, *J. Chem. Soc.*, **1959**, 551-556.
- [218] B. Quiclet-Sire, S. Z. Zard, *J. Am. Chem. Soc.*, **1996**, 118, 9190-9191.
- [219] J. Boivin, B. Quiclet-Sire, L. Ramos, S. Z. Zard, *Chem. Comm.*, **1997**, 353-354.
- [220] (a) F. Guittard, S. Geribaldi, *J. Fluorine Chem.*, **2001**, 107, 363-374. (b) J. Visjager, T. A. Tervoort, P. Smith, *Polymer*, **1999**, 40, 4533-4542. (c) M. P. Turberg, J. E. Brady, *J. Am. Chem. Soc.*, **1988**, 10, 7797-7801.
- [221] O. F. Aebischer, *Investigation of a new hexa-peri-hexaphenylbenzocoronene bearing per-fluorinated chains*, **2003**, Diploma work, University of Fribourg.
- [222] Y. Li, M. Hesse, *Helv. Chim. Acta*, **2003**, 86, 310-323.
- [223] R. E. Banks, J. C. Tatlow, *J. Fluorine Chem.*, **1986**, 33, 227-346.
- [224] L. Friedman, A. Shani, *J. Am. Chem. Soc.*, **1974**, 96, 7101-7103.
- [225] (a) P. A. Wender, R. Ternansky, M. DeLong, S. Singh, A. Olivero, K. Rice, *Pure & Appl. Chem.*, **1990**, 62, 1697-1602. (b) P. A. Wender, J. J. Howbert, *J. Am. Chem. Soc.*, **1981**, 103, 688-690.
- [226] T. Hayashi, M. Konishi, Y. Kobori, M. Kumada, T. Higuchi, K. Hirotsu, *J. Am. Chem. Soc.*, **1984**, 106, 158-163.
- [227] (a) H. Lebel, M. K. Janes, A. B. Charette, S. P. Nolan, *J. Am. Chem. Soc.*, **2004**, 126, 5046-5047. (b) J. Huang, S. P. Nolan, *J. Am. Chem. Soc.*, **1999**, 121, 9889-9890.
- [228] M. K. Schindler, *Synthesis of new HBC derivatives and investigation of their  $\pi$ - $\pi$ -stacking properties*, **2006**, Master Thesis, University of Fribourg.
- [229] T. Jeffery, *Tetrahedron*, **1996**, 52, 10113-10130.
- [230] M. Wende, F. Seidel, J. A. Gladysz, *J. Fluorine Chem.*, **2003**, 124, 45-54.
- [231] K. Maruoka, H. Sano, K. Shindoa, S. Nakai, H. Yamamoto, *J. Am. Chem. Soc.*, **1986**, 108, 6036-6038.
- [232] W. L. Collier, R. S. Macomber, *J. Org. Chem.*, **1973**, 38, 1367-1369.
- [233] P. Vinczer, R. Kovacs, L. Novak, C. Szantay, *OPPI Briefs*, **1989**, 21, 232-237.
- [234] (a) D. Käfer, G. Witte, P. Cyganik, A. Terfort, C. Wöll, *J. Am. Chem. Soc.*, **2006**, 128, 1723-1732. (b) J. C. Love, L. A. Estroff, J. K. Kriebel, R. G. Nuzzo, G. M. Whitesides, *Chem.*

- Rev.*, **2005**, 105, 1103-1169. (c) J. W. Ciszek, T. M. Tour, *Chem. Mater.*, **2005**, 17, 5684-5690.
- [235] (a) B. K. Spraul, S. Suresh, S. Glaser, D. Perahia, J. Ballato, D. W. Smith, Jr., *J. Am. Chem. Soc.*, **2004**, 126, 12772-12773. (b) P. Samori, X. Yin, N. Tchegbotareva, Z. Wang, T. Pakula, F. Jäckel, M. D. Watson, A. Venturini, K. Müllen, J. P. Rabe, *J. Am. Chem. Soc.*, **2004**, 126, 3567-3575. (c) M. Lee, J.-W. Kim, S. Peleshanko, K. Larson, Y.-S. Yoo, D. Vaknin, S. Markutsya, V. V. Tsukruk, *J. Am. Chem. Soc.*, **2002**, 124, 9121-9128. (d) Z. Li, N. T. Lucas, Z. Wang, D. Zhu, *J. Org. Chem.*, **2007**, 72, 3917-3920.
- [236] K. Weiss, G. Beernink, F. Dötz, A. Birkner, K. Müllen, C. H. Wöll, *Angew. Chem. Int. Ed.*, **1999**, 38, 3748-3752.
- [237] (a) X. Shen, D. M. Ho, R. A. Pascal, Jr., *J. Am. Chem. Soc.*, **2004**, 126, 5789-5805. (b) M. Schlupp, T. Weil, A. J. Berresheim, U. M. Wiesler, J. Bargon, K. Müllen, *Angew. Chem. Int. Ed.*, **2001**, 40, 4011-4015. (c) E. C. Constable, O. Eich, D. Fenske, C. E. Housecroft, L. A. Johnston, *Chem. Eur. J.*, **2000**, 6, 4364-4370.
- [238] E. Brenna, C. Fuganti, S. Serra, *J. Chem. Soc., Perkin, Trans. I*, **1998**, 901-904.
- [239] E. O. Stejskal, J. D. Memory, *High Resolution NMR in the Solid State – Fundamentals of CP / MAS*, **1994**, Oxford University Press.
- [240] J. Duer, *Solid-State NMR Spectroscopy, principles and applications*, **2001**, Blackwell Science
- [241] D. D. Laws, H.-M. L. Bitter, A. Jerschow, *Angew. Chem. Int. Ed.*, **2002**, 114, 3224-3259. (b) N. J. Clayden, *Ann. Rep. MMR Spectro.*, **1992**, 24, 1-74.
- [242] S. Antonijevic, G. Bodenhausen, *Angew. Chem. Int. Ed.*, **2005**, 44, 2935-2938.
- [243] (a) S. Trimpin, A. Rouhanipour, R. Az, H. J. Räder, K. Müllen, *Rapid Commun. Mass Spectrom.*, **2001**, 15, 1364-1373. (b) L. Przybilla, J.-D. Brand, K. Yoshimura, H. J. Räder, K. Müllen, *Anal. Chem.*, **2000**, 72, 4591-4597.
- [244] M. A. T. Meier, N. Adams, U. S. Schubert, *Anal. Chem.*, **2007**, 79, 863-869.
- [245] P. Echlin, *Low-Temperature Microscope and Analysis*, **1992**, Plenum Press, New York.
- [246] (a) M. Kastler, J. Schmidt, W. Pisula, D. Sebastiani, K. Müllen, *J. Am. Chem. Soc.*, **2006**, 128, 9526-9534. (b) A. J. Fleming, J. N. Coleman, A. B. Dalton, A. Fechtenkötter, M. D. Watson, K. Müllen, H. J. Byrne, W. J. Blau, *J. Phys. Chem. B*, **2003**, 107, 37-43.
- [247] (a) M. Zander, *Fluorimetrie*, **1981**, Springer-Verlag, Berlin. (b) J. N. Murrell, *The Theory of the Electronic Spectra of Organic Molecules*, **1963**, Methuen & Co Ltd, London.
- [248] K. Suhling, J. Siegel, D. Phillips, P. M. W. French, S. Lévêque-Fort, S. E. D. Webb, D. M. Davis, *Biophys. J.*, **2002**, 83, 3589-3595.
- [249] S. J. Strickler, R. A. Berg, *J. Chem. Phys.*, **1962**, 37, 814-822.
- [250] P. Attard, *Molec. Phys.*, **1996**, 89, 691-709.
- [251] J. Wu, W. Pisula, K. Müllen, *Chem. Rev.*, **2007**, 107, 718-747.



- [252] T.-Q. Nguyen, R. Martel, P. Avouris, M. L. Bushey, L. Brus, C. Nuckolls, *J. Am. Chem. Soc.*, **2004**, 126, 5234-5242.
- [253] (a) C. A. Hunter, K. R. Lawson, J. Perkins, C. J. Urch, *J. Chem. Soc., Perkin Trans. 2*, **2001**, 651-669. (b) L. Schanne, H. A. Staab, *Tetrahedron Lett.*, **1984**, 25, 1721-1724.
- [254] (a) E. W. Meijer et al., *J. Mater. Chem.*, **2007**, in press. (b) T. Nishizawa, K. Tajima, K. Hashimoto, *J. Mater. Chem.*, **2007**, in press.
- [255] D. Muñoz, *Synthesis of new HBC derivatives carrying branched perfluoroalkylated side chains and investigation of their  $\pi$ - $\pi$ -stacking behaviour*, **2007**, Master Thesis, University of Fribourg.
- [256] M. A. Biasutti, J. Rommens, A. Vaes, S. De Feyter, F. D. De Schryver, P. Herwig, K. Müllen, *Bull. Soc. Chim. Belg.*, **1997**, 106, 659-664.
- [257] (a) F. Morale, R. W. Date, D. Guillon, D. W. Bruce, R. L. Finn, C. Wilson, A. J. Blake, M. Schröder, B. Donnio, *Chem. Eur. J.*, **2003**, 9, 2484-2501. (b) D. Guillon, *Struct. Bonding*, **1999**, 95, 42-82.
- [258] (a) M. Tonouchi, *Nature Photonics*, **2007**, 1, 97-105. (b) A. Schneider, M. Stillhart, P. Günter, *Optic Express*, **2006**, 14, 5376-5384.
- [259] (a) A. Schneider, M. Neis, M. Stillhart, B. Ruiz, R. U. A. Khan, P. Günter, *J. Opt. Soc. Am. B*, **2006**, 23, 1822-1835. (b) A. Schneider, I. Biaggio, P. Günter, *Appl. Phys. Lett.*, **2004**, 84, 2229-2231.
- [260] B. Ferguson, X.-C. Zhang, *Nature Materials*, **2002**, 1, 26-33.
- [261] P. Ruffieux, O. Gröning, R. Fasel, M. Kastler, D. Wasserfallen, K. Müllen, O. Gröning, *J. Phys. Chem. B*, **2006**, 110, 11253-11258.
- [262] M. B. Pangborn, M. A. Giardello, R. H. Grubbs, R. K. Rosen, F. J. Timmers, *Organometallics*, **1996**, 15, 1518-1520.